

Metal Cutting and Design of Cutting Tools, Jigs & Fixtures

About the Author



N K Mehta retired as Professor from IIT Roorkee (former University of Roorkee) in 2010 after serving in the Department of Mechanical and Industrial Engineering for almost 40 years. He also served as Counselor (Science and Technology) at the Embassy of India in Moscow from 1995 to 1998. Dr Mehta has done extensive research in the areas of Machine Tool Design, Machining Science and Computer Aided Manufacturing. He has more than 125 research papers to his credit and has supervised 13 PhD theses and over 55 MTech dissertations. In addition, Dr Mehta was Translation Editor of the *Soviet Journal of Structural Mechanics and Design of Structures* for four years and has translated nine textbooks and monographs in English. He was also the Convenor of the First International and Twenty-second AIMTDR Conference in 2006. Dr Mehta's contribution to teaching and research has been widely acknowledged and he has been the recipient of numerous awards and honors such as G C Sen Memorial Prize for Best Research Paper at the Tenth AIMTDR conference in 1982, the A N Khosla Research Prize and silver medal in 1984, Member Program Advisory Committee of Mechanical Engineering and Robotics of the Department of Science and Technology, Govt. of India, Member Core Advisory Group for R&D in Machine Tool sector constituted by the Principal Scientific Advisor to the Govt. of India, Member, Subject Expert Committee on Engineering Sciences, FIST Program of Dept. of Science and Technology, Govt. of India, and Member Task Force on Equity and Empowerment of the Science & Engineering Research Board, Govt. of India.

Metal Cutting and Design of Cutting Tools, Jigs & Fixtures

N K Mehta

Former Professor

*Indian Institute of Technology Roorkee
Uttarakhand*



McGraw Hill Education (India) Private Limited

NEW DELHI

McGraw Hill Education Offices

New Delhi New York St Louis San Francisco Auckland Bogotá Caracas
Kuala Lumpur Lisbon London Madrid Mexico City Milan Montreal
San Juan Santiago Singapore Sydney Tokyo Toronto



McGraw Hill Education (India) Private Limited

Published by McGraw Hill Education (India) Private Limited
P-24, Green Park Extension, New Delhi 110 016

Metal Cutting and Design of Cutting Tools, Jigs & Fixtures

Copyright © 2015 by McGraw Hill Education (India) Private Limited.

No part of this publication may be reproduced or distributed in any form or by any means, electronic, mechanical, photocopying, recording, or otherwise or stored in a database or retrieval system without the prior written permission of the publishers. The program listings (if any) may be entered, stored and executed in a computer system, but they may not be reproduced for publication.

This edition can be exported from India only by the publishers,
McGraw Hill Education (India) Private Limited.

Print Edition:

ISBN-13: 978-93-3921-319-0

ISBN-10: 93-3921-319-X

eBook Edition:

ISBN-13: 978-93-3921-320-6

ISBN-10: 93-3921-320-3

Managing Director: *Kaushik Bellani*

Head—Higher Education (Publishing and Marketing): *Vibha Mahajan*

Senior Publishing Manager (SEM & Tech. Ed.): *Shalini Jha*

Editorial Executive: *Harsha Singh*

Manager—Production Systems: *Satinder S Baveja*

Assistant Manager—Editorial Services: *Sohini Mukherjee*

Senior Production Executive: *Suhaib Ali*

Assistant General Manager (Marketing)—Higher Education: *Vijay Sarathi*

Senior Graphic Designer—Cover: *Meenu Raghav*

General Manager—Production: *Rajender P Ghansela*

Manager—Production: *Reji Kumar*

Information contained in this work has been obtained by McGraw-Hill Education (India), from sources believed to be reliable. However, neither McGraw-Hill Education (India) nor its authors guarantee the accuracy or completeness of any information published herein, and neither McGraw-Hill Education (India) nor its authors shall be responsible for any errors, omissions, or damages arising out of use of this information. This work is published with the understanding that McGraw-Hill Education (India) and its authors are supplying information but are not attempting to render engineering or other professional services. If such services are required, the assistance of an appropriate professional should be sought.

Typeset at Mukesh Technologies Pvt. Ltd., Puducherry, India 605 008 and printed at

Cover Printer:

*In Memory
of
My Parents*

Contents

Preface

xi

1. Introduction to Machining Process **1**

- 1.1 Introduction 1
 - 1.1.1 *Basics of Metal Cutting* 1
 - 1.1.2 *Working and Auxiliary Motions in Machine Tools* 2
- 1.2 Concept of Speed, Feed, Depth of Cut, and Machining Time 4
- 1.3 Lathe Operations 5
- 1.4 Drilling and Allied Operations 19
- 1.5 Milling Operations 24
 - 1.5.1 *Indexing Based on Periodic Rotation* 32
 - 1.5.2 *Indexing Based on Continuous Rotation* 36
- 1.6 Shaping and Allied Operations 38
- 1.7 Grinding Operations 41
 - 1.7.1 *External Cylindrical Grinding* 41
 - 1.7.2 *Internal Cylindrical Grinding* 43
 - 1.7.3 *Surface Grinding* 44
- 1.8 Geometry of Single-Point Tool 46
 - 1.8.1 *Orthogonal System* 47
 - 1.8.2 *Machine Tool Reference System* 49
- Review Questions* 51

2. Geometry of Chip Formation **55**

- 2.1 Process of Chip Formation 55
- 2.2 Parameters of Undeformed Chip in Turning, Drilling, and Milling 58
 - 2.2.1 *Undeformed Chip in Turning* 59
 - 2.2.2 *Undeformed Chip in Drilling* 59
 - 2.2.3 *Undeformed Chip in Plain Milling* 60
 - 2.2.4 *Undeformed Chip in Face Milling* 64
- 2.3 Shear Angle and Shear Strain in Chip Formation 70
 - 2.3.1 *Shear Angle* 72
 - 2.3.2 *Shear Strain* 73
- 2.4 Types of Chips 76
 - 2.4.1 *Discontinuous Chips* 76
 - 2.4.2 *Continuous Chips* 77

- 2.4.3 *Partially Continuous Chips* 77
- 2.4.4 *Element Chips* 78
- 2.5 *Chip Flow Control and Chip Breaking* 78
 - 2.5.1 *Control of Chip Flow* 79
 - 2.5.2 *Chip Breaking* 80
 - Review Questions* 86

3. Mechanics of Machining Process

88

- 3.1 *Orthogonal and Oblique Machining* 88
- 3.2 *Force Velocity and Energy Relations in Orthogonal Machining* 91
 - 3.2.1 *Force Relations* 92
 - 3.2.2 *Velocity Relations* 95
 - 3.2.3 *Energy Relations* 96
- 3.3 *Theoretical Determination of Cutting Force* 102
 - 3.3.1 *Determination of Dynamic Shear Stress* 104
 - 3.3.2 *Shear Angle Relations* 107
 - 3.3.3 *Forces in Drilling* 117
 - 3.3.4 *Forces in Milling* 119
- 3.4 *Built-Up Edge* 121
 - 3.4.1 *Characteristic Features of BUE* 122
- 3.5 *Effect of Tool Geometry and Machining Parameters on Cutting Force* 124
 - Review Questions* 132

4. Tool Wear and Thermodynamics of Chip Formation

134

- 4.1 *Heat Sources and Its Distribution* 134
- 4.2 *Tool Failure and Tool Wear* 137
- 4.3 *Growth of Tool Wear with Cutting Time, Wear Criteria, and Wear Mechanisms* 140
 - 4.3.1 *Tool Wear Criteria* 142
 - 4.3.2 *Tool Wear Mechanisms* 146
- 4.4 *Tool Life and Machinability* 149
- 4.5 *Tool Life Testing* 158
 - 4.5.1 *Facing Test* 159
 - 4.5.2 *Variable Speed Test* 162
- 4.6 *Effect of Various Factors on Tool Life* 163
 - 4.6.1 *Effect of Work Material* 163
 - 4.6.2 *Effect of Tool Material* 165
 - 4.6.3 *Effect of Tool Geometry* 175
- 4.7 *Machinability* 179
 - 4.7.1 *Surface Finish* 180
 - 4.7.2 *Machinability Index* 183
- 4.8 *Theoretical Determination of Cutting Temperature* 185
 - 4.8.1 *Temperature Relations for Various Heat Sources* 185

- 4.8.2 *Shear Plane Temperature* 188
- 4.8.3 *Tool–chip Interface Temperature and Cutting Temperature* 190
- 4.9 Economics of Machining 191
 - 4.9.1 *Sequence of Assigning the Machining Parameters* 192
 - 4.9.2 *Selection of Depth of Cut* 195
 - 4.9.3 *Selection of Feed* 195
 - 4.9.4 *Selection of Optimum Cutting Speed* 199
- Review Questions* 205

5. Geometry of Cutting Tools

208

- 5.1 Issues in Geometry of Single-Point Tools 209
 - 5.1.1 *Effect of Tool Setting and Feed on Rake and Clearance Angles* 209
 - 5.1.2 *Selection of Optimum Tool Angles* 212
- 5.2 Geometry of Form Tool 214
- 5.3 Geometry of Drill 216
- 5.4 Geometry of Milling Cutters 223
 - 5.4.1 *Geometry of Plain Milling Cutter* 225
 - 5.4.2 *Geometry of Face Milling Cutter* 227
- 5.5 Geometry of Broach 230
- 5.6 Geometry of Thread Cutting Tools 233
 - 5.6.1 *Geometry of Single-Point Thread Cutting Tool* 235
 - 5.6.2 *Geometry of Thread Chasers* 237
 - 5.6.3 *Geometry of Thread Cutting Taps* 240
 - 5.6.4 *Geometry of Thread-Cutting Die* 241
- 5.7 Geometry of Gear Cutting Tools 243
 - Review Questions* 244

6. Design of Cutting Tools

246

- 6.1 Design of Single-Point Tool 246
 - 6.1.1 *Features Related to Cutting Bit* 249
- 6.2 Design of Form Tool 256
 - 6.2.1 *Design of Circular Form Tool* 256
 - 6.2.2 *Design of Flat Form Tool* 262
- 6.3 Design of Drills 266
- 6.4 Design of Milling Cutters 272
 - 6.4.1 *Design of Plain Milling Cutter* 272
 - 6.4.2 *Design of Face Milling Cutters* 276
- 6.5 Design of Broach 278
- 6.6 Design of Thread Cutting Tools 287
 - 6.6.1 *Design of Taps* 287
 - 6.6.2 *Design of Thread Cutting Dies* 292
- 6.7 Geometry and Design of Gear Cutting Tools 296
 - 6.7.1 *Geometry and Design of Module Cutter* 296

- 6.7.2 *Geometry and Design of Gear Shaping Cutter* 299
- 6.7.3 *Geometry and Design of Hob* 306
- Review Questions* 313

7. Design of Jigs and Fixtures

315

- 7.1 *Introduction* 315
- 7.2 *Location Principles, Methods, and Elements* 317
 - 7.2.1 *Concept of Design, Setting, and Measuring Datum Surfaces* 317
 - 7.2.2 *Locating Scheme, Error Analysis, and Elements for Prismatic Parts* 324
 - 7.2.3 *Locating Scheme, Error Analysis, and Elements for Long Cylindrical Parts* 325
 - 7.2.4 *Locating Scheme, Error Analysis, and Elements for Short Cylindrical Parts* 333
 - 7.2.5 *Locating Scheme, Error Analysis, and Elements for Parts with Through Hole* 333
 - 7.2.6 *Locating Scheme, Error Analysis, and Elements for Parts with Flat Base and Two Predrilled Holes* 339
 - 7.2.7 *Locating Scheme, Error Analysis, and Elements for Parts with Center Holes at End Faces* 343
- 7.3 *Clamping Principles, Methods, and Elements* 344
 - 7.3.1 *Clamping Principles* 345
 - 7.3.2 *Clamping Force Calculation* 348
 - 7.3.3 *Clamping Mechanisms and Applied Force Calculation* 355
 - 7.3.4 *Clamping Elements and Devices* 375
- 7.4 *Tool Guiding Elements* 379
- 7.5 *Indexing Devices* 383
- 7.6 *Body of Jigs and Fixtures* 386
- 7.7 *Power Devices* 389
 - Review Questions* 397

8. Classification of Jigs and Fixtures and Their Economic Analysis

402

- 8.1 *Classification of Jigs and Fixtures* 402
 - 8.1.1 *Universal General-Purpose Fixture(UGP)* 402
 - 8.1.2 *Universal Adjustable Fixture(UAF)* 403
 - 8.1.3 *Special Adjustable Fixture(SAF)* 404
 - 8.1.4 *Reassemblable Fixture(RAF)* 404
 - 8.1.5 *Universal Built-Up Fixture(UBF)* 405
 - 8.1.6 *Special Fixtures(SPF)* 411
- 8.2 *Economics of Jigs and Fixtures* 419
 - 8.2.1 *Calculation of Annual Cost of Fixture* 419
 - 8.2.2 *Relative Economic Analysis* 423
 - Review Questions* 427

Preface

About the Book

The topics ‘Cutting Tool Design’ and ‘Design of Jigs & Fixtures’ are included in the undergraduate curriculum of Mechanical Engineering, Production Engineering and Industrial Engineering disciplines of a large number of engineering institutions, often, as supplementary material in subjects such as ‘Metal Cutting’, ‘Advanced Machine Tool Processes’, ‘Theory of Production Processes’, etc. Both ‘Cutting Tool Design’ and ‘Design of Jigs & Fixtures’ are applied engineering topics that rely on common fundamentals derived from the theory of metal cutting and machining practices. It, therefore, makes sense to combine them into an independent subject. This realization lies at the root of the increasing trend that in many institutions these topics are now combined and offered as an independent subject under various names such as ‘Tool Design’, ‘Tooling Design’, ‘Tool Engineering’, etc. There are very few texts that deal with both these topics in sufficient detail. The present book has been written primarily to fulfill the need of a text that can serve as basic reference when these topics constitute an independent subject and supplementary reference when one or both of them are taught as part of another subject.

As mentioned above, both ‘Cutting Tool Design’ and ‘Design of Jigs & Fixtures’ cannot be studied or taught without a good understanding of the fundamental concepts, and theory of metal cutting and knowledge of machining operations and practices. Therefore, a major section on ‘Metal Cutting’ is included in the book to serve as the foundation for the subsequent sections on ‘Cutting Tool Design’ and ‘Design of Jigs & Fixtures’. The detailed coverage of these three sections in a single text is perhaps unique to the present book and is meant to provide a common platform for studying metal cutting theory and machining practices and their application to the design of cutting tools, jigs and fixtures.

In the available texts, the topics of ‘Cutting Tool Design’ and ‘Design of Jigs & Fixtures’ are presented mostly as a compilation of the existing designs. The analysis that supports the design is either absent altogether or very elementary in treatment. In the present book, there is strong emphasis on discussion and analysis of the design fundamentals and how they are applied to the design of individual cutting tools, jigs and fixtures. This approach makes the text extremely teacher-friendly’ allowing the teacher to organize the content easily into a structured set of lectures for classroom delivery.

Another unique feature of the present book is the large number of solved examples for better understanding of the concepts, elaboration of design procedures and illustration of design practices. Also, a large number of review questions have been given at the end of each chapter. These measures are aimed at making the book ‘student-friendly’, both from the viewpoint of independent study of the text and practice and self-evaluation of the studied material.

Wherever relevant, the necessary data, empirical relations, tables and design curves have been included in the text to avoid cross-referencing to handbooks and manuals in the interest of smooth reading. The overall endeavor has been to present the material in a form that is easy to understand and assimilate and is at the same time comprehensive enough to enable students and practicing engineers to apply it for solution of actual problems.

The practices adopted for the design of cutting tools, jigs and fixtures display significant variation between various manufacturers. It is, therefore, possible that the methods, procedures and even the theory presented in the present book may not entirely agree with the practices prevailing in individual organizations. However, this should not detract from the merit of the book in its potential to stimulate systematic and logical application of the metal cutting theory and machining practices to the design of cutting tools, jigs and fixtures.

The subject material has been taken mostly from various books, handbooks, manufacturer's catalogues and technical papers. A sincere effort has been made to acknowledge all the sources in the bibliography. Any failure to give credit to the original source is only due to oversight and I offer my apologies for the same. Although metal cutting, cutting tool design and design of jigs and fixtures are well-established topics, a discerning reader will notice an occasional new way of presentation of material, elaboration of a point or a line diagram that is simpler. This is all I can claim by way of originality. Otherwise, the main objective of the present endeavor was to organize and present the wealth of available information in a coherent form, suitable for an undergraduate textbook. I would like to think I have been able to do this with modest success and hope the book will meet the approval of students, teachers and practicing engineers dealing with the topics of metal cutting, cutting tool design and design of jigs and fixtures in their different capacities.

Salient Features

- Strong emphasis on discussion and analysis of design fundamentals and how they are applied to the design of individual cutting tools, jigs and fixtures
- Elaboration of design procedures and illustration of design practices
- Necessary data, empirical relations, tables and design curves included in the text for smooth reading
- Large and clear diagrams for better comprehension
- Rich pedagogy:
 - Diagrams: 318
 - Solved Examples: 65
 - Practice Problems: 185
 - Tables: 51

Structure of the Book

The material presented in the book can be broadly classified into three distinct sections. *Section 1* deals with the concepts and theory of metal cutting and is covered in chapters 1 thru 4. *Section 2* deals with cutting tool design and is covered in chapters 5 and 6. Finally, *Section 3* deals with the design of jigs and fixtures and is covered in chapters 7 and 8.

Chapter 1 is an introductory chapter that provides a review of the concepts of working and auxiliary motions in machine tools. It describes the tools used and operations carried out on lathe, drilling, milling, shaping and grinding machines with the help of simple sketches, and illustrates the calculation of machining time for these operations. The geometry of single-point tool in the orthogonal and machine-tool reference system is discussed. The chapter contains 16 solved examples and 39 review questions.

Chapter 2 describes the various models of chip formation and gives the derivations for determining the parameters of undeformed chip in turning, drilling, and milling operations. A general approach has been applied in all the derivations, many of which are being reported for the first time. Theoretical expressions have been derived for shear angle and shear strain. Formation of various types of chips is discussed and methods of controlling the flow of chips and chip breaking in continuous chips are described. The theoretical fundamentals for design of chip breakers are presented with derivations. The chapter contains 3 solved examples and 13 review questions.

Chapter 3 discusses the difference between orthogonal and oblique machining and presents the derivations of force, velocity and energy relations for orthogonal machining. Theoretical determination of cutting force has been discussed in detail. The relations proposed by Bridgman, Zorev, and Rozenberg and Eremin for determining dynamic shear stress have been presented. Shear angle relations of Ernst and Merchant (including Merchant's second relation), Kronenberg, and Lee and Schaffer have been derived from first principles. Empirical relations for cutting forces in drilling and milling operations are presented with the necessary data. The formation of built-up edge and its characteristic features are discussed in detail. Finally, the effect of work material, machining parameters (feed, depth of cut, cutting speed) and tool geometry (rake angle, clearance angle, primary cutting edge angle, cutting edge inclination angle and nose radius) has been presented with suitable empirical relations and necessary data. The chapter contains 6 solved examples and 13 review questions.

Chapter 4 presents a discussion of heat sources in metal cutting and distribution of heat between the workpiece, tool, and chip. Various models of tool failure have been presented. Tool wear mechanisms and criteria have been described and expressions for optimum tool wear have been derived. Tool life and its testing have been presented with a detailed discussion of the effect of work material, tool material, and tool geometry on tool life. An interesting feature of this part is the description of important tool materials in the chronological order of their development. The concept of machinability has been discussed with reference to various parameters, including surface finish. Theoretical determination of cutting temperature has been described in considerable detail and expressions for shear plane temperature and tool-chip interface temperature have been derived. The economics of machining has been presented in detail and expressions of optimum tool life and cutting speed for minimum cost and maximum production rate have been derived. An interesting feature of this part is the discussion on the correct sequence of assigning the machining parameters, including the effect of various constraints while selecting the feed. The chapter contains 7 solved examples and 22 review questions.

Chapter 5 is the first of the two chapters dealing with design of cutting tools. The cutting wedge in all cutting tools performs more or less the same function and its geometry displays a remarkably high degree of similarity among various cutting tools. Therefore, some general issues such as effect of tool setting and feed on actual rake and clearance angles are discussed along with recommendations for selection of optimum tool geometry of single-point tool

in the beginning. This is followed by the discussion of the geometry of individual tools to highlight their specific distinguishing features. The tools covered for this purpose are form tool, drill, milling cutters, broach and thread-cutting tools (single-point threading tool, thread chasers, taps, and thread-cutting dies). The chapter contains 8 solved examples and 11 review questions.

Chapter 6 deals with the design of cutting tools, focusing on the features other than the cutting wedge and their parameters. The discussion on design of single-point cutting tool is accompanied by a brief description of the types of bits and tool holders. The design of the rest of the tools discussed in this chapter is based partially on analysis, but is largely dependent on empirical knowledge in the form of relations, recommendations, tables and charts. All this information has been provided for the individual cutting tools in a manner which makes for its seamless integration with the design procedure. The tools covered in this section are single-point tool, form tool, drill, milling cutters, broach, thread-cutting taps and dies, and gear-cutting tools (module cutter, gear shaping cutter, and hob). A unique feature of this chapter is that the discussion of the design of every tool is illustrated with a solved example in which some critical parameter(s) is kept for cross check to verify the correctness of design and thereby inspire confidence in the credibility of the empirical data used in the design process. In fact, with some effort, most of the solved examples can be developed into design assignments for minor projects. The chapter contains 11 solved examples and 23 review questions.

Chapter 7 is the first of the two chapters devoted to the design of jigs and fixtures. The concept of design, setting, and measuring datum surfaces has been introduced as a prelude to understanding of location principles and locating error. Engineered parts have been classified into six broad categories as prismatic parts, long cylindrical parts, short cylindrical parts, parts with through hole, parts with flat base and two predrilled holes and parts with center holes at the end faces. A subsection is devoted to the description of locating scheme, error analysis, and locating elements for each category of parts. Clamping principles have been discussed from the viewpoint of calculation of clamping force, and its point and direction of application. The general principles have been summarized and illustrated with representative examples for turning, drilling, and milling operations. A major subsection is devoted to description and analysis of the mechanisms employed for application of clamping force. The mechanisms covered are screw type, eccentric type, wedge type, lever type and toggle type. The application of various clamps is illustrated with the help of simple sketches. A subsection each is devoted to guiding elements, indexing devices, and bodies of jigs and fixtures which have been illustrated with the help of simple sketches. Finally, a subsection is devoted to pneumatic, hydraulic and hydro pneumatic power devices for large jigs and fixtures in which manual application of the clamping force is beyond human capability. A brief description of vacuum-operated and magnetic devices is also included in this subsection. The chapter contains 11 solved examples and 48 review questions.

Chapter 8 presents an interesting classification of jigs and fixtures into six categories, namely, universal general purpose (UGP), universal adjustable (UAF), special adjustable (SAF), re-assemblable (RAF), universal built-up (UBF) and special (SPF). The functioning and distinguishing characteristics of each category are illustrated with simple diagrams. Special fixtures have been further classified based on machine tools for which they are designed as lathe fixtures, milling fixtures, drill jigs, etc. For each of these types, a few representative jigs/fixtures have been presented in the form of simple line diagrams with the main objective of illustrating

how the various aspects of design of jigs and fixtures discussed in Chapter 7 are applied in actual practice. A detailed cost analysis based on break-even and total cost is discussed for all the six general categories of jigs and fixtures. The chapter contains 3 solved examples and 16 review questions

Online Learning Center

The Online Learning Center can be accessed at <http://www.mhhe.com/mehta/mcd1> and contains the following material:

For Instructors

- Lecture PowerPoint slides

For Students

- Interactive quizzes
- Sample chapter

Acknowledgements

I would like to take this opportunity to remember with gratitude the late Prof. A Ya. Malkin and Prof. A D Shustikov who were my PhD supervisors at Peoples Friendship University, Moscow, and all through my professional career have been my inspiration for their brilliant intellect and work ethics. I would also like to gratefully thank Prof. P C Pandey, one of the leading authorities in metal cutting and a former senior colleague for taking me under his mentorship early in my career. From him I learnt the importance of the core values of simplicity, honesty, and discipline for a career in teaching and research. I would also like to thank Prof. P K Jain, Head of the Department of Mechanical and Industrial Engineering at IIT Roorkee, for providing the environment, facilities, and support for creative study and work during the period of writing and manuscript preparation of this book. Thanks are due to my PhD student Vikas Upadhyaya for assistance in collecting reference material for the section on metal cutting and to my MTech students Nitin Saini and Amol Dudhbale for the section on jigs and fixtures. Finally, I would like to thank Sri Rajesh Kumar for typing the manuscript and drawing the technical figures and providing technical assistance of varied nature.

Note of Thanks to Reviewers

Both the author as well as the publisher would like to thank the following reviewers for their valuable comments.

| | |
|------------------------|--|
| Gaurav Bartarya | <i>Harcourt Butler Technological Institute (HBTI), Kanpur, Uttar Pradesh</i> |
| Abid Ali Khan | <i>Aligarh Muslim University, Aligarh, Uttar Pradesh</i> |
| Jagannath De | <i>National Institute of Technology (NIT) Durgapur, West Bengal</i> |
| Alok Kumar Das | <i>Indian School of Mines (ISM) Dhanbad, Jharkhand</i> |

| | |
|-------------------------------|--|
| Ajay D Diwate | <i>TSSM's Bhivarabai Sawant College of Engineering and Research, Pune, Maharashtra</i> |
| G L Samuel | <i>Indian Institute of Technology (IIT) Madras, Tamil Nadu</i> |
| Krishnaswamy Marimuthu | <i>Coimbatore Institute of Technology, Coimbatore, Tamil Nadu</i> |
| K Prabhakaran Nair | <i>National Institute of Technology (NIT) Calicut, Kerala</i> |
| Anne Venu Gopal | <i>National Institute of Technology (NIT) Warangal, Telangana</i> |

Publisher's Note

McGraw-Hill Education (India) invites suggestions and comments from you, all of which can be sent to info.india@mheducation.com (kindly mention the title and author name in the subject line).

Piracy-related issues may also be reported.

Chapter

1

INTRODUCTION TO MACHINING PROCESS

1.1 Introduction

1.1.1 Basics of Metal Cutting

Metal cutting is a process by which a workpiece is converted into a component of the desired specifications by removing excess material from the workpiece in the form of chips by using a wedge-shaped tool. In its simplest form, metal cutting may be visualized as shown in Figure 1.1a, where the wedge moves relative to the workpiece with a velocity v and, in this process, undeformed workpiece layer A is converted into chip B. The transition from undeformed layer to chip occurs by shearing along plane C, which is known as shear plane. Surface D of the wedge along which the chip flows is known as face, and surface E facing the machined surface F is known as flank. The angle that the flank makes with the velocity vector is known as clearance angle and is denoted as α , whereas the angle that the face makes with the normal to the vector is known as rake angle and denoted by γ .

Now consider the situation depicted in Figure 1.1b, where a wedge with $\alpha = 0$ is shown. Although, in principle, it is possible to carry out machining with this tool, it is not desirable, because the flank rubs against the machined surface and damages it in the process. In the case of a wedge with a negative clearance angle α (Figure 1.1c), machining is simply not possible because at the beginning of the cut itself, the wedge hits the workpiece not as a cutting tool, but as a punch and proceeds to indent the workpiece material around the wedge, rather than shearing and converting it into a chip.

Having come to the important conclusion that the clearance angle must always be positive, we may now consider the relative merits of machining with tools having positive rake angle (Figure 1.1a), zero rake angle (Figure 1.1d), and negative rake angle (Figure 1.1e). It is evident that positive rake angle produces a narrow acute wedge (Figure 1.1a), which shears the workpiece material with less force, whereas, a tool with a negative rake angle has a wide, obtuse wedge (Figure 1.1e), which requires a larger force for removing the same layer of workpiece material. On the contrary, thanks to its larger bulk, the negative rake angle tool can withstand heavier loads and its cutting edge gets less heated because the heat generated in the cutting process is spread over a larger volume. From the above discussion, it follows that in general positive rake angle tools are to be preferred on account of their better cutting efficiency, except in the cases when the tool is subjected to heavy mechanical loading (e.g. while machining of high strength alloys), impact loading (e.g. while machining brittle materials), and heavy thermal loading (e.g. machining of heat resistant alloys and materials having poor thermal conductivity). In all such cases, the heavier

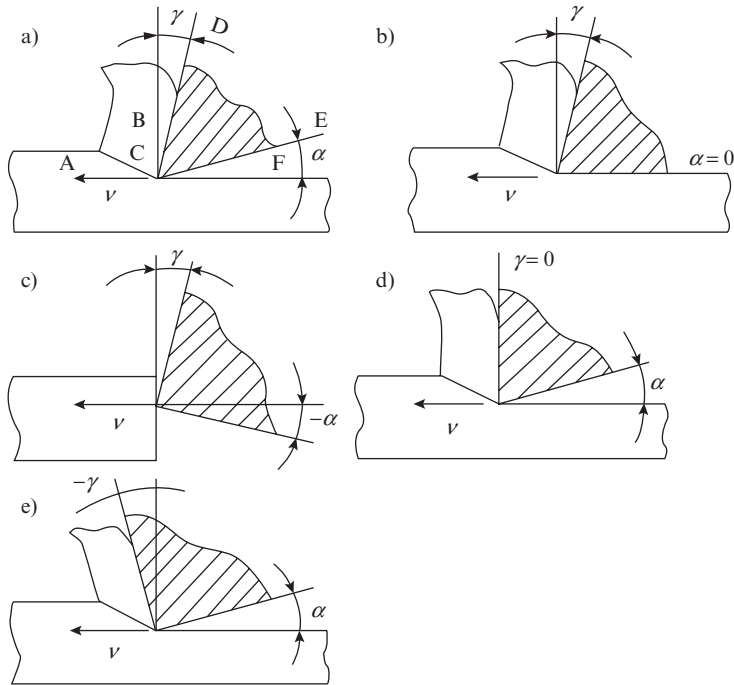


Figure 1.1 Schematic depicting chip formation: (a) cutting tool as a wedge and definition of rake face, flank, rake angle, and clearance angle; (b) cutting with wedge having clearance angle $\alpha = 0$; (c) cutting with wedge having negative clearance angle; (d) cutting with wedge having zero rake angle; and (e) cutting with wedge having negative rake angle

bulk and larger volume of negative rake tools will become the predominant factor and favour the selection of negative rake angle tools. The tools with zero rake angle occupy an intermediate position in terms of tool geometry and may be the right choice at some compromise level between the conflicting requirements of cutting efficiency epitomized by positive rake angle and robustness to withstand mechanical and thermal loads distinctive of negative rake angle.

1.1.2 Working and Auxiliary Motions in Machine Tools

For obtaining the required shape on the workpiece, it is necessary that the cutting edge of the cutting tool should move in a particular manner with respect to the workpiece. The relative movement between the workpiece and the cutting edge can be obtained either by the motion of the workpiece, the cutting tool, or by a combination of the motions of both the workpiece and cutting tool. These motions that are essential to impart the required shape to the workpiece are known as working motions. Working motions are further classified into two categories:

- (i) Drive motion or primary cutting motion
- (ii) Feed motion

Working motions in machine tools are generally of two types: rotary and translatory. Working motions of some important groups of machine tools are shown in Figure 1.2.

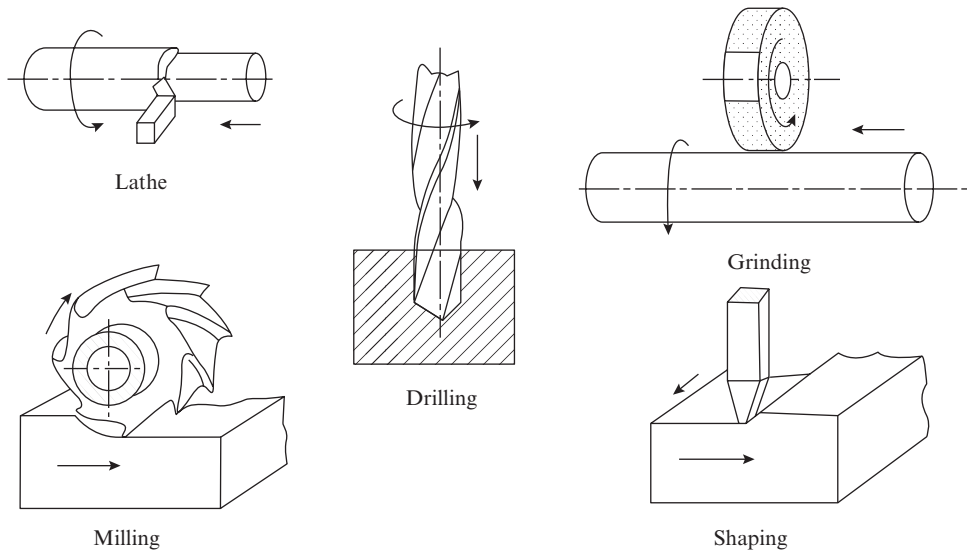


Figure 1.2 Working motions for some machine tools

- (i) *For lathes and boring machines:*
 Drive motion—rotary motion of workpiece
 Feed motion—translatory motion of cutting tool in the axial or radial direction
- (ii) *For drilling machines:*
 Drive motion—rotary motion of drill
 Feed motion—translatory motion of drill
- (iii) *For milling machines:*
 Drive motion—rotary motion of the cutter
 Feed motion—translatory motion of the workpiece
- (iv) *For shaping, planing, and slotting machines:*
 Drive motion—reciprocating motion of cutting tool
 Feed motion—intermittent translatory motion of workpiece
- (v) *For grinding machines:*
 Drive motion—rotary motion of the grinding wheel
 Feed motion—rotary as well as translatory motion of the workpiece

Besides the working motions, a machine tool also has provision for auxiliary motions. The auxiliary motions do not participate in the process of formation of the required surface but are nonetheless necessary to make the working motions fulfill their assigned function. Examples of auxiliary motions in machine tools are clamping and unclamping of the workpiece, idle travel of the cutting tool to the position from where cutting is to proceed, changing the speed of drive and feed motions, engaging and disengaging of working motions, etc.

In machine tools, the working motions are powered by an external source of energy (electrical or hydraulic motor). The auxiliary motions may be carried out manually or may also be power-operated depending on the degree of automation of the machine tool. In general-purpose machine tools, most of the auxiliary motions are executed manually. On the contrary, in automatic machines, all auxiliary motions are automated and performed by the machine tool itself. In between these

two extremes, there are machine tools in which the auxiliary motions are automated to various degrees, that is, some auxiliary motions are automated while others are performed manually.

1.2 Concept of Speed, Feed, Depth of Cut, and Machining Time

The working motions of a machine tool are numerically defined by their velocity. The velocity of the primary cutting motion or drive motion is known as cutting speed, whereas the velocity of feed motion is known as feed.

The cutting speed is denoted by v and measured in the units m/min. Feed is denoted by s and measured in the following units:

- (i) mm/rev in machine tools with rotary-drive motion, for example, lathes, boring machines, etc.
- (ii) mm/tooth in machine tools using multiple-tooth cutters, for example, milling machines,
- (iii) mm/stroke in machine tools with reciprocating-drive motion, for example, shaping and planing machines,
- (iv) mm/min in machine tools that have a separate power source for feed motion, for example, milling machines.

In machine tools with rotary primary cutting motion, the cutting speed is determined by the following relation:

$$v = \frac{\pi dn}{1000} \text{ m/min} \quad (1.1)$$

where d = diameter of workpiece (as in lathes) or cutter (as in milling machines) in millimeter

n = revolutions per minute (rpm) of the workpiece or cutter

In machine tools with reciprocating primary cutting motion, the cutting speed is determined as follows:

$$v = \frac{L}{1000T_c} \text{ m/min} \quad (1.2)$$

where L = length of stroke in millimeter

T_c = time of cutting stroke in minutes

If the time of the idle stroke in minutes is denoted by T_i , the number of strokes per minute can be determined as follows:

$$n = \frac{1}{T_c + T_i}$$

Generally, the time of idle stroke T_i is less than the time of cutting stroke; if the ratio T_c/T_i is denoted by K , the expression for number of strokes per minute may be rewritten as follows:

$$n = \frac{1}{T_c(1 + T_i/T_c)} = \frac{K}{T_c(1 + K)} \quad (1.3)$$

Now, combining Eqs (1.2) and (1.3), the relationship between cutting speed and number of strokes per minute may be written as follows:

$$v = \frac{n \cdot L(K+1)}{1000K} \quad (1.4)$$

The feed per revolution and feed per stroke are related to the feed per minute by the following relation:

$$s_m = s \cdot n \quad (1.5)$$

where s_m = feed per minute

s = feed per revolution or feed per stroke

n = number of revolutions or strokes per minute

The feed per tooth in multiple-tooth cutters is related to the feed per revolution as follows:

$$s = s_z \cdot Z \quad (1.6)$$

where s = feed per revolution

s_z = feed per tooth of the cutter

Z = number of teeth on the cutter

The machining time of any operation can be determined from the following basic expression:

$$T_m = \frac{L}{s_m} \text{ min} \quad (1.7)$$

where T_m = machining time in minutes

L = length of machined surface in millimeter

s_m = feed per minute

The thickness of the layer that is required to be removed in a machining operation is known as allowance. Depending on the machine capacity, this allowance may be removed in one or more passes (cuts). The thickness of the layer removed in one pass, measured perpendicular to the direction of feed, is known as depth of cut and is denoted by t .

1.3 Lathe Operations

Lathes are used primarily for machining axisymmetric parts on which a wide variety of operations can be carried out, such as simple turning, facing, boring, grooving, parting off, taper turning, forming, thread cutting, drilling, etc. In all these operations, the rotation of the workpiece clamped in the spindle is the primary cutting motion, whereas the translatory movement of the cutting tool is the feed or auxiliary motion.

A typical single-point tool used on lathe is shown in Figure 1.3, and the various features labeled on the figure are defined here. The face is the surface along which the chip flows. The tool surfaces facing the workpiece are known as flanks. The flank facing the current workpiece layer being cut is known as primary flank, whereas the flank facing the machined surface is known as auxiliary flank. The cutting edge produced by the intersection of the face and primary flank is known as the primary cutting edge and does the bulk of metal removal. The auxiliary cutting edge that is obtained as a result of the intersection of the face and auxiliary flank is a geometric necessity, although it plays little role in the metal removal process. The tip of the tool is formed by the

intersection of the primary and auxiliary cutting edges. If the tip is sharp, it has a tendency to chip or crumble. Therefore, a small radius is provided at the tip. The rounded tip is known as nose and the radius of the tip is known as nose radius.

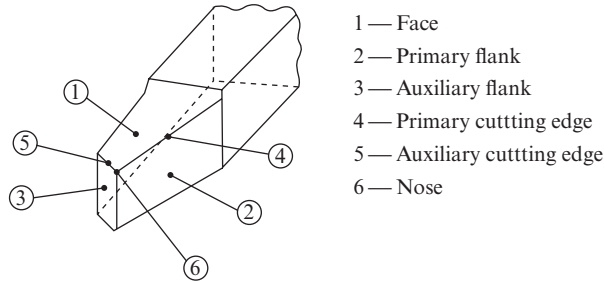


Figure 1.3 Definition of the features of single-point tool

The tool shown in Figure 1.3 is a right-hand tool, and the definition of features given above is valid only for a right-hand tool. There arises a logical question: What is a right-hand tool? In a right-hand tool, the primary cutting edge falls on the thumb side, if the palm of the right hand is placed on top of the tool with the fingers pointing toward the tip (Figure 1.4a). By the same convention, a tool in which the primary cutting edge falls under the thumb of the left hand when placed in a similar manner is defined as a left-hand tool (Figure 1.4b).

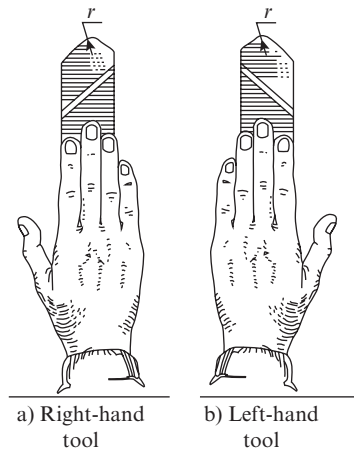


Figure 1.4 Left-hand and right-hand tools

The commonly used tools for various lathe operations are shown in Figure 1.5. To the right hand tools, feed is imparted from right to left, and to the left hand tools, feed is imparted from left to right. The straight shank tools (Figure 1.5a–d) are used for turning with axial feed, whereas bent shank tools may be used for facing operations with cross feed (Figure 1.5e and f) as well as for turning and facing operations both with axial and crossfeed, respectively (Figure 1.5g and h). In the last-named tools, there is a common primary cutting edge A, but

two auxiliary cutting edges B and C, of which B participates in cutting during the turning operation and C during the facing operation. The tool shown in Figure 1.5i is used for parting and grooving operations, whereas the round-nosed tool shown in Figure 1.5j is used when very high surface finish is desired.

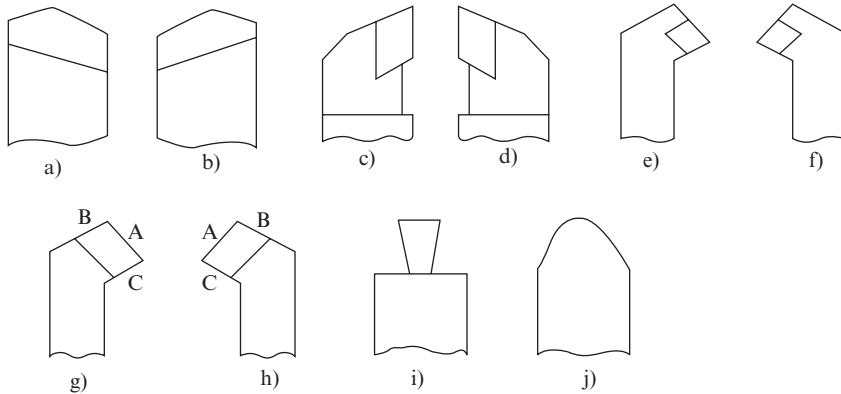


Figure 1.5 Tools used in lathe operations: (a) and (c) straight shank left-hand turning tool for turning operation with axial feed, (b) and (d) straight shank right-hand turning tool for turning operation with axial feed, (e) bent shank left-hand facing tool for facing operation with crossfeed, (f) bent shank right-hand facing tool for facing operation with crossfeed, (g) bent shank left-hand turning and facing tool, (h) bent shank right-hand turning and facing tool, (i) parting and grooving tool, and (j) round-nose tool for finishing cuts

Common lathe operations are explained below with the help of simple sketches, wherein the cutting speed, feed, and depth of cut are indicated by their respective symbols n (for rev/min), s and t .

As mentioned above, the machining time of various operations is determined using Eqn. (1.7), wherein s_m is found from Eqn. (1.5) for single-point tools and Eqn. (1.6) for multiple tooth cutters. Further, for a given work-tool pair, an optimum cutting speed is specified for which the corresponding rpm or strokes per minute is calculated using Eqs (1.1) and (1.4), respectively. It may further be noted that for a given length l of a workpiece, the actual tool travel is greater on account of the need to provide an approach of $\Delta 1$ for safe entry of tool (on commencement of machining) and over travel of $\Delta 2$ for safe exit of tool (on completion of the machining cut). Generally, $\Delta 1$ and $\Delta 2$ are taken equal to 2–3 mm. The difference in the formulae of machining time calculation for various operations arises from the individual process geometry, which is reflected in the corresponding tool travel. Hence, the calculation of tool travel for various operations is described below instead of calculation of machining time. In the figures of all the operations discussed below, I indicates the tool position at the commencement of cut and II indicates the tool position at the end of cut.

- (i) *Turning operation on workpiece held between centers* (Figure 1.6):

$$\text{Length of tool travel } L = l + \Delta 1 + \Delta 2 + \Delta 3$$

where l = length of workpiece

$\Delta 1$ = approach; generally equal to 2–3 mm

$\Delta 2$ = over travel; generally equal to 2–3 mm

$\Delta 3 = t/\cot \phi$; where t is depth of cut and ϕ is primary cutting-edge angle; for straight-edged tools $\phi = 90^\circ$, hence $\Delta 3 = 0$

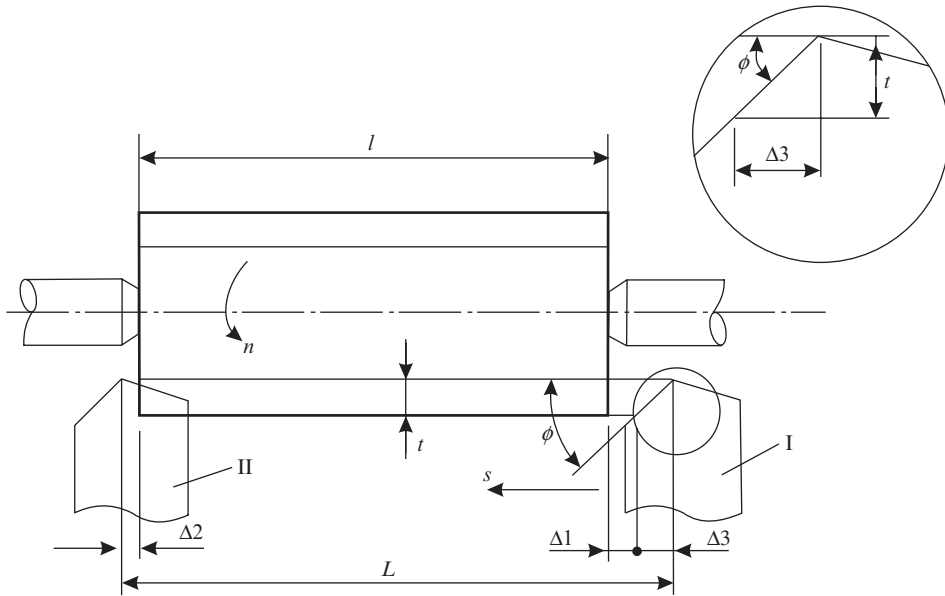


Figure 1.6 Turning operation on workpiece supported between centers

(ii) Turning operation on workpiece clamped in chuck (Figure 1.7):

Length of tool travel $L = l + \Delta 1 + \Delta 3$,

where l = length of machined surface

$\Delta 1$ and $\Delta 3$ are the same as in turning of workpiece held between centers.

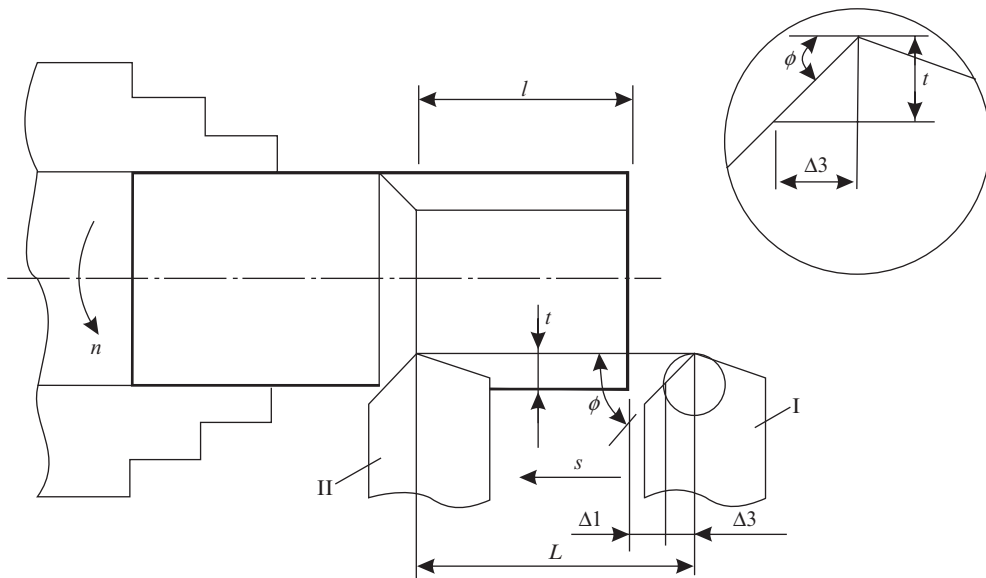


Figure 1.7 Turning operation on workpiece clamped in chuck

(iii) *Facing operation* (Figure 1.8):

Length of tool travel $L = D/2 + \Delta 1 + \Delta 2 + \Delta 3$,

where D = diameter of workpiece

$\Delta 1$ = approach; generally equal to 2–3 mm

$\Delta 2$ = over travel; generally equal to 1–2 mm; overtravel is essential in facing operation to ensure that a protruding stem is not left attached to the face of the machined workpiece

$\Delta 3 = t/\cot \phi$; where t is depth of cut and ϕ is primary cutting-edge angle; for straight-edged tools $\phi = 90^\circ$, hence $\Delta 3 = 0$

The length of tool travel for parting and grooving operations is determined in a similar manner.

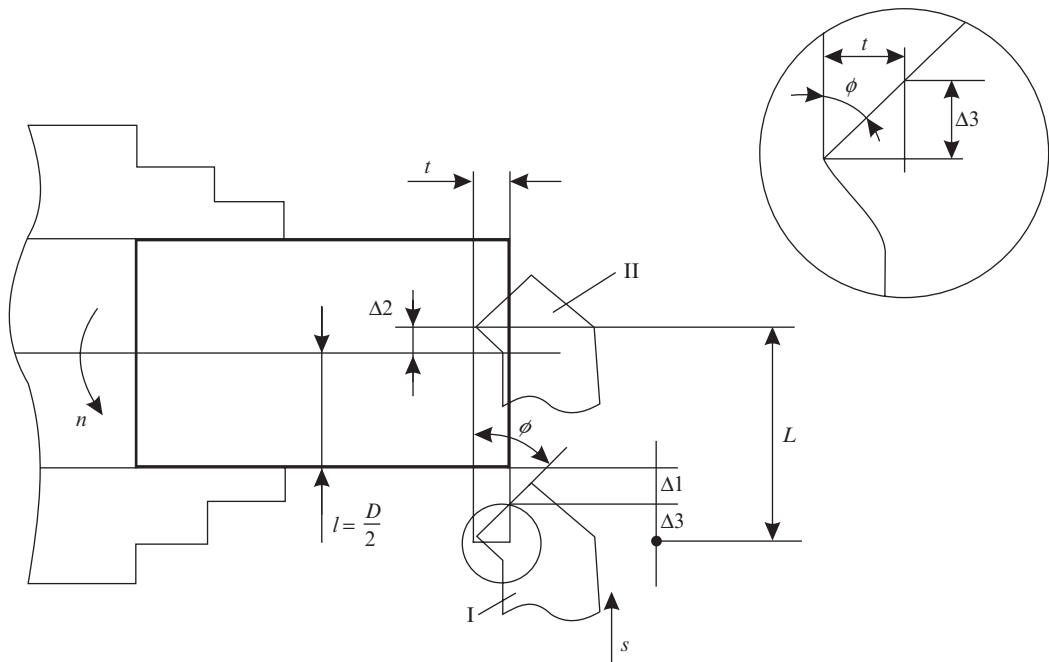


Figure 1.8 Facing operation

(iv) *Boring operation in partial length of workpiece; hole ϕd to be enlarged to ϕD* (Figure 1.9):

Length of tool travel $L = l + \Delta 1 + \Delta 3$,

where l = length of bore

$\Delta 1$ = approach; generally equal to 2–3 mm

$\Delta 3 = t/\cot \phi$; where t is depth of cut and ϕ is principal or side cutting-edge angle; for straight edged tools $\phi = 90^\circ$, hence $\Delta 3 = 0$

(v) *Boring operation in full length of workpiece; hole ϕd to be enlarged to ϕD* (Figure 1.10):

Length of tool travel $L = l + \Delta 1 + \Delta 2 + \Delta 3$,

where l = length of bore

$\Delta 2$ = over travel; generally equal to 2–3 mm

$\Delta 1$ and $\Delta 3$ are the same as in boring operation in partial length of workpiece

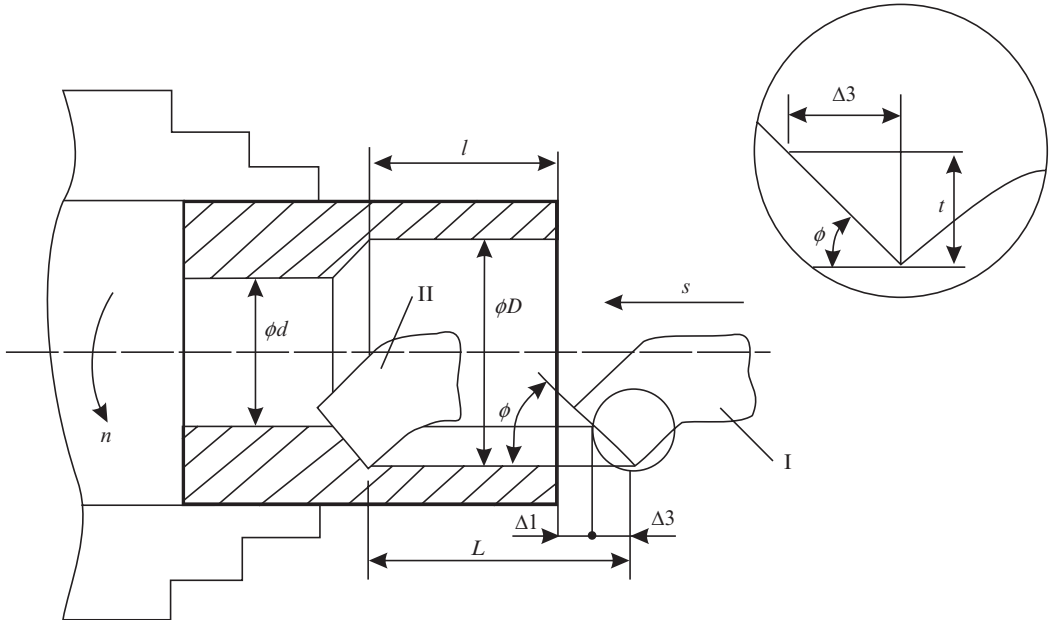


Figure 1.9 Boring operation in partial length of workpiece

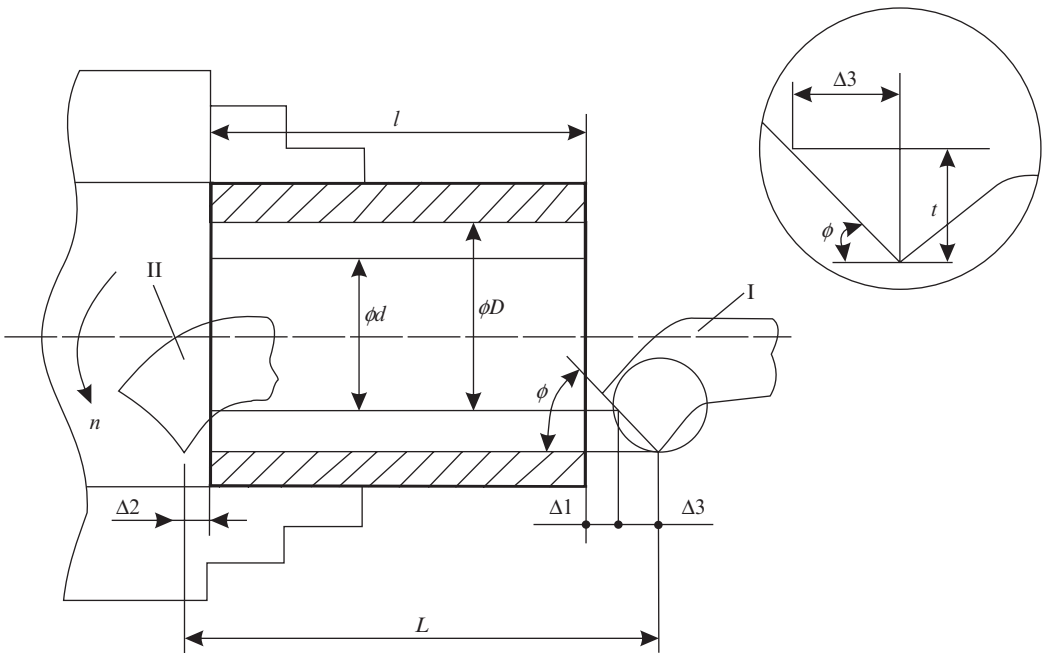


Figure 1.10 Boring operation in full length of workpiece

Example 1.1

Determine the machining time for turning a shaft from $\phi 70$ mm to $\phi 64$ mm over a length of 200 mm at $n = 600$ rpm and $s = 0.4$ mm/rev. The turning tool has primary cutting-edge angle $\phi = 45^\circ$.

$$\text{Depth of cut} = \frac{70 - 64}{2} = 3 \text{ mm}$$

$$\text{Length of travel } L = 200 + t/\cot \phi + \Delta 1 + \Delta 2$$

Assuming $\Delta 1$ and $\Delta 2 = 2$ mm each

$$L = 200 + 3 \times 1 + 2 + 2 = 207 \text{ mm}$$

$$\text{Machining time} = \frac{207}{600 \times 0.4} = 0.8625 \text{ mm.}$$

Example 1.2

A ring has to be cut out from a pipe of outside diameter $D = 100$ mm and inside diameter $d = 84$ mm at 250 rpm and feed 0.14 mm/rev. Calculate the machining time.

Length of travel in a pipe cutting operation is

$$L = \frac{D - d}{2} + \Delta 1 + \Delta 2$$

Assuming $\Delta 1 = \Delta 2 = 2$ mm

$$L = \frac{100 - 84}{2} + 2 + 2 = 12 \text{ mm}$$

$$\text{Machining time, } T_m = \frac{L}{n \cdot s_0} = \frac{12}{250 \times 0.14} = 0.342 \text{ mm}$$

Example 1.3

The diameter of a mild steel rod is to be reduced from 70 mm to 65 mm by turning in a single pass at $n = 300$ rpm and $s = 0.4$ mm/rev. Determine the material removal rate in cubic centimeter per minute.

$$\text{Machining time} = \frac{L}{s \cdot n}$$

Hence, length machined in unit time = $s \cdot n = 0.4 \times 300 = 120$ mm

$$\text{The volume of material removed in unit time} = \frac{\pi}{4} (70^2 - 65^2) \times 120 = 63585 \text{ mm}^3$$

Hence, material removal rate in cubic centimeter per minute = $63.585 \text{ cm}^3/\text{min}$

(vi) Taper turning

For a workpiece requiring taper turning (Figure 1.11), the first step is to determine the taper angle from the following expression:

$$\tan \frac{\alpha}{2} = \frac{D - d}{2l} \quad (1.8)$$

Taper turning may be done by using the following methods:

- (a) Form tool method
- (b) Compound rest method
- (c) Tail stock displacement method
- (d) Taper turning attachment method

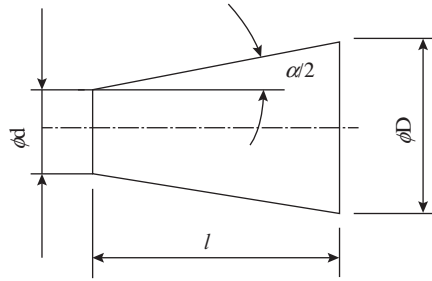


Figure 1.11 Parameters defining a taper

The first two methods are used for making short tapers (< 30 mm long), and the third method is used for making long tapers. The last method is equally suitable for all tapers.

In the form tool method (Figure 1.12), a special tool with primary cutting-edge angle equal to $\frac{\alpha}{2}$ is made. The length of the forming edge must be greater than the length of the tapered surface, and the desired surface is generated by translatory crossfeed of the tool. In the compound rest setting method (Figure 1.13), the compound rest is rotated through angle $\frac{\alpha}{2}$ and locked in this position on the cross slide of the lathe. The feed is imparted to the tool manually by rotating the compound rest wheel.

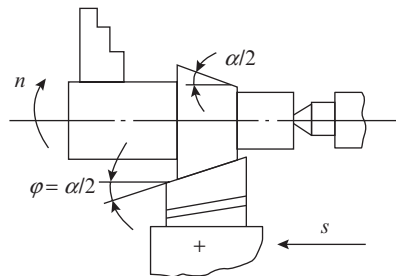


Figure 1.12 Taper turning with a form tool

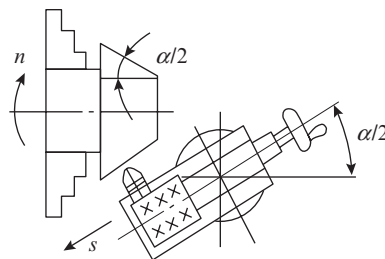


Figure 1.13 Taper turning by compound rest setting

For making long tapers on workpiece supported between centers, the tailstock center is displaced horizontally by a distance that is calculated from the following expression:

$$h = L \sin \frac{\alpha}{2} \quad (1.9)$$

This method (Figure 1.14) is generally used for long tapered surfaces having $\alpha < 20^\circ$. The longitudinal translatory motion of the tool serves as the feed motion. From the original round blank, the material shown as hatched is removed by the tool to produce the tapered job. Both long and short tapers can be made by using a taper turning attachment (Figure 1.15). It consists of a slotted arm 1 that can be set at any desired angle on the graduated arc scales 2 mounted on the attachment base. Slider 3 can move along the slot in arm 1 and can be fixed in any position. The cross slide (4) of the lathe is disconnected from the crossfeed screw by unloosening nut 5 and is connected to the slider (3) of the taper turning attachment. Now when the longitudinal feed of the lathe is engaged, the tool follows the path parallel to the slot, thereby producing the tapered surface of angle $\frac{\alpha}{2}$. For carrying out the taper turning operation, the slotted arm is set at angle $\frac{\alpha}{2}$.

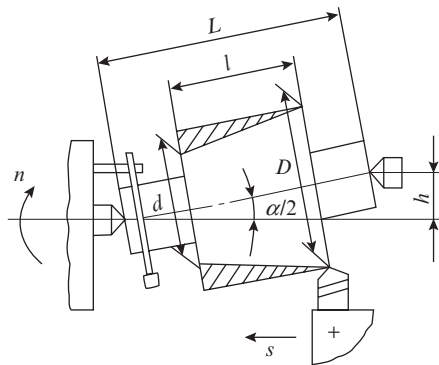


Figure 1.14 Taper turning by tail stock off setting

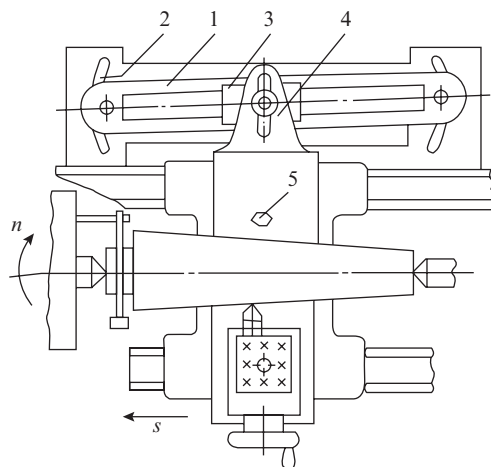


Figure 1.15 Taper turning using taper turning attachment

(vii) Thread cutting

Thread-cutting operation requires a particular kinematic relation between the spindle rotation and tool motion that may be expressed as follows: By the time the spindle completes one revolution, the tool should move by a distance equal to the pitch of the thread. In thread-cutting lathes, satisfying this kinematic relationship presents no difficulty because all that is required is to set the feed rate value on the feed box equal to the pitch of the thread to be cut.

However, in ordinary lathe machines, the required feed rate has to be calculated and set with the help of change gears. The kinematic train in this case is very simple as shown in Figure 1.16, but the calculations demand considerable ingenuity as will become evident from the discussion below.

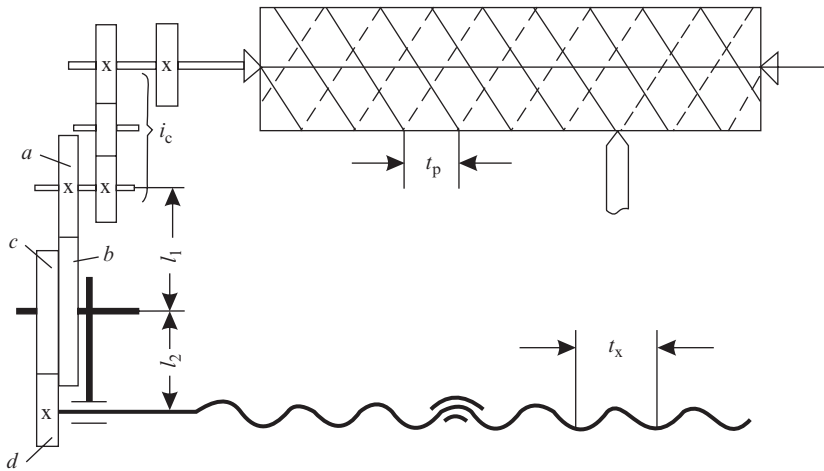


Figure 1.16 Kinematics of thread cutting operation

The kinematic relationship for thread cutting may be expressed as follows:

$$s = t_p = 1 \text{ spindle revolution } i_c \cdot i_x \cdot t_x \tag{1.10}$$

where s = feed per revolution of the threading tool;

t_p = pitch of the thread to be cut,

i_c = transmission ratio of gear pairs in constant mesh, generally $i_c = 1$

i_x = transmission ratio of change gears $a, b, c,$ and d

t_x = pitch of the lead screw of the lathe

After calculating transmission ratio i_x of the change gears from formula (2.34), the next step is to determine the number of teeth of the change gears. For a single pair of change gears,

$$i_x = \frac{a}{b}$$

whereas for two pairs of change gear,

$$i_x = \frac{a}{b} \times \frac{c}{d}$$

The change gear set consists of the following two series:

Series 1: Gears having teeth in multiples of 5:

20, 20, 25, 30, 35, 40, 45, 50, 55, 60, 65, 70, 75, 80, 85, 90, 95, 100, 105, 110, 115, 120

Series 2: Gears having teeth in multiples of 4:

20, 20, 24, 28, 32, 36, 40, 44, 48, 52, 56, 60, 64, 68, 72, 76, 80

Besides, the change gear sets are also provided with gears having 47, 97, 127, and 157 teeth.

This necessity of having gears 47, 97, 127, and 157 in the change gear set deserves special mention. While cutting threads and setting the lathe for this purpose, one may come across the following cases:

- (i) The pitch of thread and lead screw are expressed in identical units.
- (ii) The units in which t_p and t_x are expressed are different; that is, cutting metric thread when the lead screw has British Standard Whitworth (BSW) thread and vice versa.
- (iii) The pitch of the thread to be cut is a multiple of π , for example, modular thread used in worm–worm gear transmission in which the pitch of the worm is expressed as $t_p = \pi m$, m being the module of the worm gear.

In case (1), the setting calculations are done in accordance with Eqn (1.10). In case (2), the pitch of lead screw and thread to be cut must be expressed in identical units. For instance, if BSW thread is to be cut on a lathe having lead screw with metric thread, the pitch of the thread to be cut must be first determined by the following expression:

$$t_p = \frac{25.4}{TPI} = \frac{127}{5} \times \frac{1}{TPI}$$

To handle this situation, it is essential to have a gear with 127 teeth in the change gear set.

In case (3), the transmission ratio of the change gears is determined in accordance with expression (1.10) as follows:

$$i_x = \frac{t_p}{i_c \cdot t_x}$$

Keeping in mind that $i_c = 1$ and $t_p = \pi m$, the transmission ratio may be expressed as follows:

$$i_x = \frac{\pi m}{t_x}, \text{ if the lead screw has metric threads} \quad (1.11)$$

and
$$i_x = \frac{\pi m TPI}{25.4} = \frac{5\pi m TPI}{127} \text{ if the lead screw has BSW threads} \quad (1.12)$$

The quantities π and $\frac{5}{127} \pi$ may be expressed through different combinations of whole numbers.

Each combination entails a certain error; and depending on the accuracy required, any of the combinations may be selected. These combinations dictate the necessity of having gears with 47, 97, and 157 teeth, respectively, in the change gear set.

For formula (1.11),

$$\pi = \frac{22}{7}, \text{ error} = 0.04, \text{ no special gear required}$$

$$\pi = \frac{157}{50}, \text{ error} = 0.05, \text{ gear 157 required}$$

For formula (1.12),

$$\pi = \frac{47}{380} \frac{127}{5}, \text{ error} = -0.005, \text{ gear 47 required}$$

$$\pi = \frac{12}{97} \frac{127}{5}, \text{ error} = 0.021, \text{ gear 97 required}$$

$$\pi = \frac{19 \times 21}{127}, \text{ error} = +0.004, \text{ gear 127 required}$$

While selecting the change gears, the following two constraints must be satisfied:

Constraint 1: The sum of radii of gears a and b must be greater than the radius of gear c .

Constraint 2: The sum of radii of gears c and d must be greater than the radius of gear b .

If constraint 1 is violated, gear c cannot be mounted on shaft II; whereas if constraint 2 is violated, gear b cannot be mounted on shaft II.

The radius of a gear of module m and number of teeth z is $= \frac{mz}{2}$. If gears a , b , c , and d are assumed to have a , b , c , and d teeth, respectively, then constraints 1 and 2 may be expressed as follows:

$$\frac{m}{2}(a+b) > \frac{mc}{2}$$

$$\frac{m}{2}(c+d) > \frac{mb}{2}$$

Wherefrom, we get the condition

$$\begin{pmatrix} a+b > c \\ c+d > b \end{pmatrix} \quad (1.13)$$

Suppose that for a particular operation, we get

$$(a) \quad i_x = \frac{5}{9}$$

By multiplying the numerator and denominator by 5,

$$i_x = \frac{a}{b} = \frac{5}{9} \times \frac{5}{5} = \frac{25}{45}$$

Gears 25 and 45 are available in series 1.

$$(b) i_x = \frac{120}{127} = \frac{40 \times 3}{127}$$

This ratio may be obtained in the following combinations of gear:

$$(i) i_x = \frac{a c}{b d} = \frac{40}{127} \times \frac{60}{20}$$

This is not acceptable because $c + d = 60 + 20 = 80$; whereas $b = 127$, that is, constraint 2 is violated as $c + d < b$.

$$(ii) i_x = \frac{60}{20} \times \frac{40}{127}$$

This is acceptable because $a + b = 60 + 20 = 80$, $c = 40$; hence, $a + b > c$
 $c + d = 40 + 127 = 167$, $b = 20$, hence $c + d > b$

That is, both constraints 1 and 2 are satisfied.

For cutting multiple start threads, the lathe is set for the pitch value:

$$t_m = t_p k \quad (1.14)$$

where t_m = distance between adjacent threads of a particular start

t_p = distance between adjacent peaks

k = number of starts of the thread

After cutting one start, the kinematic linkage between the spindle and lead screw is disconnected and the spindle with workpiece is rotated precisely through an angle = $360/k$. The kinematic train is again connected, and the next start of the thread is cut.

If the number of teeth on the first change gear a is a multiple of the number of starts of the thread, then accurate rotation of the workpiece through $360/k$ can be achieved with the help of gear a ; for this purpose, a chalk mark is made on gear a after disconnecting the spindle from the lead screw, the gear is rotated through a/k teeth, and the kinematic train is again engaged. Multiple-start threads are also cut in a spindle chuck, which can be indexed through any desired angle. This chuck (Figure 1.17) consists of two halves: 1 and 2. During the threading operation, the halves are tightened by bolts. When one start has been cut, the two halves are unfastened. Half 1 remains attached to the spindle, whereas half 2 along with the workpiece is indexed through the desired angle that can be easily read on the graduated scale.

Example 1.4

It is required to cut screw thread of pitch 3 mm on a lathe with lead screw of pitch 10 mm. Determine the required change gears.

$$i_x = \frac{t_p}{t_x} = \frac{3}{10} = \frac{3}{5} \times \frac{1}{2} = \frac{30}{50} \times \frac{20}{40}$$

Transmission ratio of the change gears:

Check: $a + b > c$, that is, $30 + 50 > 20$

$c + d > b$, that is, $20 + 40 > 50$

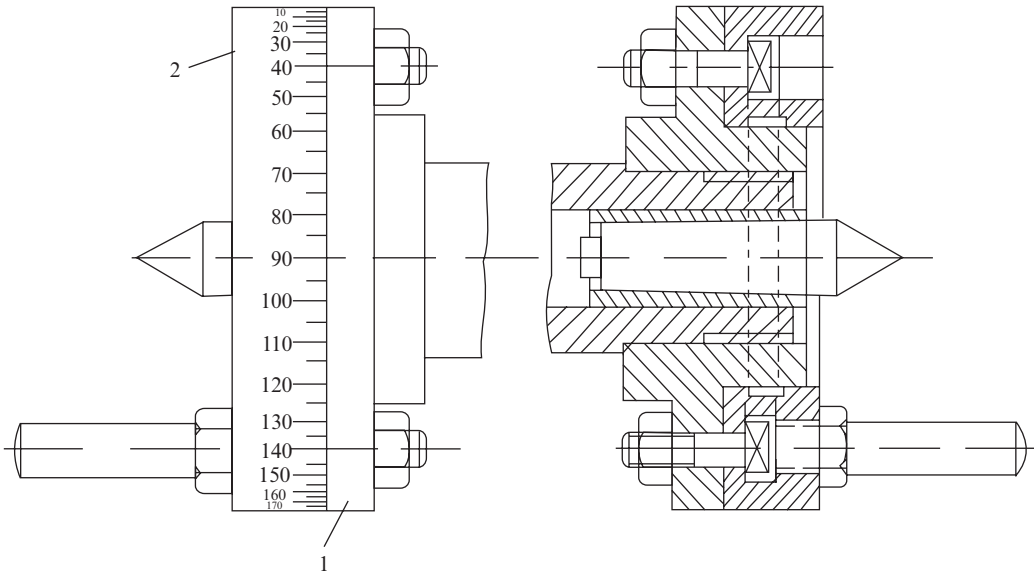


Figure 1.17 Special chuck for cutting multiple start threads

Example 1.5

It is required to cut screw thread of pitch 1.5 mm on a lathe with lead screw having BSW thread of 2TPI. Determine the required change gears.

$$\text{Pitch of the lead screw} = \frac{1}{2} \text{ inch} = \frac{25.4}{2} = \frac{127}{5 \times 2} \text{ mm}$$

$$\text{Transmission ratio of the change gears, } i_x = \frac{t_p}{t_x} = \frac{1.5 \times 5 \times 2}{127} = \frac{15}{127}$$

As no gear of 15 teeth is available in the set of change gears, i_x is represented as follows:

$$i_x = \frac{1}{2} \times \frac{30}{127} = \frac{20}{40} \times \frac{30}{127}$$

Check: $a + b > c$, that is, $20 + 40 > 30$

$c + d > b$, that is, $30 + 127 > 40$

Example 1.6

It is required to cut double start thread of pitch 4 mm on a lathe with lead screw of pitch 6 mm. Determine the required change gears.

Lead of the thread to be cut = pitch of the thread \times number of starts = $4 \times 2 = 8$ mm

$$\text{Transmission ratio of the change gears} = \frac{\text{Lead of thread to be cut}}{\text{Pitch of lead screw}}$$

$$= \frac{8}{6} = \frac{4}{3} = \frac{4}{3} \times 1 = \frac{40}{30} \times \frac{20}{20}$$

Check: $a + b > c$; $40 + 30 > 20$
 $c + d > b$; $20 + 20 > 30$

Example 1.7

It is required to cut modular thread on the worm of a worm–worm gear pair of module 4 mm on a lathe with lead screw of pitch 6 mm. Determine the required change gears.

Pitch of the worm thread = $\pi m = 4\pi$

Transmission ratio of change gears, $i_x = \frac{4\pi}{6}$

Representing $\pi = 3.14 = \frac{22}{7} = \frac{157}{50}$, we find

$$i_x = \frac{157}{50} \times \frac{2}{3} = \frac{157}{50} \times \frac{40}{60}$$

Check: $a + b > c$; $157 + 50 > 40$
 $c + d > b$; $60 + 40 > 50$

1.4 Drilling and Allied Operations

Drilling is the operation of making holes in a workpiece. When the operation is carried out on a drilling machine, both the primary cutting motion (rotation) and the secondary cutting motion (axial feed) are imparted to the drill, while the job is stationary. However, when the drilling operation is carried out on a lathe, the rotation is imparted to the workpiece clamped in chuck, whereas, the axial movement is imparted to the drill held in the tail stock. The salient geometrical features of a drill are shown in Figure 1.18.

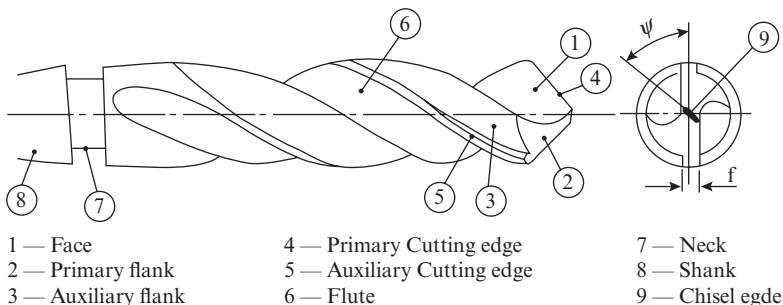


Figure 1.18 Geometrical features of drill

In drilling operation (Figure 1.19,) the depth of cut = $\frac{d}{2}$, where d is the drill diameter. The length of tool travel $L = l + \Delta_1 + \Delta_2 + \Delta_3$

where l = height of workpiece

Δ_1 = approach: generally equal to 2–3 mm

$\Delta 2$ = overtravel; generally equal to 2–3mm

$$\Delta 3 = \frac{d}{2} \cot \phi$$

where d is the drill diameter and 2ϕ is the lip angle of the drill.

The length of tool travel for counter boring and reaming operations can be determined in a similar manner.

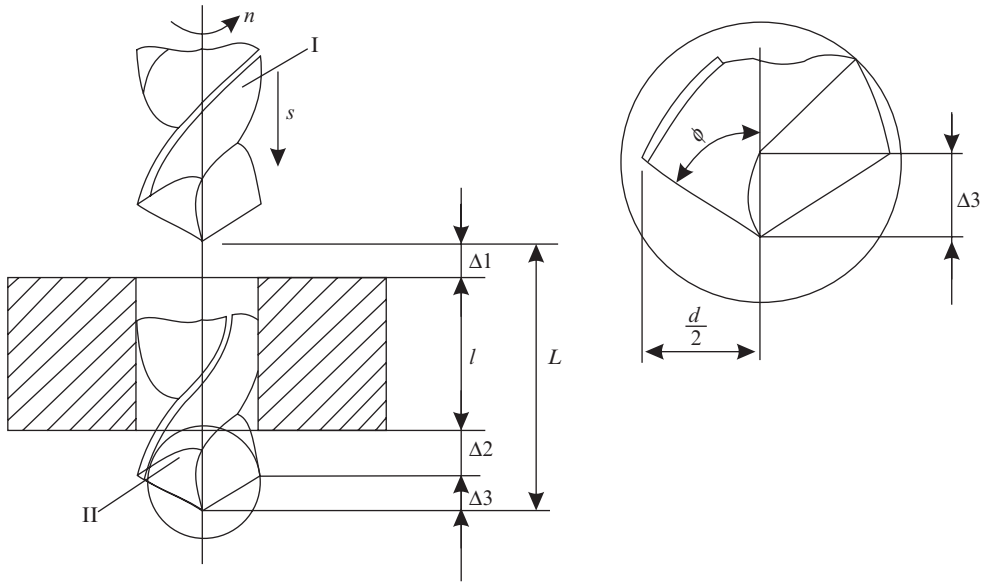


Figure 1.19 Parameters describing drilling operation

Example 1.8

Calculate the machining time for drilling a $\phi 30$ through hole in a 30-mm-thick plate at a speed of 30 m/min and feed 0.1 mm/tooth.

Length of travel $L = 30 + \Delta 1 + \Delta 2 + \frac{d}{2} \cot \phi$

Assuming $\Delta 1 = \Delta 2 = 2$ mm and $\phi = 60^\circ$ (half of lip angle)

$$L = 30 + 2 + 2 + \frac{30}{2} \cot 60^\circ = 42.66 \text{ mm}$$

The rpm of the drill is

$$n = \frac{1000v}{\pi d} = \frac{1000 \times 30}{\pi \times 30} = \frac{1000}{\pi}$$

Feed per revolution of drill = 2 × feed per tooth because a drill has two cutting teeth.

Therefore,

$$s_o = 2 \times 0.1 = 0.2 \text{ mm/rev}$$

Hence, feed per minute $s_m = \frac{1000}{\pi} \times 0.2 = \frac{200}{\pi}$, mm/min

Machining time, $T_m = \frac{L}{s_m} = \frac{42.66}{200/\pi} = 0.67$ min

Allied operations carried out on drilling machines are described below. For calculating the machining time of these operations, the length of tool travel is determined based on workpiece height and tool geometry and feed per minute is found from Eqs (1.5) and (1.6) using the given values of feed per tooth (s_z) and revolution per minute of the tool.

Core drilling is the operation of enlarging a cast or drilled hole (Figure 1.20). The core drill has 3–4 teeth, unlike a drill that has 2 teeth.

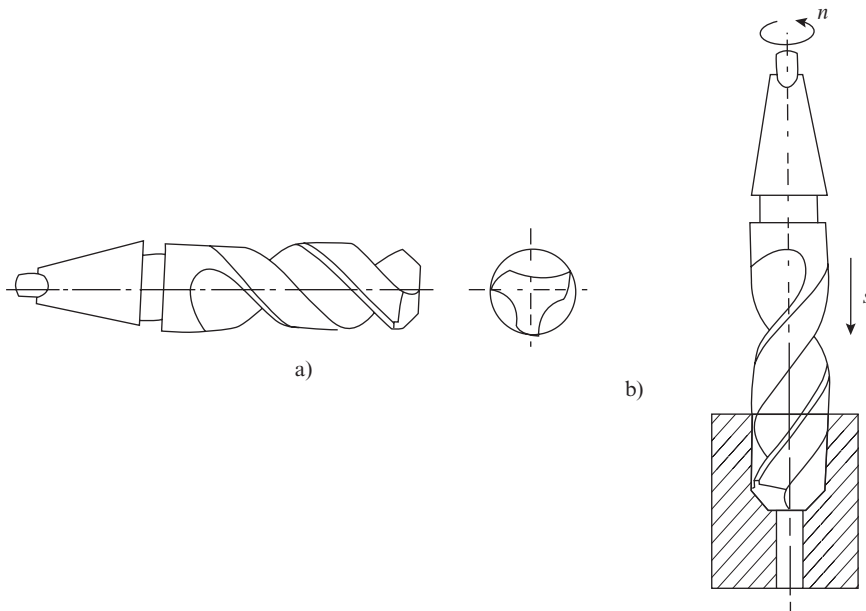


Figure 1.20 Core drilling: (a) schematic of core drill and (b) core drilling operation

Reaming is an operation used for finishing of drilled holes (Figure 1.21). The number of teeth of reamer may be found from the following relation:

$$z = 1.5\sqrt{D} + G$$

where D = hole diameter in millimeter

$G = 2$ (for normal accuracy reamers)

$G = 4$ (for precision reamers)

Counter boring is the operation used for enlarging one end of a drilled hole up to a certain depth (Figure 1.22). The counter boring tool has 4–6 teeth at the end face as well as the periphery. The diameter of the pilot is equal to the predrilled hole, and it serves to guide the counterboring tool.

Countersinking is the operation used for countersinking one end of a drilled hole up to a certain depth (Figure 1.23). The taper angle of the cutting portion of the tool matches the angle required on the countersunk portion of the hole.

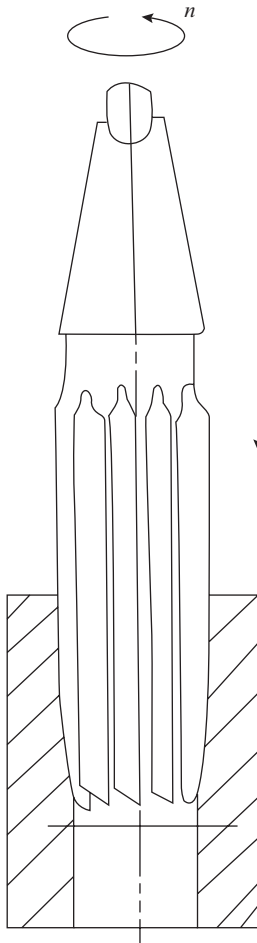


Figure 1.21 Reaming

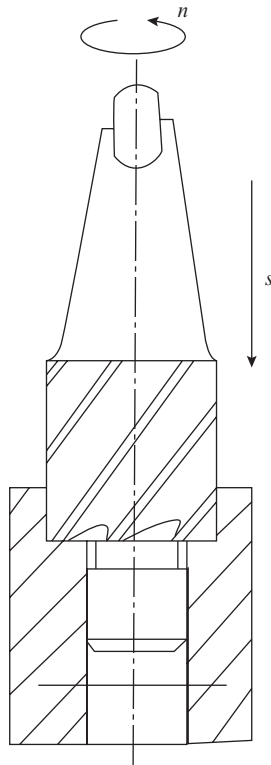


Figure 1.22 Counterboring operation

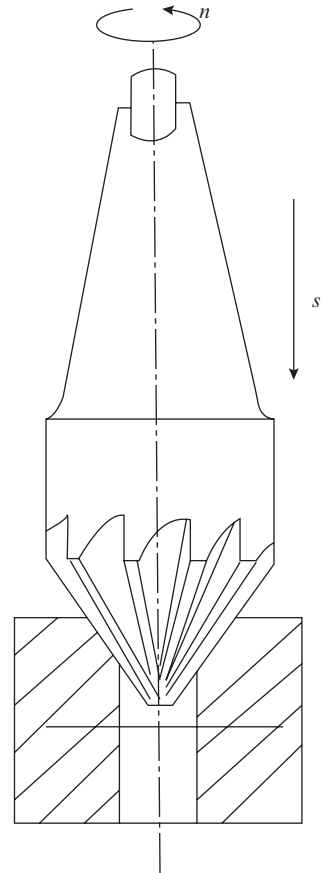


Figure 1.23 Countersinking operation

Spot facing is the operation carried out for machining the top surface of a bossing or the component in which a hole has already been drilled (Figure 1.24). The spot facing tool has cutting teeth only on the face. The pilot has the same function as in the counterboring tool.

Tapping is an operation used for cutting internal threads in an existing hole obtained after drilling or boring (Figure 1.25). Rotation and axial motion are imparted simultaneously to the tap either manually or with the tap clamped in the drilling machine spindle for which a special adaptor with a square hole corresponding to the tap shank at one end is used. The thread is cut during the forward motion of the tap. While withdrawing the tap from the workpiece, its direction

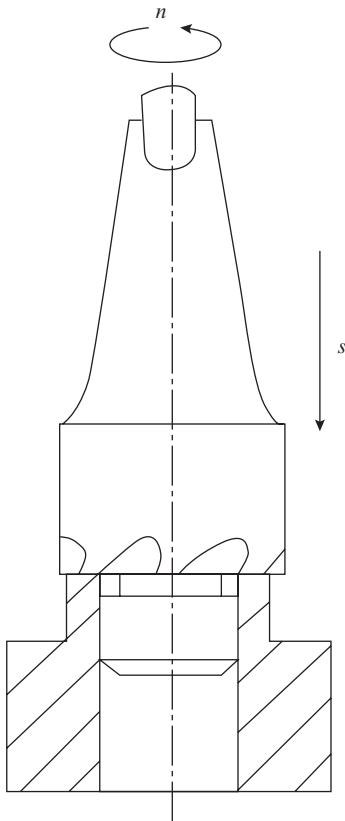


Figure 1.24 Spot facing operation

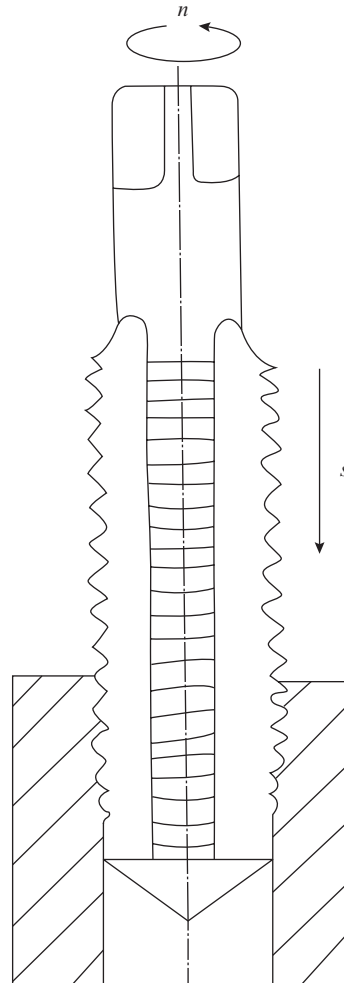


Figure 1.25 Tapping operation

of rotation is reversed. A single tap or sets of 2 and 3 taps may be used for cutting threads, depending on the pitch (p) of the thread and whether the thread is cut manually or on a drilling/boring machine (Table 1.1)

Table 1.1 Tap sets

| S. No | Number of taps | Application | |
|-------|----------------|----------------|-----------------|
| | | Manual tapping | Machine tapping |
| 1 | 1 | $p < 2$ mm | $p < 3$ mm |
| 2 | 2 | $p < 3$ mm | $p < 5$ mm |
| 3 | 3 | $p < 3$ mm | - |

1.5 Milling Operations

Milling is a metal-cutting process in which machining is carried out by a multiple teeth tool called milling cutter. The primary cutting motion in milling operations is rotation of the milling cutter, whereas the feed motion is imparted to the workpiece clamped on the milling machine table.

The main type of milling cutters are plain, face, end, side, angle, and form cutters (Figure 1.26). The plain and form milling cutters have teeth only on the periphery; the face milling cutter has teeth only on the end face; the end milling cutters (also called end mills) have cutting teeth both on the periphery and end face; and the side and angle cutters have teeth on the periphery and side face(s). Form cutters are used for machining of complex profiles.

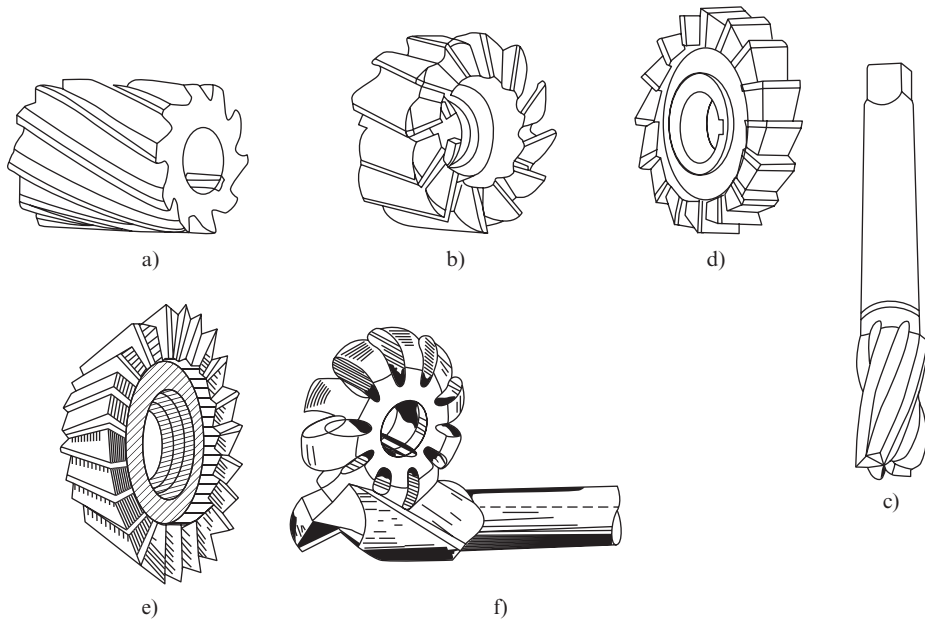


Figure 1.26 Milling cutters (a) plain milling cutter, (b) face milling cutter, (c) end milling cutter, (d) side milling cutter, (e) angle cutter, and (f) form cutter

Plain milling cutters are used mainly for machining flat surface and may have straight or helical teeth. Light duty plain milling cutters have width < 20 mm and have teeth parallel to the axis. Helical teeth cutters provide relatively smoother cutting and may be of two types: coarse teeth for rough work and fine teeth for finishing work. Plain milling operation in two variants: up and down milling is shown in (Figure 1.27). In the case of down milling, the vertical component of the cutting force acts downward, pressing the workpiece against the table. In the case of up milling, the vertical component of the cutting force acts upward, tending to lift the workpiece from the table. In up milling, the chip section increases from zero at the point of entry to maximum at the point of exit of the cutter; whereas in down milling, it is just the reverse. Down milling is generally preferred for its higher stability, except when the workpiece is very hard and may damage the cutter teeth at the time of entry as the engagement commences with maximum undeformed chip thickness.

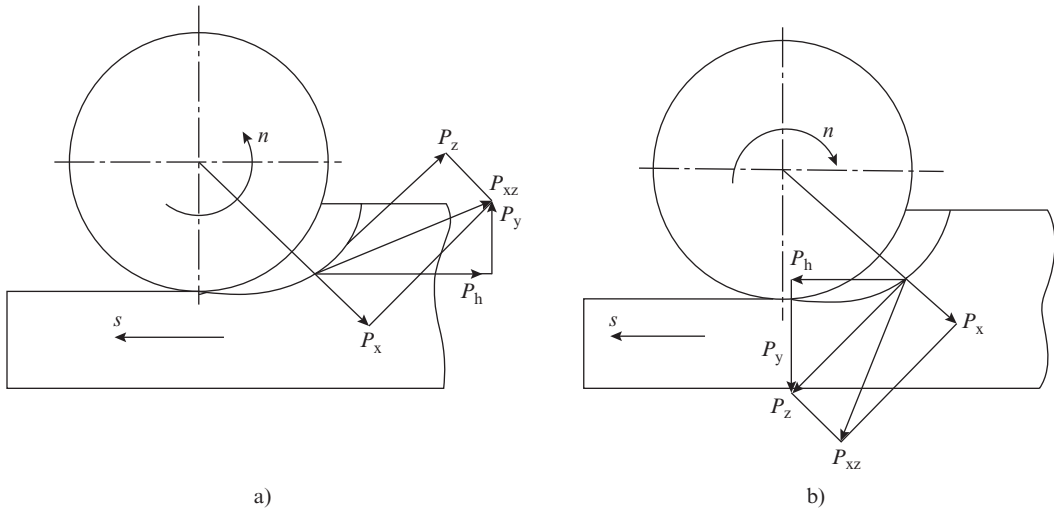


Figure 1.27 Plain milling operation: (a) up milling and (b) down milling

Face milling cutters are also used mainly for machining flat surfaces that may be horizontal, vertical, and inclined. Horizontal surfaces are machined on a vertical milling machine (Figure 1.28a), vertical surfaces on planomilling machine (Figure 1.28b), and inclined surfaces on vertical milling machine by swiveling the milling head (Figure 1.28c).

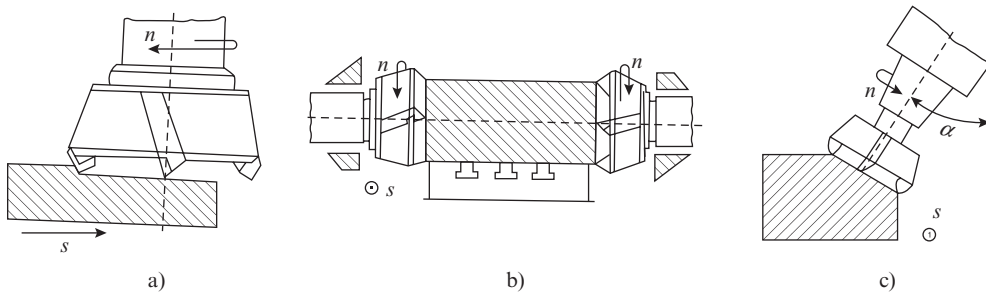


Figure 1.28 Operations using face milling cutters: (a) machining of horizontal flat surface on vertical milling machine, (b) machining of vertical face on planomilling machine, and (c) machining of inclined surface by swiveling the spindle head on vertical milling machine

End mill cutters have smaller diameter than plain and face milling cutters. During the cutting operation, they may act as a plain milling cutter, a face milling cutter, or as a combination of both, because they are long just like plain milling cutters, but have, in addition, teeth on the end face like a face milling cutter. In view of this in-built versatility, end mill cutters are used in a wider range of operations, namely machining of vertical surface (Figure 1.29a) and profile (Figure 1.29b) with teeth on the periphery and milling of slot (Figure 1.29c), keyway (Figure 1.29d), and pocket (Figure 1.29e) with teeth on the cutter periphery and face both. Operations using end mill cutters are mostly carried out on vertical milling machines.

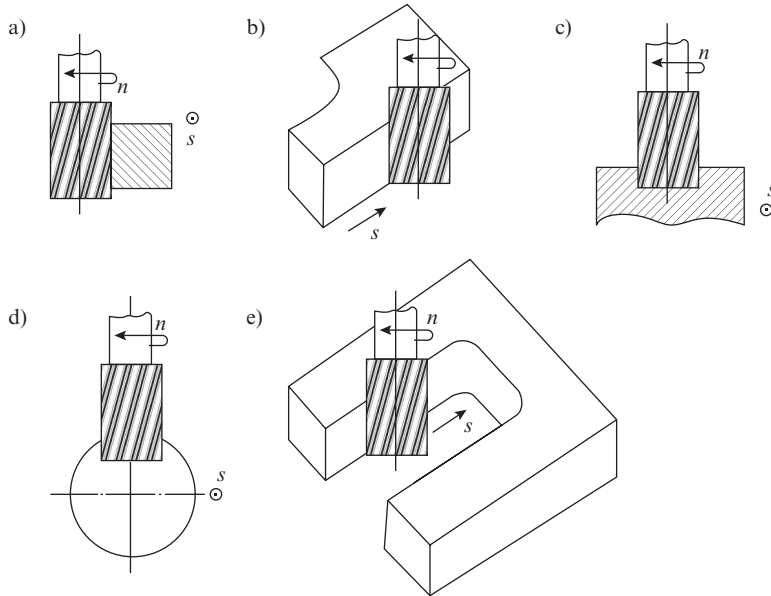


Figure 1.29 Operation using end mill cutters: (a) Machining of a vertical surface, (b) contour milling, (c) slot milling, (d) keyway milling, and (e) pocket milling

A side milling cutter with teeth on the periphery and both the side faces is known as plain side milling cutter, whereas a side milling cutter with teeth on the periphery and only on one side face is known as a half-side milling cutter. A thin side milling cutter (width < 5 mm) with teeth only on the periphery is known as slotting cutter.

Typical examples of operations using these cutters on horizontal milling machine are machining a vertical surface (Figure 1.30a) and a groove (Figure 1.30b). Machining of a T-slot with a plain side milling cutter on a vertical milling machine is shown in (Figure 1.28c). Simultaneous machining of two sides of a projection is carried out by using two half-side milling cutters on a horizontal milling machine in an operation known as straddle milling (Figure 1.30d)

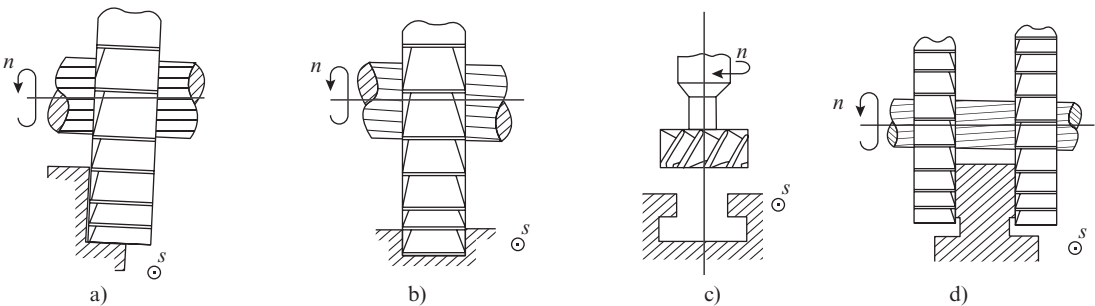


Figure 1.30 Operation using side milling cutters: (a) machining of a vertical surface, (b) groove milling, (c) T-slot milling, and (d) straddle milling

Angle milling cutters are used mainly for machining of grooves. They may be single angle (Figure 1.31a) and double angle (Figure 1.31b) with angle of 45° or 60°. Typical operations carried out with these

cutters are machining of an inclined surface on a horizontal milling machine using a single-angle cutter (Figure 1.31c), machining of an angular slot on a horizontal milling machine with a double-angle cutter (Figure 1.31d), and machining a dove tail slot on a vertical milling machine with a single-angle cutter (Figure 1.31e).

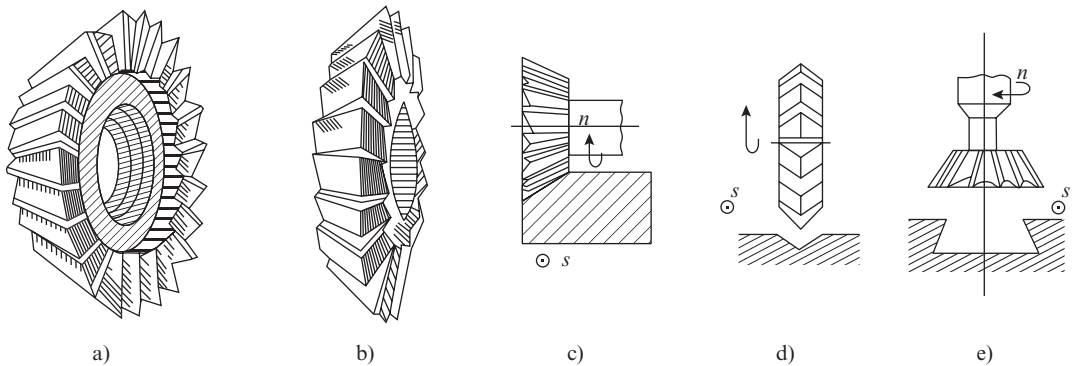


Figure 1.31 Operations using angle milling cutters: (a) single-angle cutter, (b) double-angle cutter, (c) machining of inclined surface on horizontal milling machine, (d) machining of angular slot on horizontal milling machine, and (e) machining of dove tail slot on vertical milling machine

Form milling cutters come in various profiles, depending on the specific shape of the surface to be machined. Form milling operations are generally carried out on a horizontal milling machine and some typical examples of form milling are milling of a groove (Figure 1.32a) with a convex form milling cutter, milling of a protruding surface with a concave form milling cutter (Figure 1.32b), and milling of a gear using a module cutter (Figure 1.32c). Complex features can be machined on a horizontal or planomilling machine by combining several milling cutters of different types in an operation known as gang milling (Figure 1.32d).

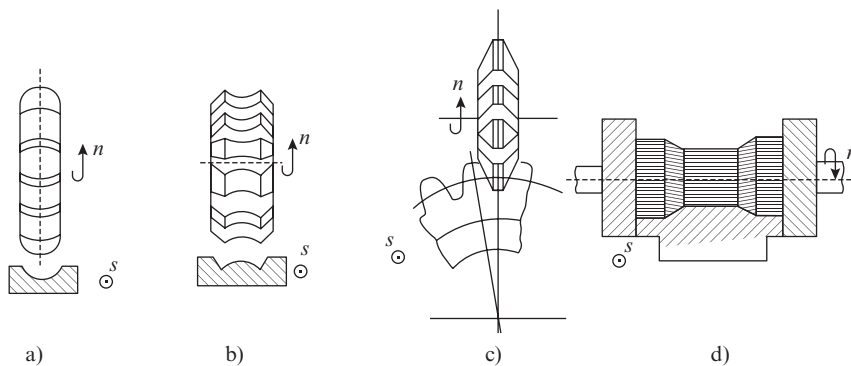


Figure 1.32 Operations using form milling cutters: (a) groove milling, (b) profile milling, (c) gear cutting, and (d) gang milling

Calculation of machining time is described below for two representative cases, one of plain (slab) milling using plain milling cutter that has teeth on the periphery and the other of face milling using face milling cutter that has teeth on the end face of the cutter. The machining time of opera-

tions with end milling cutters, side milling cutters, angle cutters, and profile cutters can be determined on similar lines, of course, with due consideration of the cutter geometry.

In all the milling operations described below,

$\Delta 1$ = approach; generally equal to 2–3 mm

$\Delta 2$ = over travel; generally equal to 2–3 mm

- (i) *Horizontal milling machine: Plain milling operation* (Figure 1.33)

Length of cutter travel $L = l + \Delta 1 + \Delta 2 + \Delta 3$

where, l = length of the workpiece

$$\begin{aligned} \Delta 3 = BC &= \sqrt{OC^2 - OB^2} = \sqrt{R^2 - OB^2} = \sqrt{R^2 - (R-t)^2} = \sqrt{R^2 - (R^2 + t^2 - 2Rt)} \\ &= \sqrt{2Rt - t^2} = \sqrt{t(D-t)} \end{aligned}$$

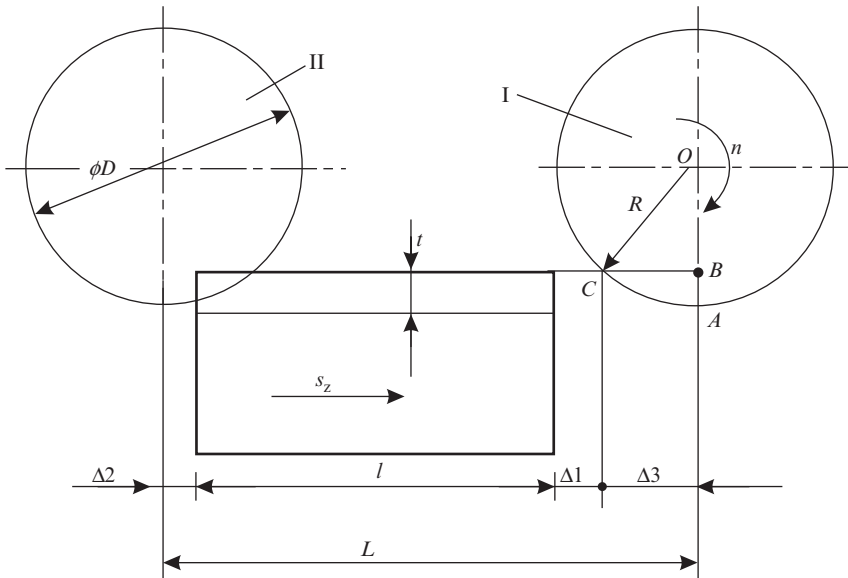


Figure 1.33 Plain milling operation

- (ii) *Vertical milling machine: Symmetrical face milling operation* (Figure 1.34):

Length of cutter travel $L = l + \Delta 1 + \Delta 2 + \Delta 3$

where, l = length of the workpiece

$$\Delta 3 = AB = OA - OB = R - \sqrt{OC^2 - BC^2} = R - \sqrt{R^2 - \left(\frac{B}{2}\right)^2} = 0.5(D - \sqrt{D^2 - B^2})$$

- (iii) *Vertical milling machine: Asymmetrical face milling operation* $B > \frac{D}{2}$ (Figure 1.35):

As shown, $B_1 > B_2$ and $B_1 + B_2 = B$. The approach is determined by the larger of the two asymmetrical portions, that is, B_1 in the given case.

Length of cutter travel $L = l + \Delta 1 + \Delta 2 + \Delta 3$,

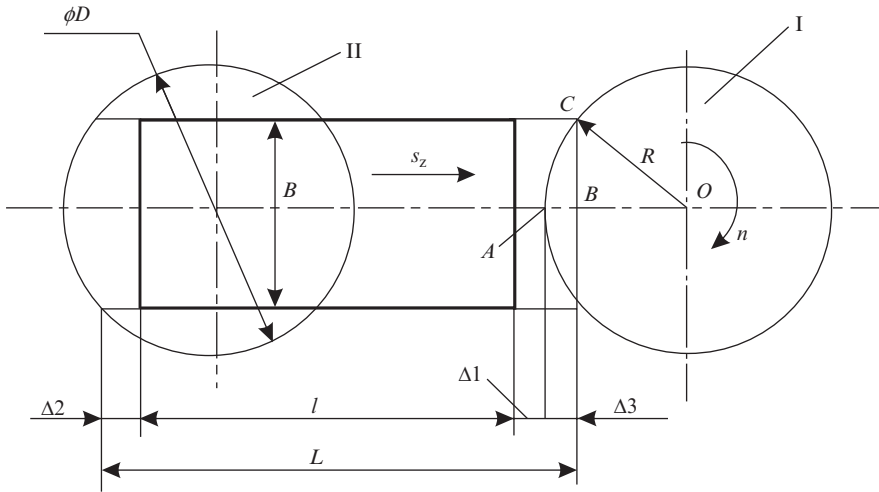


Figure 1.34 Symmetrical face milling operation

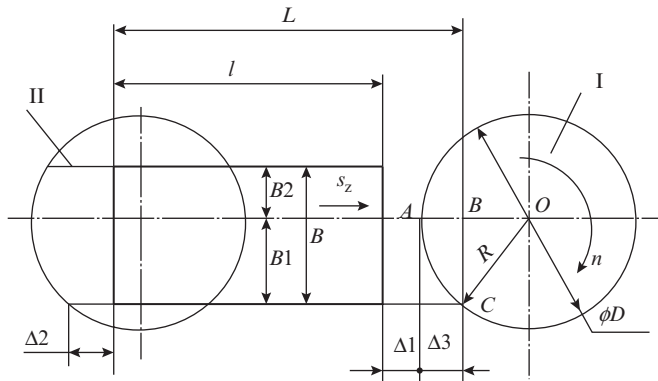


Figure 1.35 Asymmetrical face milling operation, $B > \frac{D}{2}$

where, l = length of the workpiece

$$\Delta 3 = AB = OA - OB = R - \sqrt{OC^2 - BC^2} = R - \sqrt{R^2 - (B1)^2}$$

(iv) Vertical milling machine: Asymmetrical face milling operation $B < \frac{D}{2}$ (Figure 1.36):
Length of cutter travel $L = l + \Delta 1 + \Delta 2 + \Delta 3$,

where l = length of the workpiece

$$\Delta 3 = AB = \sqrt{OA^2 - OB^2} = \sqrt{R^2 - (R - B)^2} = \sqrt{R^2 - R^2 - B^2 + 2BR} = \sqrt{B(D - B)}$$

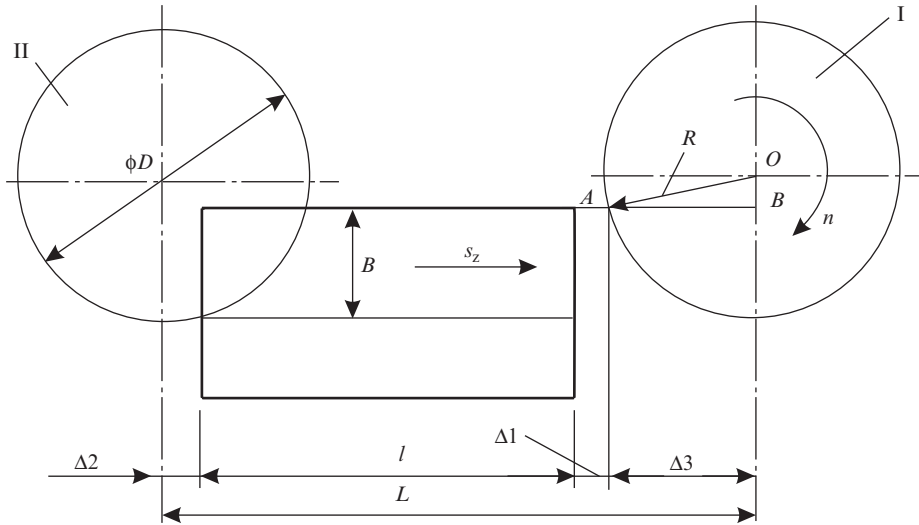


Figure 1.36 Asymmetrical face milling operation, $B < \frac{D}{2}$

Example 1.9

A 200-mm-long job is to be machined by a plain milling cutter of diameter $D = 40$ mm and 10 teeth. If the cutting speed is 30 m/min and feed is 0.08 mm/tooth, calculate the machining time for a depth of cut of 4 mm. Assume suitable approach and overtravel.

Length of travel $L = 200 + \sqrt{t(D - t)} + \Delta 1 + \Delta 2$

Assuming $\Delta 1 = \Delta 2 = 2$ mm each

$$L = 200 + \sqrt{4(40 - 4)} + 2 + 2 = 216 \text{ mm}$$

The rpm of the milling cutter is

$$n = \frac{1000v}{\pi D} = \frac{1000 \times 30}{\pi \times 40}$$

Feed per minute $s_m = s_z \times z \times n$

$$= 0.08 \times 1 \times \frac{1000 \times 30}{\pi \times 40} = 191 \text{ mm/min}$$

Machining time $T_m = \frac{L}{s_m} = \frac{216}{191} = 1.13 \text{ min.}$

Example 1.10

A 80 mm × 160 mm surface is rough machined using a face milling cutter of diameter 150 mm and 10 teeth. The cutter center is offset by 15 mm from the line of symmetry of the surface. Estimate

the machining time if $s_z = 0.25$ mm and $v = 20$ m/min. Assume approach and overtravel of 5 mm each. What will be the machining time if the tool axis is symmetrical with the job?

This is a case of asymmetrical face milling operation with $B > \frac{D}{2}$

$$\text{Cutter rpm} = \frac{1000v}{\pi D} = \frac{1000 \times 20}{\pi \times 150} = 42.4$$

$$\text{Feed per min} = s_z \times z \times n = 0.25 \times 10 \times 42.4 = 106 \text{ mm/min}$$

For the given offset of 15 mm, $B_1 = 55$ mm and $B_2 = 25$ mm.

Hence, the length of cutter travel will be

$$160 + 5 + 5 + \left\{ 75 - \sqrt{75^2 - 55^2} \right\} = 160 + 5 + 5 + 51 = 221 \text{ mm}$$

Machining time is

$$\frac{221}{106} = 2.084 \text{ min}$$

If the workpiece is symmetrically placed, then the length of cutter travel will be

$$160 + 5 + 5 + \left\{ 75 - \sqrt{75^2 - 40^2} \right\} = 233.4 \text{ mm}$$

The machining time will therefore be

$$\frac{233.4}{106} = 2.20 \text{ min}$$

Aside from the milling operations discussed above, there are operations such as gear cutting and machining of multiple grooves in which precise indexing of the workpiece is required. This indexing is carried out with the help of a special fixture called indexing head.

The indexing head is clamped on the machine tool table. The job is supported between the indexing head centre and tail stock and clamped in a chuck or with the help of dog and face plate mounted on the indexing head spindle. The spindle is rotated manually by means of a crank wheel for obtaining the following two types of motions:

- (i) Periodic rotation of the workpiece through a certain angle.
- (ii) Continuous rotation of the workpiece that is related to the longitudinal feed of the machine table.

The construction of the indexing head is shown in Figure 1.37. It consists of two pairs of spur gears of transmission ratio 1, one pair of bevel gears of transmission ratio 1 and a worm–worm gear transmission. If the number of starts of the worm is k and the number of teeth of the worm gear is z_w , then the ratio $N = z_w/k$ is called the indexing head characteristic.

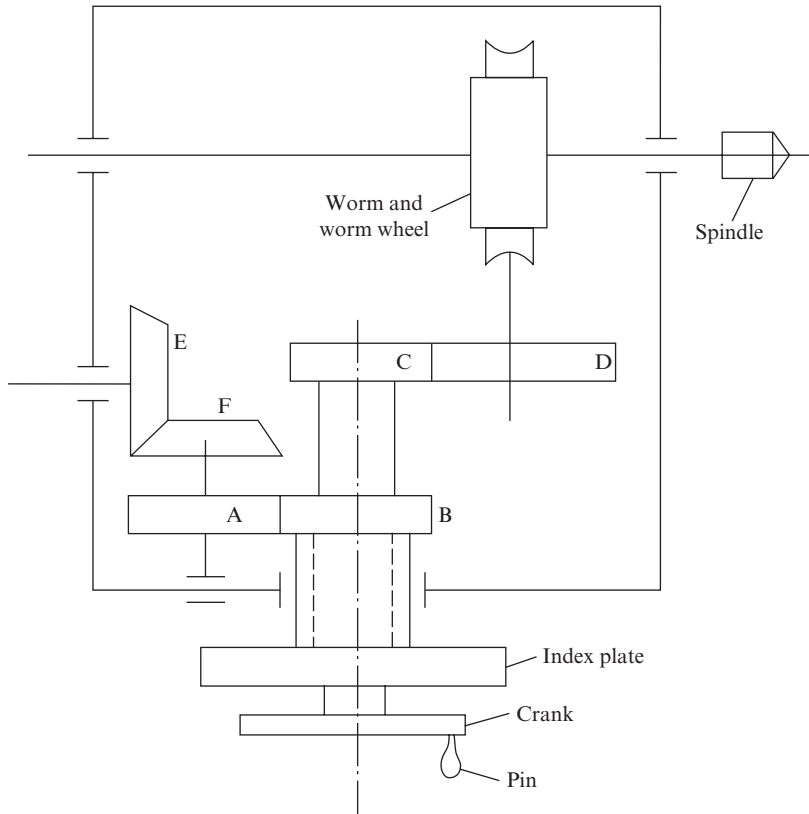


Figure 1.37 Schematic of indexing head

Generally, the transmission ratio of the worm–worm gear transmission, and hence the index head characteristic is equal to 40. The worm gear and the spindle of the indexing head have a common axis. Indexing of the spindle is achieved by rotating the crank wheel. Rotation from the crank is transmitted to the spindle through spur gears *C–D* and the worm–worm gear pair. Accurate indexing through a given angle is carried out with the help of an index plate (Figure 1.38). The index plate has several concentric circles with different number of holes on each side. There is an adjustable sector that can be opened to cover the required number of holes of a particular circle of the index plate. Generally, two index plates are supplied with an indexing head.

Plate no. 1 has 20, 23, 33, and 43 holes on one side and 18, 21, 31, and 41 on the other. Plate no. 2 has 16, 19, 29, 39, and 49 holes on one side and 15, 17, 27, 37, and 47 on the other. However, index plates with other hole combinations are also available. The index plate is mounted on a hollow shaft that is concentric with the crank wheel axis and can freely rotate about it.

1.5.1 Indexing Based on Periodic Rotation

There are three distinct types of indexing operations based on periodic rotation of the workpiece, namely plain indexing, differential indexing, and angular indexing. The kinematics of each of these three modes of indexing is described below:

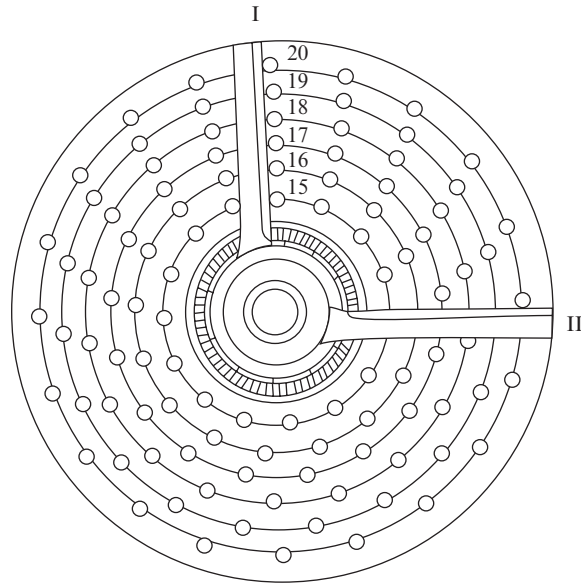


Figure 1.38 Index plate

1. *Plain indexing for periodic rotation* is used when the number of crank rotations is
 - (i) a whole number
 - (ii) a fraction in which the denominator matches the number of holes in one of the circles of the index plate
 - (iii) a whole number cum fraction as described in (ii) above.

Suppose we have to index for n divisions on an indexing head of characteristic $N = 40$. Then, the turns through which the crank must be moved, that is, the crank rotation $R = \frac{40}{n}$

Example 1.11

- (i) If n is say 8, then $R = \frac{40}{8} = 5$, that is, the crank will be rotated through 5 full turns.
- (ii) If n is say 80, then $R = \frac{40}{80} = \frac{1}{2} = \frac{10}{20}$, that is, the crank will be rotated through 10 holes of the circle with 20 holes on plate No. 1. After each indexing, the adjustable sector is moved forward by 10 holes.
- (iii) If n is say 6, then $R = \frac{40}{6} = 6 \frac{4}{6} = 6 \frac{2}{3} = 6 \frac{22}{33}$, that is, the crank will be rotated through 6 full turns plus 22 holes of the circle with 33 holes on plate no. 1. After each indexing, the adjustable sector will be moved through 22 holes and the crank will be rotated through 6 full turns and 22 holes.

2. *Differential indexing for periodic rotation* is resorted to when the indexing for the required number of divisions n involves a fraction whose denominator does not match with the number of holes in any of the circles of plates 1 and 2. In this case, indexing is carried out for n_x

such that n_x is close to n and $\frac{N}{n_x}$ involves a fraction whose denominator matches with the number of holes in one of the circle of plate 1 or plate 2.

When indexing is carried out for n_x divisions, the error in rotation of the crank per indexing = $\frac{N}{n} - \frac{N}{n_x}$. Therefore, the error in one rotation of the indexing head spindle is

$$x = \left(\frac{N}{n} - \frac{N}{n_x} \right) n$$

$$= \frac{N(n_x - n)}{n_x}$$

The above error must be compensated by imparting a corresponding additional rotation to the indexing plate in the proper direction. While rotating the crank through the requisite turn for n_x divisions, the crank pin is withdrawn from the index plate that can now receive additional rotation through the kinematic train starting from the indexing head spindle via change gears $\frac{a}{b} \times \frac{c}{d}$, bevel gear pair $E-F$, and spur gear pair $A-B$ (Figure 1.39)

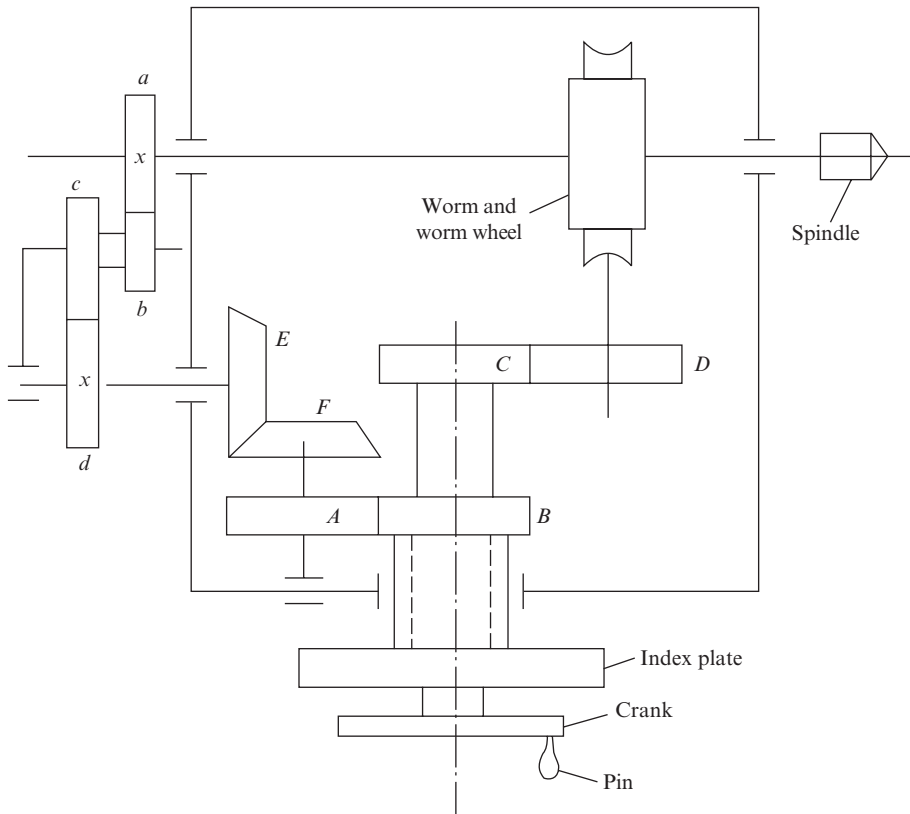


Figure 1.39 Schematic of differential indexing

The change gear ratio

$$x = \frac{a}{b} \times \frac{c}{d} = \frac{N(n_x - n)}{n_x}$$

If $n_x > n$, then the index plate should rotate in the same direction as the crank. However if $n_x < n$, the index plate should rotate in a direction opposite to that of the crank for which an idle gear is inserted between the change gears c and d . Here, it is pertinent to remember that the spur gear pairs $A-B$ and $C-D$ and the bevel gear pair $E-F$ all have transmission ratio equal to unity

Example 1.12

It is required to make a gear of 109 teeth using an indexing head with which the following change gear set is provided: 20, 25, 30, 35, 40, 45, 50, 55, 60, 65, 70, 80, 90, and 100. As $n = 109$ and no circle of 109 holes or its multiple is available on plates 1 and 2, we will have to take recourse to differential indexing for which we select $n_x = 110$. Therefore, indexing will involve the following:

- (i) Rotation of crank through $R = \frac{40}{110} = \frac{4}{11} = \frac{12}{33}$, that is, through 12 holes of the circle with 33 holes on plate 1.
- (ii) Selection of appropriate change gears of transmission ratio:

$$x = \frac{a}{b} \times \frac{c}{d} = \frac{40(110 - 109)}{110} = \frac{4}{11} = \frac{4}{5.5} \times \frac{1}{2} = \frac{40}{55} \times \frac{25}{50}$$

As $n_x > n$, the index plate and crank rotate in the same direction, and there is no need of an idle gear to be inserted between change gears c and d .

(iii) check $\frac{4}{11} + \frac{4}{11 \times 109} = \frac{4 \times 109 + 4}{11 \times 109} = \frac{436 + 4}{11 \times 109} = \frac{440}{11 \times 109} = \frac{40}{109}$

3. *Angular indexing* is used when the job has to be indexed through a given angle. Since 40 turns of the crank turn the job through one complete revolution (i.e. 360°), one turn of the crank evidently turns it through $\frac{360}{40} = 9^\circ = 540' = 32400''$. To determine the required crank rotation for angular indexing, the given angle is divided by 9, 540 or 32400, depending on whether the angle is expressed in degrees, minutes, and seconds, respectively. The quantity thus obtained is then treated as a whole number or a fraction or a whole number cum fraction and tackled as a problem of plain or differential indexing, as the case may be.

Example 1.13

- (i) The job has to be indexed through 50° . The required crank rotation will be

$$\frac{50}{9} = 5 \frac{5}{9}$$

That is, 5 full turns and 10 holes of the circle with 18 holes on plate 1.

- (ii) The job has to be indexed through $31^\circ 20'$

The required crank rotation will be

$$\frac{31 \times 60 + 20}{540} = \frac{1860 + 20}{540} = \frac{1880}{540} = 3 \frac{18}{54} = 3 \frac{1}{3} = 3 \frac{6}{18}$$

That is, 3 full turns and 6 holes of the circle of 18 holes on plate 1.

- (iii) The job has to be indexed through $4^{\circ}56'1''$
The required crank rotation will be

$$\frac{4 \times 60 \times 60 + 56 \times 6 + 1}{32400} = \frac{17761}{32400}$$

The above value can be interpreted in terms of number divisions of the jobs as

$$\text{No. of divisions} = \frac{40}{\frac{17761}{32400}} = 72.968 \approx 73$$

Thus, the indexing through $4^{\circ}56'1''$ is equivalent to indexing of a job for 73 divisions. As no circle of 73 holes or its multiple is available on any of the index plates, this becomes a problem of differential indexing for which we select $n_x = 75$. Hence, indexing will involve the following

- (i) Rotation of crank through $R = \frac{40}{75} = \frac{8}{15}$, that is, through eight holes of the circle of 15 holes on plate 2
(ii) Selection of appropriate change gears of transmission ratio

$$x = \frac{a}{b} \times \frac{c}{d} = \frac{40(75 - 73)}{75} = \frac{16}{15} = \frac{4}{3} \times \frac{4}{5} = \frac{40}{30} \times \frac{40}{50}$$

As $n_x > n$, the index plate and crank rotate in the same direction, and there is no need of an idle gear to be inserted between change gears c .

- (iii) Check $\frac{8}{15} + \frac{16}{15 \times 73} = \frac{8 \times 73 + 16}{15 \times 73} = \frac{584 + 16}{15 \times 73} = \frac{600}{15 \times 73} = \frac{40}{73}$

1.5.2 Indexing Based on Continuous Rotation

This type of indexing is used for machining of helical grooves on milling machine. The kinematic relation that must be satisfied is that by the time the indexing head spindle completes one rotation, the milling machining table should travel a distance equal to the pitch of the helix. First, the table of the milling machine is rotated and set at an angle equal to the helix angle. Next, rotation of the index head spindle and the longitudinal feed of the table are coordinated by using change gears a_1, b_1, c_1 , and d_1 between the lead screw of the milling machine responsible for longitudinal travel of the table and the output shaft of the bevel gear pair $E-F$ (Figure 1.40) such that they satisfy the following relation:

$$1 \text{ spindle rotation} \times N \left(\frac{d_1 \cdot b_1}{c_1 \cdot a_1} \right) \times t_x = t_p$$

where N is the index head characteristic

t_x is the pitch of the lead screw of the milling machine

t_p is the pitch of the helix to be machined

$$t_p = \frac{\pi D}{\tan \beta}$$

where β is helix angle and D is diameter of the job on which the helical groove is to be machined.

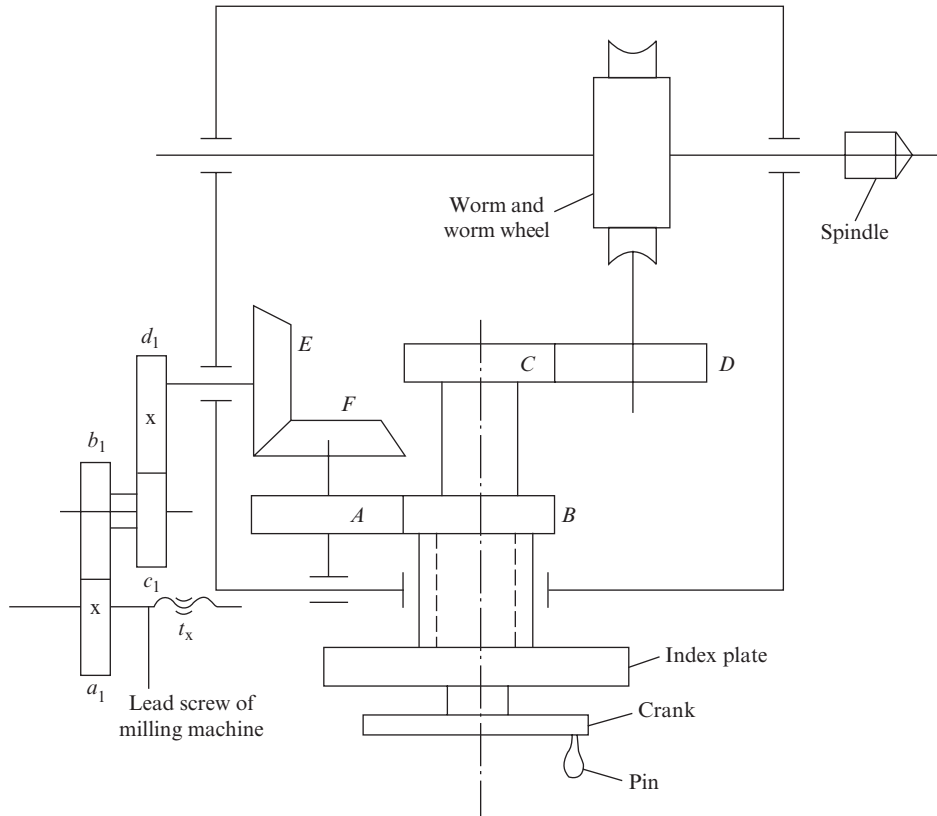


Figure 1.40 Schematic of machining of a helical flute

Again, it must be borne in mind that the above relation implies that the spur gear pairs $A-B$ and $C-D$ and the level gear pair $E-F$ all have transmission ratio equal to unity.

If the transmission ratio of the change gears is represented by $x = \frac{a_1}{b_1} \times \frac{c_1}{d_1}$, then the above relation may be written as follows:

$$\frac{N \cdot t_x}{x} = t_p$$

wherefrom $x = \frac{N t_x}{t_p}$

Here, it may be interesting to note that as the bevel gear pair $E-F$ is engaged in machining of the helix, it is not available for differential indexing. Hence, only such helical grooves can be machined that require only plain indexing. Further, since the table of the milling machine has to be rotated through an angle equal to the helix angle, the groove milling operation can only be carried out on a universal milling machine.

Example 1.14

It is required to make a helical gear of teeth $z = 35$, module $m = 5$, and helix angle $\beta = 22.5^\circ$. The milling machine on which the gear is machined has lead screw of pitch 6 mm and is provided with a change gear set 20, 25, 30, 35, 40, 45, 50, 55, 60, 70, 80, 90, and 100.

Diameter of the gear $D = mz = 5 \times 35 = 175$ mm

$$t_p = \frac{\pi D}{\tan \beta} = \frac{\pi 175}{\tan 22.5^\circ} = \frac{3.14 \times 175}{0.422} = 1302.1 \approx 1300 \text{ mm}$$

$$x = \frac{Nt_x}{t_p} = \frac{40 \times 6}{1300} = \frac{24}{130} = \frac{6 \times 4}{10 \times 13} = \frac{30}{50} \times \frac{20}{65}$$

Before cutting the gear, the table of the milling machine is rotated and set at an angle of 22.5° . After milling one tooth, the gear blank is index for 35 division for which the crank is rotated by

$\frac{40}{35} = 1 \frac{5}{35} = 1 \frac{1}{7} = 1 \frac{7}{49}$ turns, that is, one full turn plus rotation through 7 holes of the circle

with 49 holes on plate 2.

1.6 Shaping and Allied Operations

Shaping, planing, and slotting machines are characterized by linear reciprocating primary cutting motion that consists of a forward-cutting stroke and an idle-return stroke. The feed motion in all these machines is intermittent in nature and is imparted at the end of full (forward + return) stroke. In shaping machines, the primary cutting motion is imparted to the tool mounted on a reciprocating ram, whereas the feed motion is imparted to the workpiece clamped on the table. In planing machines, the roles are reversed because they are meant for machining of bigger jobs that require large length of travel. Hence, in planing machines, the primary cutting motion is imparted to the workpiece mounted on the reciprocating table and the feed motion to the tool mounted on the cross rail. The difference between the slotting machine and the shaping machine is that in the former the primary cutting motion is imparted to the tool in the vertical direction, and typically the stroke length in slotting machines is much less than in shaping machines.

In shaping, planing, and slotting operations, machining is carried out during the forward-cutting stroke and the reverse stroke is idle. The feed is given intermittently to the table (in shaping and slotting machines) or the tool (in planing machines) after the end of the idle stroke or just before the beginning of the cutting stroke. Thus, in each forward stroke, the cutting process begins with an impact. In view of this, single-point tools used in shaping, planing, and slotting operations are provided negative or small positive rake angle that is $5\text{--}10^\circ$ less than on the corresponding turning tools. In addition, due to higher vulnerability of the tips of these tools to chipping on account of impact loading at the commencement of cut, the tool nose radius is kept 1–2 mm larger than on the corresponding turning tools.

Another feature of shaping, planing, and slotting operations is that if the tool has a straight shank, it bends about point O as shown in Figure 1.41a under the effect of the cutting force. In this process, the tool tip inscribes a circle of radius R and digs into the workpiece, damaging the machined surface. The solution lies in using bent shank or goose neck tools such that point O about which the tool bends is aligned with the tip of the tool as shown in Figure 1.41b.

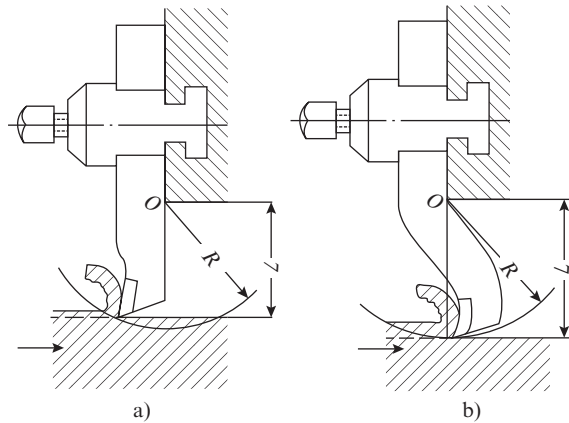


Figure 1.41 Schematic of shaping operation with (a) straight shank tool and (b) bent shank tool

Typical shaping operations are shown in Figure 1.42.

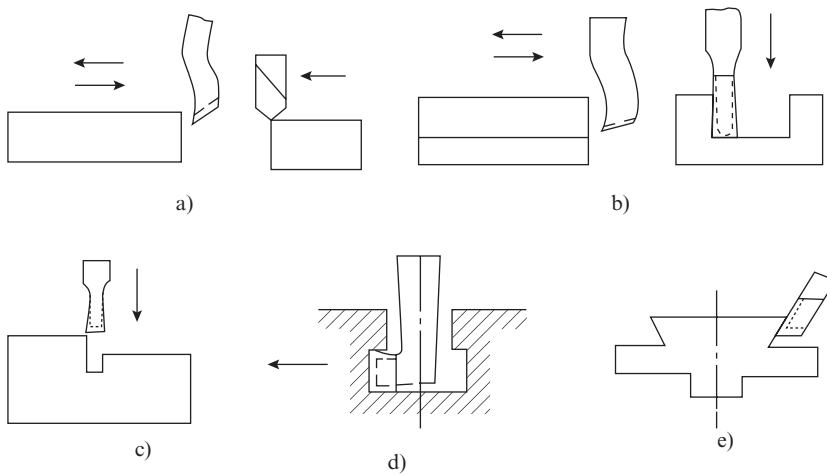


Figure 1.42 Shaping operations: (a) planing of flat surface, (b) machining of slot, (c) machining of groove, (d) machining of T-slot, and (e) machining of dove tail

Typical slotting operations are shown in Figure 1.43.

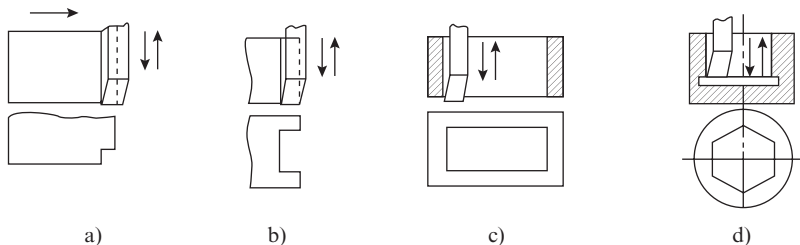


Figure 1.43 Slotting operations: (a) machining of a flat surface, (b) machining of open slot, (c) machining of rectangular slot, and (d) machining of blind hexagonal slot

Calculation of machining time is illustrated below for a shaping operation (Figure 1.44). It can be determined for the other shaping and allied operations in a similar manner.

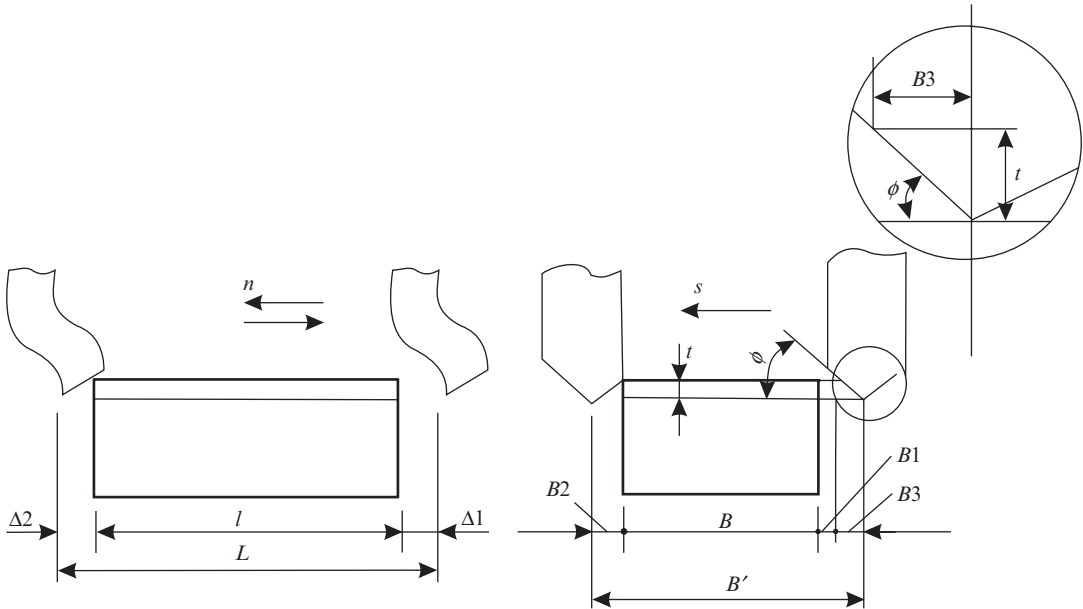


Figure 1.44 Shaping operation

$$\text{Machining time} = \frac{B'}{s \cdot n}$$

where, $B' = B + B1 + B2 + B3$

B = width of workpiece

$B1$ = approach, generally equal to 2–3 mm

$B2$ = over travel, generally equal to 2–3 mm

$B3 = t/\cot \phi$; where t is depth of cut and ϕ is primary cutting-edge angle; for straight-edged tools $\phi = 90^\circ$, hence $\Delta3 = 0$

s = feed per stroke

n = strokes/min which is found from Eqn. (1.4)

The machining time of planing and slotting operations can be determined in a similar manner.

Example 1.15

A 100-mm-wide and 200-mm-long surface is to be machined on a shaper, using feed per stroke of 0.3 mm. If the cutting speed is 20 m/min and the ratio of return time to cutting time is 1:1.25, calculate the time required to machine the job. Assume suitable approach and over travel.

Strokes per minute of the shaper is

$$n = \frac{1000vK}{L(K + 1)}$$

For a job of length 200 mm, the typical stroke length will be approximately 20 percent greater.

Hence,

$$L = 1.2 \times 200 = 240 \text{ mm}$$

Therefore,

$$n = \frac{1000 \times 20 \times 1.25}{240(1.25 + 1)} = 46.29 \text{ strokes/min}$$

Correcting this value to the nearest available value available on the shaper, say 50 strokes/min and assuming that the operation is carried out with a straight-edged tool and that $B_1 = B_2 = 2$ mm each

$$\text{Machining time, } T_m = B + B_1 + B_2 = \frac{100 + 2 + 2}{0.3 \times 50} = 6.934 \text{ min}$$

1.7 Grinding Operations

Grinding is the method of removing metal by an abrasive tool called the grinding wheel. It is carried out as a finishing operation on workpieces that have been machined by the conventional metal-cutting tools and then heat treated to attain higher mechanical properties such as hardness and strength. The increased hardness is beyond the capability of the conventional cutting tools of HSS or cemented carbides and grinding remains the only avenue of completing the machining of the workpiece to achieve the desired tolerance and surface finish. Generally, an allowance of <1 mm is left for the grinding operation.

The grinding methods generally used in practice are the following:

1. External cylindrical grinding
2. Internal cylindrical grinding
3. Surface grinding

1.7.1 External Cylindrical Grinding

(i) *Traverse cut.* Rotation of the grinding wheel is the primary cutting motion (Figure 1.45). The workpiece rotates (rotary feed) and reciprocates (longitudinal feed). At the end of each pass, the grinding wheel is given radial (cross) feed

$$\text{Grinding time, } T = \frac{Lh}{n_{\text{wp}} k B t} K, \text{ min,}$$

where L = length of workpiece

$s_1 = kB$ mm/rev of workpiece is the longitudinal feed of the reciprocating motion of the workpiece; $k = 0.3 - 0.5$ for rough grinding and $D_{\text{wp}} < 20$ mm; $k = 0.7 - 0.85$ for rough grinding and $D_{\text{wp}} \geq 20$ mm; and $k = 0.2 - 0.4$ for finish grinding

h = allowance, mm

$t = s_r$ = radial feed/stroke, mm is akin to depth of cut and is given intermittently at the end of stroke, that is, on traversing the length of the workpiece; typically $t = 0.01 - 0.025$ mm

$K = 1.2$ for rough grinding and 1.4 for finish grinding

n_{wp} = rpm of the workpiece

B = width of the grinding wheel

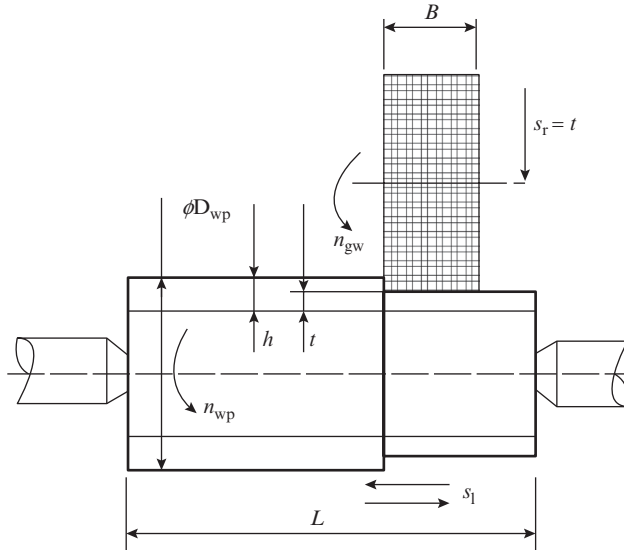


Figure 1.45 External cylindrical grinding—traverse cut

(ii) *Plunge cut.* In plunge cut grinding, (Figure 1.46), there is no longitudinal movement of the grinding wheel or of the workpiece because the width of the grinding wheel is greater than the length of the surface being machined. The grinding wheel rotates and is continuously fed into the workpiece, whereas the latter only rotates.

$$\text{Grinding time, } T = \frac{h}{s_t n_{wp}} K,$$

where $s_t = 0.0025 - 0.20$ mm per revolution of workpiece is the transverse feed h , n_{wp} , and K are the same as in traverse cut external grinding.

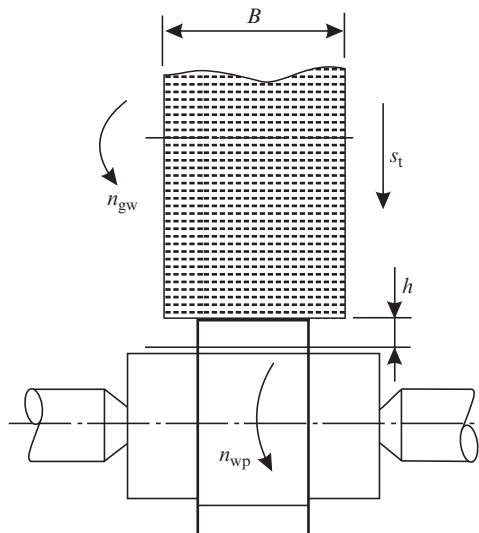


Figure 1.46 External cylindrical grinding—plunge cut

1.7.2 Internal Cylindrical Grinding

Internal cylindrical grinding is used for machining of holes (Figure 1.47). The diameter of the grinding wheel is therefore always less than that of the hole.

Internal cylindrical grinding is carried out in one of the following two ways: with a rotating workpiece or with a stationary workpiece. In the latter case, the grinding wheel not only rotates about its own axis but also executes a planetary motion such that its center moves along the planetary motion circle (PMC). This method is used for large workpieces.

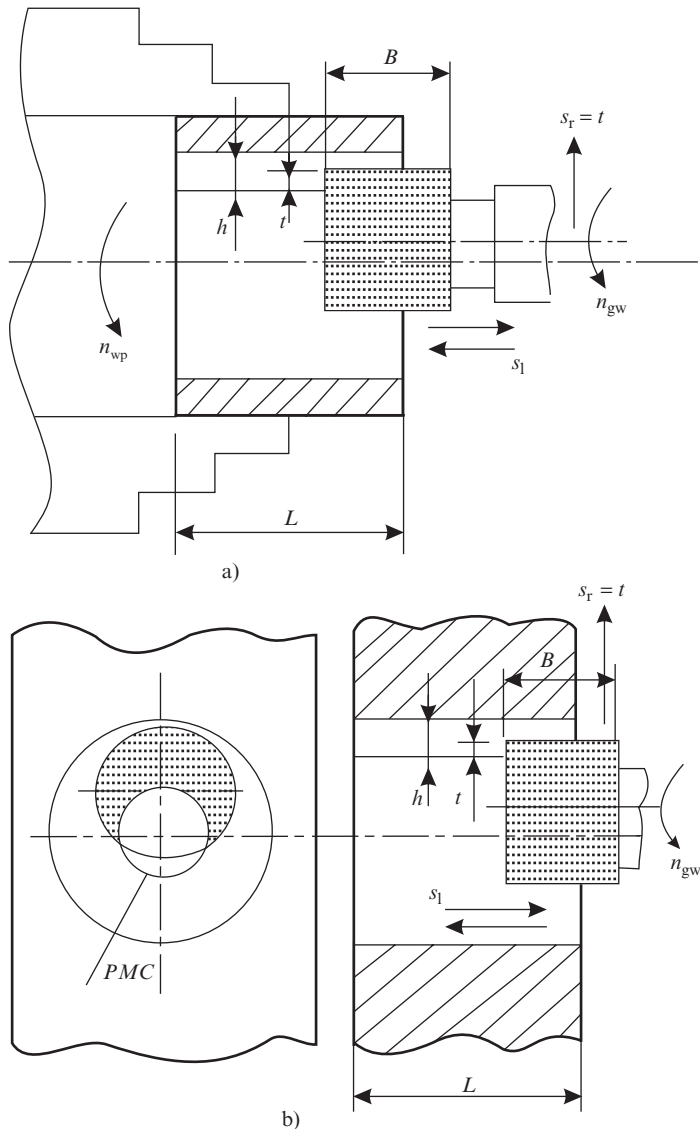


Figure 1.47 Internal cylindrical grinding: (a) with rotating workpiece and (b) with stationary workpiece

Grinding time, $T = \frac{2Lh}{n_{wp}kBt}$ K, min for internal grinding with rotating workpiece

Grinding time, $T = \frac{2Lh}{n_{PMC}kBt}$ K, min for internal grinding with stationary workpiece,

where L = length of workpiece

$s_l = kB$ mm/rev of workpiece is longitudinal feed; $k = 0.4 - 0.8$ for rough grinding and $0.25 - 0.45$ for finish grinding

$s_r = t$ = radial feed/double stroke, mm; typically $t = 0.005 - 0.03$ mm for rough grinding and $0.002 - 0.1$ for finish grinding. It is given at the end of one complete to-and-fro stroke (double stroke), which explains the presence of $2L$ in the formula of machining time calculation

n_{wp} = rpm of the workpiece

n_{PMC} = rpm of planetary motion of the grinding wheel

B = width of the grinding wheel

h = allowance, mm

$K = 1.3$ for rough grinding and $K = 1.6$ for finish grinding

1.7.3 Surface Grinding

Surface grinding is used for grinding plane surfaces. The grinding process may be carried out either by the periphery of the grinding wheel or by its face (Figure 1.48).

(i) *Peripheral-planer feed.*

$$\text{Grinding time, } T = \frac{LhH}{s_m kBt} \text{ K, min,}$$

where L = length of stroke; $L = l + 10$ mm, where l is length of workpiece

$s_t = kB$, mm/stroke is the transverse feed which is given at the end of stroke, that is, on traversing the length of the workpiece; $k = 0.4 - 0.7$ for rough grinding and $0.25 - 0.35$ for finish grinding

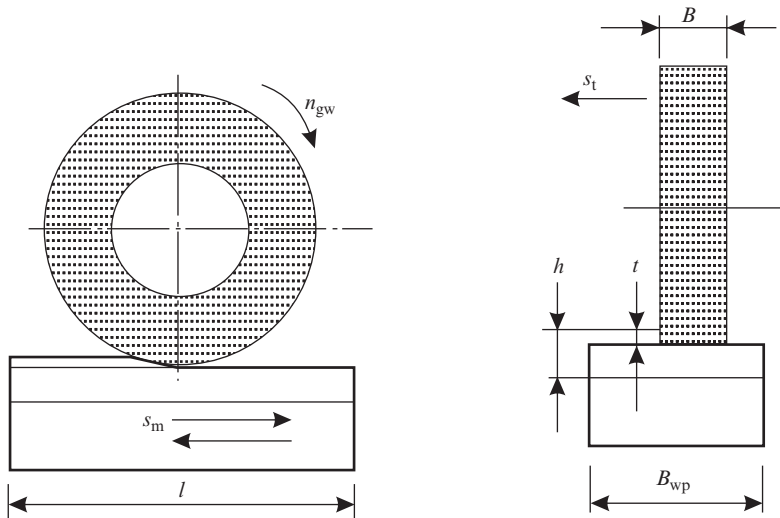


Figure 1.48 Peripheral surface grinding

$t = 0.015 - 0.15$ mm for rough grinding and $0.005 - 0.015$ for finish grinding. It is akin to depth of cut and is given intermittently at the end of stroke, that is, on traversing the length of the workpiece

$$H = B_{wp} + B + 5 \text{ mm};$$

s_m = feed of table, mm/min

h = allowance, mm

$K = 1.25$ for rough grinding and $K = 1.4$ for finish grinding

(ii) *Face-planer feed.* Surface grinding with the face of grinding wheel is generally carried out with grinding wheels having diameter D greater than the width of the workpiece B (Figure 1.49). Therefore, the transverse feed s_t is not required (see Figure 1.49a).

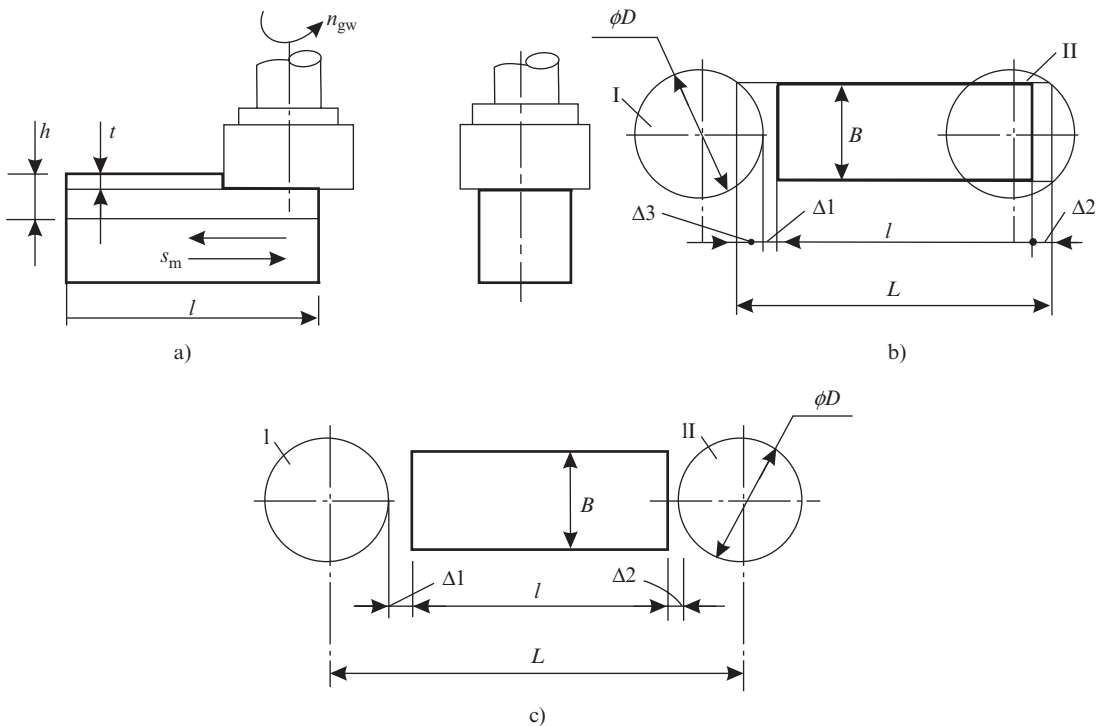


Figure 1.49 Face surface grinding

If the feed in depth is given at the end of stroke, that is, on traversing the length of the workpiece, then grinding time is determined from the following expression:

$$T = \frac{Lh}{s_m t} K; \text{ min}$$

where $L = l + \Delta 1 + \Delta 2 + D$ (see Figure 1.49c)

If the feed in depth is given at the end of one complete to-and-fro stroke (double stroke), then grinding time is determined from the following expression:

$$T = \frac{2Lh}{s_m t} K; \text{ min}$$

where $L = l + \Delta 1 + \Delta 2 + \Delta 3$

l = length of workpiece

$\Delta 1$ = approach; generally equal to 2–3 mm

$\Delta 2$ = over travel; generally equal to 2–3 mm

$\Delta 3 = 0.5(D - \sqrt{D^2 - B^2})$ as in symmetrical face milling (see Figure 1.49b)

s_m , t , and h are the same as in peripheral surface grinding

Example 1.16

A $\phi 40$ - and 210-mm-long step is to be machined on a cylindrical grinding machine. Grinding wheel diameter is 600 mm and its width 63 mm. Allowance is 0.2 mm and radial feed 0.005 mm per stroke. Transverse feed (mm per revolution of work) $s_1 = kB$, where $k = 0.3$. If peripheral speed of the grinding wheel and workpiece is 30 m/s and 35 m/min, respectively, determine the machining time.

Length of stroke of the table = 210 mm

$$\text{rpm of the workpiece, } n_{wp} = \frac{1000v_{wp}}{\pi D_{wp}} = \frac{1000 \times 35}{\pi \times 40} = \frac{875}{\pi}$$

Allowance, $h = 0.2$ mm

Longitudinal feed of reciprocating motion of workpiece, $s_1 = k \cdot B = 0.3 \times 63 = 18.9$ mm/rev.

Radial feed $t = 0.005$ mm/stroke

Assuming it to be case of finish grinding, we take $K = 1.4$

$$\text{Machining time, } T_m = \frac{Lh}{n_{wp} s_1 t}$$

$$K = \frac{210 \times 0.2}{\frac{875}{\pi} \times 18.9 \times 0.005} \times 1.4 = 2.22 \text{ min}$$

1.8 Geometry of Single-Point Tool

As mentioned in Section 1.1, Metal cutting is a process by which a workpiece is converted into a component of the desired specifications by removing excess material from the workpiece in the form of chips by using a wedge-shaped tool. By defining tool geometry, we seek to specify the parameters of this wedge and the location of the cutting edge that is obtained as the intersection of tool face and flank. For this purpose, it is first necessary to select the coordinate system. On the basis of the planes constituting the coordinate system, a large number of systems of defining tool geometry have been developed. Amongst these, the two systems that are most widely used are (i) orthogonal system and (ii) machine tool reference system.

1.8.1 Orthogonal System

Consider the turning operation shown in Figure 1.50. Here, one can identify two planes: (i) the base plane that is a horizontal plane coinciding with the base of the tool and (ii) the cutting plane that includes the primary cutting edge and is a vertical plane perpendicular to the base plane. These two planes along with an orthogonal plane that is also a vertical plane perpendicular to both of them comprise the coordinate system for defining the wedge parameters (Figure 1.51). As these planes are related to the tool cutting edge, this system is also known as the tool reference system.

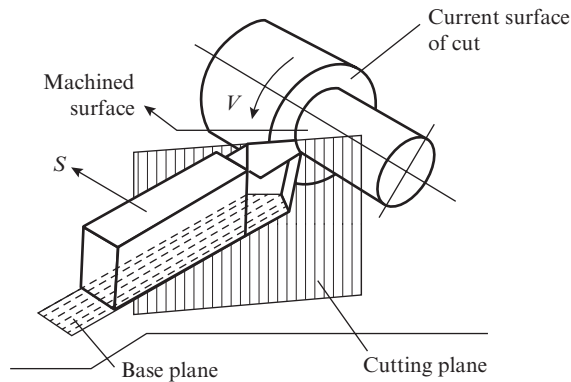


Figure 1.50 Schematic depicting the cutting plane and base plane in a turning operation

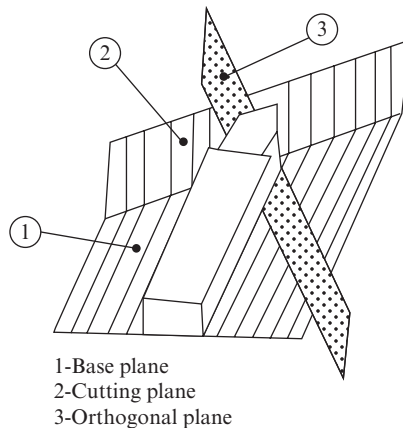


Figure 1.51 Planes of the coordinate system for defining tool geometry in the orthogonal system

Here, it is important to note that if the orthogonal plane is used as a sectioning plane, the tool section obtained is the true wedge. The angles that define the wedge of the primary cutting edge are the orthogonal clearance angle (α_0) and orthogonal rake angle (γ_0) (Figure 1.52). The wedge sections corresponding to positive, zero, and negative rake angles are shown in the figure. As discussed earlier in Section 1.1, α_0 is always positive.

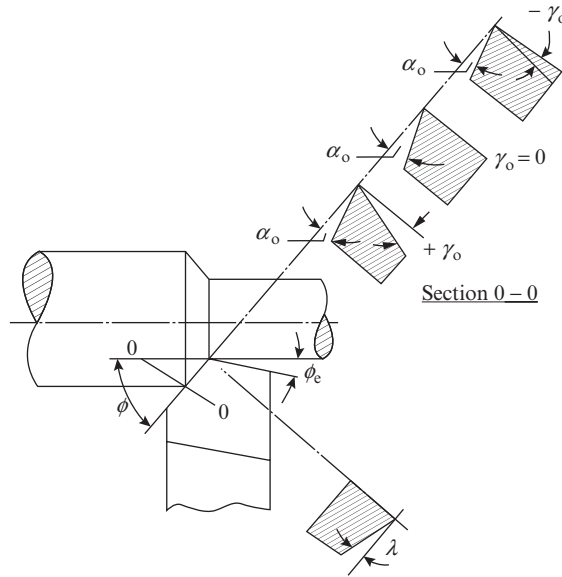


Figure 1.52 Schematic depicting the tool angles in the orthogonal system

The geometry of the auxiliary cutting edge can be defined in a similar manner with the help of an auxiliary cutting plane and an auxiliary orthogonal plane. The location of the primary and auxiliary cutting edges in the horizontal plane is fixed by defining the following two angles:

- Primary cutting edge angle (ϕ), which is the angle that the primary cutting edge makes with the direction of feed
- Auxiliary cutting edge angle (ϕ_e), which is the angle that the auxiliary cutting edge makes with the direction of feed

Although the location of the cutting edges is fixed in the horizontal plane by means of angles ϕ and ϕ_e , the primary cutting edge is still not uniquely defined as it can occupy different positions in the vertical plane (perpendicular to the plane of the page) by rotating about the tip of the tool as the pivot. Hence, the location of the primary cutting edge in the vertical plane is fixed by defining the cutting inclination angle λ as shown in Figure 1.52. This is the angle that the cutting edge makes with a line drawn from the tool tip parallel to the base plane. Angle λ may be positive, zero, and negative, and the corresponding tools are shown in Figure 1.53.

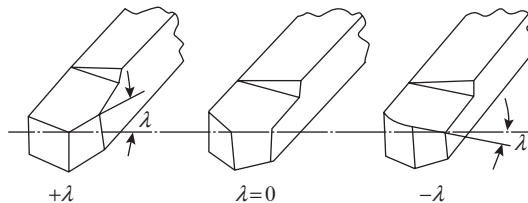


Figure 1.53 Cutting edge inclination angle

Tool nomenclature in the orthogonal system is represented by the parameters in the sequence given below

$$\lambda - \gamma_o - \alpha_o - \alpha'_o - \phi_e - \phi - r$$

where r is the nose radius and α'_o is the clearance angle on the auxiliary flank.

1.8.2 Machine Tool Reference System

The orthogonal system discussed earlier is based on a coordinate system related to the cutting edge of the tool. For making a new tool, the orthogonal system is not applicable because there is yet no cutting edge. Therefore for defining the geometry to make (grind) a new tool, the coordinate system has to be related to the axes of the tool grinder. It comprises the following three planes (Figure 1.54):

- Base plane, which is a horizontal plane coinciding with the base of the tool
- Machine longitudinal plane, which includes the direction of the longitudinal feed and is a vertical plane perpendicular to the base plane
- Machine transverse plane, which includes the direction of the transverse (cross) feed and is a vertical plane perpendicular to both the planes defined above.

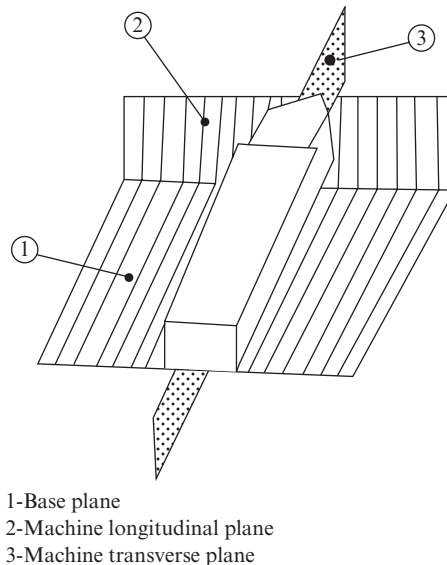


Figure 1.54 Planes of the coordinate system for defining tool geometry in the machine tool reference system

Since neither the machine longitudinal plane nor the machine transverse plane is perpendicular to the cutting edge, using just one of them as the sectioning plane does not give the true wedge in the section. Therefore, both the machine longitudinal plane and the machine transverse plane are used as sectioning planes to yield the projections of the tool section in the corresponding planes. The angles that define the geometry of the wedge in these two sections are side-rake angle (γ'_s), back-rake angle (γ'_b), side-clearance angle (α'_s), and end-clearance angle (α'_e). (See Figure 1.55.)

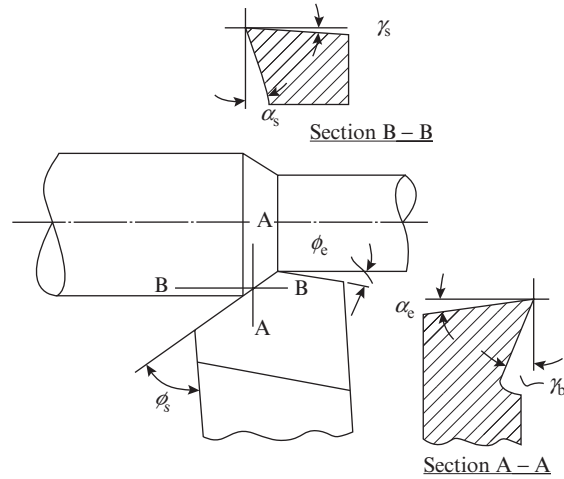


Figure 1.55 Schematic depicting the tool angles in the machine tool reference system

The location of the cutting edge is defined as in the orthogonal system with the help of the angles ϕ , ϕ_e , and λ . Tool nomenclature in the machine tool reference system is represented by the parameters in the sequence given below:

$$\gamma_b - \gamma_s - \alpha_e - \alpha_s - \phi_e - (90 - \phi), r$$

The angle $\phi_s = 90 - \phi$ is commonly referred to as side cutting-edge angle. The rake and clearance angles in the orthogonal and machine tool reference systems are geometrically correlated. This is obvious from the observation that the orthogonal system when rotated through an angle $(90 - \phi)$ gets converted to the machine tool reference system.

The rake angles in the orthogonal and machine tool reference system are related by the following expressions:

For $+\lambda$,

$$\begin{bmatrix} \tan \gamma_0 \\ \tan \lambda \end{bmatrix} = \begin{bmatrix} \cos \phi, \sin \phi \\ \sin \phi, -\cos \phi \end{bmatrix} \begin{bmatrix} \tan \gamma_b \\ \tan \gamma_s \end{bmatrix}$$

$$\begin{bmatrix} \tan \gamma_b \\ \tan \gamma_s \end{bmatrix} = \begin{bmatrix} \cos \phi, \sin \phi \\ \sin \phi, -\cos \phi \end{bmatrix} \begin{bmatrix} \tan \gamma_0 \\ \tan \lambda \end{bmatrix}$$

For $-\lambda$,

$$\begin{bmatrix} \tan \gamma_0 \\ \tan \lambda \end{bmatrix} = \begin{bmatrix} \cos \phi, \sin \phi \\ -\sin \phi, \cos \phi \end{bmatrix} \begin{bmatrix} \tan \gamma_b \\ \tan \gamma_s \end{bmatrix}$$

$$\begin{bmatrix} \tan \gamma_b \\ \tan \gamma_s \end{bmatrix} = \begin{bmatrix} \cos \phi, -\sin \phi \\ \sin \phi, \cos \phi \end{bmatrix} \begin{bmatrix} \tan \gamma_0 \\ \tan \lambda \end{bmatrix}$$

The clearance angles in the two systems are related by the following expressions:

$$\begin{bmatrix} \cot \alpha_0 \\ \tan \lambda \end{bmatrix} = \begin{bmatrix} \sin \phi, \cos \phi \\ \cos \phi, -\sin \phi \end{bmatrix} \begin{bmatrix} \cot \alpha_s \\ \cot \alpha_c \end{bmatrix}$$

$$\begin{bmatrix} \cot \alpha_s \\ \cot \alpha_c \end{bmatrix} = \begin{bmatrix} \sin \phi, \cos \phi \\ \cos \phi, -\sin \phi \end{bmatrix} \begin{bmatrix} \cot \alpha_0 \\ \tan \lambda \end{bmatrix}$$

It may be noted that the orthogonal or tool reference system is more suited for analytical study of metal cutting because the tool angles in this system define the true wedge, whereas the machine tool reference system is essential for imparting the desired geometry while grinding a new cutting tool.

Review Questions

- 1.1 Determine the rpm of a lathe spindle if a workpiece of diameter 100 mm is to be turned at a cutting speed of 88 m/min.
- 1.2 A 175-mm-long workpiece is to be machined on a shaper that has a cutting stroke to idle stroke velocity ratio of 0.84. Calculate the strokes/min of the shaping tool if the cutting speed is 30 m/min. Assume an approach and overshoot of 5 mm.
- 1.3 A 40-mm hole is drilled at a speed of 30 m/min and feed of 0.1 mm/tooth. Calculate the feed per minute of the operation.
- 1.4 A 10-teeth face milling cutter of diameter 125 mm machines a flat surface of length $L = 200$ mm and width $B = 100$ mm at a speed of 80 m/min and feed of 0.15 mm/tooth. Calculate the machining time, assuming an approach and overshoot of 5 mm.
(Hint: Travel = $L + 0.5\sqrt{(D^2 - B^2)} + 10$)
- 1.5 A 120-mm diameter workpiece is being turned on a lathe at 400 rpm and a feed of 0.3 mm/rev. The tangential, radial, and axial components of the cutting force were measured on a dynamometer and found to be 325, 120, and 130 kgf, respectively. Calculate the power rating of the motor assuming a coefficient of efficiency of 0.85 for the drive.
- 1.6 A $\phi 40$ shaft is machined at a speed of 80 m/min and feed of 0.1 mm/rev. Calculate machining time. Given shaft length = 100 mm. Assume suitable approach and over travel and sketch the operation.
- 1.7 A $\phi 72$ workpiece is faced at a speed of 40 m/min and feed of 0.15 mm/rev. Sketch the operation and calculate the machine time.
- 1.8 A $\phi 20$ blind hole is to be drilled to a depth of 30 mm at a speed of 30 m/min and feed of 0.1 mm/teeth. Calculate the machine time, assuming a suitable approach.
- 1.9 A $\phi 40$ hole is to be enlarged to $\phi 50$ in a boring operation. The cutting speed and feed is 40 m/min and 0.1 mm/rev, respectively, and the job diameter is $\phi 70$. Calculate the machining time if the permissible depth of cut is 2 mm. Assume a suitable approach and make a neat sketch of the operation. Job length = 70 mm.

- 1.10 Single-pass slab milling operation is carried out on a 500-mm-long job by a $\phi 70$ plain milling cutter at $n = 300$ rpm depth of cut 5mm and feed of 200 mm/min. If the cutter has 12 teeth, determine the feed per tooth and machining time. Assume suitable approach and over travel.
- 1.11 A $\phi 80$ face milling cutter is used for facing a 60-mm-wide and 300-mm-long job. The speed is 40 m/min and the feed is 40 mm/min. Calculate the machining time if the allowance is 10 mm and the permissible depth of cut is 5 mm. Assume a suitable feed rate of accelerated travel and time for manual vertical setting of the table.
- 1.12 A shaping operation is carried out at 20 m/min. If the length of stroke is 250 mm and the ratio of return time to cutting time is 2:3, find the strokes per minute of the arm.
- 1.13 A $\phi 60$ hole is to be ground by a $\phi 50$ grinding wheel of width 50 mm. The length of the hole is 65 mm, allowance is 0.2 mm, and radial feed 0.005 mm per stroke. Transverse feed (mm per revolution of work) $s_1 = kB$, where $k = 0.3$. If peripheral speed of the grinding wheel and workpiece is 30 m/s and 35 m/min, respectively, determine the machining time.
- 1.14 A flat plate of width 110 mm and length 280 mm is to be ground on a planer-type surface grinder using the periphery of a grinding wheel of diameter 450 mm and width 63 mm. Six plates are ground in one setting, placed 3 along length. Assume approach of 5 mm in width and 15 mm in length. The speed of reciprocation of the table is 15 m/min. The rest of the data are the same as in Q.13.
- 1.15 A slab of 50 mm width and 200 mm length is rough machined in a symmetrical face milling operation. If the cutter diameter is 75 mm, what will be the length of travel of the cutter?
- 1.16 In a slab milling operation, the diameter of cutter is 50 mm and number of teeth of cutter is 12. If the cutter spindle speed is 300 rpm, depth of cut is 2 mm, length of job is 500 mm, and table longitudinal feed is 200 m/min, what will be the feed per tooth during the milling operation? If the cutter over travel is 2 mm, what is the machining time for the single-pass milling operation?
- 1.17 BSW thread of 12 TPI is to be cut on a lathe with lead screw of 8 TPI. Determine the required change gears.
- 1.18 BSW thread of 27 TPI is to be cut on a lathe with lead screw of 6 TPI. Determine the required change gears.
- 1.19 Screw thread of pitch 0.25 inch is to be cut on a lathe with lead screw of pitch 8 mm. Determine the required change gears.
- 1.20 A double start thread of pitch 0.5 inch is to be cut on a lathe with lead screw of 6 TPI. Determine the required change gears.
- 1.21 Modular thread of module 3 mm is to be cut on a lathe with lead screw of 2 TPI. Determine the required change gears.
- 1.22 Determine the required crank rotation of the indexing head to index for
 (i) 33 divisions (ii) 24 divisions (iii) 5 divisions
- 1.23 Determine the required crank rotation and change gears for differential indexing for
 (i) 83 divisions (ii) 73 divisions (iii) 55 divisions
- 1.24 Determine the required crank rotation for indexing through
 (i) $3^\circ 30'$ (ii) $42^\circ 40'$ (iii) $34^\circ 12'$

- 1.25** Five helical flutes of pitch 500 mm have to be milled on a job of diameter 500 mm on a milling machine with a lead screw of pitch 6.35 mm. Determine the required crank rotation, table setting angle, and change gears.
- 1.26** A grinding wheel of diameter 150 mm is rotating at 3000 rpm. The speed of the grinding wheel is
 (a) 7.5π m/s (b) 15π m/s
 (c) 45π m/s (d) 450π m/s
- 1.27** Consider the following statements: In up-milling process,
 1. the cut starts from the machined surface and proceeds upward
 2. the cut starts from the top surface and proceeds downward
 3. the job is fed in a direction opposite to that of cutter rotation
 4. the job is fed in the same direction as that of cutter rotation
 The correct statements are
 (a) 1 and 3 (b) 1 and 4
 (c) 2 and 3 (d) 2 and 4
- 1.28** A 400-mm-long shaft has a 100-mm tapered step at the middle with 4° included angle. The tailstock offset required to produce this taper on a lathe would be
 (a) $400 \sin 4^\circ$ (b) $400 \sin 2^\circ$
 (c) $100 \sin 4^\circ$ (d) $100 \sin 2^\circ$
- 1.29** A single start thread of pitch 2 mm is to be produced on a lathe having a lead screw with double start thread of pitch 4 mm. The ratio of speeds between the spindle and lead screw for this operation is
 (a) 1:2 (b) 2:1
 (c) 1:4 (d) 4:1
- 1.30** An index plate of a milling machine dividing head has the following hole circles: 15, 16, 17, 18, 19, 20. A gear of 34 teeth has to be milled by simple indexing method. To machine each tooth the crank needs to be rotated through
 (a) 17 holes in the 20-hole circle
 (b) 18 hole in the 20-hole circle
 (c) 1 revolution and 3 holes in the 17-hole circle
 (d) 1 revolution and 2 holes in the 18-hole circle
- 1.31** A 31.8-mm drill is used to drill a hole in a 100-mm-thick block at $v = 20$ m/min and $s = 0.3$ mm/rev. If the approach = 9 mm and overtravel = 4 mm, the machining time is
 (a) 1 min 40 s (b) 1 min 44 s
 (c) 1 min 49 s (d) 1 min 53 s
- 1.32** A side- and face-milling cutter of diameter 125 mm and 10 teeth operates at $v = 14$ m/min and table traverse of $s_m = 100$ mm/min. The feed per tooth of the cutter is
 (a) 10 mm (b) 2.86mm
 (c) 0.286mm (d) 0.8mm
- 1.33** A bar of diameter 72 mm is faced at $v = 80$ m min and cross feed $s = 0.3$ mm/rev. The machining time is
 (a) 1.5min (b) 3.0 min
 (c) 5.4min (d) 8.5min
- 1.34** A workpiece is turned on a lathe at $v = 50$ m/min, $s = 0.8$ mm/rev and $t = 1.5$ mm. What is the metal removal rate?
 (a) $1000 \text{ mm}^3/\text{min}$ (b) $6000 \text{ mm}^3/\text{min}$
 (c) $2000 \text{ mm}^3/\text{min}$ (d) It cannot be calculated with the given data.

- 1.35 For taper turning on center lathe, the method of swiveling the compound rest is used for
- (a) long job with small taper angle
 - (b) long job with steep taper angle
 - (c) short job with small taper angle
 - (d) short job with steep taper angle
- 1.36 A double start thread of pitch 2 mm is to be cut on a lathe having lead screw pitch of 6 mm. What is the speed ratio between the lathe spindle and lead screw?
- (a) 1:3
 - (b) 3:1
 - (c) 2:3
 - (d) 3:2
- 1.37 The following tool signature is specified for a single-point tool in the machine tool reference system: 10, 12, 8, 6, 15, 20, 3. What does the angle 12 represent?
- (a) side cutting-edge angle
 - (b) side-rake angle
 - (c) back-rake angle
 - (d) side-clearance angle
- 1.38 A lathe tool has the following angle: $\gamma_s = -5^\circ$, $\gamma_b = -5^\circ$, and $\phi = 80^\circ$. Calculate the orthogonal rake angle and the cutting-edge inclination angle.
- 1.39 A lathe tool having $\gamma_b = -8^\circ$ and $\phi = 45^\circ$ is to be used for orthogonal machining. Determine γ_s to ensure orthogonality.

GEOMETRY OF CHIP FORMATION

2.1 Process of Chip Formation

As mentioned earlier in Section 1.1, metal cutting involves the use of a wedge-shaped tool that is used to convert a workpiece into a component of the desired specifications by removing the excess material in the form of chips. As the cutting tool is fed into the workpiece (Figure 2.1), the material that lies ahead of the tool tip is deformed, first elastically and then plastically. As the tool moves forward, the stresses in the deformed material increase, till they reach a level that causes the deformed material to shear in the plane of the maximum shear stresses at a particular angle to the direction of feed. As the first element shears off, the next element begins to get deformed, and so on. Thus, the successively removed elements form a stack, analogous to a stack of cards (Figure 2.2). The degree of connection between the elements determines whether the chip will be discontinuous, partially continuous, or continuous.

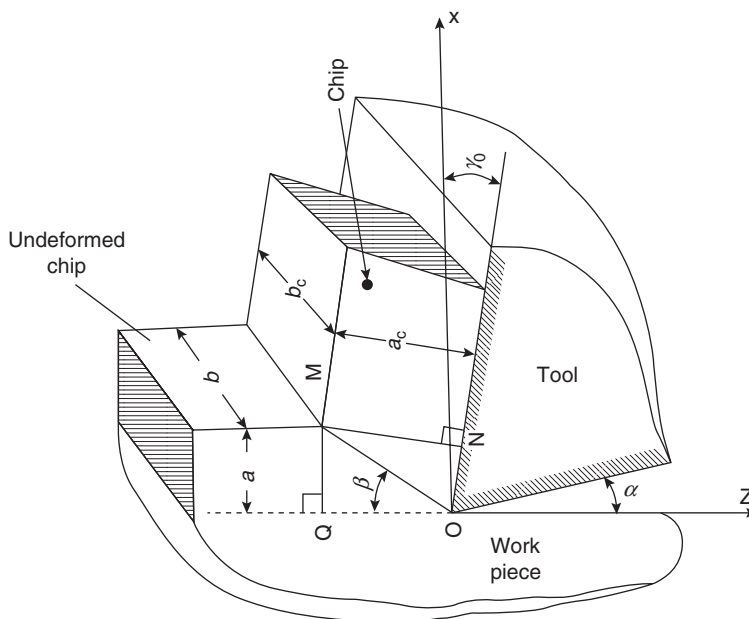


Figure 2.1 Schematic of chip formation in metal cutting

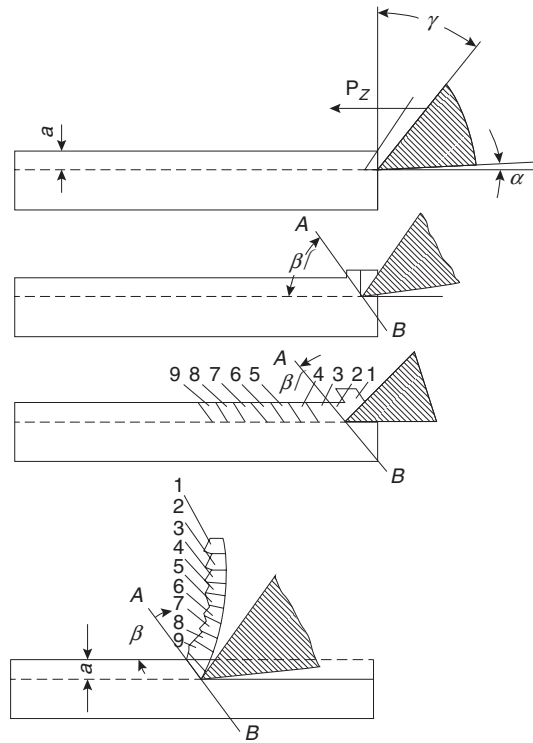


Figure 2.2 Schematic depicting the formation of continuous chip by stacking of elements

In the simplified model of chip formation described above, a sharp line separates the undeformed and deformed material. The material below this line is undeformed and is known as undeformed chip, whereas the material above this line is deformed and constitutes the chip. The line is known as slip line. When it is projected parallel to itself and perpendicular to the plane of the page, it forms a plane known as shear plane. A simplified representation of this process is shown in Figure 2.3, which may be articulated as follows: an undeformed layer of thickness a , moving at velocity v with respect to the tool tip is converted into a chip of thickness a_c moving at velocity v_c parallel to the tool face.

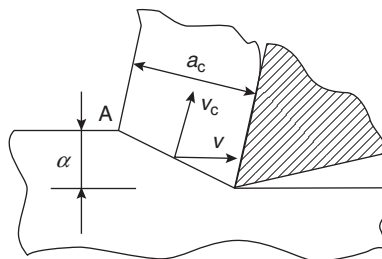


Figure 2.3 Single-shear plane model of metal cutting

The above model of chip formation is characterized by the following two features:

- (i) presence of a single-shear plane OA
- (ii) absence of smooth connection between the undeformed material and chip at the outer surface of the latter, that is, point A is an abrupt junction

The existence of a single-shear plane is impossible for two reasons. First, the yield points of the deformed and undeformed material differ by two to four times. Second, a particle of the undeformed material must receive infinite acceleration as its velocity changes from v to v_c during the instantaneous transition from the undeformed state to deformed state while crossing the shear plane.

Therefore, it follows that the deformed and undeformed materials should be separated not by a plane, but by a zone of plastic deformation in which the stresses and velocities change gradually from values corresponding to the undeformed material to those of the chip. Such a model is shown in Figure 2.4.

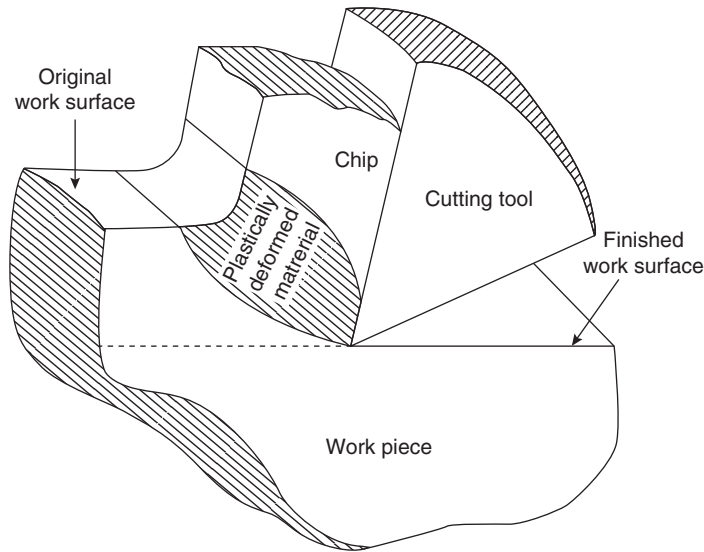


Figure 2.4 Thick plastic zone model of metal cutting with curved shear zone boundaries

In this model, the outer surface of the chip and the undeformed material do not intersect directly, but they are separated by a curved transition surface and within the transition zone, plastic shear occurs in a family of planes arranged fan-like and starting from the cutting edge. Analysis of the stressed and deformed state using the above model presents considerable difficulties. A simplified model that gives a reasonably accurate description of the state of stress and strain is obtained by replacing the curved shear lines by straight lines (Figure 2.5).

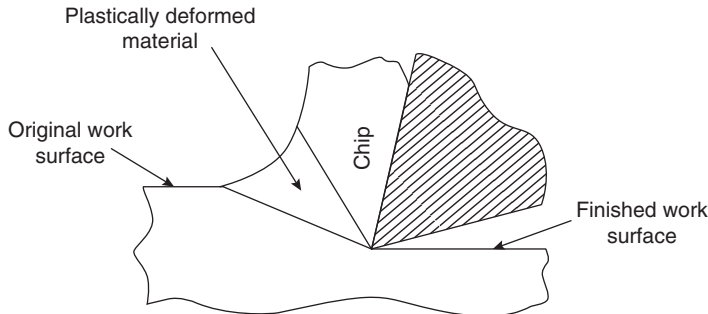


Figure 2.5 Thick plastic zone model of metal cutting with straight shear zone boundaries

The thickness of the shear zone is comparable with the thickness of the undeformed zone only under conditions of very small rake angle, very large undeformed chip thickness and very low cutting speed. For the values of rake angle, undeformed chip thickness and cutting speed that are typical of normal cutting practice, the thickness of the shear zone is very small—of the order of a few microns—and the boundaries of the shear zone OA and OB come so close that it becomes possible to consider that shear deformation is localized in an extremely thin layer of thickness Δx , and the shear zone can be replaced by a single line at an angle β (Figure 2.6).

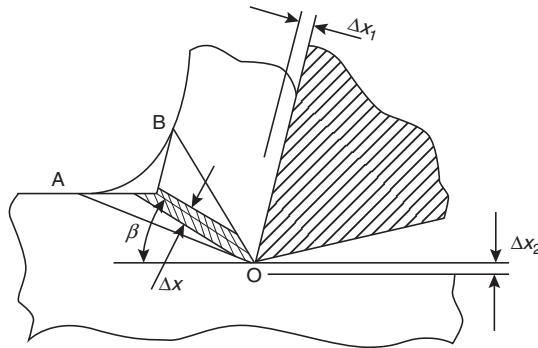


Figure 2.6 Model of metal cutting depicting narrow primary shear zone and secondary shear zones

The model considered above pertains to deformation in the vicinity of the shear plane that is known as primary shear zone. In fact, as shown in Figure 2.6, deformation also occurs in a thin layer of the chip (Δx_1) due to friction between the chip and tool face and also in a thin layer of the machined surface (Δx_2) due to friction between the tool flank and the machined surface. These two deformations, referred to as secondary shear, are generally much smaller in magnitude than the primary shear and may be ignored for the sake of simplicity of the model. The simplified, idealized model thus obtained (Figure 2.7) is used for theoretical analysis of metal cutting in all subsequent discussions.

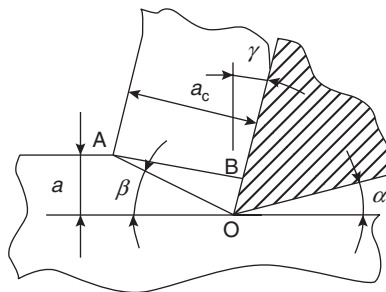


Figure 2.7 Simplified model of chip formation

2.2 Parameters of Undeformed Chip in Turning, Drilling, and Milling

Undeformed chip is defined as the volume of work material that is converted into chip as the tool moves through a distance equal to feed per revolution in case of single-point tool and feed per tooth in case of multiple tooth cutters, for example, milling cutters. The outline of the undeformed

chip is obtained by graphically representing the cutting tool in two adjacent locations separated by feed per revolution in single-point tools and feed per tooth in multiple tooth cutters. The overlapped work material between the two tool locations represents the undeformed chip.

2.2.1 Undeformed Chip in Turning

The turning operation is shown in Figure 2.8(a), where the single-point tool has been sketched in two positions 1 and 2 separated by the distance s representing the feed per revolution. The parallelogram $ABCD$ represents the undeformed chip and is shown separately on an enlarged scale in Figure 2.8(b).

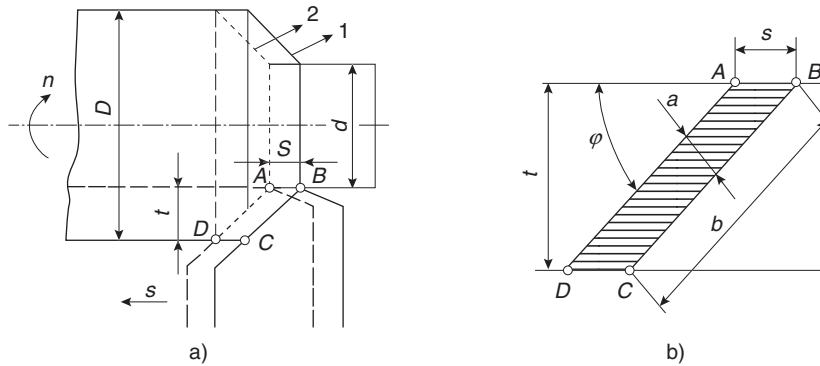


Figure 2.8 Undeformed chip parameters in turning operation

From the geometry of the undeformed chip, its thickness a and width b are found from the following relations:

$$a = s \sin \phi \quad (2.1)$$

$$b = t / \sin \phi \quad (2.2)$$

Where s , t , and ϕ represent feed per revolution, depth of cut, and primary cutting-edge angle, respectively

The working length of the cutting edge l_{ce} is equal to the undeformed chip width b when cutting-edge inclination angle $\lambda = 0$. For λ not exceeding $\pm 10^\circ$, l_{ce} can be determined from the following expression:

$$l_{ce} = \frac{t}{\sin \phi \cos \lambda} \quad (2.3a)$$

From Eqs (2.1) and (2.2), it is evident that irrespective of the value of ϕ , the undeformed chip area

$$A = a b = s t \quad (2.3b)$$

2.2.2 Undeformed Chip in Drilling

The drilling operation is shown in Figure 2.9, where the drill is shown in two positions 1 and 2, separated by the distance $s_z = s/2$, because a drill has two cutting edges. The undeformed chip is represented by the parallelogram with vertical hatching. Again, from the geometry of this parallelogram, thickness a and width b of the undeformed chip are found from the following relations:

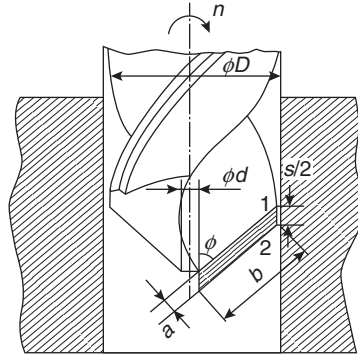


Figure 2.9 Undeformed chip parameters in drilling operation

$$a = s_z \sin \phi = \frac{s}{2} \sin \phi \tag{2.4}$$

$$b = \frac{D - d}{2 \sin \phi} \tag{2.5}$$

Where D is the drill diameter, d the diameter of the chisel edge of the drill, and 2ϕ is the point angle of the drill. It may be noted that the depth of cut in the drilling operation is $t = \frac{D - d}{2}$.

2.2.3 Undeformed Chip in Plain Milling

The plain milling operation is shown in Figure 2.10(a) in the up milling version. The plain milling cutter is shown in two positions 1 and 2 separated by the distance s_z equal to the feed per tooth. A particular cutting tooth enters the job when the angle of engagement $\psi = 0$ and exits the job when $\psi = \delta$. The undeformed chip has the shape of a comma (,) as shown in Figure 2.10(b) and its thickness varies from zero at the entry to maximum at the exit.

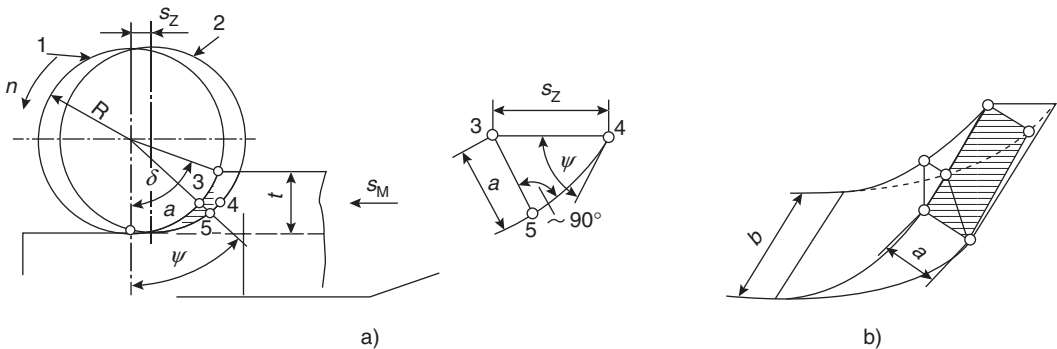


Figure 2.10 Undeformed chip parameters in plain milling operation

At an arbitrary angle of engagement ψ , the undeformed chip thickness is given by the following expression:

$$a = s_z \sin \psi \tag{2.6}$$

Therefore, at the maximum angle of engagement δ , the maximum undeformed chip thickness is found as follows:

$$a_{\max} = s_z \sin \delta \quad (2.7)$$

From ΔOAB ,

$$\cos \delta = \frac{\frac{D}{2} - t}{D/2} = \left(1 - \frac{2t}{D}\right) \quad (2.8)$$

$$\begin{aligned} \therefore \sin \delta &= \sqrt{1 - \cos^2 \delta} = \sqrt{1 - \left(1 - \frac{2t}{D}\right)^2} \\ &= 2\sqrt{\frac{t}{D}\left(1 - \frac{t}{D}\right)} \end{aligned}$$

Hence, substituting for $\sin \delta$ in Eqn. (2.7), we find

$$a_{\max} = 2s_z \sqrt{\frac{t}{D}\left(1 - \frac{t}{D}\right)} \quad (2.9)$$

The average undeformed chip thickness may be looked upon in two ways as

- (i) the thickness a_{av1} at the middle of the arc of contact, that is, $\delta/2$.
- (ii) the constant thickness a_{av2} that provides the same undeformed chip area as that of the actual undeformed chip of varying thickness.

For case 1:

$$a_{av1} = s_z \sin \frac{\delta}{2}$$

$$\text{As } \cos \delta = 1 - 2 \sin^2 \frac{\delta}{2},$$

$$\sin \frac{\delta}{2} = \sqrt{\frac{1}{2}(1 - \cos \delta)}$$

Substituting for $\cos \delta$ from Eqn. (2.8), we get

$$\sin \frac{\delta}{2} = \sqrt{\frac{1}{2}\left\{1 - \left(1 - \frac{2t}{D}\right)\right\}} = \sqrt{\frac{t}{D}} \quad (2.10)$$

Therefore,

$$a_{av1} = s_z \sqrt{\frac{t}{D}} \quad (2.11)$$

For case 2:

$$\begin{aligned} \frac{D}{2} \delta a_{av2} &= \frac{D}{2} \int_0^\delta s_z \sin \psi . d\psi \\ \therefore a_{av2} &= \frac{s_z (1 - \cos \delta)}{\delta} = \frac{s_z \left\{ 1 - \left(1 - \frac{2t}{D} \right) \right\}}{\cos^{-1} \left(1 - \frac{2t}{D} \right)} \\ a_{av2} &= \frac{s_z \frac{2t}{D}}{\cos^{-1} \left(1 - \frac{2t}{D} \right)} \end{aligned} \tag{2.12}$$

Length of the undeformed chip is

$$l = \frac{D}{2} \delta = \frac{D}{2} \left\{ \cos^{-1} \left(1 - \frac{2t}{D} \right) \right\} \tag{2.13}$$

The expressions for a_{max} , a_{av2} , and l can be simplified if it is assumed that the depth of cut t is much less than the cutter diameter D .

Let us first consider the following expression for a_{max} :

$$a_{max} = 2s_z \sqrt{\frac{t}{D} \left[1 - \frac{2t}{D} \right]} = 2s_z \sqrt{\frac{t}{D} - \frac{2t^2}{D^2}}$$

Neglecting, the higher order terms, the following simplified relation is obtained for a_{max} :

$$a_{max} = 2s_z \sqrt{\frac{t}{D}} \tag{2.14}$$

Now consider the following expression for a_{av2} :

$$a_{av2} = \frac{s_z (1 - \cos \delta)}{\delta}$$

Expressing $\cos \delta$ as a series, we have

$$\cos \delta = 1 - \frac{\delta^2}{2} + \frac{\delta^4}{4} + \dots$$

Ignoring the higher order terms, we may write

$$\cos \delta = 1 - \frac{\delta^2}{2} = 1 - \frac{2t}{D},$$

Wherefrom,

$$\delta = 2\sqrt{\frac{t}{D}} \tag{2.15}$$

Now substituting for $\cos\delta$ from Eqn. (2.8) and δ from Eqn. (2.15), we get

$$a_{av2} = \frac{s_z \left\{ 1 - \left(1 - \frac{2t}{D} \right) \right\}}{2\sqrt{\frac{t}{D}}} = s_z \sqrt{\frac{t}{D}} \quad (2.16)$$

It can be noted from Eqs (2.11), (2.14), and (2.16) that with the assumption t is much less than D , $a_{av2} = a_{av1} = a_{max}/2$.

Finally, let us consider the expression for undeformed chip length:

$$l = \frac{D}{2} \delta$$

Substituting for δ from Eqn. (2.15), we get the following simplified expression:

$$l = \frac{D}{2} \times 2\sqrt{\frac{t}{D}} = \sqrt{tD} \quad (2.17)$$

Undeformed chip width:

$$b = B \quad (2.18)$$

where B is the width of the workpiece.

All the above expressions for undeformed chip parameters in plain milling have been derived for a plain milling cutter with straight teeth, parallel to the cutter axis. In cutters with helical teeth with helix angle θ , the general expressions for a_{max} , a_{av1} , a_{av2} , and l get modified as follows:

$$a_{max} = 2s_z \sqrt{\frac{t}{D} \left(1 - \frac{t}{D} \right)} \cos \theta \quad (2.19)$$

$$a_{av1} = s_z \sqrt{\frac{t}{D}} \cos \theta \quad (2.20)$$

$$a_{av2} = \frac{s_z \frac{2t}{D}}{\cos^{-1} \left(1 - \frac{2t}{D} \right)} \cos \theta \quad (2.21)$$

$$l = \frac{D}{2 \sin \theta} \left\{ \cos^{-1} \left(1 - \frac{2t}{D} \right) \right\} \quad (2.22)$$

While the corresponding simplified expressions are

$$a_{max} = 2s_z \sqrt{\frac{t}{D}} \cos \theta \quad (2.23)$$

$$a_{av1} = s_z \sqrt{\frac{t}{D}} \cos \theta \quad (2.24)$$

$$a_{av2} = s_z \sqrt{\frac{t}{D}} \cos \theta \quad (2.25)$$

$$l = \frac{\sqrt{tD}}{\sin \theta} \quad (2.26)$$

In a helical tooth cutter, the undeformed chip width is different for each tooth at a given instant and is given by the following expression:

$$b_x = \frac{D}{2 \sin \theta} (\cos \psi_{en} - \cos \psi_{ex}) \quad (2.27)$$

Where

ψ_{ex} = angle of contact when the given tooth exits the workpiece in the particular position of the cutter.

ψ_{en} = angle of contact when the given tooth enters the workpiece in the particular position of the cutter.

Example 2.1

A slab milling operation is being carried out with a 100-mm diameter milling cutter having 8 teeth at 30 m/min. The depth of cut is 4 mm and table feed rate is 150 mm/min. The width of the workpiece is 120 mm. Find the average cross-sectional area of the undeformed chip:

$$\text{Cutter rpm, } n = \frac{1000v}{\pi D} = \frac{1000 \times 30}{\pi \times 100} = \frac{300}{\pi}$$

$$\text{Feed per tooth, } s_z = \frac{\text{feed per min}}{\text{number of teeth of cutter} \times \text{cutter rpm}} = \frac{150 \times \pi}{8 \times 300}$$

Applying the relation $a_{av} = s_z \sqrt{\frac{t}{D}}$, the average width of the undeformed chip is found as follows:

$$a_{av} = \frac{150\pi}{2400} \sqrt{\frac{4}{100}} = \frac{150\pi}{2400 \times 5}$$

Hence for a work piece of width 120 mm, the average cross-sectional area of the undeformed chip is

$$= \frac{150 \times \pi \times 120}{2400 \times 5} = 4.71 \text{ mm}^2$$

2.2.4 Undeformed Chip in Face Milling

Undeformed Chip in Unsymmetrical Face Milling when $B < 0.5D$ The operation is shown in Figure 2.11, where it is evident that the process is similar to plain milling, except that the depth of cut t in plain milling is replaced by width of milling B . However, unlike

in plain milling, the assumption that B is much less than D is not valid. In addition, instead of the helix angle θ , the primary cutting-edge angle ϕ of the face milling cutter should be used.

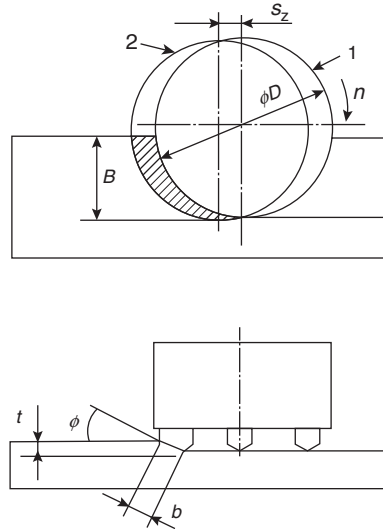


Figure 2.11 Undeformed chip parameters in unsymmetrical face milling operation when $B < 0.5D$

Bearing the above in mind, the parameters of undeformed chip (shown hatched in Figure 2.11) for the given case of face milling may be expressed by the following relations:

$$a_{\max} = 2s_z \sqrt{\frac{B}{D} \left(1 - \frac{B}{D}\right)} \sin \phi \quad (2.28)$$

$$a_{\text{av1}} = 2s_z \sqrt{\frac{B}{D}} \sin \phi \quad (2.29)$$

$$a_{\text{av2}} = \frac{s_z \frac{2B}{D}}{\cos^{-1} \left(1 - \frac{2B}{D}\right)} \sin \phi \quad (2.30)$$

$$l = \frac{D}{2} \cos^{-1} \left(1 - \frac{2B}{D}\right) \quad (2.31)$$

$$b = \frac{t}{\sin \phi} \quad (2.32)$$

Undeformed Chip in Symmetrical Face Milling The operation is shown in Figure 2.12 and the undeformed chip is shown hatched in the figure.

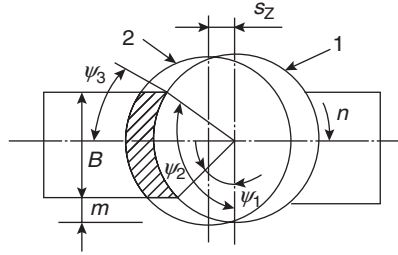


Figure 2.12 Undeformed chip parameters in symmetrical face milling operation

Considering that in the given case $m = \frac{D}{2} - \frac{B}{2}$ as shown in Figure 2.12 and considering Eqn. (2.10) of the plain milling operation for the analogous parameters, we may write

$$\sin \frac{\psi_1}{2} = \sqrt{\frac{\left(\frac{D}{2} - \frac{B}{2}\right)}{D}} \quad \text{and} \quad \sin \frac{\psi_2}{2} = \sqrt{\frac{\left(\frac{D}{2} + \frac{B}{2}\right)}{D}}$$

Wherefrom,

$$\frac{\psi_1}{2} = \sin^{-1} \left\{ \sqrt{\frac{\left(\frac{D}{2} - \frac{B}{2}\right)}{D}} \right\} \quad \text{and} \quad \frac{\psi_2}{2} = \sin^{-1} \left\{ \sqrt{\frac{\left(\frac{D}{2} + \frac{B}{2}\right)}{D}} \right\}$$

The thickness of the undeformed chip is maximum at the middle where

$$\psi_0 = \frac{\psi_1 + \psi_2}{2} = \frac{\psi_1}{2} + \frac{\psi_2}{2}$$

Hence,

$$\begin{aligned} \psi_0 &= \sin^{-1} \sqrt{\frac{\frac{D}{2} - \frac{B}{2}}{D}} + \sin^{-1} \sqrt{\frac{\frac{D}{2} + \frac{B}{2}}{D}} \\ \psi_0 &= \sin^{-1} \left[\left\{ \left(\sqrt{\frac{\frac{D}{2} + \frac{B}{2}}{D}} \right) \left(\sqrt{1 - \frac{\frac{D}{2} - \frac{B}{2}}{D}} \right) \right\} + \left\{ \left(\sqrt{\frac{\frac{D}{2} - \frac{B}{2}}{D}} \right) \left(\sqrt{1 - \frac{\frac{D}{2} + \frac{B}{2}}{D}} \right) \right\} \right] \\ \psi_0 &= \sin^{-1} \left[\left\{ \left(\sqrt{\frac{D+B}{2D}} \right) \left(\sqrt{\frac{D+B}{2D}} \right) \right\} + \left\{ \left(\sqrt{\frac{D-B}{2D}} \right) \left(\sqrt{\frac{D-B}{2D}} \right) \right\} \right] \\ \psi_0 &= \sin^{-1} \left[\left(\frac{D+B}{2D} \right) + \left(\frac{D-B}{2D} \right) \right] = \sin^{-1} (1) \end{aligned}$$

Hence, $\sin \psi_0 = 1$, that is, $\psi_0 = 90^\circ$, that is, the maximum undeformed chip thickness occurs at the middle, along the line of symmetry and

$$a_{\max} = s_z \sin \phi \quad (2.33)$$

The average undeformed chip thickness a_{av1} at the middle of the arc of contact is given by an expression analogous to Eqn. (2.6) at $(90 - \psi_1)/2$; hence,

$$\begin{aligned} a_{\text{av1}} &= s_z \sin \left(\frac{90 - \psi_1}{2} \right) \sin \phi \\ &= s_z \left[\sin 45^\circ \cos \frac{\psi_1}{2} - \cos 45^\circ \sin \frac{\psi_1}{2} \right] \sin \phi \end{aligned}$$

We have already derived

$$\sin \frac{\psi_1}{2} = \sqrt{\frac{\frac{D}{2} - \frac{B}{2}}{D}}$$

Therefore,

$$\cos \frac{\psi_1}{2} = \sqrt{1 - \sin^2 \frac{\psi_1}{2}} = \sqrt{1 - \frac{\frac{D}{2} - \frac{B}{2}}{D}} = \sqrt{\frac{D+B}{2D}}$$

Hence,

$$\begin{aligned} a_{\text{av1}} &= s_z \left[\frac{1}{\sqrt{2}} \sqrt{\frac{D+B}{2D}} - \frac{1}{\sqrt{2}} \sqrt{\frac{D-B}{2D}} \right] \sin \phi \\ &= \frac{s_z}{2\sqrt{D}} \left[(\sqrt{D+B}) - (\sqrt{D-B}) \right] \sin \phi \end{aligned} \quad (2.34)$$

The average undeformed chip thickness a_{av2} based on the concept of equivalent constant thickness is found from the following relation:

$$\frac{D}{2} \left(\frac{\pi}{2} - \psi_1 \right) a_{\text{av2}} = \frac{D}{2} \int_{\psi_1}^{\frac{\pi}{2}} s_z \sin \psi \, d\psi$$

Hence,

$$a_{\text{av2}} = \frac{s_z \left[\cos \psi \right]_{\frac{\pi}{2}}^{\psi_1}}{\frac{\pi}{2} - \psi_1} \sin \phi = \frac{s_z \cos \psi_1}{\frac{\pi}{2} - \psi_1} \sin \phi$$

Now

$$\begin{aligned} \cos \psi_1 &= 2 \cos^2 \frac{\psi_1}{2} - 1 = 2 \left(\sqrt{\frac{D+B}{2D}} \right)^2 - 1 \\ &= \frac{D+B}{D} - 1 = \frac{B}{D} \end{aligned}$$

Hence,

$$a_{av2} = \frac{s_z \frac{B}{D}}{\frac{\pi}{2} - \cos^{-1}\left(\frac{B}{D}\right)} \sin \phi \tag{2.35}$$

The length of undeformed chip is given by the expression:

$$l = \frac{D}{2} \left(\frac{\pi}{2} + \psi_3 - \psi_1 \right)$$

$$= \frac{\pi D}{4} + \frac{D}{2} (\psi_3 - \psi_1)$$

From Figure 2.12, it can be noted that

$$\cos \psi_1 = \frac{B/2}{D/2} = \frac{B}{D}$$

i.e. $\psi_1 = \cos^{-1}\left(\frac{B}{D}\right)$

$$\sin \psi_3 = \frac{B/2}{D/2} = \frac{B}{D}$$

i.e. $\psi_3 = \sin^{-1}\left(\frac{B}{D}\right)$

Hence,

$$l = \frac{\pi D}{4} + \frac{D}{2} \left[\cos^{-1}\left(\frac{B}{D}\right) + \sin^{-1}\left(\frac{B}{D}\right) \right] \tag{2.36}$$

In this case too, the width of the undeformed chip is given by Eqn. (2.32).

Undeformed Chip in Face Milling when $B > 0.5D$ The operation is shown in Figure 2.13, and the undeformed chip is shown hatched in the figure.

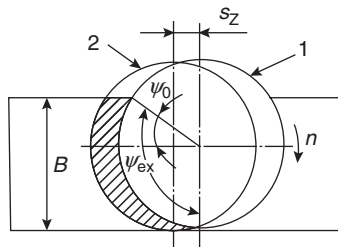


Figure 2.13 Undeformed chip parameters in unsymmetrical face milling operation when $B > 0.5D$

Based on the analysis of symmetrical face milling operation, it is evident that the maximum undeformed chip thickness will occur when the engagement angle $\Psi = 90^\circ$; consequently, a_{\max} will be given by Eqn. (2.33).

The average undeformed chip thickness at the middle of the arc of contact:

$$a_{av1} = s_z \sin \frac{\psi_{ex}}{2} \sin \phi$$

Where

$$\sin \frac{\psi_{ex}}{2} = \sqrt{\frac{1}{2}(1 - \cos \psi_{ex})}$$

It is can be noted from Figure 2.13 that

$$\cos \psi_{ex} = \cos(90 + \psi_0) = -\sin \psi_0 = -\left(\frac{B - \frac{D}{2}}{D/2}\right) = 1 - \frac{2B}{D}$$

Therefore,

$$\sin \frac{\psi_{ex}}{2} = \sqrt{\frac{1}{2}\left[1 - \left(1 - \frac{2B}{D}\right)\right]} = \sqrt{\frac{B}{D}}$$

Hence,

$$a_{av1} = s_z \sqrt{\frac{B}{D}} \sin \phi \quad (2.37)$$

The average undeformed chip thickness a_{av2} based on the concept of equivalent constant thickness is found from the following relation:

$$\frac{D}{2} \left(\frac{\pi}{2} + \psi_0\right) a_{av2} = \frac{D}{2} \int_0^{\frac{\pi}{2} + \psi_0} s_z \sin \psi d\psi \sin \phi$$

$$\begin{aligned} \left(\frac{\pi}{2} + \psi_0\right) a_{av2} &= -s_z [\cos \psi]_0^{\frac{\pi}{2} + \psi_0} \sin \phi \\ &= -s_z [-\sin \psi_0 - 1] \sin \phi \end{aligned}$$

Therefore,

$$a_{av2} = \frac{s_z (1 + \sin \psi_0)}{\frac{\pi}{2} + \psi_0} \sin \phi$$

It can be noted from Figure 2.13 that

$$\sin \psi_0 = \frac{B - \frac{D}{2}}{D/2} = \frac{2B}{D} - 1$$

Hence, substituting for $\sin \psi_0$ and Ψ_0 , we obtain

$$a_{av2} = \frac{s_z \left[1 + \left(\frac{2B}{D} - 1 \right) \right]}{\frac{\pi}{2} + \sin^{-1} \left(\frac{2B}{D} - 1 \right)} \sin \phi$$

Hence,

$$a_{av2} = \frac{s_z \frac{2B}{D}}{\frac{\pi}{2} + \sin^{-1} \left(\frac{2B}{D} - 1 \right)} \sin \phi \quad (2.38)$$

The length of the undeformed chip is given by the following expression:

$$l = \frac{D}{2} \left(\frac{\pi}{2} + \psi_0 \right)$$

$$l = \frac{D}{2} \left[\frac{\pi}{2} + \sin^{-1} \left(\frac{2B}{D} - 1 \right) \right] \quad (2.39)$$

As in the previous two cases of face milling discussed above, the undeformed chip width is given by Eqn. (2.32).

2.3 Shear Angle and Shear Strain in Chip Formation

It was established in Section 2.1 that the idealized, simplified model can be used for analysis of chip formation under normal conditions. As chip formation is the result of plastic deformation, it is necessary to state two axioms from the theory of plasticity that are relevant to the discussion that will follow.

Axiom 1: Condition of constant volume—This axiom states that the volume of a body subjected to plastic deformation remains constant, that is, the volume before plastic deformation is equal to the volume after plastic deformation.

Axiom 2: Principle of minimum perimeter—The principle states that any prismatic or cylindrical cross section after plastic deformation tends to acquire a shape that has minimum perimeter, that is, ultimately every cross section tends to acquire a circular profile after plastic deformation.

Now consider the process of chip formation based on the single-shear plane model (Figure 2.7), whereby a layer of the workpiece material of dimensions $a \times b \times l$ is converted to a chip of dimensions $a_c \times b_c \times l_c$ (Figure 2.14).

This is subject to the following four assumptions:

- (i) The chip formed is continuous.
- (ii) b is much greater than a .
- (iii) The cutting is orthogonal, that is, the cutting edge is perpendicular to the direction of feed.
- (iv) The width of the cutting edge is greater than b .

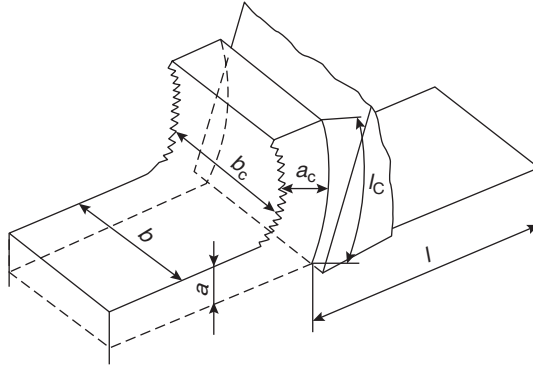


Figure 2.14 Schematic depicting the parameters of undeformed chip and chip in orthogonal machining

The cross section of the undeformed chip will be a narrow rectangle of sides $a \times b$, as it is assumed that b is much greater than a , which is actually the case in most metal cutting operations. When axiom 2 is applied to this section, it follows that after plastic deformation the narrow rectangle will tend to acquire a shape closer to a square and finally to a circle. This implies that as a result of plastic deformation, the side b of the section will remain unchanged, that is, $b = b_c$, whereas the side a will increase to a_c . Now applying axiom 1 of constant volume to this case, we get

$$a \times b \times l = a_c \times b_c \times l_c$$

But since $b = b_c$,

$$a \times l = a_c \times l_c$$

i.e.

$$\frac{a_c}{a} = \frac{l}{l_c} = \xi$$

Obviously, as $a_c > a$, the chip length $l_c < l$.

Coefficient ξ is known as chip reduction coefficient. It is a measure of the degree of plastic deformation in the chip and its value may typically vary between 1.5 and 4.0, but it may go as high as 8.0 for extremely tough cutting conditions. In general, a smaller value of ξ is indicative of the ease of plastic deformation in chip formation, and hence associated with less energy consumption for the cutting process.

Chip reduction ξ is determined experimentally by the slotted pipe test in case of good continuous chips. For performing this test, a narrow slot is cut along the length of a pipe of diameter D . The pipe is clamped in a lathe chuck and is turned by a tool with $\phi = 90^\circ$ and length of the cutting edge greater than the pipe thickness at a particular value of feed s as shown in Figure 2.15(a). Due to discontinuity created by the slot, ring-shaped chips will be formed in the turning operation as shown in Figure 2.15(b).

The thickness of the chip is measured by a micrometer and its length along the perimeter with the help of a thread and scale. This will give us the values of a_c and l_c , respectively. As per axiom 1, $b = b_c =$ pipe thickness. The parameters of the undeformed chip are known, being $a = s$ and $l = \pi D$.

Hence, ξ is found as the ratio of $\frac{a_c}{a}$ or $\frac{l}{l_c}$.

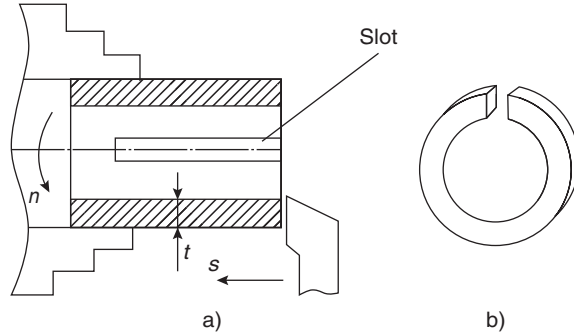


Figure 2.15 Schematic of slotted pipe test for determination of chip reduction coefficient

If it is not possible to obtain a good continuous chip in the shape of a full ring under the selected cutting conditions (v, s, t) or due to limited ductility of the workpiece material, then ξ is determined from orthogonal turning of a nonslotted pipe as follows:

- (i) A small straight piece of length 5–6 mm is cut out from the chip and its length l_c is accurately measured.
- (ii) This piece is weighed to find its weight W .
- (iii) The chip cross-section area is found from the relation $A_c = \frac{W}{\gamma l_c}$, where γ is the specific weight of the chip material.
- (iv) Undeformed chip area is found as per Eqn. (2.3b) as $A = st$.
- (v) Chip reduction coefficient is determined as follows:

$$\xi = \frac{A_c}{A} = \frac{W}{\gamma l_c st}$$

2.3.1 Shear Angle

The angle that the shear plane makes with the direction of feed is known as shear angle and is denoted as β . From Figure 2.7, it can be noted that

$$\sin \beta = \frac{a}{OA}$$

In $\triangle AOB$, Angle $AOB = 90 + \gamma - \beta$ and

$$\sin (90 + \gamma - \beta) = \frac{AB}{OA} = \frac{a_c}{OA}$$

Therefore,

$$\frac{a_c/OA}{a/OA} = \frac{a_c}{a} = \xi = \frac{\sin(90 + \gamma - \beta)}{\sin \beta} = \frac{\sin\{90 - (\beta - \gamma)\}}{\sin \beta}$$

Hence,

$$\xi = \frac{\cos(\beta - \gamma)}{\sin \beta} \tag{2.40}$$

On expanding the right-hand side of the above expression, we get the following:

$$\begin{aligned}\frac{\cos \beta \cos \gamma + \sin \beta \sin \gamma}{\sin \beta} &= \xi \\ \cot \beta \cos \gamma &= \xi - \sin \gamma \\ \cot \beta &= \frac{\xi - \sin \gamma}{\cos \gamma} \\ \beta &= \tan^{-1} \frac{\cos \gamma}{\xi - \sin \gamma}\end{aligned}\quad (2.41)$$

Example 2.2

In turning of a slotted pipe of diameter 90 mm, the chip produced was 125-mm long. If $\phi = 90^\circ$, $\gamma = 20^\circ$, and $s = 0.2$ mm/rev determine the length of the shear plane.

Length of undeformed chip = $\pi D = \pi \times 90$ mm

Length of the chip produced = 125 mm

Hence, chip reduction coefficient $\xi = \frac{\pi \times 90}{125} = 2.262$

Shear angle $\beta = \tan^{-1} \left(\frac{\cos \gamma_0}{\xi - \sin \gamma_0} \right) = \tan^{-1} \left(\frac{\cos 20}{2.262 - \sin 20} \right) = 26.08^\circ$

Hence length of shear plane $a_s = \frac{a_0}{\sin \beta} = \frac{0.2 \times \sin 90}{\sin 26.08} = 0.45$ mm

2.3.2 Shear Strain

In the idealized simplified model of chip formation discussed in Section 2.1 (Figure 2.2), a continuous chip is considered to be formed by stacking of a succession of elements. This process is illustrated in Figure 2.16(a), where an undeformed element $ABCD$ has been shown to be deformed into $ADPQ$ and aligned along the tool face. In a similar manner, the next undeformed element $RADS$ will be deformed and stacked underneath $ADPQ$, pushing the latter up. A series of such deformed elements stacked one over the other will comprise the chip. For the purpose of analysis, consider the side DC of the undeformed element, which upon shearing occupies the position DP (Figure 2.16b) and in this process undergoes shear strain.

$$\varepsilon = \frac{CP}{DM} = \frac{CM}{DM} + \frac{PM}{DM}$$

where DM represents the normal drawn from point D on CP .

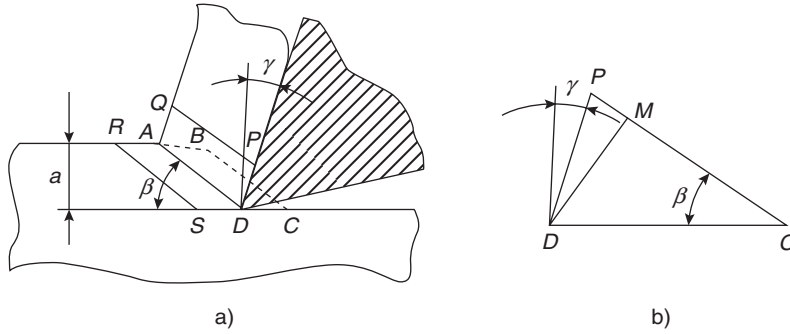


Figure 2.16 Schematic for determination of shear strain

In $\triangle DCM$, angle $DCM = \beta$; therefore, $\frac{CM}{DM} = \cot \beta$.

In $\triangle DPM$, angle $PDM = 90 - \gamma - (90 - \beta) = \beta - \gamma$.

Therefore, $\frac{PM}{DM} = \tan(\beta - \gamma)$

Hence,

$$\begin{aligned} \epsilon &= \cot \beta + \tan(\beta - \gamma) \\ &= \cot \beta + \frac{\tan \beta - \tan \gamma}{1 + \tan \beta \tan \gamma} \end{aligned} \tag{2.42}$$

Substituting for $\cot \beta$ and $\tan \beta$ in the expressions derived above, we get

$$\begin{aligned} \epsilon &= \frac{\xi - \sin \gamma}{\cos \gamma} + \frac{\frac{\cos \gamma}{\xi - \sin \gamma} - \tan \gamma}{1 + \frac{\cos \gamma}{\xi - \sin \gamma} \tan \gamma} \\ &= \frac{\xi - \sin \gamma}{\cos \gamma} + \frac{\cos^2 \gamma - \xi \sin \gamma + \sin^2 \gamma}{(\xi - \sin \gamma) \cos \gamma + \cos \gamma \sin \gamma} \\ &= \frac{\xi - \sin \gamma}{\cos \gamma} + \frac{1 - \xi \sin \gamma}{\xi \cos \gamma} \end{aligned}$$

Hence,

$$\epsilon = \frac{\xi^2 - 2\xi \sin \gamma + 1}{\xi \cos \gamma} \tag{2.43}$$

The value of ξ at which shear strain is minimum is obtained from the condition $\frac{\partial \epsilon}{\partial \xi} = 0$, that is,

$$\frac{\partial \epsilon}{\partial \xi} = \frac{\partial}{\partial \xi} \left\{ \frac{\xi^2 - 2\xi \sin \gamma + 1}{\xi \cos \gamma} \right\} = 0$$

$$\frac{\xi \cos \gamma (2\xi - 2 \sin \gamma) - (\xi^2 - 2\xi \sin \gamma + 1) \cos \gamma}{\xi^2 \cos^2 \gamma} = 0$$

$$\frac{(\xi^2 - 1) \cos \gamma}{\xi^2 \cos^2 \gamma} = 0$$

$$\xi^2 - 1 = 0$$

i.e., $\xi = \pm 1$

A negative value of ξ is theoretically not possible; hence, the unique correct value is $\xi = 1$, which implies that $a = a_c$ and $l = l_c$ and that the chip has been formed without any plastic deformation. Substituting this value of $\xi = 1$ in Eqn. (2.40), we get

$$\frac{\cos(\beta - \gamma)}{\sin \beta} = 1$$

$$\sin \beta = \cos(\beta - \gamma) = \sin \left[\frac{\pi}{2} - (\beta - \gamma) \right]$$

$$\beta = \frac{\pi}{2} - \beta + \gamma$$

Hence,

$$\beta = \frac{\pi}{4} + \frac{\gamma}{2}$$

Example 2.3

A tool of nomenclature 0, 10, 6, 8, 75, 1 in the machine tool reference system is used for machining at $s = 0.2$ mm/rev, $t = 2$ mm, and $v = 140$ m/min. The chip produced was 0.36-mm thick. Determine the shear strain.

For the given tool nomenclature in the machine tool reference system, the side cutting-edge angle = 75° . Therefore,

$$\text{Primary cutting-edge angle } \phi = 90 - 75 = 15^\circ$$

In addition, for the given tool nomenclature $\gamma_b = 0$, $\gamma_s = 10^\circ$

Therefore, applying the relation $\tan \gamma_0 = \cos \phi \tan \gamma_b + \sin \phi \tan \gamma_s$,

We obtain

$$\tan \gamma_0 = \cos 15 \tan 0 + \sin 15 \tan 10,$$

Wherefrom $\gamma_0 = 2.61^\circ$

$$\text{Chip reduction coefficient } \xi = \frac{0.36}{0.2 \sin 15^\circ} = 6.954$$

Applying the relation $\varepsilon = \frac{\xi^2 - 2\xi \sin \gamma_0 + 1}{\xi \cos \gamma}$, we find

$$\text{Shear strain } \varepsilon = \frac{(6.954)^2 - 2 \times 6.954 \sin(2.61) + 1}{6.954 \times \cos 2.61} = 7.014$$

Alternately, we can find

$$\beta = \tan^{-1} \left[\frac{\cos \gamma_0}{\xi - \sin \gamma_0} \right] = \tan^{-1} \left[\frac{\cos 2.61}{6.954 - \sin 2.61} \right] = 8.228^\circ$$

Applying the relation $\varepsilon = \cot \beta + \tan(\beta - \gamma_0)$, we find

$$\varepsilon = \cot(8.228) + \tan(8.228 - 2.61) = 7.014$$

2.4 Types of Chips

Depending on the work material and cutting conditions, four types of chips are formed. Discontinuous chips are formed while machining brittle materials. When ductile materials are machined, continuous, partially continuous, and element chips may be formed depending on the ductility of the work material and the cutting conditions. The main difference between the formation of chips in ductile and brittle materials is that in ductile materials there is continuous shearing of the chip ahead of the tool tip without fracture, whereas in brittle materials, a crack initiated ahead of the tool tip propagates almost instantaneously across the chip thickness, causing fracture before any noticeable plastic deformation has taken place.

While discussing the chip formation process in Section 2.1, it was explained that the chip is subjected to primary shear in the vicinity of the shear plane and secondary shear as it flows along the tool face (Figure 2.6). These are referred to as cutting strain (ε_c) and secondary strain (ε_s), respectively. The chip breaks only when the total strain in the chip exceeds the fracture strain (ε_f) of the chip material. With this knowledge, the conditions for formation of various types of chips can now be discussed.

2.4.1 Discontinuous Chips

As mentioned earlier, discontinuous chips are produced in machining of brittle materials. As the chip is produced due to instantaneous fracture immediately on initiation of cutting, it does not slide along the tool face at all and does not experience any secondary strain (Figure 2.17a).

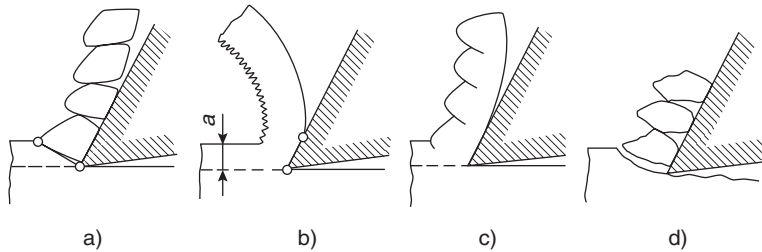


Figure 2.17 Schematic depicting various types of chips: (a) discontinuous chip, (b) continuous chip, (c) partially continuous chip, and (d) element chip

However, the cutting strain itself is so large that it exceeds the fracture strain; that is,

$$\varepsilon_c > \varepsilon_f$$

Discontinuous chips are very small in size and look like metal powder. All factors that tend to increase the cutting force promote the formation of discontinuous chips, for example, brittleness of work material, large undeformed chip thickness, low cutting speed, and small rake angle. Under these conditions, materials that are not brittle but that have relatively poor ductility may also produce discontinuous chips.

2.4.2 Continuous Chips

Continuous chips are produced in machining of ductile materials as successively sheared elements of the work material get stacked one above the other without getting separated (Figure 2.17b). Either no cracks are formed ahead of the tool tip; or even if microcracks are formed, they are effectively incapable of propagating to any noticeable depth. As the continuous chip flows along the tool face, it undergoes secondary strain, but even the addition of this strain to the cutting strain is not enough to cause fracture of the chip; that is,

$$\varepsilon_c + \varepsilon_s < \varepsilon_f$$

If there is no obstacle in the path of the chip, it continues to flow as a ribbon or spiral until it breaks due to its own weight. The inner chip surface in contact with the tool face is smooth on account of friction with the tool face, but the outer surface has the appearance of fine saw teeth, where the “teeth” are the visible ends of the interconnected sheared elements comprising the continuous chip. All factors that tend to decrease the cutting force promote the formation of continuous chips, for example, high ductility of work material, large rake angle, small undeformed chip thickness, high cutting speed, and low frictional resistance at the tool–chip interface due to the use of coolant.

2.4.3 Partially Continuous Chips

Partially continuous chips (Figure 2.17c), also known as arc chips, are formed when the ductility of the work material and the cutting parameters are such that $\varepsilon_c + \varepsilon_s$ is approximately equal to or slightly $> \varepsilon_s$. Under these, continuous cracks do appear ahead of the tool tip, but they are not large enough to propagate across the whole thickness of the chip. The chip therefore consists of loosely jointed arc-shaped elements that appear in the form of prominent saw teeth on the

outer chip surface. As the ductility of the work material decreases (i.e. its strength and hardness increases), a continuous chip may change to a partially continuous chip. The same occurs with reduction of rake angle, increase of feed, reduction of cutting speed, and increase of friction at the tool–chip interface.

2.4.4 Element Chips

Element chips (Figure 2.17d) are produced in machining of materials of relatively poor ductility under such conditions that

$$\varepsilon_c + \varepsilon_s > \varepsilon_f$$

Under conditions of low cutting speed, large feed, and small rake angle, the cutting strain developed in the primary shear zone is substantial, but not sufficient enough on its own to produce cracks large enough to cause rupture of the chip. However, as the chip slides along the tool face, the secondary strain gets added to the cutting strain, and the two together exceed the fracture strain causing the chip to fracture. Unlike discontinuous chips, the element chips are basically produced by the shearing mechanism, and the chips consist of identical segments that are either very loosely connected to each other or not connected at all. Machining under conditions that produce element chip is not desirable because every time an elemental chip segment breaks, it produces an impact on the cutting tool that in turn adversely affects the surface finish of the machined component.

2.5 Chip Flow Control and Chip Breaking

A long continuous chip can get entangled with the cutting tool, workpiece, and machine tool elements and can damage them. If a coolant is being used, the chip may interfere with the free flow of coolant into the cutting zone. A chip flowing outward may pose hazard to the operator. Therefore, when long continuous chips are produced in a machining operation, they can sometimes become unmanageable, and it is extremely important to know how to control the direction of chip flow and the size of the chips. Before these aspects are discussed, it is necessary to understand the phenomenon of chip curling that is a characteristic feature of most continuous chips.

Chip curling (Figure 2.18) occurs due to deformation of the layer of chip adjacent to the tool face. It is assisted by uneven cooling across the chip section because the outer free surface of the chip that is exposed to air is cooled more than the inner surface that is in contact with the hot tool face. Consequently, the inner chip surface shrinks more, causing the chip to curl. Here, it may be noted that the chip starts to curl away only at the end of the tool–chip contact length and then maintains a constant radius of curvature.

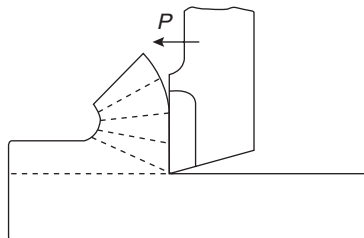


Figure 2.18 Schematic depicting chip curling

Although no reliable method of predicting chip curl radius is available, the knowledge of the effect of some of the factors that influence chip curl radius can be helpful in handling of continuous chips. Briefly, it may be summed up that the chip curvature increases with

- (i) the increase in rake angle
- (ii) the increase in undeformed chip thickness, that is, increase in feed and primary cutting-edge angle
- (iii) the increase in cutting speed
- (iv) the increase in friction at the tool-chip interface, that is, the absence or inadequate supply of coolant

2.5.1 Control of Chip Flow

Consider the turning operation with a tool having cutting-edge inclination angle $\lambda = 0$ and its tip set at the height of the job axis (Figure 2.19). For a given rpm of the job, the cutting speed v_D at the periphery is greater than that at the depth of cut v_{D_0} ; therefore, the chip that initially starts flowing normal to the cutting edge deflects toward the machined surface and begins to move in a direction opposite to that of the feed.

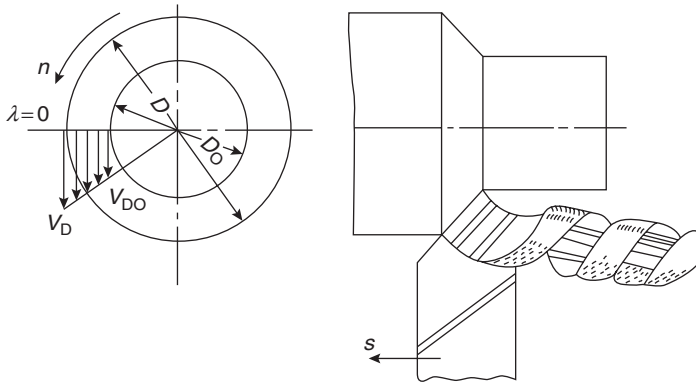


Figure 2.19 Schematic depicting chip flow

Now consider two cases of turning (i) with a tool having $\lambda = 0$, but mounted below the height of the job axis by height h and (ii) a tool with $+\lambda$ and its tip set at the height of the job axis (Figure 2.20a). In this case, the average velocity assumed to be acting at the middle of the length of contact of the cutting edge can be resolved into two components: a component v_x normal to the cutting edge and a component v_s along the cutting edge but directed inward, that is, toward the job center. Because of this direction of v_s , the initial flow of the chip is directed toward the axis of the job and not along the normal to the cutting edge. This, coupled with the natural tendency of the chip to move toward the machined surface as discussed earlier (Figure 2.19), deflects the chip further toward the machined surface and increases the likelihood of the chip damaging the machined surface.

The opposite picture prevails when we consider turning with (i) a tool having $\lambda = 0$, but mounted above the height of the job axis by h and (ii) a tool with $-\lambda$ and its tip at the height of the job axis (Figure 2.20b). Following the same logic as in the preceding case, we find that velocity component

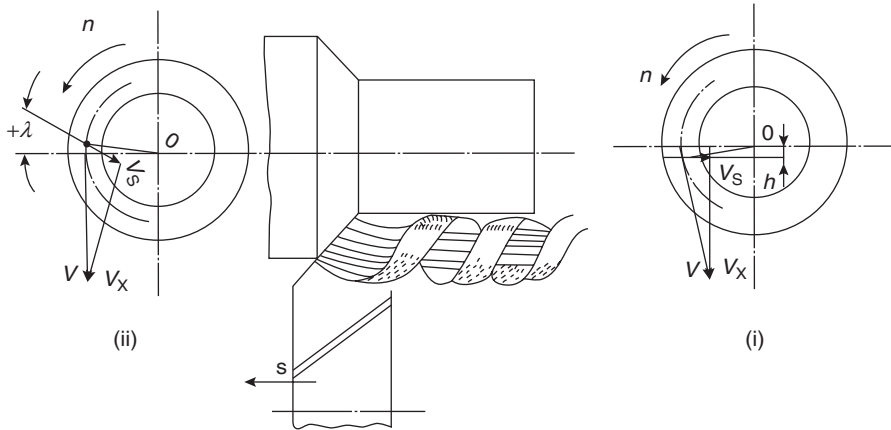


Figure 2.20a Schematic depicting chip flow direction with tool set below the center (i) or tool with $+\lambda$ (ii)

v_s is in this case directed outward, that is, away from the job center; therefore, the initial flow of the chip is directed away from the axis of the job and not along the normal to the cutting edge. This type of chip flow is more likely to pose a hazard to the operator.

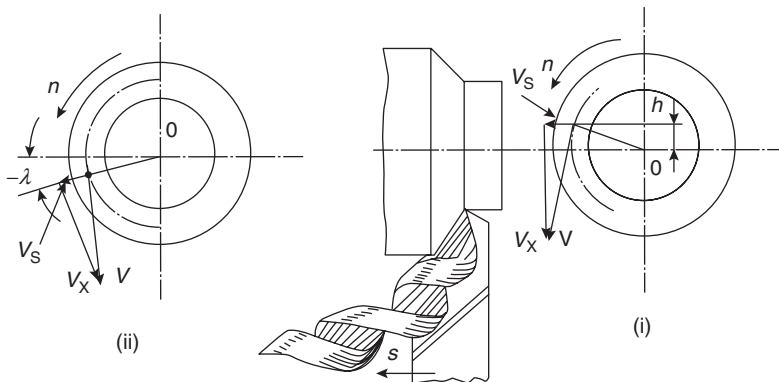


Figure 2.20b Schematic depicting chip flow direction with tool set above the center (i) or tool with $-\lambda$ (ii)

From the above analysis, it follows that one should strive to obtain chip flow as per (Figure 2.20b) for finishing cuts with value of $\lambda = -5$ or so, or by setting the tool above the height of the job axis. However, it should be kept in mind that $+\lambda$ is associated with greater bulk of the tool. Therefore, for rough cuts in which the surface finish of the machined surface is not of serious concern, chip flow as per (Figure 2.20a) may be preferred.

2.5.2 Chip Breaking

Up until a few decades ago, most of the machining was carried out at low-to-moderate cutting speeds. The chips produced under these conditions were heavily curled (small curling radius) and tended to break before they became uncomfortably long. With the advent of cemented carbides,

coated cemented carbides, ceramics, cubic boron nitride (CBN), etc., machining at very high cutting speeds has now become the norm rather than exception in modern machining practice. The chips produced under these conditions are less curled, unmanageably long, and extremely difficult to handle. Given the fact that due to the high productivity of the modern machining operations enormous volumes of chips are produced every hour of machining, the problem of controlling chip flow direction, shape, and size acquires great significance. The measures that can be adopted for controlling chip flow direction have been discussed earlier.

The shape of the continuous chip depends on the cutting conditions. Spiral chips are formed during parting operation and orthogonal turning ($\phi = 90^\circ$, $\lambda = 0$) of a shoulder in the absence of crater wear on the tool face. At very high cutting speeds, the chip ceases to curl and a ribbon chip is formed that can get snarled. These chips are shown in Figure 2.21.

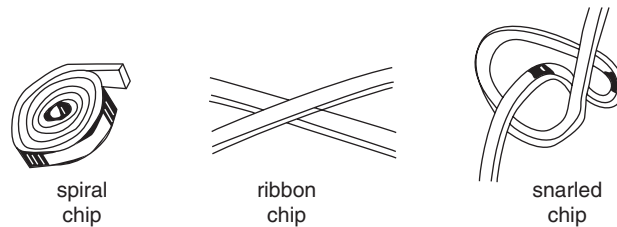


Figure 2.21 Shapes of continuous chips produced in parting and orthogonal turning operations

In the case of oblique cutting ($\phi \neq 90^\circ$, $\lambda \neq 0$), the chips produced may be cylindrical (tubular), conical (helical), and washer type. Cylindrical chips are produced when the undeformed chip thickness is large, but the depth of cut is small, so that the cutting speed does not vary much along the effective length of the cutting edge that is in contact with the workpiece. If there is considerable variation of cutting speed along the cutting edge of the tool as in a drill, then washer type and conical chips may be formed—the former when the undeformed chip thickness is small and the latter when it is large. These chips are shown in Figure 2.22.

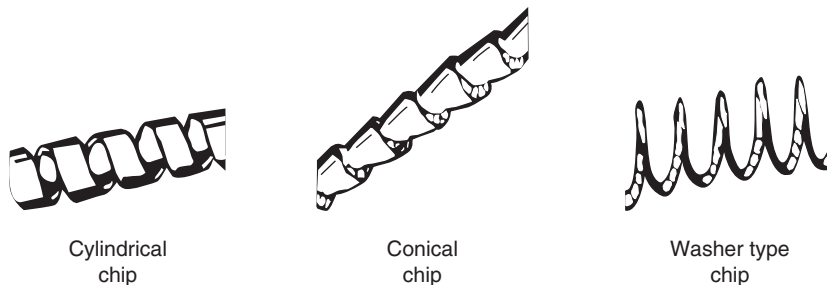


Figure 2.22 Shapes of continuous chips produced in oblique cutting operations

All continuous chips, irrespective of their shape, must be efficiently broken in order to facilitate their handling and disposal. The enormity of this task can be judged by introducing a term called *bulk ratio* (BR), which is expressed as follows:

$$BR = \frac{\text{Total volume of the chips}}{\text{Solid volume from which the chips are produced}}$$

Bulk ratio is approximately 50 for long continuous chips, 15 for tightly wound chips, and 3 for well-broken chips. Obviously, if long continuous chip can be somehow converted to a well-broken chip, their handling and disposal will become considerably easier.

To some extent, chip breaking may be achieved by varying the feed, because increase of feed increases the undeformed chip thickness that is one of the measures of facilitating the transition from a continuous chip to a partially continuous chip. Achieving a similar transition by reducing the cutting speed is not desirable as it will adversely affect the productivity of the machining operation.

Generally, for efficient chip breaking, it is necessary that a chip breaker be used. Chip breakers may be of (i) groove type, (ii) step obstruction type, and (iii) attached obstruction type.

A groove-type breaker is obtained by making a groove of small radius r_g on the tool face as shown in Figure 2.23.

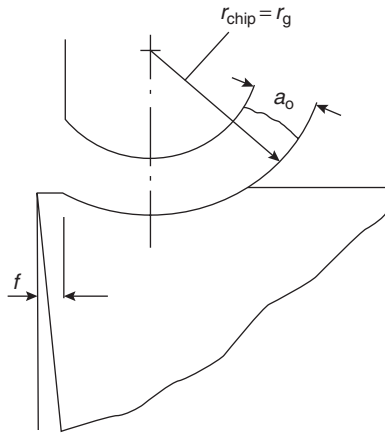


Figure 2.23 Schematic depicting flow of chip conforming to groove on tool face

When the groove is made at a distance f less than the tool–chip contact length C_L , the chip tends to flow into the groove and curl with the adopted radius, that is, $r_{\text{chip}} = r_g$. If this radius is properly selected, then the chip gets tightly wound and gets efficiently broken. If r_g is too large, then tight curling of the chip may not take place and it may fail to break. On the contrary, if r_g is too small, the chip may fail to conform to the groove profile and slide above it, as if the groove did not exist at all. In this case, chip breaking may begin only much later after the groove has been substantially enlarged by crater wear on the tool face. Recommended groove geometry is shown in Figure 2.24 and the associated parameters are as follows:

- $d = 0.2 \text{ mm}$, $m = 1.5\text{--}2.0 \text{ mm}$, $r_g = 0.8\text{--}1.8 \text{ mm}$
- $f = 0.1\text{--}0.2$ less than the feed for $s < 0.6 \text{ mm/rev}$
- $= \text{feed}$ for $s > 0.6 \text{ mm/rev}$
- $K = 0.1\text{--}0.5 \text{ mm}$
- $l = \text{undeformed chip width plus } 1.5\text{--}2.0 \text{ mm}$

A tool with a step obstruction-type chip breaker is shown in Figure 2.25(a). As schematically shown in Figure 2.25(b), the step obstruction should ideally be such that the chip strikes the top edge of the step and breaks. On the one hand, if the step is shorter in height or placed

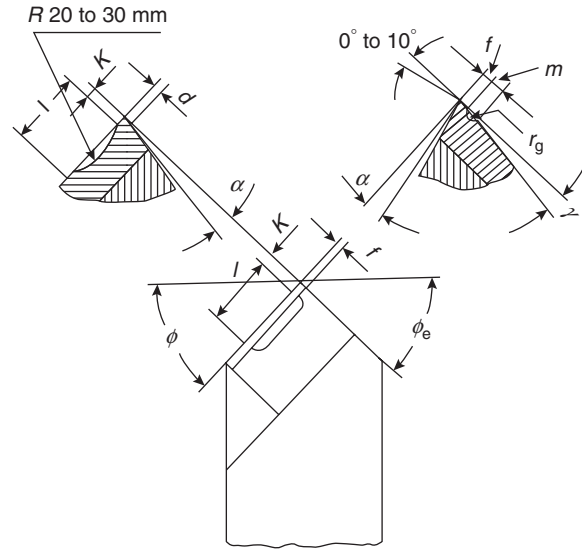


Figure 2.24 Recommended groove geometry

farther than shown in the figure, then no chip breaking will occur. On the other hand, if the step is of greater height or is placed closer than that shown, then the chip will strike the step with considerable impact. The reactive force of the impact will be transmitted back to the workpiece and will adversely affect the finish of the machined surface. It will also impinge on the tool face and aggravate crater wear on the tool face, thus adversely affecting tool life.

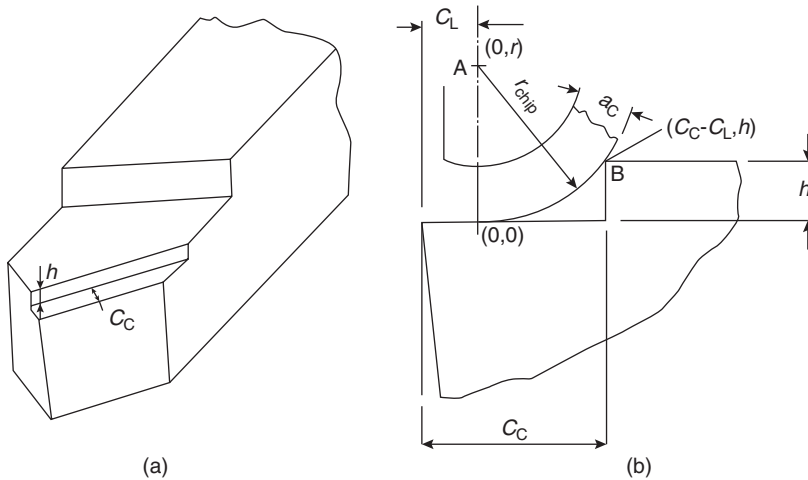


Figure 2.25 Step obstruction-type chip breaker: (a) tool with step obstruction and (b) schematic for determining step parameters

From the geometry of Figure 2.25(b), it can be noted that

$$AB = r_{\text{chip}} = \sqrt{(C_C - C_L)^2 + (h - r_{\text{chip}})^2}$$

where

- r_{chip} = chip curl radius
- C_L = tool–chip contact length
- C_C = length of the step
- h = height of the step

$$\begin{aligned} r_{\text{chip}}^2 &= (C_C - C_L)^2 + (h - r_{\text{chip}})^2 \\ &= (C_C - C_L)^2 + (h^2 - 2hr_{\text{chip}} + r_{\text{chip}}^2) \end{aligned}$$

Hence,

$$r_{\text{chip}} = \frac{(C_C - C_L)^2}{2h} + \frac{h}{2} \tag{2.44}$$

The tool–chip contact length can be found from the following approximate relation:

$$C_L = 2a[\xi(1 - \tan \gamma) + \sec \gamma]$$

However, a simpler relation $\frac{C_L}{a_C} = K$ can be used with a reasonably accurate approximation. For steel $K = 1$, although it may vary, though not significantly, for other materials. Thus, substituting $C_L = a_C$, Eqn. (2.44) may be written as follows:

$$r_{\text{chip}} = \frac{(C_C - a_C)^2}{2h} + \frac{h}{2} \tag{2.45}$$

For given r_{chip} and a_C , the above equation can be used for selecting the step parameters C_C and h . On the contrary, for a tool with a given step, efficient chip breaking can be achieved by controlling r_{chip} with proper selection of the parameters that influence chip curling as discussed with reference to Figure 2.18.

A tool with an attached obstructing-type chip breaker is shown in Figure 2.26(a). This type of chip breaker is common in tools with mechanical clamping of cutting inserts, as the clamping plate itself serves as the chip breaker. The basic principle of chip breaking with this type of chip breaking is the same as that of a step obstruction-type discussed earlier, except that the attached obstruction is inclined and its location is easily adjustable. The attached obstruction-type chip breaker is represented by the simplified schematic of Figure 2.26(b).

It can be noted from Figure 2.26(b) that

$$\begin{aligned} r_{\text{chip}} &= AB \\ AB &= BC \cot \frac{\theta}{2} \\ BC &= C_C - C_L - CD \\ &= C_C - C_L - h \cot \theta \end{aligned}$$

Review Questions

- 2.1** An orthogonal cutting operation is conducted at $t = 0.5$ mm, $v = 2$ m/s. If the chip thickness is 0.75 mm, the chip velocity is
- (a) 1.33 m/s (b) 2 m/s
(c) 2.5 m/s (d) 3 m/s
- 2.2** In a machining operation, the chip reduction coefficient is 3.33 and the rake angle is 10° . What is the value of shear strain?
- (a) 0.31 (b) 0.13
(c) 3.0 (d) 3.34
- 2.3** In a turning operation, a continuous ribbon-like chip is produced in machining
- (1) at high cutting speed (2) at low cutting speed
(3) of brittle material (4) of ductile material
- Which of the following are correct?
- (a) (1) and (3) (b) (1) and (4)
(c) (2) and (3) (d) (2) and (4)
- 2.4** Continuous chips without built-up edge will be produced in machining
- (1) of ductile material (2) at high cutting speed
(3) at small rake angle (4) small undeformed chip thickness
- Which of the following are correct?
- (a) (1), (2), and (4) (b) (1), (2), and (3)
(c) (2), (3), and (4) (d) (1), (3), and (4)
- 2.5** While machining with a tool of rake angle 15° , the shear angle was found to be 45° . The chip reduction coefficient is
- (a) 1.228 (b) 1.282
(c) 1.382 (d) 1.489
- 2.6** In an orthogonal cutting operation, the chip reduction coefficient is 1.33, $v = 60$ m/min and $t = 2.4$ mm, two of the following are correct:
- (1) chip velocity = 45 m/min (2) chip velocity = 80 m/min
(3) chip thickness = 1.8 mm (4) chip thickness = 3.2 mm
- The correct answers are
- (a) (1) and (3) (b) (1) and (4)
(c) (2) and (3) (d) (2) and (4)
- 2.7** During turning of a mild steel tube with a tool having $\phi = 90^\circ$ and tool of 6° rake angle, the chip reduction coefficient was equal to 3.0. Determine the shear strain.
- 2.8** In machining with a tool having $\phi = 90^\circ$ and $\gamma = 10^\circ$ at $s = 0.2$ mm/rev, the shear angle was found to be 25° . The thickness of the chip is
- (a) $0.2 \frac{\cos 15}{\sin 25}$ (b) $0.2 \frac{\cos 25}{\sin 15}$
(c) $0.2 \frac{\cos 25}{\sin 25}$ (d) $0.2 \frac{\sin 25}{\cos 15}$

- 2.9** A bar of diameter 75 mm is reduced to 73 mm by turning with a tool having $\phi = 90^\circ$ and $\gamma = 15^\circ$. If the length of the chip produced is 73.9 mm, what is the shear angle?
- 2.10** A plane milling operation is carried out by a straight teeth 40 mm diameter cutter of 10 teeth at 60 rpm at a feed of 30 mm/min. Determine the average undeformed chip thickness if depth of cut is 1.0 mm.
- 2.11** In orthogonal turning of a pipe with a tool of rake angle 10° at feed of 0.25 mm/rev, the shear angle is 27.75° . The thickness of the chip produced is
- | | |
|--------------|--------------|
| (a) 0.511 mm | (b) 0.528 mm |
| (c) 0.818 mm | (d) 0.846 mm |
- 2.12** In an orthogonal machining operation with a tool of rake angle 15° , the undeformed chip thickness was 0.5 mm and the chip produced was 0.7 mm thick. The shear angle and shear strain, respectively, are
- | | |
|---------------------------|---------------------------|
| (a) 30.3° and 1.98 | (b) 30.3° and 4.23 |
| (c) 40.2° and 2.97 | (d) 40.2° and 1.65 |
- 2.13** In orthogonal turning of a bar with a tool of rake angle 0° at a feed of 0.24 mm/rev, the chip produced was 0.48 mm thick. What is the shear angle?
- | | |
|-------------------|-------------------|
| (a) 20.56° | (b) 26.56° |
| (c) 30.56° | (d) 36.56° |

3.1 Orthogonal and Oblique Machining

Mechanics of the cutting process deals with the study of force and velocity relationships with a view to determine

- (i) the power requirement of the machine tool for selection of a proper electric motor.
- (ii) the reactions on machine tool elements such as spindle, bed, guide ways, tailstock, etc., as they are basic inputs for their design.
- (iii) the force acting on the cutting tool and jigs and fixtures as it is the basic input for the design of cutting tools and jigs and fixtures.
- (iv) the force acting on the work piece as it affects its deflection, and hence the accuracy of the machined surface.

The undeformed chip presses on the tool with a force R that is the geometrical resultant of the normal and frictional force components acting on the tool face and flank. In the general case of turning, R is represented by its components P_x , P_y , and P_z in the x , y , and z directions, respectively (Figure 3.1). The force component P_x is known as feed force, P_y as radial force and P_z as cutting force, respectively. Here, it may be noted that the x - and y - axis coincide with the direction of axial feed and radial feed, respectively, and lie in the horizontal plane. The z -axis coincides with the direction of velocity vector v and is vertical.

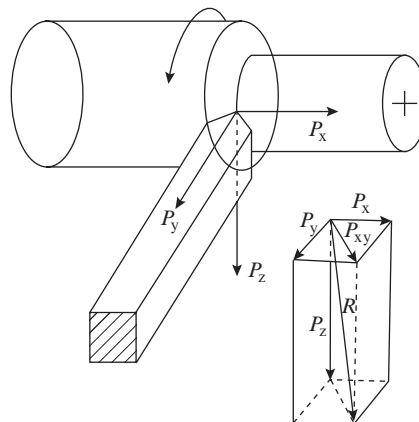


Figure 3.1 Schematic representation of resultant cutting force and its components

In the general case of metal cutting with a wedge, the cutting edge is inclined at an angle λ with respect to the normal to the direction of cutting velocity (Figure 3.2). The chip formed in this case does not flow perpendicular to the cutting edge, but deviates from the normal by an angle approximately equal to λ . This type of cutting is known as oblique cutting. Analysis of oblique cutting as a three-dimensional force process is difficult. The problem is further aggravated by the fact that the direction of chip flow does not coincide with any of the axis of the force system. For theoretical study of the cutting process, the latter can be simplified if we

- (i) eliminate the effect of cutting edge obliquity so that the chip flow occurs perpendicular to the cutting edge.
- (ii) reduce the three-dimensional force system to a two-dimensional force system in the plane perpendicular to the cutting edge.

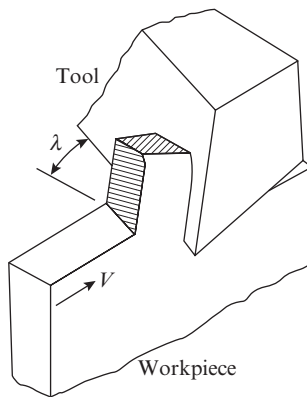


Figure 3.2 Schematic representation of oblique cutting

For the general case of turning, condition (i) is achieved by using a tool with $\lambda = 0$. Condition (ii) requires that P_{xy} , the resultant of P_x and P_y , should be perpendicular to the cutting edge. This is possible only when $P_x = P_y \tan \phi$. (Figure 3.3) In actual practice, it is virtually impossible to manipulate the cutting conditions to obtain the P_x and P_y values that would exactly fit the above relation. Therefore, in order to achieve a practically feasible two-dimensional force system, it is necessary to make angle $\phi = 90^\circ$, as this would eliminate component P_y in case of turning or P_x in case of grooving/parting (Figure 3.4).

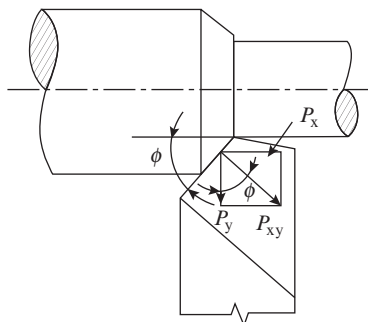


Figure 3.3 Schematic depicting condition of two-dimensional cutting when $\phi \neq 90^\circ$

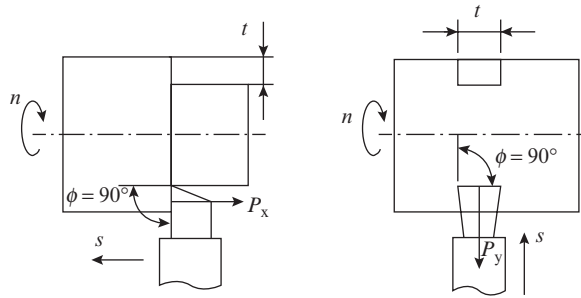


Figure 3.4 Schematic representation of two-dimensional turning and parting when $\phi = 90^\circ$

However, even after making $\lambda = 0$ and $\phi = 90^\circ$, the deviation of resultant cutting force and chip flow from the normal to the cutting edge persists because of the “restriction” effect of the auxiliary cutting edge. The auxiliary cutting edge generally does not play an important part in the cutting process; but although its contribution to the magnitude of the overall cutting force is small, its role in causing deviation of the cutting force and chip flow from the normal to the cutting edge is significant. As is evident from Figure 3.5, on account of force P_a from the auxiliary cutting edge, the resultant force on primary cutting edge is P_{xa} that acts at an angle η to the normal to the cutting edge. Hence, in order to achieve full conformance to conditions (i) and (ii) specified earlier, it is necessary to prevent the auxiliary cutting from participating in the cutting process. Two practical cases in which this is achieved are shown in Figure 3.6, representing machining of a pipe with a tool edge longer than the pipe thickness (Figure 3.6a) and machining of a step with a tool edge wider than the step length (Figure 3.6b). The above two cases are true representatives of what is known as orthogonal cutting, where the resultant cutting force is a two-dimensional system and the resultant cutting force and cutting velocity lie in one plane that is perpendicular to the cutting edge.

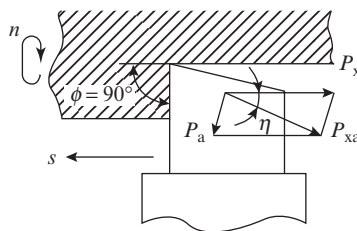


Figure 3.5 Deviation of cutting force and chip flow due to “restriction” effect of auxiliary cutting edge

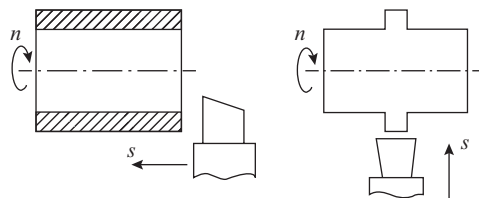


Figure 3.6 Schematics depicting two cases of fully orthogonal cutting

Based on the above discussion, the assumptions inherent in a true orthogonal system may be summarized as follows:

- (i) Cutting-edge inclination angle $\lambda = 0$.
- (ii) Primary cutting-edge angle $\varphi = 90^\circ$.
- (iii) The width of cutting edge of the tool is greater than the undeformed chip width (depth of cut) to prevent the auxiliary cutting edge from participating in the cutting process.

3.2 Force Velocity and Energy Relations in Orthogonal Machining

Consider the case of orthogonal cutting depicted in Figure 3.7. The undeformed chip undergoes elastic and plastic deformation before it separates from the work material in the form of chip. On account of the resistance that the undeformed chip offers to the above deformations a force $P_r = P_{el} + P_{pl}$ is exerted by the chip on the tool face. Similarly a force $P_{fl} = P'_{el} + P'_{pl}$ is exerted by the machined surface on the tool flank. The forces P_r and P_{fl} are directed normal to the tool face and tool flank, respectively. As the chip slides along the tool face and the machined surface advances past the tool flank, the normal forces give rise to frictional force $F_f = \mu (P_{el} + P_{pl})$ and $F_{fl} = \mu'(P'_{el} + P'_{pl})$ on the tool face and flank respectively, where μ and μ' is the coefficient of friction between the chip and tool face and the machined surface and tool flank respectively. The projection of P_r , P_{fl} , F_f and F_{fl} on the horizontal axis gives the component P_h . For chip removal to take place a force R must be applied on the tool such, that its horizontal component P_z (cutting force) is able to overcome P_h . The projection of P_r , P_{fl} , F_f and F_{fl} on the vertical axis gives the component P_v that tends to push the tool away from the work piece. To prevent this, the tool is rigidly clamped. The reaction produced due to this restraint appears as thrust force P_y .

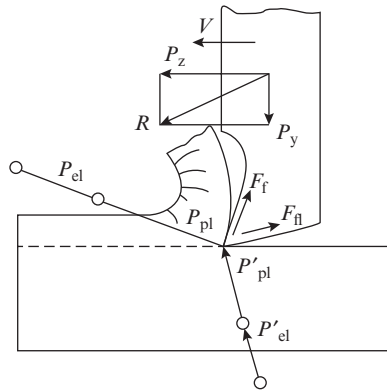


Figure 3.7 Forces acting on the cutting tool in orthogonal machining

The force system discussed above is an accurate representation of the phenomena involved in metal cutting, but it is too complex for the purpose of theoretical analysis. A much simplified system is obtained if it is assumed that:

- (i) the elastic force P_{el} and P'_{el} are negligible in comparison with the forces of plastic deformation P_{pl} and P'_{pl} . This assumption can be safely accepted for metal cutting with formation of continuous chip involving large strains. However, it may not be valid in machining of brittle materials with formation of discontinuous chips because of the small levels of strain at which chip separation takes place.

(ii) the forces on tool flank P_{fl} and F_{fl} are small as compared to forces on the tool face P_f and F_f . Here, it may be pertinent to mention that the forces P_{fl} and F_{fl} arise only if there is a significant amount of tool wear on the flank. If the flank wear is negligible, then the forces acting on the tool flank may be ignored. This indeed would be the case at the start of machining with a new sharp tool.

Bearing in mind the factors defining orthogonal machining in Section 3.1 and the simplifications of the force system discussed above, the assumptions for theoretical analysis of cutting force in orthogonal machining may be summarized as follows:

- (i) Perfectly sharp tool cutting edge
- (ii) Formation of continuous chip
- (iii) Cutting edge inclination angle $\lambda = 0$ and primary cutting edge angle $\phi = 90^\circ$
- (iv) Width of tool edge being greater than the undeformed chip width
- (v) Chip formation taking place according to the simplified idealized, single-plane model (Figure 2.7)
- (vi) Metal cutting occurring under condition of plan strain, that is, no lateral flow of chip along the width and $b = b_c$ (Figure 2.14)

3.2.1 Force Relations

The theoretical analysis of the force system is based on the idea that the chip is a body in a state of equilibrium under the action of force R acting in the shear plane representing the resistance of the work material and an equal and opposite force R' applied on the tool face to overcome the force R and cause the chip to shear in the shear plane (Figure 3.8).

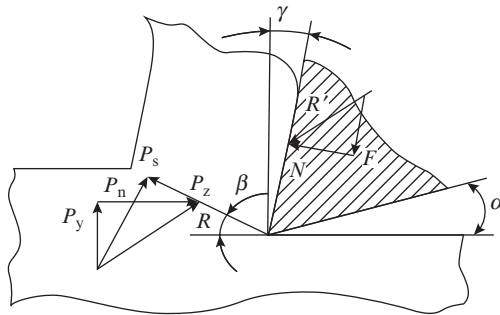


Figure 3.8 Forces acting on the tool face and the shear plane

Force R can be resolved into components P_s and P_n acting along and normal to the shear plane, respectively, and force R' into components F and N representing the frictional and normal force acting on the tool face. Force R can also be resolved into cutting force P_z and thrust force P_y . Since R and R' are equal and opposite forces, we may represent their components as components of a single vector located for convenience at the tool tip. Thus, R and R' that are coincident are made the diameter of a circle. Resultant R can be graphically resolved into pairs of mutually perpendicular forces (P_s, P_n) , (F, N) , and (P_z, P_y) by virtue of the property that for a right-angled triangle with the diameter of a circle as base, the tip of the triangle will lie on the circle. This construction was suggested by V.E. Merchant in 1945 and is popularly known as Merchant's circle (Figure 3.9).

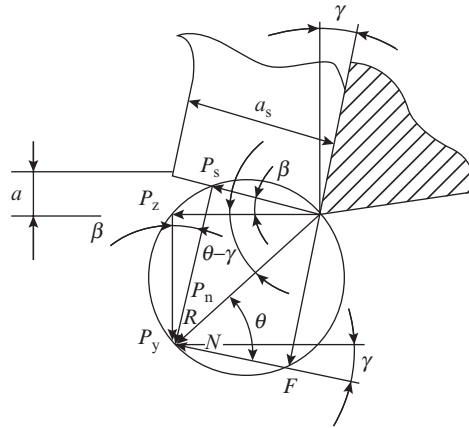


Figure 3.9 Construction of Mohr's circle for orthogonal cutting

From among the quantities shown in Figure 3.9, the following quantities are directly measurable: P_z , P_y , a , a_c , γ . With known a_c and a , and bearing in mind that $\xi = \frac{a_c}{a}$, shear angle β can be calculated from Eqn. (2.39).

The rest of the quantities can be represented in terms of the above known parameters with the help of simple geometrical constructions Figures 3.10(a) and 3.10(b) in which the firm lines show the relevant portion lifted from Merchant's circle and the dotted lines indicate the additional constructs necessary for deriving the relations.

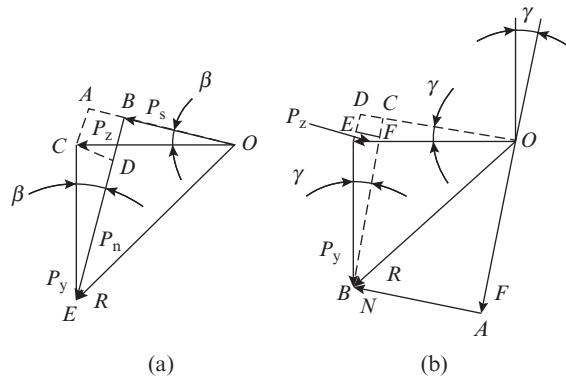


Figure 3.10 Graphic constructions for determining (a) force components in the shear plane (b) force components on the tool face

The force component P_s and P_n acting in the shear plane are found from Figure 3.10(a), where it can be noted that

$$P_s = OA - AB = OA - CD$$

$$P_s = P_z \cos \beta - P_y \sin \beta \quad (3.1)$$

$$P_n = ED + DB = ED + AC$$

$$P_n = P_y \cos \beta + P_z \sin \beta \quad (3.2)$$

The force components F and N acting on the tool face are found from Figure 3.10(b), where it can be noted that

$$F = OA = BC = BF + CF = BF + ED$$

$$F = P_y \cos \gamma + P_z \sin \gamma \tag{3.3}$$

$$N = AB = OC = OD - DC = OD - EF$$

$$N = P_z \cos \gamma - P_y \sin \gamma \tag{3.4}$$

The coefficient of friction between the chip and tool face can be found from the following relation (see Figure 3.9):

$$\mu = \tan \theta = \frac{F}{N} = \frac{P_z \sin \gamma + P_y \cos \gamma}{P_z \cos \gamma - P_y \sin \gamma} \tag{3.5}$$

where

θ is the mean angle of friction between the chip and the tool face.

It can be noted from Figure (3.9) that

$$\frac{a}{a_s} = \sin \beta$$

In view of the absence of lateral flow $b = b_s$,

Hence,

$$\frac{a}{a_s} = \sin \beta$$

Therefore,

$$A_s = \frac{A}{\sin \beta} \tag{3.6}$$

where

A = undeformed chip area

A_s = area of the shear plane

The mean stress on the shear plane, known as dynamic shear stress is now found as follows:

$$\tau_s = \frac{P_s}{A_s} = \frac{P_z \cos \beta - P_y \sin \beta}{\frac{A}{\sin \beta}}$$

$$\tau_s = \frac{P_z \sin \beta \cos \beta - P_y \sin^2 \beta}{a.b} \tag{3.7}$$

Example 3.1

During orthogonal machining of a pipe with a 6° rake angle tool at $v = 20$ m/min, the following data were recorded: $\xi = 3.05$, friction angle $\theta = 35^\circ$, $N = 1000$ N. Determine P_x and P_z .

Friction force $F = \mu N = \tan 35^\circ \times 1000 = 700.2$ N

Applying the relations for friction and normal force at the tool face, we have

$$\begin{aligned} P_z \cos 6^\circ - P_x \sin 6^\circ &= 1000 \\ P_x \cos 6^\circ + P_z \sin 6^\circ &= 700.2 \end{aligned}$$

On solving the above equations, we find

$$P_x = 591.85 \text{ N}, \quad P_z = 1067.71 \text{ N}$$

3.2.2 Velocity Relations

The following three velocities are involved in the process of chip formation:

- (i) cutting velocity v_z that is the velocity of the cutting edge relative to the workpiece and directed parallel to P_z
- (ii) chip velocity v_c that is the velocity of the chip relative to the tool face and directed along the tool face
- (iii) shear velocity v_s that is the velocity of the chip relative to the workpiece and directed along the shear plane

As the chip is considered to be a body in equilibrium, the vectors of the three velocities must form a closed velocity diagram as shown in Figure 3.11.

That is,

$$\bar{v}_s = \bar{v}_z + \bar{v}_c$$

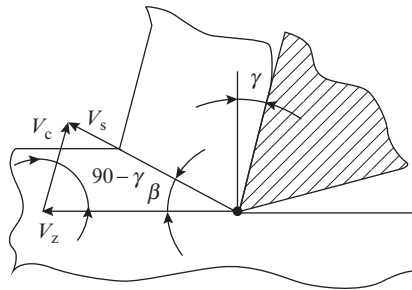


Figure 3.11 Schematic depicting cutting velocity, chip velocity, and shear velocity in orthogonal cutting

Applying the sine rule, it can be noted from Figure 3.11 that

$$\frac{v_z}{\sin[90 - (\beta - \gamma)]} = \frac{v_s}{\sin(90 - \gamma)} = \frac{v_c}{\sin \beta}$$

Expressing v_s in terms of cutting speed v_z , we have

$$v_s = \frac{v_z \sin(90 - \gamma)}{\sin[180 - (90 - \gamma) - \beta]} = \frac{v_z \sin(90 - \gamma)}{\sin[90 - (\beta - \gamma)]} = \frac{v_z \cos \gamma}{\cos(\beta - \gamma)} \quad (3.8)$$

Similarly, expressing v_c in terms of v_z , we have

$$v_c = \frac{v_z \sin \beta}{\sin[90 - (\beta - \gamma)]} = \frac{v_z \sin \beta}{\cos(\beta - \gamma)} \quad (3.9)$$

Reverting to Eqn. (2.38), we obtain

$$v_c = \frac{v_z}{\xi} \quad (3.10)$$

The method of determining ξ from cutting tests was described in Section 2.3. Therefore, for a known value of γ , shear angle β can be found from Eqn. (2.39). Thus, for given cutting speed v_z and rake angle γ , Eqs (3.8)–(3.10) can be used for determining v_c and v_s .

3.2.3 Energy Relations

The energy spent per unit volume of metal removed in an operation is consumed

- (i) in overcoming the shear resistance per unit volume in the shear plane.
- (ii) in overcoming the frictional resistance per unit volume at the tool–chip interface.
- (iii) as surface energy per unit volume in formation of a new cutting surface.
- (iv) as momentum energy per unit volume due to momentum change when metal is converted from undeformed state to deformed state while crossing the shear plane.

The last two factors are negligible as compared to the first two and can therefore be ignored in the calculation of energy balance.

The work done in overcoming shear resistance per unit volume of metal in unit time, i.e. shear energy consumed per unit volume of metal removed is

$$W_s = \frac{P_s v_s}{A v_z} \quad (3.11)$$

Substituting for A from Eqn. (3.6) and for v_s from Eqn. (3.8), we obtain

$$W_s = \frac{P_s}{A_s \sin \beta} \frac{v_z \cos \gamma}{\cos (\beta - \gamma) v_z}$$

$$W_s = \tau_s \frac{\cos \gamma}{\sin \beta \cos (\beta - \gamma)} \quad (3.12)$$

The above expression is written in a modified form to derive an expression for W_s in terms of shear strain:

$$W_s = \tau_s \frac{\cos [\beta - (\beta - \gamma)]}{\sin \beta \cos (\beta - \gamma)}$$

$$= \tau_s \frac{\cos \beta \cos (\beta - \gamma) + \sin \beta \sin (\beta - \gamma)}{\sin \beta \cos (\beta - \gamma)}$$

$$= \tau_s [\cot \beta + \tan (\beta - \gamma)]$$

Reverting to Eqn. (2.40), we get

$$W_s = \tau_s \epsilon \quad (3.13)$$

The work done in overcoming frictional resistance per unit volume of metal in unit time, i.e. frictional energy consumed per unit volume of metal removed is

$$W_f = \frac{Fv_c}{Av_z} \quad (3.14)$$

Substituting for v_c from Eqn. (3.10), we get

$$W_f = \frac{Fv_z}{A\xi v_z} = \frac{F}{A\xi}$$

But we know that $A\xi = A_c$. Hence,

$$W_f = \frac{F}{A_c} \quad (3.15)$$

The energy spent in metal cutting per unit volume of metal removed can be expressed as follows:

$$W_z = \frac{P_z v_z}{Av_z} \quad (3.16)$$

With reference to Figure 3.12, we see that

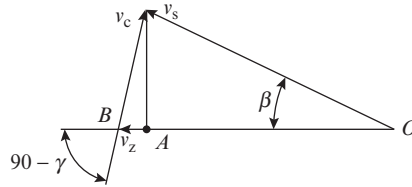


Figure 3.12 Construction of velocity triangle in orthogonal cutting

$$\begin{aligned} v_z &= OA + AB \\ v_z &= v_s \cos \beta + v_c \cos (90 - \gamma) \end{aligned}$$

or

$$v_z = v_s \cos \beta + v_c \sin \gamma \quad (3.17)$$

Substituting Eqn. (3.17) in Eqn. (3.16), we get

$$W_z = \frac{P_z}{A} \left(\frac{v_s}{v_z} \cos \beta + \frac{v_c}{v_z} \sin \gamma \right)$$

Now substituting for $\frac{v_s}{v_z}$ and $\frac{v_c}{v_z}$ from Eqs (3.8) and (3.9), respectively, we obtain

$$W_z = \frac{P_z}{A} \left[\cos \beta \frac{\cos \gamma}{\cos (\beta - \gamma)} + \sin \gamma \frac{\sin \beta}{\cos (\beta - \gamma)} \right]$$

From Merchant's circle (Figure 3.9), it can be that

$$P_z = R \cos (\theta - \gamma)$$

Substituting for P_z the expression for W_z becomes

$$W_z = \frac{R}{A} \left[\frac{\cos \beta \cos \gamma \cos (\theta - \gamma) + \sin \beta \sin \gamma \cos (\theta - \gamma)}{\cos (\beta - \gamma)} \right]$$

On adding and subtracting $\sin \beta \sin \gamma \cos (\theta - \gamma)$ in the numerator, we get

$$\begin{aligned} W_z &= \frac{R}{A} \left[\frac{[\cos \beta \cos \gamma \cos (\theta - \gamma) - \sin \beta \cos \gamma \sin (\theta - \gamma)] + \sin \beta \cos \gamma \sin (\theta - \gamma) + \sin \beta \sin \gamma \cos (\theta - \gamma)}{\cos (\beta - \gamma)} \right] \\ &= \frac{R}{A} \left[\frac{\cos \gamma \cos (\beta + \theta - \gamma) + \sin \beta \cos \gamma \sin (\theta - \gamma)}{\cos (\beta - \gamma)} + \frac{\sin \beta \sin \gamma \cos (\theta - \gamma)}{\cos (\beta - \gamma)} \right] \end{aligned}$$

Again, From Merchant's circle (Figure 3.9), we see that

$$P_s = R \cos (\beta + \theta - \gamma)$$

Substituting for P_s in the above expression, we get

$$W_z = \frac{P_s \cos \gamma}{A \cos (\beta - \gamma)} + \frac{R \sin \beta}{A \cos (\beta - \gamma)} [\cos \gamma \sin (\theta - \gamma) + \sin \gamma \cos (\theta - \gamma)] \quad (3.18)$$

Let us represent W_z as a sum of two factors:

$$W_z = W_{z1} + W_{z2}$$

Now let us consider the first factor on the right hand side of Eqn. (3.18)

$$W_{z1} = \frac{P_s \cos \gamma}{A \cos (\beta - \gamma)}$$

Substituting $A = A_s \sin \beta$ (see Eqn. (3.6)) we get

$$\begin{aligned} W_{z1} &= \frac{P_s \cos \gamma}{A_s \sin \beta \cos (\beta - \gamma)} = \frac{P_s \cos [\beta - (\beta - \gamma)]}{A_s \sin \beta \cos (\beta - \gamma)} \\ &= \tau_s \left[\frac{\cos \beta}{\sin \beta} + \frac{\sin (\beta - \gamma)}{\cos (\beta - \gamma)} \right] \\ &= \tau_s [\cot \beta + \tan (\beta - \gamma)] \end{aligned}$$

On reverting to Eqn. (2.40), we find

$$W_{z1} = \tau_s \varepsilon \quad (3.19)$$

Now let us analyze the second factor on the right-hand side of Eqn. (3.18):

$$W_{z2} = \frac{R \sin \beta}{A \cos (\beta - \gamma)} [\cos \gamma \sin (\theta - \gamma) + \sin \gamma \cos (\theta - \gamma)]$$

$$= \frac{R \sin \beta \sin (\theta - \gamma) \cos \gamma}{A \cos (\beta - \gamma)} + \frac{R \sin \beta \cos (\theta - \gamma) \sin \gamma}{A \cos (\beta - \gamma)}$$

Again from Merchant's circle (Figure 3.9), we note that

$$\begin{aligned} R \cos (\theta - \gamma) &= P_z \\ R \sin (\theta - \gamma) &= P_y \end{aligned}$$

On substituting these values in the expression of W_{z2} , we obtain

$$W_{z2} = \frac{(P_y \cos \gamma + P_z \sin \gamma) \sin \beta}{A \cos (\beta - \gamma)}$$

Substituting $\frac{\sin \beta}{\cos (\beta - \gamma)} = \frac{1}{\xi}$ (see Eqn. 2.38) and

$P_y \cos \gamma + P_z \sin \gamma = F$ (see Eqn. 3.3), we get

$$W_{z2} = \frac{F}{A\xi} = \frac{F}{A_c} \quad (3.20)$$

Hence, the total energy spent in removing unit volume of work material is found as the sum of Eqs (3.19) and (3.20), i.e.

$$W_z = \tau_s \varepsilon + \frac{F}{A_c}$$

Now referring to Eqs (3.13) and (3.15), we see that

$$W_z = W_s + W_f \quad (3.21)$$

In fact, the actual energy spent in metal removal will be slightly more than the W_z value given by Eqn. (3.21) on account of the surface energy and momentum energy factors that were ignored in the above analysis because they are negligibly small. It is also important to note that the energy consumed in overcoming the shear resistance in the shear plane and frictional resistance at the tool-chip interface comes exclusively from the force component P_z . This is why it is considered the main component of the resultant cutting force and often referred as the cutting force. Force component P_y balances the thrust from the shear and frictional forces, whereas component P_x is responsible for overcoming the resistance from the feed mechanism of the machine tool.

Example 3.2

A tool having $\gamma_b = 8^\circ$ and $\theta = 45^\circ$ is used for orthogonal machining. Determine γ_s for orthogonality. If $\xi = 2.75$, $P_z = 1.7$ kN, $P_{xy} = 0.8$ kN, and $v = 100$ m/min, calculate the coefficient of friction and energy consumed in friction per unit volume of metal removed, given that $t = 2$ mm and $s = 0.2$ mm/rev.

The condition for orthogonality is $\lambda = 0$. From the relation $\tan \lambda = \sin \phi \tan \gamma_b - \cos \phi \tan \gamma_s$, at $\lambda = 0$, we obtain

$$\tan \gamma_s = \tan \phi \tan \gamma_b = \tan 45^\circ \times \tan 8^\circ$$

Hence,

$$\gamma_s = 8^\circ$$

The orthogonal rake angle is found from the following relation:

$$\tan \gamma_o = \cos \phi \tan \gamma_b + \sin \phi \tan \gamma_s$$

On substituting for γ_s, γ_b , and ϕ , we get $\gamma_o = 11.24^\circ$.

Coefficient of friction

$$\mu = \frac{F}{N} = \frac{P_{xy} + P_z \tan \gamma_o}{P_z - P_{xy} \tan \gamma_o} = \frac{0.8 + 1.7 \tan 11.24^\circ}{1.7 - 0.8 \tan 11.24^\circ} = 0.738$$

Energy consumed in friction $E_f = Fv_c$. Therefore, the friction energy consumed per unit volume of metal removed will be

$$e_f = \frac{Fv_c}{\text{undeformed chip area} \times \text{cutting speed}} = \frac{Fv_c}{stv}$$

As $F = P_{xy} \cos \gamma_o + P_z \sin \gamma_o$ and $\frac{v_c}{v} = \frac{1}{\xi}$, we get

$$e_f = \frac{0.8 \times \cos 11.24 + 1.7 \sin 11.24}{0.2 \times 2 \times 2.75} = 1.0145 \frac{\text{kN}}{\text{mm}^2}$$

Example 3.3

While turning a carbon steel rod of diameter 160 mm by a cemented carbide tool of geometry 0, 0, 10, 8, 15, 75, 0 in the orthogonal system at $n = 400$ rpm, $s = 0.4$ mm/rev, and $t = 4.0$ mm, the following observations were made: $P_z = 1200$ N, $P_x = 800$ N, and chip thickness = 0.8 mm. Determine friction force and normal force acting on the tool face, shear yield strength of the work material under the given conditions and cutting power consumption in kW.

For the given tool signature $\gamma = 0$, $\phi = 75^\circ$ Hence, the orthogonal force components will be $P_z = 1200$ N and $P_{xy} = P_x \cos (90 - 75) = 800 \cos 15 = 828.22$ N

Applying the relation for friction and normal force on the tool face, we find

$$N = P_z \cos \gamma - P_{xy} \sin \gamma = 1200 \cos 0^\circ - 828.22 \sin 0^\circ = 1200 \text{ N}$$

$$F = P_{xy} \cos \gamma + P_z \sin \gamma = 828.22 \cos 0^\circ + 1200 \sin 0^\circ = 828.22 \text{ N}$$

Shear angle is found as $\beta = \tan^{-1} \left(\frac{\cos \gamma}{\xi - \sin \gamma} \right)$

$$\text{As } \xi = \frac{0.8}{0.32} = 2.5, \beta = \tan^{-1} \left(\frac{\cos 0^\circ}{2.5 - \sin 0^\circ} \right) = 21.18^\circ$$

The shear force in the shear plane is found as follows:

$$\begin{aligned}
 P_s &= P_z \cos \beta - P_{xy} \sin \beta \\
 &= 1200 \cos 21.18^\circ - 828.22 \sin 21.8^\circ = 819.7 \text{ N} \\
 \tau_s &= \frac{P_s}{A_s} = \frac{P_s \sin \beta}{s.t} = \frac{819.7 \sin 21.18^\circ}{0.32 \times 4} = 233.1 \text{ N/mm}^2
 \end{aligned}$$

Cutting power consumed is given by the following expression:

$$\begin{aligned}
 E &= P_z v \\
 v &= \frac{\pi D n}{1000} = \frac{\pi \times 160 \times 400}{60 \times 1000} = 3.35 \text{ m/s}
 \end{aligned}$$

Hence,

$$E = 1200 \times 3.35 = 4020 \text{ W} = 4.02 \text{ kW}$$

Example 3.4

In an orthogonal machining operation with a tool of rake angle 15° , the cutting force and thrust force were measured as 1200 N and 200 N, respectively, under the following cutting conditions: $v = 20 \text{ m/min}$., undeformed chip thickness = 0.5 mm, thickness of chip produced = 0.7 mm. Show that 30 percent of total energy is dissipated due to friction.

$$\text{Chip reduction coefficient } \xi = \frac{0.7}{0.5} = 1.4$$

$$\text{Shear angle } \phi = \tan^{-1} \frac{\cos \gamma}{\xi - \sin \gamma} = \frac{\cos 15^\circ}{1.4 - \sin 15^\circ} = 40.2^\circ$$

$$\begin{aligned}
 \text{Frictional force } F &= P_x \cos \gamma + P_z \sin \gamma \\
 &= 200 \cos 15^\circ + 1200 \sin 15^\circ = 503.8 \text{ N}
 \end{aligned}$$

$$\text{Chip velocity} = v_c = \frac{v}{\xi} = \frac{20}{1.4} = 14.28 \text{ m/min}$$

$$\text{Total power consumed} = P_z v = 1200 \times 20 = 24 \frac{\text{kN.m}}{\text{min}}$$

$$\text{Power consumed due to friction} = F v_c = 503.8 \times 14.28 = 7.2 \frac{\text{kN.m}}{\text{min}}$$

$$\text{Hence, percentage of power consumed in friction} = \frac{7.2}{24} \times 100 = 30\%$$

3.3 Theoretical Determination of Cutting Force

Knowledge of cutting force is necessary for successfully solving many practical problems, such as design of machine tool elements, cutting tools, jigs and fixtures, and analysis of the cutting process. Empirical relations for determination of cutting forces based on experimental studies are plenty, but they all suffer from a disadvantage inherent in all empirical equations—they are valid only for the experimental conditions in which the particular study was conducted.

Theoretical relations for determining cutting force are inherently imprecise because of the large number of assumptions that have to be made to render the cutting process amenable to a reasonably simple analysis. However in the absence of a suitable empirical relation or experimental data, they are useful as a tool for obtaining an idea, though approximate, of the magnitude and direction of the cutting forces for a preliminary design of machine tool elements, cutting tool, etc.

From Merchant's circle (Figure 3.9), it can be noted that

$$P_z = R \cos(\theta - \gamma) \quad (3.22)$$

$$P_y = R \cos(\beta + \theta - \gamma) \quad (3.23)$$

Substituting for R from Eqn. (3.23) in Eqn. (3.22), we obtain

$$\begin{aligned} P_z &= \frac{P_s \cos(\theta - \gamma)}{\cos(\beta + \theta - \gamma)} \\ &= \tau_s A_s \frac{\cos(\theta - \gamma)}{\cos(\beta + \theta - \gamma)} \end{aligned}$$

We know that $A_s = \frac{A}{\sin \beta}$ (Eqn. 3.6) and $A = ab = st$ (see Eqs (2.1) and (2.2)). Therefore, the above expression becomes

$$P_z = \tau_s st \left[\frac{\cos(\theta - \gamma)}{\sin \beta \cos(\beta + \theta - \gamma)} \right] \quad (3.24)$$

Here, $(\theta - \gamma)$ represents the angle that the resultant cutting force makes with the main cutting component P_z and is referred as cutting angle. Denoting $(\theta - \gamma) = \delta$, Eqn. (3.24) may be written as follows:

$$\begin{aligned} P_z &= \tau_s st \frac{\cos \delta}{\sin \beta \cos(\beta + \delta)} \\ P_z &= \tau_s st \frac{\cos[(\beta + \delta) - \delta]}{\sin \beta \cos(\beta + \delta)} \\ &= \tau_s st \cot \beta \tan(\beta + \delta) \end{aligned} \quad (3.25)$$

Cutting angle δ and shear angle β are related to each other. An increase of δ produces in its wake an almost corresponding reduction of β . Based on extensive experimental studies, Zorev established that under the cutting conditions commonly used in machining practice angle $\beta + \delta$ remained practically constant.

Denoting $\beta + \delta = c$ and substituting $\cot \beta = \frac{\xi - \sin \gamma}{\cos \gamma}$ (see Eqn. 2.39), Eqn. (3.25) may be written as follows:

$$P_z = \tau_s s t \left[\frac{\xi - \sin \gamma}{\cos \gamma} + \tan c \right] \quad (3.26)$$

$c = 40^\circ$ for low carbon steels with carbon ≤ 0.15 percent

$c = 46^\circ$ for mild and medium carbon steels with carbon = 0.15–0.5 percent and for low alloyed steels

$c = 50^\circ$ for high alloyed steels

The value of c reduces slightly with increase of rake angle. For instance, for $\gamma > 20^\circ$, c is 4° less than the values given above.

In Eqs (3.24)–(3.26) s , t and γ are known parameters. Therefore, the task of determining P_z from Eqn. (3.26) can be solved by determining ξ and dynamic shear stress τ_s . If Zorev's assumption regarding $\beta + \delta = c$ is ignored, then P_z is to be found from Eqn. (3.24) for which it is necessary to determine

- (i) τ_s
- (ii) the value within the bracketed term

Here, it may be recalled that β can be calculated for known value of γ and experimentally determined value of ξ . Therefore, if a relation correlating β with θ can be established, then it would be possible to estimate the bracketed term. Several such relations, known as shear angle relations have been proposed, based on different approaches and various assumptions,

The method of determination of dynamic shear stress τ_s and description of some of the popular shear angle relations are presented below.

Example 3.5

While machining with a 0, 5, 6, 6, 8, 90, 1 tool (in orthogonal system) at $v = 180$ m/min, $s = 0.2$ mm/rev, and $t = 2.0$ mm, a chip thickness 0.42 mm was formed. If $\tau_s = 40$ kgf/mm², calculate the friction force using the shear angle relation $2\beta + \theta - \gamma = 77^\circ$.

For the given tool signature, $\gamma_0 = 5^\circ$, $\phi = 90^\circ$, Hence

$$\text{Chip reduction coefficient } \xi = \frac{0.4}{0.2 \sin 90^\circ} = 2.1$$

$$\text{Shear angle } \beta = \tan^{-1} \left(\frac{\cos \gamma}{\xi - \sin \gamma} \right) = \tan^{-1} \left(\frac{\cos 5^\circ}{2.1 - \sin 5^\circ} \right) = 26.33^\circ$$

On substituting for β and γ in the shear angle relation $2\beta + \theta - \gamma = 77^\circ$, we get

$$\text{Friction angle } \theta = 77 - 2 \times 26.33 + 5 = 29.33$$

Applying the relations for P_z and P_x , we find

$$P_z = \tau_s \times s \times t \left[\frac{\cos(\theta - \gamma)}{\sin \beta \cos(\beta + \theta - \gamma)} \right]$$

$$= 40 \times 0.2 \times 2 \left[\frac{\cos(29.33 - 5)}{\sin 29.33 \cos(26.33 + 29.33 - 5)} \right] = 47.18 \text{ kgf}$$

$$P_x = \tau_s \times s \times t \left[\frac{\sin(\theta - \gamma)}{\sin \beta \cos(\beta + \theta - \gamma)} \right]$$

$$= 40 \times 0.2 \times 2 \left[\frac{\sin(29.33 - 5)}{\sin 29.33 \cos(26.33 + 29.33 - 5)} \right] = 21.25 \text{ kgf}$$

Substituting these values in the relation

$$F = P_x \cos \gamma + P_z \sin \gamma, \text{ we obtain}$$

$$F = 21.25 \times \cos 5^\circ + 47.18 \times \sin 5^\circ = 25.28 \text{ kgf}$$

3.3.1 Determination of Dynamic Shear Stress

Plastic deformation in the shear plane with formation of continuous chips is characterized by high strain rate and high temperature. They are considered to have opposing effects on the shear yield strength of a material. But since the strain rate and shear zone temperature are both high in metal cutting, they tend to cancel the effect of each other. Another feature of plastic flow in the shear plane is that it occurs at large values of strain, typically more than two. At this value of strain, the capacity of work material to strain harden is largely exhausted; therefore, the dynamic shear stress remains unaffected by the degree of deformation. It would therefore seem that under typical metal cutting conditions, dynamic shear stress may be regarded as constant. This, in fact, is borne out by various experimental studies that have not found any significant effect of cutting speed, feed, depth of cut, and rake angle on the dynamic shear stress. This observation makes it possible to think of treating dynamic shear stress akin to a material constant and look at the possibilities of determining it from mechanical properties obtained from standard mechanical tests.

Bridgman's Relation For relating τ_s with the flow stress obtained from the mechanical test under uniaxial tensile or compressive loading, a basic assumption has to be made that for equal values of strain in cutting and mechanical test, the stresses are also equal.

In case of compressive test, the flow curve is plotted between true stress σ_c and true strain ϵ_c that are found from the following relations:

$$\sigma_c = \frac{P}{A}$$

$$\epsilon_c = l_n \frac{l}{l_0}$$

Where

A = current area of cross section of specimen

l_0 = original length of specimen

l = current length of specimen

If the stress corresponding to cutting strain is σ_{oc} , then assuming that the state of stress in the shear zone is that of simple shear, dynamic shear stress τ_s is found as $\tau_s = \frac{\sigma_{oc}}{\sqrt{3}}$.

In case of tensile test, the conventional stress–strain diagram for large strain cannot be plotted directly from the test data on account of necking. Instead, the flow curve is plotted between the corrected uniaxial tensile stress σ_{ct} and true strain ϵ_t , where σ_{ct} is found from Bridgman's relation given below (Figure 3.13)

$$\sigma_{ct} = \frac{P}{\pi r^2} \left[\frac{1}{1 + 2 \frac{R}{r} \log_e \left(1 + \frac{r}{2R} \right)} \right] \quad (3.27)$$

where

P = axial load

R = profile radius at the neck

r = neck radius

Generally, it is not possible to reliably conduct tensile test up to strain values typical of the cutting process. Therefore, the $\sigma_{ct} = f(\epsilon_t)$ curve has to be extrapolated to the range of metal cutting strain. Here, it is important to remember that in the elastic range, the stress–strain curve is plotted between engineering stress $\sigma = \frac{P}{A_0}$ and engineering strain $e = \frac{\Delta l}{l}$. However, in the plastic range, the curve is plotted between σ_{ct} given by Eqn. (3.37) and $\epsilon_t = l_n \frac{l}{l_0}$. Therefore, while extrapolating the flow curve under tensile loading, considerable error can occur if the difference in the slope of the flow curve in the elastic and plastic ranges is ignored. The extrapolation should be done only based on the gradient in the plastic zone. Again, as in the case of compressive test, having determined σ_{oc} corresponding to the metal cutting strain, the dynamic shear stress is found as follows:

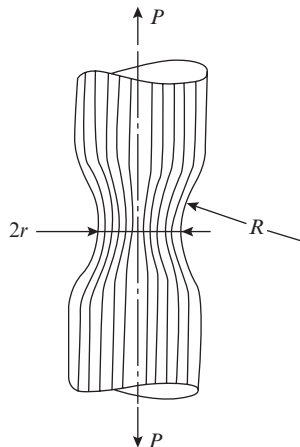


Figure 3.13 Schematic depicting neck parameters in tensile specimen

$$\tau_s = \frac{\sigma_{\text{oct}}}{\sqrt{3}}$$

Zorev's Relation Relation between shear stress τ and true strain ϵ_t determined from uniaxial compression or tensile test is well described by the following relation suggested by Zorev:

$$\tau = K \epsilon_t^m \quad (3.28)$$

where K and m are constants.

If this relation is extrapolated into the region of metal cutting strain, then at $\epsilon_t \approx 2.5$, the shear stress in mechanical test is approximately equal to the shear stress in cutting and the following relation is obtained for dynamic shear stress

$$\tau_s = K(2.5)^m \quad (3.29)$$

Constants K and m are found by plotting the tensile test data in double-log coordinates. For this, the tensile test data are used to plot $\sigma_t = f(\psi)$, where σ_t is true stress and ψ the relative reduction of the cross section, here

$$\sigma_t = \frac{P}{A} \quad \text{and}$$

$$\psi = \frac{A_0 - A}{A_0}$$

where

A_0 = original area of cross section

A = current area of cross section

From the $\sigma_t = f(\psi)$ curve, we determine

$$\tau = \frac{\sigma_t}{2} \quad \text{and} \quad \epsilon_t = 1.5 \ln \frac{1}{1-\psi} \quad \text{at different points.}$$

When this data representing $\tau = K(\epsilon_t)^m$ is plotted in the double-log coordinates, it yields a straight line described by the expression

$$\log \tau = \log K + m \log(\epsilon_t)$$

From which K is found as the ordinate at $\log(\epsilon_t) = 0$, i.e. $\epsilon_t = 1$ and m as the gradient of the line, i.e.

$$m = \frac{\log \tau - \log K}{\log \epsilon_t}.$$

The quantity $\tau_s = K(2.5)^m$ is often denoted as $K_{2.5}$ for the sake of brevity. Zorev also proposed the following relation for determining the dynamic shear stress directly from the mechanical properties of the work material without conducting any tensile test specifically for this purpose

$$\tau_s = K_{2.5} = \frac{0.6\sigma_u}{1-1.7\psi_u} \quad (3.30)$$

where

σ_u = ultimate strength of the work material

$\psi = \frac{A_o - A_u}{A_o}$ is the relative reduction of cross section at rupture, wherein A_o and A_u represent

the original area of cross section and the area of the rupture section, respectively.

If the value of ψ_u is not known, then τ_s can be found from the following empirical relations:

$\tau_s = \sigma_u$ for annealed structural steels and austenitic steels

$\tau_s = 0.9 \sigma_u$ for normalized carbon steels and alloyed steels

$\tau_s = 0.8 \sigma_u$ for hardened steel

Rosenberg and Eremín's Relation Based on analysis of the indentation process similar to the one used in determining the hardness of materials and extensive experimental studies, Rosenberg and Eremín proposed the following relation for determining τ_s :

$$\tau_s = k(BHN) \quad (3.31)$$

where BHN represents the Brinell's hardness of the work piece material in kg/mm²

$k = 0.185$ for ductile materials, e.g. steel

$k = 0.175$ for brittle materials, e.g. cast iron

3.3.2 Shear Angle Relations

As mentioned earlier, expressions correlating shear angle β and friction angle θ are required for theoretical determination of cutting force P_z . Realizing the importance of these relations, several researchers directed their attention on this task. As successive researchers strived for higher precision, the expressions became increasingly complex. Some of the early simple relations only are described here as befitting the scope of this text book, but a large array of expressions is summarized in a table at the end of this section.

Ernst and Merchant's Shear Angle Relation Ernst and Merchant assumed that the dynamic shear stress is a true property of the work material, hence it may be treated as a material constant i.e. $\tau_s = C$. With this assumption Eqn. (3.24) may be written as follows:

$$P_z = Cst \left[\frac{\cos(\theta - \gamma)}{\sin \beta \cos(\beta + \theta - \gamma)} \right] \quad (3.32)$$

Ernst and Merchant further assumed that the minimum energy principle was applicable to metal cutting, implying that shear angle β would adjust itself to a minimum energy condition, i.e. P_z

would be minimum when $\frac{dP_z}{d\beta} = 0$. On differentiating the above expression, we get

$$\frac{dP_z}{d\beta} = Cst \left[\frac{-\cos(\theta - \gamma) \{-\sin \beta \sin(\beta + \theta - \gamma) + \cos \beta \cos(\beta + \theta - \gamma)\}}{\sin^2 \beta \cos^2(\beta + \theta - \gamma)} \right] = 0$$

Hence,

$$\cos \beta \cos(\beta + \theta - \gamma) - \sin \beta \sin(\beta + \theta - \gamma) = 0$$

or

$$\cos[\beta + (\beta + \theta - \gamma)] = 0$$

$$\cos(2\beta + \theta - \gamma) = 0$$

$$2\beta + \theta - \gamma = \frac{\pi}{2} \quad (3.33)$$

This is Ernst and Merchant's shear angle relation. On substituting for θ from Eqn. (3.33) in Eqn. (3.32), we get

$$\begin{aligned} P_z &= Cst \left[\frac{\cos(\frac{\pi}{2} - 2\beta)}{\sin \beta \cos(\frac{\pi}{2} - \beta)} \right] \\ &= Cst \frac{\sin 2\beta}{\sin \beta} \\ P_z &= 2Cst \cot \beta \end{aligned} \quad (3.34)$$

And on substituting for $\cot \beta$ from Eqn. (2.39), the final expression for P_z is obtained as follows:

$$P_z = 2Cst \left(\frac{\xi - \sin \gamma}{\cos \gamma} \right) \quad (3.35)$$

Example 3.6

In orthogonal turning of a workpiece of shear strength 250 MPa with a tool of rake angle 7° at $v = 180$ m/min, $t = 3$ mm, and feed of 0.2 mm/rev, the chip produced was 0.5 mm thick. Applying Merchant's shear angle relationship determine the shear angle, shear force, cutting force, and radial force.

$$\text{Chip reduction coefficient } \xi = \frac{0.5}{0.2} = 2.5$$

$$\text{Shear angle } \beta = \tan^{-1} \frac{\cos \gamma}{\xi - \sin \gamma} = \tan^{-1} \frac{\cos 7^\circ}{2.5 - \sin 7^\circ} = 28^\circ$$

Applying Merchant's shear angle relation, we find

$$\text{Friction angle } \theta = 90 - 2\beta + \gamma = 90 - 2 \times 28 + 7^\circ = 41^\circ$$

$$\text{Area of shear plane } A_s = \frac{a \times b}{\sin \beta} = \frac{s \times t}{\sin \beta} = \frac{0.2 \times 3}{\sin 28^\circ}$$

$$\text{Hence, shear force } P_s = \tau_s A_s = \frac{250 \times 3 \times 0.2}{\sin 28^\circ} = 319.5 \text{ N}$$

We also know that

$$P_z = P_s \frac{\cos(\theta - \gamma)}{\cos(\beta + \theta - \gamma)}$$

Therefore,

$$P_z = \frac{319.5 \cos(41 - 7)}{\cos(28 + 41 - 7)} = 565.08 \text{ N}$$

$$\text{Radial force } P_y = P_z \tan(\theta - \gamma) = 565.08 \tan(41 - 7) = 381.55 \text{ N}$$

Merchant's Second Shear Angle Relation Experimental studies did not fully validate Eqn. (3.34), and it was observed that Ernst and Merchant's shear angle relation provided upper bound solution. The discrepancy could be attributed to two main sources:

- (i) inadequacy of the minimum energy hypotheses, when applied to non conservative processes, such as metal cutting
- (ii) inadequacy of the hypothesis of constant dynamic shear stress, because it was observed that the flow stress in the shear plane increased with the presence of a normal stress in this plane (Figure 3.14)

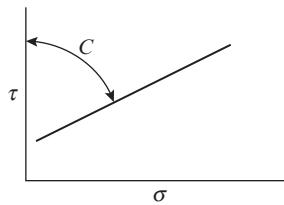


Figure 3.14 Relation between the flow stress in shear plane and normal stress

Merchant addressed the second of the two short comings in a new shear angle relation. He represented the behavior represented in Figure 3.14 in the form of the relation

$$\tau_s = \tau_o + K \sigma_n \quad (3.36)$$

Where K is a material constant and σ_n is normal stress in the shear plane.

From Merchant's circle (Figure 3.9), it can be noted that

$$P_n = P_s \tan(\beta + \theta - \gamma)$$

Dividing both sides of the equation by the shear plane area A_s , we obtain

$$\sigma_n = \tau_s \tan(\beta + \theta - \gamma)$$

Substituting the above expression in Eqn. (3.36), we obtain

$$\tau_s = \tau_o + K \tau_s \tan(\beta + \theta - \gamma)$$

That is,

$$\tau_s = \frac{\tau_o}{1 - K \tan(\beta + \theta - \gamma)}$$

Hence, Eqn. (3.24) for P_z may be written as follows:

$$P_z = st \frac{\tau_o \cos(\theta - \gamma)}{[1 - K \tan(\beta + \theta - \gamma)] \sin \beta \cos(\beta + \theta - \gamma)} \quad (3.37)$$

Again, applying the minimum energy principle, we conclude that for P_z to be minimum, the denominator of Eqn. (3.37) should be maximum, i.e. $\frac{d}{d\beta} (\text{denominator}) = 0$

Denoting

$$\begin{aligned} D &= [1 - K \tan(\beta + \theta - \gamma)] \sin \beta \cos(\beta + \theta - \gamma) \\ &= \sin \beta \cos(\beta + \theta - \gamma) - K \sin \beta \sin(\beta + \theta - \gamma) \end{aligned}$$

$$\frac{dD}{d\beta} = \cos \beta \cos(\beta + \theta - \gamma) - \sin \beta \sin(\beta + \theta - \gamma) - K [\sin \beta \cos(\beta + \theta - \gamma) + \cos \beta \sin(\beta + \theta - \gamma)] = 0$$

$$\cos(\beta + \beta + \theta - \gamma) - K \sin(\beta + \beta + \theta - \gamma) = 0$$

$$\cos(2\beta + \theta - \gamma) = K \sin(2\beta + \theta - \gamma)$$

$$\cot(2\beta + \theta - \gamma) = K$$

$$2\beta + \theta - \gamma = \cot^{-1} K = C \quad (3.38)$$

This is Merchant's second shear angle relation. Here C is known as machining constant. In fact, it is represented by the angle that the $\tau = f(\sigma)$ line makes with the τ -axis (see Figure 3.14). Its value is less than $\frac{\pi}{2}$ and varies between 70° for low carbon steel to about 80° for stainless steel.

Obviously, When $C = \frac{\pi}{2}$, Merchant's second shear angle relation coincides with the first relation of Ernst and Merchant.

On substituting for θ from Eqn. (3.38) in Eqn. (3.24), we obtain

$$\begin{aligned} P_z &= \tau_s st \frac{\cos(C - 2\beta)}{\sin \beta \cos(C - \beta)} \\ &= \tau_s st \frac{\cos[(C - \beta) - \beta]}{\sin \beta \cos(C - \beta)} \\ &= \tau_s st \frac{\cos(C - \beta) \cos \beta + \sin(C - \beta) \sin \beta}{\sin \beta \cos(C - \beta)} \end{aligned}$$

$$P_z = \tau_s st [\tan \beta (C - \beta) + \cot \beta] \quad (3.39)$$

On substituting for $\tan \beta$ from Eqn. (2.39), we obtain

$$P_z = \tau_s st \left[\frac{\xi - \sin \gamma}{\cos \gamma} + \tan \left\{ C - \tan^{-1} \frac{\cos \gamma}{\xi - \sin \gamma} \right\} \right] \quad (3.40)$$

Kronenberg's Shear Angle Relation In order to apply Merchant's second shear angle relation, it is necessary to plot $\tau_s = f(\sigma_n)$ curve and for this purpose it is necessary to measure cutting force components from which P_s and P_n may be calculated using Eqs (3.1) and (3.2). This goes contrary to the basic idea of shear relations as a tool of theoretically determining cutting force without taking recourse to its measurement. This objective can be met if a direct relation is established between machining constant C and chip reduction coefficient ξ .

It is customary to consider the chip as a stationary body in static equilibrium. However, the fact is that the chip decelerates as it moves along the tool face on account of friction. This leads to a reduction of chip velocity (see Eqn. 3.10)

Applying the principle of constant volume to metal removed in unit time (axiom 1 of the theory of plasticity, see Section 2.3),

$$\frac{a_c}{a} = \frac{v}{v_c} = \xi$$

That is, the reduction of chip velocity is accompanied by a corresponding increase of chip thickness. Assuming that deceleration is caused only by the frictional force we may write

$$\frac{mdv}{dt} = -F = -\mu N \quad (3.41)$$

where F and N are the frictional and normal forces, respectively, on the tool face.

Now if the path taken by an elementary mass m of the work material while moving from undeformed state I (velocity v) to deformed state II (velocity v_c) is represented by a circular arc (Figure 3.15), then the centrifugal force on the mass = $\frac{mv^2}{n} = mv \frac{d\theta}{dt}$, where $\frac{d\theta}{dt}$ is the angular velocity of the deflected chip.

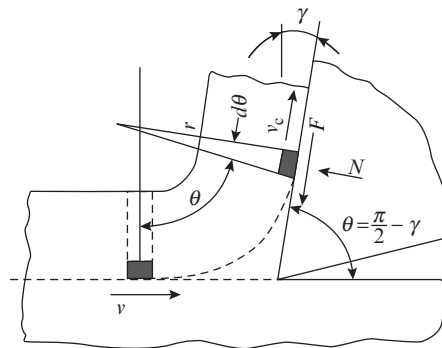


Figure 3.15 Schematic depicting deceleration of chip during transition from undeformed state to deformed state

This force must obviously balance the normal force N , i.e.

$$mv \frac{d\theta}{dt} = N \quad (3.42)$$

Substituting for N from Eqn. (3.42) in Eqn. (3.41), we obtain

$$m \frac{dv}{dt} = -\mu mv \frac{d\theta}{dt}$$

$$\frac{dv}{dt} = -\mu v \frac{d\theta}{dt}$$

As the velocity changes from v to v_c , the elementary mass is deflected through an angle $(\frac{\pi}{2} - \gamma)$. Therefore, on integrating the above relation we have

$$\int_v^{v_c} \frac{dv}{v} = -\mu \int_0^{\frac{\pi}{2}-\gamma} d\theta$$

$$[l_n v]_v^{v_c} = -\mu [\theta]_0^{\frac{\pi}{2}-\gamma}$$

$$l_n \frac{v_c}{v} = -\mu \left(\frac{\pi}{2} - \gamma \right)$$

$$\frac{v_c}{v} = \frac{1}{\xi} = e^{-\mu \left(\frac{\pi}{2} - \gamma \right)}$$

Hence,

$$\xi = e^{-\mu \left(\frac{\pi}{2} - \gamma \right)} \quad (3.43)$$

or

$$\mu = \tan \theta = \frac{\log \xi}{\frac{\pi}{2} - \gamma} \quad (3.44)$$

This is an important relation as it directly correlates the friction angle θ with chip reduction coefficient ξ . The relation between θ and shear angle β can also be derived. We know from Eqn. (2.39) that

$$\tan \beta = \frac{\cos \gamma}{\xi - \sin \gamma}$$

On substituting for ξ from Eqn. (3.43) in the above expression, we obtain

$$\tan \beta = \frac{\cos \gamma}{e^{\mu \left(\frac{\pi}{2} - \gamma \right)} - \sin \gamma} \quad (3.45)$$

This gives the approximate solution

$$\beta = \frac{\pi}{4} + \frac{\gamma}{2} - \theta(0.75 + 0.0045\gamma) \quad (3.46)$$

Having found expressions for θ and β in terms of ξ and γ these values can be put in Eqn. (3.38) to determine C without having to measure the cutting force.

Slip Line Field Solutions—Lee and Shaffer's Shear Angle Relation In general, the three-dimensional deformation problem is difficult to analyze. However, often it can be reduced to a two-dimensional (plane strain) problem, or at least a solution of the analogous plane strain problem can be obtained to get a fair idea of the stresses and deformation in the actual three-dimensional problem.

Slip line field theory is an approach that has been widely used for solution of plane strain problems. It is based on the fact that any general state of stress in plane strain consists of pure shear and hydrostatic pressure. The slip lines are lines of maximum shear stress and show the direction of shear yield strength in pure shear τ_y at a given point. They come in orthogonal pairs and are designated as α and β lines (Figure 3.16a).

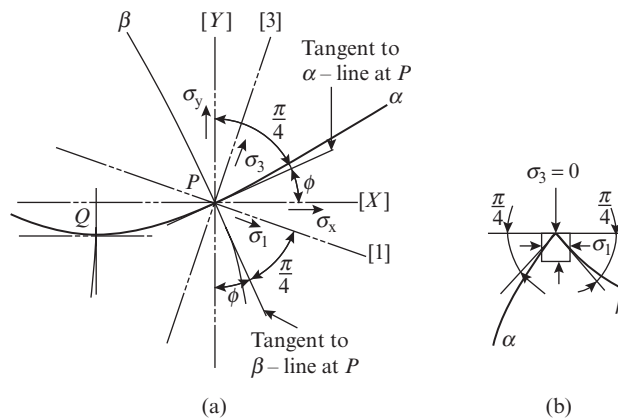


Figure 3.16 Slip line field: (a) general representation of α and β slip lines (b) slip lines on a free surface

The salient properties of slip lines are as follows:

- (i) Shear strain is maximum along the slip lines.
- (ii) Linear strain is zero along the tangent to the slip lines.
- (iii) Slip lines may in general be curved; but if the stress distribution in the deformed zone is uniform, then they are represented as straight lines.
- (iv) The tangents to α and β lines, i.e. the directions of maximum shear stresses make an angle $\frac{\pi}{4}$ with the direction of principal stresses.
- (v) The line of action of the algebraically largest principal stress lies in the first and third quadrants.

(vi) On the free surface, there can be no normal stress therefore $\sigma_3 = 0$. Assuming the hydrostatic compressive stress acting on all the faces of an element of the free surface equal to p (Figure 3.16b),

$$\sigma_3 = -p + \tau_y = 0, \text{ hence } p = \tau_y$$

And
$$\sigma_1 = -p - \tau_y = -2\tau_y$$

Several shear angle relations based on slip line field approach have been developed. The earliest and the simplest of them all, proposed by Lee and Shaffer is discussed below. They assumed that the material ahead of the tool is ideally plastic and that the shear plane coincides with the direction of maximum shear stress. They further assumed that a slip field exists within the chip to transmit the cutting forces from the shear plane to the tool face (Figure 3.17). Hence, although the chip shears in plane OA, it retains some shearing stress in a certain deformed zone OAB and only in plane AB the shearing becomes complete, i.e. plane AB is a free surface on which the shear stress and normal stress both are equal to zero. Hence, AB is a principal plane in which the principal stress is zero.

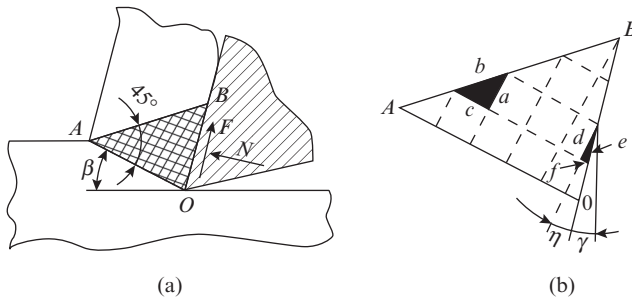


Figure 3.17 Slip line field solution for shear angle (a) slip line field proposed by Lee and Shaffer (b) schematic to explain the construction of slip lines in the deformed zone

The following points regarding the slip line field shown in Figure 3.17(a) need clarification:

1. As per property (iv) of the slip lines, two sets of orthogonal slip line will emanate from different points of AB at an angle $\frac{\pi}{4}$. Assuming uniform stress distribution in deformed zone OAB, the slip lines are shown as straight lines.
2. As OA is assumed to be coincident with the direction of maximum shear stress and AB is coincident with the direction of one of the principal stresses, $\angle OAB = 45^\circ$.
3. In view of (1) and (2) above, one set of slip lines emanating from points on AB must be incident on OA at right angle to it. Further, considering property (v) of the slip lines, this set of slip lines must be associated with the algebraically largest principal stress. As one of the principal stress that lies along the free surface AB is zero, the other perpendicular to it will be $= 2\tau_y$ (see Figure 3.16b).

Let us consider an element abc in plane AB and another element def on the tool face, (Figure 3.17b). If the Mohr's circle is drawn for the state of stress in the deformed zone OAB (Figure 3.18), the centre of the circle where the shear and normal stress are both zero will represent the stress in plane b of element abc. Plane a of element abc and d of element def are inclined to b at $\frac{\pi}{4}$ in the

positive direction. Accordingly, their state of stress is represented by point (a,d) on the Mohr's circle. Similarly, the state of stress of planes c and f that are inclined to b at $\frac{\pi}{4}$ in the negative direction is represented by point (c,f) on the Mohr's circle.

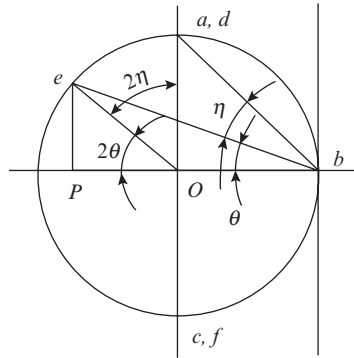


Figure 3.18 Mohr's circle representing the state of stress in the deformed zone

The stresses at the tool face are given by plane e of element def . Since plane e makes angle η with plane d , the location of point e on the Mohr's circle is obtained by drawing a line making angle 2η with the line $[O, (a,d)]$. Applying the theorem that the angle subtended by a chord at the center of a circle is twice the angle subtended by it at the periphery, we observe that

$$\text{Angle } [(a,d), O, e] = 2\eta$$

$$\text{Angle } [(a,d), b, e] = \eta$$

The ordinate of point e gives the shear (frictional) stress and the abscissa the normal stress on the tool face. Hence, the friction angle θ is found from the following relation:

$$\mu = \tan \theta = \frac{Pe}{Pb}$$

From the Mohr's circle (Figure 3.18), it can be noted that

$$\eta = \frac{\pi}{4} - \theta$$

Also, from the geometrical construction of the deformed zone (Figure 3.17), it can be noted that

$$\beta = \eta + \gamma$$

Substituting for η in the above expression, the shear angle relation of Lee and Shaffer is obtained as follows:

$$\beta = \frac{\pi}{4} - \theta + \gamma \quad (3.47)$$

On substituting for θ from E (3.47) in Eqn. (3.24), we obtain

$$P_z = \tau_s st \frac{\cos\left(\frac{\pi}{4} - \beta\right)}{\sin \beta \cos \frac{\pi}{4}}$$

$$P_z = \tau_s st (1 + \cot \beta) \tag{3.48}$$

And on substituting for $\cot \beta$ from Eqn. (2.39), we obtain

$$P_z = \tau_s st \left[1 + \frac{\xi - \sin \gamma}{\cos \gamma} \right] \tag{3.49}$$

Armarego suggests that most of the shear angle relations can be reduced to the form

$$\beta = C_1 - C_2 (\theta - \gamma) \tag{3.50}$$

where C_1 and C_2 are constants. A summary of some of the well-known shear angle relations is tabulated below (see Table 3.1).

Table 3.1 Summary of shear angle relations

| Author | Year | Shear angle relation | C_1 | C_2 |
|--------------------|------|--|------------------------------------|---------------|
| Ernst and Merchant | 1941 | $\beta = \frac{\pi}{4} + \frac{\gamma}{2} - \frac{\theta}{2} =$ $= \frac{\pi}{4} - \frac{1}{2}(\theta - \gamma)$ | $\frac{\pi}{4}$ | $\frac{1}{2}$ |
| Merchant | 1945 | $\beta = \frac{C}{2} - \frac{1}{2}(\theta - \gamma)$ | $\frac{C}{2}$ | $\frac{1}{2}$ |
| Lee and Shaffer | 1951 | $\beta = \frac{\pi}{4} - (\theta - \gamma)$ | $\frac{\pi}{4}$ | 1 |
| Stabler | 1952 | $\beta = \frac{\pi}{4} - \theta + \frac{\gamma}{2}$ $= \frac{\pi}{4} - \frac{\gamma}{2} - (\theta - \gamma)$ | $\frac{\pi}{4} - \frac{\gamma}{2}$ | 1 |
| Zorev | 1952 | $\beta = \frac{\pi}{4} + \frac{\gamma}{2} - \frac{\theta}{2} - \frac{\psi}{2}$ $= \frac{\pi}{4} - \frac{\psi}{2} - \frac{1}{2}(\theta - \gamma)$ | $\frac{\pi}{4} - \frac{\psi}{2}$ | $\frac{1}{2}$ |

ψ = angle that the tangent to the chip outer boundary makes with the velocity vector

It may be noted that in Ernst and Merchant's relations, C_1 is maximum and C_2 is minimum. It therefore gives the upper bound solution. On the contrary, in Stabler's relation C_1 is minimum and C_2 is maximum. It therefore gives the lower bound solution. The other relations lie in between these two.

3.3.3 Forces in Drilling

In drilling operation, two primary cutting edges, two auxiliary cutting edges, and a chisel edge are involved in the process of chip removal. The cutting force acting on each primary cutting edge may be resolved into three mutually perpendicular components P_x , P_y , and P_z (Figure 3.19). Force P_x is directed parallel to the drill axis, force P_y is directed towards the drill axis (centre) and force P_z , the cutting force component is directed along the tangent at the given point. The components P_y on the two primary cutting edges should be theoretically equal and balance each other. However, inaccuracy of grinding results in different values of primary cutting edge angle φ on the two edges and the resultant force $\Delta P_y = P_{y1} - P_{y2}$ tends to bend the drill to one side. This leads to oversizing that is characteristic of drilled holes.

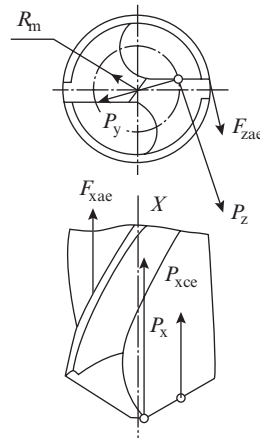


Figure 3.19 Forces acting on a drill

The force on the half chisel edge may also be resolved into three components. However, the components P_{yce} and P_{zce} are negligibly small and only the axial component P_{xce} is of some significance.

On the auxiliary (spiral) edges running along the length of the flutes, the clearance angle is zero. A friction force therefore develops between the drill and the hole surface. This force has a peripheral component F_{zae} and an axial component F_{xae} , but the latter is very small and may be easily neglected. The drilling forces described above are used to calculate the torque and thrust of the drilling operation. The torque is required for determining the power of the drilling machine motor and design of the spindle and components of the main drive system. The thrust force is required for designing the components of the feed mechanism of the drilling machine. Based on the preceding discussion, the expressions for torque and thrust force in drilling may be written as follows:

Torque

$$T = 2P_z R_m + 2F_{zae} R \quad (3.51)$$

where

R = drill radius

$$R_m = \frac{R}{2} = \text{mean radius of the primary cutting edge}$$

Thrust

$$P = 2P_x + 2P_{x_{ce}} \tag{3.52}$$

The contribution of primary cutting edge, auxiliary cutting edge, and chisel edge to the torque and thrust force in drilling is summarized in Table 3.2.

Table 3.2 Contribution of primary, auxiliary, and chisel edge to torque and thrust force in drilling

| Factor | Cutting edge | | |
|--------|--------------|-----------|--------|
| | Primary | Auxiliary | chisel |
| Thrust | 40 | 3 | 57 |
| Torque | 80 | 12 | 8 |

The above data justify our neglecting of $F_{x_{ae}}$ (contribution 3 percent) and $P_{z_{ce}}$ (contribution 8 percent) in Eqs (3.51) and (3.52), respectively.

Drilling is an oblique cutting process and drill has a very complex geometry. Therefore, theoretical determination of torque and thrust force, though possible is rather complicated and beyond the scope of the present text. However, for the completeness of the discussion, a few empirical relations for calculation of torque and thrust are given below.

In these relations, D is the drill diameter in mm and s is the feed in mm/rev.

Drilling of stainless steel with HSS drill:

$$T = 41.6D^2s^{0.7}, \text{ kg. mm}$$

$$P = 189Ds^{0.7}, \text{ kg}$$

Drilling of heat-resistant steel with HSS drill:

$$T = 45.8D^2s^{0.7}, \text{ kg. mm}$$

$$P = 208Ds^{0.7}, \text{ kg}$$

Drilling of carbon and low alloyed steels with HSS drill:

$$T = 39D^2s^{0.8} \left(\frac{\sigma_u}{75} \right)^{0.75}, \text{ kg. mm}$$

$$P = 98.8Ds^{0.7} \left(\frac{\sigma_u}{75} \right)^{0.75}, \text{ kg}$$

Here,

σ_u = ultimate strength of work material in kg/mm²

Drilling of gray cast iron with HSS drill

$$T = 23.6D^2s^{0.8} \left(\frac{HB}{190} \right)^{0.6}, \text{ kg. mm}$$

$$P = 62Ds^{0.8} \left(\frac{HB}{190} \right)^{0.6}, \text{ kg}$$

Here,

HB = Brinell's hardness of work material

Drilling of carbon and structural steels using drill with cemented carbide bits and emulsion cooling:

$$T = 3D^2s\sigma_u^{0.7}, \text{ kg. mm}$$

$$P = 2D^{1.4}s^{0.8}\sigma_u^{0.75}, \text{ kg}$$

Drilling of gray and ductile cast iron using drill with cemented carbide bits in dry machining:

$$T = 1.43D^2s^{0.94} (HB)^{0.6}, \text{ kg. mm}$$

$$P = 7.2D^{0.9}s(HB)^{0.6}, \text{ kg}$$

3.3.4 Forces in Milling

In plain milling operation using a cutter with spiral teeth, the resultant force can be resolved into three components, tangential P_z , radial P_x , and axial P_y . The tangential component P_z produces a torque $\frac{P_z D}{2}$ and is used for determining the power of the main motor and in the design of the arbor, spindle, and components of the main drive system. The radial component P_x also bends the arbor. Therefore, the arbor design is based on consideration of P_z and P_x both. Axial force P_y is directed toward the spindle. To prevent sliding of the cutter along the arbor under the effect of P_y , its location on the arbor is fixed by means of sleeves. The effect of P_y can be eliminated by using plain milling cutters in pairs with opposite but equal helix angle, akin to herringbone gears. In plain milling cutters with straight teeth, P_y is absent. The force system in face milling is basically similar to that in plain milling. Milling being a multiple-tooth operation, the cutting force in milling continuously changes with the rotation of the cutter as the chip section removed by an individual tooth changes with the engagement angle and also due to engagement and disengagement of successive teeth. The tangential component P_z is the main component of the cutting force. A simple method of its determination was suggested by Vulf based on his experimental studies. According to Vulf, the average value of tangential force P_{zav} in milling may be found from the following relation:

$$P_{zav} = \frac{C_p A_{av}}{(a_{av})^{\lambda}}, \text{ kg} \quad (3.53)$$

where

A_{av} = average chip cross section for the number of teeth in engagement

a_{av} = average undeformed chip thickness

C_p and λ are constants for a given work material

The volume of metal removed in milling operation in unit time is

$$V = B t s_m \quad (3.54)$$

where

B = width of the work piece, mm

t = depth of cut, mm

s_m = feed per min, mm/min

Referring to Eqs (1.5) and (1.6), s_m may be expressed as follows:

$$s_m = s_z z n \quad (3.55)$$

where

s_z = feed per tooth, mm

z = number of teeth of the cutter

n = rev/mm of the cutter

Average chip area A_{av} is found as the ratio of Volume V to the linear chip removal rate πDn , i.e.

$$A_{av} = \frac{V}{\pi Dn}$$

Combining (3.54) and (3.55), we obtain

$$A_{av} = \frac{Bts_zzn}{\pi Dn}$$

Or

$$A_{av} = \frac{Bts_zz}{\pi D} \quad (3.56)$$

Substituting (3.56) in (3.53), we obtain

$$P_{zav} = \frac{C_p}{(a_{av})^\lambda} \frac{Bts_zz}{\pi D} \quad (3.57)$$

The value of a_{av} can be taken for the relevant case of milling from Section 2.2. For instance, for the case of plain milling considering that

$$a_{av1} = s_z \sqrt{\frac{t}{D}} \quad (\text{Eqn. 2.10}), \text{ we obtain}$$

$$\begin{aligned} P_{zav} &= C_p \frac{1}{\left(s_z \sqrt{\frac{t}{D}}\right)^\lambda} \frac{Bts_zz}{\pi D} \\ &= \frac{C_p}{\pi} \frac{s_z^{1-\lambda} t^{1-\frac{\lambda}{2}}}{D^{1-\frac{\lambda}{2}}} Bz \end{aligned} \quad (3.58)$$

The values of C_p and λ for a few materials are given in Table 3.3.

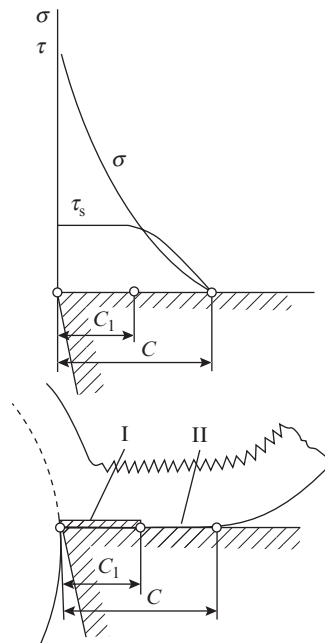
Table 3.3 Values of C_p and λ

| Material | C_p | λ |
|-------------|-------|-----------|
| Alloy steel | 210 | 0.28 |
| Mild steel | 140 | 0.28 |
| Bronze | 40 | 0.40 |

Force components P_x and P_y are generally expressed as ratios with respect to P_z . The ratio $\frac{P_x}{P_z}$ depends on undeformed chip thickness and the helix angle of the cutter, decreasing with increase of both. For a cutter with helix angle 25–35°, the ratio $\frac{P_x}{P_z}$ varies between 0.4 and 0.6 in the commonly used range of machining parameters. The ratio $\frac{P_y}{P_z}$ depends mainly on the helix angle of the cutter, increasing with the increase of the helix angle. In the commonly used range of machining parameter $P_y = (0.2-0.4) P_z \tan \theta$, where θ is the helix angle of the cutter.

3.4 Built-Up Edge

Machining under certain conditions is accompanied by the built-up edge (BUE) formation, which essentially is a wedge-shaped deposition of strain hardened work material on the tool face. BUE plays a major role in the cutting process, and several aspects of machining especially concerning cutting force and tool wear cannot be explained without a proper understanding of the BUE phe-


Figure 3.20 Variation of tangential and normal stress along tool–chip contact length

nomenon. It has been discussed in Section 2.5 that all chips have a natural tendency to curl (Figure 2.18), thereby restricting the tool–chip contact length. Over this length of contact with the tool face, the chip exerts normal force $P_f = P_{el} + P_{pl}$ and as it slides along the tool face this gives rise to frictional force $F_f = \mu (P_{el} + P_{pl})$ (Figure 3.7). The normal and frictional forces give rise to normal stress σ and tangential stress τ that vary along the tool chip contact length as shown in Figure 3.20. The normal stress σ is zero at the point where the chip departs from the tool face. It increases following a hyperbolic distribution and becomes maximum at the cutting edge. The tangential stress is also zero at the point where the chip leaves the tool face. Over the length $C-C_1$, it increases proportionally with the normal stress. However, this increase is arrested when the tangential stress attains a value equal to shear yield strength of the work material τ_s , because any further increase of τ is impossible. The tool–chip contact can thus be divided into two distinct zones as follows:

- (i) Zone I of length C_1 , of plastic contact characterized by conditions of sticking friction,
- (ii) Zone II of length $C-C_1$ of elastic contact characterized by conditions of sliding friction.

Zone I acts as a stagnant zone in which the lower-most layers of the chip stick to the tool face and external sliding of the chip is replaced by internal plastic shear of the upper layers of the chip. Under certain cutting conditions, the combination of temperature and pressure at the tool chip interface in the stagnant zone becomes favorable for formation of microwelds. As these microwelds increase in number, they produce a layered deposition of hardened work material on the tool face, known as BUE as shown in Figure 3.21(a). A few characteristic features of BUE are worth highlighting as they will be required later on for explanation of several phenomena related to metal cutting.

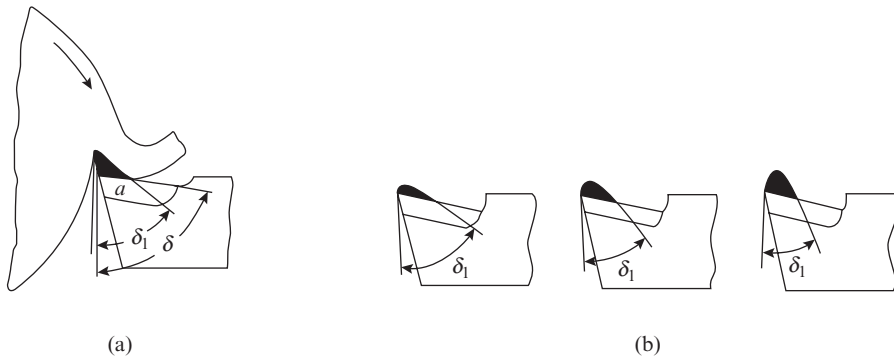


Figure 3.21 Build-up edge: (a) depicted as a deposition of hardened work material on the tool face and (b) schematic depicting the reduction of BUE wedge angle with the increase of its height

3.4.1 Characteristic Features of BUE

1. The base of the BUE is initially equal in length to the length of the stagnant zone, which can be found from the following relation:

$$C_1 = a [\xi (1 - \tan \gamma) + \sec \gamma]$$

where

a = undeformed chip thickness

γ = rake angle

ξ = chip reduction coefficient

2. The BUE is shaped like a wedge that slightly protrudes beyond the cutting edge, acting like an overhang above the tool flank and in a way isolating the tool flank from the cutting process and protecting it against wear
3. The BUE is made up of severely deformed work material that is 2–3 times harder than the original work material. This makes the BUE comparable to the tool material in terms of hardness. Therefore, under conditions in which the BUE is stable, it effectively becomes an extension of the cutting tool and the cutting is effectively carried out by the BUE of action angle δ_1 rather than the wedge of action angle δ of the original tool.
4. As the height of the BUE increases, its wedge angle decreases (Figure 3.21b). This eases the plastic deformation associated with chip formation. Hence, increase of BUE height is accompanied by a reduction of chip reduction coefficient ξ .
5. On account of friction between the chip and BUE and between the machined surface and BUE, particles of the BUE are continuously picked up by the chip and the machined surface. At the same time, the BUE is also continuously replenished by new particles of the work material. The BUE is therefore an unstable wedge whose size keeps on changing all the time. Within a fraction of a second, it originates and grows in size reaching a maximum and then breaks. It may be mentioned that generally this breaking is partial. The lower portion of the BUE in the immediate vicinity of the tool face keeps sticking to the latter, but the upper portion separates and disintegrates; part of the disintegrated BUE is carried away by the chip and part of it escapes with the machined surface. This process of BUE formation and disintegration may be repeated 3000–4000 times per minute
6. As the essential condition for formation of BUE is the presence of a stagnant zone based on sticking friction, all the factors that tend to reduce friction on the tool face will hinder the formation of BUE. Important among these factors are use of coolant, improving the surface finish of the tool face, and reducing the wedge angle of the tool, i.e. increasing its rake angle.
7. In intermittent cutting operations (shaping, milling, etc.), and when the chips formed in machining are discontinuous or elemental (see Section 2.4), the BUE phenomenon is absent because either BUE formation fails to take place or separation of BUE occurs before it acquires a practically meaningful size.
8. The single most important actor that affects BUE formation and its size is the cutting speed (Figure 3.22).

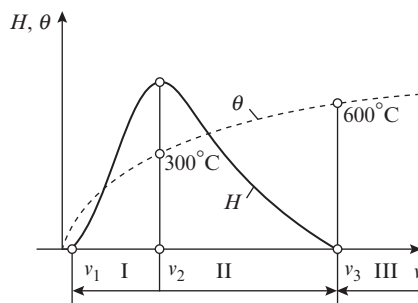


Figure 3.22 Effect of cutting speed on BUE height and cutting temperature

Three distinct zones can be identified in the figure. At very low cutting speed up to $v_1 = 2\text{--}5$ m/min, element chips are produced. In addition, the cutting temperature is too low for formation

of microwelds. Because of the combination of these two factors no BUE is observed at very low cutting speeds. As the cutting speed increases, the chip changes from elemental to continuous and conditions become conducive for formation of microwelds between the chip and the tool face. Consequently, the BUE becomes increasingly more stable and also increases in height, reaching a maximum at $v_2 = 15\text{--}30$ m/min (zone I). With further increase of cutting speed and the accompanying rise of cutting temperature, the stagnant zone begins to soften and the BUE begins to decrease till at a particular speed $v_3 = 80\text{--}100$ m/min the BUE disappears completely (zone II). Any further increase has no effect on the BUE phenomenon (zone III). As already mentioned, the BUE is maximum at a cutting speed of 10–20 m/min depending on the work material and this generally corresponds to cutting temperature of 300°C. Similarly, the cutting speed at which BUE disappears may vary between 80–100 m/min, but it will generally correspond to a cutting temperature of 600°C.

9. To a less extent, the size of the BUE is also affected by rake angle γ and undeformed chip thickness a . The height of BUE increases with the decrease of γ and increase of a (Figure 3.23), because the cutting temperatures of 300°C and 600°C are attained at a lower cutting speed.

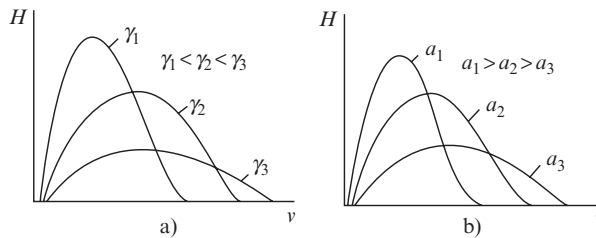


Figure 3.23 Variation of BUE height with cutting speed at (a) different values of rake angle γ and (b) at different values of undeformed chip thickness a

3.5 Effect of Tool Geometry and Machining Parameters on Cutting Force

The factors that affect the cutting force components P_x , P_y , and P_z are the work material, the machining parameters, namely speed, feed, and depth of cut and the tool geometry mainly through the rake angle γ , primary cutting edge angle ϕ , cutting-edge inclination angle λ , and nose radius r . The rest of the parameters of tool nomenclature namely, the clearance angle, auxiliary cutting edge angle and rake angle of the auxiliary cutting edge have little effect on P_x , P_y , and P_z in the range of their commonly used values and have therefore been excluded from the discussion.

Effect of Work Material The mechanical properties of work material have a complex relationship with cutting forces. On the one hand, the increase in hardness and strength of the work material increases the shear angle β and reduces the chip reduction coefficient ξ , thereby reducing the shear strain ε and consequently the cutting force. On the other hand, the increase in hardness and strength of work material increases the dynamic shear stress in the shear plane τ_s , and hence the cutting force. Depending on which of the two factors predominates, the cutting force components P_x , P_y , and P_z will increase or decrease. Cutting data for some common engineering materials are given in the table below to illustrate the point.

| Work material | Shear angle β | τ_s (kg/mm ²) | ξ | P_z (kg) |
|-------------------------|---------------------|--------------------------------|-------|------------|
| Copper | 9°05' | 32 | 6.2 | 500 |
| 20 Cr1 Structural steel | 17°40' | 58 | 3.3 | 500 |
| Stainless steel | 22°45' | 103 | 2.6 | 740 |

Despite the fact that the ultimate tensile strength of copper (30 kg/mm²) is much less than that of structural steel (58 kg/mm²), P_z is the same for both as it is evident from the table above. The reason is that though the τ_s value of structural steel is $\frac{58}{32} = 1.81$ times more than that of copper, the ξ value is $\frac{6.2}{3.3} = 1.87$ less. These two conflicting phenomena balance each other, resulting in the same P_z value for both the materials. The comparison of the tabulated data for stainless steel and structural steel shows that for stainless steel the τ_s value is 1.77 times more, but the ξ value is only 1.26 times less. As the effect of dynamic shear stress is stronger, this is reflected in the higher value of P_z for stainless steel.

However, it should be kept in mind that for a particular category of materials, say structural steels or cast iron the effect of τ_s far exceeds that of ξ for various grades within the same category. Hence, one would generally observe the cutting force to increase with the strength and hardness of the work material. The following relations may be used for determining the cutting forces:

$$\text{For steels} \quad P_i = C_1 \sigma_u^n \quad (3.59)$$

$$\text{For cast iron} \quad P_i = C_2 (HB)^n \quad (3.60)$$

where

σ_u = ultimate tensile strength of steel, kg/mm²

HB = Brinell's hardness of cast iron

C_1, C_2 = constants that depend on machining conditions and tool geometry

n = exponent; values of n are given in Table 3.4

Table 3.4 Values of exponent n in Eqs (3.59) and (3.60)

| Work material | Exponent n | | | | | |
|---|--------------|----------|--------------|----------|--------------|----------|
| | P_z | | P_y | | P_x | |
| | Carbide tool | HSS tool | Carbide tool | HSS tool | Carbide tool | HSS tool |
| Steel, $\sigma_u < 60$ kg/mm ² | 0.35 | 0.35 | 1.35 | 2.0 | 1.0 | 1.5 |
| Steel, $\sigma_u > 60$ kg/mm ² | 0.35 | 0.75 | 1.35 | 2.0 | 1.0 | 1.5 |
| Cast iron | 0.4 | 0.55 | 1.0 | 1.3 | 0.8 | 1.1 |

Effect of Feed and Depth of Cut Depth of cut t and feed s both affect the cutting force through the change in undeformed chip area. It is evident from Eqs (2.1) and (2.2) that increase of t and s produces a proportional increase of undeformed chip width b and undeformed chip thickness, respectively, resulting in a higher value of P_x , P_y , and P_z . However, the increase of cutting force components due to increase of s is less than that due to an equal increase of t . The reason is that an increase of t is accompanied by a proportional increase of b without any affect on chip reduction coefficient. However, increase of a due to increase of s is accompanied by a decrease of ξ , which explains the weaker affect of s on the cutting force. The following relations represent the effect of s and t on the cutting force:

$$P_z = C_{z1} t^x s^y \quad (3.61)$$

$$P_y = C_{y1} t^x s^y \quad (3.62)$$

$$P_x = C_{x1} t^x s^y \quad (3.63)$$

Here C_{x1} , C_{y1} , and C_{z1} are constants that depend on the work material, cutting speed, and tool geometry; whereas x and y are exponents of t and s , respectively and their values are given in the Table 3.5, where it can be noted that the exponent of feed y is less than that of depth of cut x for all the force components

Table 3.5 Values of exponents x and y in Eqs (3.61)–(3.63)

| Cutting tool material | Exponents x and y in Eqs (3.61)–(3.63) | | | | | |
|-----------------------|--|------|-------|------|-------|------|
| | P_z | | P_y | | P_x | |
| | x | y | x | y | x | y |
| Cemented carbide | 1 | 0.75 | 0.9 | 0.6 | 1.0 | 0.5 |
| HSS | 1 | 0.75 | 0.9 | 0.75 | 1.2 | 0.65 |

In view of the unequal effect of t and s on the cutting force, for a given undeformed chip area $A = ab$, the cutting force will be more for the combination with higher $\frac{t}{s}$ value. Therefore, in order to achieve lower cutting force while maintaining the same productivity of the machining operation, it is preferable to work with large feed and small depth of cut, so that the $\frac{t}{s}$ value is as small as possible.

Effect of Cutting Speed Cutting speed influences the cutting force by the manner in which it affects the chip reduction coefficient ξ . While machining metals that do not have a tendency of BUE formation, ξ decreases with increase of cutting speed v . The rate of decrease is fast at low cutting speed, but it slows down at higher speeds. The same trend is observed in the variation of all the force components (Figure 3.24a). While machining materials that have a tendency of BUE formation, the variation of P_z and ξ is fully explained by the BUE phenomenon (Figure 3.24b).

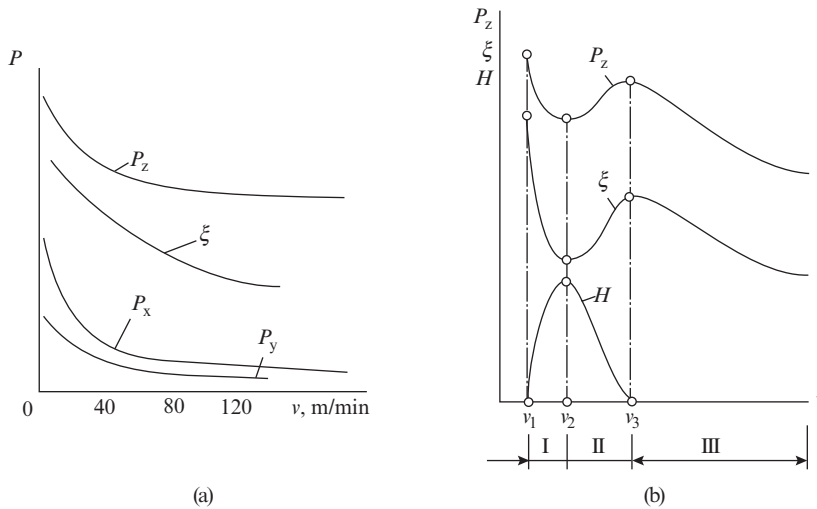


Figure 3.24 Effect of cutting speed on chip reduction coefficient ξ and cutting force components P_x , P_y , and P_z (a) without BUE formation (b) with BUE formation

Here, the following three distinct zones can be identified:

Zone I: zone of stable BUE, in which the increase of BUE height is accompanied by a corresponding reduction of the angle of the wedge constituting the BUE (see Section 3.4.1, point 4) and consequently that of ξ . This is reflected in decrease of P_z with v in zone I.

Zone II: zone of softening of the stagnant zone that is accompanied by reduction of the height of BUE, with a corresponding increase of the angle of the wedge constituting the BUE and increase of ξ . This is reflected in increase of P_z in zone II.

Zone III: the reduction of P_z with v in zone III is attributed to the reduction of friction at the tool-chip interface that occurs due to local softening of the contact zone as the cutting temperature increases.

Nowadays, turning operation is usually carried out with cemented carbide tools at cutting speeds of 80 m/min and above at which BUE is not formed, and hence does not interfere with the cutting process. Under these conditions, only zone III of the cutting force vs cutting speed relation is relevant. In this zone, for reasons explained above, all the cutting force components display a trend of continuous reduction with cutting speed that may be represented by the following expressions:

$$P_z = \frac{C_{zv}}{v^{zv}} \quad (3.64)$$

$$P_y = \frac{C_{yv}}{v^{yv}} \quad (3.65)$$

$$P_x = \frac{C_{xv}}{v^{xv}} \quad (3.66)$$

Here C_{xv} , C_{yv} , and C_{zv} are constants that depend on the work material, s , t , and tool geometry and xv , yv , and zv are exponents of the cutting speed; $zv = 0.35-1.0$, $yv = 0.25-0.50$, and $xv = 0.3-0.50$.

At $v > 400$ m/min, the cutting speed practically ceases to have any effect on the cutting force and the exponents zv , yv , and $zv \rightarrow 0$

Effect of Rake Angle Reduction of rake angle increases the angle of the cutting wedge, thereby making chip removal relatively more difficult and increasing the chip reduction coefficient. As can be seen from Figure 3.25, the variation of rake angle from +20° to -20° results in a continuous increase of all the cutting force components. It can also be noted from the figure that the rate of increase of axial force P_x is more than that of the cutting force P_z and radial force P_y . It is convenient to represent the effect of γ on P_x , P_y , and P_z through the angle of action $\delta = 90 - \gamma$ by the following relations:

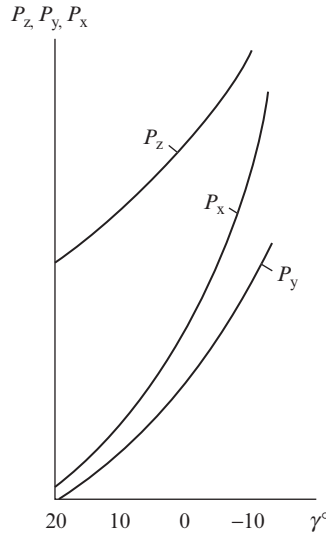


Figure 3.25 Effect of rake angle γ on cutting force components P_x , P_y , and P_z

$$P_z = C_{zy} \delta^{zy} \tag{3.67}$$

$$P_y = C_{yy} \delta^{yy} \tag{3.68}$$

$$P_x = C_{xy} \delta^{xy} \tag{3.69}$$

Here C_{xy} , C_{yy} , and C_{zy} are constants that depend on the work material, tool geometry (except γ), and the machining parameters v , s , and t . The exponents of rake angle $x\gamma$, $y\gamma$, and $z\gamma$ have the following values: $z\gamma = 0.95-1.05$, $y\gamma = 2.0-2.5$, and $x\gamma = 2.5-3.5$.

Effect of Primary Cutting-Edge Angle In order to understand the effect of primary cutting angle ϕ on the cutting force, it is first necessary to recall that cutting tools typically have a nose radius r of a few mm. The cutting edge therefore consists of two segments—a straight segment defined by ϕ and a curved segment defined by r . For a given depth of cut, as ϕ increases, the straight line segment decreases and the curved segment increases in the total length of the cutting edge (Figure 3.26). However, with reference to Eqn. (2.2), it can be noted that increase of ϕ is accompanied by reduction of undeformed chip width b . Thus, increase of ϕ is associated with two conflicting phenomena:

- (i) Increased role of the curved segment of the cutting edge is accompanied with increase of cutting force.
- (ii) Reduction of b is accompanied with the decrease of cutting force.

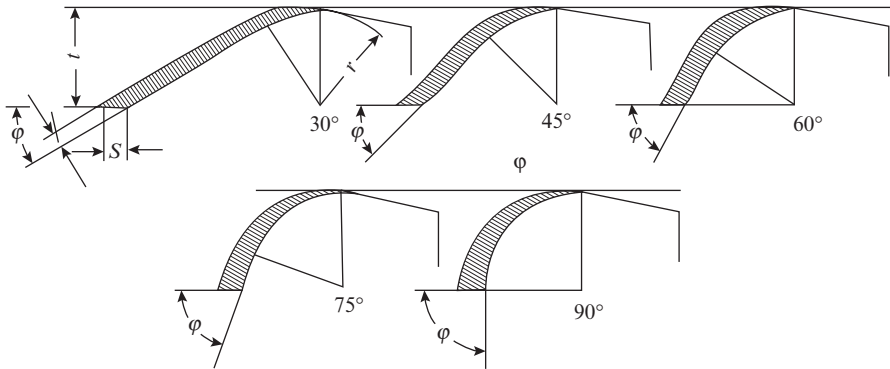


Figure 3.26 Schematic depicting the decrease of straight segment and increase of curved segment of the cutting edge with increase of primary cutting-edge angle ϕ

The net effect of ϕ on the cutting force will depend on which of the two factors dominates in a particular range of ϕ . As can be seen on curve (1) in Figure 3.27, P_z decreases in the range $\phi = 30\text{--}60^\circ$ in which the second factor predominates, but increases in the range $\phi = 60\text{--}90^\circ$ in which the first factor predominates. It would be logical to think that if $r = 0$, then the first factor will cease to play any role and the effect of ϕ on the cutting force will be governed solely by the second factor, i.e. increase of ϕ will be accompanied by a continuous reduction of the cutting force. This is actually the case as can be seen on curve (2) in Figure 3.27.

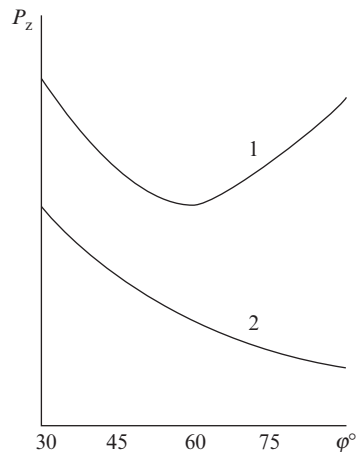


Figure 3.27 Effect of primary cutting-edge angle ϕ on cutting force P_z (1) for ductile work material (2) for brittle work material

In machining of brittle materials, the chips formed are discontinuous and the plastic deformation for chip formation is much less than in machining of ductile materials. Therefore, the effect of the curved segment on the cutting force is negligible and the variation of cutting force follows the trend shown on curve (2) in Figure 3.27.

Force components P_x and P_y are the projections of the horizontal resultant P_{xy} on the X - and Y -axis, respectively (Figure 3.3) wherefrom it can be noted that

$$P_x = P_{xy} \sin \phi \quad (3.70)$$

$$P_y = P_{xy} \cos \phi \quad (3.71)$$

Obviously, P_y will decrease and P_x will increase with the increase of ϕ as is shown in Figure 3.28.

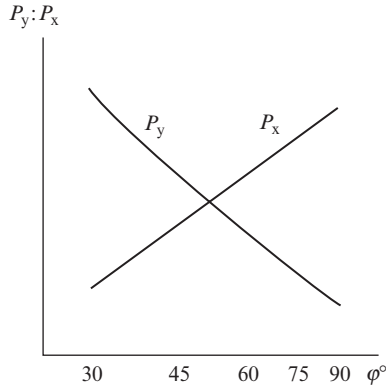


Figure 3.28 Effect of primary cutting-edge angle ϕ on cutting force components P_x and P_y .

The effect of ϕ on cutting force components can be expressed by the relations given below.

For steel:

$$P_z = \frac{C_{z\phi}}{\phi^{0.16}} \text{ for } \phi = 30-50^\circ$$

$$P_z = C_{z\phi} \phi^{0.22} \text{ for } \phi = 50-90^\circ$$

$$P_y = \frac{C_{y\phi}}{\phi^{1.03}} \text{ for } \phi = 30-50^\circ$$

$$P_y = \frac{C_{y\phi}}{\phi^{0.86}} \text{ for } \phi = 50-90^\circ$$

$$P_x = C_{x\phi} \phi^{0.72} \text{ for } \phi = 30-90^\circ$$

For cast iron:

$$P_z = \frac{C_{z\phi}}{\phi^{0.13}}, P_y = \frac{C_{y\phi}}{\phi^{0.51}}$$

$$P_x = C_{x\phi} \phi^{1.08} \text{ for } \phi = 30-45^\circ$$

$$P_x = C_{x\phi} \phi^{0.35} \text{ for } \phi = 45-90^\circ$$

Here, $C_{x\phi}$, $C_{y\phi}$, and $C_{z\phi}$ are constants that depend on the work material, tool geometry (except ϕ), and the machining parameters v , s , and t .

Effect of Cutting-Edge Inclination Angle As can be noted from Figures 1.51 and 1.54, cutting-edge inclination angle λ affects the position of the tool face in the XYZ coordinate system. Increase of λ increases the working length of the cutting edge. Angle λ also affects chip reduction coefficient ξ . Increase of $+\lambda$ increases ξ , whereas increase of $-\lambda$ reduces ξ . Generally λ lies within $\pm 10^\circ$ in most turning tools. In this range it has almost no effect on P_z . However P_x decreases and P_y increases as λ values increase from negative-to-zero-to-positive as shown in Figure 3.29.

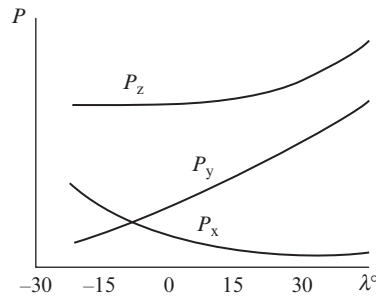


Figure 3.29 Effect of cutting edge inclination angle λ on force component P_x , P_y , and P_z

The effect of λ on cutting force can be expressed by the following relations:

$$P_z = P_{z0}(1 + 0.007\lambda)$$

$$P_y = P_{y0}(1 + 0.02\lambda)$$

$$P_x = P_{x0}(1 - 0.01\lambda)$$

Where P_{z0} , P_{y0} , and P_{x0} are the values of the respective force components at $\lambda = 0$.

Effect of Nose Radius As was shown in Figure 3.26, the larger the nose radius r , the longer will be the curved segment of the cutting-edge length, and hence the greater will be the cutting force component P_z . This was also pointed out while discussing the effect of ϕ on the cutting force. Tangents at points on the curved segment represent a virtual cutting edge. Depending on the location of the point, the angle that the tangent makes with the direction of feed varies from zero at the tool tip to ϕ at the point where the nose radius merges with the linear segment of the cutting edge (Figure 3.30).

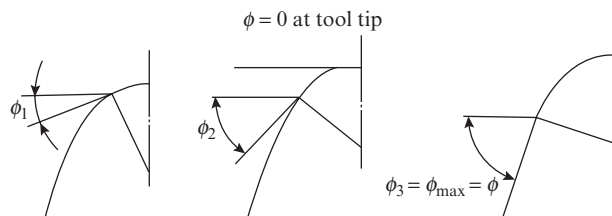


Figure 3.30 Schematic depicting the variation of effective primary cutting edge angle ϕ at different locations on the nose radius

Thus, increase of r is akin to reduction of ϕ in the curved segment. Therefore, the effect of r on P_x and P_y can be approximately described by Eqs (3.70) and (3.71). Based on the above discussion, the effect of r on P_x , P_y , and P_z is shown in Figure 3.31.

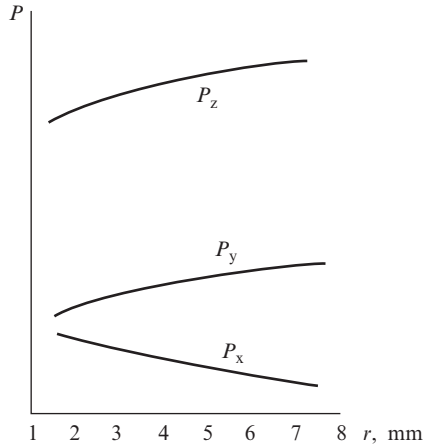


Figure 3.31 Effect of nose radius r on cutting force components P_x , P_y , and P_z

The effect of r on P_x , P_y , and P_z can be expressed by the following relations:

$$P_z = C_{zr} r^{zr}$$

$$P_y = C_{yr} r^{yr}$$

$$P_x = C_{xr} r^{xr}$$

Here C_{xr} , C_{yr} , and C_{zr} are constants that depend on the work material, tool geometry (except r), and the machining parameters, v , s , and t . The exponents of nose radius xr , yr , and zr have the following values: $zr = 0.1$, $yr = 0.3$, $xr = 0.3$ for steels; $zr = 0.07$, $yr = 0.2$, $xr = 0.2$ for cast iron.

Review Questions

- 3.1** In turning of slender rod between centers it is necessary to keep the radial force minimum mainly to
- improve surface finish
 - increase productivity
 - improve cutting efficiency
 - reduce barreling
- 3.2** Which of the following sets of forces are encountered by a parting tool while making a groove on a lathe?
- Tangential, radial, and axial
 - Tangential and radial
 - Tangential and axial
 - Radial and axial
- 3.3** In an orthogonal cutting test with a zero rake angle tool, the cutting force and thrust force were observed to be 1000 N and 500 N, respectively. The coefficient of friction at the chip interface is
- $\frac{1}{2}$
 - 2
 - $\frac{1}{\sqrt{2}}$
 - $\sqrt{2}$

- 3.4** The following data are obtained from an orthogonal cutting test: $\gamma = 10^\circ$, $\xi = 2.86$, undeformed chip thickness = 0.51 mm, undeformed chip width = 3 mm, shear yield stress of work material = 285 N/mm², mean coefficient of friction on tool face = 0.65. Determine the cutting force, radial force, normal force on tool face, and shear force.
- 3.5** If the cutting force = 900 N, thrust force = 600 N, and shear angle = 30° in an orthogonal cutting test, what is the magnitude of the shear force?
 (a) 1079.4N (b) 969.6N
 (c) 479.4 N (d) 69.6N
- 3.6** Which of the following is the correct expression for Merchant's machinability constant? Given that ϕ = shear angle, θ = friction angle, γ = rake angle.
 (a) $2\phi + \theta - \gamma$ (b) $2\phi - \theta + \gamma$
 (c) $2\phi - \theta - \gamma$ (d) $\phi + \theta - \gamma$
- 3.7** Consider the following statements:
 (1) Cutting edge is normal to cutting velocity.
 (2) Cutting force occurs in two directions only.
 (3) Cutting edge is wider than the depth of cut.
 The characteristics applicable to orthogonal cutting are
 (a) (1) and (2) (b) (1) and (3)
 (c) (2) and (3) (d) (1), (2), and (3)
- 3.8** Thrust force will decrease with increase of
 (a) primary cutting-edge angle (b) tool nose radius
 (c) rake angle (d) auxiliary cutting-edge angle
- 3.9** A carbide tipped tool of designation 0, 10, 5, 5, 8, 90, 1 in the orthogonal system is used to turn a 50 mm diameter workpiece at $v = 240$ m/min and $s = 0.25$ mm/rev. The data from the cutting test are $P_z = 180$ kg, $P_x = 100$ kg and chip thickness = 0.32 mm. Calculate the shear angle, normal force in the shear plane, friction force, coefficient of friction, friction angle, and chip velocity.
- 3.10** An orthogonal cutting test on mild steel was conducted with a 5° rake angle and the cutting force and thrust force were found to be 900 N and 450 N, respectively. What is the friction angle?
 (a) 26.6° (b) 31.5°
 (c) 45° (d) 63.4°
- 3.11** In orthogonal turning of a pipe with a tool of rake angle 10° , the shear angle is 27.75° . Applying Merchant's shear angle relation, the coefficient of friction at the tool-chip interface is
 (a) 0.18 (b) 0.36
 (c) 0.71 (d) 0.98
- 3.12** In an orthogonal cutting test with a tool of rake angle 10° , the chip reduction coefficient was found to be 3.33 and the cutting and thrust components of the cutting force were found to be 1290 N and 1650 N, respectively. Determine the coefficient of friction at the tool-chip interface and the shear and normal forces acting on the shear plane.
- 3.13** While turning a 90 mm diameter pipe at $v = 50$ m/min and $s = 0.2$ mm/rev, the following values were recorded: $P_z = 41.8$ kgf, $P_x = 10.9$ kgf, length of chip = 125 mm. If $\gamma = 20^\circ$ and $\theta = 90^\circ$, calculate the friction angle and shear angle. Also determine the resultant cutting force and its inclination to the shear plane.

Chapter

4

TOOL WEAR AND THERMODYNAMICS OF CHIP FORMATION

4.1 Heat Sources and Its Distribution

Heat is produced in a metal cutting operation due to conversion of mechanical energy when work is done to produce a chip. Extensive experimental studies have established that during machining of most of the industrial materials, around 99 percent of the work of cutting is converted into heat. Work of cutting may be expressed as follows:

$$W_c = P_z v \text{ kg m/min} \quad (4.1)$$

where

$$P_z = \text{cutting force, kg} \\ v = \text{cutting speed, m/min}$$

The heat produced by this work is found as follows:

$$Q = \frac{P_z v}{E}, \text{ cal/min} \quad (4.2)$$

where

$$E = \text{mechanical equivalent of heat} = 427 \text{ kgm/cal}$$

As the total heat produced is proportional to the work of cutting, its magnitude will depend on all the factors that affect P_z , that is, mechanical properties of the work material, tool geometry, and the machining conditions.

The main sources of heat produced in metal cutting are as follows:

- (i) Primary shear zone where most of the plastic deformation takes place; heat produced is say Q_s .
- (ii) Tool–chip interface where heat is produced due to secondary plastic deformation in a thin layer of the chip and the friction between the chip and the tool face; heat produced is say Q_f .
- (iii) Flank–machined surface interface due to plastic deformation in a thin layer of the machined surface and the rubbing between the tool flank and the machined surface; heat produced is say Q_{fl} .

The total heat produced in cutting operation can thus be expressed as the sum of the heat from the above three sources; that is,

$$Q = Q_s + Q_f + Q_{fl} \quad (4.3)$$

The distribution of heat generated at the above locations is shown in Figure 4.1, wherefrom it is seen that

- (i) heat produced in the shear zone is shared between the workpiece (Q_{swp}) and the chip (Q_{sc}).
- (ii) heat produced at the tool–chip interface is shared between the chip (Q_{fc}) and the tool (Q_{ft}).
- (iii) heat produced at the flank–machined surface interface is shared between the tool (Q_{flt}) and the workpiece ($Q_{fl.wp}$).

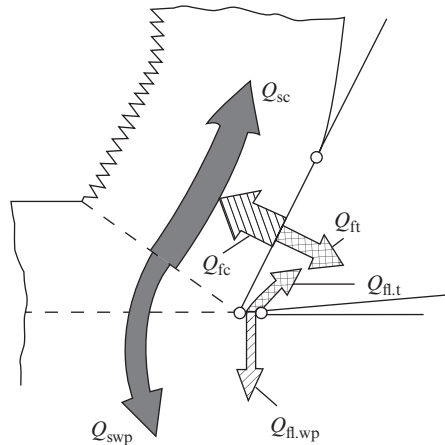


Figure 4.1 Flow of heat in workpiece, tool, and chip

The heat balance in metal cutting may therefore be represented by the following relation:

$$Q = Q_{wp} + Q_t + Q_c + Q_o$$

where

- Q_{wp} = heat transmitted to the workpiece
- Q_t = heat transmitted to the cutting tool
- Q_c = heat carried away by the chip
- Q_o = heat lost by radiation in the surrounding environment

The relative distribution of the total heat between the workpiece, chip, and tool depends mainly on the mechanical and thermal properties of the work material. This data are given in Table 4.1 for three materials.

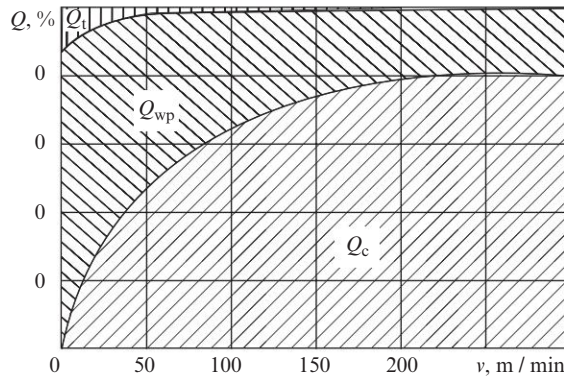
The data are quite illustrative in highlighting the effect of work material. Less heat going into the chip in the case of cast iron as compared to structural steel is due to the formation of discontinuous chips. In the case of aluminum, the remarkably low percentage of heat going into the chip is due to its high thermal conductivity, which is approximately 5–6 times that of structural

Table 4.1 Relative distribution of heat between chip, workpiece, and tool

| Work material | Percent of heat going into | | | |
|------------------|----------------------------|-----------|------|-------------|
| | Chip | Workpiece | Tool | Environment |
| Structural steel | 71 | 26 | 1.9 | 1.1 |
| Cast iron | 42 | 50 | 1.5 | 6.5 |
| Aluminum | 21 | 73 | 2.2 | 3.8 |

steel and cast iron. All tool materials have very poor thermal conductivity, which explains the very small percentage of heat going into the tool irrespective of the work material being machined. This is especially true of cemented carbide and ceramic tools

Cutting speed also plays an important role in relative distribution of total heat between the workpiece, chip, and tool. As shown in Figure 4.2, with the increase of cutting speed, the heat going in the chip increases, whereas that going in the tool and workpiece decreases. With the increase of cutting speed, shearing of the chip proceeds faster. Therefore, there is little time for heat generated in the shear plane to be transferred to the workpiece, and most of it is carried away by the chip. The reduction in percentage of heat going into the tool with the increase of cutting speed is due to reduction of the width of tool–chip contact on the tool face and the consequent reduction of the area through which heat from the chip is transmitted to the tool.

**Figure 4.2** Effect of cutting speed on flow of heat in workpiece, tool, and chip

With the increase of cutting speed, the average chip temperature θ_{cav} increases rapidly in the beginning, but as the cutting speed is increased further, the rate of increase of θ_{cav} slows down and finally stabilizes at a certain level that depends on the mechanical properties of the work material, tool geometry, feed s , and depth of cut t (Figure 4.3). As discussed earlier, a very small fraction of the total heat generated in metal cutting goes in the tool. However, due to the poor thermal conductivity of the tool material and continuously moving heat source (chip flowing along the tool face), bulk of the heat transmitted to the tool remains concentrated at the tool face, resulting in high temperature at the tool–chip interface θ_{t-c} , which rises continuously with the increase of cutting speed. To illustrate this, while machining structural steel with a P-grade cemented carbide tool, the average chip temperature θ_{cav} stabilizes at about 400°C at a cutting speed of 200 m/min,

but the tool–chip interface temperature θ_{t-c} at the same speed is about 800°C and may rise up to 900°C at $v = 400$ m/min and 950°C at $v = 600$ m/min.

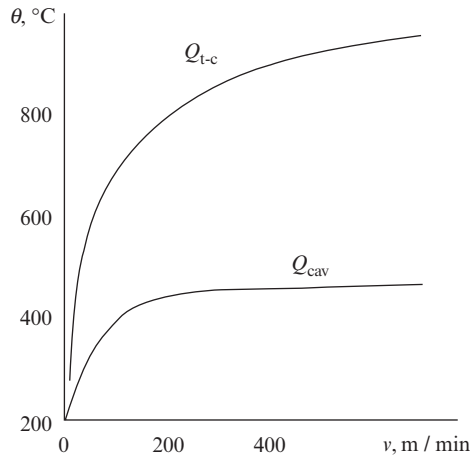


Figure 4.3 Effect of cutting speed on average chip temperature and tool–chip interface temperature

It may be mentioned in conclusion that depth of cut t and feed s have little effect on the heat generated per unit volume of the chip removed. On the contrary, increase of t and s is accompanied by a slight reduction of θ_{cav} on account of the increased undeformed chip area.

4.2 Tool Failure and Tool Wear

The combination of high tool–chip interface temperature and high pressure leads to failure of the tool by one of the following methods:

- (i) microchipping
- (ii) gross fracture
- (iii) plastic deformation
- (iv) gradual wear

Microchipping refers to the separation of small pieces up to 0.3 mm in size from various points of the cutting edge. When the size of the disintegrating pieces is between 0.3 and 1.0 mm, the mode of tool failure is referred to as gross fracture. Both these modes of failure occur when the tool is subjected to too high a cutting force or when machining is accompanied by the formation of too large a built-up edge (BUE). The likelihood of these modes of failure increases when the tool material is extremely brittle. To a large extent, these modes of failure can be avoided by proper selection of machining parameters, tool material, and its geometry.

Tool failure by plastic deformation occurs when the cutting temperature is too high relative to the softening point of the tool material. This is observed mostly while machining with cemented carbide tools at very high cutting speed. As a result of plastic deformation, the tool wedge becomes curved due to which a part of the tool face adjoining the cutting edge is lowered by h_1 and a part of the tool flank adjoining the cutting edge bulges out by h_2 (Figure 4.4). Lowering of the tool face creates a large negative rake angle near the cutting edge, resulting in very high cutting force. Bulging of the flank creates a zero- or negative-clearance angle that causes rapid wear of the tool flank. This mode of failure just as microchipping and gross fracture is mainly the result

of poor machining practice and can largely be avoided by proper selection of the tool material and cutting speed.

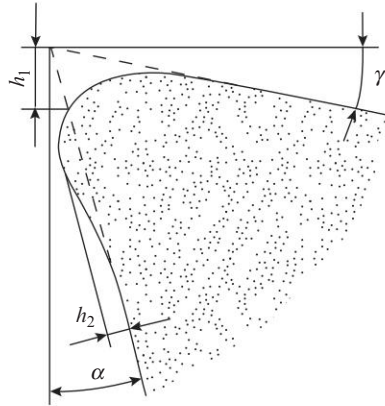


Figure 4.4 Plastic deformation of the tool wedge

If cutting is being carried out with proper selection of tool material, tool geometry, and machining parameters, then degeneration of the cutting ability of the tool should occur by gradual wear, and the tool should be deemed to have failed when the cumulative wear reaches a certain predefined level known as wear criterion. Tool wear is mainly of two types:

- (i) Type-1 wear that takes place only on the tool flank
- (ii) Type-2 wear that takes place simultaneously on both the tool flank and face

A third type of wear that takes place only on the tool face is observed while machining with HSS tools when faulty selection of machining parameters leads to heat generation in excess of the thermal resistance of the tool material. This type of wear is indicative of poor machining practice and must not be permitted.

Type-1 wear appears as a land of width h_z on the tool flank (Figure 4.5a). This width in general varies along the length of the primary cutting edge but is usually maximum at the tool tip (Figure 4.5b). However, another maximum in the form of a thin groove may sometimes be observed at the other end of the wear land coinciding with the external surface of the workpiece (Figure 4.5c).

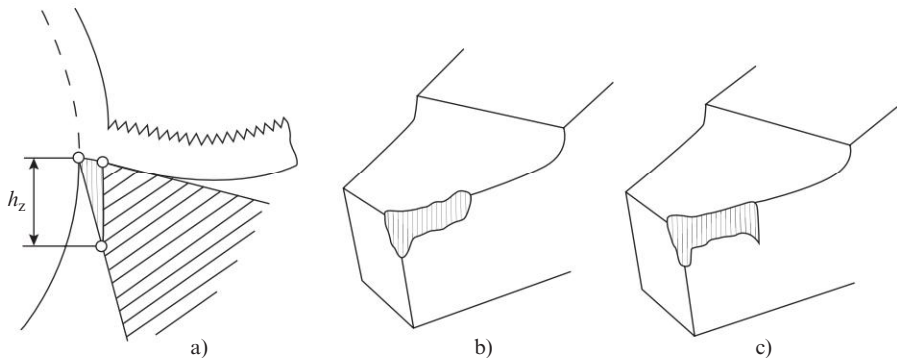


Figure 4.5 Flank wear depicting (a) width of flank wear land, (b) maximum flank wear at tool tip, and (c) maximum flank wear at tool tip and end point of tool-workpiece contact

In type-2 wear, the wear on the tool flank described earlier is accompanied by simultaneous wear on the tool face. The friction between the chip and tool face produces a crater of width b_c and depth h_c (Figure 4.6a). This crater is located roughly parallel to the primary cutting edge and its length l_c is equal to the effective length of the primary cutting edge.

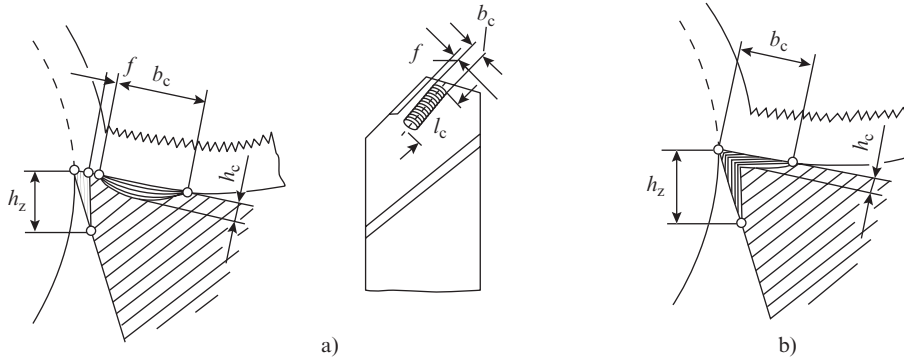


Figure 4.6 Crater wear depicting (a) width and depth of crater and (b) location of crater relative to the primary cutting edge

The crater is located at a distance f from the primary cutting edge that varies with the cutting speed. At low cutting speeds (using HSS tool), a thin strip of width f separates the edge of the crater from the primary cutting edge. Cutting at low speed is accompanied by formation of built-up edge; therefore, wear on the tool face proceeds only beyond the limits of the stagnant zone (Figure 3.20). This explains the presence of the thin strip of width f . Of course, as wear increases with cutting time, f continuously decreases and the edge of the crater comes closer to the primary cutting edge. Cutting must be stopped when f reaches a prespecified minimum value; otherwise, it may lead to catastrophic failure of the primary cutting edge. When machining is carried out at high cutting speeds at which BUE is not formed, the edge of the crater virtually coincides with the primary cutting edge, that is, $f \approx 0$ (Figure 4.6b). On a worn tool, the crater on the tool face merges with the wear land on the tool flank, and it becomes difficult to distinguish between the two.

The type of wear that a cutting tool will experience depends mainly on the type of work material, undeformed chip thickness (feed), and cutting speed.

While machining brittle materials, wear occurs mostly on the tool flank (type-1 wear). For explanation, refer to Eqn. (3.10) that clearly shows that the relative velocity v_z between the tool flank and workpiece is ξ times the relative velocity v_c between the chip and the tool face. As the value of chip reduction coefficient ξ typically lies between 1.5 and 4.0 (see Section 2.3), rubbing on the tool flank is that many times more than at the tool face. This is the reason for the predominant prevalence of type-1 wear in machining of brittle materials. While machining these materials, crater wear may be observed only at very high cutting speeds.

The picture is more complicated in machining of ductile materials. At very low cutting speeds (<5 m/min), wear at the tool flank is more dominant for the reasons explained above. In the range of cutting speed in which BUE phenomenon is significant (10–50 m/min), the BUE virtually becomes an extension of the cutting edge, thus protecting the tool flank. Under these conditions, the wear is initially concentrated mainly on the tool face. However, as the crater width increases with cutting time, the support width f of the BUE continuously decreases till a stage is reached when it is no longer able to support the BUE. At this stage, flank wear also begins to take place.

At high cutting speeds, wear is more at the tool flank for thin chips ($a < 0.1$ mm). However, as chip thickness increases, crater wear begins to play a more important role, because of the higher pressure exerted by a thicker chip on the tool face resulting in higher temperature at the tool face as compared to that at the tool flank. In general, the larger the values of v and a , the greater is the magnitude of crater wear and correspondingly less is the flank wear. Cutting data on machining of mild steel with a cemented carbide tool at $v = 50\text{--}200$ m/min are illustrative of the above pattern of change of wear with a . At $s = 0.08$ mm/rev, flank wear comprised 60–80 percent of the total wear; at $s = 0.24$ mm/rev, flank and crater wear were almost equal; and at $s = 0.46$ mm/rev, crater wear comprised 60–90 percent of the total wear.

4.3 Growth of Tool Wear with Cutting Time, Wear Criteria, and Wear Mechanisms

The growth of tool wear with cutting time is represented by means of wear curves. A typical wear curve of type-2 wear when the wear on tool flank and rake face is more or less equal is shown in Figure 4.7(a). This curve consists of three distinct zones: Zone I (OA) is the zone of initial wear during which the surface asperities of the tool and workpiece contacting surfaces rub heavily against each other. This zone represents the run-in period of the cutting tool and is distinguished by a high rate of wear. As the contacting surfaces smooth out, the rate of wear decreases and a period of more or less gradual uniform wear sets in. This is represented by zone II (AB). When the cumulative wear attains a certain level, there is a sharp rise in the wear, especially on the tool flank. Thus, zone III (BC) represents the zone of accelerated wear. With the onset of accelerated wear, cutting must be stopped immediately; otherwise, it may lead to catastrophic failure of the entire cutting edge. If machining parameters are properly selected, zone II comprises approximately 85–90 percent of the tool life. As cutting speed is increased, the length of zone II decreases. At excessively high cutting speeds, zone II may disappear completely and catastrophic failure of the tool may occur immediately after the run-in period.

When wear on the tool face is much less than that on the tool flank, the wear curve appears as shown in Figure 4.7(b). In this case, the zone of the run-in period is absent. In the zone of gradual uniform wear, the wear initially proceeds slowly, but picks up pace as cutting time increases. The rate of wear continuously increases till catastrophic failure of the tool sets in at point B.

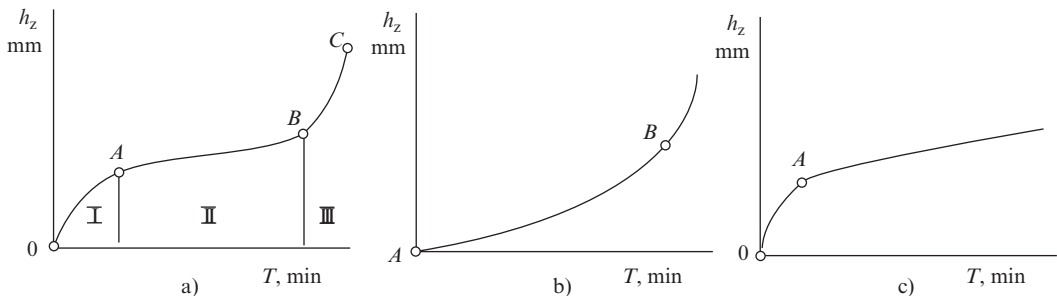


Figure 4.7 Variation of tool wear with cutting time (a) when wear occurs equally on tool flank and rake face, (b) when wear on tool flank is significantly higher than at the rake face, and (c) when wear occurs only on the tool flank

If the tool wears only on the flank (type-1 wear), the wear curve appears as shown in Figure 4.7(c). In this case, the zone of initial wear (OA) is similar to that shown in Figure 4.7(a), but the zone of gradual uniform wear continues for much longer than in the first two cases. In fact, the duration of this period is so large that cutting with the tool is terminated before accelerated wear has set in due to unacceptably high deterioration of quality of the machined surface.

As can be noted from a comparison of Figures 4.5 and 4.6, crater wear is more complicated than flank wear. The variation of crater wear parameters with cutting time is shown in Figure 4.8. The crater length l_c that is equal to the effective length of the cutting edge remains practically constant. Variation of h_c follows the same trend as the wear curve of Figure 4.7(a) with three distinct zones as explained earlier. With the increase of cutting time, crater width b_c increases. As the enlarging crater moves toward the primary cutting edge, it encroaches on the strip separating the crater from the cutting edge. Thus, increase of b_c is accompanied by a corresponding reduction of f , as can be noted from the relevant curves in Figure 4.8.

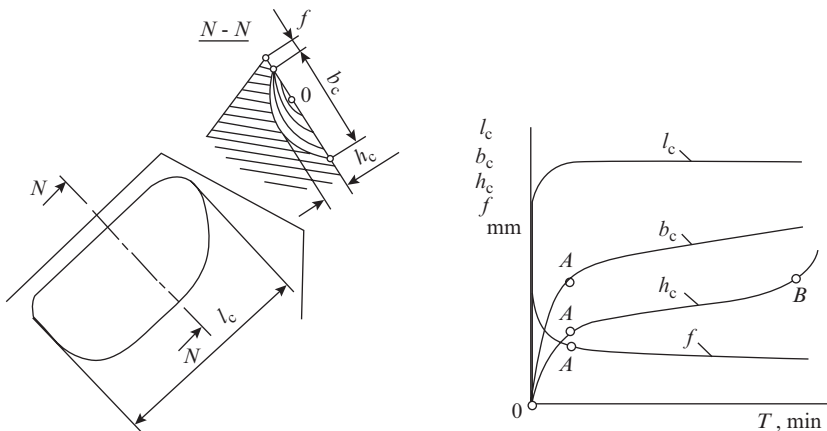


Figure 4.8 Variation of crater parameters with cutting time

Tool wear can also be assessed by volumetric measurements. The loss in weight of the cutting tool serves as measure of the wear. This method has been found useful in determining the wear of grinding wheels, but has not found favor in the case of cutting tools, because of the difficulty of distinguishing between the contribution of flank and crater wear in the total volumetric wear. In addition, the weight loss due to wear being very small as compared to the weight of the tool, the accuracy of this method is somewhat suspect.

Radioactive tracing has also been attempted as a method of volumetric wear measurement. In this method, radioactive isotopes are produced in the cutting tool by bombarding it with nuclear particles. These isotopes are carried away by the chips as a part of the wear particles. The radioactivity of the chip segments is measured by a scintillation detector and serves as measure of the tool wear. This method allows measurement of tool wear without interrupting the cutting process, and therefore appears to be particularly suitable for rapid evaluation of tool wear. However, one has to bear in mind that tool wear is not uniform along the cutting edge, nor does it follow a uniform pattern in time as well as location on different parts of the face and flank. Such odd variations cannot be detected by this method. All these factors considered together with the high initial cost and mandatory safety precautions restrict the use of this method only to laboratory experiments.

4.3.1 Tool Wear Criteria

If cutting with a tool is stopped and the tool sent for regrinding well short of point B on the wear curve (Figure 4.7a), then the total cost of tool usage will go up due to frequent regrinding. On the contrary, if cutting is allowed to continue well beyond point B, then the severe damage caused to the cutting edge by accelerated wear will require a large layer of tool material to be removed during regrinding. This will increase the regrinding cost and also reduce the number of times a tool may be reground during its total life span, thereby again increasing the total cost of tool usage. Continuing to use a cutting tool till it is badly worn out is not desirable also because this will be accompanied by a sharp increase of cutting force and temperature and will adversely affect the accuracy and finish of the machined surface. It is thus seen how important it is to decide a rational level of wear, known as “wear criterion” for economical and technically proper use of the cutting tool. Here, it may be recalled that flank wear takes place in machining of all types of materials and under all types of machining conditions. Crater wear, on the contrary, is absent in machining of brittle materials; and even in machining of ductile materials, it is significant only at high cutting speed and large feed rate. Flank wear is therefore a more universal criterion. What makes it even more attractive for adoption as “wear criterion” is that it is far easier to measure the flank wear land width h_z compared with the parameters h_c , b_c , l_c , and f associated with crater wear. Hence, h_z is used as the wear criterion in general, but h_c or a combination of h_c with other parameters of crater wear is used as the wear criterion when crater wear is overwhelmingly predominant. The important wear criteria that are used in machining practice are described below.

Optimum Wear Criterion for Flank Wear The tool is considered to be worn out and in need of regrinding when the width of the flank wear land attains an optimum value, which maximizes the total service life of the tool, that is, it maximizes

$$Z = NT \quad (4.4)$$

where

Z = total service life of cutting tool

N = number of possible regrindings of the tool

T = tool life, that is, cutting time between two regrindings

Figure 4.9 shows flank wear of a tool with a cutting bit of width B . The width of the flank wear land is h_z . For restoring the worn edge, it would be necessary to remove a layer of thickness y parallel to the tool flank to restore the cutting edge. Successive such layers can be removed till we reach the limit of the usable width of the cutting bit H , which is generally $2/3$ of the original width B .

The number of possible regrindings of this tool is

$$N = \frac{H}{y}$$

where

$$y = p + \Delta$$

where Δ is tolerance on grinding of the flank that is generally taken equal to 0.1–0.15 mm.

From Figure 4.9, it can be noted that

$$p = \frac{a}{\cos \gamma}$$

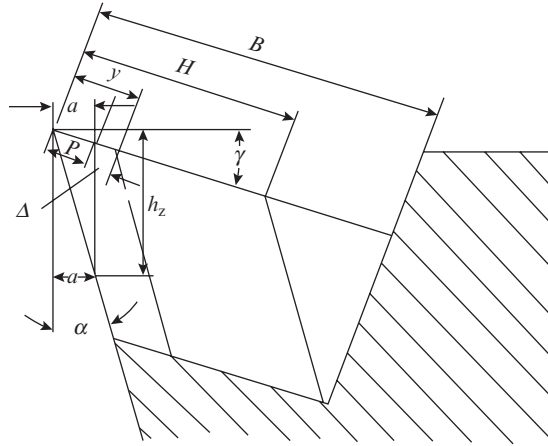


Figure 4.9 Elements of flank wear and regrinding of tool flank

and

$$a = h_z \tan \alpha$$

Therefore,

$$p = \frac{h_z \tan \alpha}{\cos \gamma}$$

Hence,

$$N = \frac{H}{\frac{h_z \tan \alpha}{\cos \gamma} + \Delta}$$

For a particular tool, clearance angle α and rake angle γ are constant, therefore representing $\frac{\tan \alpha}{\cos \gamma} = c$, the above expression for N may be simplified as follows:

$$N = \frac{H}{ch_z + \Delta}$$

If T is the tool life, then, the total service life of the tool may be expressed as follows:

$$Z = NT = \frac{HT}{ch_z + \Delta} \tag{4.5}$$

The value of h_z at which Z is maximum is found from the condition $\frac{dZ}{dh_z} = 0$; applying this condition to Eqn. (4.5), we get

$$\frac{dZ}{dh_z} = \frac{H \left[\frac{dT}{dh_z} (ch_z + \Delta) - cT \right]}{(ch_z + \Delta)^2} = 0$$

Wherefrom

$$\frac{dT}{dh_z} = \frac{cT}{ch_z + \Delta} = \frac{T}{h_z + \frac{\Delta}{c}}$$

Hence,

$$\frac{dh_z}{dT} = \frac{1}{T} \left(h_z + \frac{\Delta}{c} \right) \tag{4.6}$$

From the wear curve of flank wear shown in Figure 4.10, it can be noted that Eqn. (4.6) is satisfied by a tangent to the wear curve, such that it produces an intercept Δ/c on the negative side of the h_z axis. It can also be noted from Figure 4.10 that practically the point where such a tangent can be drawn will be the point of inflexion B on the wear curve that denotes the onset of accelerated flank wear. The width of flank wear land h_z corresponding to point B of the wear curve is taken as the wear criterion.

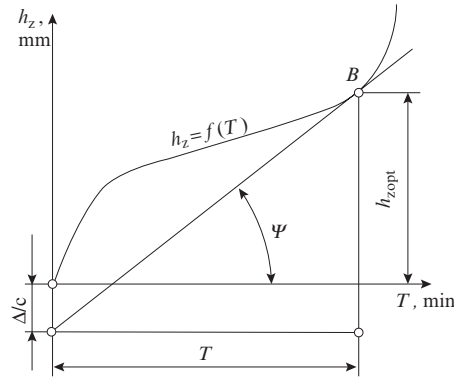


Figure 4.10 Schematic for determining optimum flank wear land width

Optimum Wear Criterion for Crater Wear The tool is considered to be worn out and in need of regrinding when the crater depth attains an optimum value that maximizes the total service life of the tool as expressed by Eqn. (4.4). Figure 4.11(a) shows crater wear on a tool with a cutting bit of height C.

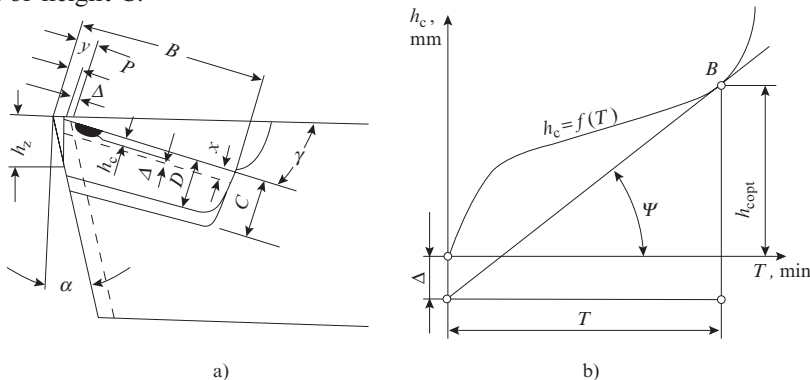


Figure 4.11 Crater wear (a) elements of crater wear and regrinding of tool face and (b) schematic for determining optimum crater depth

The depth of the crater is h_c , and it would be necessary to remove a layer of thickness $h_c + \Delta$ parallel to the tool face to restore the cutting edge. Successive such layers can be removed till we reach the limit of the usable height of the bit D , which is generally $2/3$ of the original height C . The number of possible regrindings of this tool is

$$N = \frac{D}{x} = \frac{D}{h_c + \Delta}$$

Where Δ is the tolerance on grinding of the tool face, which is generally taken equal to 0.1–0.15 mm.

If T is the tool life, then the total service life of the tool may be expressed as follows:

$$Z = NT = \frac{DT}{h_c + \Delta} \quad (4.7)$$

The value of h_c at which Z is maximum is found from the condition $\frac{dZ}{dh_c} = 0$; applying this condition to Eqn. (4.7), we get

$$\frac{dZ}{dh_c} = \frac{D \left[\frac{dT}{dh_c} (h_c + \Delta) - T \right]}{(h_c + \Delta)^2} = 0$$

Wherefrom

$$\frac{dT}{dh_c} = \frac{T}{h_c + \Delta}$$

Hence,

$$\frac{dh_c}{dT} = \frac{1}{T} (h_c + \Delta) \quad (4.8)$$

From the crater depth-cutting time wear curve shown in Figure 4.11(b), it can be noted that Eqn. (4.8) is satisfied by a tangent to the wear curve such that it produces an intercept Δ on the negative side of the h_c axis. It can also be seen from Figure 4.11(b) that the point where such a tangent can be drawn will be the point of inflexion B on the wear curve that denotes the onset of accelerated crater wear. Crater depth h_c corresponding to point B of the wear curve is taken as the wear criterion.

A major drawback of the optimum wear criteria discussed above is that they cannot be applied if a distinct point of inflexion denoting the onset of accelerated wear cannot be identified on the wear curve. This happens while machining relatively soft materials with cemented carbide tools where it can be noted that the tool wear might gradually build up to the level at which the tool is unfit for further use without showing any sign of the onset of accelerated wear. Another drawback of the optimum wear criteria is that for their application wear curves have to be plotted almost upto the point of catastrophic tool failure. This process is quite lengthy and may involve consumption of large amount of workpiece material. In such cases, it is more feasible to adopt wear criteria that do not involve plotting of the wear curve. A few of these criteria are described below.

Bright Band Criterion The tool is considered to be worn out and in need of regrinding when a bright band appears on the cutting surface while machining steels or when dark spots appear while machining cast iron. This happens when small chunks of the cutting edge begin to chip off. The damaged portion of the cutting edge loses the capability of chip formation by shearing and only ends up burnishing the cutting surface which is seen as a bright band. The appearance of bright band corresponds to the onset of accelerated wear, and it is the signal for cutting to be stopped immediately. The width of the flank wear land h_z when the bright band appears is taken as the wear criterion.

Force Criterion The tool is considered to be worn out and in need of regrinding when the cutting force, especially its radial component P_y and axial component P_x register a sharp increase. The width of the flank wear land h_z when the sharp increase of cutting force takes place is taken as the wear criterion. The drawback of this method is that it is necessary to continuously monitor the cutting force by means of a dynamometer. Therefore, this method is not suitable for shop floor applications.

Processing Criterion This criterion is applied for tools used in finishing operations. The tool is considered to be worn out and in need of regrinding when the machined surface fails to meet the quality requirements in terms of dimensional tolerance and/or surface finish. The width of the flank wear land h_z at which this occurs is taken as the wear criterion. This criterion is much smaller in magnitude compared to the rest of the criteria discussed above because the tool becomes unfit for cutting due to process limitation much before its wear is anywhere near the onset of accelerated wear.

Recommended values of h_z for some typical cases are give below:

(i) HSS tool

$h_z = 0.6\text{--}1.0$ mm for semirough machining of steel

$h_z = 1.5\text{--}2.0$ mm for semirough machining of cast iron

(ii) Cemented carbide tool

$h_z = 1.0\text{--}1.4$ mm for rough turning of steel

$h_z = 0.4\text{--}0.6$ mm for finish turning of steel

$h_z = 0.8\text{--}1.0$ mm for rough turning of cast iron

$h_z = 0.6\text{--}0.8$ mm for finish turning of cast iron

$h_z = 0.8\text{--}1.0$ mm for parting and cut-off tools

(iii) Ceramic tool

$h_z = 0.6\text{--}0.8$ mm

When crater wear is used as wear criterion an index h_i is calculated from the following relation:

$$h_i = \frac{h_c}{\frac{b_c}{2} + f}$$

Recommend value of h_i is 0.4 for cemented carbide tools and 0.6 for HSS tools.

4.3.2 Tool Wear Mechanisms

Wear of cutting tool limits its useful life and should therefore be minimized to the extent it is possible under the conditions in which cutting is carried out. Knowledge of how wear takes place, that is, the wear mechanism can help in this exercise. Here, it is important to understand that friction between

the rubbing surfaces of the tool and the workpiece in a cutting operation is different from the common sliding friction between mechanical bodies for the following reasons:

- (i) Rubbing between the tool and workpiece contacting surface takes place under conditions of high temperature and pressure.
- (ii) The workpiece-contacting surface is a continuously newly exposed nascent surface that is free of contaminants and oxides and, therefore, has a strong tendency of bonding.

These characteristics of friction in metal cutting are the cause of wear of the cutting tool that occurs due to macrotransfer of material by abrasion and adhesion.

Abrasion Wear is a direct consequence of the characteristics stated earlier and occurs due to ploughing of the tool matrix by hard constituents of the work material such as complex carbides of the alloying elements in steels, cementite, and phosphides in cast iron, silicon carbide in Al–Si base alloys (silumins) and intermetallics in heat resistant alloys. The ploughing action on the tool face and flank may also come from the built-up edge. Abrasion wear is prominent at low-to-moderate cutting speeds and is relatively more severe on the tool flank because the work shoulder provides a much harder backing as compared to the chip. Abrasion wear intensifies with the reduction of the tool/work hardness ratio; therefore, it is more common in high carbon and high-speed steels as compared to cemented carbide and other harder tool materials.

Adhesive Wear At relatively higher cutting temperatures, the two characteristics that describe friction in metal cutting jointly create conditions that are highly conducive for adhesion between the contacting surfaces of the tool and workpiece in the form of microwelds. When these bonds rupture, they pluck out elementary particles of the tool material, resulting in adhesion wear. Between identical materials, adhesion generally begins at a temperature equal to $(0.35–0.50)T_{\text{melting}}$, where T_{melting} is the lower of the melting temperatures of the metal pair. The tendency to form microwelds intensifies at temperatures close to the recrystallization temperature and the magnitude of adhesion wear increases with the reduction of the tool/work hardness ratio. The intensity of adhesion wear of tool materials depends on their fatigue strength and ductility. A material with higher fatigue strength and ductility will experience less adhesion wear than a material that is more brittle and has poorer fatigue strength, though both may have identical temperature resistance. At relatively low cutting temperatures, the temperature resistance of the tool material is not a critical factor; therefore at cutting temperature up to 500°C, the wear resistance of cemented carbides may be less than that of high speed steels on account of the higher fatigue strength and ductility of the latter. At higher temperatures, the ductility of cemented carbides improves and at the same time the temperature resistance of high-speed steels reaches its limit; therefore in the cutting temperature range of 500–750°C, the wear resistance of cemented carbide tools improves and their performance is superior to that of high speed steels. Adhesion wear can be reduced by using cutting fluids that produce a protective film on the contact surfaces, thereby creating a barrier to the formation of micro welds. However, it is necessary to make sure that the cutting fluid does not cause chemical wear of the tool material by dissolving the hard constituents of the tool material.

Wear is an extremely complex phenomenon as it depends on several factors such as tool and work material, cutting environment, cutting temperature, machining parameters, etc. It is therefore difficult to pin point exactly when the wear mechanism changes from abrasion to adhesion. In addition, pure adhesion wear is uncommon because the material transfer that occurs during adhesion wear also simultaneously produces some abrasion.

Diffusion Wear A sharp increase in tool wear at cutting temperatures above 800°C is attributed to diffusion wear due to diffusion mass transfer of the tool material into the work material. It is a process based on microtransfer of atoms from the crystal lattice of one material to that of another. In general, the diffusion process between any two materials follows a parabolic law according to which the rate of diffusion is initially very high but gradually diminishes and asymptotically approaches zero rate. In case of metal cutting, a fresh nascent surface of the workpiece and a new chip surface are continuously engaged in contact with the tool flank and rake face, respectively. Therefore, the initial high rate of diffusion is steadily sustained over a long period of time and can result in a substantial mass of the cutting tool getting diffused into the workpiece and chip. Diffusion rate is a temperature dependent process and is a direct function of the cutting speed. However, the amount of material transferred by diffusion depends on the duration of contact between the rubbing surfaces and is therefore an inverse function of cutting speed. The relation between cutting speed and diffusion wear is therefore a complex one. For instance, the belief that an increase of cutting temperature with increase of cutting speed will cause higher diffusion metal transfer is not confirmed by actual wear studies.

The temperature threshold of 800–850°C above which diffusion wear becomes important is far too high for high-speed steel tools with typical temperature resistance of 600–700°C. Therefore, diffusion wear studies have mainly focused on cemented carbide tools. The various components of cemented carbide diffuse into the work material at different rates. The rate of diffusion is fastest for carbon, whereas that of tungsten, cobalt, and titanium is slower. On account of the different rates of diffusion between the tool, chip, and workpiece, three distinct diffusion layers are observed while machining steel with a cemented carbide tool. The carbon enriched layer is located the farthest from the contact interface. The next is a white layer that represents the solid solution of carbon + tungsten or carbon + tungsten + titanium in γ -iron. The third layer that lies at the contact interface is an intermetallic of iron and tungsten. This layer experiences structural changes due to reverse diffusion of iron from the workpiece and is softer and at the same time more brittle than the main body. This weakened layer is therefore prone to separation from the contact surfaces of the tool and is carried away by the flowing chip or the workpiece. The wear of cemented carbide tools thus occurs owing to a combination of two mechanisms: diffusion and adhesion. The diffusion wear by direct micrometal transfer is the primary mechanism, whereas the breaking away of the surface layers weakened by structural transformation and their macroremoval with the chip and workpiece is the secondary mechanism. It has been observed from wear studies that although the amount of tool metal transfer through diffusion per unit time increases with the increase of cutting speed as a result of direct diffusion, the percentage of diffusion wear as a fraction of total wear actually decreases because of the increased role of the secondary mechanism.

Diffusion is also influenced significantly by the bonding affinity of the metals of the contact surfaces. While machining steel with a single carbide tool (tungsten + cobalt), the strong affinity of cobalt binder of the tungsten carbide with some of the alloying elements of steel can result in diffusion of cobalt out of the tool and cause rapid wear of the tool in the form of severe cratering. To some extent this problem can be controlled by addition of titanium and tantalum in the cemented carbide. A more glaring example of the role of affinity is seen in machining of steels with diamond tools. Being one of the allotropic forms of carbon, diamond has a strong affinity with the carbon in other materials. When heated in air at 700–800°C diamond undergoes graphitization and the outer layers of the diamond crystal are transformed to amorphous carbon. When steel is machined with a diamond tool, intensive diffusion of diamond in iron takes place at temperature of 700–750°C,

rendering the diamond tool useless for cutting in a very short time. In view of the above, diamond tools are never used for machining of steels, though given their exceptionally high hardness they are widely used in precision machining of plastics, nonferrous alloys, semiconductors, and other engineering materials, where the low temperature resistance of diamond is not a limiting factor.

Chemical Wear Metal cutting is often carried out with the application of a cutting fluid to reduce the cutting temperature. If the cutting fluid is chemically active with respect to the tool material, then the wear rate may be greatly enhanced by the chemical reaction. Such cutting fluids form a layer of low shear strength solid lubricant at the tool–work interface resulting in less friction and better surface finish. Hence, sometimes when surface finish of the machined component is a primary concern, the use of chemically active cutting fluids is accepted even though it involves higher tool wear rate and shorter tool life. A special form of chemical wear in cemented carbide tools is related to oxidation of the various carbide constituents. At cutting temperature of 700–800°C, the cobalt binder in cemented carbide enters into a chemical reaction with atmospheric air forming CoO and Co₃O₄. Similarly, WC and TiC also react with the atmospheric oxygen forming WO₃ and TiO₂. These oxides are not restricted to the contact surfaces and partially affect the subsurface tool material too up to a certain depth. The hardness of the oxides is 40–60 times less than that of the cemented carbide; therefore, the drastic softening of the cobalt binder creates favorable condition for plucking of cobalt particles out of the carbide grains by the frictional forces acting on the tool flank and rake face, and hence their rapid wear. The tendency of cobalt oxidation is stronger in single carbide tools as compared to double carbide tools and increases with the cobalt percentage in the cemented carbide. The effect of oxidation wear can be countered to a large extent by cutting in an environment of inert gases such as argon, helium, and nitrogen up to cutting temperature of 900°C.

In conclusion, it may be pointed out that the specific temperature ranges mentioned for the various wear mechanisms discussed above are to a considerable extent notional, because wear mechanisms can co exist in different combinations depending on the tool–work pair and the cutting conditions. It may also be mentioned that only abrasion and adhesion wear mechanisms have been confirmed to exist in metals beyond any doubt. Studies confirming the existence and importance of diffusion, chemical, and oxidation wear are few and far less conclusive.

4.4 Tool Life and Machinability

Tool life refers to the useful life of a tool and is the period during which a tool cuts satisfactorily or the time elapsed between two successive grindings. Tool life can be expressed in a number of ways as follows:

- (i) time of actual operation, that is, the time during which the tool is actually engaged with the workpiece, converting the work material into chips
- (ii) total time of operation, including the idle time as in intermittent cutting operations such as shaping, milling, etc.
- (iii) volume of material removed
- (iv) number of workpieces machined
- (v) total length of work machined

In machining practice, the time of actual operation is the commonly used measure of tool life. A tool is considered to have failed when it can no longer perform satisfactorily in its designated

function. Therefore, the failure criterion is linked to the requirements associated with the component being machined. For instance, in a roughing operation, surface finish and dimensional accuracy will be of little importance; therefore, tool failure may be linked to the onset of accelerated tool wear or sharp rise of cutting force. On the other hand, in a finishing operation, surface finish and dimensional accuracy will be of primary concern, and therefore tool failure will be linked to its inability to provide the desired surface finish or accuracy, although the tool wear and cutting force may be well within safe limits. Tool life will depend on the failure criterion used, and it is therefore important that the failure criterion should be clearly stated when tool life values are quoted and compared. For instance, for a given tool–work pair the tool life for wear criterion $h_z = 0.3$ mm will be substantially less than the tool life for the same pair if the wear criterion is $h_z = 1.0$ mm.

From among the wear criteria (discussed in Section 4.3.1), the width of flank wear land h_z is the one that is most widely used in machining practice for several reasons. Its biggest virtue is that it can be easily measured with a Brinell microscope. An added advantage is that h_z is related to the performance parameters of the cutting process such as surface finish and cutting force. However, a major short coming of using h_z as wear criterion is that it is not uniform along the length and for convenience the maximum value of h_z is taken as the measure of flank wear. The value of h_z selected as wear criterion depends on several factors such as desired dimensional accuracy and surface finish, maximum permissible cutting force and tool regrinding cost etc. Obviously, a small value of h_z will be adopted as wear criterion for finishing cuts where dimensional accuracy and surface finish are crucial, but a larger value of h_z will be appropriate for roughing cuts to derive the economic benefit of a longer tool life.

It was mentioned in Section 4.3.1 that a performance measure such as surface finish may be used as wear criterion in finishing operations. For this, it is necessary to measure the surface finish of the machined components continuously, so that the use of the tool can be stopped as soon as the surface roughness exceeds a certain prespecified limit. This type of measurement requires portable surface analyzers and taking of several repeat observations to account for the scatter in the readings. In view of these difficulties, even in the case of finishing operations, the process criterion is related to h_z and a suitably small value is adopted as the wear criterion.

Crater wear is also an important wear criterion. However, the problem with crater wear is that it is difficult to decide as to which crater parameter should be adopted as the wear criterion. Crater depth is a common criterion used in Europe. However, it is well known that crater wear parameters, including crater depth, are far more difficult to measure as compared to flank wear land width.

When limiting force is used as wear criterion, this requires a dynamometer, preferably coupled to a recorder. As the tool/workpiece is mounted on the dynamometer rather than directly on the carriage/slide/table, this reduces the stiffness of the machining system. The limiting force criterion is therefore used mainly in laboratory conditions for research studies. In actual shop floor machining practice, suitable value of h_z corresponding to the limiting force is determined and used as the wear criterion.

From the above discussion, it follows that notwithstanding the large number of wear criteria that exist in principle, only the flank wear land width h_z is universally used as the wear criterion conditions. Among the various performance measures of cutting process discussed above tool life is considered the most important because it is an indicator not only of tool performance but also of machinability of work material. Besides, it is a major factor in the economics of the cutting process. Tool life is related to the wear criterion. The time at which the wear criterion h_z is reached

is the tool life. From the h_z vs time curve or wear curve shown in Figure 4.12, it can be noted that tool life will change with the h_z value taken as the wear criterion.

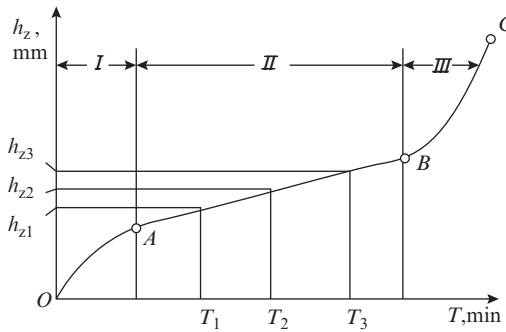


Figure 4.12 Relation between wear criterion and tool life

The parameter that has maximum effect on tool life is cutting speed. The wear curves at four different cutting speeds shown in Figure 4.13 clearly demonstrate that the gradient of the zone of gradual wear increases with the cutting speed. Therefore, for a particular value of wear criterion h_z , the tool life is found to reduce with the increase of cutting speed.

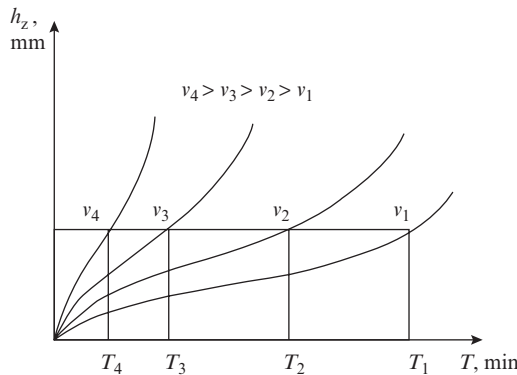


Figure 4.13 Effect of cutting speed on the gradient of wear curve or wear rate

The data presented in Figure 4.13 can be used to plot a curve relating tool life with cutting speed (Figure 4.14).

This relation can be expressed by the following equation, popularly known as Taylor's tool life equation:

$$vT^n = C \tag{4.9}$$

where

v = cutting speed, m/min

T = tool life, min

n = exponent of tool life

C = constant, known as Taylor's constant

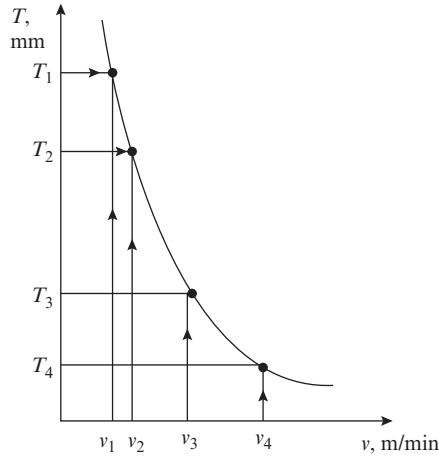


Figure 4.14 Effect of cutting speed on tool life

The parameters n and C are constant for a given pair of tool and work material and machining parameters (feed, depth of cut, tool geometry, etc.) other than cutting speed. If the tool life vs cutting speed data is plotted in log–log coordinates, a straight line as shown in Figure 4.15 is obtained.

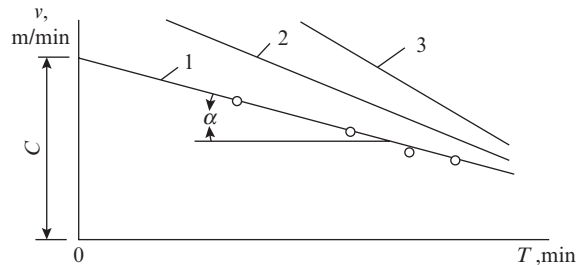


Figure 4.15 Log–log representation of the relation between cutting speed and tool life (1—HSS tool, 2—cemented carbide tool, and 3—ceramic tool)

In the log–log representation, Eqn. (4.9) may be written as follows:

$$\log vT^n = \log C$$

$$\log v = \log C - n \log T$$

$$n = \frac{\log C - \log v}{\log T}$$

Also for $T = 1$, $\log T = 0$, therefore

$$\log v = \log C$$

It is thus noted that C is the intercept on the velocity axis in Figure 4.15 and is the cutting speed that gives a 1 min tool life. The slope of the line gives the value of n . For a given work material, the slope increases with the hardness of tool material as is evident from the lines for three tool materials shown in Figure 4.15.

Example 4.1

A batch of 10 cutting tool could produce 500 components at 50 rpm, $t = 1$ mm, and $s = 0.25$ mm/rev. A similar batch of 10 tools could produce 122 components at 80 rpm and same feed and depth of cut. How many components can be produced at 60 rpm?

Feed per minute of the first tool = $50 \times 0.25 = 12.5$ mm/min

Feed per minute of the second tool = $80 \times 0.25 = 20$ mm/min

Consider that the job under consideration has length L and diameter D .

For a job of length L :

Machining time of one part with first tool = $\frac{L}{12.5}$ min

Machining time of one part with second tool = $\frac{L}{20}$ min

As 10 tools are used for producing the batches in both cases,

$$\text{Life of tool 1} = \frac{500}{10} \times \frac{L}{12.5} = \frac{50L}{12.5}$$

$$\text{Life of tool 2} = \frac{122}{10} \times \frac{L}{20} = \frac{12.2L}{20}$$

For a job of diameter D :

$$\text{Cutting speed of tool 1} = \frac{\pi D \times 50}{1000} = \frac{\pi D}{20}$$

$$\text{Cutting speed of tool 2} = \frac{\pi D \times 80}{1000} = \frac{\pi D}{12.5}$$

Applying both sets of data to Taylor's tool life equation:

$$\left(\frac{\pi D}{20}\right)\left(\frac{50L}{12.5}\right)^n = \left(\frac{\pi D}{12.5}\right)\left(\frac{12.2L}{20}\right)^n$$

$$\left(\frac{50}{12.5} \times \frac{20}{12.2}\right)^n = \frac{20}{12.5}$$

$$(6.557)^n = 1.6$$

Hence, $n = 0.25$

Now at 60 rpm, we have for tool 3

Feed per minute = $0.25 \times 60 = 15$ mm/min

Machining time of 1 part = $\frac{L}{15}$ min

$$\text{Cutting speed} = \frac{\pi D \times 60}{1000} = \frac{\pi D}{16.67}$$

If number of parts produced by this tool is X , then tool life of the third tool = $X \frac{L}{15}$

Again applying Taylor's tool life equation to tool numbers 1 and 3, we get

$$\begin{aligned} \left(\frac{\pi D}{20}\right)\left(\frac{50L}{12.5}\right)^{0.25} &= \left(\frac{\pi D}{16.67}\right)\left(\frac{XL}{15}\right)^{0.25} \\ \left(\frac{50}{12.5} \times \frac{15}{X}\right)^{0.25} &= \frac{20}{16.67} = 1.2 \\ X^{0.25} &= \frac{2.783}{1.2} = 2.319 \end{aligned}$$

Hence $X = 29$ parts.

Example 4.2

In machining tests with two tools A and B , the exponent n and constant C were found to be 0.45 and 90 for tool A and 0.3 and 60 for tool B . Determine the cutting speed above which tool A will have higher tool life than tool B .

Let v be the cutting speed above which tool A will have higher tool life than tool B . At v , the tool life is same for both, hence

$$vT_A^{0.45} = 90 \text{ and } vT_B^{0.3} = 60$$

Taking log on both the sides,

$$\begin{aligned} l_n v + 0.45 l_n T_A &= l_n 90 \text{ and} \\ l_n v + 0.3 l_n T_B &= l_n 60 \\ l_n T_A - l_n T_B &= \frac{l_n 90 - l_n v}{0.45} - \frac{l_n 60 - l_n v}{0.30} \end{aligned}$$

As $T_A = T_B$ at cutting speed of v , we get

$$\begin{aligned} 0 &= \frac{0.3 l_n 90 - 0.3 l_n v - 0.45 l_n 60 + 0.45 l_n v}{0.45 \times 0.3} \\ 0.15 l_n v &= 0.4925 \end{aligned}$$

Hence, $v = 26.67$ m/min

Tool life is also affected by feed and depth of cut, though to a much less extent than cutting speed. It reduces with the increase of feed and depth of cut. To accommodate the effect of feed and depth of cut, tool life is expressed by the following three relations:

$$\begin{aligned} T &= \frac{C_1}{v^m} \\ T &= \frac{C_2}{f^q} \\ T &= \frac{C_3}{s^p} \end{aligned}$$

Upon combining these three relations, we get

$$T = \frac{C_4}{v^m t^q s^p}$$

which yields the following expression, known as Taylor’s generalized tool life equation:

$$v = \frac{C_v}{T^{\frac{1}{m}} s^{y_v} t^{x_v}} \tag{4.10}$$

where

$\frac{1}{m} = n$ is the Taylor’s tool life exponent

$x_v = \frac{q}{m}$ is the exponent of depth of cut

$y_v = \frac{p}{m}$ is the exponent of feed

C_v = modified Taylor’s constant

Considering that the maximum impact on tool life is that of cutting speed, followed by feed and depth of cut in the given order, it ensues that $m > p > q$, therefore $y_v > x_v$. The values of x_v and y_v depend on the type of cutting tool, work material, and machining conditions. Typical values of C_v , n , x_v , and y_v are given in Table 4.2.

Table 4.2 Constants of Taylor’s generalized tool life equation

| Work material | Tool material | C_v | $\frac{1}{m} = n$ | x_v | y_v | Restriction |
|---------------|----------------------|-------|-------------------|-------|-------|----------------------|
| Steel | HSS | | | 0.26 | 0.66 | $s > 0.4, t > 1$ |
| | | | 0.125 | 0.26 | 0.36 | $s = 0.2-0.4, t > 1$ |
| | | | | 0.18 | 0.66 | $s > 0.4, t > 1$ |
| Steel | Single carbide | 273 | | 0.15 | 0.2 | $s < 0.3$ |
| | 10% Co | 227 | 0.2 | | | 0.35 |
| | Double carbide 6% Co | 221 | | 0.3 | 0.15 | $s > 0.75$ |
| | | 292 | 0.18 | | | 0.15 |
| Cast iron | Single carbide | 292 | 0.20 | 0.15 | 0.2 | $t > s$ |
| | | 243 | | 0.15 | 0.4 | $s > 0.4$ |

Here, s is in mm/rev and t in millimeter.

Among the exponents in Eqn. (4.10), the tool life exponent $n = 1/m$ is by far the most important. Although it is customary to refer to it as a constant, it actually increases with the increase of feed, but it decreases with the increase of rake angle, cutting speed, and wear criterion value of h_z . It is higher for intermittent cutting operations and increases with the reduction of the ratio of cutting time to total time. Typical values of n for commonly used cutting tools are given in Table 4.3.

Table 4.3 Typical values of tool life exponent n for various cutting tools

| Cutting tool | Work material | <i>n</i> for different tool materials | | |
|----------------------|---------------|---------------------------------------|----------------|----------------|
| | | HSS | Double carbide | Single carbide |
| Turning tool | Steel | 0.125 | 0.25 | – |
| | Cast iron | – | – | – |
| Drill | Steel | 0.1 | – | 0.2 |
| | Cast iron | 0.2 | – | 0.25 |
| Reamer | Steel | 0.4 | 0.75 | – |
| | Cast iron | 0.3 | – | 0.45 |
| Plain milling cutter | Steel | 0.33 | 0.33 | – |
| | Cast iron | 0.25 | – | – |
| Face milling cutter | Steel | 0.2 | 0.2 | – |
| | Cast iron | 0.15 | – | 0.35 |
| Broach | Steel | 0.62 | – | – |
| | Cast iron | 0.5 | – | – |

Example 4.3

The following tool life equation was obtained for a HSS tool $V T^{0.13} s^{0.6} t^{0.3} = C$. Tool life of 60 min was obtained at $v = 40$ m/min, $s = 0.25$ mm/rev, and $t = 2.0$ mm. Calculate the effect on tool life if v , s , and t are together increased by 25 percent.

$$\text{Given, } v T^{0.13} s^{0.6} t^{0.3} = C$$

Substituting $v = 40$ m/min, $s = 0.25$ mm/rev, $t = 2.0$ mm, and $T = 60$ min in the above expression, we obtain $C = 36.5$.

With the increase of 25 percent, the increased values will be

$$v = 1.25 \times 40 = 50 \text{ m/min; } s = 1.25 \times 0.25 = 0.3125 \text{ mm/rev, and } t = 1.25 \times 2.0 = 2.5 \text{ mm}$$

On substituting these values in the tool life equation, we obtain

$$T = \frac{36.5}{50(0.3125)^{0.6} (2.5)^{0.3}}$$

Hence, $T = 2.30$ min

Like n , exponents x_v and y_v are also not constant, but depend on the absolute values of t and s . They increase with increase of s and t , but at different rates. Thus, for a two-fold increase of s and t , the increase of y_v will be more than that of x_v and the higher the t/s ratio, the lower will be the absolute values of x_v and y_v .

Let us consider the case of turning for which $n = 0.125 = 1/8$. From Taylor's Eqn. (4.9), it follows that

$$v = \frac{C}{T^{\frac{1}{8}}}$$

If tool life is doubled, the denominator will increase by $(2)^{\frac{1}{8}} = 1.09$ times. Now consider the same expression in the following form:

$$T = \frac{C_1}{v^8}$$

If the cutting speed is doubled, the denominator will increase by $(2)^{\frac{1}{8}} = 256$ times. It thus follows that variation of tool life has little effect on the cutting speed, but even a small variation of cutting speed has a very strong effect on the tool life.

In this context, it is important to remember that Eqn. (4.9) represents not a law, but an empirical relation, and therefore the values of C and n are valid only for the range of the cutting speed in which the tool life curve shown in Figures 4.14 and 4.15 is plotted. Consider for example the rela-

tion $vT^{\frac{1}{8}} = 35$ that represents the tool life curve for machining of steel by HSS tool in the cutting speed range of $v = 20$ – 25 m/min. On substituting in the above relation, we find that

at $v = 20$ m/min, $T = 87.9$ min; at $v = 21$ m/min, $T = 59.5$ min

at $v = 22$ m/min, $T = 41.0$ min; at $v = 23$ m/min, $T = 28.75$ min

at $v = 24$ m/min, $T = 20.45$ min; at $v = 25$ m/min, $T = 14.75$ min

Even within the narrow range considered above, the tool life at $v = 20$ m/min is somewhat too large; and that at $v = 25$ m/min, it is somewhat too small compared with the typical tool life of 30–60 min that is considered to be economically feasible for HSS tools. Now let us see what happens when we apply the above tool life relation for values of cutting speed much different from the range for which the tool life curve was plotted.

at $v = 5$ m/min, $T = 5,764,800$ min ≈ 11 years

at $v = 35$ m/min, $T = 1$ min

If actual tool life tests were conducted at 5 m/min and 35 m/min, the tool life values obtained from these tests would be more realistic. The ridiculously large value of tool life at $v = 5$ m/min and an equally ridiculously small value of tool life at $v = 35$ m/min have been obtained because the

relation $vT^{\frac{1}{8}} = 35$ is not applicable to these values of cutting speed. The example discussed above serves as a pointer that the constants tabulated in Tables 4.2 and 4.3 should be used with caution with the understanding that they are valid only for cutting conditions that are commensurate with good machining practices for the given tool–work pair.

From the point of view of economic feasibility of cutting operation, neither high nor very low cutting speeds are desirable, as the former will lead to frequent tool regrinding/replacement, and the latter will lead to loss of productivity. Therefore, some optimum cutting speed and its corresponding tool life should be the desired objective for any machining operation. Typical recommended values of tool life for a few production conditions are as follows:

$T = 60$ min for single point tools used on general-purpose machine tools in job shop and batch production

$T = 1$ shift for transfer lines

$T = 20\text{--}30$ min for cutting tools used on CNC machine tools

$T = 120\text{--}180$ min for plain, face, and side milling cutters

$T = 60\text{--}120$ min for end mill and form cutters

4.5 Tool Life Testing

As has been discussed above, tool wear and tool life depend on a large number of factors, including work material, tool geometry, and machining parameters; but among all the parameters, they are affected the most by cutting speed. As will be noted later, conventional tool life tests are inherently long involving consumption of large amount of work material. Therefore, they are mostly restricted to investigation of the effect of cutting speed in order to determine the constants of Taylor's tool life equation, so that the test results can be used for predicting tool life at cutting speeds other than the values at which the tests were conducted.

For conducting the tool life test, a bar of the work material is machined on a lathe by a suitable tool of a particular geometry at fixed values of feed and depth of cut. The test is conducted at rpm value found from Eqn. (1.1) at the cutting speed recommended for the given tool-work pair. Machining is interrupted at suitable intervals to measure flank wear land width h_z and the test is continued till h_z attains the value specified as wear criterion. The h_z vs cutting time curve similar to Figure 4.7 is plotted, and the tool life is found from this curve as the cutting time corresponding to the wear criterion. These tests are repeated at other values of cutting speeds and a set of wear curves is obtained as shown in Figure 4.13. From these curves, the tool life curve similar to Figure 4.14 is plotted and by representing the data in the log-log coordinates as in Figure 4.15, the constants C and n of Taylor's tool life equation are obtained as explained in Section 4.4. Usually, it is sufficient to plot the wear curves at four different cutting speeds. If it is desired to study the effect of feed rate and depth of cut on tool life, then sets of curves similar to those shown in Figure 4.13 are plotted by repeating the tests at different values of feed and depth of cut. A similar approach will be adopted for studying the effect of tool geometry on tool life.

As stated earlier, tool life tests are lengthy and expensive. To illustrate, let us try to calculate the time spent and work material consumed in a single test for a mild steel-cemented carbide work-tool pair conducted on a $D = 50$ mm diameter bar with a tool of a given geometry at fixed value of feed $s = 0.3$ mm/rev, depth of cut $t = 2$ mm and cutting speed $v = 94.2$ m/min. From Eqn. (1.1),

the rpm is found as $n = \frac{1000 \times 94.2}{\pi \times 50} = 600$. From Eqn. (1.5), the feed per minute is found as

$s_m = 0.3 \times 600 = 180$ mm/min. Now, for a tool life of 60 min, the length of job machined is found from Eqn. (1.7) as $L = T \times s_m = 60 \times 180 = 10,800$ mm. The volume of material removed in this single test = $\pi D \times L \times t = \pi \times 50 \times 10800 \times 2 = 3391200$ mm³ = 3391.2 cm³. Taking density of steel

= 7.8 g/cm³, the mass of steel consumed in the test is found as $\frac{3391.2 \times 7.8}{1000} = 26.45$ kg. As it is

generally required to conduct the test at four different speeds in order to obtain the constants of Taylor's tool life equation, it follows that close to 100 kg of the work material will be consumed in this exercise. Even for a common work material such as steel, the cost of the material will be substantial. However, for more costly material such as Cu, Ti, Mg, etc., the cost would become prohibitive. To address this problem, several methods of accelerated tool life testing have been developed. Two of these are described below.

4.5.1 Facing Test

In the facing test, a facing operation is carried out on a disc of the work material, moving the tool from the center of the job towards the periphery (Figure 4.16). A disc of diameter $D = 300\text{--}350$ mm is clamped in the lathe chuck. A hole of diameter D_o is predrilled in the disc to provide access to the facing tool. The test is conducted at feed of $s = 0.3$ mm/rev and depth of cut $t = 2$ mm. As the facing tool moves from the center toward the periphery, the cutting speed continuously increases linearly and the tool is subjected to gradually increasing wear. At a certain diameter D_z , the wear reaches the wear criterion signifying the onset of accelerated wear that is accompanied by a sharp whistling sound. At this point, cutting is stopped and the diameter D_z is measured. The rpm of the disc should be selected such that D_z is greater than $2D_o$, but less than D . The test is conducted at two different rpm values n_1 and n_2 and the corresponding diameters D_{z1} and D_{z2} at which tool failure occurs are measured. The related cutting speeds v_{z1} and v_{z2} are then calculated using Eqn. (1.1)

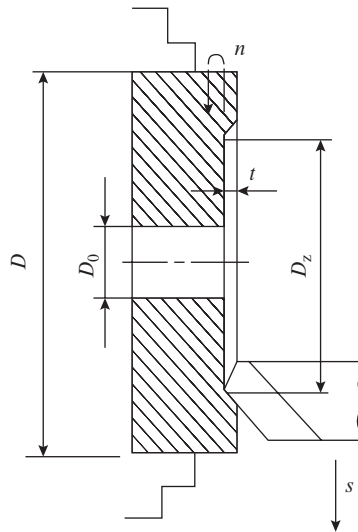


Figure 4.16 Schematic of facing test

Taylor’s equation $VT^n = C$ can be written in modified form as follows:

$$Tv^m = C^m \tag{4.11}$$

As cutting speed changes from v_o (corresponding to D_o) to v_z (corresponding to D_z), tool life may be expressed through an average speed v_{av} (see Figure 4.17):

$$Tv_{av}^m = C^m \tag{4.12}$$

From Figure (4.17), it can be noted that the area $ABCD = \text{area } ABEF$; hence,

$$(v_z - v_o) \left(\frac{C^m}{T} \right)_{av} = \int_{v_o}^{v_z} \left(\frac{C^m}{T} \right) dv$$

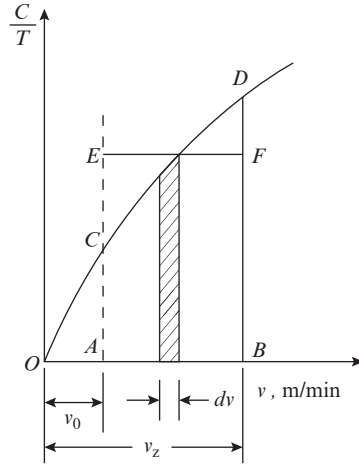


Figure 4.17 Schematic for determining average cutting speed in facing test

From Eqn. (4.12), we see that $\left(\frac{C^m}{T}\right)_{av} = v_{av}^m$, hence,

$$(v_z - v_o)v_{av}^m = \int_{v_o}^{v_z} v^m dv$$

$$v_{av}^m = \frac{v_z^{m+1} - v_o^{m+1}}{(m+1)(v_z - v_o)} \tag{4.13}$$

The time of the facing operation from diameter D_o to D_z is

$$T = \frac{D_z - D_o}{2ns}$$

On substituting for D from Eqn. (1.1), we get

$$T = \frac{100(v_z - v_o)}{2\pi n^2 s} \tag{4.14}$$

Now substituting for T from Eqn. (4.14) and v_{av}^m from Eqn. (4.13) in Eqn. (4.12), we get

$$\frac{100(v_z - v_o)}{2\pi n^2 s} \frac{v_z^{m+1} - v_o^{m+1}}{(m+1)(v_z - v_o)} = C^m$$

As $D_z > 2D_o$, for the practical values of n , it is found that v_z^{m+1} is much greater than v_o^{m+1} , and therefore the latter may be ignored. Consequently, the above expression may be written as follows:

$$1000v_z^{m+1} = 2\pi n^2 s(m+1)C^m \tag{4.15}$$

As mentioned earlier, the test is conducted at two rpm values n_1 and n_2 . For reliable results, these rpm values should be widely spaced apart (recommended $\frac{n_2}{n_1} \geq 8$). For these conditions, we obtain

$$1000v_{z1}^{m+1} = 2\pi n_1^2 s(m+1)C^m$$

$$1000v_{z2}^{m+1} = 2\pi n_2^2 s(m+1)C^m$$

On dividing the first expression by the second, we get

$$\left(\frac{v_{z1}}{v_{z2}}\right)^{m+1} = \left(\frac{n_1}{n_2}\right)^2$$

Wherefrom we get

$$(m+1)\log\left(\frac{v_{z1}}{v_{z2}}\right) = 2\log\frac{n_1}{n_2}$$

And finally

$$m = \frac{2\log\frac{n_1}{n_2}}{\log\frac{v_{z1}}{v_{z2}}} - 1 \quad (4.16)$$

From Eqn. (4.15), we have

$$\begin{aligned} C^m &= v_z^m \frac{1000v_z}{\pi n} \frac{1}{2ns(m+1)} \\ &= v_z^m \frac{D_z}{2ns(m+1)} \end{aligned}$$

Hence,

$$C = v_z \left[\frac{D_z}{2ns(m+1)} \right]^{\frac{1}{m}} \quad (4.17)$$

Substituting for any one set of values of v_{z1} , n_1 , D_{z1} or v_{z2} , n_2 , D_{z2} in the above expression along with the value of m from Eqn. (4.16), the Taylor's constant C can be calculated from Eqn. (4.17).

Example 4.4

In a facing test, the critical wear of 1 mm was observed at radius 150 mm at 200 rpm. At what radius is the same amount of wear expected to occur at 300 rpm if the tool life equation is $vT^{0.12} = 60$.

Given $vT^{0.12} = 60$. On rearranging, we get

$$Tv^{\frac{1}{0.12}} = 60^{\frac{1}{0.12}}$$

$$Tv^{8.33} = 6.575 \times 10^{14}$$

On comparing with the expression $Tv^m = C$, we find $m = 8.33$

Applying the following relation for the facing test,

$$\left(\frac{v_{n2}}{v_{n1}}\right)^{m+1} = \left(\frac{N_2}{N_1}\right)^2$$

On rearranging, we get

$$\left(\frac{v_{n2}}{v_{n1}}\right) = \left(\frac{N_2}{N_1}\right)^{\frac{2}{m+1}}$$

$$\frac{\pi D_2 N_2}{\pi D_1 N_1} = \left(\frac{N_2}{N_1}\right)^{\frac{2}{m+1}}$$

$$\frac{D_2}{D_1} = \left(\frac{N_1}{N_2}\right) \left(\frac{N_2}{N_1}\right)^{\frac{2}{m+1}} = \left(\frac{N_2}{N_1}\right)^{\frac{2}{m+1}-1} = \left(\frac{N_2}{N_1}\right)^{\frac{1-m}{m+1}}$$

$$\frac{D_2}{D_1} = \left(\frac{N_1}{N_2}\right)^{\frac{1-m}{m+1}}$$

Given $D_1 = 300$ mm, $N_1 = 200$ rpm, and $N_2 = 300$ rpm.

On substituting these values, we get

$$D_2 = 300 \left(\frac{200}{300}\right)^{\frac{8.33-1}{8.33+1}} = 218.54 \text{ mm}$$

Hence, the same amount of wear will occur at the radius $\frac{218.54}{2} = 109$ mm

4.5.2 Variable Speed Test

This test is based on the assumption that in the zone of gradual wear (zone II, Figure 4.7a), the wear rate is practically independent of the magnitude of wear h_z . In this test, a bar of the work material is turned at constant values of feed rate s and depth of cut t by a tool of particular geometry. After the completion of the initial run-in period, several cuts are taken at different cutting speeds $v_1, v_2, v_3, \dots, v_n$. The cutting time $T_1, T_2, T_3, \dots, T_n$ corresponding to each cutting speed is recorded or calculated. After each cut, the machining is stopped and the corresponding increment of wear band width $\Delta h_{z1}, \Delta h_{z2}, \Delta h_{z3}, \dots, \Delta h_{zn}$ is measured on the tool. The wear rate (WR) at each of the cutting speeds is then found as follows:

$$\frac{\Delta h_{z1}}{T_1}, \frac{\Delta h_{z2}}{T_2}, \frac{\Delta h_{z3}}{T_3} \dots \frac{\Delta h_{zn}}{T_n}$$

The selection of cutting speed and planning of the cuts are such that wear reaches the wear criterion on completion of the final cut.

The wear rate vs cutting speed data plotted in log–log coordinates appears as shown in Figure 4.18. The tangent of angle ψ that this line makes with the WR axis gives the value of tool life exponent n , that is, $n = \tan\psi$ in Taylor's tool life equation. The equivalent wear rate corresponding to the tool life is found as follows:

$$WR_{eq} = \frac{\Delta h_{z1} + \Delta h_{z2} + \Delta h_{z3} \dots \Delta h_{zn}}{T_1 + T_2 + T_3 \dots T_n}$$

Now from Figure 4.18, the equivalent cutting speed v_{eq} corresponding to WR_{eq} is found and Taylor's constant C is found by substituting for v as v_{eq} and n as $\tan\psi$ in Taylor's tool life equation, thus yielding $C = v_{eq} T^{\tan\psi}$.

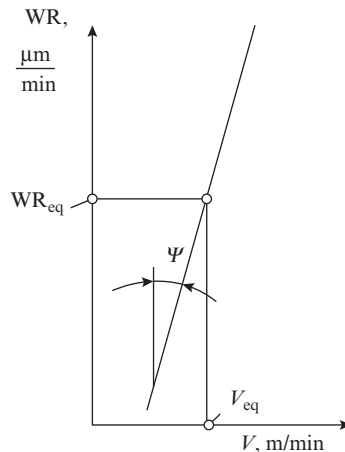


Figure 4.18 Log–log representation of the effect of cutting speed on wear rate in accelerated test

This method is simple and reliable and cuts down the test duration by 6–10 times as compared to the classical method.

4.6 Effect of Various Factors on Tool Life

4.6.1 Effect of Work Material

The effect of work material on tool life depends to a large extent on its physical and mechanical properties, because they determine the amount of heat generated in the cutting process and its distribution between the tool, chip, and workpiece. This effect is directly attributable to the machinability of the work material—the better the machinability of the work material, the higher the tool life, with other parameters remaining the same.

Within a particular material group, machinability can be significantly influenced by chemical composition. For instance, in structural steels, reduction of carbon content and the percentage of alloying elements (Cr, Mn, etc.) improve machinability. In addition, steels with ferritic microstructure have better machinability than those with pearlitic microstructure. Addition of

small amount of sulphur (up to 0.1 percent), lead (0.2–0.25 percent), and phosphorus (up to 0.15 percent) improve machinability of steel without any noticeable effect on its mechanical properties.

Heat-resistant steels have very poor machinability, because of their high ultimate strength that they can retain without noticeable loss right up to 800°C. This results in generation of large amount of heat during cutting. The problem is aggravated by the fact that these alloys have poor thermal conductivity; therefore, the heat generated remains concentrated in a narrow area near the cutting edge leading to intensive tool wear and poor tool life.

Nonferrous alloys, especially Al alloys have very good machinability thanks to the combination of low ultimate strength, tendency to soften with increase of temperature and high thermal conductivity. It is not surprising, therefore, that for a particular tool life (say 60 min), Al alloys can be machined at 4–6 times higher cutting speed than structural steels.

Gray cast iron has relatively poorer machinability compared with structural steel because of lower thermal conductivity, higher contact pressure due to the formation of discontinuous chip, and greater abrasive action of the hard constituents (cementite, ledeburite). Machinability of SG iron and malleable iron is better than that of gray cast iron on account of their higher ductility and because arc chips are produced during their machining.

It is not feasible to discuss the machinability of all engineering materials that are used in industry. However, as a thumb rule it may be stated that the harder is the work material and the higher is its ultimate strength, the lower will be the tool life or the permissible cutting speed (v_p) for a given tool life. A few empirical relations representative of the above statement are given below.

Structural and Low-Alloy Steels

$$v_p = \frac{C}{\sigma_u^x} \quad (4.18)$$

where

v_p = permissible cutting speed in m/min

σ_u = ultimate tensile strength in kg/mm²

x = exponent that depends on the tool work combination

$x = 1$ in machining of structural and low alloy steels with cemented carbide tool

$x = 1.25$ for Cr–Mo, Cr–Mo–Al steels while machining with HSS tools

$x = 1.50$ for Cr–Ni, Ni, Mn, Cr–Mn, Cr–Si, Si–Mn, Cr–Ni–Mn steels while machining with HSS tools

$x = 1.75$ for structural and low alloy steels while machining with HSS tools

The values of coefficient x are given above for steel having $\sigma_u = 75$ kg/mm². For other steels, the permissible cutting speed should be multiplied by the following coefficient:

$$K_v = \left(\frac{75}{\sigma_u} \right)^x$$

Cast Iron

$$v_p = \frac{C}{(HB)^y} \quad (4.19)$$

where

HB = Brinell's hardness of cast iron

$y = 1.7$ for machining with HSS tool

$y = 2.2$ for machining of gray cast iron with tungsten carbide tool

$y = 1.5$ for machining of SG iron with tungsten carbide tool

The values of coefficient y are given above for gray CI of hardness HB = 190 and SG and malleable iron of hardness HB = 150. For other cast irons, the permissible cutting speed should

be multiplied by coefficient $K_v = \left(\frac{190}{HB}\right)^y$ or $\left(\frac{150}{HB}\right)^y$ as the case may be.

Heat-Resistant Steels In view of the characteristic features of heat resistant steels discussed above, their machinability is defined with the help of coefficient of thermal conductivity (λ) and the true failures stress σ_t (in place of σ_u). For 20 min tool life, the suggested relation for permissible cutting speed is

$$v_{20} = C \frac{\lambda^{0.8}}{\sigma_t^{1.8}} \quad (4.20)$$

4.6.2 Effect of Tool Material

The wear of cutting tool and consequently tool life depends primarily on the properties of the tool material. Among the mechanical properties that determine the performance of a tool material the most important are high hardness, strength, toughness and wear resistance and the ability to retain these properties at the temperatures that prevail during cutting. Tool wear is significantly affected by the thermal conductivity of the tool material. A material having high thermal conductivity will be less prone to cracking during fabrication and regrinding. In addition, high thermal conductivity of the tool material facilitates the flow of heat from the cutting zone, thereby reducing the cutting temperature and consequently the tool wear. Finally, the cost of tool material and the ease of fabrication of the tool represented by its grindability also play an important role in determining the economic feasibility of a tool material for a given application.

The materials that satisfy the above requirements and have found application in industry are high carbon and alloyed steels, high-speed steels, cemented carbides, ceramics, and super hard materials such as diamond and cubic boron nitride (CBN).

In view of the fact that the cutting temperatures may be quite high, the loss of hardness with increase of temperature is often the factor that restricts the use of a tool material for a particular application. A tool loses its ability to cut when its hardness falls below a certain level. The maximum temperature at which the cutting tool retains its cutting ability is known as critical temperature and is an important parameter in defining the performance of tool materials. The variation of hardness with temperature is shown in Figure 4.19 for some important tool materials. It may be mentioned here that an ideal tool material that combines in it all the properties discussed above does not exist. High hardness gives good wear resistance, but is associated with poor grindability and low toughness. This explains the existence of a wide range of tool materials, each suitable in its own way for niche areas of application. The important tool materials will be briefly discussed below with an attempt to highlight their main applications and, wherever possible, to give a comparative assessment of their performance.

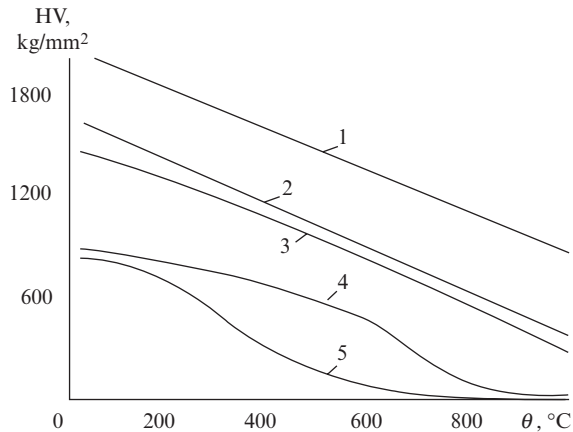


Figure 4.19 Effect of temperature on hardness of tool materials (1—ceramic, 2—P-group cemented carbide, 3—K-group cemented carbide, 4—high-speed steel, and 5—high carbon steel)

High Carbon Steels These are steels containing 0.7–1.4 percent C. To improve their hardness, they are subjected to quenching at 760–820°C which imparts to them hardness of HRC 61–63. Their critical temperature lies between 200 and 250°C, which restricts their application to hand tools such as chisels, hammers, swages, etc., and cutting tools operating at low cutting speed such as taps, thread cutting dies, and reamers. Complex cutting tools such as drills, end mills, and form tools are also sometimes made from these steels for machining of free cutting materials such as wood and soft nonferrous materials such as magnesium, brass, and aluminum.

Alloyed Steels In addition to high carbon content, these steels contain a small percentage of Cr, Mn, W, and Si, which helps in significantly enhancing their wear resistance. Some of the alloyed tool steels used for metal cutting are T90Mn1Cr1W1, T90Si1Cr1, T90Cr6W1, T90Cr1W5. These steels are quenched at 820–875°C, followed by tempering at 150–180°C. This treatment produces small amount of complex carbides of the alloying elements in addition to martensite, resulting in a hardness of HRC = 63–67. The critical temperature of these steels lies in the range 250–300°C, which makes it possible to use them for cutting at speeds that are 20–40 percent higher than those possible with high carbon steels. These tools are mainly used for cutting tools operating at low cutting speeds such as drills, taps, reamers, etc. Although their range of application is similar to that of high carbon steels, their productivity is much higher.

High-Speed Steels The development of high-speed steels in the first decade of the past century was a landmark in cutting-tool technology. These are basically high carbon steels to which carbide-forming alloying elements such as W, Mo, Cr, Co, and V are added in larger percentages. The complex carbides formed in large amounts by these alloying elements are stable up to a much higher temperature than in carbon and alloyed steels raising their cutting temperature to 600°C and above, thereby permitting a dramatic increase of cutting speed. This explains the tag of “high” speed attached to them. Subsequently, other materials that allow much higher cutting speeds have been developed; but for historical reasons, the term high speed still continues to be associated with these steels.

Tungsten and molybdenum are the main elements responsible for the hardness of HSS. They are similar in the manner in which they influence tool properties; therefore, a particular

hardness can be achieved by reducing the percentage of one, but increasing that of the other. On a weight basis 1 percent Mo can replace 2 percent of W without any detriment to hardness. The first of the typical high-speed steels contained high percentage of tungsten. Molybdenum substitutes were developed later, thus paving the way for two basic types of HSS that are in use till today—T type for tungsten predominant alloy and M type for molybdenum predominant alloy.

The function of vanadium is to inhibit grain growth at the high temperature (1200–1300°C) at which these steels are quenched. Therefore, 1–2 percent V is essential in all HSSs. Vanadium forms vanadium iron carbide that is exceptionally hard and provides very high wear resistance. Therefore, high vanadium HSSs constitute a separate category for particular applications. However, it needs to be mentioned that vanadium adversely affects grindability and high vanadium content reduces toughness; therefore, its content in HSS rarely exceeds 5 percent.

Cobalt does not form complex carbide, but it makes a solid solution in the ferrite (α —iron) matrix. Cobalt HSSs are more ductile than the plain (T- and M-type) HSSs. Therefore, their hardness can be increased by strain hardening. As cobalt tends to raise the recrystallization temperature of alloy, the cobalt HSSs are able to retain their hardness up to a much higher temperature. These features together with better grindability and higher thermal conductivity make cobalt HSSs particularly suitable for rough machining with heavy cuts.

All grades of HSS contain approximately 4–5 percent Cr. Its main function is to provide uniform hardenability, so that even tools of large section may form a martensitic structure throughout the section.

Typical compositions, properties, and application of the various types of HSSs are given in Table 4.4.

Table 4.4 Major HSSs, their properties, and applications

| Type | Composition | Critical temperature (°C) | HardnessHRC | Application |
|-------------------|---|----------------------------------|--------------------|---|
| Plain T-type HSSs | T75W18Cr4V1 T90W9Cr4V2 T85W9Cr4V2 | 600 | 62–64 | Single-point tools, drills, and reamers Turning of carbon steels, alloy steels, and cast iron |
| M-type HSSs | T85W6Mo5Cr4V1 | | | |
| Vanadium HSSs | T85W9 V5Cr4 T125W14 V4Cr4 | 625–635 | 66–67 | Single-point tools, flat and circular-form tools, broaches, drills, machining of materials with high thermal conductivity |
| Cobalt HSSs | T95W9 Co5Cr4 T95W9 Co10Cr4 T95W9 Co5Cr4V2 | 640–670 | 65–68 | Drills, milling cutters form tools, broaches, hobs, taps, and tool bits. Machining of heat-treated steels and titanium alloys |

It may be mentioned here that in view of the fast depletion of tungsten reserves worldwide, there is increasing tendency of replacing tungsten dominant HSSs with molybdenum dominant HSSs as the latter are cheaper and equal, if not superior, in performance. In recent years, a special category of HSSs with very high percentage of cobalt and very small percentage of carbon (<0.06 percent) have been developed for machining of difficult to machine materials such as heat resistant steels and titanium alloys. They are also known as carbonless HSSs or super HSSs and have hardness of HRC = 68–69 and critical temperature in the range 700–720°C. A few typical compositions of these steels are C05Co25W18Mo3, C05Co25W18Mo7, and C05Co25W10Mo5. Finally, it may be mentioned, that in view of their higher cost, all special HSSs (vanadium, cobalt, carbonless) should be used only for machining of high strength and difficult to machine materials. The plain HSSs, both T and M types, should be preferred for machining of carbon steels, low-alloy steels and nonferrous alloys on account of their lower cost. In single-point tools, the cutting portion is made of HSS bits that are brazed to the shank. In complex tools such as drills, reamers, taps, etc., the cutting portion is made of HSS and the shank of structural steel. The two are joined by friction welding or some other suitable joining method.

Cast Alloys About 1915, a new category of cobalt base alloys was developed. These alloys contain four primary elements, namely Co, Cr, W, and C. Chromium is the main alloying element comprising 25–35 percent as it forms the most important carbide in the tool. Tungsten varies between 12 percent and 25 percent and contributes to overall hardness. Carbon content varies between 1 percent and 3 percent—lower carbon percentage gives a relatively soft and ductile tool, whereas higher carbon percentage gives a harder and more wear resistant tool. Other elements may be added in small quantities for specific properties, for example, vanadium for hardness and wear resistance.

These materials are not heat treatable and are used as cast, which is why they came to be known as cast alloys. They have a critical temperature of about 750°C, low coefficient of friction, excellent resistance to corrosion, and high resistance to shock and impact. They are less tough, but more wear resistant than HSS. In general, they have properties intermediate between HSS and cemented carbides and work at cutting speeds higher than those with HSS but lower than those with carbides. Cast alloys are used for machining cast iron, malleable iron, alloy steels, stainless steels, nonferrous metals, bronze, inconel, monel, graphite, and plastics. Because of good shock and impact resistance, they perform better than carbides on interrupted cuts. Because they are used as cast, it makes them more suitable for form tools and tools of complex shapes.

Some important compositions of cast alloys and their preferred application are given in Table 4.5.

Table 4.5 Typical compositions of cast alloys and their application

| Group | Composition (%) | | | | | Hardness HRC | Application |
|-------|-----------------|----|----|-----|-------|-----------------|--|
| | Co | Cr | W | C | Other | | |
| A | 55 | 30 | 12 | 1.7 | – | 55 | Heavy roughing with impact loads |
| B | 52 | 30 | 13 | 2.5 | – | 59 | -----”----- |
| C | 46 | 32 | 17 | 2.5 | – | 62 | Roughing and cut-off operations at 20–30 percent higher speed than HSS |

| | | | | | | | |
|---|----|----|----|-----|---|----|---|
| D | 45 | 30 | 18 | 2.5 | 5 | 64 | Finishing operations at 30–50 percent higher speed than HSS |
| E | 42 | 25 | 25 | 3.0 | 5 | 66 | -----”----- |

Commercial cast alloy tool materials are marketed under various trade names with different grades for particular range of applications such as Blackalloy 525, Blackalloy Tx90, Crobalt 1, Crobalt 2, Crobalt 3, Haynes Stellite R Star J, Haynes Stellite R19, Haynes Stellite R98M2, Tantung G and Tantung 144. Broadly speaking, stellites belong to group A and B, Tantung’s to group C and D, and Blackalloy to group E.

Cemented Carbides After high-speed steels and cast alloys, the next major breakthrough in cutting tools technology was the development of cemented carbides in the third decade of the past century. Earlier, tool materials were mostly produced by molten metallurgy and depended on proper heat treatment for hardness and other properties. Their hardness was therefore affected by the cutting temperature and was limited by the hardness of the available cutting tools. The cemented carbides are produced by powder metallurgy, and can therefore possess much higher hardness and temperature resistance. Hardness in the range of HRA 87–92 and critical temperature in the range of 800–900°C allow cemented carbides to carry out machining at much higher cutting speed as compared to HSSs. With the development of diamond grinding wheels and nonconventional machining methods in the past few decades, the fabrication of cemented carbide tools has become easier and cheaper. Therefore, increasingly they are replacing HSS tools in all cutting applications.

Cemented carbides are carbides made of mainly three high-temperature materials, namely W, Ti, and Ta that are sintered with cobalt binder. The hardness of a particular carbide grade depends on the carbide percentage; the higher the carbide percentage, the greater the hardness. Between different grades of cemented carbides, the hardness is determined by the relative percentage of WC, TiC, and TaC in a particular grade. The microhardness of TiC, WC, and TaC is 3200, 2500, and 1800 kg/mm², respectively. Therefore, a given percentage of TiC will contribute more to the hardness of a cemented carbide than the same percentage of WC and TaC. Cobalt in comparison is much softer. Increase of Co content in cemented carbide reduces its hardness and temperature resistance, but increases its strength.

Cemented carbides are of three types:

- (i) single carbides
- (ii) double carbides
- (iii) triple and fine-grain carbides

- (i) *Single carbides* are designated as K-group carbides in the ISO classification system. They consist of WC with Co as binder. The hardness of these carbides lies in the range HRA = 87–90 and their critical temperature in the range 800–850°C. On account of their high ductility and relatively lower cutting temperature, K-group carbides are mainly used for machining of brittle materials such as cast iron, machining of soft nonferrous alloys, rough machining of steels on low rigidity machines and machining of Ti alloys because of their high thermal conductivity that is three times higher than that of HSS and double carbides.

The approximate composition of single (K-group) carbides and their application is summarized in Table 4.6.

Table 4.6 Composition and application of single (K-group) carbide

| Symbol | WC | Co | Microstructure | Application |
|---------------|-----------|-----------|-----------------------|---------------------------|
| K01 | 97 | 3 | Normal | Finishing of CI |
| K10 | 94 | 6 | Fine | -----”----- |
| K20 | 96 | 4 | Normal | Semi finishing of CI |
| K30 | 94 | 6 | Normal | Rough machining of CI |
| K40 | 92 | 8 | Normal | Rough machining of steels |
| K50 | 90 | 10 | Normal | -----”----- |

Within the group the hardness of grades increases and their toughness decreases with the increase of WC percentage. Thus, K01 will have the maximum hardness and minimum toughness; whereas for K50, it will be just the reverse, which explains the recommended use of K01 for machining at high speed under light load conditions such as finish machining of cast iron and that of K50 for tough machining conditions such as rough machining of steels. Here, it may be pointed out that although K10 and K30 have the same chemical composition. K10 is harder and stronger on account of a special treatment that imparts to it a fine microstructure.

- (ii) *Double carbides* designated as P-group carbides in the ISO classification system were developed in response to the need for a tool material for machining of carbon and alloyed steels. The chip produced in machining of these steels is continuous, which provides stable cutting and exerts less load on the tool; but at the same time, continuous rubbing at the tool–chip interface increases the tool wear. Therefore, the need was to develop a material of greater hardness, even if it involved some compromise with toughness. Such a new type of cemented carbide was developed by addition of TiC to the single carbide and came to be known as double carbide. The hardness of double or P-group carbides lies in the range HRA = 89–92 and their critical temperature in the range 850–900°C. The P-group carbides also have lower coefficient of friction and lower tendency of adhesion with chip. Therefore, they are also used in machining of heat-resistant steels that have high toughness and low thermal conductivity.

The approximate composition of P-group carbides and their application is summarized in Table 4.7.

Table 4.7 Composition and application of double (P-group) carbides

| Symbol | WC | TiC | Co | Microstructure | Application |
|---------------|-----------|------------|-----------|-----------------------|---------------------------|
| P01 | 66 | 30 | 4 | Normal | Finishing of steels |
| P10 | 79 | 15 | 6 | Normal | Semifinishing of steels |
| P20 | 78 | 14 | 8 | Normal | -----”----- |
| P30 | 85 | 5 | 10 | Normal | Rough machining of steels |
| P40 | 83 | 5 | 12 | Normal | -----”----- |

Within the group, the hardness of grades increases with carbide percentage and reduction of Co percentage, but this is accompanied by a corresponding reduction of toughness. On account of its greater hardness, every single percentage increase of TiC contributes more to the hardness of a particular grade compared with a similar increase in WC. Grade P01 being the hardest in the group is used for finish machining of steels at high speeds, whereas P40 being the toughest is used for their rough machining.

- (iii) *Triple and fine-grain carbides* designated as M-group carbides in the ISO classification system have hardness in the range HRA = 87–90 and critical temperature of 750–780°C. They are obtained by adding TaC to the basic single-carbide or double-carbide composition for greater impact strength. In addition, a special treatment allows these carbides to be obtained with extra fine-grain size that reduces the chances of crack formation. Generally, TaC addition is restricted to 3–4 percent as larger additions reduce the hardness below the required limit. Although their wear resistance and strength lie somewhere between that of the K-group and P-group carbides, the combination of high impact strength and crack resistance makes them suitable for tough machining conditions such as intermittent cutting and machining of stainless steel, ductile iron, and high temperature alloys.

The approximate composition of M-group carbides and their application is summarized in Table 4.8.

Table 4.8 Composition and application of triple (M-group) carbides

| Symbol | WC | TiC | TaC | Co | Microstructure | Application |
|---------------|-----------|------------|------------|-----------|-----------------------|---|
| M05 | 94 | – | – | 6 | Extra fine | Finishing of difficult to machine materials |
| M10 | 84 | 6 | 4 | 6 | Normal | Intermittent cutting |
| M30 | 82 | 5 | 5 | 8 | Normal | -----”----- |
| M40 | 90 | – | 2 | 8 | Extrafine | Semifinishing of difficult to machine materials |
| M50 | 85 | – | – | 15 | Extrafine | Rough machining of difficult to machine materials |

In recent years, the advances in materials technology have made it possible to develop cemented carbides that are in a sense customized for specific applications. Three such group of cemented carbides are H for tempered and hardened steels, S for heat-resistant alloys, super alloys, and titanium alloys and N for nonferrous and particularly aluminum alloys. The symbol is followed by a two-digit number (01–40). As in K, P, and M groups, the lower numbers correspond to the harder grades, whereas the higher numbers stand for greater toughness.

Partly due to low tensile strength and partly due to high cost, cemented carbides were originally used as small tips or inserts that were brazed to a rigid shank of less-costly material. However, brazing has certain drawbacks such as internal stresses in the carbide owing to different coefficients of expansion of carbide and steel shank. These stresses when they get coupled with the normal cutting stresses may cause failure of the tip. The geometry and consequently the performance of the brazed carbide tool depend on the skill of the operator. This problem acquires serious

proportions in multiple point tools such as milling cutters where accurate relative position of the cutting edges is important. In addition, some of the grades of cemented carbides are difficult to braze. Subsequently, clamped tools were developed in which throwaway indexable inserts with multiple cutting edges on each side are used. Elimination of regrinding and substantial reduction of tool changing downtime cost in clamped bits allows machining to be carried out at higher cutting speeds than those possible with brazed tips. Improved and simpler chip flow control and chip breaking make the mechanically clamped throw away inserts even more attractive. This explains why brazed tools are increasingly being replaced in industry by mechanically clamped tool holders with indexable throwaway inserts. Regrinding of throw away bits and recycling of scrap inserts is further enhancing their economic feasibility.

Tungsten Less Cemented Carbides The high cost of tungsten and its depleting reserves worldwide motivated the development of tungsten less cemented carbides (TCC). These carbides are mainly divided into two groups: one based on TiC and the other based on TiCN. Both use Ni and Mo as binder. The main drawback of these carbides is their poor impact strength, but this problem has been solved to some extent by addition of small amounts of Nb and Ta. The TiC-based TCCs contain about 60–90 percent TiC and the rest Ni + Mo. They serve as substitutes for P01- and P10-grade cemented carbides. The TiCN-based TCCs contain 70–85 percent TiCN and the rest Ni + Mo. They serve as substitutes for P10- and M-group carbides. On account of their poor toughness, TCCs have not been found suitable for intermittent cutting operations. These carbides have a good future in India in view of its rich titanium reserves.

Coated Bits In these tools, a thin hard coating is deposited on the cutting bit. The strength and ductility of the bit is determined by the base material or substrate, whereas its hardness is determined by the hard coating. These coatings are particularly useful under high cutting temperature conditions when wear of the tool is predominantly due to diffusion. The coating acts as a diffusion barrier and greatly reduces diffusion wear. Coatings are used on HSS as well as carbide substrates. In general, the application of the coated bit continues to be governed by that of the substrate, though with improved performance. For example, coated bits of P-group carbide substrates are used mainly for steels whereas those of K-group carbide substrates are used mainly for cast irons, which is commensurate with the uncoated P- and K-group carbide inserts.

The most popular coating used on cutting bits is that of TiC, followed by TiN. The TiC coating has a tendency to flake under dynamic loading due to the formation of a brittle η -phase. The TiN coating does not form a brittle phase, but has poor bonding with the base. Therefore, there is now a tendency to use multiple layer coatings which combine the positive features of both TiC and TiN. This coating consists of a 1–2 μ thick layer of TiC followed by a gradually increasing percentage of titanium carbonitride, till, at the surface the coating consists of 40 percent TiN. Such coatings have slightly less wear resistance than TiC coatings, but they are more reliable. The TiC coating has a thickness between 3 microns and 7 microns, TiN coating between 8 microns and 12 microns and the multiple layer coating between 10 microns and 15 microns. Coatings of other materials such as Al_2O_3 and aluminum oxynitride, have also been developed as substitutes of P10 and P30 carbides. Multiple composition hybrid coatings consisting of TiC and Al_2O_3 and coatings of various other combinations have also been developed. Coatings is an area that is developing fast; and with the advances in coating technologies, it holds the promise of becoming the latest landmark in cutting tool materials.

Ceramics Cemented carbide tools are expensive because they contain costly materials such as W, Ti, Ta, Co, etc. Ceramics are much cheaper and equally, if not more, efficient if used properly. The main component of ceramics is Al_2O_3 with addition of small amount of Ti, Cr, and Zr to increase fracture strength. The binder is 5 percent solution of rubber in petrol. A small amount of MgO (0.5–1.0 percent) TiO or Y_2O_3 is added at the time of sintering to promote densification and restricting grain size. This ceramic known as white oxide ceramic has a hardness of HRA = 89–95 and critical temperature of 1200°C, which allows it to be used for high speed, high metal removal rate finish machining of medium hard steels, chilled cast iron, malleable cast iron, and nonferrous metals and alloys. However, it is not suitable for machining of Al alloys, Ti alloys, and other materials that react with alumina (Al_2O_3). The cutting speed with ceramic tools may be 1.5–2 times higher than that possible with carbide tools while machining steels and 3–4 times higher while machining cast iron.

A serious drawback of white oxide ceramic that restricts its application is its low impact and transverse rupture strength. Therefore, recently considerable attention has been devoted to development of newer carbides with improved mechanical properties. One such development is related to black oxide ceramic that contains 5–40 percent of TiC/TiN and 10 percent of ZrO_2 . An altogether different category of nitride ceramics has also been developed. These ceramics mainly consist of Si_3N_4 , with TiC, TiN, SiO_2 , and Al_2O_3 as additives. One particular grade of this category known as SiAlON is a combination of Si_3N_4 , aluminum nitride, aluminum oxide, and Y_2O_3 . It is reported to be much tougher than the oxide ceramics and even capable of taking interrupted cuts. It is reportedly being used in machining of Ni based gas turbine blades and aerospace alloys.

Another development in producing improved ceramics is based on addition of metals such as W, Mo, B, Ti with the Al_2O_3 base. These composites consisting of a combination of ceramic and metals are known as cermets and combine the good toughness of the metals with the high refractoriness of the ceramics. They perform best in high-speed machining of hard cast irons and relatively hard steels under conditions of limited mechanical impact.

Ceramics are acid resistant, nonmagnetic, nonconducting, and noncorrosive and have high resistance to reactivity with most work materials. This combined with their poor wettability minimizes built-up edge formation and tool wear and is helpful in maintaining close dimensional tolerances and surface finish when machining long shafts. Ceramics are used in the form of bits or inserts of the same shape and size as carbide bits and are either mechanically clamped or brazed. Because of the brittleness of ceramics, a very important consideration in the use of ceramic tools is the rigidity of the machine tool. The tool holder too should be rigid and there should be perfect contact between the ceramic insert and the seating surface of the shank.

Superhard Materials Materials of tetrahedron composition (C, B, N, Si) are unusually hard, which immediately draws attention to them as potential tool materials. Among these materials, diamond is the earliest known superhard material adopted for cutting operations.

Diamond is the hardest of all known substances with hardness of approximately HV = 10,000. Its high modulus of elasticity and chemical inertness combined with exceptionally high hardness makes it an ideal material for obtaining fine surface finish and accuracy. Diamond has small coefficient of thermal expansion and the highest thermal conductivity among cutting tool materials—about 2–3 times that of carbides—and this result in lower cutting temperatures. Large natural industrial diamonds are used as single-point cutting tools for finishing operations on nonferrous alloys. Diamond bits vary in size from 0.3 to 1.0 carat (1 carat = 0.2 g). Small diamond bits (<0.6 carat) are brazed to the shank with the help of silver, brass, and bronze brazing compounds.

Larger bits (>0.6 carat) are pressed into a soft bronze base (80 percent Cu + 20 percent Sn) and their cutting surface is exposed by machining out the base material around the bit. A single crystal diamond has a hard and a soft axis. It wears much faster if used in the direction of soft axis. Therefore, it is important to know the cleavage plane of diamond and mount it in such a way that the tool approaches the workpiece at a plane not parallel to the cleavage plane. Although the initial cost of diamond is high as compared to other tool materials, the cost per machined component may be lower if the diamond tool is used properly. Under proper conditions, a diamond tool may machine 10,000–50,000 and even 100,000 pieces where a carbide tool can machine only 300–500 pieces before it needs sharpening.

As a cutting tool, diamond is used mainly for finish machining of nonferrous metals and alloys such as aluminum, brass, copper, bronze, etc., and nonmetallic materials such as plastic, epoxy resins, hard rubber, glass, and precious metals such as gold, silver, and platinum in turning boring face milling and drilling operations.

Diamond is extremely brittle, and it easily chips or fractures. It should therefore be used on machines with minimum vibration and chatter and should be completely protected from impact loading. For higher strength and shock resistance polycrystalline diamond has been developed as an alternative to single crystal diamond. Polycrystalline diamond (PCD) is made of synthetic diamond powder that is sintered into molded shapes similar to carbide and ceramic inserts that can be used on the standard tool holders for carbide inserts. Synthetic diamond is produced from graphite by a controlled high temperature, high-pressure treatment in the presence of catalysts. A bit is composed of millions of tiny randomly oriented diamond crystals fused together. Hardness of the crystals provides wear resistance, while their random orientation provides strength and toughness. Polycrystalline diamond bits are in general used in the same applications as single crystal diamonds, but have the added advantage of relatively better robustness. Diamond powder is also used in grinding wheels, dressing tools, hones, lapping compounds, and drawing dies.

Cutting speeds for diamond tools should be as high as possible, the speed being limited by the onset of vibrations. Feeds should be low between 0.02 mm/rev and 0.1 mm/rev and depth of cut between 0.05 mm and 0.5 mm.

Apart from low strength and high brittleness, a major drawback of diamond is its predisposition to oxidation. When heated in air at 700–800°C, diamond undergoes graphitization and the outer surface of diamond crystal quickly turns to amorphous carbon. During machining steels and other ferrous alloys, rapid dissolution of diamond in iron takes place at 700–750°C, rendering the cutting tool useless in no time. In view of the above, diamond is not used in machining of ferrous alloys. In addition, despite all the positive features, the above drawback effectively restricts the critical temperature of diamond to 700–800°C. Therefore, diamond tools should be used with abundant supply of cutting fluid.

Cubic Boron Nitride The high cost of diamond and its limitations as regards the machining of ferrous alloys motivated the search for alternate superhard materials that may replace diamond in industrial applications. The material that has met the maximum success in this regard is cubic boron nitride (CBN). It is a chemical compound of boron and nitrogen with a special structural configuration similar to diamond. Boron nitride exists in three polymorphic forms, namely hexagonal graphite structure, ultrahard cubic structure, and ultrahard hexagonal structure. The last named structure when subjected to a high-temperature, high-pressure treatment similar to that used for producing polycrystalline diamond in the presence of a catalyst yields CBN. The CBN grains are monocrystals of dark color up to 1.0 mm in size. The hardness of CBN is less than that of diamond (HV = 8500–9000), but many times more than that of all other tool materials.

Its thermal conductivity is about three times less than that of diamond, but its greatest advantage lies in its chemical inertness that allows it to remain stable up to 1200–1300°C. In particular, its chemical inertness with respect to carbon-based alloys has promoted its wide use for finish machining of steels and cast iron.

Large-size CBN polycrystals of diameter 3–4 mm and length 5–6 mm are used as cutting bits on single-point tools and face milling cutters that have successfully replaced the grinding of hardened steels and cast irons by conventional turning and milling operations with 4–5 times higher productivity. One such example is the replacement of grinding of machine tool guide ways by milling with a CBN fly face milling cutter. Polycrystalline CBN can be used to make solid inserts or as a surface coating (= 0.5 mm thick) on a cemented carbide substrate. These inserts can be used on standard-type tool holders and may be brazed on to the steel shank or mechanically clamped.

CBN is not suitable for nonhardened steels. In fact, CBN compacts perform best on extremely hard steels (HRC > 45) and chilled cast iron. CBN can successfully machine HSS at 70 m/min and high-temperature alloys at 100–250 m/min. CBN is also successfully used as an abrasive in grinding wheels for grinding of high-speed steels, titanium, stainless steels, and satellites.

UCON Another interesting material that is technically sound but that has a narrow area of application has been developed by Union Carbide, USA, under the trade name UCON. It is a nitrated refractory metal alloy containing 50 percent Columbium, 30 percent Titanium and 20 percent Tungsten. The alloy is cast into ingots that are rolled into sheets and then slit to strips from which blanks are formed. These blanks are ground to the desired indexable insert geometry. The untreated inserts have a hardness of only about BHN = 200, but after nitriding in nitrogen atmosphere at 1650°C, the surface layer acquires a hardness of HV = 3000, which is greater than that of ceramic. However, the hardness at the centre is only around HRC = 60. Because of this inhomogeneity, the application of UCON is limited to throwaway inserts.

UCON has excellent thermal shock resistance, high hardness, and toughness because of which it is primarily recommended for roughing, semifinishing, and finishing cuts in turning, facing, and boring operations in the speed range of 200–500 m/min on steels of 200 BHN. It is not suitable for intermittent cutting or for parting off operations and for machining of iron, stainless steel and super alloys having Ni, Co, and Ti base. If properly used it has 3–5 times higher tool life than the conventional cemented carbides.

4.6.3 Effect of Tool Geometry

Effect of Rake Angle γ Increase of positive rake angle reduces the angle of the cutting wedge, thereby making chip removal less difficult, reducing the chip reduction coefficient and the cutting force (see Figure 3.25). This in turn implies less heat generation, lower cutting temperature, and higher tool life. However, the increase of positive rake angle also means reduction of the tool mass, which implies reduced tool strength and poorer heat removal from the contact surfaces resulting in higher cutting temperature and lower tool life. In view of the presence of two conflicting phenomena, the tool life vs rake angle relation is represented by a hill-type curve (Figure 4.20a) on which γ_{opt} corresponding to maximum tool life depends on the mechanical and physical properties of the tool–work pair. For $\gamma < \gamma_{opt}$, the first phenomenon predominates leading to increase of tool life; whereas for $\gamma > \gamma_{opt}$, the second factor predominates leading to reduction of tool life. The factor that has maximum effect on γ_{opt} is the strength and hardness of the work material. With the increase in strength and hardness of the work material, the amount of heat generated and the cutting temperature also increase. Therefore increase in strength and

hardness of work material is accompanied by a reduction of tool life as well as the optimum rake angle (Figure 4.20b). Applying the same logic to the tool material, a reduction of the strength and hardness of the tool material will also be accompanied by reduction of tool life and optimum rake angle.

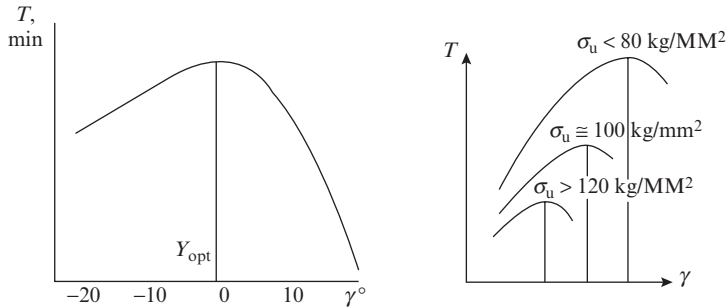


Figure 4.20 Effect of rake angle on tool life depicting the (a) presence of an optimum rake angle and (b) effect of the strength of workpiece material on optimum rake angle and tool life

Empirical relations to determine γ_{opt} for high-speed steel tools and carbide inserts are given below.

For high-speed steel tools,

$$\gamma_{\text{opt}} = 42 - \frac{55}{\xi} \quad (4.21)$$

Where ξ = chip reduction coefficient determined from cutting test on the tool–work pair at $\gamma = 10^\circ$, undeformed chip thickness $a = 0.5$ mm, and cutting speed $v = 10$ m/min.

For cemented carbide tool in machining of cast iron,

$$\gamma_{\text{opt}} = 17.2 - 0.066 \text{ BHN}$$

where BHN represents the Brinell's hardness of the cast iron.

For cemented carbide tool in machining of steel having $\sigma_u < 80 \text{ kg/mm}^2$,

$$\gamma_{\text{opt}} = \frac{25 \times 10^4}{\sigma_u^8} \quad (4.22)$$

Machining of steels under intermittent cutting conditions and of steels having $\sigma_u > 80 \text{ kg/mm}^2$ requires tools with negative rake angle because the positive rake angle tools are unable to withstand the stress produced by the impact loading and the excessively larger cutting forces. In this case, the optimum rake angle may be found from the following relation:

$$-\gamma_{\text{opt}} = 5 \times 10^{-16} \sigma_u^8 \quad (4.23)$$

Effect of Clearance Angle γ The effect of clearance angle on tool life is determined by the same two conflicting phenomena that were described with relation to the rake angle. A large clearance angle not only reduces the angle of the cutting wedge but also the friction on the tool flank, resulting in smaller cutting force, less heat generation, lower cutting temperature,

and longer tool life. However, beyond a certain value of clearance angle, the weakening of the cutting wedge and the reduction of tool mass become the dominant factors and the poorer conditions of heat removal from the contact surface see an increase of cutting temperature and reduction of tool life. The effect of α on tool life is shown in Figure 4.21(a). As was discussed in Section 1.1, the clearance angle must always be positive. As compared to rake angle, it does not vary much under different cutting conditions. For most cutting tools, it lies in the range $\alpha = 6\text{--}15^\circ$. The exception are cutters that are used for operations in which the undeformed chip thickness is extremely small throughout the cut (undeformed chip thickness is less than nose radius) or during part of the cut as in milling operations in which undeformed chip thickness is zero at the beginning of cut. On these cutters, the clearance angle is of the order of $20\text{--}30^\circ$. Optimum clearance angle is affected the most by the feed. Tool life and α_{opt} both decrease with the increase of feed (Figure 4.21b).

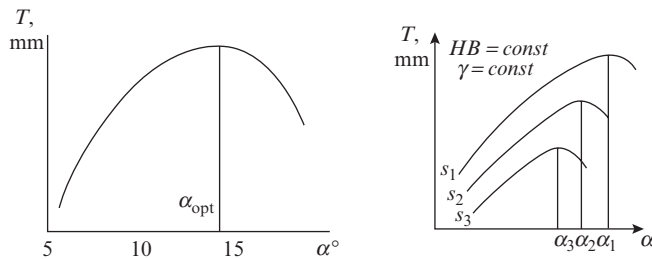


Figure 4.21 Effect of clearance angle on tool life depicting the (a) presence of an optimum clearance angle and (b) effect of feed on optimum rake angle and tool life

Effect of Primary Cutting Angle ϕ For the same depth of cut and feed, increase of ϕ leads to reduction of undeformed chip width (see Eqn. 2.2) and working length of the cutting edge (see Eqn. 2.3). The net effect is a reduction of b/a ratio and the volume of the tool resulting in poorer heat removal from the cutting zone, higher cutting temperature, and lower tool life as shown in Figure 4.22.

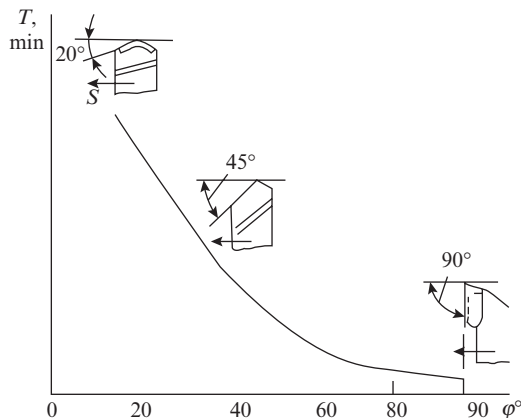


Figure 4.22 Effect of primary cutting-edge angle on tool life

Effect of Auxiliary Cutting-Edge Angle ϕ_c The effect of ϕ_c on tool life is determined by two conflicting phenomena. At small values of ϕ_c , the auxiliary tool flank rubs more vigorously against the machined surface, producing more heat, and reducing tool life. As ϕ_c is increased, the rubbing decreases but due to reduced volume of the tool the heat removal from the cutting zone also becomes poorer. Beyond a certain value of $\phi_c = \phi_{c\text{opt}}$, the second factor begins to predominate and tool life begins to decrease. This effect of ϕ_c on tool life is shown in Figure 4.23. Generally, $\phi_{c\text{opt}}$ lies between 5° and 10° .

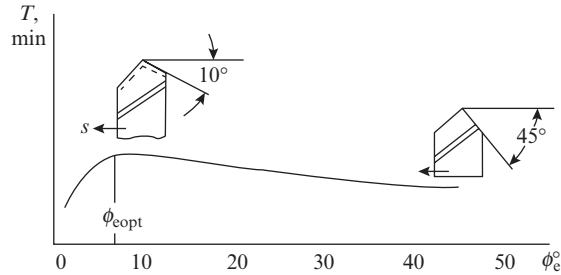


Figure 4.23 Effect of auxiliary cutting-edge angle on tool life

Effect of Cutting-Edge Inclination Angle λ The effect of λ on tool life is determined by two conflicting phenomena. An increase of λ from negative-to-zero-to positive value increases the bulk of the tool body that provides for better heat removal from the cutting zone and hence higher tool life. On the contrary, the increase of λ from negative-to-zero-to positive value is accompanied by an increase in chip reduction coefficient, which in turn leads to higher cutting forces, higher heat generation, and lower tool life. The variation of tool life with λ is represented by a hill-type curve (Figure 4.24) with optimum occurring at $\lambda = 3 - 4^\circ$. To the left of this point, an increase of λ from -15° to λ_{opt} is accompanied by increase of tool life due to predominance of the first factor and to the right of λ_{opt} , tool life decreases as λ is increased from λ_{opt} to $+30$ to 40° due to predominance of the second factor.

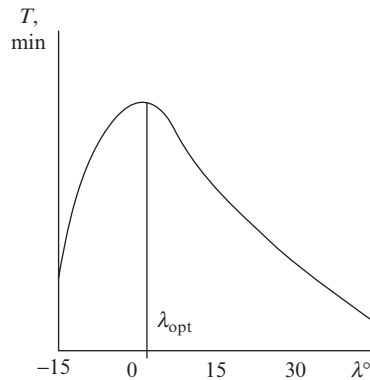


Figure 4.24 Effect of cutting-edge inclination angle on tool life

Effect of Nose Radius r While discussing the effect of nose radius r on cutting force in Section 3.5, it was shown that increase of r was akin to reduction of ϕ in the curved segment of the cutting edge (Figure 3.30). Hence, referring to Figure 4.22, it follows that increase of r is accompanied by increase of tool life. However, increase of r is also accompanied by increase of cutting force (Figure 3.31) and increase of tool volume. The former leads to reduction of tool life, and the latter leads to higher tool life on account of the improved heat removal from the cutting zone. The net result of the three effects considered together indicates an increase of tool life with increase of r as shown in Figure 4.25. However, it may be mentioned that this effect is not very strong and an increase of r from 1 mm to 5 mm may only produce approximately 10 percent improvement in tool life.

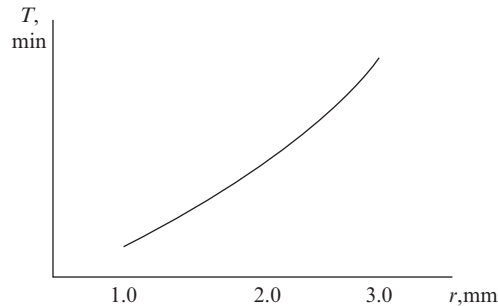


Figure 4.25 Effect of tool nose radius on tool life

Effect of Intermittent Cutting Intermittent cutting is characteristic of cutting operations in which a cutting period/stroke during which chip is removed alternates with an idle period/stroke. Common examples of intermittent cutting operation are shaping, planing, and milling.

Intermittent cutting has little effect on the life of HSS tools. For instance, if the time of idle strokes is deleted from the total cutting time in a shaping operation, then the life of a shaping tool of HSS based on cutting time will be almost the same as that of a similar turning tool doing continuous cutting under identical machining conditions.

However, intermittent cutting adversely affects tool life of cemented carbide tools. In intermittent cutting, the tool surface is heated during the cutting period/stroke and cooled during the idle period/stroke. Thus, expansion of the tool surface during the cutting period/stroke alternates with compression during the idle period/stroke, giving rise to tensile stresses in the surface layers of the carbide bit. This cyclic thermomechanical loading produces cracks in the carbide bit, because of the poor fatigue strength and high brittleness of cemented carbide. The HSS tools remain more or less immune to this effect because of their good fatigue strength. The loss of tool life in carbide tools increases with the degree of intermittence, that is, the ratio of the idle time to cutting time in a cycle. The use of cutting fluid in an intermittent cutting operation such as face milling reduces tool life because it intensifies the cooling and hence the thermal shock during the idle period. On the contrary, flame heating of the face milling cutter during the idle period is found to improve tool life as it reduces the thermal shock.

4.7 Machinability

Whereas tool life is a characteristic parameter of the cutting tool, machinability is concerned with the workpiece and defines the ease with which a work material may be machined. Machinability of a material depends on its chemical composition, microstructure, mechanical and physical

properties, and the machining parameters. It may be judged in terms of parameters such as tool life, cutting forces, and surface finish. It is conventionally accepted that a material has good machinability if tool wear is low and tools life is long, cutting forces are small and surface finish produced is good. Ease of chip control implying chip size, chip shape, chip flow direction, and chip breakability is also an important indicator of machinability. Each of these parameters that define machinability depends in turn, on several variables such as tool material, tool geometry, cutting conditions and so on. Among the indicators of machinability, cutting force has been discussed in detail in Chapter 3 and specifically the effect of various factors has been dealt with in Section 3.5. Tool wear and tool life has been discussed in detail in Chapter 4 and specifically the effect of various factors on tool life has been dealt with in Section 4.6. All aspects of chip control, including chip size, chip flow direction, and chip breaking have been covered in Section 2.4. The only remaining indicator of machinability namely surface finish will now be discussed in this section.

4.7.1 Surface Finish

The roughness of a machined surface is defined by the shape and height of the surface microirregularities. For a systematic study of surface finish, it is useful to distinguish between theoretical surface profile and actual surface profile. The theoretical surface profile represents the feed marks of the cutting tool on the machined surface with the following assumptions:

- (i) work material is absolutely rigid (undeformable)
- (ii) machine–fixture–tool–work (MFTW) system is absolutely rigid

The actual surface profile is the profile that is obtained after machining and represents a combination of the theoretical profile with superimposed fluctuations arising due to flexibility of the MFTW system, built-up edge formation and its breakage in ductile materials, crack formation in brittle materials, and so on. The actual profile can not be predicted analytically. It can only be measured with a profilometer or some similar instrument.

The theoretical profile generated in turning by a tool of nose radius r is shown in Figure 4.26(a). It is obtained as the overlapping work material when the cutting tool is sketched in successive positions spaced apart at a distance equal to the feed per revolution.

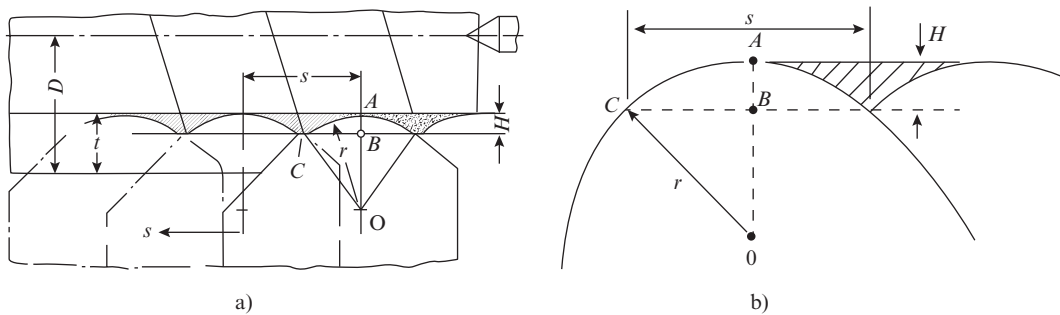


Figure 4.26 Surface finish with a round nose tool (a) theoretical profile and (b) schematic for determining the height of theoretical profile

From the geometry of the theoretical profile shown on an enlarged scale (Figure 4.26b), it can be noted that the height of the surface profile is

$$\begin{aligned}
 H &= OA - OB \\
 &= OA - \sqrt{OC^2 - BC^2} \\
 &= r - \sqrt{r^2 - \left(\frac{s}{2}\right)^2}
 \end{aligned}$$

Hence,

$$(H - r)^2 = r^2 - \frac{s^2}{4}$$

$$H^2 + r^2 - 2Hr = r^2 - \frac{s^2}{4}$$

Assuming H to be small in comparison with r , the term H^2 may be neglected, therefore

$$H = \frac{s^2}{8r} \tag{4.24}$$

The theoretical profile generated by a tool having nose radius $r = 0$ is shown in Figure 4.27(a).

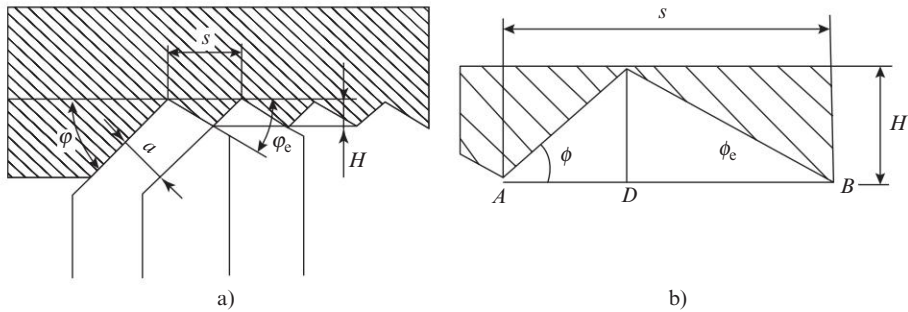


Figure 4.27 Surface finish with a tool of zero nose radius (a) theoretical profile and (b) schematic for determining the height of theoretical profile

From the geometry of the theoretical profile shown on an enlarged scale (Figure 4.27b), it can be noted that

$$H = AD \tan \phi = DB \tan \phi_c$$

Therefore, $\frac{AD}{DB} = \frac{\tan \phi_c}{\tan \phi}$

$$1 + \frac{AD}{DB} = 1 + \frac{\tan \phi_c}{\tan \phi}$$

$$\frac{DB + AD}{DB} = \frac{\tan \phi + \tan \phi_c}{\tan \phi}$$

As can be noted from the figure $DB + AD = s$, hence

$$DB = \frac{s \tan \phi}{\tan \phi + \tan \phi_c}$$

and

$$H = DB \tan \phi_c = \frac{s \tan \phi \tan \phi_c}{\tan \phi + \tan \phi_c}$$

Finally,

$$H = \frac{s}{\cot \phi + \cot \phi_c} \tag{4.25}$$

For a tool in which the nose radius and the primary and auxiliary cutting edges, all participate in generation of the surface profile, H that depends on s , r , ϕ , and ϕ_c may be found from the relations given in Table 4.9.

Table 4.9 Formulae for determining height of surface profile

| ϕ_c | $\phi < \sin^{-1} \frac{s}{2r}$ | $\phi > \sin^{-1} \frac{s}{2r}$ |
|----------------------------|--|--|
| $< \sin^{-1} \frac{s}{2r}$ | $H = \frac{\sin \phi \sin \phi_c}{\sin(\phi + \phi_c)} \times \left[s - r \left(\tan \frac{\phi}{2} + \frac{\tan \phi_c}{2} \right) \right]$ | $H = r(1 - \cos \phi_c) + s \sin \phi_c \cos \phi - \sin \phi \sqrt{s \sin \phi_c (2r - s \sin \phi_c)}$ |
| $> \sin^{-1} \frac{s}{2r}$ | $H = r(1 - \cos \phi) + s \sin \phi \cos \phi - \sin \phi \sqrt{s \sin \phi (2r - s \sin \phi)}$ | $H = r - \frac{\sqrt{4r^2 - s^2}}{2}$ |

As mentioned earlier, the actual surface profile differs from the theoretical profile. A typical profile of a turned surface recorded by a profilometer is shown in Figure 4.28.

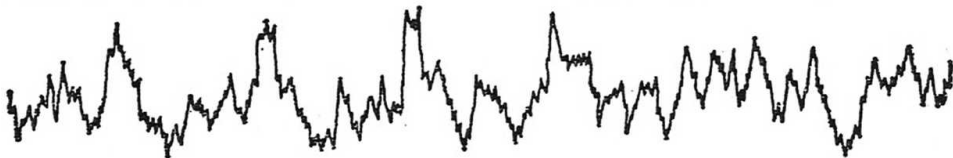


Figure 4.28 Actual surface profile of a machined surface

Here, it may be mentioned that actual height of surface microirregularities H_a is always greater than the theoretical height H due to the following reasons:

- (i) plastic flow of work material
- (ii) vibration of the tool and the workpiece

- (iii) rubbing between the tool flank and the machined surface
- (iv) unevenness of the cutting edge that increases with tool wear

Aside from the factors that affect the height of microirregularities of the theoretical surface profile, namely s , r , ϕ , and ϕ_c , the actual surface finish is also affected by the rake angle, cutting fluid, work material, and cutting speed. Increase of rake angle reduces H_a , which may be attributed to reduction of cutting force. The use of cutting fluid also reduces H_a due to less friction at the contact surfaces that eases the process of plastic deformation in chip forming. The effect of work material on H_a depends on its strength and hardness. The higher the strength and hardness of the work material and the lower its ductility, the less will be the plastic deformation and cutting strain at the time of rupture, and hence the lower will be the value of H_a . Notches, indents and serrations on the cutting edge are copied on to the machined surface, therefore the greater the unevenness of the cutting edge, the higher the value of H_a . Wear of the cutting edge also influences the surface finish. Generally, flank wear land width h_z up to 0.5 mm has little effect on H_a ; but at higher values of h_z , the increased rubbing and unevenness of the cutting edge lead to increase of H_a .

The effect of cutting speed on H_a is shown in Figure 4.29. For materials that do not have tendency of built-up edge formation, the increase of cutting speed is accompanied by continuous reduction of H_a due to reduced friction and less plastic deformation of chip formation (curve 2). For materials that have tendency of built-up edge formation, the effect of cutting speed on H_a is determined by the variation of the height of the BUE. Thus, the effect of cutting speed on H_a is represented by curve 1 on Figure 4.29, which is fully explained by the effect of cutting speed on the height of built-up edge that has been discussed in detail in Section 3.4.1 (see Figure 3.22) and Section 3.5 (see Figure 3.24b)

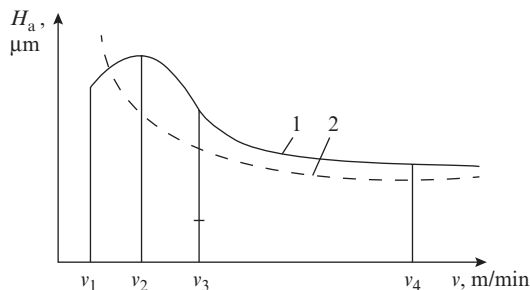


Figure 4.29 Effect of cutting speed on the actual height of surface microirregularities

4.7.2 Machinability Index

As mentioned earlier, a simple definition of machinability has remained elusive, because it is difficult to identify a particular material property capable of accurately predicting how machinable a material is. From among the indicators of machinability discussed earlier, namely tool life, cutting force, surface finish, chip control, etc., a particular parameter or a combination of parameters may be chosen as indicator of machinability depending on the type of operation and its requirements. The relative importance of four machinability parameters is given below for three production conditions.

| Importance in decreasing order | Roughing operation | Finishing operation | Machining on automat |
|---------------------------------------|---------------------------|----------------------------|-----------------------------|
| 1 | Tool life | Surface finish | Type of chips |
| 2 | Cutting force | Type of chips | Surface finish |
| 3 | Type of chips | Tool life | Tool life |
| 4 | Surface finish | Cutting force | Cutting force |

Note: 1—maximum importance and 4—least importance.

Being a vague quantity, machinability is difficult to define in absolute terms. Hence, there is no unit of machinability, and it is generally assessed in relative terms using the machinability parameters of a particular material as bench mark.

One common method is to express machinability in terms of cutting speed for a given tool life in minutes. A particular material is taken as a reference or standard and the cutting speed v_{60} corresponding to 60 min tool life is determined for this material as explained in Section 4.4. The machinability of any other material may be compared to the standard by determining v_{60} for this material and taking the ratio $v_{60} \text{ material}/v_{60} \text{ standard}$ and expressing it as a percentage. This ratio is called relative machinability. Obviously, a material with a higher value of v_{60} will be considered to have better machinability. The tool life at which the machinability of materials is compared may change with type of operation and cutting tool. For finishing operations, the comparison based on v_{20} or v_{30} may obviously be more appropriate. Similarly for milling cutters with recommended tool life of 90–180 min, a comparison based on v_{90} , v_{120} , or v_{180} would be more to the point. The value of v_{60} is found from the conventional or accelerated tool life test (see Section 4.5). However, if the tool life Eqn. (4.9) for a particular material is known, then v_{60} may be found by substituting the known values of n and C and putting $T = 60$ in the tool life equation. Alternately, some empirical relations for v_{60} can also be used.

Studies on cutting forces indicate that for a wide range of cutting conditions the cutting force component P_z and the shear force component P_s are linear functions of shear plane area, that is, $P_z = K_z A_s$ and $P_s = K_s A_s$. The ratio $\frac{K_z}{K_s} = \frac{P_z}{P_s}$ being a constant can serve as a machinability index. This is a comprehensive index in the sense that P_z and P_s encompass within themselves the effect of several factors such as machining parameters, tool geometry, etc.; it was therefore named universal machinability index (UMI). From Eqs (3.22) and (3.23) we find that

$$UMI = \frac{P_z}{P_s} = \frac{\cos(\theta - \gamma)}{\cos(\beta + \theta - \gamma)} \quad (4.26)$$

Obviously, the larger the UMI, the easier it would be to machine a material.

It may be summarized that machinability is difficult to define and may only be expressed in general terms, for example, a material that provides longer tool life or less cutting force or better surface finish has a relatively better machinability. However, this assessment is valid only for the conditions in which the tool life or cutting force or surface finish was determined. Under different cutting conditions or with a different tool material, the machinability rating may change. The search for a meaningful, unambiguous, and reliable machinability criterion/index is yet not over; and till such time that such an index is found, the term *machinability* can only be taken as a rough guide to adopt the proper measures for machining a given material.

4.8 Theoretical Determination of Cutting Temperature

Cutting temperature is an important parameter of the cutting process as it affects the quality of machined surface, tool wear and tool life, built-up edge formation, cutting forces, cutting fluid selection, and almost everything else related to the cutting process. The sources of heat in metal cutting and the distribution of heat generated at the various sources between the chip, tool, and workpiece have been discussed in Section 4.1. Here, it is important to mention that among the three sources of heat, about 80–85 percent of the heat is generated in the shear zone, about 15–20 percent at the tool–chip interface, and only 1–3 percent at the flank–machined surface interface. The cutting temperature therefore consists of two main constituents, namely shear plane temperature θ_s due to shearing of the chip to which is added the tool–chip interface temperature θ_i due to rubbing as the sheared chip flows along the tool face. The heat generated at the flank–machined surface interface is much less than that produced at the other two sources therefore its contribution to cutting temperature is neglected.

4.8.1 Temperature Relations for Various Heat Sources

For analytical determination of cutting temperature, consider the simplified model of heat sources and their distribution shown in Figure 4.30, where the chip, tool, and workpiece have been placed apart for ease of representation. For reasons explained above, the heat distribution on the flank–machined surface is not shown in Figure 4.30.

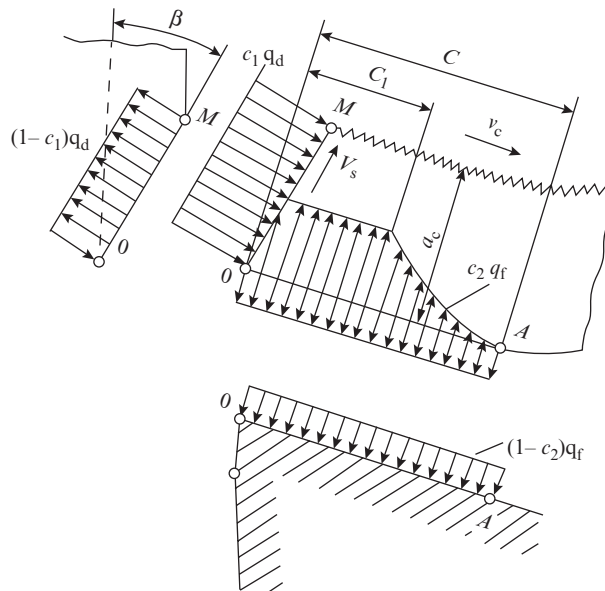


Figure 4.30 Simplified model of heat sources and their distribution

The chip may be treated as an infinite bar of thickness a_c in which the temperature distribution is governed by the following two heat sources:

- (i) heat source of uniform intensity $c_1 q_d$ in the shear plane which is a plane source moving with velocity v_s ; c_1 is the fraction of heat of the shear plane going into the chip.

- (ii) heat source of variable intensity at the tool face with the variation following the pattern of shear stresses (Figure 3.20); however, it may be treated as a plane source of uniform intensity of a certain equivalent average value $c_2 q_f$ moving with velocity v ; c_2 is the fraction of the tool–chip interface heat going into the chip.

The workpiece may be considered a semiinfinite body in which the temperature field is governed by the plane heat source of uniform intensity $(1 - c_1)q_d$ moving with velocity v , and the tool may be analyzed as an infinite wedge in which the temperature field is governed by a stationary plane heat source of intensity $(1 - c_2)q_f$.

The temperature field in a body is obtained by applying the heat source method, which states that the temperature field in a conducting body can be found for any type of heat source as a combination of temperature fields produced by a system of instantaneous point sources.

The fundamental equation of heat conduction known as the Fourier's equation of heat conduction is

$$\frac{\partial \theta}{\partial t} = K \left(\frac{\partial^2 \theta}{\partial x^2} + \frac{\partial^2 \theta}{\partial y^2} + \frac{\partial^2 \theta}{\partial z^2} \right) \quad (4.27)$$

where

$$K = \frac{k}{c\rho}$$

K = coefficient of thermal diffusivity

k = coefficient of thermal conductivity

c = specific heat

ρ = density

The heat propagation in an infinite body due to an instantaneous point source that releases energy q calories is found by solving Eqn. (4.27) with the assumption that the body had uniform temperature throughout before the release of heat from the source, and there is no heat exchange between the body and the environment. The temperature at a point having coordinates (x, y, z) after t sec of the release of heat from the source located at (x', y', z') is given by the following expression:

$$\theta_{(x,y,z,t)} = \frac{q}{k\sqrt{K}(4\pi t)^{\frac{3}{2}}} e^{-\frac{r^2}{4Kt}} \quad (4.28)$$

where

$$r^2 = [(x - x')^2 + (y - y')^2 + (z - z')^2]$$

The solution for heat propagation under the effect other type of heat sources is obtained from Eqn. (4.28). The solution for a continuous point source is obtained by integrating with respect to time with a given rate of heat liberation. Line or plane source solutions are obtained by integrating with respect to the appropriate space variables. The solution for a moving heat source is obtained by shifting of one coordinate with a certain velocity and integrating with respect to time.

Some of the solutions that are relevant to the problem of metal cutting are given below.

Continuous Point Source

$$\theta_{(x,y,z)} = \frac{q}{4\pi k r} \quad (4.29)$$

Instantaneous line source parallel to z axis:

$$\theta_{(x,y,t)} = \frac{q}{4\pi k t} e^{-\left[\frac{(x'-x)^2 + (y'-y)^2}{4Kt}\right]} \quad (4.30)$$

Instantaneous plane source parallel to xz plane at a distance y_i from it:

$$\theta_{(y,t)} = \frac{q\sqrt{K}}{2k\sqrt{\pi t}} e^{-\left[\frac{(y'-y)^2}{4Kt}\right]} \quad (4.31)$$

Here, q is the heat released per unit area of the source.

Moving line source moving with velocity v that is much greater than the velocity of heat propagation in the body:

$$\theta_{(x,y)} = \frac{q\sqrt{K}}{2k\sqrt{\pi x v}} e^{-\left[\frac{vy^2}{4Kx}\right]} \quad (4.32)$$

Here, q is the heat released per unit length of the source.

Moving Plane Source The solution for a moving heat source can be simulated as a slider moving with velocity v (Figure 4.31). If the slider is moving in the x -direction; and if $\frac{m}{l} > 2$, then the effect of dimension m is negligible and the maximum temperature occurs at the end of contact, that is, at $x = l$.

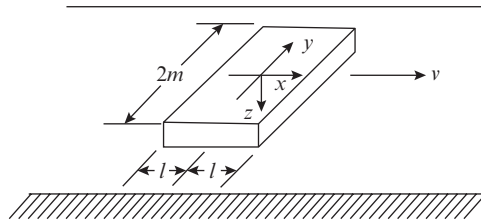


Figure 4.31 Moving slider on conducting surface

The maximum surface temperature at $z = 0$ is given by following the expression:

$$\theta_{\max} = \frac{ql}{k\sqrt{\pi L}} \quad (4.33)$$

For a semiinfinite solid, the maximum temperature is twice the above and the average temperature over the area therefore is

$$\theta_{av} = 2 \times \frac{2}{3} \frac{ql}{k\sqrt{\pi L}}$$

$$\theta_{av} = 0.754 \frac{ql}{k\sqrt{L}} \quad (4.34)$$

where

$$L = \frac{vl}{2K}$$

4.8.2 Shear Plane Temperature

When the plastic strain energy is as large as that involved in metal cutting, all but a percent or so of the energy appears as thermal energy, the rest appearing in the form of permanent lattice deformation. The rate at which the shear energy is expended along the shear plane is

$$E_s = P_s v_s \quad (4.35)$$

While discussing the energy relations in Section 3.2, it was shown that the total strain energy of metal removal consists of the energy spent on shearing and the energy spent on overcoming friction at the tool–chip interface, that is,

$$P_s v_s = P_z v - F v_c \quad (4.36)$$

where v_s , v , and v_c represent shear, cutting, and chip velocity, respectively, and P_s , P_z , and F represent the shear plane force, cutting force, and friction force on rake face, respectively.

Shear plane area $A_s = \frac{ab}{\sin \beta} = ab \operatorname{cosec} \beta$. Therefore, the shear zone heat per unit time per unit area is found as follows:

$$q_d = \frac{P_z v - F v_c}{J ab \operatorname{cosec} \beta} \text{ cal/cm}^2\text{s} \quad (4.37)$$

where J = mechanical equivalent of heat, kg.cm/cal

As mentioned in Section 4.8.1, the fraction $c_1 q_d$ of this heat is conducted into the chip and the rest $(1 - c_1) q_d$ goes into the workpiece. The heat going into the chip is used in raising its temperature from ambient temperature θ_0 to θ_s . Assuming zero loss to the environment, the energy balance may be expressed as follows:

$$\frac{c_1}{J} (P_z v - F v_c) = s_c \rho_c v ab (\theta_s - \theta_0)$$

where

s_c = specific heat of chip material, cal/kg. °C

ρ_c = density of chip material, kg/cm³

ab = A = area of undeformed chip section

$s_c \rho_c$ = volumetric specific heat of chip material, cal/cm³. °C

From the above expression, we find

$$\theta_s = \theta_0 + \frac{c_1(P_z v - F v_c)}{J s_c \rho_c v a b} \quad (4.38)$$

Substituting from Eqn. (4.37),

$$\theta_s = \theta_0 + \frac{c_1 q_d \operatorname{cosec} \beta}{s_c \rho_c v} \quad (4.39)$$

The temperature rise in the shear plane can also be simulated as that in a slider due to a moving heat source of intensity $(1 - c_1)q_d$ moving with velocity v_s . Referring to Eqn. (4.34), the average temperature on the slider surface (i.e. the shear plane) will be

$$\theta_s = \theta_0 + \frac{0.754(1 - c_1)q_d \left(\frac{a}{2} \operatorname{cosec} \beta \right)}{k_1 \sqrt{L_1}} \quad (4.40)$$

where k_1 is thermal conductivity of work material at temperature θ_s

$$L_1 = \frac{v_s \left(\frac{a}{2} \operatorname{cosec} \beta \right)}{2K_1} = \frac{v_s a}{4K_1 \sin \beta}$$

K_1 = thermal diffusivity of work material at temperature θ_s

From Eqs (2.40) and (3.8), it can be noted that

$$\frac{v_s}{\sin \beta} = v \varepsilon$$

where ε is shear strain

Hence,

$$L_1 = \frac{v \varepsilon a}{4K_1}$$

On equating Eqs (4.39) and (4.40),

$$\frac{c_1 q_d \operatorname{cosec} \beta}{s_c \rho_c v} = \frac{0.754(1 - c_1)q_d \left(\frac{a}{2} \operatorname{cosec} \beta \right)}{k_1 \sqrt{L_1}}$$

On substituting for L_1 , we find that

$$\frac{c_1}{s_c \rho_c v} = \frac{0.754(1 - c_1)a\sqrt{4K_1}}{2k_1\sqrt{v\varepsilon a}}$$

On simplification,

$$\frac{c_1}{s_c \rho_c \sqrt{v}} = \frac{0.754(1-c_1)\sqrt{aK_1}}{k_1 \sqrt{\epsilon}}$$

On substituting $K_1 = \frac{k_1}{\rho_c s_c}$, we find

$$\begin{aligned} \frac{c_1 K_1}{\sqrt{v}} &= \frac{0.754(1-c_1)\sqrt{aK_1}}{\sqrt{\epsilon}} \\ c_1 \sqrt{K_1 \epsilon} &= 0.754(1-c_1)\sqrt{av} \\ \frac{1-c_1}{c_1} &= \frac{\sqrt{K_1 \epsilon}}{0.754\sqrt{av}} \\ \frac{1}{c_1} - 1 &= 1.326\sqrt{\frac{K_1 \epsilon}{av}} \end{aligned}$$

Hence,

$$c_1 = \frac{1}{1 + 1.326\sqrt{\frac{K_1 \epsilon}{av}}} \quad (4.41)$$

On substituting this expression in Eqn. (4.38), we finally get the relation for shear plane temperature as follows:

$$\theta_s = \theta_0 + \frac{P_z v - F v_c}{\left[1 + 1.326\sqrt{\frac{K_1 \epsilon}{av}} \right] J s_c \rho_c v a b} \quad (4.42)$$

4.8.3 Tool–chip Interface Temperature and Cutting Temperature

The temperature at a particular point of an infinite body at time t due to an instantaneous point heat source is given by Eqn. (4.28). For a continuous plane heat source of finite area like the one prevailing at the tool–chip interface, the steady-state solution ($t \rightarrow \infty$) for temperature inside a semiinfinite body extending between $-l$ to $+l$ in the X direction and $-m$ to $+m$ in the Y direction is obtained by integrating Eqn. (4.28) for time and area. The analytical solution is quite complicated, although the general approach is similar to the one adopted for determining the shear plane temperature. For the sake of simplicity, it is assumed that of the mechanical energy associated with friction at the tool–chip interface 10 percent goes into the tool and 90 percent into the chip, that is, $c_2 = 0.9$. This relieves us of the detailed exercise of calculating partition coefficient c_2 .

The intensity of heat produced at the tool chip interface is

$$q_f = \frac{F v_c}{J b l} \quad (4.43)$$

where l = tool–chip contact length.

Out of this, $c_2 q_f = 0.9 q_f$ goes into the chip and $0.1 q_f$ into the tool.

Again, using the analogy of a plane slider moving with velocity v_c , we get the average rise in tool–chip interface temperature due to friction as follows:

$$\Delta\theta_i = \frac{0.754 \times 0.9 q_f \frac{l}{2}}{k_2 \sqrt{L_2}} \quad (4.44)$$

where

$$L_2 = \frac{v_c \frac{l}{2}}{2K_2}$$

k_2 and K_2 are thermal conductivity and thermal diffusivity, respectively, of the chip material at its final temperature or cutting temperature.

Substituting for L_2 in Eqn. (4.44), we get

$$\Delta\theta_i = \frac{0.3393 \times q_f l}{k_2 \sqrt{v_c \frac{l}{4K_2}}} \quad (4.45)$$

The average cutting temperature at the tool face is found as the sum of Eqs (4.42) and (4.45), that is,

$$\theta_s = \theta_0 + \frac{P_2 v - F v_c}{\left[1 + 1.326 \sqrt{\frac{K_1 \varepsilon}{av}} \right] J s_c \rho_c v a b} + \frac{0.3393 \times q_f l}{k_2 \sqrt{v_c \frac{l}{4K_2}}} \quad (4.46)$$

A large number of methods exist for experimental determination of cutting temperature. However, a limitation of all these methods is that they cannot be used to get a reliable temperature field in the tool–chip interface and workpiece even for steady-state orthogonal cutting. Moreover, from the measured values, it is not possible to identify the individual contribution of shear plane temperature and tool–chip interface temperature to the final cutting temperature, although this distinction is important for insight in to the influence of θ_s on flow stress and $(\theta_s + \Delta\theta_i)$ on crater wear at the tool face. In view of the above, the analytical method of evaluating cutting temperature, though rather complex, occupies an important place in the study of all the important thermal aspects of metal cutting.

4.9 Economics of Machining

The primary objective of any machining operation is to produce a component of assigned specifications in terms of dimensional accuracy and surface finish. A related objective is that this should be achieved at minimum possible cost. For a particular component of given work material, there are a large number of factors that need to be selected properly to achieve the above objectives, namely tool material, tool geometry, cutting fluid, and machining parameters (speed, feed, depth of cut). Selection of tool material, tool geometry, and cutting fluid is guided essentially by the

imperatives of the primary objective mentioned earlier. They also play a role in determining the machining cost through their effect on tool wear and tool life, but this aspect is peripheral.

Selection of proper machining parameters is equally important for achieving dimensional accuracy and surface finish of the machined components; but in addition, their role in determining the machining cost far exceeds that of the other factors mentioned above. Machining parameters directly impact on the machining cost as they determine the machining time of an operation (Eqs (1.4)–(1.7)) and indirectly by their effect on tool life. It therefore follows that economics of machining is mainly dependent on proper selection of the machining parameters.

4.9.1 Sequence of Assigning the Machining Parameters

The first question that arises is, what should be the order in which speed, feed, and depth of cut should be assigned? That is, which of them should be fixed first, which of them second, and which of them the last?

Let us first consider feed and depth of cut to decide which of the two should be assigned first. For analysis, consider the turning of a bar of length l (Figure 4.32) with allowance H in the following two ways:

Case I: depth of cut $t_1 = H = t$, feed $s_1 = s$; single-pass machining

Case II: depth of cut $t_{II} = \frac{H}{2} = \frac{t}{2}$ feed $s_{II} = 2s$; double-pass machining

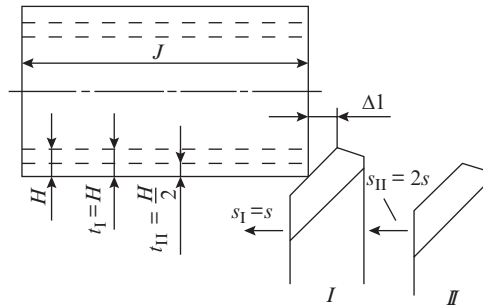


Figure 4.32 Schematic depicting the removal of allowance in one and two cuts

The undeformed chip area in the two cases is the same as $t_1 s_1 = t_{II} s_{II} = t s$. As discussed in Section 1.2, the length of tool travel for machining job of length l is

$$L = l + \Delta 1 + \Delta 2$$

where $\Delta 1 =$ tool approach

$\Delta 2 =$ tool over travel; for simplicity $\Delta 2$ is not considered in this example.

If the rpm of the job for case I and II is n_1 and n_{II} , respectively, then referring to Eqn. (1.7), the machining time for Case I will be as follows:

$$T_{mI} = \frac{L}{n_1 s}$$

And for Case II, it will be as follows:

$$T_{mII} = \frac{2L}{n_{II}2s} = \frac{L}{n_{II}s}$$

Here,

$$n_I = \frac{1000v_I}{\pi D} \text{ and } n_{II} = \frac{1000v_{II}}{\pi D}$$

Referring to Eqn. (4.10),

$$v_I = \frac{C_v}{T^{\frac{1}{m}} t^{x_v} s^{y_v}} \text{ and } v_{II} = \frac{C_v}{T^{\frac{1}{m}} \left(\frac{t}{2}\right)^{x_v} (2s)^{y_v}}$$

Here, it may be noted that for a particular tool–work pair, the factor $T^{\frac{1}{m}}$ will be the same in both the cases. In addition, as mentioned in the discussion on Eqn. (4.10), for higher values of $\frac{t}{s}$ ratio, the absolute values of x_v and y_v are less. Therefore, other conditions remaining the same, a higher $\frac{t}{s}$ ratio will allow machining at a higher cutting speed. For the two cases under consideration,

$$\left(\frac{\text{depth of cut}}{\text{feed}}\right)_I = \frac{t}{s}, \left(\frac{\text{depth of cut}}{\text{feed}}\right)_{II} = \frac{t}{4s}$$

Obviously, since $\frac{t}{s} > \frac{t}{4s}$, $v_I > v_{II}$ and $n_I > n_{II}$. Hence, $T_{mI} < T_{mII}$. In case II, apart from the fact that the machining time is higher, one also has to consider that on completion of the first pass, the tool will have to return idle to the starting position for the second pass. This will further add to the total machining time in Case II. The obvious conclusion from the foregoing analysis of the two cases is that for achieving higher productivity of machining operation, it is preferable to increase the depth of cut than the feed.

Let us now extend the analysis and consider feed and cutting speed to decide which of the two should be assigned first. The productivity of a machining operation may be represented by the number of parts Q that can be processed in the period equal to tool life T , that is,

$$Q = \frac{T}{T_m}$$

where, T_m is the machining time of one component.

From Eqs (1.5) and (1.7), we know that $T_m = \frac{L}{ns}$ and from Eqn. (1.1) that $n = \frac{100v}{\pi D}$. On substituting these values in the expression for Q , we obtain

$$Q = \frac{T \times 1000vs}{\pi DL} \quad (4.47)$$

For a given job and tool–work pair, the term $\frac{1000T}{\pi DL}$ is constant; denoting it by C , we get

$$Q = Cvs \quad (4.48)$$

Again referring to Eqn. (4.10), the term $T^{\frac{1}{m}}$ and t^{x_v} being constant for a given tool-work pair and the already selected value of t , it follows that

$$v = \frac{C'_v}{s^{y_v}} \quad (4.49)$$

where, $C'_v = \frac{C_v}{T^{\frac{1}{m}} t^{x_v}}$

Combining Eqs (4.48) and (4.49), we get

$$Q = C \frac{C'_v s}{s^{y_v}} = C C'_v s^{1-y_v} \quad (4.50)$$

It follows from Eqn. (4.50) that Q will increase with the increase of feed s . For example, if $y_v = 0.4$, a two-fold increase of s will see Q being increased by $(2)^{1-0.4} = 2^{0.6} = 1.32$ times, that is, by 32 percent.

In order to ascertain the effect of v on Q , let us rewrite Eqn. (4.49) as follows:

$$s^{y_v} = \frac{C'_v}{v}$$

i. e.
$$s = \frac{(C'_v)^{\frac{1}{y_v}}}{v^{\frac{1}{y_v}}} \quad (4.51)$$

Substituting this expression of s in Eqn. (4.48), we get

$$Q = C \frac{(C'_v)^{\frac{1}{y_v}}}{v^{\frac{1}{y_v}}} v = \frac{C(C'_v)^{\frac{1}{y_v}}}{v^{\frac{1}{y_v}-1}} \quad (4.52)$$

It follows from Eqn. (4.52) that an increase of v will lead to a reduction of Q . In this case, if $y_v = 0.4$, a two-fold increase of v will see Q become $\frac{1}{2^{\frac{1}{0.4}-1}} = \frac{1}{2^{2.5-1}} = \frac{1}{(2)^{1.5}} = \frac{1}{2.83} = 0.35$ of the original value, thus getting reduced by 65 percent.

The obvious conclusion from this analysis is that for achieving higher productivity of machining operation, preference should be given to increase of feed. As seen from the above analysis, increase of cutting speed may actually have a negative impact on productivity in view of the reduction of tool life associated with the higher cutting speed.

The strategy of assigning machining parameters in cutting operations may therefore be summarized as follows:

- (i) Assign the maximum possible depth of cut first.
- (ii) Based on the selected value of depth of cut in step 1, assign the maximum possible value of feed.
- (iii) Based on the selected values of depth of cut and feed, select the appropriate value of cutting speed corresponding to optimum tool life.

The above sequence of assigning the machining parameters has been arrived at on the basis of the foregoing analysis of productivity of machining operation. It is also commensurate with the commonly accepted practice of assigning the parameters in the order of their effect on tool wear and tool life, which is minimum for depth of cut, more for feed and maximum for cutting speed.

4.9.2 Selection of Depth of Cut

Before discussing the procedure for selection of depth of cut, it is necessary to point out that there are three types of cuts: rough, semifinishing, and finishing. It also needs to be mentioned that for every machine tool, there is a maximum limit on depth of cut that is imposed by insufficient available power of the drive motor, but more often by the dynamic instability of the system that results in chatter.

Based on the requirements of accuracy and surface finish an appropriate machining strategy is adopted. If there is no restriction on accuracy and surface finish, the whole allowance is removed by rough cuts. If the allowance H is less than the limiting depth of cut t_{lim} for the particular machine tool, then the whole allowance is removed in one cut. Say, for example that $t_{lim} = 8$ mm and $H = 6$ mm. In this case, the whole allowance can be removed in one cut. If $H > t_{lim}$, then H is divided into a suitable number of cuts of equal depth. Let us consider that again $t_{lim} = 8$ mm, but $H = 14$ mm. In this case, the allowance is divided between two cuts of 7 mm each.

When there are constraints of accuracy and surface finish, then the allowance may be divided as a combination of rough cut + semifinishing cut or rough cut + semifinishing cut + finishing cut or rough cut + finishing cut. Generally, semifinishing cut is taken with a depth of cut of 0.5 – 2.0 mm and finishing cut with a depth of cut of 0.1 – 0.4 mm. The allowance for rough cut is removed by the same approach as discussed above. The allowance for the semifinishing and finishing is generally removed in one cut.

4.9.3 Selection of Feed

Having selected the depth of cut, the next step is to select the maximum possible feed. For rough cuts, this value may be restricted by one of several factors such as power, torque, strength of the lead screw of the feed mechanism, rigidity of the cutting tool, and deflection of the workpiece. In semifinishing and finishing operations, the maximum value of feed is restricted by the surface roughness of the machined component. The selection of feed based on these limiting constraints is discussed below.

Power Constraint The power consumed in cutting process is found as follows:

$$N_c = \frac{P_z v}{6120} \text{ kW} \quad (4.53)$$

where P_z is in kg and v in m/min.

Substituting for P_z from Eqn. (3.61) and for v from Eqn. (1.1), we get

$$N_c = \frac{C_2 t^x s^y \pi D n}{6120 \times 1000}$$

This power consumed in cutting ought to be less than the power capacity of the main drive N_m , hence

$$\frac{C_z t^x s^y D n}{1950000} < N_m \eta_p$$

where η_p is a factor of safety. On rearranging, the expression for feed with power constraint is found as follows:

$$s \leq \left[\frac{1950000 N_m \eta_p}{C_z t^x D n} \right]^{\frac{1}{y}} \text{ mm/rev} \quad (4.54)$$

Torque Constraint The torque absorbed by the cutting process is given by the following expression:

$$M = \frac{P_z D}{2 \times 1000} \text{ kg.m} \quad (4.55)$$

where P_z is in kg and D in millimeter.

Again, substituting for P_z from Eqn. (3.61), we get

$$M = \frac{C_z t^x s^y D}{2000}$$

This torque must be less than the torque M_s available on the spindle. Hence,

$$M = \frac{C_z t^x s^y D}{2000} \leq M_s \eta_s$$

Where η_s is a factor of safety. On rearranging, the expression for feed with torque constraint is found as follows:

$$s \leq \left[\frac{2000 M_s \eta_s}{C_z t^x D} \right]^{\frac{1}{y}} \text{ mm/rev} \quad (4.56)$$

Constraint on Strength of Weak Element in Feed Mechanism The axial force P_x in cutting operation is given by Eqn. (3.63). To avoid damage or premature failure of the lead screw, P_x must be less than the maximum load P_1 that the lead screw can withstand. Hence,

$$P_x \leq \eta_1 P_1$$

On substituting for P_x from Eqn. (3.63), we get

$$C_x t^x s^y \leq P_1 \eta_1$$

Where η_1 is a factor of safety. On rearranging, the expression for feed with constraint on load bearing capacity of lead screw is found as follows:

$$s \leq \left[\frac{P_1 \eta_1}{C_x t^x} \right]^{\frac{1}{y}} \text{ mm/rev} \quad (4.57)$$

Constraint on Workpiece Deflection The workpiece is deflected by force components P_z and P_y . If P_y is represented as a fraction of P_z , that is, $P_y = fP_z$, then the resulting force deflecting the workpiece is found as $P_{zy} = \sqrt{P_z^2 + P_y^2} = P_z\sqrt{1 + f^2}$. The maximum deflection of the workpiece is given by the expression

$$\Delta_{wp} = \frac{P_{zy}l^3}{\eta_{\Delta}EI} \quad (4.58)$$

where I = polar movement of inertia of the workpiece section

E = modulus of elasticity of the workpiece material

η_{Δ} = coefficient that depends on the condition of clamping of the workpiece, $\eta_{\Delta} = 100$ if the job is clamped between centers, $\eta_{\Delta} = 140$ if the job is clamped in chuck and supported by the tailstock, and $\eta_{\Delta} = 2.4$ when the job is clamped in chuck without any support at the other end.

Expressing P_z by Eqn. (3.61), and $I = \frac{\pi D^4}{64} \approx 0.05D^4$, we get

$$\Delta_{wp} = \frac{C_z t^x s^y \sqrt{1 + f^2} l^3}{\eta_{\Delta} 0.05D^4 E} = \frac{20C_z t^x s^y \sqrt{1 + f^2} l^3}{\eta_{\Delta} D^4 E}$$

The permissible workpiece deflection Δ_{pwp} is decided based on the accuracy of the machined surface. Applying the condition that $\Delta_{wp} \leq \Delta_{pwp}$, we get

$$\frac{20C_z t^x s^y \sqrt{1 + f^2} l^3}{\eta_{\Delta} D^4 E} \leq \Delta_{pwp}$$

On rearranging, the expression for feed with constraint on workpiece deflection is found as follows:

$$s \leq \left[\frac{\eta_{\Delta} D^4 E \Delta_{pwp}}{20C_z t^x s^y \sqrt{1 + f^2} l^3} \right]^{\frac{1}{y}} \text{ mm/rev} \quad (4.59)$$

Constraint on Tool Deflection The deflection of tool occurs under the effect of force component P_z and is given by the following relation:

$$\Delta_t = \frac{P_z l^3}{3EI} \quad (4.60)$$

where l = tool overhang.

$I = \frac{bh^3}{12}$ is moment of inertia of the tool section, where in b and h is the width and height of the section, respectively.

E = modulus of elasticity of the tool material.

Expressing P_z by Eqn. (3.61) and substituting for I , we get

$$\Delta_t = \frac{C_z t^x s^y l^3}{3E \frac{bh^3}{12}} = \frac{4C_z t^x s^y l^3}{Ebh^3}$$

The permissible tool deflection Δ_{pt} is decided on the basis of the desired accuracy of the machined surface. Applying the condition that $\Delta_t \leq \Delta_{pt}$, we get

$$\frac{4C_z t^x s^y l^3}{Ebh^3} \leq \Delta_{pt}$$

On rearranging, the expression for feed with constraint on tool deflection is found as follows:

$$s \leq \left[\frac{Ebh^3 \Delta_{pt}}{4C_z t^x l^3} \right]^{\frac{1}{y}} \text{ mm/rev} \quad (4.61)$$

For most cutting tools, the shank is sufficiently strong and failure due to breakage is extremely rare. The exceptions are small-size cutting tools of considerable length such as drills, taps, and end mill cutters, or tools that have to work with a large overhang as an operational necessity such as single-point grooving and parting tools. For such tools, a check for strength is essential and may entail reduction of depth of cut and/or feed to prevent tool breakage.

Constraint on Surface Roughness The generation of theoretical surface profile and factors affecting the height of the theoretical profile H were discussed in Section 4.7.1. For a given limiting permissible value of R_{zp} defining the surface roughness, the expression for feed with constraint on surface roughness can be found by applying the condition $H \leq R_{zp}$ to Eqs (4.24) and (4.25) for round nose tool and tool with $r = 0$, respectively. Accordingly, the following expressions are obtained:

For round nose tool

$$s \leq (8rR_{zp})^{\frac{1}{2}} \quad (4.62)$$

For tool with nose radius $r = 0$,

$$s \leq (\cot \phi + \cot \phi_e) R_{zp} \quad (4.63)$$

Similar expressions can be derived for tools in which the nose radius and primary and auxiliary cutting edges all participate in generation of the surface profile (see Table 4.9).

The actual surface profile differs significantly from the theoretical surface profile and the actual height of the surface microirregularities H_a is always greater than that of the theoretical profile H due to several factors that were discussed in see Section 4.7.1. An empirical relation for H_a in finish turning is given below:

$$H_a = \frac{C t^{x'} s^{y'} \phi^{z'} \phi_e^{z'}}{r^k} \quad (4.64)$$

Applying the condition $H \leq R_{zp}$ and rearranging, the expression for feed with constraint on surface roughness is obtained as follows:

$$s \leq \left[\frac{r^k R_{zp}}{C_t^{x'} \phi_e^{z'} \phi_c^{z'}} \right]^{\frac{1}{y'}} \text{ mm/rev} \quad (4.65)$$

In actual practice, the feed value is selected from tables given in machining data handbook and then cross checked to ensure that it does not violate the relevant constraints discussed above. In case more than one constraint is considered, the feed is determined for all the valid constraints and the minimum among them is finally selected.

4.9.4 Selection of Optimum Cutting Speed

As discussed in Section 4.4, for a given tool–work pair, cutting speed has the maximum impact on tool life, and the selection of cutting speed is intimately linked to the designated value of tool life. While deciding the value of tool life, the following two approaches are possible:

- (i) Select a high value of tool life. This will involve less tool changes and hence less tool changing cost. However, for attaining high tool life, machining will have to be done at low cutting speed, which will result in large machining time and hence high machining cost.
- (ii) Select a small value of tool life. This involves more tool changes and hence higher tool changing cost. However, small value of tool life will allow machining at high cutting speed that will reduce the machining time and hence the machining cost.

In fact, there exists an optimum tool life somewhere between the two cases outlined above and the decision regarding that optimum value will emerge only from a proper cost analysis. It may be mentioned that the analysis only deals with the cost factors that are involved with machining. Other aspects such as cost of workpiece material, cost of material handling, and storage etc are not included in this analysis.

Minimum Cost Criterion The variable cost of machining operation with a single-point tool is given by the following expression:

$$C = T_m W + T_1 W + \frac{T_t}{Q} W + \frac{C_{ot}}{Q} \quad (4.66)$$

where

T_m = machining time

T_1 = sum of loading/unloading, tool advance and withdrawal, and idle times

W = rate of one work center, that is, rate per min of one machine and one operator

T_t = time taken to remove worn-out tool and replace it with a fresh tool, that is, idle time of machine tool associated with tool change

C_{ot} = operational cost associated with tool usage

Q = number of parts machined during the period equal to tool life

Cost factor C_{ot} can be expressed as follows:

$$C_{ot} = C_{tg} + \left(\frac{C_{in} - C_d}{i + 1} \right) \psi$$

where

C_{ig} = cost of tool regrinding.

C_{in} = initial cost of tool

C_d = disposal cost of used tool

i = number of regrindings permitted till tool usage is exhausted

ψ = factor that accounts for accidental tool damage

If tool life is T , then $Q = \frac{T}{T_m}$ and Eqn. (4.66) may be written as follows:

$$C = T_m W + T_1 W + T_i W \frac{T_m}{T} + C_{ot} \frac{T_m}{T} \quad (4.67)$$

For a turning operation on a job of length L carried out at rpm = N and feed = s , we know that

$$T_m = \frac{L}{Ns}$$

On substituting $N = \frac{1000v}{\pi D}$, where v is cutting speed in m/min and D is diameter of the workpiece in mm, we get

$$T_m = \frac{\pi DL}{1000vs}$$

Further, applying Taylor's tool life equation $v = \frac{C}{T^n}$, we get

$$T_m = \frac{\pi DLT^n}{1000sC}$$

For a particular operation on a workpiece of given dimensions and material, the term $\frac{\pi DL}{1000sC}$ is constant. Denoting it by η , we find that $T_m = \eta T^n$; and therefore Eqn. (4.67) may be rewritten as follows:

$$C = W\eta T^n + WT_1 + WT_i \eta T^{n-1} + C_{ot} \eta T^{n-1} \quad (4.68)$$

Optimum tool life can be determined by applying the condition of minimum cost to Eqn. (4.68), that is, $\frac{dC}{dT} = 0$, that is

$$\begin{aligned} \frac{dC}{dT} &= \eta W \left[nT^{n-1} + (n-1)T_i T^{n-2} + \frac{C_{ot}}{W} (n-1)T^{n-2} \right] = 0 \\ &= \eta W T^{n-1} \left[n + (n-1)T_i T^{-1} + \frac{C_{ot}}{W} (n-1)T^{-1} \right] = 0 \end{aligned}$$

As $\eta W T^{n-1} \neq 0$, it follows that

$$n + (n-1)T_i T^{-1} + \frac{C_{ot}}{W} (n-1)T^{-1} = 0$$

$$n + (n-1) \left[T_i + \frac{C_{ot}}{W} \right] \frac{1}{T} = 0$$

$$n = (1-n) \left[T_i + \frac{C_{ot}}{W} \right] \frac{1}{T}$$

Hence, optimum tool life for minimum cost can be expressed as follows:

$$(T_{opt})_{min.c} = \frac{(1-n)}{n} \left[T_i + \frac{C_{ot}}{W} \right] = \left(\frac{1}{n} - 1 \right) \left(T_i + \frac{C_{ot}}{W} \right) \quad (4.69)$$

That T_{opt} expressed in Eqn. (4.69) corresponds to minimum cost can be confirmed by checking that $\frac{d^2C}{dT^2} = 0$. The cutting speed is selected corresponding to this optimum tool life from Taylor's equation, that is,

$$v \left[\frac{(1-n)}{n} \left(T_i + \frac{C_{ot}}{W} \right) \right]^n = C$$

$$v = \frac{C}{\left[\frac{(1-n)}{n} \left(T_i + \frac{C_{ot}}{W} \right) \right]^n}$$

Hence,

$$(v_{opt})_{min.c} = C \left(\frac{n}{1-n} \right)^n \left(\frac{W}{WT_i + C_{ot}} \right)^n \quad (4.70)$$

The optimum tool life should desirably be as small as possible as this will allow machining at higher cutting speed, and hence with higher productivity without violating the minimum cost consideration. From Eqn. (4.69), it is evident that this objective can be achieved by reducing T_i and C_{ot} , that is, the idle time of the machine tool associated with tool change and the operational cost associated with tool usage, that is, the initial cost of the tool and the cost of its regrinding. From Eqs (4.69) and (4.72), it is also evident that T_{opt} decreases with increase in n . Hence, tool materials that have a high value of n and are less sensitive to the effect of cutting speed on tool life can be used at higher cutting speed without affecting the machining cost.

Maximum Production Rate Criterion Production rate is the inverse of the production time per component or piece time T_{pc} which is given by the following expression:

$$T_{pc} = T_m + T_i + T_i \left(\frac{T_m}{T} \right)$$

On substituting $T_m = \eta T^n$, we get

$$T_{pc} = \eta T^n + T_i + \eta T_i T^{n-1} \quad (4.71)$$

When maximum production rate is desired, then the operational cost C_{ot} is ignored. Accordingly, Eqn. (4.69) can be written to express optimum tool life for maximum production rate as follows:

$$(T_{opt})_{max.pr} = \left(\frac{1-n}{n}\right) T_t = \left(\frac{1}{n}-1\right) T_t \tag{4.72}$$

The corresponding cutting speed is found from Taylor’s tool life equation, that is,

$$v \left[\left(\frac{1-n}{n}\right) T_t \right]^n = C$$

wherefrom,

$$v_{(opt)max.pr} = C \left(\frac{n}{1-n}\right)^n T_t^{-n} \tag{4.73}$$

The effect of tool life on machining cost C and production rate PR is shown in Figure 4.33.

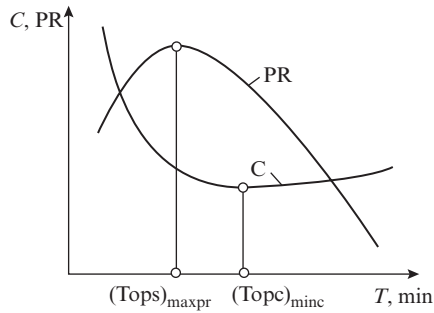


Figure 4.33 Effect of tool life on cost and production rate

It can be noted from Figure 4.33 that with the increase in tool life, the cost initially decreases rapidly, but after reaching the minimum corresponding to $(T_{opt})_{min.c}$, it tends to stabilize for a while and then begins to record a mild increase. On the contrary, the production rate, which is the inverse of piece time, initially increases, but after reaching the maximum corresponding to $(T_{opt})_{max.pr}$, begins to decrease rather sharply. Machining with $T_{opt} < (T_{opt})_{max.pr}$ and $T_{opt} > (T_{opt})_{min.c}$ carries a double penalty, both in terms of lowering of production rate as compared to $(PR)_{max}$ as well as increase of cost as compared to C_{min} . The range of tool life between $(T_{opt})_{max.pr}$ and $(T_{opt})_{min.c}$ represents the range of a sensible compromise between the production rate and cost. The corresponding range of cutting speed that lies between $(v_{opt})_{max.pr}$ and $(v_{opt})_{min.c}$ is known as high efficiency or Hi-E range. This range may be wide or narrow depending on the tool cost and the cost of tool changing and grinding. If the sum of these costs is small, $(v_{opt})_{max.pr}$ and $(v_{opt})_{min.c}$ may be within 5–10 percent of each other. But for large value of the above costs, the two optimum cutting speeds may differ by as much as 30–40 percent. From Figure 4.33, it can be noted that the cost curve has a very small gradient in the region of $(T_{opt})_{min.c}$, indicating thereby that the cost is relatively immune to the variation of $(T_{opt})_{min.c}$ and the corresponding $(v_{opt})_{min.c}$ and spindle rpm in a reasonably decent range. This allows the nearest available rpm on the machine tool to be selected without serious detriment to the machining cost.

Maximum Profit Criterion Profit rate is given by the following expression:

$$P_r = \frac{P_{pc} - C_{pc}}{T_{pc}} \quad (4.74)$$

where

P_{pc} = price per component

C_{pc} = cost per component

T_{pc} = piece time or production time per component

Price per component is the monetary value for which the component is sold. This value is arrived at by adding to the direct machining cost several other factors such as the following:

- (i) machine overheads and operator overheads that are applied as multiplication factor to W , the work centre rate
- (ii) factory overheads denominated per component
- (iii) corporate overheads denominated per component
- (iv) mark-up on the total cost per component to provide the profit

Here, it is important to remember that the material cost per component should be included or excluded in P_{pc} and C_{pc} both. As material cost has not been included in the cost Eqn. (4.68), it should also not be included in calculation of unit price P_{pc} .

Substituting for C_{pc} from Eqn. (4.68) and T_{pc} from Eqn. (4.71), the expression for P_r is obtained as follows:

$$P_r = \frac{P_{pc} - [W\eta T^n + WT_1 + WT_t\eta T^{n-1} + C_{ot}\eta T^{n-1}]}{[\eta T^n + T_1 + \eta T_t T^{n-1}]} \quad (4.75)$$

$$P_r = \frac{P_{pc} - W\eta(T^n + T_1 + \eta T_t T^{n-1}) - C_{ot}\eta T^{n-1}}{(\eta T^n + T_1 + \eta T_t T^{n-1})}$$

$$P_r = \frac{P_{pc} - C_{ot}\eta T^{n-1}}{\eta T^n + T_1 + \eta T_t T^{n-1}} - W \quad (4.76)$$

The optimum tool life corresponding to maximum profit rate is found from the condition $\frac{dP_r}{dt} = 0$, and the corresponding optimum tool life is found by substituting the value of this optimum tool life in Taylor's tool life equation. This analysis yields the following result:

When $P_{pc} = W \left(T_1 - \frac{T_m}{1-n} \right)$ zero profit

When $P_{pc} > W \left(T_1 - \frac{T_m}{1-n} \right)$ positive profit

When $P_{pc} < W \left(T_1 - \frac{T_m}{1-n} \right)$ negative profit, that is, loss

Example 4.5

The results of machining steel with two grades of tool material are given below.

| Tool | Taylor's exponent | Cutting speed for 1 min tool life (m/min) |
|-------------|--------------------------|--|
| A | 0.20 | 100 |
| B | 0.25 | 120 |

What are the standard tool life equations for these tool materials? For a 180 min tool life, which material will be preferred, and why? If the tool grinding and changing time is 15 min for tool "A", which of the two available cutting speed 45 m/min or 50 m/min will be preferred?

Tool life equations are as follows:

$$\text{For tool A: } vT^{0.2} = 100$$

$$\text{For tool B: } vT^{0.25} = 120$$

For $T = 180$ min, the cutting speed is

$$\text{For tool A: } v = \frac{100}{180^{0.2}} = 35.4 \text{ m/min}$$

$$\text{For tool B: } v = \frac{100}{180^{0.25}} = 32.76 \text{ m/min}$$

As v for tool A is greater, it should be preferred

Now for the tool A:

$$\text{At } v = 45 \text{ m/min tool life is } T = \left(\frac{100}{45}\right)^{\frac{1}{0.2}} = 54.2 \text{ min}$$

$$\text{At } v = 50 \text{ m/min tool life is } T = \left(\frac{100}{50}\right)^{\frac{1}{0.2}} = 32 \text{ min}$$

For the given tool changing and regrinding time of 15 min from consideration of maximum production rate

$$v_{\text{opt}} = \frac{C}{\left[\left(\frac{1}{n}-1\right)T_i\right]^n} = \frac{100}{\left[\left(\frac{1}{0.2}-1\right)15\right]^{0.2}} = 44.093 \text{ m/min}$$

Hence, cutting speed of 45 m/min should be selected as it is closer to the optimum cutting speed.

Example 4.6

In a machining operation conducted at $v = 50$ m/min, tool life of 45 min was observed. However at $v = 100$ m/min, tool life decreased to 10 min. Estimate the cutting speed for maximum production rate if tool changing time is 2 min.

Substituting the given values in Taylor's tool life equation, we obtain

$$50(45)^n = 100(10)^n$$

$$\left(\frac{45}{10}\right)^n = 2.0$$

$$n \ln 4.5 = \ln 2.0$$

$$\text{Hence, } n = \frac{l_n 2.0}{l_n 4.5} = 0.46$$

Substituting the above value in the tool life equation, we obtain

$$C = 50(45)^{0.46} = 100(10)^{0.46} = 288.4$$

Hence, the cutting speed for maximum production rate is found as follows:

$$v_{\text{opt}} = \frac{C}{\left[\left(\frac{1}{n} - 1\right) T_t\right]^n} = \frac{288.4}{\left[(2.17 - 1) \times 2\right]^{0.46}} = \frac{288.4}{(2.34)^{0.46}} = 195.12 \text{ m/min}$$

Example 4.7

Determine the optimum cutting speed for an operation on a lathe for the following data:

Tool changing time = 3.0 min

Tool regrinding time = 3 min

Machine running cost = ₹ 0.50/min

Depreciation on tool edge = ₹ 5

Constants in Taylor's tool life equation are 60 and 0.2

On substituting $n = 0.2$, $C = 60$, $T_t = 3$ min, $C_{\text{ot}} = ₹ 5$, and $W = 0.5 \times 3 = ₹ 1.5$, in the expression of the optimum cutting speed for minimum cost, we find

$$v_{\text{opt}} = \frac{60}{\left[\frac{1}{0.2} - 1\right] \left[3 + \frac{5}{1.5}\right]^{0.2}} = 10.73 \text{ m/min}$$

Similarly, on substituting the relevant values in the expression of optimum cutting speed for maximum production rate, we find

$$v_{\text{opt}} = \frac{60}{\left[\left(\frac{1}{0.2} - 1\right) 3\right]^{0.2}} = 36.5 \text{ m/min}$$

Review Questions

4.1 A round stock of diameter 100 mm having tensile strength of 75 kg/mm² is to be machined at $n = 1000$ rpm, $s = 0.3$ mm/rev, and $t = 3.0$ mm. Which of the following materials will be suitable for this task?

- (a) Cemented carbide (b) Ceramic (c) HSS (d) Diamond

4.2 Which of the following indicate better machinability?

- (1) Smaller shear angle (2) Higher cutting force (3) Longer tool life (4) Better surface finish
 (a) (1) and (3) (b) (2) and (4) (c) (1) and (2) (d) (3) and (4)

4.3 Consider the following factors:

- (1) Nose radius (2) Cutting speed (3) Depth of cut (4) Feed

The correct sequence of these factors in decreasing order of their influence on tool life is

- (a) (2), (4), (3), (1) (b) (4), (2), (3), (1) (c) (2), (4), (1), (3) (d) (4), (2), (1), (3)

4.4 Consider the following factors:

- (1) Feed force (2) Thrust force (3) Tangential (cutting) force

The correct sequence of these factors in decreasing order of their influence on surface finish is

- (a) (1), (2), (3) (b) (2), (3), (1) (c) (3), (1), (2) (d) (3), (2), (1)

4.5 Consider the following criteria of machinability:

- (1) Surface finish (2) Type of chips (3) Tool life (4) Power consumption

In high-speed machining with coated carbide tool, the correct sequence of these factors in decreasing order of their importance is,

- (a) (1), (2), (4), (3) (b) (2), (1), (4), (3) (c) (1), (2), (3), (4) (d) (2), (1), (3), (4)

4.6 In metal cutting operation, the approximate ratio of heat distribution between the chip, tool, and work is

- (a) 80:10:10 (b) 33:33:33 (c) 20:60:10 (d) 10:10:80

4.7 On a lathe, the actual machining time per piece is 30 min. Two types of tools both having tool life of 60 min are available: type 1—brazed tool of cost ₹ 50 and type 2—throwaway insert of cost ₹. 70. If the cost of grinding the edge is ₹ 10, the breakeven batch size will be

- (a) 2 pieces (b) 4 pieces (c) 6 pieces (d) 8 pieces

4.8 In a single-point turning operation of steel with a cemented carbide tool, the Taylor's tool life exponent is 0.25. If the cutting speed is halved, the tool life will increase by

- (a) 2 times (b) 4 times (c) 8 times (d) 16 times

4.9 For precision machining of nonferrous alloys, diamond is preferred because it has

- (1) low coefficient of thermal expansion
 (2) high wear resistance
 (3) high compressive strength
 (4) low fraction toughness

The correct answer is

- (a) (1) and (2) (b) (1) and (4) (c) (2) and (3) (d) (3) and (4)

4.10 In a turning operation, the feed is doubled to increase metal removal rate. To keep the same level of surface finish, the radius of the tool should be

- (a) halved (b) kept unchanged (c) doubled (d) increased four times

4.11 In a tool life test, doubling of cutting speed reduces tool life to 1/8th of the original. The Taylor's tool life index is

- (a) $\frac{1}{2}$ (b) $\frac{1}{3}$ (c) $\frac{1}{4}$ (d) $\frac{1}{8}$

4.12 Consider the following tool materials:

- (1) HSS (2) cemented carbide (3) ceramic (4) diamond

The correct sequence of these materials in decreasing order of hardness is

- (a) (4), (3), (1), (2) (b) (4), (3), (2), (1) (c) (3), (4), (2), (1) (d) (3), (4), (1), (2)

4.13 In a machining operation, the percentage of heat carried away by the chips is typically

- (a) 5 percent (b) 25 percent (c) 50 percent (d) 75 percent

- 4.14** Which of the following is the hardest tool material, next only to diamond?
 (a) Cemented carbide (b) Ceramic (c) Silicon (d) CBN
- 4.15** In a drilling operation, tool life was observed to decrease from 20 min to 5 min when drill speed was increased from 200 rpm to 400 rpm. What will be the drill life at 300 rpm?
- 4.16** In the selection optimal cutting conditions, the requirement of surface finish would put a limit on
 (a) maximum feed (b) maximum depth of cut
 (c) maximum speed (d) maximum number of passes
- 4.17** A HSS tool is used for turning operation. The tool life is 1 hr when turning at 30 m/min, but reduces to 2 min if cutting speed is doubled. Find the suitable rpm for turning a 300 mm diameter rod so that tool life is 30 min.
- 4.18** Consider the following statements concerning larger nose radius:
 (1) It deteriorates surface finish. (2) It increase possibility of chatter. (3) It improves tool life.
 Which of the statements is/are correct?
 (a) (2) only (b) (3) only (c) (2) and (3) (d) (1), (2), and (3)
- 4.19** Two tool P and Q have signatures 5, 5, 6, 6, 8, 30, 0 and 5, 5, 7, 7, 8, 15, 0 in the machine tool reference system. If H_p and H_q denote the height of the theoretical surface profile produced by tools P and Q, respectively, the ratio $\frac{H_p}{H_q}$ will be
 (a) $\frac{\tan 8^\circ + \cot 15^\circ}{\tan 8^\circ + \cot 30^\circ}$ (b) $\frac{\tan 15^\circ + \cot 8^\circ}{\tan 30^\circ + \cot 8^\circ}$
 (c) $\frac{\tan 15^\circ + \cot 7^\circ}{\tan 30^\circ + \cot 7^\circ}$ (d) $\frac{\tan 7^\circ + \cot 15^\circ}{\tan 7^\circ + \cot 30^\circ}$
- 4.20** While machining a bar, the observed tool lives were 24 min and 12 min at $v = 90$ m/min and 120 m/min, respectively. What is the cutting speed at 20 min tool life?
 (a) 87 m/min (b) 97 m/min (c) 107 m/min (d) 114 m/min
- 4.21** In a machining experiment tool life was found to be 81 min and 36 min at 60 m/min and 90 m/min, respectively. The exponent n and constant C of Taylor's tool life equation are
 (a) $n = 0.5, C = 540$ (b) $n = 1, C = 4860$ (c) $n = -1, C = 0.74$ (d) $n = -0.5, C = 1.155$
- 4.22** A drill of diameter 20 mm is used for making holes in a 25 mm thick plate. The drill must be changed after making 10 and 50 holes if rotated at 250 rpm and 200 rpm, respectively. How many holes can be produced if the drill is rotated at 150 rpm?

Chapter

5

GEOMETRY OF CUTTING TOOLS

All cutting tools are meant to cut a layer of work material in the form of chip to produce a surface of the desired accuracy and surface finish. The cutting element of any cutting tool is a wedge-shaped body that functions in a more or less uniform manner in all cutting tools. In multiple tooth cutters, each cutting tooth may be considered as an individual wedge defined by its flank and face. Therefore, notwithstanding the large variety of cutting tools that are used in machining practice, the cutting element, that is, the wedge is remarkably similar in all of them. The cutting element is either integral with or connected to a body. The tool body may vary in shape in order to locate and support the cutting element (s) in a particular manner that is commensurate with the type of surface the tool is supposed to produce. The variation in the shape of this supporting body is reflected in the wide range of tools such as single-point tool, drill, milling cutter, and so on, that are used in machining practice for producing variety of surfaces. Based on the method used to mount the cutting tool on the machine, the tool body must have an appropriate mounting feature or surface such as flat base in single-point tools, taper shank in drills, or cylindrical hole in milling cutters for mounting on arbor and so on.

Based on the above, the design of cutting tools may be looked upon as consisting of the following two aspects:

- (i) design of cutting element or the wedge
- (ii) design of the tool body

The shape of the wedge is determined by the tool angles—that is, the tool geometry that has been discussed in detail in Section 1.8 for a single-point tool. In multiple tooth cutters, each cutting tooth may be considered as an individual wedge whose shape is broadly described by the same tool angles as in single-point tools. The analysis of the effect of tool geometry on cutting force (Section 3.5), tool life (Section 4.6.3), and surface finish (Section 4.7.1) serves as the basis for optimization of tool angles, and hence the shape of the cutting element (wedge). The selection of optimum tool geometry will be discussed in Section 5.1.2.

As discussed above, the cutting wedge is basically similar in all cutting tools as it performs the same function. Therefore, the factors governing the optimum tool geometry in single-point cutting tools are equally valid for other cutting tools, and this aspect will not be included in the discussion of tool geometry of other tools. However, despite the general similarity of the cutting wedge, each cutting tool has its own specific geometrical features, that necessitate discussion of the geometry of various cutting tools, which is presented in Chapter 5. Both the wedge shape and the system of forces acting on it are very complex. Therefore, detailed design of the wedge for strength is extremely complicated and rarely carried out. A simple design

calculation is however carried out for individual tooth in multiple tooth cutters, treating it as a cantilever attached to the cutter body.

Design of the parameters and features, other than the wedge, will be discussed for individual cutting tools in Chapter 6. This includes the design of the main body of the tool as well as the mounting feature. Selection of some simple features of cutting tool body may be based on design calculations; but given the complex shape of the body and the force system acting on it for most cutting tools, the design is mostly based on empirical relations, practical recommendations, and even rules of thumb. For some extremely complex cutting tools, such as form tools, the design may even be based on graphical construction.

5.1 Issues in Geometry of Single-Point Tools

The geometry of single-point tools was discussed in Section 1.8. There are extraneous factors that affect the tool angles; therefore, the actual tool angles during cutting may differ from the angles provided on the tool. In addition, in the background of the knowledge about the effect of tool angles on the cutting forces, tool life, and surface finish of machined parts, it would be pertinent to attempt to determine the optimum tool angles, as they in turn will define the optimum shape of the cutting wedge. These issues will be discussed below for single-point tools; but as mentioned earlier, much of the discussion will also be relevant to other cutting tools to a large extent.

5.1.1 Effect of Tool Setting and Feed on Rake and Clearance Angles

Let us first recall the definition of clearance and rake angles from Section 1.1, which states that the clearance angle α is the angle that the tool flank makes with the velocity vector and rake angle γ is the angle that the tool face makes with the normal to the velocity vector. Now consider an orthogonal cutting operation (machining of a step, see Figure 3.6b) on a lathe machine with a tool of $\lambda = 0$ and $\phi = 90^\circ$, that is, the cutting edge of the tool is parallel to the workpiece axis. When the cutting edge is set at the height of the workpiece axis, the velocity vector B–B will be vertical and the rake and clearance angles will be as shown in Figure 5.1(a). However, if the cutting edge is set above (Figure 5.1b) or below (Figure 5.1c) the axis of the workpiece by h , then the velocity vectors $A' - A'$ and $A'' - A''$ and their normals will deviate from their previous position as shown in the corresponding figures by an angle τ , where

$$\tau = \sin^{-1} \frac{2h}{D}$$

The actual clearance and rake angles as measured from the realigned velocity vector and its normal are accordingly obtained as follows:

Tool set above the workpiece axis:

$$\alpha_{\text{act}} = \alpha - \tau \quad (5.1)$$

$$\gamma_{\text{act}} = \gamma + \tau \quad (5.2)$$

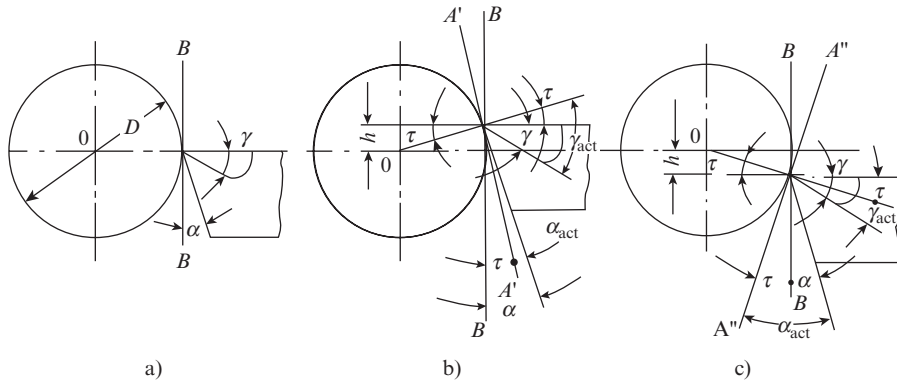


Figure 5.1 Effect of tool setting on rake and clearance angles: (a) tool tip set at the workpiece axis, (b) tool tip set above the workpiece axis, and (c) tool tip set below the workpiece axis

Tool set below the workpiece axis:

$$\alpha_{act} = \alpha + \tau \tag{5.3}$$

$$\gamma_{act} = \gamma - \tau \tag{5.4}$$

In case the primary cutting-edge angle $\phi \neq 90^\circ$, the angle τ in the above equations is replaced by angle τ_ϕ , which is found from the following relation:

$$\tan \tau_\phi = \tan \tau \sin \phi$$

In case of tools used for machining internal features, for instance a boring tool, the sign before the angle ϕ is reversed. In general, the tool is set at the height of the workpiece axis. However, for controlling the direction of chip flow, it may be set above or below the axis by $h = (0.01 - 0.02) D$ as explained in Section 2.5 (see Figure 2.20), where D is the workpiece diameter.

The working angles of the cutting tool are also affected by feed. In a simple orthogonal turning operation, the cutting surface is a helix as shown in Figure 5.2. Therefore, the actual plane of cut A–A does not coincide the static plane of cut B–B (vertical plane), but is inclined to it at an angle μ equal to the helix angle, which is found from the following relation:

$$\tan \mu = \frac{s}{\pi D}$$

where

s = feed per rev of the cutting tool

D = diameter of the workpiece

Accordingly, the actual clearance and rake angle are obtained as follows:

$$\alpha_{act} = \alpha - \mu \tag{5.5}$$

$$\gamma_{act} = \gamma + \mu \tag{5.6}$$

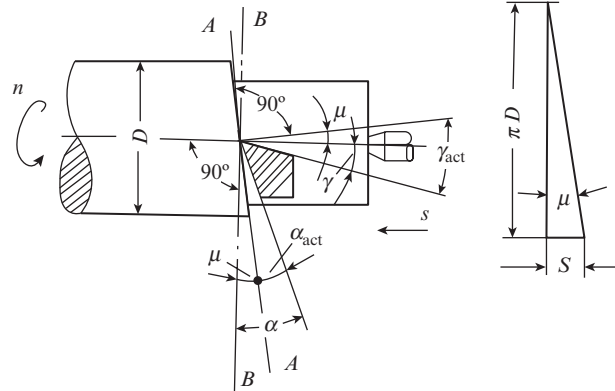


Figure 5.2 Effect of feed on rake and clearance angle

Again, if $\phi \neq 90^\circ$, the angle μ in the above equations is replaced by μ_ϕ which is found from the following relation:

$$\tan \mu_\phi = \tan \mu \sin \phi$$

By considering the effect of tool setting and feed simultaneously, the general expressions for the clearance and rake angles may be written as follows:

Tool set above the workpiece axis:

$$\alpha_{\text{act}} = \alpha - \tau_\phi - \mu_\phi \quad (5.7)$$

$$\gamma_{\text{act}} = \gamma + \tau_\phi + \mu_\phi \quad (5.8)$$

Tool set below the workpiece axis:

$$\alpha_{\text{act}} = \alpha + \tau_\phi - \mu_\phi \quad (5.9)$$

$$\gamma_{\text{act}} = \gamma - \tau_\phi + \mu_\phi \quad (5.10)$$

The knowledge of actual clearance and rake angles is important for deciding the angles to be provided on the cutting tool, that is, deciding the tool geometry. This can become a critical issue for tools with small clearance angle, because under conditions of high feed rate (large μ_ϕ) and tool set above the workpiece axis (Eqn. (5.7)), the actual clearance angle may become negative, rendering it impossible to machine with such a tool as explained in Section 1.1 (see Figure 1.1c).

Example 5.1

A job of diameter 30 mm is being machined at feed of $s = 1.0$ mm/rev and rpm of $n = 500$, with a tool of orthogonal rake angle $\gamma_0 = 5^\circ$ and primary cutting edge angle $\phi = 60^\circ$. Determine the height at which the tool tip should be set to achieve actual rake angle of 0° .

The deviation of the rake angle due to feed is

$$\tan \mu_\phi = \tan \mu \sin \phi = \frac{s}{\pi D} \sin \phi = \frac{1.0}{\pi \times 30} \times 0.866 = 0.009$$

Therefore,

$$\mu_{\phi} = 0'30'$$

As the actual rake angle is less than the static rake angle in the given problem, Eqn. (5.10) will be applicable. Substituting $\gamma_{\text{act}} = 0$ and $\gamma = 5^{\circ}$ in Eqn. (5.10), we get $0 = 5 - \tau_{\phi} + \mu_{\phi}$
Hence,

$$\tau_{\phi} = 5^{\circ} + 0'30' = 5'30'$$

Applying the relation $\tan \tau_{\phi} = \tan \tau \sin \phi$, we get

$$\tan \tau = \frac{\tan 5^{\circ}30'}{\sin 60} = \frac{0.0963}{0.866} = 0.1112$$

Hence, $\tau = 6^{\circ}20'$

Now, applying the relation $\sin \tau = \frac{2h}{D}$, we get

$$h = \frac{D}{2} \sin \tau = \frac{30}{2} \sin 6^{\circ}20' = 15 \times 0.1103 = 1.65 \text{ mm}$$

Hence, tool tip should be set 1.65 mm below the workpiece axis.

5.1.2 Selection of Optimum Tool Angles

Clearance Angle α The optimum value of clearance angle is determined mainly on the basis of its effect on tool life. This has been discussed in Section 4.6.3 (see Figure 4.21a). Among the machining parameters, α_{opt} is affected the most by feed and tends to decrease with the increase in feed (see Figure 4.21b). Therefore, finish turning tools that operate at low feed will have a larger clearance angle than tools used for rough cuts. Small clearance angle for the latter is also desirable for improved strength. The value of α_{opt} also depends on the properties of the work material. A large clearance angle is generally used for soft and ductile materials and a relatively smaller clearance angle for hard and brittle materials. In general, α_{opt} does not vary much and lies between 8° and 12° —the lower value corresponding to machining of brittle materials at low feed and the higher value corresponding to machining of ductile materials at high feed.

Rake Angle γ The optimum value of rake angle is determined on the basis of its effect on cutting force (Figure 3.25) and tool life (Figure 4.20a). The first effect favors a large rake angle, as increase of rake angle is accompanied by continuous decrease of cutting force. However, the second effect places a restriction on using very large rake angles, due to the weakening of the cutting wedge and poorer heat transfer. The recommendations for selecting γ_{opt} based on these considerations are given in Section 4.6.3. The value of γ_{opt} is affected the most by the strength of the work material and tends to decrease with the increase of strength (see Figure 4.20b). Therefore, a large rake angle is generally used for soft and ductile materials and a relatively smaller rake angle for hard and brittle materials. Selection of proper rake angle also depends on the tool material.

As a general rule, rake angles for cemented carbide and ceramic tools are less than for HSS tools. For all the tool materials, the rake angles are lower for machining brittle materials than for ductile materials.

On HSS tools, the rake angle is always positive, varying between 5° for cast iron and 25° for carbon and alloyed steels. On carbide tools, the rake angle is generally negative for improved strength of the cutting wedge varying from -10° for cast iron to -5° for carbon and alloy steels having $\sigma_u > 100 \text{ kgf/mm}^2$. For soft materials such as brass and carbon and alloy steels having $\sigma_u < 100 \text{ kgf/mm}^2$, positive rake angle in the range $5\text{--}10^\circ$ may be used on cemented carbide tools.

Primary Cutting-Edge Angle ϕ The optimum value of primary cutting-edge angle ϕ is determined on the basis of its effect on tool life (Figure 4.22), surface finish (see Eqn. 4.25) and radial cutting force component P_y (Figure 3.3). A small value of ϕ is favored by the first two factors as it leads to higher tool life and better surface finish. However, a small value of ϕ increases P_y that tends to push the tool away. As the tool is rigidly clamped, the reaction to P_y causes the workpiece to bend, resulting in loss of accuracy of the machined surface. Bearing all the above considerations in mind, the following recommendations are made for selection of ϕ based on the length-to-diameter (l/D) ratio of the workpiece:

For rigid workpiece with $\frac{l}{d} < 6$ $\phi = 10\text{--}30^\circ$

For moderately rigid workpiece with $\frac{l}{D} = 6\text{--}12$, $\phi = 45^\circ$

For workpiece of poor rigidity with $\frac{l}{D} = 12\text{--}15$ and dynamic loading, $\phi = 75^\circ$

For slender workpiece with $\frac{l}{D} > 15$, $\phi = 80\text{--}90^\circ$

For parting tools, $\phi = 90^\circ$

Auxiliary Cutting-Edge Angle ϕ_c The optimum value of auxiliary cutting-edge angle is determined on the basis of its effect on tool life (Figure 4.23) and surface finish (see Eqn. (4.25)). From the viewpoint of surface finish, ϕ_c should be as small as possible. However, as can be seen from Figure 4.23, reduction of ϕ_c below ϕ_{opt} leads to lower tool life. Therefore, it is customary to select ϕ_c close to the optimum value from tool life consideration and the recommended value is $\phi_c = 5\text{--}10^\circ$ for finishing cuts and $10\text{--}15^\circ$ for rough cuts. For tools that cut in both directions, ϕ_c acts as auxiliary cutting-edge angle in one direction and primary cutting-edge angle in the other. For such tools, the recommended value is $\phi_c = 30^\circ$.

Cutting-Edge Inclination Angle λ The selection of λ is related to three factors, namely direction of chip flow (Figure 2.20), tool life (Figure 4.24), and cutting force (Figure 3.29). The third factor does not play an important role, because the main component of the cutting force P_z is relatively immune to the variation of λ within $\pm 10^\circ$. Therefore, following Figure 4.24, $\lambda = -4^\circ$ is recommended for finishing turning and boring operations and $\lambda = +4^\circ$ for rough cuts.

In case of interrupted cutting, the impact falls on the tip of the tool with $-\lambda$, but at a certain distance from the tip in a tool with $+\lambda$ as shown in Figure 5.3a. In the former case, (Fig 5.3b) the impact can cause immediate and severe damage to the tool. Therefore, for interrupted cuts a value of $\lambda = 10\text{--}20^\circ$ is recommended, depending on the magnitude of the impact.

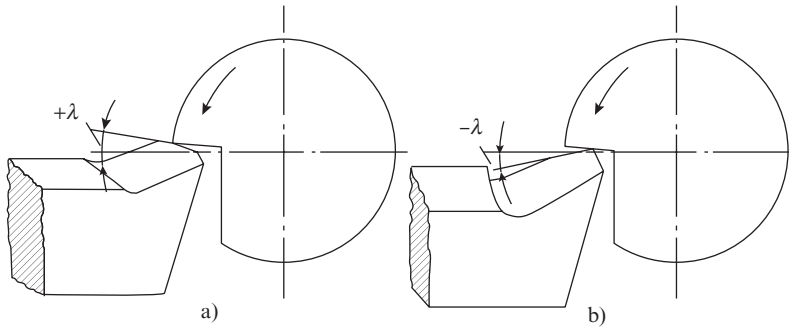


Figure 5.3 Schematic depicting the point of impact in interrupted cutting in (a) tool with $+\lambda$ (b) tool with $-\lambda$

Nose Radius r The optimum value of tool nose radius is determined by its effect on tool life (Figure 4.25), cutting force (Figure 3.31), and surface finish (Eqn. 4.24). A larger value of r is favored for good surface finish. However, restriction has to be placed on using very large values of r because this has an adverse effect on tool life and increases the cutting force components P_z and P_y . As explained in the context of angle ϕ above, a large value of P_y causes the workpiece to bend, resulting in loss of accuracy. Bearing all the above factors in mind, the value of r is recommended in the range 0.5–3.0 mm. In general, higher values of r are taken for large tool shank section and depth of cut and higher surface finish requirement.

5.2 Geometry of Form Tool

A form tool is a type of tool in which the cutting edge is of a profile that produces the desired contoured surface on the workpiece. Form tools are used on lathes for large-scale production of components with contoured surfaces of revolution such as knobs, handles, hand wheels, etc. Form tools are of two types: flat (prismatic) and circular (see Figure 5.4).

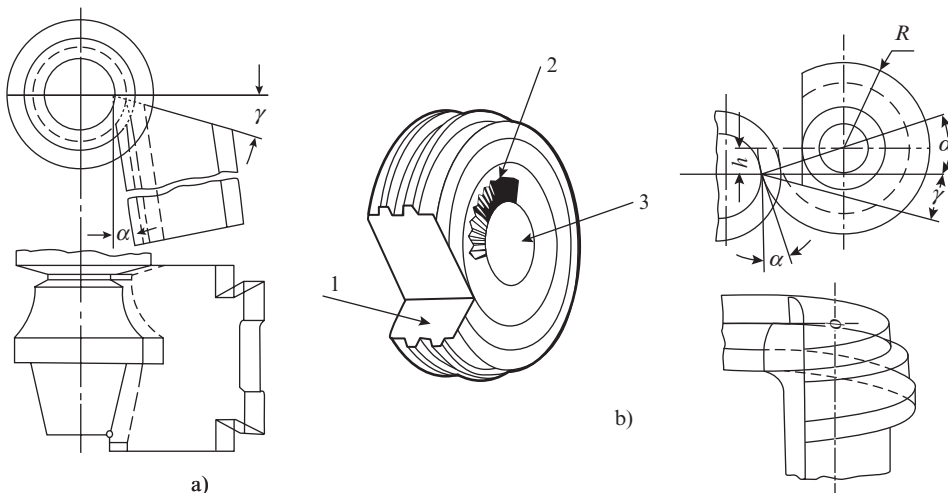


Figure 5.4 Form tool: (a) flat and (b) circular (1—face, 2—serrations, and 3—central hole)

A form tool is essentially a negative image of the work to be produced for which the tool is ground with appropriate cutting angles. On flat form tools (Figure 5.4a), the flank is a prismatic contoured surface; whereas on circular form tools, it is a contoured surface of revolution. The face on both types of form tools is a plane surface. Flat form tools are easy to make and cheaper, but have limited life as re sharpening alters the tool profile. Form tools may also be classified on the basis of the direction of feed as radial and tangential form tools. In tangential form tools, the feed is at a tangent to the surface being machined, whereas in radial form tools, it is directed along the radius of the tool at the base point. The base point is the outermost point on the cutting edge of the tool.

The flat form tool is mounted such that its cutting edge is at the level of the workpiece axis. The clearance and rake angles on a flat form tool are obtained by grinding the flank and face at the appropriate angles. The clearance angle on circular form tools (Figure 5.4b) is obtained by mounting the tool above the level of the workpiece axis. At the outermost point of the profile, the clearance angle is found from the following expression:

$$\sin \alpha = \frac{h}{R}$$

where

h = height of the form tool axis from the workpiece axis

R = radius of the form tool at the outermost point of the profile

The rake face 1 of a circular form tool is obtained by cutting away a section of the disc to provide enough space for easy flow of the chip. Serrations or teeth 2 on the side of the tool are provided to mate with similar serrations on the tool holder to prevent its rotation during operation. For clamping the form tool a clamping bolt attached to the tool holder is passed through the central hole 3 and the tool is held in position by means of a nut. The rake angle on circular form tool is also obtained by grinding the face at the appropriate angle. The recommended value of clearance angle is 10–12° for circular form tools and 12–15° for prismatic tools. The value of rake angle γ depends on the work material. The recommended values of γ are given below:

| | | | | |
|---|--------------|---------|-------|-----|
| Aluminum and copper | 25–30° | | | |
| Steel, σ_u , kgf/mm ² | <50 | 50–60 | 60–80 | >80 |
| $\gamma =$ | 20 | 15 | 10 | 5 |
| Cast iron, BHN | <180 | 180–200 | >200 | |
| $\gamma =$ | 10 | 5 | 0 | |
| Bronze, brass | $\gamma = 0$ | | | |

The values of α and γ are given above for the outer most point of the form tool profile. At other points of the profile closer to the center in case of circular tool and the base in case of prismatic tool, the clearance angle continuously increases while the rake angle continuously decreases. At an arbitrary point on the profile where the radius from the center (in circular tool) or the distance from the base (in prismatic tool) is R_x , the clearance angle α_x is found from the following expression:

$$\tan \alpha_x = \frac{R}{R_x} \tan \alpha \sin \phi_x$$

where ϕ_x is the angle between the tangent to the profile at point x and the normal to the tool axis. It is necessary to ensure that the actual clearance angle with consideration of the deviation of the actual plane of cut from the theoretical plane of cut (see Eqn. 5.5) should be at least 2–3°.

5.3 Geometry of Drill

As discussed briefly in Section 1.4, twist drills are used for making and enlarging holes whose depth does not exceed 10 times the diameter of the drill. A conventional twist drill and its elements are labeled and shown in Figure 1.18(a). Basically, a twist drill consists of two parts: the cutting portion and the shank. The cutting portion, in turn, also consists of two parts, the cutting element that does the bulk of metal removal and the guiding or sizing portion. The sizing portion does very little cutting, but it serves mainly for guiding the drill during operation and to accommodate the chips produced by the cutting element.

The cutting element has two primary cutting edges: (lips) 1 and a chisel edge 2 (see Figure 5.5). The geometry of the cutting element of drill may be simulated to a single-point tool by viewing the drill as a combination of two cutting edges twisted to join at the chisel edge.

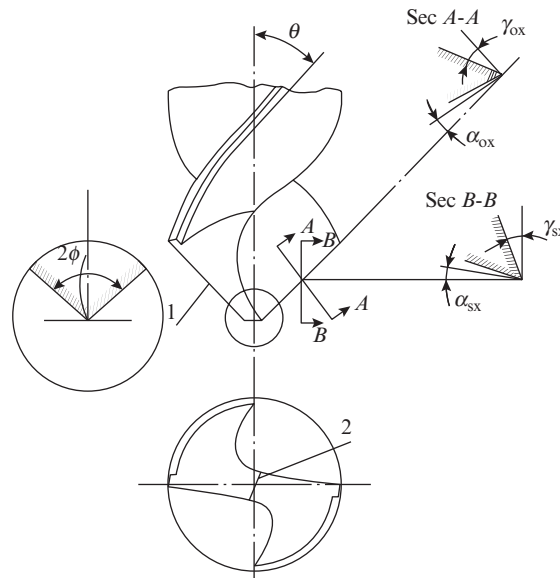


Figure 5.5 Schematic depicting drill geometry (1—primary cutting edge and 2—chisel edge)

Drill geometry is shown in Figure 5.5 where one of the two cutting wedges is depicted in an orthogonal section (A–A) and a section in the direction of feed (Section B–B) at the radius $R_x = \frac{D_x}{2}$.

Angles α_{ox} and γ_{ox} in section A–A represent the orthogonal clearance and orthogonal rake angle respectively at radius R_x , whereas angles α_{sx} and γ_{sx} in section B–B represent the side clearance and side rake angle, respectively, of the wedge in the machine tool reference system at radius R_x .

At the outer edge of the drill, $R_x = R = \frac{D}{2}$; here, the angle γ_{sx} is maximum and is equal to the helix angle of the drill flute θ . The variation of γ_{sx} with the change of radius can be understood by referring to Figure 5.6.

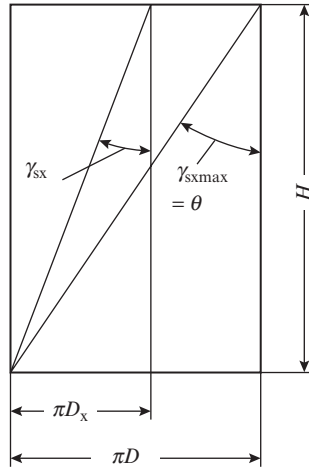


Figure 5.6 Schematic depicting the variation of γ_{sx} along the primary cutting edge of drill

$$\tan \theta = \tan \gamma_{sx \max} = \frac{\pi D}{H} \quad (5.11)$$

where

D = diameter of the drill

H = pitch of the helix of drill flute

At an arbitrary diameter $D_x = 2R_x$,

$$\tan \gamma_{sx} = \frac{\pi D_x}{H} \quad (5.12)$$

From Eqs (5.11) and (5.12), we find

$$\frac{\tan \gamma_{sx}}{\tan \theta} = \frac{D_x}{D}$$

Therefore,

$$\tan \gamma_{sx} = \frac{D_x}{D} \tan \theta \quad (5.13)$$

One-half of the lip angle shown in Figure 5.5 can be considered as the primary cutting-edge angle ϕ . At the outer edge of the drill, the cutting-edge inclination angle λ is equal to ϕ . The cutting-edge inclination angle λ_x at an arbitrary radius R_x may be determined from the following relation:

$$\sin \lambda_x = \frac{D_o}{D_x} \sin \phi \quad (5.14)$$

where

D_o = diameter of the chisel edge

Now considering the relations correlating the tool angle in the orthogonal and machine tool reference systems given in Section 1.8, we find that for the case of negative cutting-edge inclination angle:

$$\tan \gamma_{sx} = \tan \gamma_{ox} \sin \phi + \tan \lambda_x \cos \phi \tag{5.15}$$

wherefrom

$$\tan \gamma_{ox} = \frac{\tan \gamma_{sx} - \tan \lambda_x \cos \phi}{\sin \phi}$$

Substituting for $\tan \gamma_{sx}$ from Eq (5.13) and $\tan \lambda_x$ from Eq(5.14) in the above expression, we finally obtain

$$\tan \gamma_{ox} = \frac{\left(\frac{D_x}{D}\right) \tan \theta - \tan \left[\sin^{-1} \left\{ \frac{D_o}{D_x} \sin \phi \right\} \right] \cos \phi}{\sin \phi} \tag{5.16}$$

The variation of γ_{ox} with the ratio R_x/R is shown in Figure 5.7, where it can be noted that the rake angle is maximum at the outer edge of the drill (periphery) and reduces as we move toward the centre of the drill. At the chisel edge, the rake angle has a large negative value that creates tough conditions for machining because of thick wedge. At the periphery of the drill where cutting speed and heat produced are maximum, it would be desirable to have a small rake angle and a correspondingly thick wedge. However, the actual situation is just the opposite, resulting in severe heating of the cutting edge at the periphery. This type of undesirable variation of the rake angle along the cutting edge of the drill explains the large contribution of chisel edge to the thrust force (Table 3.2) produced in drilling and that the wear of the cutting edge is not uniform along its length, but is concentrated mostly near the periphery.

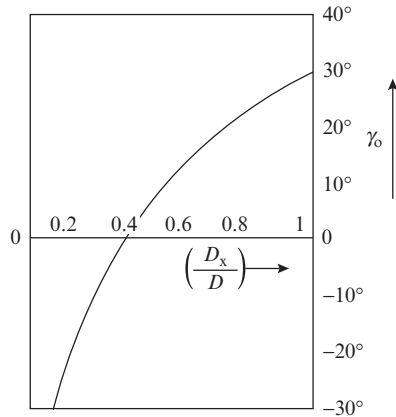


Figure 5.7 Variation of orthogonal rake angle along the primary cutting edge of drill

The normal clearance angle of the drill at radius R_x is given by the following relation:

$$\tan \alpha_{nx} = \tan \alpha_{sx} \sin \phi \tag{5.17}$$

An important feature of drill geometry is that the actual rake and clearance angles during cutting are noticeably different from the corresponding static angles provided on the drill at the time of

grinding. This is due to the fact that during the cutting operation, the drill not only rotates but also moves axially. The trajectory of a point on the cutting edge of a rotating drill is not a circle but a helix. Consequently, the cutting surface generated by the primary cutting edge is not a tapered cone but a spiral as shown in Figure 5.8.

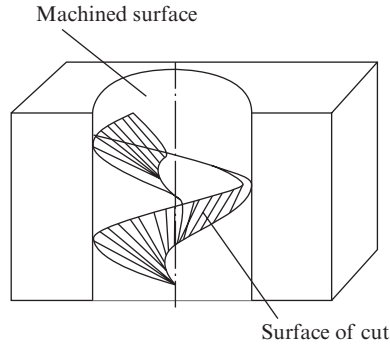


Figure 5.8 Surface of cut in drilling operation

Hence, the actual cutting plane at a given point of the cutting edge during cutting is inclined to the static cutting plane by an angle μ as shown in Figure 5.9(a). This angle is found from the relation.

$$\tan \mu = \frac{s}{\pi D_x} \quad (5.18)$$

The actual clearance and rake angles on a drill are therefore given by the following relations as is shown in Figures 5.9(a) and 5.9(b), respectively:

$$\alpha_{\text{sact}} = \alpha_s - \mu \quad (5.19)$$

$$\gamma_{\text{sact}} = \gamma_s + \mu \quad (5.20)$$

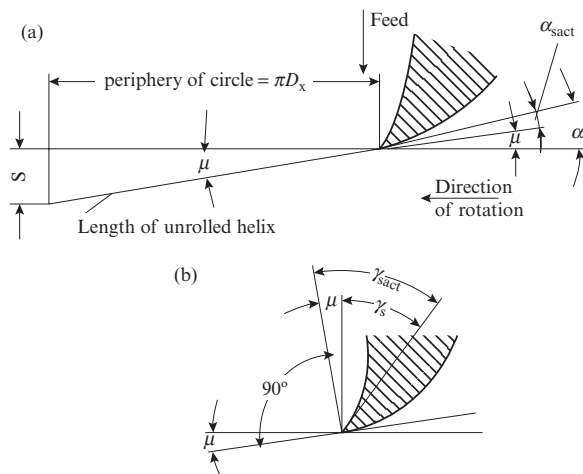


Figure 5.9 Schematic depicting the effect of feed on (a) actual clearance angle and (b) actual rake angle

The value of μ increases with the increase of feed s and reduction of R_x . Hence, it is maximum at the point where the primary cutting edge meets the chisel edge. Correspondingly, the actual clearance angle is minimum at this point. For very large value of μ (at large feed), the actual clearance angle may become extremely small or even negative. This is unacceptable as was explained in Section 1.1 (see Figure 1c). Therefore, in order to ensure sufficient clearance angle on the cutting edge near the drill axis, a variable clearance angle is provided on the primary cutting edge of the drill at the time of grinding. Correspondingly, in order to provide a more or less uniform thickness of the cutting wedge, the rake angle is also made variable along the length of the primary cutting edge. The recommended values of clearance and rake angles are given below.

- (i) For HSS drills:
 $\alpha_s = 20\text{--}27^\circ$ at the center and $8\text{--}14^\circ$ at the periphery; the larger values pertain to smaller drills.
 $\gamma_0 = 20\text{--}30^\circ$ at the periphery and approximately zero at the end of the chisel edge.
- (ii) For cemented carbide tipped drills:
 $\alpha_s = 16\text{--}20^\circ$ at the center and $4\text{--}6^\circ$ at the periphery.
 $\gamma_0 = 0\text{--}6^\circ$ at the periphery and large negative value of approximately -15° to -20° at the end of the chisel edge.
- (iii) The chisel edge angle ψ does not vary much and is taken as $\psi = 50^\circ$ for HSS drills of diameter 1–12 mm and 55° for HSS drills of diameter >12 mm. For cemented carbide-tipped drills, the chisel edge angle is taken 55° , irrespective of the drill diameter.
- (iv) Helix angle θ is the angle that the tangent to the flute spiral makes with the drill axis. It can be seen from Eqn. (5.13) that the increase of helix angle is accompanied by the increase of the rake angle, thereby weakening the cutting wedge. On the contrary, torque and thrust force reduce with the increase of helix angle. Thus, an optimum value of θ exists for each drill, depending on its diameter. For machining of steels with HSS drills of diameter 4–80 mm, the value of θ varies from 25° to 30° . For small drills of diameter 0.25–4.0 mm, the value of θ varies from 18° to 25° . For nonferrous materials (copper, aluminum, etc.), it varies from 35° to 45° ; and for brass, bronze, bakelite, and other plastics, it varies from 8° to 12° . For cemented carbide-tipped drills, the recommend values of θ , depending on drill diameter are given below:

| | | | | |
|-------------------------|----|------|-------|-----|
| Drill diameter D (mm) | <8 | 8–15 | 15–25 | >25 |
| θ (degrees) | 13 | 15 | 18 | 20 |

In all the above recommendations regarding θ , the lower values of the range pertain to smaller drills.

- (v) Lip angle 2ϕ plays a role similar to that of primary cutting-edge angle ϕ in single-point tools. With the increase of lip angle, the torque decreases, but the thrust force increases. Increasing the lip angle also reduces tool life (see Figure 4.22). Thus, an optimum value of lip angle exists, which depends on the work material. This optimum value increases as the work material becomes more brittle and harder. In fact, the helix angle also depends on the work material. The recommended values of lip angle and helix angle for carbon steel, alloyed steel, and HSS drills of diameter >10 mm are given in Table 5.1.

The recommend values of lip angle for cemented carbide-tipped drills are given in Table 5.2.

Table 5.1 Recommended values of lip angle and helix angle for carbon steel, alloy steel and HSS twist drills

| S. No. | Material | Helix angle (degrees) | Lip angle (degrees) |
|--------|--|-----------------------|---------------------|
| 1. | Steel, $\sigma_u < 70$ kgf/mm ² | 30 | 116–118 |
| 2. | Steel, $\sigma_u = 70$ –100 kgf/mm ² | 25 | 120 |
| 3. | Steel, $\sigma_u = 100$ –140 kgf/mm ² | 20 | 125 |
| 4. | Stainless steel | 25 | 125 |
| 5. | Cast iron | 25–30 | 116–120 |
| 6. | Copper | 34–45 | 125 |
| 7. | Brass | 25–30 | 130 |
| 8. | Bronze, BHN >100 | 15–20 | 135 |
| 9. | Soft bronze, BHN <100 | 8–12 | 125 |
| 10. | Aluminum alloys | 35–45 | 130–140 |
| 11. | Plastics, ebonite, bakelite | 8–12 | 60–100 |

Table 5.2 Recommend values of lip angle for cemented carbide-tipped drills

| S. No. | Material | Lip angle (degrees) |
|--------|---|---------------------|
| 1. | Steel, $\sigma_u = 60$ –100 kgf/mm ² | 116–118 |
| 2. | Cast iron, BHN <220 | 116–118 |
| 3. | Steel, $\sigma_u > 100$ kgf/mm ² | 130–135 |
| 4. | Babbitt, tin | 140 |

Example 5.2

In a twist drill, the helix angle $\phi = 30^\circ$ and lip angle $2\phi = 120^\circ$. If the chisel edge diameter is 5.0 mm and drill diameter is 30 mm, determine the minimum and maximum orthogonal rake angle.

The minimum rake angle occurs at the end of the chisel edge where $D_x = 5.0$ mm and the maximum at the end of the primary cutting edge where $D = 30$ mm. On substituting these values and the given values of $D_o = 5$ mm, $\theta = 30^\circ$, and $\phi = 60^\circ$ in Eqn. (5.16), we find

$$\begin{aligned}
 (\tan \gamma_{ox})_{\min} &= \frac{\frac{5}{30} \tan 30 - \tan \left[\sin^{-1} \left(\frac{5}{5} \sin 60 \right) \right] \cos 60}{\sin 60} \\
 &= \frac{\frac{5}{30} \times 0.5774 - \tan \left[\sin^{-1} 60 \right] \times 0.5}{0.866}
 \end{aligned}$$

$$= \frac{0.0962 - \tan(60^\circ) \times 0.5}{0.866} = \frac{0.0963 - 0.866}{0.866}$$

$$= -0.8889$$

Hence, γ_o minimum = -41°

$$\tan \gamma_{o \max} = \frac{\frac{30}{30} \tan 30 - \tan \left[\sin^{-1} \left(\frac{5}{30} \sin 60 \right) \right] \cos 60}{\sin 60}$$

$$= \frac{0.5774 - \tan \left[\sin^{-1} 0.1443 \right] \times 0.5}{0.866} = \frac{0.5774 - \tan 8^\circ 20' \times 0.5}{0.866}$$

$$= \frac{0.5774 - 0.1465}{0.866} = 0.4975$$

Hence, γ_o maximum = $26^\circ 25'$

Example 5.3

A ϕ 20 hole is made by a drill of chisel edge diameter 5 mm. If the clearance angle in the normal plane at the junction of primary cutting edge and chisel edge is 5° and the primary cutting edge angle $\phi = 60^\circ$, determine the feed at which it is safe to carry out the drilling operation.

The deviation of clearance angle due to feed is given by the following relation:

$$\tan \mu = \frac{s}{\pi D_x}$$

Obviously, this angle increases with reduction of D_x and is maximum at the point where the chisel edge meets the primary cutting edge, that is, where $D_x = D_o = 5$ mm

Hence,

$$\mu_{\max} = \tan^{-1} \left(\frac{s}{\pi \times 5} \right)$$

The side clearance angle α_{sx} is found from Eqn. (5.17):

$$\tan \alpha_{sx} = \frac{\tan \alpha_{nx}}{\sin \phi} = \frac{\tan 5^\circ}{\sin 60^\circ} = \frac{0.0875}{0.866} = 0.101$$

The side clearance angle $\alpha_{sx} = 6^\circ$

For safe drilling, α_{sact} must be ≥ 0 . Hence from Eqn. (5.19), we find

$$\mu_{\max} = \tan^{-1} \left(\frac{s}{\pi \times 5} \right) \alpha_{sx} = 6^\circ$$

Hence, safe feed is $s = \pi \times 5 \times \tan 6^\circ = \pi \times 5 \times 0.101 = 1.58$ mm/rev

Example 5.4

Select the appropriate tool angles for an HSS taper shank twist drill to make a hole for M27 thread in a 50-mm-long job.

For making a M27 thread, the required drill size is 23.9 mm. The nearest available drill of 23.5 mm is therefore selected. The remaining diametric allowance of 0.4 mm is to be removed by reaming or boring to enlarge the drilled hole to the required size.

Medium carbon steel has $\sigma_u < 70 \text{ kg/mm}^2$. Hence, from Table 5.1, we select lip angle $2\phi = 118^\circ$ helix angle $\theta = 30^\circ$.

The chisel edge angle ψ for drill of diameter $>12 \text{ mm}$ is recommended as $\psi = 55^\circ$. Hence, this value is selected for the drill of diameter 23.5 mm.

The clearance angle at the periphery is recommended as $8\text{--}14^\circ$; a value of $\alpha = 12^\circ$ is selected for the drill of diameter 23.5 mm.

5.4 Geometry of Milling Cutters

As mentioned in Section 1.5, milling cutters can be broadly classified into four groups:

Group 1: cutters that have cutting teeth only on the periphery, for example, plain milling cutter

Group 2: cutters that have cutting teeth only on the face, for example, face milling cutter

Group 3: cutters that have cutting teeth on the periphery and end face, for example, end milling cutter

Group 4: cutters that have cutting teeth on the periphery and side face, for example, side milling cutter

From the above classification, it is evident that the geometry of all the milling cutters can be established based on the geometry of two distinct cutters: one with the cutting teeth on the periphery and the other with the cutting teeth on the face. As the most popular representatives of these two situations, the plain and face milling cutter will be the subject of a detailed description of their geometry in this section.

However, before undertaking this exercise, it is necessary to tackle an issue that is central to the geometry of all milling cutters, namely the profile of the cutting teeth. Based on the shape of the tooth profile, all milling cutters are classified into two groups:

- (i) profile sharpened cutters
- (ii) form-relieved cutters

All general-purpose milling cutters, namely plain, face, end, and side milling cutters machine a straight surface that is generated by a combination of cutter rotation and feed imparted to the job (see Figures 1.26–1.30). In these cutters, the reduction in size of the cutter after resharpening is not important, and the profile shape and size is determined from the following considerations:

- (i) adequate tooth strength
- (ii) adequate space between adjacent teeth to accommodate the chip produced
- (iii) maximum number of regrindings allowed for overall maximum total cutter life
- (iv) ease of regrinding

The cutting teeth that meet the above requirements are sharpened by grinding the flank on a narrow land behind the cutting edges. They are therefore known as profile sharpened and the cutters with such teeth are known as profile sharpened cutters. Three types of shapes used in profile sharpened teeth are shown in Figure 5.10.

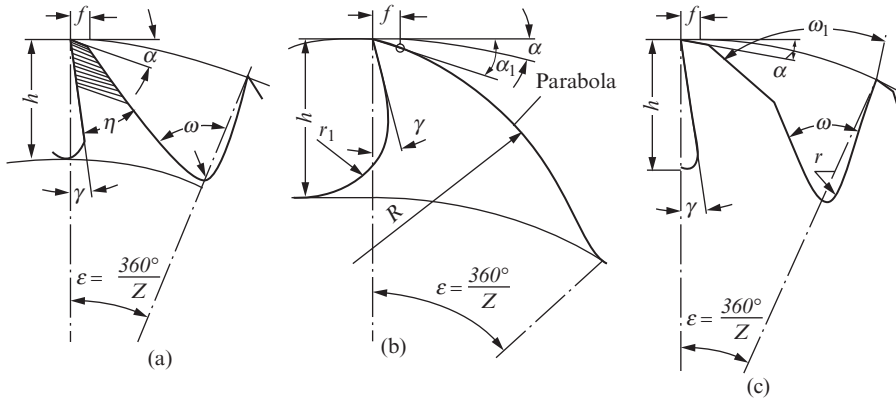


Figure 5.10 Tooth shapes of profile sharpened milling cutters: (a) trapezoidal, (b) parabolic, and (c) heavy duty shape with two clearance surfaces

The trapezoidal shape shown in Figure 5.10(a) is the simplest to manufacture and resharpen. However, the tooth is relatively weak, and this shape is therefore mostly used in fine-tooth milling cutters for finishing cuts. The parabolic shape, as can be seen in Figure 5.10(b), is designed based on the equistrength principle—that is, equal bending strength in all sections of the tooth. In view of the difficulty of making a parabolic profile, a compromise shape consisting of two straight clearance surfaces (Figure 5.10c) that is close to the equistrength principle in performance is more popular. The shapes shown in Figure 5.10(b) and (c) are used in coarse-tooth milling cutters for rough cuts.

The parameters of the trapezoidal tooth profile shown in Figure 5.10(a) are as follows:

$$\eta = 45\text{--}50^\circ, f = 1\text{--}2 \text{ mm}, r = 0.5\text{--}2.0 \text{ mm}, h = (0.5\text{--}0.65)p, \epsilon = \frac{360}{Z}, \omega = \eta + \epsilon$$

where

p = pitch of the cutter teeth

Z = number of teeth of the cutter

To reduce the required number of flute milling cutters, the values of ω are established in the range 45–110° in steps of 5°.

The parameters of the parabolic tooth profile shown in Figure 5.10(b) are as follows:

$$f = 1\text{--}2 \text{ mm}, \alpha = \text{clearance angle at the tip} + (10\text{--}15^\circ), \epsilon = \frac{360}{Z}, h = (0.3\text{--}0.45)p, r_1 = (0.4 - 0.75)h, R = (0.3\text{--}0.45)D$$

The parameters of the tooth profile shown in Figure 5.10(c) are as follows:

$$f = 1\text{--}2 \text{ mm}, h = (0.3\text{--}0.45)p, r = 0.5\text{--}2.0 \text{ mm}, \epsilon = \frac{360}{Z}, \eta = 45\text{--}50^\circ, \omega = \eta + \epsilon, \omega_1 = 60\text{--}65^\circ, \alpha_1 = 20\text{--}30^\circ$$

The cutters used in form milling and gear cutting operations shown in Figure 1.31(a)–(c) work on a different principle. For these operations, the negative image of the volume of metal to be removed is provided on the cutter, which later copies this profile on the workpiece during the operation to produce the desired feature. The main requirement for the profile of such cutters is that after resharpening the profile should ideally remain unchanged or at least the change should be minimal. The curve that best meets this requirement is the Archimedean spiral. Therefore, the flank of these cutters is made to follow the Archimedean spiral.

The teeth of this profile are sharpened on the face and are known as form relieved, and the cutters with teeth of such a profile are known as form-relieved cutters. The shape of the form-relieved tooth is shown in Figure 5.11.

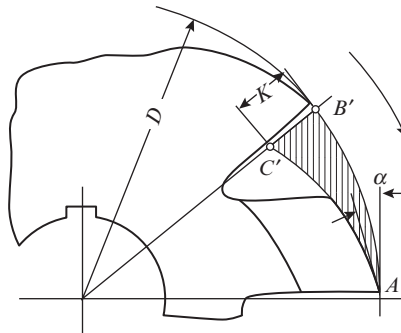


Figure 5.11 Tooth shape of form-relieved milling cutter

The main parameters of form-relieved tooth are clearance angle α and the relief height K . For a cutter of diameter D and number of teeth Z , relief height K can be found from the following relation:

$$K = AB' \tan \alpha = \frac{\pi D}{Z} \tan \alpha \quad (5.21)$$

The value of K varies from 0.5 mm to 12 mm depending on the cutter size and number of teeth. The minimum value pertains to fine-tooth cutter of small size and the maximum to rough tooth cutter of larger size. The rake angle in form-relieved cutters is taken equal to zero; otherwise after every resharpening, the cutter outer diameter will reduce in direct proportion to the magnitude of the rake angle. However, machining with $\gamma = 0$ cutters is difficult; therefore, if some distortion of the tooth profile is acceptable, a small rake angle is provided for ease of cutting.

5.4.1 Geometry of Plain Milling Cutter

The geometry of plain milling cutter can be described with the help of Figure 5.12.

The clearance angle α is generally defined in the plane, normal to the cutter axis (Section A–A). It represents the angle between the tangent to the tooth flank and the tangent to the circle at the same point of the primary cutting edge. Sometimes, the clearance angle is defined in the plane normal to the primary cutting edge α_n in (Section B–B). It represents the angle between the tangent to

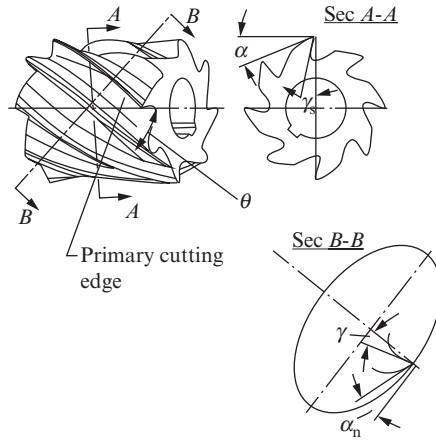


Figure 5.12 Schematic depicting geometry of plain milling cutter

the tooth flank and the tangent to the ellipse in the normal section at the same point. The angles α and α_n are related by the following expression:

$$\tan \alpha = \tan \alpha_n \cos \theta \tag{5.22a}$$

where

θ = helix angle of the cutter

The rake angle γ is generally defined in the normal Section B–B. It represents the angle between the tangent to the tooth face and the radial line of the cutter in the normal section at the same point. Sometimes, the rake angle is defined in the plane normal to the cutter axis (γ_s in Section A–A). It represents the angle between the tangent to the tool face and the circle at the same point of the primary cutting edge. As the Section A–A lies in the direction of feed, the rake angle in the plane may be considered as the equivalent of side rake angle in a single-point tool. The angles γ and γ_s are related by the following expression:

$$\tan \gamma = \tan \gamma_s \cos \theta \tag{5.22b}$$

The recommended values of rake and clearance angles for HSS plain milling cutters are as follows:

Rake angle $\gamma = 10\text{--}20^\circ$, where the larger values pertain to relatively softer materials

Clearance angle $\alpha_n = 12\text{--}16^\circ$, where the larger values pertain to fine-tooth cutters

The helix angle θ represents the angle that the tangent to the helix of the primary cutting edge at a given point makes with the cutter axis. For coarse-tooth cutters used for rough cuts and having number of teeth $Z = 6\text{--}12$, the helix angle is taken as $\theta = 40^\circ$; whereas for fine-tooth cutters used for semifinishing and finishing cuts having $Z = 10\text{--}18$, the helix angle is taken $\theta = 30\text{--}35^\circ$. For assembled HSS cutters, the recommended value is $\theta = 20^\circ$ and for assembled cutters with cemented carbide blades $\theta = 12\text{--}15^\circ$

Example 5.5

A HSS plain milling cutter of diameter 100 mm and 12 teeth is designed for finish machining of low- and medium-strength steel parts. Select the appropriate cutting angles and tooth profile of the cutter and determine the profile parameters.

As the cutter is used for finishing operations, we will select the trapezoidal tooth profile (Figure 5.1a).

As recommended for fine-tooth cutters used for finishing cuts, we select clearance angle $\alpha_n = 16^\circ$.

As the work material is mild and medium-strength steel, we select the mean value in the recommended range, that is, $\gamma = 15^\circ$.

As per the recommendation, we select helix angle $\theta = 30^\circ$.

The pitch of the cutter is

$$p = \frac{\pi D}{Z} = \frac{\pi \times 100}{12} = 26.167 \text{ mm}$$

The pitch angle is

$$\varepsilon = \frac{360}{Z} = \frac{360}{12} = 30^\circ$$

The profile parameters are found as follows:

$$\eta = 45^\circ, f = 1.5 \text{ mm}, r = 1.0 \text{ mm}, h = 0.6p = 0.6 \times 26.167 = 15.7 \text{ mm, flute angle}$$

$$\omega = \eta + \varepsilon = 45^\circ + 30^\circ = 75^\circ.$$

5.4.2 Geometry of Face Milling Cutter

The geometry of face milling cutter can be described with the help of Figure 5.13.

It is evident from the figure that each tooth of the face milling cutter can be treated as a single tip. Therefore, the geometry of face milling cutter can be described in a manner similar to the single-point tool (see Section 1.8). The orthogonal rake and clearance angles are defined in the orthogonal section (Section A–A) exactly as in a single-point tool. The geometry in the coordinate system of the machine tool is defined with the help of an axial section (Section B–B) and a radial section (Section C–C) that are equivalent to the machine transverse plane and machine longitudinal plane respectively used for defining the geometry of single point tool in the machine tool reference system. Hence axial clearance angle α_y and axial rake angle γ_y in Section B–B are identical to end clearance angle α_e and back rake angle γ_b of single-point tool. Similarly, the radial clearance angle α_x and radial rake angle γ_x in Section C–C are identical to side clearance angle α_s and side rake angle γ_s of single point tool.

The meaning and role of primary cutting edge angle ϕ , auxiliary cutting edge angle ϕ_c and cutting edge inclination angle λ in face milling cutter is similar to that in single point tool. Consequently, the orthogonal rake angle is related to the axial and radial rake angles by an expression similar to that in single-point tool:

$$\tan \gamma_o = \tan \gamma_x \sin \phi + \tan \gamma_y \cos \phi \quad (5.23)$$

In view of the fact that face milling cutter operates under impact load conditions, the primary cutting edge is provided with an intermediate step of length 1–2 mm at an angle $\phi_o = \frac{1}{2}\phi$.

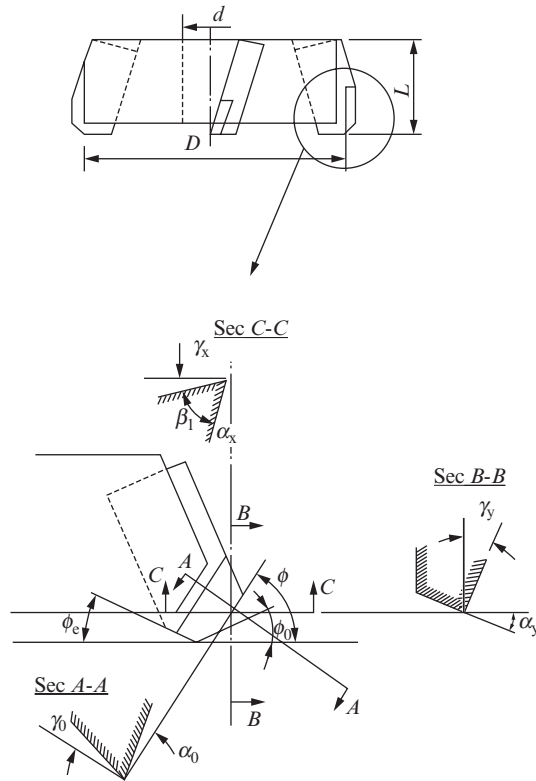


Figure 5.13 Schematic depicting geometry of face milling cutter

Solid (shell-type) HSS face milling cutters (Figure 5.14) have teeth both on the end face and the periphery. The teeth on the periphery are made at a helix angle θ in a manner similar to that in plain milling. For a smooth transition and continuity between the teeth on the end face and the periphery, the helix angle θ is taken equal to the back rake angle. The helix angle is taken $\theta = 25\text{--}30^\circ$ for fine-tooth solid HSS cutters and $35\text{--}40^\circ$ for coarse-tooth cutters. In case of assembled cutters, $\theta = 10^\circ$ is taken for HSS and $\theta = 0^\circ$ for cemented carbide cutters.

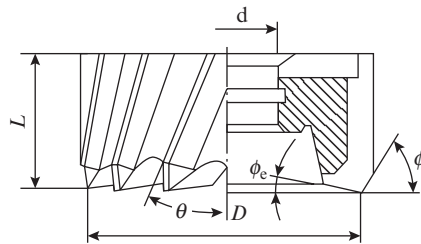


Figure 5.14 Shell-type face milling cutter

The recommended angles for face milling cutters are given below:

Solid HSS face milling cutters:

$$\gamma = 12^\circ, \quad \alpha = 14^\circ, \quad \phi = 90^\circ, \quad \phi_c = 2^\circ$$

Assembled HSS face milling cutters:

$$\gamma = 15^\circ, \quad \alpha = 12^\circ, \quad \phi = 45\text{--}60^\circ, \quad \phi_c = 2^\circ$$

Assembled cemented carbide cutters for machining cast iron:

$$\gamma = 8^\circ, \quad \alpha = 15^\circ, \quad \phi = 90^\circ, \quad \phi_c = 5^\circ$$

Assembled cemented carbide cutters for machining steel:

$$\gamma = -5^\circ, \quad \alpha = 15^\circ, \quad \phi = 15\text{--}60^\circ, \quad \phi_c = 5^\circ$$

The values of ϕ in the range 15–30° are used for milling machines with good rigidity and the larger values for machines with relatively poor rigidity.

Some empirical relations for optimum rake angle in plain as well as face milling cutters are given below:

HSS milling cutters for machining steel and cast iron:

$$\gamma_{\text{opt}} = 7.0\xi^{1.15}$$

where

ξ = chip reduction coefficient

Carbide-tipped milling cutters for machining steel:

$$\gamma_{\text{opt}} = 0.22 \times 10^{-11} \sigma_u^{5.7}$$

where

σ_u = ultimate strength of work material in kgf/mm²

Carbide-tipped milling cutters for machining cast iron

$$\gamma_{\text{opt}} = 17.2 - 0.066 \text{ BHN}$$

where

BHN represents the Brinell's hardness of cast iron

From the values of clearance angle given above, it can be noted that they are higher than for single-point tools. The reason is that in milling operations, the undeformed chip thickness may be very small during some stage of the chip removal process (see Section 2.2). In fact, in plain milling operation, it is actually zero at the start of cut in up milling and at the end of cut in down milling (see Figure 1.26). Under these conditions, the undeformed chip thickness may become less than the tool nose radius. A comparison of the chip removal process for the case $a > r$ and $a < r$ is shown in Figure 5.15 (a) and (b), respectively. The static and actual rake angle remains the same for $a > r$. However, when $a < r$ the actual rake angle acquires a very large negative value $-\gamma_a$ (Figure 5.15), and the original wedge of angle δ effectively becomes an obtuse wedge of angle δ_a .

Cutting with such a wedge becomes extremely difficult. The solution lies in reducing r . Ideally, for milling operations where a can become zero, it would be desirable to also have $r = 0$. However, in practice, this is not possible for two reasons: First, a small natural edge radius is inevitable in any tool-grinding operation. Second, even if one concedes the possibility of producing a cutting edge with $r = 0$, it is not desirable to have such an edge because it would crumble immediately on start of cutting. Consequently, for milling cutters, one should strive to reduce r as much as possible to make the cutting edge suitable for the geometry of chip to be removed. As can be seen from Figure 5.15, the easiest way to achieve this is by increasing clearance angle α , which explain its relatively higher values in milling cutters.

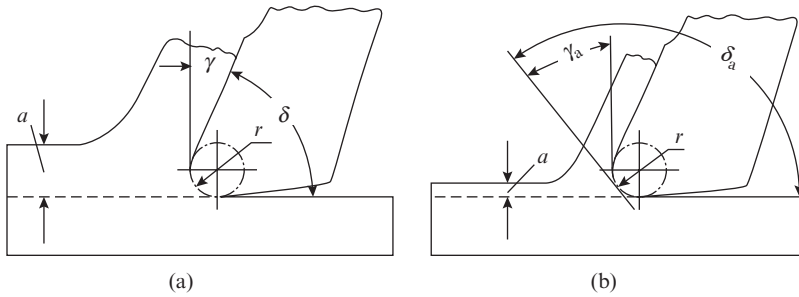


Figure 5.15 Schematic depicting chip removal: (a) when $a > r$ and (b) when $a < r$

5.5 Geometry of Broach

Broaching is an operation that is widely used in industry for making round and irregular shaped through holes, external, and internal gears and external profile shapes of any complexity. In broaching, the material is removed by a long tool called broach. Broaches may be of push or pull type. The push-type broach (Figure 5.16) is shorter in length to avoid bending during the application of the pushing force. The length of push-type broach should not exceed 15 times its diameter, and these broaches are generally used on vertical broaching machines that are similar in construction to a hydraulic press.

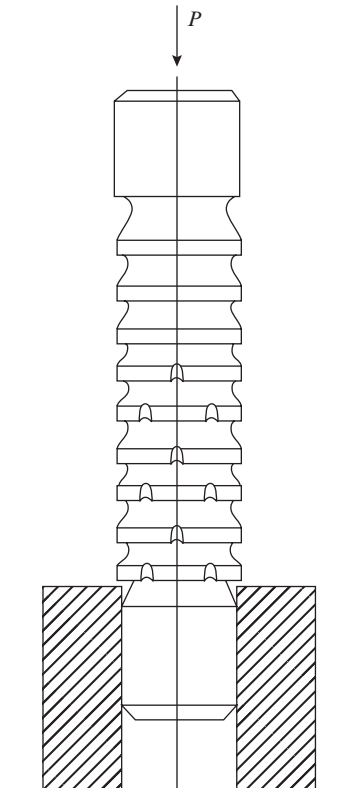


Figure 5.16 Push-type broach

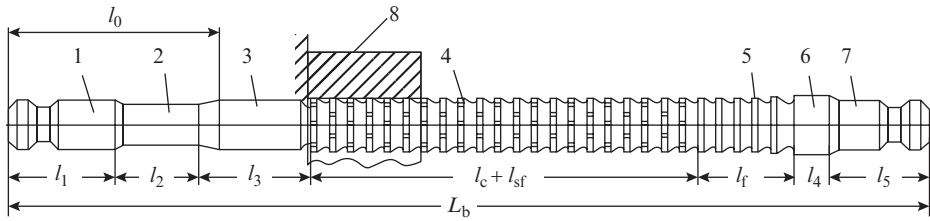


Figure 5.17 Pull-type broach and its main elements (1—pull end, 2—neck, 3—front pilot, 4—roughing teeth, 5—finishing teeth, 6—rear pilot, 7—rear support, 8—workpiece)

The pull-type broach is not subject to any limitation of length and is therefore more widely used. In view of excessive length, it is used on horizontal broaching machines. A pull-type broach and its elements are shown in Figure 5.17, and the schematic of a horizontal broaching machine is shown in Figure 5.18.

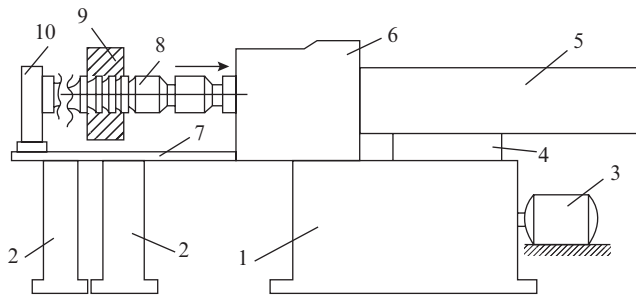


Figure 5.18 Schematic of horizontal pull-type broaching machine (1—housing with hydraulic drive, 2—supporting column, 3—electric motor, 4—direction control system, 5—hydraulic cylinder, 6—carriage with ram, 7—guideways, 8—broach, 9—workpiece, 10—follower)

The hydraulic drive located inside the housing of the broaching machine consists of a pump, reservoir, flow control valve, and pressure valve. The drive along with the direction control valve powers the reversible translatory motion of the cylinder. The pull end of the broach is gripped by an attachment on the piston of the hydraulic cylinder. Now as the piston is moved under hydraulic pressure, it pulls the broach through the component and each of its cutting teeth removes metal in succession to make the final desired profile. The front pilot aligns the broach, whereas the rear support rests on a follower that moves in guideways along with the broach.

External profiles are made on continuous broaching machines that may have a rotary or a translatory cutting motion (Figure 5.19).

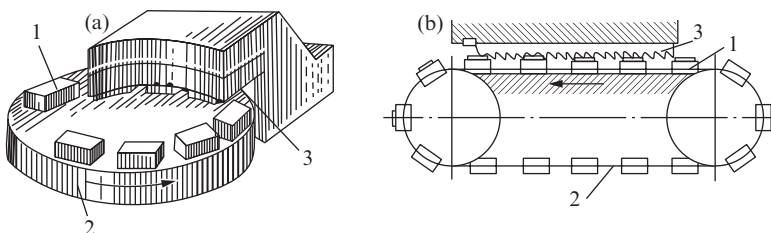


Figure 5.19 Broaching of external profiles on continuous broaching machine with (a) rotary cutting motion (1—workpiece, 2—rotary table, 3—fixed broach) and (b) translatory cutting motion (1—workpiece, 2—endless chain, 3—fixed broach)

Broach is a fragile tool and can be easily damaged if overloaded. To prevent such accidental damage, broaching machines are mostly provided with hydraulic drive, because of the ease of implementing overload protection in hydraulic circuits. A unique feature of broaching machines is that unlike all other metal cutting machines, they have only one cutting motion: the speed motion. The feed motion is not required, because it is in-built in the broach as each of its successive teeth is higher than the previous one. The machining of the workpiece is completed in a single cutting stroke as the roughing, semifinishing, and finishing teeth all are provided on the broach itself.

Here, it also needs to be mentioned that broach is an expensive tool; therefore, broaching is used mainly for making complex profiles, especially internal ones and for machining of small holes that cannot be easily enlarged by boring because of the difficulty of accommodating the boring bar in the hole. As a rule, broaching is a final finishing operation and broached surfaces are not subject to further machining. Some typical examples of the profiles produced by broaching are shown in Figure 5.20.

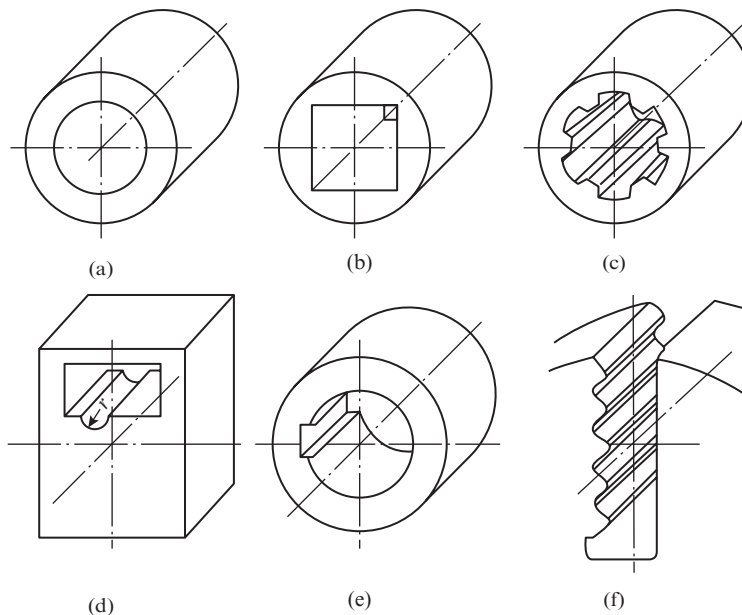


Figure 5.20 Typical examples of parts made by broaching operation: (a) round hole, (b) square hole, (c) splined hole, (d) square hole with groove, (e) round hole with key way, and (f) vice jaw

Broaches are mostly made of high-speed steel. The cutting speed in broaching lies in the range 2–10 m/min and is purposely kept low to avoid cutting with built-up edge formation that starts at about $v = 10$ m/min. Despite low cutting speed, the productivity of broaching is very high on account of the large number of cutting edges removing metal in a single stroke. The machining time in one pass of a broach can be found from the following relation:

$$T_m = \frac{L}{1000vq}K \quad (5.24)$$

where

L = length of stroke of the broach, mm

v = cutting speed, m/min

q = number of components broached simultaneously

K = ratio of the reverse stroke speed to cutting stroke speed; generally $K = 1.4$ – 1.5

The geometry of the cutting and finishing teeth of broach is shown in Figure 5.21.

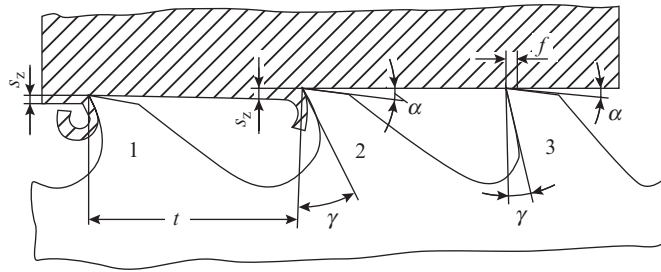


Figure 5.21 Geometry of broach (1 and 2—rough cutting teeth, 3—finishing tooth, s_z —rise per tooth, t —pitch)

The clearance angle is $\alpha = 3^\circ$ for roughing teeth and 2° for finishing teeth. A narrow cylindrical band of width $f = 0.05$ – 0.2 mm is made on the finishing teeth to minimize profile change after resharpening. The reason for small value of clearance angle is that being in principle a form tool (the broach tooth profile is negative image of the surface removed by it); the broach is ground only at the face just like form relieved milling cutters (see Figure 5.11). Therefore, to minimize variation of the broach dimension after regrinding, the clearance angle is kept as small as possible.

Rake angle of broach is selected for different materials from Table 5.3.

Table 5.3 Rake angle on broach

| S. No. | Material | Hardness | Rake angle γ for | |
|--------|--------------------------------|----------------|-------------------------|-----------------|
| | | | Roughing teeth | Finishing teeth |
| 1. | Steel | BHN ≤ 197 | 16–18 | 5 |
| | | BHN 198–229 | 15 | |
| | | BHN > 229 | 10 | |
| 2. | Cast iron | BHN ≤ 180 | 10 | –5 |
| | | BHN > 180 | 5 | |
| 3. | Al, Al alloys, copper, babbitt | – | 20 | 20 |
| 4. | Bronze, brass | – | 5 | –10 |

5.6 Geometry of Thread Cutting Tools

Thread cutting by machining involves removal of large volume of material. Therefore, there are fundamentally two different approaches of thread cutting as shown in Figure 5.22.

- (i) Cutting of threads with a single-point tool in multiple passes; these tools can be used both for cutting external and internal threads,
- (ii) Cutting of threads with multiple-point tool in a single pass; thread chasers and thread cutting dies are multiple-point tools for cutting external threads and taps are multiple point tools for cutting internal threads.

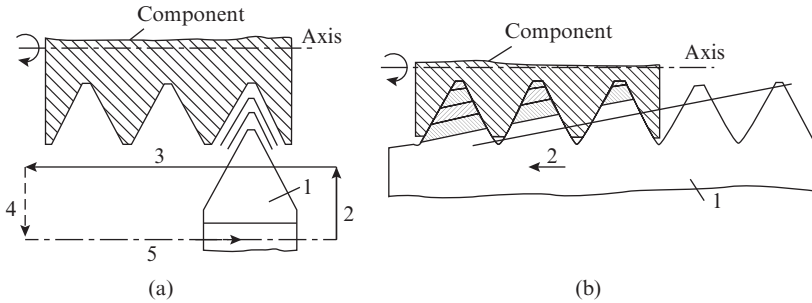


Figure 5.22 Thread cutting with (a) single-point tool in multiple passes (1—thread cutting tool, 2—in feed, 3—cutting motion, 4—withdrawal, 5—reverse motion) (b) multiple-point tool (chaser) in single pass (1—thread chaser, 2—cutting motion)

The number of passes required for machining threads with single-point tool depends on the thread pitch. To achieve accuracy of the thread profile, cutting has to be done in several rough and finishing passes. The recommended number of passes for cutting metric thread by HSS single-point tool is given in Table 5.4 and for cutting trapezoidal (Acme) thread in Table 5.5. These values are given for external threads. For cutting internal threads, one extra roughing pass may be taken for short jobs and 2 for long jobs.

Table 5.4 Recommended number of passes for cutting metric thread in steel, cast iron, bronze, and brass with single-point HSS tool

| Thread pitch (mm) | 0.75–1.0 | 1.25–1.50 | 1.75 | 2–3 | 3.5–4.5 | 5–5.5 | 6 |
|----------------------------|----------|-----------|------|-----|---------|-------|---|
| Number of rough passes | 3 | 4 | 5 | 6 | 7 | 8 | 9 |
| Number of finishing passes | 3 | 3 | 3 | 3 | 4 | 4 | 4 |

The use of large number of rough passes for cutting thread of large pitch is due to the fact that with less passes, the undeformed chip section to be removed will become excessively large, thereby causing heating of the part and its deformation. This is particularly important while cutting threads on long parts such as lead screws with trapezoidal (Acme) thread.

In view of the large number of passes required for cutting threads by a single-point tool, it would appear that this method is inherently at a disadvantage in comparison with thread cutting with multiple-point tools. However, this disadvantage is offset by two factors:

- (i) Cutting speed in single-point HSS threading tools lies in the range 30–40 m/min; whereas for multiple-point tools such as thread chasers, taps, and dies, it lies in the range 6–15 m/min. Nowadays, single-point thread-cutting tools are increasingly being made with cemented carbide tips that allow machining at 120–150 m/min.
- (ii) Multiple teeth thread cutting tools are much more expensive than single-point tools

Table 5.5 Recommended number of passes for cutting trapezoidal thread with single-point HSS tool

| Thread pitch (mm) | Number of passes while cutting thread in | | | | | |
|-------------------|--|-----------|-------------|-----------|--------------------------|-----------|
| | Carbon steel | | Alloy steel | | Cast iron, bronze, brass | |
| | Rough | Finishing | Rough | Finishing | Rough | Finishing |
| 2–12 | 14 | 6 | 12 | 5 | 20 | 10 |
| 16 | 15 | 8 | 12 | 5 | 20 | 10 |
| 20 | 17 | 10 | 13 | 7 | 30 | 15 |
| 24 | 21 | 11 | 15 | 8 | 35 | 18 |
| 32 | 27 | 13 | 20 | 10 | 40 | 20 |
| 40 | 32 | 16 | 25 | 12 | 45 | 20 |

5.6.1 Geometry of Single-Point Thread Cutting Tool

Thread cutting with a single-point tool is shown in Figure 5.23 where it is evident that the side of the thread is a helix of pitch t_p , where t_p is the pitch of the thread to be cut. The helix of the thread θ is defined at the pitch circle of the thread and is found from the following relation:

$$\tan \theta = \frac{t_p}{\pi D_{pc}}$$

where D_{pc} = pitch circle diameter of the thread

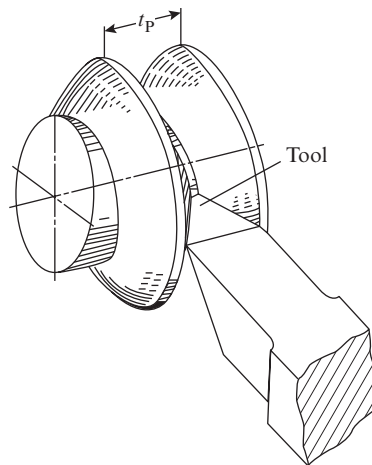


Figure 5.23 Thread cutting with a single-point tool

In view of the large values of feed at which thread cutting is done, the actual plane of cut deviates significantly from the static plane in which the tool angles are defined (see Figure 5.2). The angle of deviation μ is found from the following relation:

$$\tan \mu = \tan \theta \tan \varepsilon$$

where ε = half angle of the thread profile

On account of the deviation of the actual cutting plane from the static plane, the actual cutting angles also change. For instance, while cutting right-hand thread with a tool having static clearance angle α on both flanks, the actual clearance angle on the two flanks of the threading tool (Figure 5.24) will be as follows:

On the right flank (Section A–A),

$$\alpha_2 = \alpha + \mu$$

On the left flank (Section B–B),

$$\alpha_1 = \alpha - \mu$$

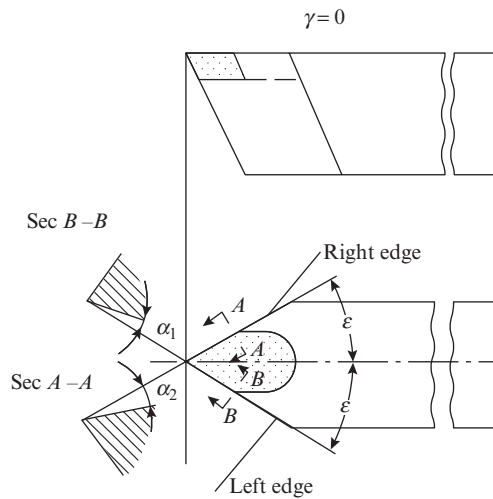


Figure 5.24 Schematic depicting the cutting angles on single-point thread cutting tool

Table 5.6 Recommended values of rake angle for single-point thread-cutting tools

| Work material | γ (degrees) |
|--|--------------------|
| Aluminum | 20–15 |
| Bronze | 0–5 |
| Soft steel, $\sigma_u < 50$ kgf/mm ² | 25 |
| Medium-strength steel, $\sigma_u = 50$ –80 kgf/mm ² | 20–25 |
| Hard steel, $\sigma_u = 80$ –100 kgf/mm ² | 12–20 |
| Cast iron, BHN < 150 | 15 |
| Cast iron, BHN = 150–200 | 12 |
| Cast iron, BHN = 200–250 | 8 |

In metric thread $\theta = 3\text{--}4^\circ$ and $2\varepsilon = 55\text{--}60^\circ$; therefore, the value of μ is small and may be ignored. However, in trapezoidal (Acme) thread, the value of μ is significant and must be taken into consideration while deciding the tool angles. For a given thread profile, the profile of the cutting tool is determined by the same procedure as that adopted for prismatic form tools. The clearance and rake angles are also taken similar to those for form tools. For metric thread, the recommended value of clearance angle is $\alpha = 12\text{--}15^\circ$; but for Acme thread $\alpha = 25\text{--}30^\circ$ because in this case, the angle μ may be of the order of $10\text{--}15^\circ$. The value of the rake angle γ depends on the work material and increases with its strength and hardness. The recommended values of γ are given in Table 5.6.

Example 5.6

A M60 metric thread is to be cut on a medium strength steel point using a single-point tool. Select appropriate number of passes and cutting tool angles and determine the actual clearance angle on the tool flanks.

From thread standards, the following data can be obtained for a metric M60 thread:

Profile angle $2\varepsilon = 60^\circ$, pitch $p = 4.0$ mm, pitch circle diameter $D_{pc} = 57.402$ mm, and minor diameter $d_m = 55.76$ mm

From Table 5.4, we find the following for pitch $p = 4.0$ mm:

Number of rough passes = 7

Number of finishing passes = 4

Clearance angle is selected as $\alpha = 12^\circ$

From Table 5.6, the rake angle for medium strength steel is selected as $\gamma = 20^\circ$

Helix angle of the thread is found as follows:

$$\theta = \tan^{-1}\left(\frac{p}{\pi D_{pc}}\right) = \tan^{-1}\left(\frac{4.0}{\pi \times 57.402}\right) = 1^\circ 15'$$

The angle of deviation is found as follows:

$$\mu = \tan^{-1}[\tan \theta \tan \varepsilon] = \tan^{-1}[0.0222 \times 0.5774] = 0'45'$$

Hence, the actual clearance angle on the two flanks will be $12 - 0^\circ 45' = 11^\circ 15'$ and $12 + 0'45' = 12^\circ 45'$, respectively

5.6.2 Geometry of Thread Chasers

Thread chasers are multiple-point thread cutting tools that may be shank, block, and circular type (Figure 5.25). These tools are similar to form tools in construction. The difference is that they are designed for producing a specific surface of revolution, namely the helical surface of thread. In principle, a chaser may be looked upon as a tool with several single-point tools embedded in one body. A chamfer of angle ϕ on the entry side of the chaser provides a set of cutting points among which the first point is the shortest in height and each successive point is higher than the preceding one. The increment in height determines the volume of metal removed by a particular tooth. Generally, a chamfer angle of $25\text{--}30^\circ$ is sufficient to provide the required number of teeth for completing rough machining of the thread profile. The chamfer is followed by a sizing section consisting of 2–6 points for finishing of the thread.

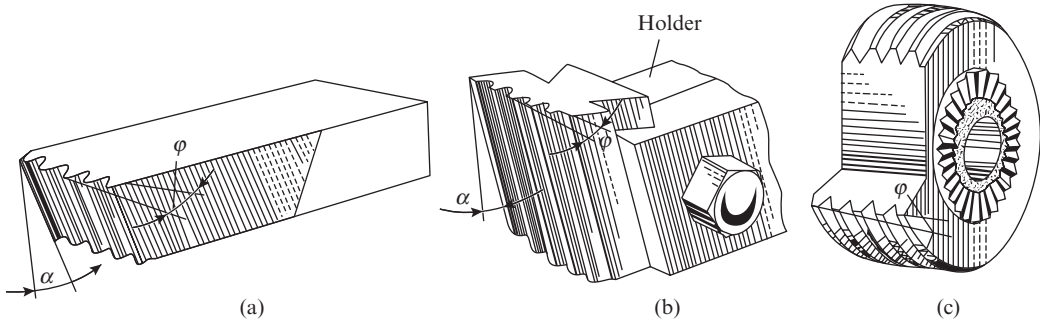


Figure 5.25 Thread chasers: (a) shank type, (b) block type, and (c) circular

Due to the difficulty associated with their manufacturing, shank- and block-type thread chasers have not found much application. Circular chasers may be made in two ways: either with a series of circular threads or with a single continuous helical thread. The former are easier to manufacture, but they can be used only for making threads with small helix angle. Circular chasers with helical thread can be used even if the helix angle of the thread to be cut is large and are therefore the most popular type of chasers used in practice although they are more difficult to manufacture. The helix of the tool should have the same direction as that of the thread while making internal threads and opposite direction while making external threads. For example, for making right-hand external thread, the chaser must have left-hand thread. This arrangement allows the clearance angle on the two flanks of the cutting teeth to be kept equal, thereby providing better cutting conditions and uniform wear of the chaser teeth.

The diameter of the thread chaser for making internal thread must be less than that of the threaded hole to be made, although the pitch of the threads on the two must be the same. If D_{wp} and D_c represent the mean diameter of the threaded hole and chaser, respectively, then the pitch is

$$p = \pi D_{wp} \tan \theta_{wp} = \pi D_c \tan \theta_c$$

As $D_{wp} > D_c$, it follows that $\theta_c > \theta_{wp}$. Thus, the helix angle of the chaser thread must be greater than that of the thread to be cut and can be found from the following relation:

$$\theta_c = \tan^{-1} \left(\frac{D_{wp}}{D_c} \tan \theta_{wp} \right)$$

In circular chasers used for making external thread, there is no constraint on the size of the chaser. These chasers are therefore generally made of a diameter larger than the diameter of the threaded part for greater robustness. However, to maintain the same helix angle, the thread on the chaser is made multiple-start. If n be the number of starts, the diameter of the circular chaser is found from the following relation:

$$D_c = n D_{wp}$$

The rake and clearance angles of the chaser teeth are taken the same as for single-point thread cutting tools. As in the case of circular form tool (see Section 5.2), the required clearance angle is obtained in circular chasers by mounting the tool at a height $h = R \sin \alpha$ above the axis of

the workpiece, where R is the maximum radius of the chaser. The profiles of the solid, block, and circular chasers are determined by the same procedure as that used for the corresponding form tools.

Example 5.7

A circular thread chaser is to be designed for making M20 right-hand internal thread. If the mean diameter of the chaser is 0.8 of the thread diameter, determine the helix angle of the cutter teeth.

From thread standards, we obtain the following data for a M20 internal thread.

Pitch circle diameter $D_{wp} = 18.376$ mm, pitch $p = 2.5$ mm.

Helix angle of the thread:

$$\theta_{wp} = \tan^{-1} \left(\frac{p}{\pi D_{wp}} \right) = \tan^{-1} \left(\frac{2.5}{\pi \times 18.376} \right) = 2^\circ 30'$$

The helix angle of the cutter teeth is found from the following relation:

$$\theta_c = \tan^{-1} \left(\frac{D_{wp}}{D_c} \tan \theta_{wp} \right) = \tan^{-1} \left[\frac{D_{wp}}{0.8 D_{wp}} \tan 2^\circ 30' \right] = 3^\circ 8'$$

The cutter helix will be of the same direction as the internal thread, that is, right hand.

Example 5.8

A circular thread chaser is to be designed for making M30 right-hand external metric thread in a mild steel part. If the number of starts on the cutter thread is $n = 2$, determine the helix angle of the cutter teeth, select suitable cutting angles of the chaser, and determine the height at which it should be mounted above the workpiece axis.

From thread standards, we obtain the following data for M30 external thread:

Pitch circle diameter $D_{wp} = 27.727$ mm, pitch $p = 3.5$ mm, minor diameter $D_m = 26.211$ mm, thread height $h = 1.894$ mm.

Helix angle of the thread:

$$\theta_{wp} = \tan^{-1} \left(\frac{p}{\pi D_{wp}} \right) = \tan^{-1} \left(\frac{3.5}{\pi \times 27.727} \right) = 2^\circ 20'$$

Pitch circle diameter of the cutter:

$$D_c = n D_{wp} = 2 \times 27.727 = 55.454 \text{ mm}$$

Hence, helix angle of the cutter teeth is found from the following relation:

$$\theta_c = \tan^{-1} \left(\frac{D_{wp}}{D_c} \tan \theta_{wp} \right) = \tan^{-1} \left(\frac{27.727}{55.454} \tan 2^\circ 20' \right) = 0^\circ 35'$$

As recommended for single-point threading tool, we select $\alpha = 12^\circ$ and referring to Table 5.6, we select $\gamma = 25^\circ$ for mild steel.

Diameter of the cutter $D = D_c + h = 55.454 + 1.894 = 57.348$ mm

The height at which the cutter is mounted to achieve the select clearance angle is found from the following relation:

$$h = \frac{D}{2} \sin \alpha = 57.348 \sin 12^\circ = 11.92 \text{ mm} .$$

5.6.3 Geometry of Thread Cutting Taps

As was mentioned in Section 1.4, tapping is an operation used for cutting internal threads in an existing hole (Figure 1.24) using a cutting tool called tap. A tap is basically a threaded bolt on which longitudinal flutes have been cut to form cutting edges and to provide space for accommodating the chips formed in cutting. A tap and its main elements are shown in Figure 5.26.

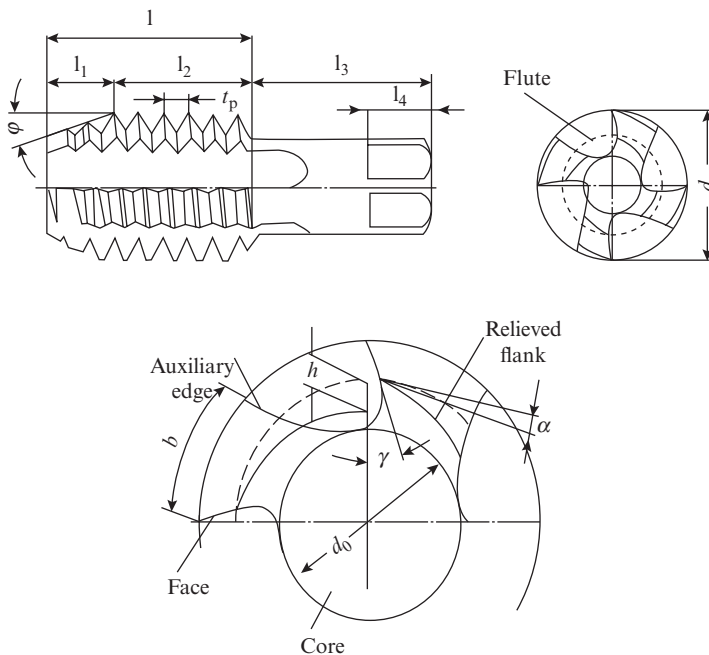


Figure 5.26 Schematic of tap and its main elements (l_1 —chamfer length, l_2 —sizing length, l_3 —Shank length, l_4 —square end length, h —flank relief height, ϕ —chamfer angle, d_0 —core diameter, d —tap diameter)

The working length of a tap consists of two distinct portions, a chamfer that contains the cutting teeth that do the bulk of metal removal and a sizing length that contains the finishing teeth. The purpose of the chamfer and sizing length is the same as explained in Section 5.6.2 with reference to thread chasers. The shank serves for clamping the tap in a chuck and the square at the end for applying torque.

The total allowance to be removed is divided between two or three taps. The chamfer angle that is specified in terms of the length of the chamfered portion depends on the cutting load on the tap. For a set of three taps, the typical data are tabulated below.

| Tap No. | Purpose | Percent of metal removed | Chamfer length |
|---------|----------------|--------------------------|----------------|
| 1 | Rough | 50–60 | $4 t_p$ |
| 2 | Semi finishing | 28–30 | $3 t_p$ |
| 3 | Finishing | 10–20 | $(1.5-2) t_p$ |

Here, t_p = pitch of the thread

Most taps have straight flutes, that is, the helix angle of the flutes $\theta = 0^\circ$. However, a small helix angle of $\theta = 8-10^\circ$ may be used to control the direction of chip flow as shown in Figure 5.27. When the helix of the flute is opposite to that of the thread, the chip flows forward as shown in Figure 5.27(a). This is convenient when cutting threads in a through hole. The helix direction shown in Figure 4.27(b) is more suitable when cutting threads in a blind hole. Even in taps with straight flutes, a small taper of $\lambda = 5-15^\circ$ at the end as shown in Figure 4.27(c) can be made to control the direction of chip flow.

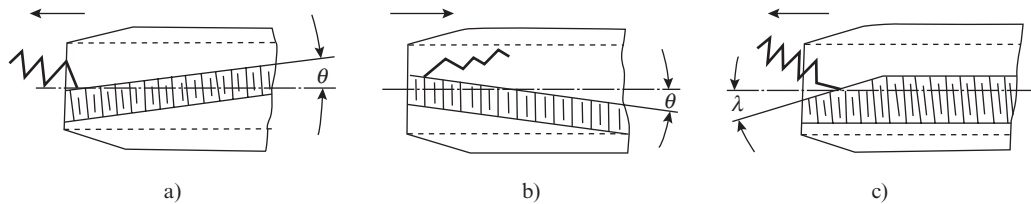


Figure 5.27 Schematic depicting the effect of helix angle of flute on direction of chip flow in tapping operation when (a) flute helix direction is opposite to that of thread to be cut, (b) flute helix direction coincides with that of thread to be cut, and (c) taper is made on straight flute tap to control chip flow direction

The rake angle in HSS taps varies from 5° to 30° depending on the work material. The softer the work material, the larger is the rake angle. Typical values are $\gamma = 10^\circ$ and 5° for making threads in steel and cast iron, respectively. The clearance angle on the finishing teeth is generally zero. On the cutting teeth in the chamfered length a clearance angle of $\alpha = 4-8^\circ$ for hand taps and $8-12^\circ$ for machine taps is provided. The flanks of these teeth are form relieved (see Figure 5.11) and the desired clearance angle is obtained by relieving the flank by the height

$$h = \frac{\pi D}{Z} \tan \alpha$$

where

D = external point diameter of the tap thread

Z = number of flutes on the tap.

5.6.4 Geometry of Thread-Cutting Die

Thread-cutting dies are used for cutting external threads. A thread-cutting die is shown in Figure 5.28(a) and its main elements in Figure 5.28(b). The working principle of threading die is similar to that of tap. It also consists of roughing teeth on a particular chamfered length for bulk removal of metal and a sizing length with finishing teeth. However, unlike the tap, in

thread cutting dies the chamfer is provided on both sides and the sizing length is sandwiched between the two chamfers. The chamfer angle ϕ is generally taken 20–25° to provide sufficient number of cutting teeth.

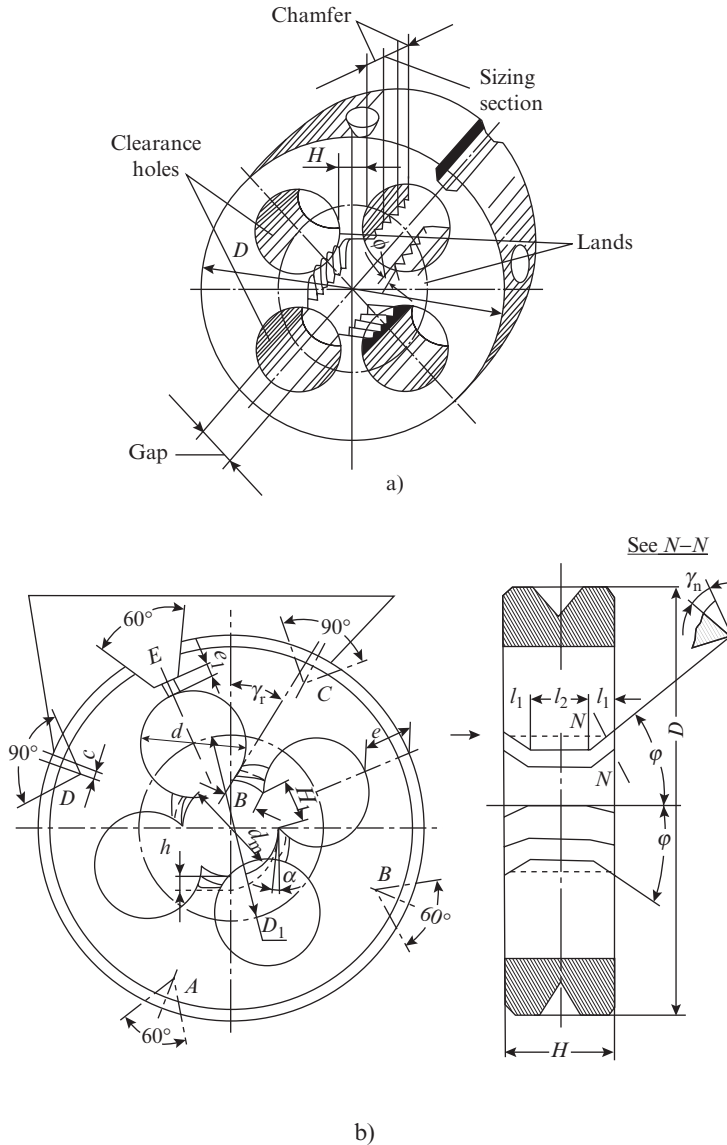


Figure 5.28 Geometry of thread-cutting die: (a) nomenclature and (b) main elements (l_1 —chamfer length, l_2 —sizing length, d_m —minor diameter of the thread to be cut, B —land width, H —gap width, d —diameter of clearance hole, D_1 —pitch circle diameter of clearance holes, H —die height, D —die diameter, and ϕ —chamfer angle)

Radial rake angle γ_r measured in the plane perpendicular to the axis is $\gamma_r = 10\text{--}12^\circ$ for hard materials, $10\text{--}20^\circ$ for medium hard materials and $20\text{--}25^\circ$ for soft materials. The normal rake angle in section N–N perpendicular to the chamfer is found from the following relation:

$$\tan \gamma_n = \tan \gamma_r \cos \phi$$

In standard thread-cutting dies $\gamma_r = 15\text{--}20^\circ$. A clearance angle $\alpha = 6\text{--}12^\circ$ is provided on the teeth in the chamfered length. The flank of the cutting teeth is form relieved by a suitable height h to obtain the desired clearance angle α as per the following expression:

$$h = \frac{\pi D}{Z} \tan \alpha$$

where

D = minor diameter of the threading die

Z = number of clearance holes.

5.7 Geometry of Gear Cutting Tools

There are two fundamentally different approaches of gear cutting based on the following:

- (i) form cutting
- (ii) generation of gear

Form cutting is done by a special form tool called module cutter on which the shape and size of the cutting teeth correspond exactly to the shape and size of the space between two adjacent teeth of the gear to be cut. Modular cutters may be disc or end mill type (Figure 5.29a), but the former is more commonly used thanks to their greater robustness. In the generating method, the gear to be produced and the cutter are made to mesh in such a way that they imitate the relative motion of the gear with another gear or a worm. The method based on meshing of work gear blank with a cutter gear is known as gear shaping (Figure 5.29b) and that based on meshing of work gear blank with a cutter worm as gear hobbing (Figure 5.29c).

For a gear of a particular module and pressure angle, the shape of the tooth profile depends on the number of teeth of the gear. This means that for each module, we must have, in principle, as many form cutters as the gears with different number of teeth that we want to cut. This is not economically feasible; therefore, module cutters come in sets of 8, 15, and 26 cutters, depending on the desired profile accuracy of the gear tooth. Each cutter of a set is supposed to cut gears having a certain range of number of teeth. A particular cutter can actually cut the correct profile only on one of the gears and the profiles of the remaining gears are produced with an inherent inaccuracy. This is a major drawback of the form cutting method, which along with its low productivity limits its application to job shop production and repair works.

In the generating method, the gear tooth profile is generated by successive removal of small chips through relative motions between the gear blank and the cutter gear (in gear shaping) or cutter worm (in gear hobbing) that are strictly coordinated. Consequently, a single cutter of a particular module can cut a gear of the same module having any number of teeth. The generating methods not only produce more accurate gears, they are also more versatile and economical.

Gear cutting methods, especially gear shaping and gear hobbing, that are based on generating approach involve complex kinematics. A description of the kinematic relations between the motions involved in the various gear cutting methods is therefore essential before taking up the geometry and design of the cutting tools used in these operations. In view of this, the geometry of

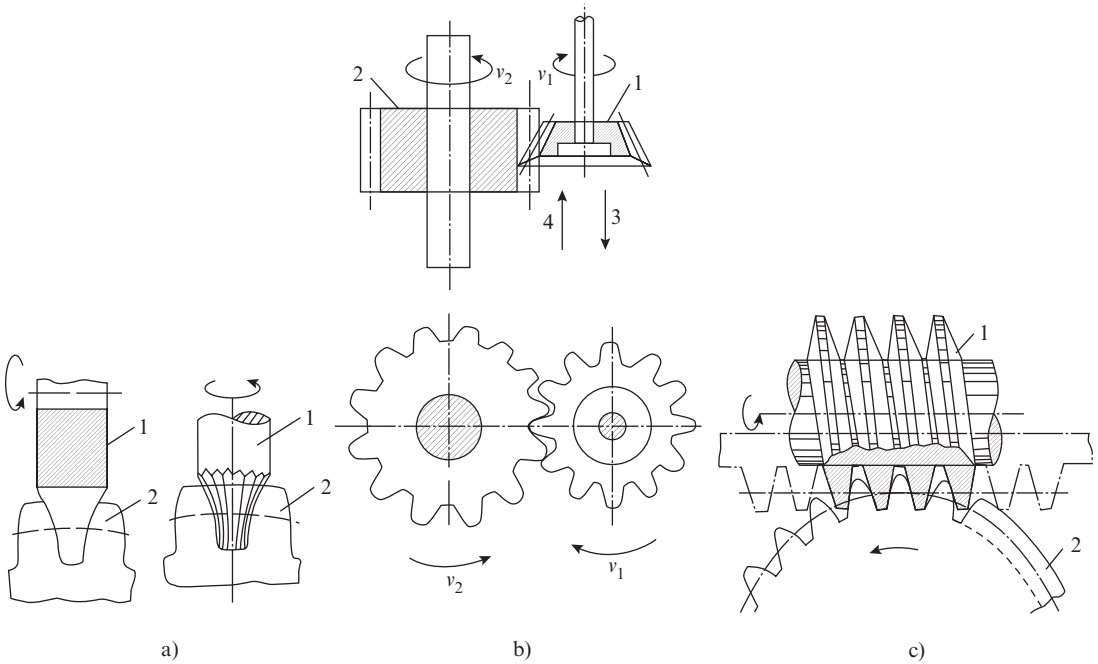


Figure 5.29 Gear cutting methods (a) using a module cutter (1—module cutter, 2—gear blank); (b) gear shaping using a cutter gear (1—cutter gear, 2—gear blank, 3—cutting stroke, 4—idle stroke); and (c) gear hobbing using a cutter worm (1—cutter worm, 2—gear blank)

gear cutting tools is not discussed here and will be taken up along with the description of operation and design of relevant cutter in Chapter 6.

Review Questions

- 5.1 In a turning operation on a job of diameter 50 mm at $s = 1.5$ mm/rev, the tool having clearance angle $\alpha = 8^\circ$ and primary cutting-edge angle $\phi = 30^\circ$ is set 4.0 mm above the workpiece axis. Determine the actual clearance angle.
- 5.2 A groove of depth 10 mm is made in a job of diameter 40 mm at $s = 1.0$ mm/rev with a tool having clearance angle $\alpha = 10^\circ$ and primary cutting-edge angle $\phi = 90^\circ$. If the tool is set 2 mm above the workpiece axis, determine the ratio of actual clearance angle at the beginning and end of the operation.
- 5.3 Select the appropriate tool angles for straight shank HSS drill to make a hole for M16 thread in a 30-mm-long job of steel having $\sigma_u = 90$ kg/mm².
- 5.4 Select the appropriate tool angles for a drill with brazed carbide bits for making a hole of diameter 30 mm in a 150-mm-long job of medium-carbon steel having $\sigma_u = 60$ kg/mm².
- 5.5 In a drill of diameter 30 mm, chisel-edge diameter 5 mm, maximum side rake angle $\gamma_s = 30^\circ$, and lip angle $2\phi = 120^\circ$, determine the maximum orthogonal rake angle and the pitch of the drill flute helix.
- 5.6 In Q. 5.5, if the drill operation is being carried out at a feed of $s = 1.0$ mm/rev, determine the actual orthogonal rake angle.

- 5.7** A HSS plain milling cutter of diameter 100 mm and 8 teeth is designed for rough machining of alloy steel parts. Select the appropriate cutting angles and tooth profile and determine the profile parameters.
- 5.8** Determine the number of passes, cutting angles, and actual clearance angles for a single-point thread cutting tool for making M42 metric thread in a cast iron part.
- 5.9** Determine the number of passes, cutting angles, and actual clearance angle for cutting Acme thread of the following data with a single point tool: external diameter = 40 mm, pitch circle diameter = 38.5 mm, minor diameter = 36.5 mm, pitch = 3.0 mm, and included angle of thread = 30° .
- 5.10** For the data given in Example 5.6, determine the diameter, helix angle, and height of setting above the workpiece axis for a double-start circular thread chaser.
- 5.11** For the data given in Q. 5.9, determine the diameter, helix angle, and height of setting above the workpiece axis for a triple-start circular thread chaser.

Chapter

6

DESIGN OF CUTTING TOOLS

In Chapter 5, the parameters that define the cutting wedge of various tools were discussed. In this chapter, the main focus will be on determination of the overall dimensions of the cutting tools and their mounting features. However, other issues that have a bearing on better understanding of the design and completeness of the design of individual cutters will also be discussed, where necessary.

6.1 Design of Single-Point Tool

The shank of a single-point tool is designed from considerations of strength and rigidity. The tool is assumed to be loaded as a cantilever by cutting forces acting at its tip as shown in Figure 6.1.

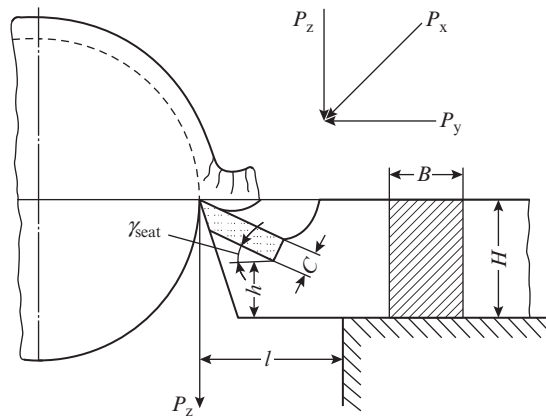


Figure 6.1 Schematic for the design of single-point tool

If only the main cutting force P_z is considered, then the maximum stress is found from the following relation:

$$\sigma_z = \frac{M_z z}{I_{xx}}$$

where

M = bending moment

z = height of the outer most layer of the section from the neutral axis

I_{xx} = moment of inertia of the section about x axis

For a tool of rectangular section $B \times H$ mounted with overhang l , we have

$$M_z = P_z l, \quad z = \frac{H}{2} \quad \text{and} \quad I_{xx} = \frac{BH^3}{12}$$

$$\sigma_z = \frac{P_z l \frac{H}{2}}{\frac{BH^3}{12}} = \frac{6P_z l}{BH^2}$$

If the permissible bending strength of the tool material is σ_{bp} , then the condition for design of tool shank based on strength is expressed as follows:

$$\frac{6P_z l}{BH^2} \leq \sigma_{bp} \quad (6.1)$$

If the force component P_x is also considered, then we have

$$\sigma_x = \frac{M_x x}{I_{zz}}$$

where

$$M_x = P_x l, \quad x = \frac{B}{2}, \quad I_{zz} = \frac{HB^3}{12}$$

Consequently,

$$\sigma_x = \frac{P_x l \frac{B}{2}}{\frac{HB^3}{12}} = \frac{6P_x l}{HB^2}$$

The total stress in this case is

$$\sigma = \sigma_z + \sigma_x = \frac{6l}{BH} \left(\frac{P_z}{H} + \frac{P_x}{B} \right)$$

And the condition for design of tool shank based on strength is expressed as follows

$$\frac{6l}{BH} \left(\frac{P_z}{H} + \frac{P_x}{B} \right) \leq \sigma_{bp} \quad (6.2)$$

For a tool of square section $B = H$, therefore, knowing P_z , P_x , and σ_{bp} , the shank dimensions can be determined straightaway from Eqn. (6.1) or (6.2) as the case may be. However, in the case of a tool with rectangular section, a particular H/B ratio has to be assumed to determine the shank dimensions. Generally, it is recommended to select $H/B = 1.6$ for roughing tools. The design based on Eqn. (6.2) can be simplified by assuming $P_x = (0.3-0.4)P_z$, which is typical of turning in a fairly wide range of the machining parameters.

Nowadays, the cutting portion of single-point tools is in the form of bit or insert that may be brazed or mechanically clamped on the shank. The shank is made of structural steel, irrespective of bit material (HSS, cemented carbide, ceramic, etc). The permissible bending strength of structural steel is given in Table 6.1.

Table 6.1 Bending strength of structural steel used in tool shank

| Shank steel | σ_{bp} , kgf/mm ² at $\varphi=$ | | | | | |
|-------------|---|-----|-----|-----|-----|---------------|
| | 30° | 45° | 60° | 75° | 90° | 45° bent sank |
| Nonhardened | 12 | 10 | 8 | 6.5 | 5.5 | 13 |
| Hardened | 24 | 20 | 16 | 13 | 11 | 26 |

The design of tool shank for stiffness is based on the deflection of the tool tip. Again, assuming the tool to be a cantilever of overhang l , the deflection of the tool tip is found from the following relation:

$$\delta = \frac{P_z l^3}{3EI_{xx}}$$

where E is the modulus of elasticity of the tool material. On substituting $I_{xx} = \frac{BH^3}{12}$, we obtain

$$\delta = \frac{P_z l^3}{3E \frac{BH^3}{12}} = \frac{4P_z l^3}{EBH^3}$$

If the permissible deflection of the tool tip is δ_p , then the condition for design of tool shank based on stiffness can be expressed as follows:

$$\frac{4P_z l^3}{EBH^3} \leq \delta_p \quad (6.3)$$

Generally, it is recommended to take $E = 2.0 - 2.2 \times 10^4$ kgf/mm² for structural steel shank, $\delta_p = 0.1$ mm for roughing tools and 0.05 mm for finishing tools. The value of cutting force components P_x and P_z in Eqs (6.1) and (6.3) is taken for a standard undeformed chip of $t = \frac{h}{40}$ and $s = \frac{h}{140}$, where h is the height of the machine tool center.

The rectangular cross section is most common among lathe tools. Square tools have better strength and stiffness under compound bending stresses; therefore, the square section is preferred for tools used on boring machines, turret lathes, and automats. Boring and threading tools generally have a round section as it allows the tool to be rotated about its axis to set the tip precisely at the desired point. The area of cross section of shaping, planing, and slotting tools is taken 25–50 percent greater than that of a lathe tool operating under identical conditions, because the former are subjected to impact loading. Tools of round section are also designed using Eqs (6.1)–(6.3), taking $I = \frac{\pi D^4}{64}$, where D is the diameter of the tool shank.

The tool shank dimensions determined as discussed above are used as the basis for selection of the nearest standard section from among the set given in Table 6.2.

Table 6.2 Standard sections of single-point tools

| Undeformed chip area (mm ²) | 1.5 | 2.5 | 4 | 6 | 9 | 12 | 16–25 |
|---|---------|---------|---------|---------|---------|---------|---------|
| Tool shank rectangular (mm) | 10 × 16 | 12 × 20 | 16 × 25 | 20 × 30 | 25 × 40 | 30 × 45 | 40 × 60 |
| Tool shank square (mm) | 12 × 12 | 16 × 16 | 20 × 20 | 25 × 25 | 30 × 30 | 40 × 40 | 50 × 50 |
| Tool shank round, diameter (mm) | 12 | 16 | 20 | 25 | 30 | 40 | 50 |

Standard tool shank dimensions related to machine tool size are given in Table 6.3.

Table 6.3 Standard tool shank size for different lathe sizes

| Height of lathe center (mm) | Rectangular (mm) | Shank size Square (mm) | Round, diameter (mm) |
|-----------------------------|------------------|------------------------|----------------------|
| 150–200 | 12 × 20 | 16 × 16 | 16 |
| 260 | 16 × 25 | 20 × 20 | 20 |
| 300 | 20 × 30 | 25 × 25 | 25 |
| 350–400 | 25 × 40 | 30 × 30 | 30 |

The tool length should be approximately 10 times the height of its cross section and should be selected from among the following set of standard values (in mm): 125, 150, 175, 200, 225, 250, 300, 350, 400, 450, 500, and 600.

6.1.1 Features Related to Cutting Bit

In modern manufacturing practice around 80–90 percent of machining is nowadays done by cutting bits of cemented carbide, ceramics, and other superhard materials. The cutting bits, also known as inserts, are either brazed or mechanically clamped on the tool shank.

The shapes of cemented carbide bits that are commonly used in brazed tools are shown in Figure 6.2. The bit is placed in a seat cut in the shank and brazed. The types of seats are shown in Figure 6.3. The open seat shown in Figure 6.3(a) is the simplest and the most commonly used. The semiclosed seat (Figure 6.3b) is used for bits with round profile, whereas the closed and grooved seats (Figure 6.3(c) and (d)) are preferred for small sized bits as they ensure more reliable joint with the shank. The bit is brazed with the shank using a spelter containing 90 percent brass and 5 percent each of nickel and ferromanganese. Brazing is done in induction or gas furnace to provide a thin spelter layer of 0.1 mm or so.

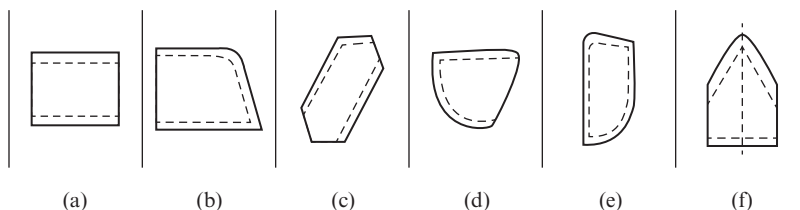


Figure 6.2 Typical shapes of cemented carbide bits used in brazed single-point tools: (a) for straight and bent shank turning, boring, and grooving tools, (b) for heavy duty bent shank turning tools, (c) for straight shank turning tools, (d) for facing and boring tools, (e) for turning and facing tools, and (f) for thread cutting tools

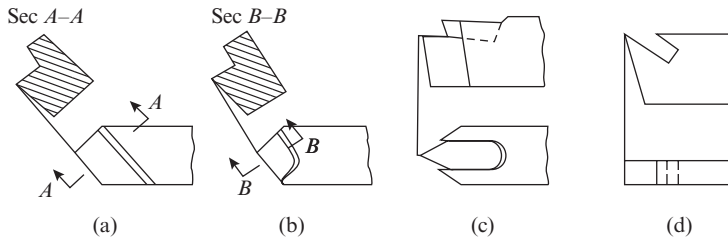


Figure 6.3 Types of seats for bits in brazed single-point tools: (a) open, (b) semiclosed, (c) closed, and (d) grooved

The carbide tip, whether brazed or mechanically clamped, should be designed in such a way that the resultant cutting force passes through its nest in the shank to keep the bit in compression (Figure 6.4). This is achieved by proper selection of the bit thickness and seat angle so that the resultant force P_r acting on the tip always presses the bit against the shoulder and keeps the bit in compression.

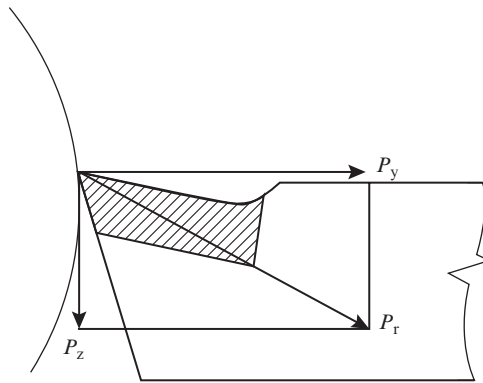


Figure 6.4 Forces acting on tool tip

The bit height C (Figure 6.1) is governed mainly by its strength and the number of times the face may be resharpened. In standard tools, the bit height is taken 0.16–0.2 times the height of the tool shank H . The seat angle is generally taken as $\gamma_{\text{seat}} = \gamma + 5^\circ$ and is equal to 12° in standard tools. Having selected C and γ_{seat} , it is necessary to check as a safeguard that $h \geq \frac{2}{3}H$, where h is the height of the lowermost point of the bit from the tool base.

The recommended shapes and dimension for a few important single-point tools are shown in Figure 6.5.

A major drawback of brazed tools is that cracks appear in the bit during brazing due to residual stresses arising from nonuniform cooling of the bit and the difference in the coefficient of linear expansion of the bit and shank material. These cracks reduce the strength of the bit and are the root cause of chipping of the cutting edge during operation. Another drawback of brazed tools is that a step- or groove-type chip breaker has to be ground on the tool face, or provision has to be made for a special attached-type chip breaker (see Figures 2.23–2.26). All these measures increase the cost of the tool. In addition, while using brazed tools, the cutting speed and feed are kept low to prolong tool life so as to limit the downtime due to regrinding and tool changing.

Disposable insert tools overcome these limitations of brazed tools. With total elimination of regrinding with these tools, the machine downtime is reduced to minimum, involving only indexing

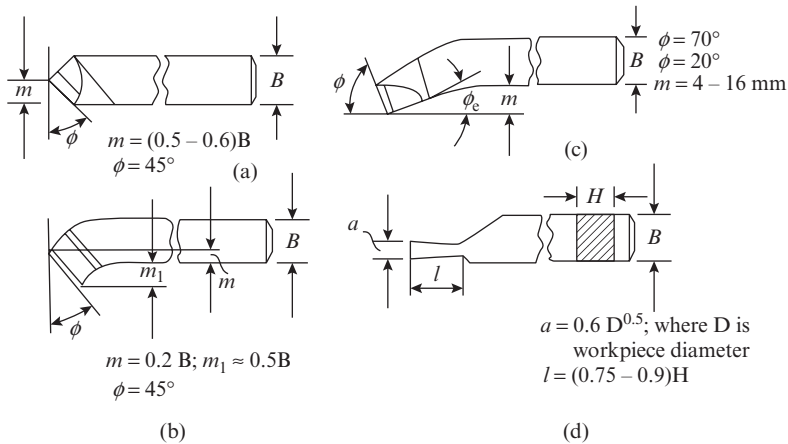


Figure 6.5 Typical shapes and dimensions of brazed single-point tools: (a) straight shank turning tool, (b) bent shank turning tool, (c) facing tool, and (d) parting tool

of the insert and its change when all the insert edges have worn out. This allows machining to be carried out at higher speed and feed, thereby increasing productivity. Another advantage of these tools is that the tool holders designed for cemented carbide bits can be easily adapted for inserts of ceramic, CBN, PCD, coated carbides, etc.

Disposable inserts are available in different shapes in two versions: flat plain and flat with molded grooves. The flat plain inserts may be solid or with a center hole, but the inserts with grooves are always made with a center hole. An example of each type of insert is shown in Figure 6.6. The various shapes of disposable inserts are shown in Figure 6.7. In general, fewer edges are a cost disadvantage. In this sense, the round insert is most cost-effective as it can be indexed multiple times for more cuts per insert. The strength of the cutting edge of an insert depends on its shape: the smaller the included angle of the edge, the lower its strength. Thus, the rhombus shape shown in Figure 6.7(g) is the weakest, and the round shape shown in Figure 6.7(a) is the strongest.

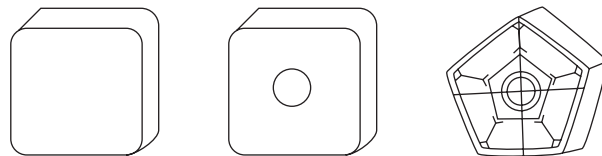


Figure 6.6 Types of disposable inserts: (a) flat plain solid, (b) flat plain with center hole, and (c) flat with molded grooves and center hole

The flat inserts may have positive rake angle or negative rake angle. In the case of flat plain inserts with positive rake angle, the shank seat under the insert is ground at the corresponding angle, and the clearance angle is obtained by grinding the flank on the insert (Figure 6.8a). These inserts can therefore be used for cutting only on one side. In flat plain inserts with negative rake angle, the shank seat under the insert is again ground at the corresponding angle, but the clearance angle is obtained automatically without grinding the flank (Figure 6.8b). In this case, both sides of the insert can be used for cutting. Thus, a square insert with positive rake angle will have four cutting edges, whereas the one with negative rake angle will have eight.

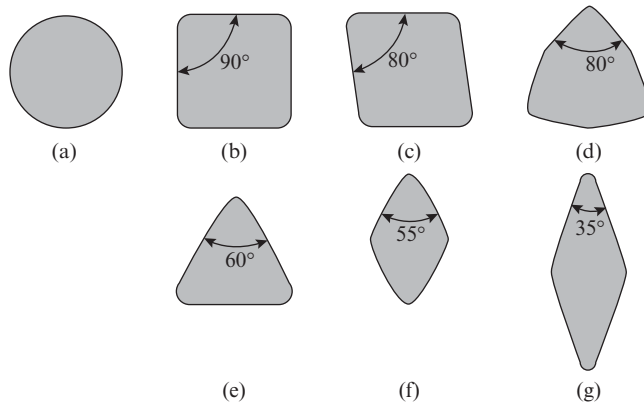


Figure 6.7 Common shapes of disposable inserts: (a) round, (b) square, (c) rhombus with two 80° point angles, (d) hexagon with three 80° point angles, (e) triangle, (f) rhombus with 55° point angles, and (g) rhombus with 35° point angles

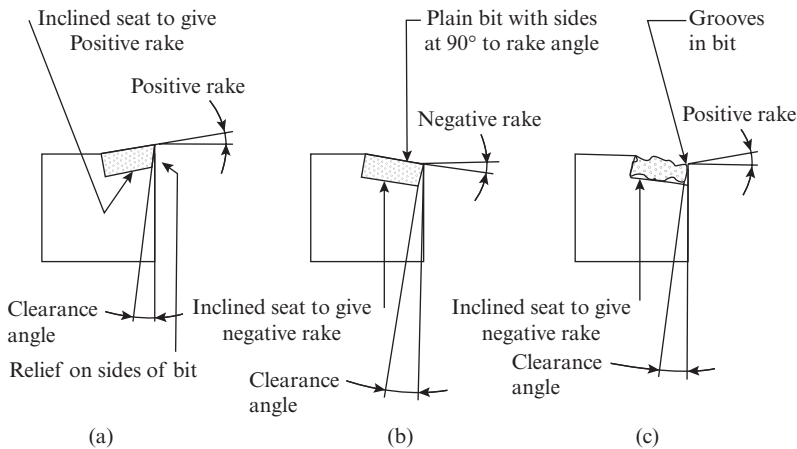


Figure 6.8 Rake and clearance angles in disposable inserts: (a) plain insert with positive rake angle, (b) plain insert with negative rake angle, and (c) insert with molded grooves and positive rake angle

Flat inserts with molded grooves have a positive rake angle but with negative rake seating (Figure 6.8c), which allows these inserts to be used on both sides. Thus, they combine the negative rake economy with positive rake cutting action. The tool holders for disposable inserts are designed for extreme rigidity. Tool holders are made of steel that is heat treated to a hardness of HRC = 40–45 to resist damage from clamping screw and chip impact. Basically, all tool holders have a solid base with a seat to accommodate the insert. In larger tool holders, a carbide pad is provided as a support to the insert to facilitate transfer of heat away from the cutting edge and to protect the seat in case of insert breakage or chipping. Tool holders come in a wide range of sizes and designs, using one of the three methods for holding the inserts namely bridge, pin, and screw type. A bridge-type tool holder for solid plain insert is shown in Figure 2.26(a). The bridge varies in shape and size

depending on the manufacturer, but the principle is similar in all designs. In this type of tool holders, a chip breaker is provided, which may either be a permanent part of the bridge or a separate replaceable chip breaker that is similar to the cutting bit but smaller. The main disadvantage of bridge-type clamps is that the top of the tool becomes bulky, making it difficult to use in cutting with space constraints.

A pin-type tool holder for inserts with center hole is shown in Figure 6.9. These holders are mainly designed for negative rake inserts. The insert 2 fits on pin 4 with a clearance of 0.1–0.15 mm. Wedge 3 holds the insert against the pin and the bearing surface of shank 1. This design does away with clamps, plates, and chip-control devices from the top of the tool, thus eliminating many of the disadvantages of bridge clamps. Shorter tool overhang allows heavier cuts with smaller shanks.

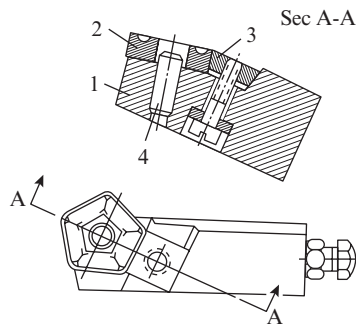


Figure 6.9 Pin-type tool holder for insert with center hole

The screw type or center-lock-type tool holder is used for inserts with a center hole and holds the insert in place with a lock pin (Figure 6.10) or screw. The insert is released from the top and is located against the seat shoulders. The holder screw hole is slightly oversize, which allows the insert to float. This design is used where the design or size of holder does not permit the use of other types of mechanisms, and its typical applications are in small boring bars and automatic tooling. The disadvantage of the screw -type design is that minute chips or swarf sometimes work their way into the threads. In addition, swarf may fill up and clog the key socket, making it difficult for key insertion.

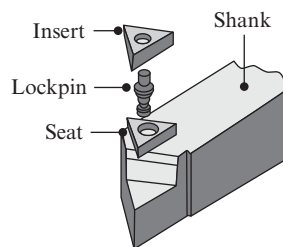


Figure 6.10 Screw or center-lock-type tool holder for insert with center hole

Example 6.1

In a rough turning operation with a straight shank brazed tool of rectangular section mounted with an overhang of 60 mm, the main cutting force was found to be 232 kgf. The tool body is made of carbon steel having permissible bending strength $\sigma_{bp} = 20 \text{ kgf/mm}^2$ and modulus of elasticity $E = 2 \times 10^4 \text{ kgf/mm}^2$. If the permissible deflection of the tool tip is $\delta_p = 0.1 \text{ mm}$, determine the tool dimensions

We first determine the tool cross-section dimensions. From Eqn. (6.1), assuming $H = 1.6B$, we obtain

$$\frac{6P_z l}{B \times (1.6B)^2} \leq \sigma_{bp}$$

wherefrom

$$B = \left[\frac{6 \times 232 \times 60}{2.56 \times 20} \right]^{\frac{1}{3}} = 16.31 \text{ mm}$$

From, among the recommended standard dimensions we select $B = 16 \text{ mm}$, therefore $H = 1.6 \times 16 = 25.6 \text{ mm}$. Again we select the standard value of $H = 25 \text{ mm}$. Hence, the selected tool section is $16 \times 25 \text{ mm}$. It is now subjected to the checks for strength and stiffness.

The maximum load that the selected section can bear from consideration of strength is again found from Eqn. (6.1) as follows:

$$P_{z\max 1} = \frac{BH^2 \sigma_{bp}}{6l} = \frac{16 \times (25)^2 \times 20}{6 \times 60} = 555 \text{ kgf}$$

The maximum load that the selected section can bear from consideration of stiffness is found from Eqn. (6.3) as follows:

$$P_{z\max 2} = \frac{EBH^3 \delta_p}{4l^3} = \frac{20000 \times 16 (25)^3 \times 0.1}{4 \times (60)^3} = 578.7 \text{ kgf}$$

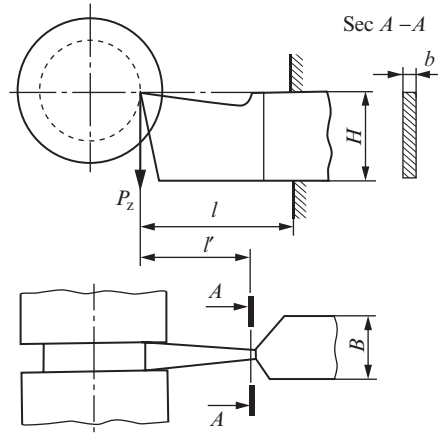
As both the values of maximum load capacity of the tool are greater than the cutting force acting on the tool, it can be concluded that the selected tool section $16 \times 25 \text{ mm}$ is safe.

As per the recommendation, the length of the tool is $L = 10 \times 25 = 250 \text{ mm}$. Finally, referring to Figure 6.6(a) for straight shank turning tool, it is recommended that $m = (0.5-0.6)B$.

Taking the mean value, we find $m = 0.55 \times 16 = 8.8 \text{ mm}$.

Example 6.2

In a parting operation on a job of diameter 22 mm with a brazed tool of cutting length 20 mm, the cutting force was 162 kgf. If the tool body is made of carbon steel have $\sigma_{bp} = 20 \text{ kgf/mm}^2$, determine the tool dimensions.



From the schematic of parting operation shown in the figure, it is evident that the weakest section of a parting tool is the neck where the transition from the cutting portion to be main body of the tool occurs. For such tools, the ratio of the width of neck b to the height of section H is recommended to be $\frac{b}{H} = \frac{1}{6}$.

Applying Eqn. (6.1) to the cutting length of the tool $l' = 20$ mm and assuming $\frac{b}{H} = \frac{1}{6}$ as recommended, we obtain

$$\frac{6P_z l'}{b(6b)^2} \leq \sigma_{bp}$$

Wherefrom,

$$b = \left[\frac{6 \times 162 \times 20}{36 \times 20} \right]^{\frac{1}{3}} = 3 \text{ mm}$$

Hence, $H = 6b = 3 \times 6 = 18$ mm. Now, applying the recommendation $\frac{B}{H} = 1.6$, we obtain $B = 11.25$. From among the standard sections, we select the tool section as 12×20 mm.

The maximum load that the tool can bear is

$$P_{\max} = \frac{b(H)^2 \sigma_{bp}}{6l'} = \frac{3 \times (20)^2 \times 20}{6 \times 20} = 200 \text{ kgf}.$$

As P_{\max} is greater than the cutting force acting on the tool, the selected tool section is safe. Now following the recommendation regarding length of the tool $L = 10H$, we obtain tool length $L = 10 \times 20 = 200$ mm. Finally, referring to Figure 6.5(d), we obtain $l' = (0.75 - 0.9)H = 15 - 18$ mm.

Hence, the cutting portion length should be reduced to 18 mm. Further, we check the width of the cutting edge for the condition $b = 0.6(D)^{0.5} = 0.6(22)^{0.5} = 2.81$ mm. Hence, the selected value of $b = 3.0$ mm is safe.

6.2 Design of Form Tool

As discussed in Section 5.2, form tools may be prismatic or circular in shape. Having already determined the parameters related to form tool geometry, the remaining aspects of the design of form tools will be discussed in this section.

6.2.1 Design of Circular Form Tool

The parameters that need to be determined for complete design of circular form tool are as follows:

- (i) diameter
- (ii) profile
- (iii) auxiliary features

The inputs required for the design of form tool are the contour and dimensions of the component features.

(i) *Determination of the diameter of circular form tool (Figure 6.11):*

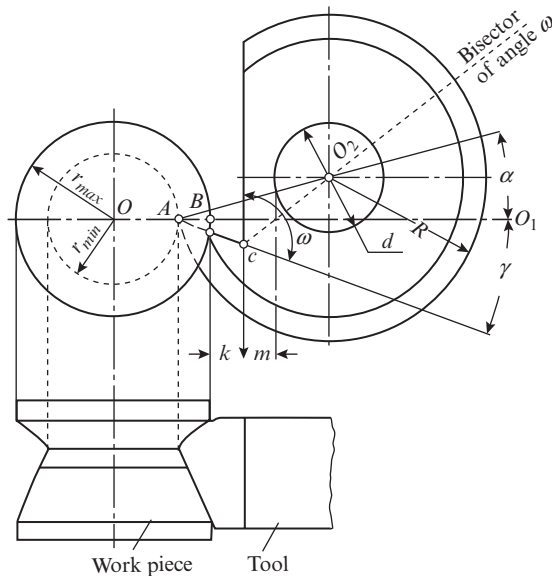


Figure 6.11 Graphic construction for determining the diameter of circular form tool

For a given component, the procedure involves the following steps:

1. Draw the component.
2. Draw concentric circles corresponding to the maximum and minimum diameter of the workpiece.
3. Draw a horizontal line OO_1 from the center of the concentric circles.
4. From point A on the circle of the minimum diameter, draw a line making angle γ with the line OO_1 , taking the value of γ from the table given in Section 5.2. This line represents the tool face.

5. Draw a line perpendicular to OO_1 at a distance K from the point B on the circle of maximum diameter. This distance K is the minimum gap required for easy flow of the chip. It lies between 3 mm and 12 mm depending on the chip thickness and its volume.
6. Draw a line bisecting the lines drawn in steps 4 and 5 above.
7. Draw a line at an angle α from point A, taking the value of α as per the recommendations given in Section 5.2.
8. The point O_2 of intersection of the lines drawn in steps 6 and 7 above represents the center of the form tool.
9. Having determined the center location, the various radii of the form tool corresponding to characteristic points of the part profile can be drawn. The term “characteristic point” refers to a point where a new feature commences or a previous one terminates.

The form tool diameter at the basic point is generally 6–8 times the depth of profile, which is the difference between the maximum and minimum radius of the component.

(ii) (a) *Determination of profile of circular form cutter by graphical method:*

By profiling we mean the determination of the shape of the normal cross section of the form tool; that is, the shape and dimensions of the line formed by the intersection of the tool flank and the radial section. Profiling of a circular form tool can be carried out graphically as well as analytically.

The graphical procedure of determination of the profile of circular form cutter for a given component (Figure 6.12a) consists of the following steps:

1. Draw two projections of the component.
2. Select appropriate values of α and γ as recommended in Section 5.2 and determine the location of the center of form tool as described above. The height of the form tool center from that of the workpiece is $H_t = R_{\max} \sin \alpha$, where R_{\max} is the maximum radius of the form tool corresponding to the characteristic point of least radial dimension on the component.
3. On the line of tool face, draw normals O_1a and O_2M from the center of the workpiece and form tool, respectively.
4. Mark points of intersection 1, 2, and 3 between the line of tool face and the concentric circles of radius r_1 , r_2 , and r_3 in the top view of the component.
5. with O_2 as center, draw circles of radius O_21 , O_22 , and O_23 to obtain the radii R_1 , R_2 , and R_3 of the form tool for the characteristic points.

To obtain the tool profile in the radial cross section N–N, the following steps are involved:

1. Draw the radial line N–N.
2. Lay off dimensions l_1 and l_2 to the right and a line perpendicular to N–N and draw lines parallel to N–N from these points.
3. From the end point, lay off dimensions P_2 and P_3 in the direction parallel to N–N, where $P_2 = R_1 - R_2$ and $P_3 = R_1 - R_3$ and draw lines perpendicular to N–N from these points.
4. The intersection of the two sets of lines drawn in steps 2 and 3 above gives points of intersection $1'$, $2'$, and $3'$.
5. The profile of the form tool in the radial section is obtained by joining these points.
6. The tool flank is generated by revolving the cutting edge about the tool axis.

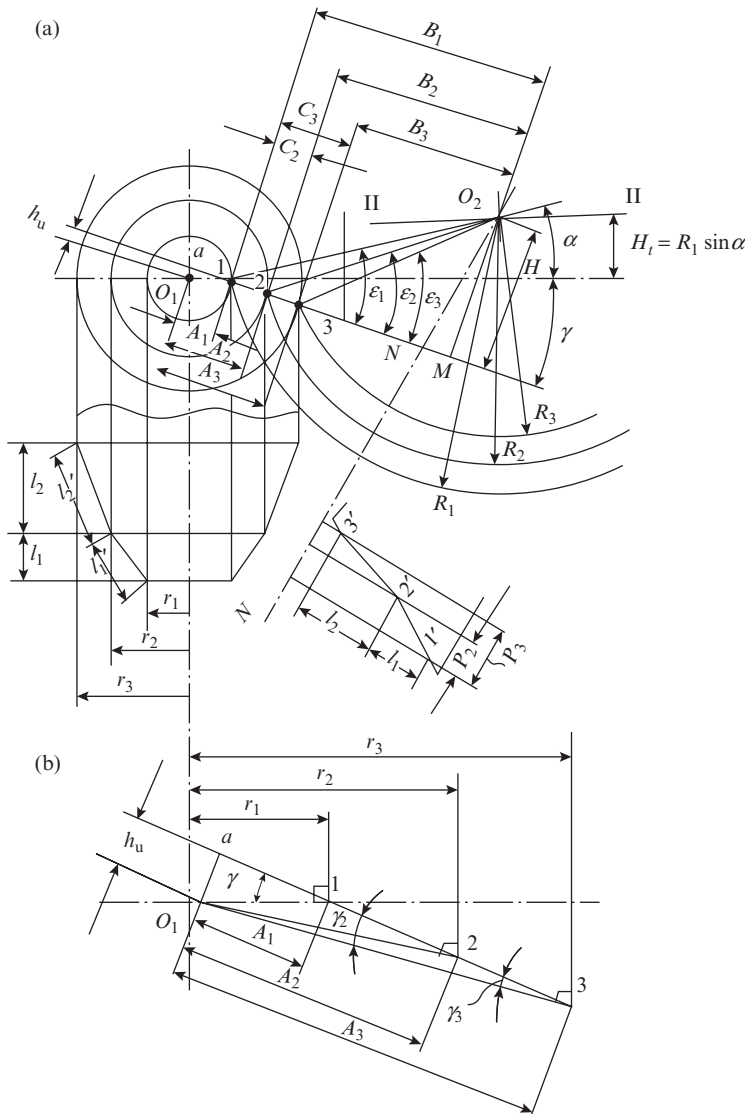


Figure 6.12 Determination of profile of circular form tool (a) by graphical construction and (b) by analytical method

(b) Determination of profile of circular form tool by analytical method:

The graphical method suffers from the drawback of being a tedious and time-consuming process. It also has in-built inaccuracies that are inherent in a graphical construction. Fortunately, the graphical construction enables us to set up a series of analytical relations that can be used to determine the form tool profile with the desired degree of accuracy. Referring to Figure 6.12(b), which has been constructed on an enlarged scale from the relevant portion of Figure 6.12(a), the necessary parameters can be determined.

Parameters defining the characteristic points on form tool face

These parameters are represented by C_2 , C_3 , etc., in Figure 6.12(a) and defined by the location of points on the tool face corresponding to the characteristic points of the component:

$$C_2 = A_2 - A_1, \text{ and } C_3 = A_3 - A_1$$

where

$$A_1 = r_1 \cos \gamma, A_2 = r_2 \cos \gamma_2, \text{ and } A_3 = r_3 \cos \gamma_3$$

The terms $\cos \gamma_2$ and $\cos \gamma_3$ are found using the following expressions:

$$\sin \gamma_2 = \frac{h_u}{r_2} \text{ and } \sin \gamma_3 = \frac{h_u}{r_3}$$

wherein

$$h_u = r_1 \sin \gamma$$

Consequently,

$$\sin \gamma_2 = \frac{r_1}{r_2} \sin \gamma \text{ and } \sin \gamma_3 = \frac{r_1}{r_3} \sin \gamma$$

Knowing r_1 , r_2 , and r_3 from the part drawing and γ as selected based on the recommendations in Section 5.2, we can first determine A_1 , A_2 , and A_3 and on substituting their values then find C_2 and C_3 .

Radii of the characteristic form tool points

Here, it is assumed that the diameter of the form tool R_1 has already been determined as described earlier and is therefore a known parameter. From Figure 6.12(a), it can also be noted that $\varepsilon_1 = \alpha + \gamma$, where the values of α and γ have been selected based on the recommendations given in Section 5.2.

From Figure 6.12(a), it can be noted that

$$R_1 = \frac{H}{\sin \varepsilon_1} = \frac{B_1}{\cos \varepsilon_1} \quad (6.4)$$

Consequently,

$$H = R_1 \sin \varepsilon_1 \text{ and } B_1 = R_1 \cos \varepsilon_1$$

From Figure 6.12(a), it can be noted that

$$R_2 = \frac{H}{\sin \varepsilon_2} = \frac{B_2}{\cos \varepsilon_2} \quad (6.5)$$

Therefore,

$$\tan \varepsilon_2 = \frac{H}{B_2} = \frac{H}{B_1 - C_2}$$

Knowing B_1 , H , and C_2 , we can find ε_2 and on substituting it in Eqn. (6.5), we can find R_2

From Figure 6.12(a), it can be noted that

$$R_3 = \frac{H}{\sin \varepsilon_3} = \frac{B_3}{\cos \varepsilon_3} \quad (6.6)$$

Therefore,

$$\tan \varepsilon_3 = \frac{H}{B_3} = \frac{H}{B_1 - C_3}$$

Knowing H , B , and C_3 , we can find ϵ_3 ; and on substituting its value in Eqn. (6.6), we can find R_3 .

The width of the form tool W is equal to the sum of the axial length of all the features of the profile to be machined, for example, for the component shown in Figure 6.12(a), we have

$$W = l_1 + l_2$$

(iii) Determination of auxiliary features of circular form tool:

For clamping the form tool, a clamping bolt attached to the tool holder is passed through the central hole of the tool, and the tool is held in position by means of a nut. Radial serrations are cut on the side face of the form tool that mate with similar serrations on the tool holder and prevent its rotation during operation.

As mentioned earlier, the outside diameter of a circular form tool is usually 6–8 times the depth of profile being machined. Circular form tools for internal turning operation have a diameter 0.6–0.85 of the hole diameter.

Diameter d of the central hole of the circular form tool depends on its outside diameter and may be taken from the table below.

| | | | | | | |
|----------|----|----|----|----|----|----|
| D (mm) | 30 | 40 | 50 | 60 | 75 | 90 |
| d (mm) | 13 | 16 | 16 | 22 | 22 | 27 |

The selected value of d should be checked for strength and stiffness of the mounting bolt, assuming it to be a cantilever of round section rigidly constrained at both ends and subjected to uniformly distributed load over its whole length.

The steps to check the strength and stiffness of the mounting bolt are as follows:

1. Calculate force P_z acting on the tool from the following relation:

$$P_z = k A$$

where k = cutting force per unit area of undeformed chip

A = undeformed chip area = $b \cdot a$

b = undeformed chip width = sum of the length of all the segments of the profile to be machined; for the component shown in Figure 6.12(a), $b = l'2' + 2'3'$ and is approximately equal to $l'_1 + l'_2$

a = undeformed chip thickness

The value of k depends on work material and is given in Table 6.4 for some common materials.

2. Calculate the maximum value of uniformly distributed load acting on the mounting bolt using the following relation:

$$q_z = \frac{P_z}{b} = ka = ks$$

Here, a has been taken equal to feed s because we know that $a = s \sin \phi$ and maximum value of a occurs at $\phi = 90^\circ$.

3. Calculate the diameter of the mounting bolt based on the criterion of maximum strength (bending moment) from the following relation:

$$d_1 \geq \left(\frac{0.053 q_z l^2}{\sigma_u} \right)^{\frac{1}{3}} \tag{6.7}$$

Table 6.4 Values of cutting force per unit undeformed chip area

| S. No. | Material | Ultimate strength σ_u (kgf/mm ²) | Hardness BHN | k (kgf/mm ²) |
|--------|--------------------------|--|--------------|----------------------------|
| 1. | Carbon and alloy steel | 30–40 | | 138 |
| | | 40–50 | | 152 |
| | | 50–60 | | 164 |
| | | 60–70 | | 178 |
| | | 70–80 | | 200 |
| | | 80–90 | | 220 |
| | | 90–100 | | 236 |
| | | 100–110 | | 256 |
| 2. | Cast iron | 110–120 | | 272 |
| | | | 140–160 | 100 |
| | | | 160–180 | 108 |
| | | | 180–200 | 114 |
| | | | 200–220 | 120 |
| | | | 220–240 | 128 |
| | | | 240–260 | 134 |
| 3. | Bronze | | | 55 |
| 4. | Brass | | | 35 |
| 5. | Copper | | | 95–115 |
| 6. | Aluminum and Al–Si alloy | | | 40 |
| 7. | Duraluminum | 25 | | 60 |
| | | 35 | | 80 |
| | | >35 | | 110 |

where

σ_u = ultimate strength of the material of the mounting bolt

l = length of the mounting bolt which is approximately equal to the width W

4. Calculate the diameter of the mounting bolt based on maximum deflection using the following relation subject to the condition that the deflection should not exceed $\frac{1}{5}$ of the tolerance on the diameter of the central bore hole, assuming sliding bit between the bore hole and the mounting bolt

$$d_2 \geq \left(\frac{0.053q_z l^4}{E y_{\max}} \right)^{\frac{1}{4}} \quad (6.8)$$

where

y_{\max} = $0.2 \times$ tolerance on diameter of mounting bolt

E = modulus of elasticity of the material of the mounting bolt

5. Compare the recommended value of d with d_1 and d_2 as calculated in steps 4 and 5, respectively

If $d < d_1$ as well as d_2 , select d

If $d >$ either d_1 or d_2 , select a new material for the mounting bolt with higher value of σ_u and E and repeat steps 3 through 5

The minimum value of wall thickness m (Figure 6.11) varies in the range 6–10 mm. Therefore, the mid value of $m = 8$ mm is taken initially. Now the off set K (Figure 6.11) is calculated from the following expression:

$$K = \frac{D}{2} - \frac{d}{2} - m - \text{depth of cut}$$

If the value of K lies between 3 mm and 12 mm, which is the recommended range, then the values of K and m are fixed as found above. However, if K lies outside the above range, then m is incremented or decremented as required.

The diameter of the radial serrations is taken (1.5–1.8) d and the serrations are cut with a profile angle of 90° .

6.2.2 Design of Flat Form Tool

The parameters that need to be determined for complete design of flat form tool are as follows:

- (i) profile
- (ii) auxiliary features

The inputs required for the design are the contour and dimensions of the component features.

- (i) (a) Determination of profile of flat form tool by graphical method:

For a given component (Figure 6.13), the procedure consists of the following steps:

1. Draw two projections of the component.
2. Select appropriate values of α and γ as recommended in Section 5.2.
3. Draw the flank and face from point 1 corresponding to the smallest radius on the component.
4. From characteristic points 1, 2, and 3, draw lines parallel to the flank.
5. To construct the tool profile in the normal section N–N, draw a line L–L parallel to N–N.
6. Draw two lines parallel to L–L at a distance of l_1 and $l_1 + l_2$, respectively.
7. Extend the lines drawn parallel to the flank in step 3 above so that they intersect the lines drawn in step 5 at points $2'$ and $3'$.
8. Join points $1'$, $2'$, and $3'$ to obtain the required profile of the flat form tool in the normal section.

- (b) Determination of profile of flat form tool by analytical method:

For determining the profile, we only need to determine P_2 and P_3 . For this, we first determine C_2 and C_3 in the same way as described for circular form tool. Now knowing that $\varepsilon = \alpha + \gamma$, P_2 and P_3 can be determined as the hypotenuse of triangle $1A2$ and $1B3$, respectively as follows:

$$P_2 = C_2 \sin[90 - (\alpha + \gamma)] = C_2 \cos \varepsilon$$

$$P_3 = C_3 \sin[90 - (\alpha + \gamma)] = C_3 \cos \varepsilon$$

- (ii) Determination of auxiliary features of flat form tools:

Flat form tools generally have a dove tail on the side opposite to that of the profile and are clamped in special tool holders with matching dove tail. The principal auxiliary dimensions are related to the tool width B by the following relations (Figure 6.14):

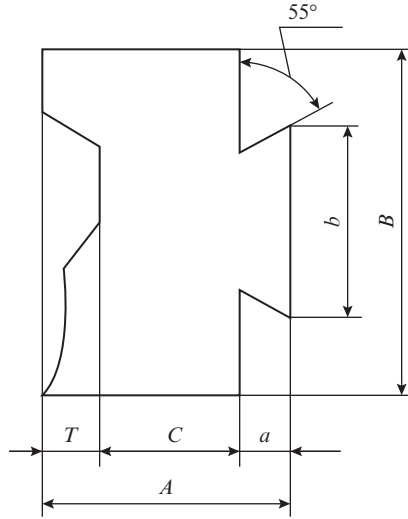


Figure 6.14 Auxiliary features of flat form tool

where

l = length of the line segment

$\Delta\phi$ = angle subtended at the center by the arc segment for which the line segment is a chord

Angle $\Delta\phi$ is found from the following expression:

$$\delta_r = r \left(1 - \cos \frac{\Delta\phi}{2} \right) \leq \frac{1}{3} \times \text{tolerance on the given feature}$$

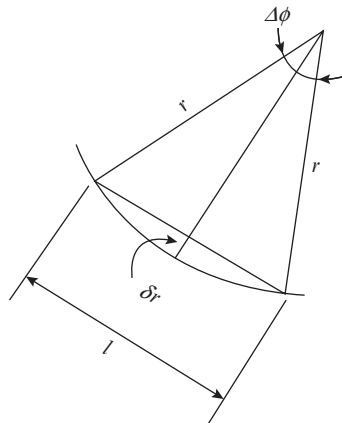


Figure 6.15 Graphical construction for determining chord length of circular arc

Example 6.3

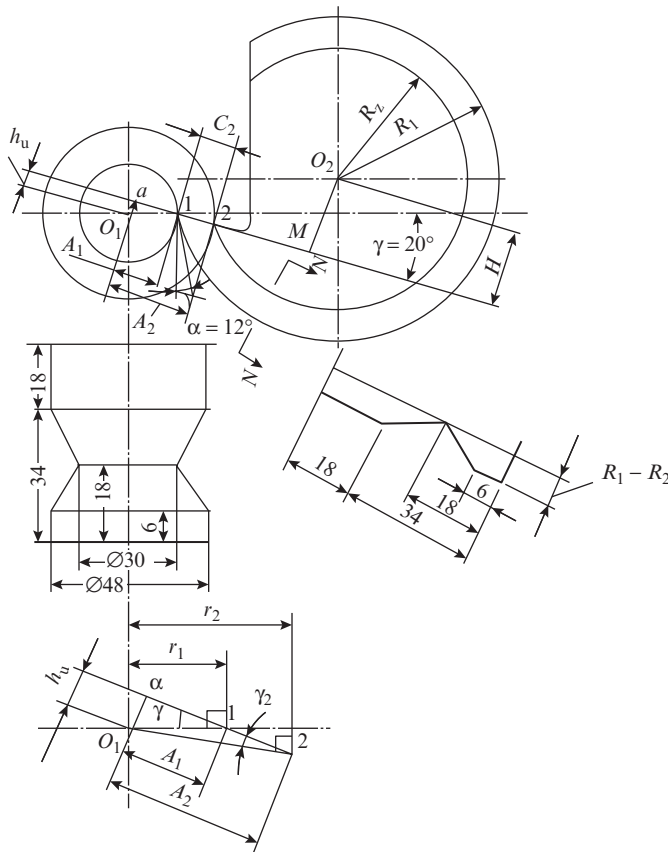
Design a circular form tool for machining of the part shown in the figure. The part is made of steel having $\sigma_u = 40 \text{ kgf/mm}^2$. The axis of the bolt on which the tool is mounted is 10 mm above the workpiece axis.

Referring to the recommendation for selection of rake angle γ and clearance angle α given in Section 5.2, we select $\gamma = 20^\circ$ and $\alpha = 12^\circ$ for the given work material. The clearance angle α is related to the height at which the tool is mounted by the following relation (see Figure 6.12a):

$$H_t = R_1 \sin \alpha$$

where R_1 is the diameter of the form tool.

For $H_t = 10 \text{ mm}$ and $\alpha = 12^\circ$, we obtain $R_1 = 48.1 \text{ mm}$. Hence, we adopt cutter diameter $D = 2R_1 \approx 100 \text{ mm}$. The actual height of tool setting is recalculated as $H_t = 50 \sin 12^\circ = 10.4 \text{ mm}$. The graphical construction of the cutter profile is illustrated in the figure, following the procedure step by step. For convenience, the symbols used are the same as in Figure 6.12(a).



The relevant expressions for determination of the cutter profile by analytical method are given below for the given values of $r_1 = 15$ mm, $r_2 = 24$ mm, $\alpha = 12^\circ$, and $\gamma = 20^\circ$. For convenience, the symbols used are the same as in Figure 6.12(b).

$$h_u = r_1 \sin \gamma = 15 \sin 20^\circ = 5.136 \text{ mm}$$

$$A_1 = r_1 \cos \gamma = 15 \cos 20^\circ = 14.1 \text{ mm}$$

$$\sin \gamma_2 = \frac{h_u}{r_2} = \frac{5.136}{24.0} = 0.214$$

Hence, $\gamma_2 = 12^\circ 20' 36''$

$$A_2 = r_2 \cos \gamma_2 = 24 \cos 12^\circ 20' 36'' = 23.445 \text{ mm}$$

$$C_2 = A_2 - A_1 = 23.445 - 14.10 = 9.345 \text{ mm}$$

$$\epsilon_1 = \alpha + \gamma = 12^\circ + 20^\circ = 32^\circ$$

$$H = R_1 \sin \epsilon_1 = 50 \sin 32^\circ = 26.496 \text{ mm}$$

$$B_1 = R_1 \cos \epsilon_1 = 50 \cos 32^\circ = 42.403 \text{ mm}$$

$$B_2 = B_1 - C_2 = 42.4 - 9.345 = 33.05 \text{ mm}$$

$$\tan \epsilon_2 = \frac{H}{B_2} = \frac{26.496}{33.05} = 0.8016$$

Hence, $\epsilon_2 = 38^\circ 40' 40''$

$$R_2 = \frac{H}{\sin \epsilon_2} = \frac{26.496}{\sin 38^\circ 40' 40''} = \frac{26.496}{0.6242} = 42.447 \text{ mm}$$

6.3 Design of Drills

Drills are used for making and enlarging holes. A variety of drills are used in industry such as flat drill, gun drill, half-round drill, twist drill, etc.; but the twist drill is most widely used. The nomenclature of the main elements of twist drill was discussed in Section 1.4 (Figure 1.18a) and its geometry was discussed in Section 5.3. The other parameters related to the shapes and dimensions of drill features will be discussed in this section for a twist drill (Figure 6.16).

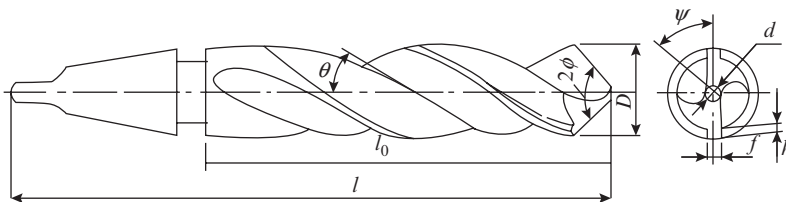


Figure 6.16 Schematic depicting the design parameters of twist drill

(i) *Diameter of drill D and reverse taper:*

Twist drills come in the range 0.25–80 mm. Various subranges within this range are graded as follows:

- 0.25 – 3.0 mm in steps of 0.05 mm
- 3.1 – 14.0 mm in steps of 0.1 mm
- 14.25 – 32.5 mm in steps of 0.25 mm
- 33.0 – 50.5 mm in steps of 0.5 mm
- >50.5 mm in steps of 1.0 mm

The diameter of the drill for drilling a particular hole is selected from standard tables. However, a general guideline is that the drill diameter must always be slightly less than the diameter of the hole.

The diameter of the guiding length of the drill reduces toward the shank to reduce friction during the drilling operation. This reverse taper depends on the drill diameter and the recommended values are given below.

| | | | |
|---------------------------|-----------|-----------|-----------|
| Drill diameter D (mm) | 1–10 | 10–18 | >18 |
| Reverse taper (mm/100 mm) | 0.03–0.08 | 0.04–0.10 | 0.05–0.12 |

For cemented carbide tipped drills, the reverse taper is provided along the length of the cutting bit as per the following recommendations:

| | | | |
|---------------------------|-----------|-----------|-----------|
| Drill diameter D (mm) | <5 | 5–10 | >10 |
| Reverse taper (mm/100 mm) | 0.01–0.03 | 0.03–0.05 | 0.05–0.08 |

(ii) *Core diameter d_o*

Adequate core diameter is essential to insure that the drill has sufficient strength and stiffness to withstand the operational load. On the contrary, excessively large core diameter increases thrust force. The recommended values of d_o for carbon steel and HSS drills are given below.

| | | | |
|--------------------------|---------------|----------------|------------------|
| Drill diameter D (mm) | 0.25–1.25 | 1.5–12 | >13 |
| Core diameter d_o (mm) | $0.24D^{0.8}$ | $(0.15–0.19)D$ | $(0.125–0.145)D$ |

For cemented carbide-tipped drills, the value of d_o may be found from the following relations:

$$d_o = (0.38–0.42)D \text{ for machining of metals}$$

$$d_o = (0.32–0.35)D \text{ for machining of non metals}$$

The core diameter increases by 1.4–1.8 mm/100 mm in the direction of the shank for greater strength and stiffness of the drill.

(iii) *Thickness of cutting blade b*

Blade thickness b is assigned from consideration of strength of the drill, whereas the width of flute that represents the gap between two blades should be such as to provide sufficient space for accommodating the chip. Generally, the blade thickness and flute width are taken equal, therefore $b = \frac{\pi D}{4}$. For drills with large helix angle, the flute width is slightly

more than b . Blade thickness is specified in the plane normal to the helix. In this plane, the blade thickness values for different drill diameters may be taken from the following data:

| | | | |
|----------|---------|---------|---------|
| D (mm) | 3–8 | 8–20 | >20 |
| b (mm) | $0.62D$ | $0.59D$ | $0.58D$ |

(iv) *Auxiliary flank height and width*

Auxiliary flank is a narrow cylindrical margin provided from the outer corner of each cutting blade and running along the length of flute. Its purpose is to guide the drill and reduce friction during operation. The following relations are recommended for determining width f and height h of the auxiliary flank:

$$f = (0.06-0.07)D$$

$$h = (0.02-0.03)D$$

where D is the drill diameter.

(v) Length of drill cutting portion l_0 and total length l :
In terms of the shank shape, drills are of two types:

1. drills with cylindrical shank
2. drills with tapered shank

Drills with cylindrical shank come in the range of diameter 0.25–20 mm, which is divided into subranges as follows:

1. short drills, diameter range 1–20 mm, length of cutting portion $l_0 = 6-65$ mm
2. medium length drills, diameter range 0.25–20 mm, length of cutting portion $l_0 = 3-140$ mm
3. long drills, diameter range 1.95–20 mm, length of cutting portion $l_0 = 55-165$ mm

The standard values of cutting length l_0 and total length l for the three types of cylindrical shank HSS drills are given in Table 6.5.

Table 6.5 Length of cutting portion l_0 and total l of HSS drills with cylindrical shank

| S. No. | Drill diameter (mm) | Drill type | | | | | |
|--------|---------------------|------------|----------|------------|----------|------------|----------|
| | | Short | | Medium | | Long | |
| | | l_0 (mm) | l (mm) | l_0 (mm) | l (mm) | l_0 (mm) | l (mm) |
| 1. | 0.25 | | | 3–5 | 20 | | |
| 2. | 0.5 | | | 6 | 22 | | |
| 3. | 1.0 | 6 | 32 | 12 | 34 | | |
| 4. | 1.5 | 9 | 36 | 18 | 40 | | |
| 5. | 2.0 | 12 | 38 | 24 | 50 | 55 | 85 |
| 6. | 5.0 | 26 | 63 | 52 | 85 | 85 | 130 |
| 7. | 10.0 | 45 | 90 | 90 | 135 | 120 | 185 |
| 8. | 15.0 | 55 | 110 | 115 | 170 | 145 | 220 |
| 9. | 20.0 | 65 | 130 | 140 | 205 | 165 | 255 |

Table 6.6 Length of cutting portion l_o and total length l of HSS drills with tapered shank

| S. No. | Drill diameter (mm) | Drill type | | | | | | | |
|--------|---------------------|------------|----------|------------|----------|-------------------------|----------|------------|----------|
| | | HSS | | | | Cemented carbide tipped | | | |
| | | Normal | | Long | | Short | | Normal | |
| | | l_o (mm) | l (mm) | l_o (mm) | l (mm) | l_o (mm) | l (mm) | l_o (mm) | l (mm) |
| 1. | 6 | 60 | 140 | 150 | 230 | – | – | – | – |
| 2. | 10 | 90 | 170 | 170 | 250 | 60 | 140 | 90 | 170 |
| 3. | 15 | 115 | 215 | 190 | 290 | 75 | 175 | 115 | 215 |
| 4. | 20 | 140 | 240 | 220 | 320 | 95 | 195 | 135 | 235 |
| 5. | 25 | 160 | 280 | 245 | 365 | 115 | 235 | 160 | 280 |
| 6. | 30 | 175 | 295 | 275 | 395 | 125 | 275 | 175 | 325 |
| 7. | 40 | 200 | 350 | | | | | | |
| 8. | 50 | 220 | 370 | | | | | | |
| 9. | 60 | 235 | 420 | | | | | | |
| 10. | 70 | 250 | 435 | | | | | | |
| 11. | 80 | 260 | 515 | | | | | | |

Drills with tapered shank are available in the range of diameter 6–80 mm. Based on length, the HSS drills come in the variants normal and long and the cemented carbide-tipped drills in the variants short and normal. The standard values of cutting length l_o and total length l for HSS and cemented carbide drill with tapered shank are given in Table 6.6.

It can be noted from Table 6.6 that for diameter >30 mm, drills are not made in the long variant, because excessive length can cause buckling of the drill during operation. As a general rule, it should be kept in mind that the length of drill affects its stiffness, therefore the shorter length should be given preference, if otherwise feasible from operational requirements. It may also be mentioned here that available drill lengths for particular diameters may vary from manufacturer to manufacturer. Therefore, the values given in Tables 6.5 and 6.6 should be taken as typical representative values only.

The tapered shanks are made with Morse taper. The recommendations for selection of particular Morse taper based on drill diameter are given in Table 6.7.

(vi) Shape of flute profile:

The drill flute is milled with a special cutter. The profile of this cutter is shown in Figure 6.17 and the empirical relations for determining the parameters defining this profile are given below. Here, it may be mentioned that the guiding principle in designing this complex profile is that it produces straight primary cutting edges on the drill.

Table 6.7 Morse taper for drill shank

| S. No. | Drill diameter (mm) | Morse taper No | Taper inch/foot | Setting angle of compound rest |
|--------|---------------------|----------------|-----------------|--------------------------------|
| 1. | 6–14 | 1 | 0.5986 | 1°25.75' |
| 2. | 14.25–23.0 | 2 | 0.5994 | 1°25.75' |
| 3. | 23.25–31.5 | 3 | 0.6023 | 1°26.25' |
| 4. | 31.75–50.5 | 4 | 0.6232 | 1°29.25' |
| 5. | 51–75 | 5 | 0.6315 | 1°30.5' |
| 6. | 76–80 | 6 | 0.6256 | 1°29.5' |

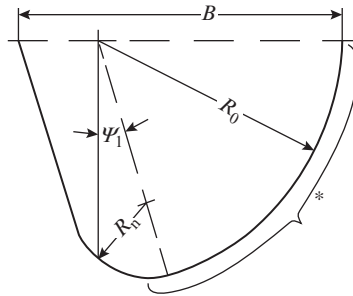


Figure 6.17 Profile of flute milling cutter (*This segment is designed to provide straight primary cutting edges on the drill.)

$$R_o = C_1 C_2 C_3 D \tag{6.9}$$

Coefficient C_1 depends on lip angle 2ϕ and helix angle θ and is given by the following relation:

$$C_1 = \frac{0.026 \times 2\phi \times \sqrt[3]{2\phi}}{\theta} \tag{6.10}$$

Coefficient C_2 depends on core diameter d_o and drill diameter D and is given by the following relation:

$$C_2 = \left(\frac{0.14D}{d_o} \right)^{0.044} \tag{6.11}$$

Coefficient C_3 takes into account the diameter of the flute milling cutter D_c and is given by the following relation:

$$C_3 = \left(\frac{13\sqrt{D}}{D_c} \right)^{0.9} \tag{6.12}$$

The nose radius of the cutter teeth R_n is expressed as follows:

$$R_n = C_n D \quad (6.13)$$

where coefficient C_n is found from the following relation:

$$C_n = 0.015\theta^{0.75} \quad (6.14)$$

Cutter width B is found from the following relation:

$$B = R_o + \frac{R_n}{\cos \psi_1} \quad (6.15)$$

Angle ψ_1 is taken as 10° . Hence, taking $\cos \psi_1 \approx 1$, the expression for B may be written as follows:

$$B = R_o + R_n$$

The profile of flute milling cutter thus determined is, strictly speaking, valid for only one particular drill of given diameter, helix angle, lip angle, and core diameter. However, these cutters are produced in a set of a few cutters and each cutter of the set is used for milling flutes in drills of a certain diameter range. The deviation of the flute shape from the theoretical and the resulting deviation of the primary cutting edges from straight line is not large and is ignored in analysis of the drilling process.

Example 6.4

Select a suitable HSS taper shank drill to make a hole for M27 thread in a 50 mm long job of medium carbon steel.

From the handbook on threaded holes, we find that the recommended drill size for a M27 thread is 23.90 mm. Since the drills in the size range of 14.25–32.50 mm are available in steps of 0.25 mm, we select a drill of 23.50 mm; the drilled hole will be subsequently enlarged to 23.90 mm by reaming or boring.

- (i) For drill of diameter $D = 23.50$ mm, the reverse taper along the length of the cutting portion will lie in the range 0.05–0.12 mm per 100 mm. We select a value of 0.07 mm per 100 mm.
- (ii) For $D = 23.50$ mm, the core diameter d_o lies in the range $(0.125\text{--}0.145)D$; we select the value of $0.135D$, and hence we obtain $d_o = 23.50 \times 0.135 = 3.17$ mm.
- (iii) For $D = 23.50$, the blade thickness b is recommended as $0.58D$, and hence we obtain $b = 0.58 \times 23.50 = 13.63$ mm.
- (iv) Auxiliary flank width f is recommended as $(0.06\text{--}0.07)D$; taking the mean value, we obtain $f = 0.065 \times 23.50 = 1.527$ mm.
- (v) Auxiliary flank height h is recommended as $(0.02\text{--}0.03)D$; taking the mean value, we obtain $h = 0.025 \times 23.50 = 0.59$ mm.
- (vi) From Table 6.6, it can be noted that for drills of diameter 20 mm and 25 mm, the length of the cutting portion for normal length drill is 140 mm and 160 mm, respectively. As the length of the job in which the hole is to be drilled is only 50 mm, we will opt for a normal length drill. Hence, for the drill of diameter $D = 23.50$ mm, the cutting length l_o will be between 140 mm and 160 mm, and the total length between 240 mm and 280 mm. The exact value will be taken from the standard table or manufacturers' catalogue.
- (vii) For $D = 23.50$, the taper of the shank is recommended as Morse taper No 3 ($1^\circ 26.25'$).

- (viii) For determining the flute profile, we will need the drill angles. Referring to Example 5.4, we retrieve the following angles that were determined for the same drill: $2\phi = 118^\circ$, $\alpha = 12^\circ$, $\psi = 55^\circ$, $\theta = 30^\circ$.

Applying the relevant values to Eqn. (6.10), we find $C_1 = 0.493$.

Applying the relevant values to Eqn. (6.11), we find $C_2 = 1.0$.

In the absence of data on flute milling cutter, its effect is neglected, and we assume $C_3 = 1.0$. Hence, substituting the above values in Eqn. (6.9), we obtain

$$R_o = 0.493 \times 1.0 \times 1.0 \times 23.50 = 11.58 \text{ mm}$$

From Eqn. (6.14), we find

$$C_n = 0.015(30)^{0.75} = 1.191$$

Now substituting this value in Eqn. (6.13), we obtain

$$R_n = 0.191 \times 23.50 = 4.48 \text{ mm}$$

Cutter width B is found from Eqn. (6.15) assuming $\psi_1 = 10^\circ$ as follows:

$$B = R_o + \frac{R_n}{\cos 10^\circ} = 11.58 + \frac{4.48}{0.9848} = 16.14 \text{ mm}$$

6.4 Design of Milling Cutters

The geometry of plain and face milling cutters, including the parameters that determine the tooth shape for profile-sharpened and form-relieved cutters were discussed in Section 5.4. The other parameters related to the shape and dimensions of plain, face, and module milling cutters will be discussed in this section.

6.4.1 Design of Plain Milling Cutter

Plain milling cutters have profile-sharpened teeth and the main parameters of a plain milling cutter are shown in Figure 6.18.

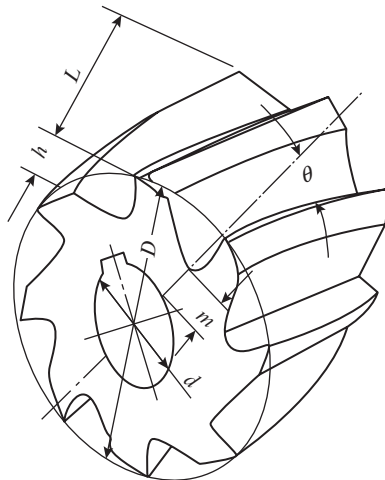


Figure 6.18 Plain milling cutter and its main parameters

(i) *Bore diameter d*

Plain milling cutters are mounted on an arbor on which their axial location is fixed by means of sleeves. The bore diameter is determined from consideration of the strength and stiffness of the arbor under the action of cutting forces. The arbor is considered as a simply supported beam subjected to combined bending and torsion, and the arbor cross section is determined at the middle of span applying the condition that the principal stress and deflection at this point should not exceed specified permissible values. The larger of the two values obtained from the strength and stiffness considerations is selected.

In regular practice, the bore diameter is usually selected from the series of standard values 16, 19, 22, 27, 32, 40, 50, and 60 mm and the design of arbor strength and stiffness is used as a check.

(ii) *Cutter diameter D*

As can be noted from Figure 6.18,

$$D = d + 2m + 2h \quad (6.16)$$

where

d = bore diameter

m = thickness of the tool body; $m = (0.3-0.5)d$

h = height of cutter tooth; if the cutter is designed for finish cuts, the value of h will be taken for the trapezoidal profile (Figure 5.10a); but if it is designed for rough cuts, the value of h will be taken for the parabolic profile (Figure 5.10b) or double clearance plane profile (Figure 5.10c) given in Section 5.4.

Cutter diameter D generally lies in the range $(2.5-3.0)d$. In industrial practice, the values of D have been standardized and constitute geometrical progression of ratio 1:26. The set of standard values are 16, 20, 25, 32, 40, 50, 60, 63, 80, 100, and so on.

The recommendations on selection of d for known D and vice versa are given in Table 6.8.

Table 6.8 Recommendation for selection of cutter diameter D and bore diameter d

| | | | | | | | | |
|-----------------------------|----|----|----|----|--------|---------|---------|---------|
| Bore diameter d (mm) | 16 | 19 | 22 | 27 | 32 | 40 | 50 | 60 |
| Cutter diameter D (mm) | 40 | 50 | 63 | 63 | 80-100 | 100-125 | 125-160 | 160-200 |

In plain milling operations, the cutter diameter is not closely associated with the size of the workpiece. In other words, a given flat surface can be milled with cutters of various diameters. Therefore, while selecting a plain milling cutter, two factors have to be borne in mind. First, a large diameter cutter enables a larger arbor to be used for mounting, permitting heavier cuts to be taken on account of the enhanced strength and stiffness of the arbor. Second, cutters with larger diameter also have better heat removal from the cutting zone, which improves cutter life. On the contrary, larger cutters are more expensive and increase machining time (see Figure 1.32).

Only a rational analysis of these conflicting factors can lead to the selection of correct cutter diameter. Table 6.9 gives recommendation on the selection of diameter D of plain milling cutters, depending on milling width B .

Table 6.9 Recommendation on selection of the diameter D depending on milling width B

| Milling width B (mm) | Diameter of plain milling cutter for depth of cut $t =$ | | | |
|------------------------|---|-------------|-------------|--------------|
| | ≤ 2 mm | ≤ 5 mm | ≤ 8 mm | ≤ 10 mm |
| 40 | 50 | 63 | 63 | 80 |
| 70 | 63 | 80 | 100 | 100 |
| 100 | 80 | 100 | 100 | 100 |
| 150 | 100 | 125 | 125 | 160 |
| 200 | 100 | 125 | 160 | 200 |
| 250 | 125 | 125 | 160 | 200 |
| 300 | 160 | 200 | 200 | 250 |

Small- and medium-sized HSS plain milling cutters ($D \leq 100$) are made solid. However, larger cutters whether HSS or carbide-tipped have a design in which individual blades with brazed or mechanically clamped bits are assembled in the cutter body

(iii) *Number of teeth of cutter Z*

The number of teeth determines the size of the teeth and the size of flute between adjacent teeth. In a coarse-pitch cutter, the number of teeth is less, but they are stronger, provide better heat removal from the cutting zone and provide more space for accommodating the chips produced. Due to these reasons, plain milling cutters are mostly designed with coarse teeth. Fine tooth cutters are used only for finish milling with small allowance.

The number of cutter teeth Z can be found from the following empirical relation:

$$Z = K\sqrt{D} \tag{6.17}$$

where coefficient K depends on the type of cutter and the cutting conditions. The values of K are given below for the various types of HSS plain milling cutters:

Solid, coarse tooth with helix angle $\theta \leq 30^\circ$, $K = 1.05$

Solid, fine tooth with helix angle $\theta = 15-20^\circ$, $K = 2.0$

The number of teeth of solid HSS plain milling cutters may also be found from the following empirical relation that takes into consideration the machining conditions:

$$Z = \frac{K_1 D}{t^{0.5} s_z^{0.5}}$$

where

K_1 = is a coefficient that depends on the type of cutter; for plain milling cutters $K_1 = 0.2$

D = cutter diameter, mm

t = depth of cut, mm

s_z = feed per tooth, mm/tooth

For assembled cutters of diameters $D \leq 200$ mm, the number of teeth may be selected from the following relations:

$$\begin{aligned} Z &= (0.04\text{--}0.06) D \text{ for machining steel} \\ Z &= (0.08\text{--}0.10) D \text{ for machining cast iron} \\ Z &= (0.02\text{--}0.03) D \text{ for machining non ferrous metals and plastics} \end{aligned}$$

For assembled milling cutters of $D \leq 200$ mm, the number of teeth calculated by the above relations is incremented by 2.

Generally, coarse teeth cutters have 6–12 teeth and fine teeth cutters have 10–18 teeth.

(iv) *Cutter length L*

Cutter length L is found from the following relation:

$$L = B + 10 \text{ mm} \quad (6.18)$$

where B = milling width, mm

Length of plain milling cutters has been standardized. The standard lengths constitute a geometrical progression of ratio 1:26, and the values in the standard set of lengths are 40, 50, 63, 100, 125, 160, and so on.

In the expression of gear diameter D (Eqn. (6.16)), tooth height h is a function of tooth pitch, that is, the number of gear teeth. Similarly, from Eqn (6.17), it can be noted that the number of teeth is a function of cutter diameter. In view of this mutual dependency, it is not possible to determine D and Z independent of each other and one of them has to be initially fixed. However, there is nothing sacrosanct about this fixed value as it may actually take several iterations to arrive at the final values of D and Z . The various recommendations given above are based on practical experience and may help in the process of iterations.

Example 6.5

Determine the design parameters of an assembled plain milling cutter with HSS blades for milling a flat surface of width $B = 100$ mm. The job is made of steel having $\sigma_u = 70$ kgf/mm² and the machining allowance is 6 mm.

From Table 6.9, we find that the diameter of the cutter $D = 100$ mm

The recommended length of the cutter is $L = D + 10 = 110$ mm. From the set of standard values for cutter length, we select the nearest higher value of $L = 125$ mm.

The helix angle for assembled HSS cutter is $\theta = 20^\circ$ (see Section 5.4.1).

From Eqn. (6.17), using a value of 0.9 for coefficient K , we obtain the number of cutter teeth:

$$Z = K\sqrt{D} = 0.9\sqrt{100} = 9$$

From Table 6.8, for $D = 100$ mm, two values of the bore diameter are possible 32 and 40 mm; for safer operation, we select bore diameter $d_o = 40$ mm.

For the selected cutter, pitch

$$p = \frac{\pi D}{Z} = \frac{\pi \times 100}{9} = 34.9 \text{ mm}$$

Assuming that the cutter teeth are made with two clearance surfaces (Figure 5.10c) as recommended for cutters used for rough cuts, we find the height of cutter teeth $h = (0.3\text{--}0.45)p$. Taking a value of 0.4, we obtain $h = 0.4 \times 34.9 = 14.0$ mm.

On substituting the selected values of h , d , and D in Eqn. (6.16), we get

$$m = \frac{100 - 40 - 2 \times 14}{2} = 16 \text{ mm}$$

The recommended range of m is $(0.3-0.5)d$. Hence for the selected value of $d = 40$ mm, the cutter body thickness m should be between 12 mm and 20 mm. The value of $m = 16$ mm is inside this range. Hence, the cutter design is safe.

6.4.2 Design of Face Milling Cutters

Face milling cutters just as plain milling cutters have profile sharpened teeth. Their geometry was described in Section 5.4.2. The main design parameters are discussed below (for reference, see Figures 5.13 and 5.14).

(i) Cutter diameter D

Unlike plain milling cutters, the diameter of face milling cutter is related to the milling width B and may be found from the following relations:

$$D = 1.1 B \text{ for HSS cutters}$$

$$D = (1.2-1.6) B \text{ for carbide-tipped cutters}$$

Diameters of face milling cutters are standardized and constitute a geometric progression of ratio 1.26. The standard values are 40, 50, 63, 80, 100, 125, 160, 200, and 250. Face milling cutters having $D \leq 80$ mm are made solid; whereas in larger cutters, individual blades with brazed or mechanically clamped HSS/cemented carbide bits are assembled in the cutter body.

(ii) Cutter length L

The prevailing relations for determining the height of face milling cutters are given below

$$L = (0.5-0.8) D \text{ for solid HSS cutters}$$

$$L = (0.2-0.5) D \text{ for assembled HSS cutters}$$

$$L = (0.25-0.5) D \text{ for assembled carbide tipped cutters}$$

Here the smaller value pertains to cutter of larger size and vice versa. For instance, $L = 0.15D$ corresponds to the largest cutter of $D = 250$ mm and $L = 0.3D$ to the smallest cutter of $D = 80$ mm in the category of assembled face milling cutters with carbide-tipped blades.

(iii) Number of teeth Z

The number of teeth Z is found from the following relations for HSS cutters:

$$Z = K\sqrt{D}$$

where

$$K = 2 \text{ for fine teeth cutters with closely spaced teeth}$$

$$K = 1.2 \text{ for coarse teeth cutters with widely spaced teeth}$$

For carbide-tipped cutters, the recommended relations are as follows:

$$Z = 0.04D \text{ for } D \leq 200 \text{ mm}$$

$$Z = 0.04D + 2 \text{ for } D > 200 \text{ mm}$$

In carbide-tipped cutters for milling of cast iron,

$$Z = 0.1D$$

Coarse teeth cutters are made only for cutter diameter > 63 mm.

(iv) Bore diameter d

Bore diameter is selected on the basis of the cutter diameter as per the recommendations given in Table 6.10.

Table 6.10 Recommendations for selection of bore diameter d based on diameter of face milling cutter D

| D (mm) | 40 | 50 | 63 | 80 | 100 | 125 | 160 | 200 | 250 |
|----------|----|----|----|-------|-----|-----|-----|-----|-----|
| d (mm) | 16 | 22 | 27 | 32/27 | 32 | 40 | 50 | 50 | 50 |

Of the two values given for $D = 80$ mm, the larger value pertains to solid cutter and the smaller to assembled cutter.

The relations and recommendations given above regarding selection of D , L , Z , and d for face milling cutters have evolved from experience of various manufacturers. The data given below in Tables 6.11–6.13 will act as a practical guide and aid in proper selection of face milling cutter parameters for machining of steel.

Table 6.11 Main parameters of solid HSS face milling cutters

| Parameter | Cutter diameter D (mm) | | | | |
|-----------|--------------------------|----|------|-------|-------|
| | 40 | 50 | 63 | 80 | 100 |
| Z | 10 | 12 | 14/8 | 16/10 | 18/12 |
| d (mm) | 16 | 22 | 27 | 32 | 32 |
| L (mm) | 32 | 36 | 40 | 45 | 50 |

Remark: For cutter diameters 63, 80, and 100 mm, the value of Z in the numerator is for fine tooth cutter and that in the denominator for coarse tooth cutter.

Table 6.12 Main parameters of assembled HSS face milling cutters

| Parameter | Cutter diameter D (mm) | | | | | |
|-----------|--------------------------|-----|-----|-----|-----|-----|
| | 80 | 100 | 125 | 160 | 200 | 250 |
| Z | 10 | 10 | 14 | 16 | 20 | 26 |
| d (mm) | 27 | 32 | 40 | 50 | 50 | 50 |
| L (mm) | 36 | 40 | 10 | 45 | 45 | 45 |

Table 6.13 Main parameters of assembled face milling cutters with carbide-tipped blades

| Parameter | Cutter diameter D (mm) | | | | | |
|-----------|--------------------------|-----|-----|-----|-----|-----|
| | 80 | 100 | 125 | 160 | 200 | 250 |
| Z | 8 | 8 | 8 | 10 | 12 | 14 |
| d (mm) | 27 | 32 | 40 | 50 | 50 | 50 |
| L (mm) | 34 | 50 | 55 | 60 | 60 | 75 |

Example 6.6

Determine the design parameters of an assembled carbide-tipped face milling cutter for milling a flat surface of width $B = 100$ mm. The job is made of cast iron with a machining allowance of 4 mm.

For carbide-tipped face milling cutter the cutter diameter lies in the range $(1.2-1.6) B$. Taking a value of 1.4, we obtain diameter $D = 1.4 \times 100 = 140$ mm. From the standard set of values, we select the nearest higher value of $D = 160$ mm.

Cutter length $L = (0.25-0.5) D$ for assembled carbide-tipped cutters. Taking a value of 0.35, we obtain $L = 0.35 \times 160 = 56$ mm.

Number of teeth $Z = 0.1D$ for carbide-tipped cutters for machining of cast iron. Hence, we obtain $Z = 0.1 \times 100 = 10$.

The value of bore diameter d is selected from Table 6.10. For $D = 160$ mm, we find $d = 50$ mm.

For confirmation of the selected values, we refer to Table 6.13, wherefrom it can be noted that for $D = 160$ mm, the conventional standard values are $Z = 10$, $d = 50$ mm and $L = 60$ mm, which are in conformance with the selected parameters.

6.5 Design of Broach

A broach machines a surface by one of the following two methods:

- (i) rising-tooth method
- (ii) progressive cut method

In the rising tooth method (Figure 6.19), each successive tooth is higher than the previous one and therefore removes a thin layer of work material along the whole width of the machined surface, for example, along the whole periphery of a circle or the whole width of a keyway or spline. Depending on the shape of the broached surface, rising tooth method may be further classified as form broaching (Figure 6.19a) in which each tooth has the same shape or generation broaching (Figure 6.16b) in which most of the cutting teeth remove metal from separate segments and only the last few teeth remove the metal from the whole profile. This is illustrated in Figure 6.19(b) in which the first tooth is circular in shape, but through a succession of intermediate teeth of increasingly wider cutting segment a stage is reached where the last tooth of square section completes the broaching operation, thereby achieving enlargement of a circular hole into a square hole.

In the progressive cut method (Figure 6.20), the total allowance to be removed is divided into a few layers. Each layer is then divided into segments and these are assigned to individual teeth of that group. Thus, if a layer is divided into say four segments, then this layer will be removed by four teeth of equal height and the shape of each of these teeth will correspond to the segment that is assigned to it.

As mentioned in Section 5.15, broaches are used for making a large variety of complex internal and external features. The design procedure is illustrated below for a round broach, but the general approach can be easily adopted for other shapes.

The initial data for broach design is the feature dimension and broaching allowance. Broaching is a finishing operation, therefore the allowance sought to be removed in this operation should not be very large. For circular holes, broaching allowance on diameter can be found from the following relation:

$$\delta D = 0.005D(0.1-0.2)\sqrt{L} \quad (6.19)$$

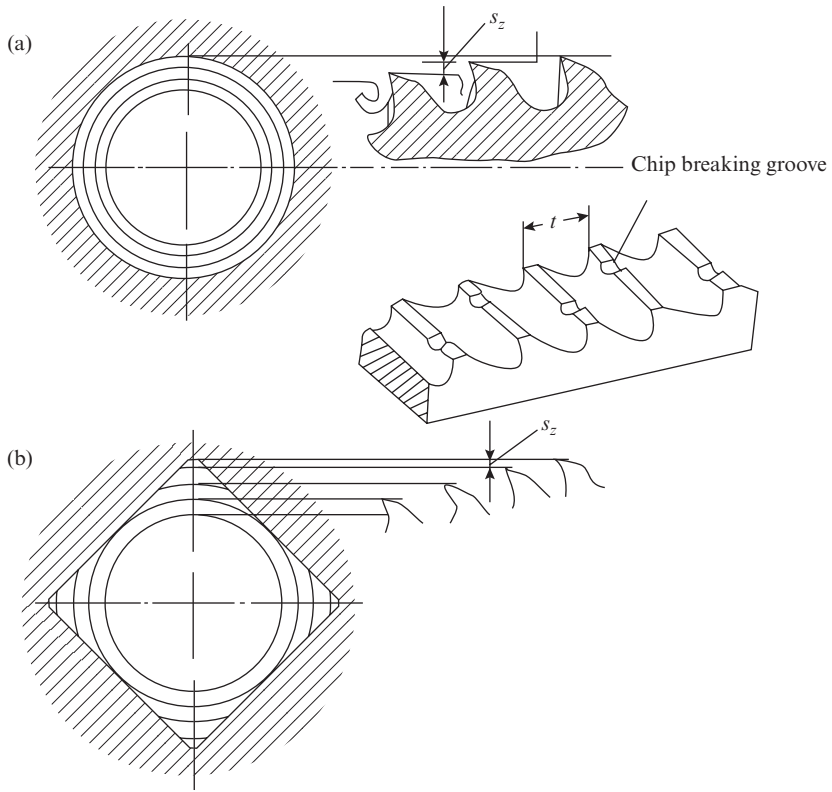


Figure 6.19 Broaching by rising tooth method: (a) form broaching and (b) generation broaching

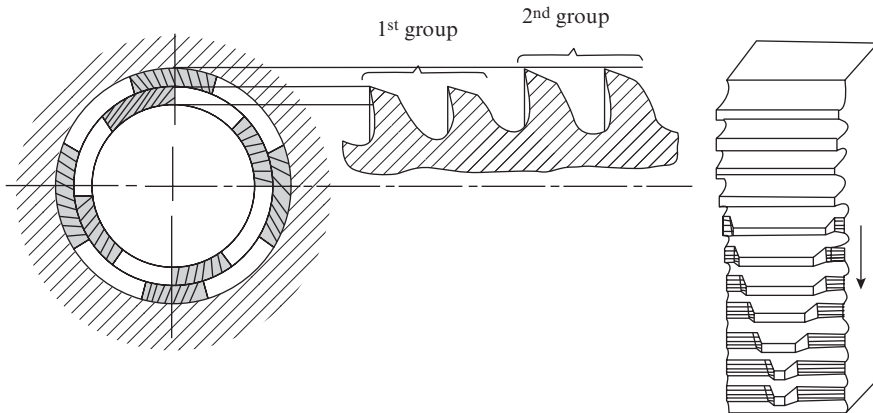


Figure 6.20 Broaching by progressive cut or group cut method

where

$$D = \text{diameter of hole, mm}$$

$$L = \text{length of hole, mm}$$

The broach design parameters are discussed below.

(i) *Rise per tooth s_z*

Rise per tooth depends on the broach profile (round, keyway, spline, etc.) and the work material. The minimum possible value is 0.02 mm that is limited by the accuracy of manufacturing and also because cutting with very small undeformed chip thickness becomes difficult as explained in Section 5.4 (see Figure 5.15). The maximum value is limited by the quality (surface finish) of the broached profile. The recommended values of s_z are given in Table 6.14 for rising tooth broaches. Generally, the last 2–4 teeth of broach are made with a small value of s_z to ensure good surface finish.

Table 6.14 Rise per tooth s_z , mm in rising tooth broaches

| Work material | Rise per tooth for broach having profile | | |
|------------------|--|-----------|-----------|
| | Round | Spline | Keyway |
| Steel | 0.02–0.05 | 0.04–0.08 | 0.03–0.20 |
| Cast iron | 0.03–0.08 | 0.04–0.10 | 0.06–0.15 |
| Bronze and brass | 0.05–0.10 | 0.05–0.12 | 0.06–0.20 |
| Aluminum | 0.02–0.05 | 0.02–0.10 | 0.05–0.20 |

In progressive cut broaches, the value of s_z is considerably higher and lies in the range 0.2–0.4 mm.

(ii) *Area of space between two broach teeth A_c*

The area of space between two broach teeth A_c depends on the undeformed chip area A .

$$A = s_z L$$

where

s_z = rise per tooth, mm

L = length of the broached surface

The area provided for chip space A_c must be greater than A and is given by the following relation:

$$A_c = KA$$

where

K is a coefficient that depends on the work material and the rise per tooth. It generally lies in the range 2.5–6, where the lower value pertains to brittle work material. Detailed recommendations for selection of K for rising tooth broach are given in Table 6.15.

For progressive cut broach, the recommended values of K are as follows for broaching of steel:

$$s_z = 0.07\text{--}0.1, \text{ mm} \quad K = 3.0$$

$$s_z = 0.10\text{--}0.15, \text{ mm} \quad K = 2.5$$

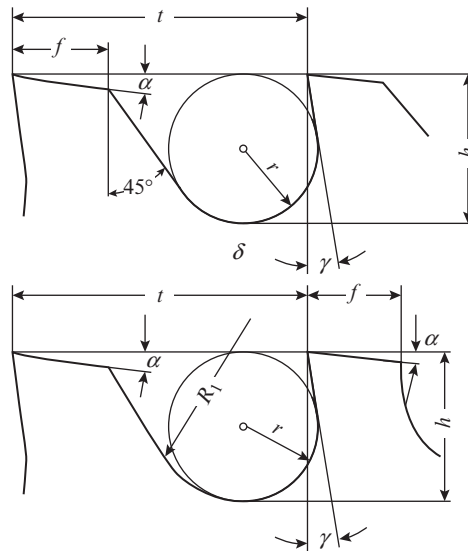
Table 6.15 Minimum required value of coefficient K for area of space in rising tooth broach

| Rise per tooth | Work material | | | | |
|----------------|---------------|---------|------|-----------------------------|---------------------|
| | Steel of BHN | | | Cast iron, bronze, brass | Copper, aluminum |
| | <197 | 198–229 | >229 | | |
| <0.03 | 3 | 2.5 | 3 | 2.5 | 2 |
| 0.03–0.07 | 4 | 3 | 3.5 | 2.5 | 3 |
| >0.07 | 4.5 | 3.5 | 4 | 2 | 3.5 |

$$s_z = 0.15-0.4, \text{ mm} \quad K = 2.2$$

(iii) Pitch of cutting teeth t and parameters of tooth profile:

The profiles of two types of broaches are shown in Figure 6.21.

**Figure 6.21** Tooth profile of (a) rising tooth broach and (b) progressive cut or group cut broach

The most important parameter of a broach is the pitch of the cutting teeth t , which is determined from the following relations:

For rising tooth broach,

$$t = (1.25-1.5)\sqrt{L} \quad (6.20)$$

For progressive cut broach,

$$t = (1.45-1.9)\sqrt{L} \quad (6.21)$$

Additionally, the pitch should be checked for the condition that there should be at least three teeth cutting simultaneously, although for very short jobs, two teeth may be accepted. This means that $t_{\max} \leq \frac{L}{3}$ for normal jobs and $\leq \frac{L}{2}$ for short jobs. The pitch of the finishing (sizing) teeth t_f may be taken 0.6–0.7 times the pitch of the cutting teeth. On the other hand, if the pitch is very small than the number of simultaneously cutting teeth may become excessively large resulting in large cutting force. This number should not exceed 6–8. Hence, $t_{\min} \geq (0.125 - 0.15)L$

The main elements of the broach tooth profile are the face, flank, cutting edge and back. The main difference between the shapes of the two profiles is in the back, which is straight for rising tooth broach (Figure 6.21a) and curved for progressive cut broach (Figure 6.21b).

The main parameters of broach tooth profile are given below.

For rising tooth broach,

$$\begin{aligned} f &= (0.3-0.4) t \\ h &= (0.2-0.4) t \\ r &= (0.1-0.25) t \end{aligned}$$

For progressive cut broach,

$$\begin{aligned} f &= 0.3t \\ h &= 0.4t \\ R_1 &= 0.7t \\ r' &= 0.5h \end{aligned}$$

As the main purpose of the space between two adjacent teeth is to accommodate the chip produced, the following condition is used as a check to ensure that the above requirement is fulfilled:

$$h \geq 1.13\sqrt{Ks_z L} \tag{6.22}$$

(iv) Number of chip breaking grooves n :

The purpose of chip breaking grooves is to break the continuous chip produced along the whole surface (a ring in case of a round hole) into smaller segments to make it easier to accommodate in the space between two adjacent teeth. For a round broach, these grooves have a pitch of 3–8 mm and it is advisable to make them with a clearance angle of 3–5°. The number of grooves for round broach may be taken from the following data:

| | | | | |
|--------------------------|-------|-------|-------|-------|
| Broach diameter D (mm) | 10–13 | 13–16 | 16–20 | 20–25 |
| Number of grooves | 6 | 8 | 10 | 12 |

(v) Number of teeth of broach Z :

The number of cutting teeth is found from the following relation:

$$Z_c = \frac{\delta D - x}{2s_z} \tag{6.23}$$

where δD is the total allowance on diameter (see Eqn. 6.19) and x is the fraction of the allowance reserved for removal by semifinishing teeth. The number of semifinishing teeth Z_{sf} is generally 3–5 and the allowance x is evenly distributed among them. The number of finishing teeth Z_f generally lies from 3 to 8, where the larger value is used for higher precision. Here, it may be mentioned that the finishing teeth only serve for sizing and effectively do not remove any material.

The diameter of the last semi finishing tooth and that of all finishing teeth is taken as follows:

$$D = D_{\max} - \delta$$

where D_{\max} is maximum limit of the diameter of the hole being broached and δ is the amount by which the broach cuts more than its own diameter. Generally, δ is taken (0.3–0.4) times the tolerance on the hole.

(vi) Length of broach L_b (see Figure 5.17):

The total length of broach consist of the length of several segments as detailed below:

(a) Length of cutting portion,

$$l_c = Z_c t_c$$

(b) Length of semifinishing portion,

$$l_{sf} = Z_{sf} t_c$$

(c) Length of finishing portion,

$$l_f = Z_f t_r$$

(d) Length of front support including pull end, neck, and front taper (l_o),

The pull end serves for engagement of the broach with the broaching machine. Its shape and size depend on the shape and size of the hole before broaching. The diameter of the pull end must be less than that of the pre machined hole by 0.5–1.0 mm and its length l_1 depends on the gripping mechanism of the broaching machine. The neck is needed so that the broach can be easily attached to the puller head of the machine. The length of the neck is found from the following relation:

$$l_2 = (10-15) \text{ mm} + n + m - l_t$$

where,

n = thickness of the platen of the broaching machine

m = thickness of the supporting flange of the fixture

l_t = length of the front taper

The front taper facilitates the alignment of the broach with the hole to be broached and lies in the range 5–20 mm. The total length of the front support of the broach l_o which includes the length of the pull end l_1 , the neck l_2 , and the front taper generally lies between 160 mm and 200 mm.

(e) Length of front pilot,

The front pilot aligns the broach with the hole to be broached and also guides it at the beginning of cut. Its shape must correspond to that of the previously cut hole and its diameter equal to the minimum dimension of the previously machined hole. The length of the front pilot is found from the following relation:

$$l_3 = L + 0.5t$$

(f) Length of rear pilot l_4 ,

The purpose of rear pilot is to insure that when the finishing teeth of the broach are disengaging from the workpiece, the direction of the cutting force should lie within the limits of the supporting surface of the machine fixture.

The length of rear pilot is taken as follows:

$$l_4 = (0.5-0.7)L$$

but not less than 20 mm.

(g) Length of rear support l_5 ,

Rear support is required on broaches used on automatic and semiautomatic machines. There is no rear pilot on broaches that are manually returned to their initial position on completion of cut. The shape, dimensions and length of the rear support, if present, are taken the same as that of the front support, that is,

$$l_5 = l_o$$

The total length of broach is found as the sum of all the above lengths, that is,

$$L_b = l_o + l_3 + l_c + l_{sf} + l_f + l_4 + l_5$$

This length must be less than the maximum length of stroke of the broaching machine. The maximum length is also limited by rigidity of the broach which is reflected by the condition $L_b \leq 40D$, where D is the broach diameter. If the design length of the broach exceeds the maximum length of stroke of the broaching machine, then the broaching allowance is divided into two-three steps and a separate broach is designed for each step, with the precaution that all broaches of the set should be of equal length and the dimension of the first cutting tooth of new broach should be equal to that of the last finishing (calibrating) tooth of the previous broach.

(vii) *Check for strength:*

As mentioned in Section 5.4, the broach is inherently a fragile tool by virtue of its very large length to diameter ratio. In addition, because each tooth removes a large chip and there are several teeth cutting simultaneously, the cutting load on the broach is high. It is therefore necessary to check the broach for strength.

The stress in the broach section, assumed to be a bar subjected to tension is given by the following expression:

$$\sigma = \frac{P_{\max}}{A_{\min}}$$

where

$$P_{\max} = P_u \sum b$$

$\sum b$ = sum of the length of simultaneously cutting edges

For a round section,

$$\sum b = \pi D Z_i$$

where

$$Z_i = \frac{L}{t} + 1$$

Here,

L = length of broached hole

t = pitch of broach teeth

P_u = unit cutting force per unit length of the cutting edge

The value of P_u depends on rise per tooth (undeformed chip thickness) and the work material and may be taken from Table 6.16.

The broach design should satisfy the following condition for strength.

$$\sigma \leq \sigma_p$$

Table 6.16 Values of cutting force per unit length (kgf/mm)

| Rise per tooth | P_c , kgf/mm for | | |
|----------------|-----------------------------|----------------------------|-----------------------------|
| | Carbon steel BHN 200–230 | Alloy steel BHN 200–230 | Gray cast iron BHN > 180 |
| 0.02 | 10.5 | 13.6 | 8.9 |
| 0.05 | 18.1 | 22.2 | 15.5 |
| 0.08 | 23.5 | 30.2 | 20.2 |
| 0.10 | 27.3 | 35.4 | 23.6 |
| 0.15 | 37.9 | 48.0 | 32.1 |
| 0.20 | 47.3 | 62.0 | 40.2 |

where σ_p is the permissible strength of broach material that depends on the type of broach. For broaches made of HSS, the value of σ_p can be taken from Table 6.17.

Table 6.17 Permissible value of σ_p , kgf/mm²

| Type of broach | σ_p (kgf/mm ²) |
|------------------|-----------------------------------|
| Round | 25 |
| Keyway, involute | 20 |
| Splined | 10 |

As was mentioned above, the minimum number of simultaneously cutting teeth is 2–3 and the maximum 6–8. Very thin components such as rings should be broached in packs. In general, a broach designed for a particular component can not be used for other components that are too long or too short as compared to the reference part. If the check indicates that the broach has insufficient strength, then either the rise per tooth is reduced or the tooth pitch is increased as both these measures reduce the total cutting force.

Example 6.7

Determine the design parameters of a rising tooth broach for making a 25 mm diameter hole in a medium strength steel part ($\sigma_u = 70$ kgf/mm²) of length 60 mm. The hole has been pre drilled to a diameter of 24 mm.

The broaching allowance on diameter is $\delta D = 25 - 24 = 1.0$ mm. From Eqn. (6.19), we find that for $D = 25$ mm and $L = 60$ mm, δD should be between 0.8995 mm and 1.674 mm. Hence, the diametric allowance provided for broaching is correct.

The rise per tooth as per Table 6.14 should lie in the range 0.02–0.05 mm. We select $s_z = 0.03$ mm.

The undeformed chip area $A = s_z L = 0.03 \times 60 = 1.8$ mm². For the selected value of s_z and given work material, we determine coefficient K from Table 6.15 and obtain $K = 3.0$.

Hence, the area for chip space,

$$A_c = K A \text{ is found as } A_c = 3 \times 1.8 = 5.4 \text{ mm}^2$$

The pitch of the cutting and semifinishing teeth is given by Eqn. (6.20). For the given value of $L = 60 \text{ mm}$, it should lie in the range 9.68–11.60 mm. We select $t_c = t_{sf} = 10 \text{ mm}$. The pitch of the finishing teeth t_f should be 0.6–0.7 times t_c , therefore we select $t_f = 7 \text{ mm}$.

For the selected value of $t = 10 \text{ mm}$, the tooth profile parameters (see Figure 6.21a) are the following:

$$\begin{aligned} f &= (0.3-0.4) t = 3-4 \text{ mm, we select } f = 3.5 \text{ mm} \\ h &= (0.2-0.4) t = 2-4 \text{ mm, we select } h = 3 \text{ mm} \\ r &= (0.1-0.25) t = 1.0-2.5 \text{ mm, we select } r = 1.75 \text{ mm} \end{aligned}$$

As per the recommendation given in the design procedure, the number of chip breaking grooves is selected as $n = 12$.

The diametric allowance allocated to semifinishing teeth is taken as $x = 0.1 \text{ mm}$ and the number of semifinishing teeth is taken as $Z_{sf} = 5$. Hence, the number of cutting teeth is found from Eqn. (6.23) as follows:

$$Z_c = \frac{1.0-0.1}{2 \times 0.03} = 15$$

We select $Z_c = 15$ and distribute the allowance of 0.90 mm equally among them. The allowance of 0.1 mm is also distributed equally among the five semifinishing teeth with $s_{zsf} = \frac{0.1}{5} = 0.02 \text{ mm}$. The number of finishing teeth should lie in the range 3–8. We select $Z_f = 5$.

The components of broach length are (see Figure 5.17):

$$\begin{aligned} \text{length of cutting portion } l_c &= Z_c t_c = 15 \times 10 = 150 \text{ mm} \\ \text{length of semifinishing portion } l_{sf} &= Z_{sf} t_{sf} = 5 \times 10 = 50 \text{ mm} \\ \text{length of finishing portion } l_f &= Z_f t_f = 5 \times 7 = 35 \text{ mm} \\ \text{length of front pilot } l_3 &= L + 0.5t = 60 + 0.5 \times 10 = 65 \text{ mm} \\ \text{length of rear pilot } l_4 &= (0.5-0.7)L = 35-42 \text{ mm ; we select } l_4 = 35 \text{ mm} \end{aligned}$$

The length of the pull end l_o and rear support l_5 depend on the machine and the tool holding fixture. In the absence of specific data, we adopt $l_o = l_5 = 180 \text{ mm}$ which represents the mean of the recommended range.

The total broach length is found as follows:

$$\begin{aligned} L_b &= l_o + l_3 + l_c + l_{sf} + l_f + l_4 + l_5 \\ &= 180 + 65 + 150 + 50 + 35 + 35 + 180 = 695 \text{ mm} \end{aligned}$$

From the consideration of rigidity, $L_{b,max} = 40D = 40 \times 25 = 1000$. As the selected value is less than the maximum allowable length, the broach design is safe.

Finally, we check the selected broach design for strength.

The number of simultaneously cutting edges is

$$Z_i = \frac{L}{t_c} + 1 = \frac{60}{10} + 1 = 7$$

The sum of the length of simultaneously cutting edges for a round section is

$$\sum b = \pi D Z_i = 3.14 \times 25 \times 7 = 549.5 \text{ mm}$$

For the selected value of $s_z = 0.3$ and the given work material, the unit cutting force per unit length is found from Table 6.16 by interpolating the P_u values for $s_z = 0.02$ mm and 0.05 mm and it is found that $P_u = 13$ kgf/mm.

Hence,

$$P_{\max} = P_u \times \sum b = 13 \times 549.5 = 7143.5 \text{ kg}$$

The minimum diameter of the broach section

$$D_{\min} = D - 2h = 25 - 2 \times 3 = 19 \text{ mm}$$

Hence, the maximum stress in the broach:

$$\sigma_{\max} = \frac{P_{\max}}{A_{\min}} = \frac{7143.5}{\frac{\pi}{4} \times (19)^2} = 25.20 \text{ kgf/mm}^2$$

On comparing σ_{\max} with the permissible stress value $\sigma_p = 25$ kgf/mm² from Table 6.17, we conclude that the broach design is not safe from the strength point of view. To address this problem, we reduce tooth height from 3.0 mm to $0.25t = 2.5$ mm, which is still within the recommended range.

The minimum diameter of the broach section now becomes $D_{\min} = 25 - 2 \times 2.5 = 20$ mm and the modified maximum stress is found as follows:

$$\sigma_{\max} = \frac{P_{\max}}{A_{\min}} = \frac{7143.5}{\frac{\pi}{4} \times (20)^2} = 22.75 \text{ kgf/mm}^2$$

Hence, the modified broach design is safe.

6.6 Design of Thread Cutting Tools

As described in Section 5.6, the tools that are used for thread cutting are single-point tools for cutting both external and internal threads, multiple-point thread chasers and thread cutting dies for making external threads and taps for making internal threads. The design of single-point threading tool is similar to that of turning tool that has been discussed in Section 6.1. Similarly, the procedure of design of thread chasers is the same as that of form tools discussed in Section 6.2. In view of the above only the design of taps and thread cutting dies will be discussed in this section.

6.6.1 Design of Taps

As the geometry of taps has already been described in Section 5.6.3, only the main design parameters related to shape and size of the various tap elements will be discussed here.

- (i) Diameters of the threaded portion of tap (see Figure 5.26):

The various diameters defining the threaded portion of tap depend on the corresponding diameters and pitch of the thread to be cut, namely external diameter d_e , pitch diameter

d_p , minor diameter d_m and pitch t_p . For 2-tap and 3-tap sets the values can be taken from the following Table 6.18.

Table 6.18 Diameters of the threaded portion of tap

| Tap diameter | Two-tap set | | Three-tap set | | |
|-------------------------------|----------------|-----------------|-----------------|-----------------|-----------------|
| | No 1: Rough | No 2: Finishing | No 1: Rough | No 2: Medium | No 3: Finishing |
| External d | $d_e - 0.2t_p$ | d_e | $d_e - 0.5t_p$ | $d_e - 0.1t_p$ | d_e |
| Minor d_{mt} | d_m | d_m | d_m | d_m | d_m |
| Pitch circle d_{pt} | $d_p - 0.1t_p$ | d_p | $d_p - 0.15t_p$ | $d_p - 0.07t_p$ | d_p |
| Distribution of metal removal | 75 | 25 | 50 | 35 | 15 |

Single tap is used for making thread of pitch ≤ 2 mm; 2-tap set for pitch ≤ 3 mm and 3-tap set for pitch > 3 mm.

(ii) *Number of flutes Z*

Flutes are provided to accommodate the chip produced in the threading operation. The number of flutes depends on the size and type of tap. A large number of flutes indirectly imply large number of cutting teeth. In this case, each tooth removes a thin chip, but the overall cutting load becomes high. On the other hand, removal of thin chips is associated with thread of better surface finish. The recommendations for selection of Z are arrived at as a compromise between the two conflicting trends and are given in Table 6.19.

Table 6.19 Number of flutes Z in taps

| Type of tap | Number of flutes Z in taps for $d =$ | | | |
|-------------|--|-----------|------------|------------|
| | 3–6 (mm) | 8–16 (mm) | 18–24 (mm) | 27–52 (mm) |
| Hand tap | 2–3 | 3–4 | 4 | 4–6 |
| Machine tap | 2–3 | 3–4 | 4 | 4–6 |
| Nut tap | 3 | 3–4 | 3–4 | 4 |
| Gauge tap | 3 | 3–4 | 4–6 | 6–8 |

(iii) *Core diameter d_o and width of cutting teeth b (see Figure 5.26):*

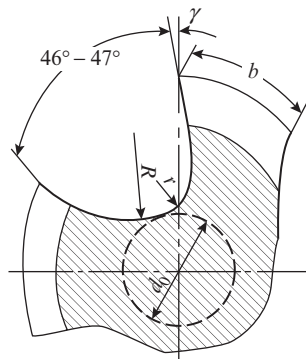
The core diameter and width of cutting teeth depend on the number of flutes. The latter also depends on the work material. For instance, b is reduced and flute width correspondingly increased for threading in aluminum because of the requirement of more space to accommodate the continuous soft chip produced. The values of d_o and b can be taken from Table 6.20.

Table 6.20 Core diameter d_o and width of cutting teeth b in taps

| Number of flutes | d_o | | b | |
|------------------|------------|---------|------------|---------|
| | Steel & CI | Al | Steel & CI | Al |
| 3 | $0.4d$ | $0.4d$ | $0.4d$ | $0.3d$ |
| 4 | $0.5d$ | $0.45d$ | $0.3d$ | $0.22d$ |
| 6 | $0.64d$ | – | $0.2d$ | – |

(iv) Flute profile

The flute profile should be such as to provide sufficient space for accommodating the chip produced, without compromising on the strength of the tap. It should also ensure that when the tap is being withdrawn from a threaded hole by reversing its direction of rotation, the flank of the tap tooth should not damage the previously cut thread. The profile that is most widely used is shown in Figure 6.22 and its parameters r and R can be taken from the following Table 6.21.

**Figure 6.22** Profile of tap flute**Table 6.21** Parameter r and R of tap profile

| Tap diameter d (mm) | Number of flutes Z | r (mm) | R (mm) |
|-----------------------|----------------------|----------|----------|
| 6 | 3 | 1.0 | 4.2 |
| 10 | 3 | 1.5 | 6.6 |
| 20 | 4 | 2.0 | 10.5 |
| 30 | 4 | 3.5 | 15.7 |
| 42 | 4 | 5.0 | 22.3 |
| 52 | 4 | 7.0 | 28.6 |

(v) Tap length (see Figure 5.26):

Tap length consists of the length of cutting portion or the chamfer length, length of the sizing portion, and the length of the shank and square.

(a) Chamfer length

If the number of teeth in the chamfer length is k , then chamfer length can be found as (Figure 6.23):

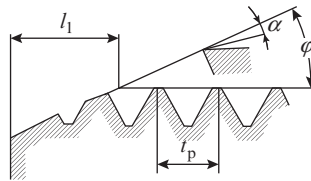


Figure 6.23 Graphical construction to determine chamfer length of tap

$$l_1 = k t_p$$

Parameter k is related to the number of flutes Z and the undeformed chip thickness per tooth a_z by following the relation:

$$a_z = \frac{h}{Zk}$$

where h is the depth of thread.

Substituting for k from the above expression in l_1 , we obtain

$$l_1 = \frac{h t_p}{a_z Z}$$

Generally $\frac{a_z}{t_p} = 0.01-0.03$ for hand and machine taps and $0.012-0.02$ for nut taps

The chamfer angle ϕ is related to a_z , Z , and t_p by the following expression:

$$\tan \phi = \frac{a_z Z}{t_p}$$

While selecting the value of a_z , it should be kept in mind that ϕ should not exceed 30° . The minimum and maximum limits of s_z are 0.02 and 0.15 , respectively.

(b) Length of sizing portion:

The length of sizing portion is taken as follows:

$$l_2 = (5-10)t_p$$

(c) Length of shank and square:

The length of the shank l_3 including the length l_4 of the square are related to the centering and torque transmission elements of the clamping fixture. These values therefore have to be taken for the specific fixture.

$$\text{Length of tap} = l_1 + l_2 + l_3$$

(vi) Reverse taper on tap length:

A small taper is provided along the tap length such that the tap diameter reduces toward the shank in order to decrease the friction during the threading operation. The taper is of the order of 0.05–0.10 mm per 100 mm length for ground machine taps and 0.08–0.12 mm per 100 mm length for hand taps.

Example 6.8

Determine the design parameter parameters of a hand tap set for making coarse—pitch metric thread M27 in a medium steel part having $\sigma_u = 80 \text{ kgf/mm}^2$.

From thread standards, the following data are obtained for the M27 thread:

Pitch $t_p = 3.0 \text{ mm}$ and external diameter $d_e = 27.242 \text{ mm}$

Minor diameter $d_m = 23.592 \text{ mm}$ and pitch circle diameter $d_p = 25.107 \text{ mm}$

As $t_p = 3 \text{ mm}$, referring to the recommendations of Table 6.18, it follows that a 2-tap set would be suitable in the given case and values of the various diameters are as follows:

| Tap parameter | Rough tap (mm) | Finishing tap (mm) |
|--------------------------------|---------------------------|--------------------|
| External diameter d | $= d_e - 0.2t_p = 26.642$ | $= d_e = 27.242$ |
| Minor diameter d_{mt} | $= d_m = 23.592$ | $= d_m = 23.592$ |
| Pitch circle diameter d_{pt} | $= d_p - 0.1t_p = 24.807$ | $= d_p = 25.107$ |

Referring to Table 6.19, for $d = 27 \text{ mm}$, the number of flutes in hand tap set is selected as $Z = 4$.

Referring to Table 6.20, for the selected number of flutes $Z = 4$ and given work material (steel), the core diameter is selected as $d_o = 0.5d = 0.5 \times 26.642 = 13.321 \text{ mm}$ for the rough tap and $0.5 \times 27.242 = 13.621 \text{ mm}$ for the finishing tap.

Referring to Table 6.20 again, the width of cutting teeth is found to be $b = 0.3d = 0.3 \times 26.642 = 8.0 \text{ mm}$ for the rough tap and $0.3 \times 27.242 = 8.172 \text{ mm}$ for the finishing tap.

The parameters of the flute profile shown in Figure 6.22 are determined from Table 6.21. For the selected values of $d = 27 \text{ mm}$ and $Z = 4$, the flute profile radii are found by extrapolating the values given in the table for $d = 20 \text{ mm}$ and $d = 30 \text{ mm}$, and it is found that $r = 3.05 \text{ mm}$ and $R = 14.14 \text{ mm}$.

The tap length consists of the chamfer length l_1 , length of the sizing portion l_2 and the length of the shank and square l_3 (see Figure 5.26).

Chamfer length,

$$l_1 = \frac{ht_p}{a_z Z},$$

Depth of thread of the rough tap $h = \frac{1}{2}(d_e - d_m) = \frac{1}{2}(26.642 - 23.592) = 1.525 \text{ mm}$;

We have already determined $t_p = 3.0 \text{ mm}$ and $Z = 4$.

The parameter $\frac{a_z}{t_p}$ lies in the range 0.01–0.03 for hand and machine taps. We select $\frac{a_z}{t_p} = 0.02$

Now substituting the values of $\frac{a_z}{t_p}$, h and Z in the expression of l_1 , we obtain

$$l_1 = \frac{1.525}{0.02 \times 4} = 19.06 \text{ mm}$$

The length of sizing portion of the rough tap is recommended as $(5-10)t_p$; selecting a value of 8, we find $l_2 = 8 \times 3 = 24$ mm.

Hence, total length of the cutting portion:

$$l = l_1 + l_2 = 19.06 + 24 = 43.06 \text{ mm}$$

For the finishing tap the total length of cutting portion is retained the same, of which the chamfer is provided over a length of $(1.5-2.0)t_p$. Selecting a value of 2, we find chamfer length of finishing tap = $2 \times 3 = 6$ mm.

The reverse taper of the order of 0.08–0.12 mm per 100 mm length is recommended. Taking a value of 0.10, the reverse taper on the length of cutting portion is found as follows:

$$\frac{0.10 \times 43.06}{100} = 0.043 \text{ mm.}$$

6.6.2 Design of Thread Cutting Dies

The geometry of thread cutting dies has been described in Section 5.6.4; therefore, only the main design parameters related to shape and size of the elements of thread cutting dies will be discussed in this section.

(i) *Diameter of thread cutting die D (see Figure 5.28b):*

The diameter of thread cutting die depends on the diameter of the thread to be cut. The recommended values are given Table 6.22.

Table 6.22 Diameter of thread cutting die D for different values of thread diameter d_o

| d_o (mm) | D (mm) | d_o (mm) | D (mm) | d_o (mm) | D (mm) |
|------------|--------|------------|--------|------------|--------|
| 1–2 | 12 | 16–22 | 45 | 62–76 | 120 |
| 2.2–3.0 | 16 | 24–27 | 55 | 78–90 | 135 |
| 3.5–6.0 | 20 | 28–39 | 65 | 95–100 | 150 |
| 7–9 | 25 | 40–45 | 75 | 105–120 | 170 |
| 10–12 | 30 | 48–52 | 90 | 125–135 | 200 |
| 14–16 | 38 | 55–60 | 105 | | |

(ii) *Number of clearance holes Z (see Figure 5.28b):*

The number of clearance holes is related to the thread pitch t_p , undeformed chip thickness a_z and chamfer angle ϕ by the following relation:

$$a_z = \frac{t_p}{Z} \tan \phi$$

In thread cutting dies, generally $a_z = 0.2\text{--}0.5$ mm for steel and $0.4\text{--}0.7$ mm for cast iron. The value of ϕ is selected on the basis of t_p and the recommended values are as follows:

$$\begin{aligned}\phi &= 25^\circ \text{ for } t_p \leq 2.0 \text{ mm} \\ \phi &= 20^\circ \text{ for } t_p = 2\text{--}3 \text{ mm} \\ \phi &= 15^\circ \text{ for } t_p > 3 \text{ mm}\end{aligned}$$

After selecting the appropriate values of a_z and ϕ based on the above recommendations, the number of clearance holes can be calculated from the relation given above. The following Table 6.23 presents the values of Z used in practice depending on the thread pitch t_p .

Table 6.23 Number of clearance holes in thread cuttings dies

| Thread pitch t_p (mm) | 1–5 | 5.5–16 | 18–27 | 30–33 | 36–48 | 52–64 |
|---------------------------|-----|--------|-------|-------|-------|-------|
| Number of clearance holes | 3 | 4 | 5 | 6 | 7 | 8 |

(iii) *Diameter d and pitch circle diameter D_1 of clearance hole:*

The dimensions of the clearance holes should be such that they can conveniently accommodate the chips produced in the threading operation. The shape of the clearance hole is shown in Figure 6.24, where it can be noted that beginning at the edge of the die land, the clearance hole is machined to give a straight rake face upto a certain height x at angle γ selected as per the recommendation given in Section 5.6.4. Generally, $x = (1.2\text{--}1.5)t_p$.

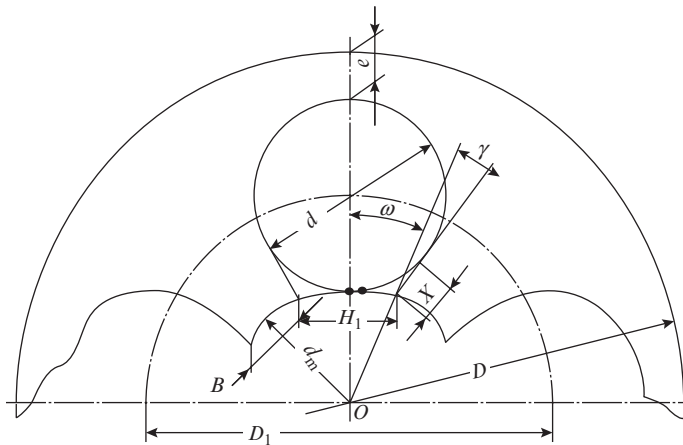


Figure 6.24 Parameters of the clearance hole in thread cutting die

The clearance hole diameter d and pitch circle diameter D_1 are found from the following relations:

$$\begin{aligned}\frac{d}{2} &= \frac{\frac{d_m}{2} \sin \omega + x \sin(\omega + \gamma)}{\cos(\omega + \gamma)} \\ \frac{D_1}{2} &= \frac{d_m}{2} \cos \omega + x \cos(\omega + \gamma) + \frac{d}{2} \sin(\omega + \gamma)\end{aligned}$$

Here,

d_m = minor diameter of the thread

ω = central angle corresponding to hole gap width

(iv) Land width B and gap width H_1 :

Land width B and gap width H_1 are found from the following two relations:

$$B + H_1 = \frac{\pi d_m}{Z}$$

$$B = (0.8-1.0)H_1$$

Having determined D , D_1 , and d , we can now determine the minimum wall thickness of the die:

$$e = \frac{D}{2} - \frac{D_1}{2} - \frac{d}{2}$$

To ensure adequate strength of the die it is required that $e \geq (0.12-0.15)D$ for dies with $Z = 3-5$ and $\geq (0.09-0.10)D$ for dies with $Z = 6-8$. An alternate recommendation is $e \geq (0.6-0.9)\sqrt{D}$.

(v) Height of die H (see Figure 5.28b):

Thread cutting dies have chamfers at both ends with a sizing portion in between.

(a) Chamfer length

$$l_1 = (h + a) \cot \phi$$

where h = height of thread

$a = (0.15-0.4)$ mm

ϕ = chamfer angle; the recommendations for selection of ϕ were given while discussing the number of clearance holes Z .

(b) Sizing length:

$$l_2 = (3-6)t_p$$

(c) Total height of die:

$$H = 2l_1 + l_2$$

(vi) Die mounting (see Figure 5.28b):

The die is mounted in a casing and tightened with the help of screws pressing on the 60° grooves A and B. The 90° grooves C and D are meant to tighten the die. To achieve tightening, the grooves C and D are off set from the radius vector by a small distance c . Groove E located between C and D has a web e_1 , in which a thin cut is made with a grinding wheel. Depending on the degree of tightening of the screws mounted in grooves C and D, the cut made in e_1 can be opened up or closed, thereby allowing minor adjustment in the diameter of the threaded hole.

Example 6.9

Determine the cutting angles and design parameters of a thread cutting die for making M12 thread in mild steel part.

From thread standards the following data is obtain for M12 thread:

Pitch circle diameter $D_{wp} = 10.86$ mm, minor diameter $d_m = 10.106$ mm

Thread height $h = 0.947$ mm, pitch $t_p = 1.75$ mm

Considering mild steel as medium hard material, the radial rake angle is selected as $\gamma_r = 18^\circ$, clearance angle $\alpha = 10^\circ$ on the teeth in the chamfered length and $\phi = 25^\circ$ (see Section 5.6.4).

The normal rake angle is found from the following relation:

$$\gamma_n = \tan^{-1} [\tan \gamma_r \cos \phi] = \tan^{-1} [\tan 18^\circ \cos 25^\circ] = 16^\circ$$

Referring to Table 6.22, for M12 thread the diameter of the die is selected as $D = 30$ mm.

Referring to Table 6.23, the number of clearance holes is selected as $Z = 3$.

For check we determine the undeformed chip thickness

$$a_z = \frac{t_p}{Z} \tan \phi = \frac{1.75}{3} \tan 25^\circ = 0.27 \text{ mm}$$

which is within the recommended range.

Assuming land width $B = H_1$ (Figure 6.24), we find $B + H_1 = \frac{\pi d_m}{Z}$, $2H_1 = \frac{\pi \times 10.106}{3}$.

Hence, gap width $H_1 = B = 5.2$ mm.

The central angle corresponding to half gap width is found from the following relation (see Figure 6.24):

$$\omega = \sin^{-1} \left(\frac{\frac{H_1}{2}}{\frac{d_m}{2}} \right) = \sin^{-1} \left(\frac{H_1}{d_m} \right) = 31^\circ$$

Assuming $x = t_p = 1.75$ mm and substituting the selected values of ω , d_m , x , and γ we find clearance hole diameter:

$$d = 2 \left[\frac{\frac{d_m}{2} \sin \omega + x \sin(\omega + \gamma)}{\cos(\omega + \gamma)} \right] = 2 \left[\frac{\frac{10.106}{2} \sin 31^\circ + 1.75 \sin 47^\circ}{\cos 47^\circ} \right]$$

$$d = \frac{2(2.06 + 1.08)}{0.682} = 11.37 \text{ mm}$$

Pitch circle diameter:

$$D_1 = 2 \left[\frac{d_m}{2} \cos \omega + x \cos(\omega + \gamma) + \frac{d}{2} \sin(\omega + \gamma) \right]$$

$$= 2 \left[\frac{10.106}{2} \cos 31^\circ + 1.75 \cos 47^\circ + \frac{11.37}{2} \sin 47^\circ \right]$$

$$= 2(2.60 + 1.19 + 4.15) = 15.88 \text{ mm}$$

Minimum wall thickness of the die is found from the following relation:

$$e = \frac{D}{2} - \frac{D_1}{2} - \frac{d}{2} = \frac{30 - 15.88 - 11.37}{2} = 1.375 \text{ mm}$$

As per the recommendation $e \geq (0.12-0.15)D$, that is, in the given case the minimum value of e should be $0.12 \times 30 = 3.6$ mm.

Hence, the diameter of the die needs to be enhanced, and we finally select a $D = 35$ mm.

Chamfer length is found as (see Figure 5.28b) follows:

$$l_1 = (h + a) \cot \phi = (0.947 + 0.3) \cot 25^\circ = 2.67 \text{ mm}$$

Sizing length is taken as follows:

$$l_2 = 5t_p = 5 \times 1.75 = 8.75$$

Hence, height of the die:

$$H = 2l_1 + l_2 = 2 \times 2.67 + 8.75 = 14.0 \text{ mm}$$

6.7 Geometry and Design of Gear Cutting Tools

As discussed in Section 5.7, module cutters are used for cutting gear teeth based on form cutting principle and gear shaping cutters and hobs based on generating principle. The geometry and design parameters of these cutters are discussed in this section.

6.7.1 Geometry and Design of Module Cutter

Module cutters have form relieved teeth. The profile of this type of teeth was discussed in Section 5.4 (see Figure 5.11). The main parameters of a disc-type module cutter are shown in Figure 6.25.

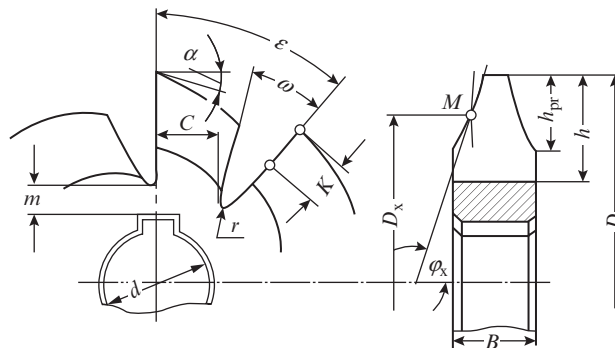


Figure 6.25 Disc-type module cutter and its main parameters

(i) Profile of module cutter:

It was mentioned in Section 5.7 that module cutters come in sets of 8, 15, and 26 cutters depending on the desired profile accuracy of the gear teeth. The 8-cutter set is used for gears of module up to 8 mm and the 15 and 26 cutter sets for larger modules. The range of number of gear teeth Z_g assigned to individual cutters is given below for the 8-cutter set.

| Cutter no | 1 | 2 | 3 | 4 | 5 | 6 | 7 | 8 |
|------------------|-------|-------|-------|-------|-------|-------|--------|------|
| Z_g gear teeth | 12–13 | 14–16 | 17–20 | 21–25 | 26–34 | 35–54 | 55–134 | >135 |

The cutter profile corresponds to the tooth space and for a particular cutter of the set it is designed for the profile of the gear with the minimum number of teeth in the range. For instance, cutter No 6 that is meant to cut gears with 35–54 teeth is designed with the profile corresponding to the gear with 35 teeth. The tooth profile may be determined graphically or analytically, but the latter is preferred because it is more accurate. The x and y coordinates of the involute at a radius r_x are given by the relations:

$$x = r_x \sin \delta_x \quad \text{and} \quad y = r_x \cos \delta_x$$

where

$$\delta_x = \frac{\pi}{2Z} + (\text{inv}\theta - \text{inv}\theta_x)$$

Here, Z = number of teeth of the cutter

θ = pressure angle of the gear (generally 20°)

θ_x = pressure angle at radius r_x ; $\theta_x = \cos^{-1} \left(\frac{D_{\text{pcc}} \cos \theta}{D_x} \right)$

D_{pcc} = pitch circle diameter of the cutter

For gears of pressure angle 20° the coordinates are also available in tabulated form which considerably simplifies the process of profile design. The total profile consists of the involute portion and the noninvolute portion. The latter consists of straight lines and circular arc (Figure 6.26). On the basis of the coordinates of the involute and noninvolute portions a template is prepared which is then used for making the desired profile of the module cutter.

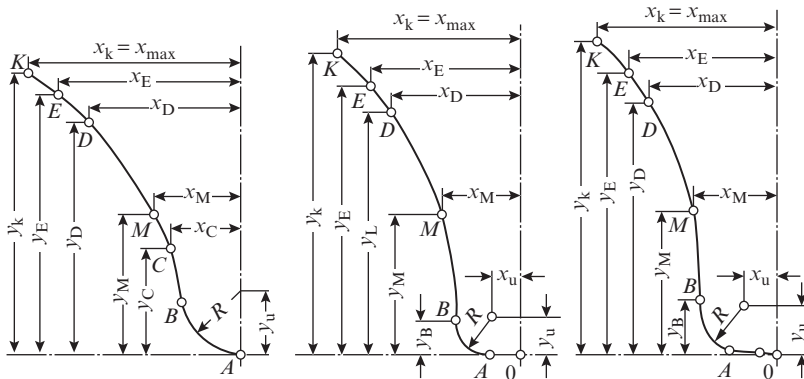


Figure 6.26 Profiles of disc-type module cutters: (a) for cutter No 1 and 2 of the set: CE involute, CB straight, and AB arc of circle; (b) for cutter No 3–7 of the set: BE involute, AO straight, and BA arc of circle; and (c) for cutter No 8 and above; EM involute, MB and AO straight, and BA arc of circle

(ii) *Geometry of module cutter teeth:*

Module cutters are of two types: rough and finishing. The rough cutters have rake angle $\gamma = 8\text{--}10^\circ$, whereas the finishing cutters have rake angle $\gamma = 0^\circ$. The clearance angle α is obtained by relieving the cutter teeth. The relief off set is related to the clearance angle on the periphery by the following relation (see Figure 5.11):

$$K = \frac{\pi D}{Z} \tan \alpha$$

where

D = diameter of the module cutter

Z = number of cutter teeth

At an arbitrary diameter D_x (point M), the clearance angle on the profile side surface α_x is related to α by the following expression:

$$\tan \alpha_x = \frac{D}{D_x} \tan \alpha \sin \phi_x$$

where

ϕ_x is the angle that the tangent to the profile side at the diameter D_x makes with the cutter axis.

As the variation of ϕ_x along the involute profile is much greater than the variation of the cutter diameter, the term $\frac{D}{D_x}$ may be ignored and a simpler relation between α and ϕ_x obtained as follows:

$$\tan \alpha_x = \tan \alpha \sin \phi_x$$

Angle α is selected such as to ensure a minimum value of $\alpha_x = 2-3^\circ$. Generally, α lies from 10° to 12° , but may be increased to $16-17^\circ$ to ensure that α_x does not become less than 2° . Angle ϕ_x varies from about 35° at the base of the tooth to 90° at the periphery where α_x becomes equal to α to ensure smooth transition of the cut from the tooth periphery to the sides.

Height of the module cutter teeth is found from the following relation:

$$H = h_{pr} + K + r$$

where

h_{pr} = height of the cutter tooth profile; depending on the cutter size it is taken 1–5 mm more than the height of gear tooth to ensure a safe gap in case the gear blank is oversize

K = relief offset

r = fillet radius; generally taken between 1 mm and 5 mm, depending on the cutter diameter

Flute angle ω varies from 18° to 30° and the tooth base thickness $C = (0.8-1.0)H$.

(iii) *Bore diameter d :*

Disc-type module cutters are used for cutting gears on horizontal milling machine with an indexing head. The module cutter is mounted on an arbor in the same manner as a plain milling cutter; therefore, the procedure of determining the bore diameter from consideration of strength and stiffness is the same as that described in Section 6.4.1 for plain milling cutters.

(iv) *Cutter diameter D :*

Diameter of module cutter D can be found from the following relation that is similar to Eqn. (6.16) that was used for determining the diameter of plain milling cutter:

$$D = d + 2m + 2H$$

In the above expression, all the terms have the same meaning and recommended values, except H which should be taken from the expression given earlier for height of module cutter teeth.

(v) *Number of teeth of module cutter Z:*

The number of teeth affects the size of the tooth and flute. It should be selected such as to provide a tooth of sufficient strength and a flute that is spacious enough to accommodate the chips produced in the operation. It can be found from the following expression:

$$Z = \frac{\pi D}{p}$$

where p is the circular pitch of the cutter teeth that is taken equal to $(1.3-1.8)H$ for finishing cutters and $(1.8-2.5)H$ for roughing cutters.

The data given in Table 6.24 may be used as a practical guide and aid in selection of module cutter parameters.

Table 6.24 Main parameter of disc-type module cutters

| | | | | | | | | | | | | |
|-------------|-----|-----|-----|-----|-----|-----|-----|-----|-----|-----|-----|-----|
| Module (mm) | 1.0 | 1.5 | 2.0 | 2.5 | 3.0 | 4.0 | 5.0 | 6.0 | 7.0 | 8.0 | 9.0 | 10 |
| D (mm) | 50 | 55 | 60 | 65 | 70 | 80 | 90 | 100 | 105 | 110 | 115 | 120 |
| d (mm) | 16 | 22 | 22 | 22 | 27 | 27 | 27 | 32 | 32 | 32 | 32 | 32 |
| Z | 14 | 14 | 14 | 12 | 12 | 12 | 11 | 11 | 11 | 11 | 10 | 10 |

(vi) *Width of module cutter B:*

The width of the module cutter depends on the profile of the cutter teeth (see Figure 6.26) and is found from the following relation:

$$B = 2x_{\max}$$

where x_{\max} is the maximum value of the x coordinate corresponding to half of the tooth profile (see Figure 6.26).

6.7.2 Geometry and Design of Gear Shaping Cutter

As was mentioned in Section 5.7 gear shaping involves cutting of gear by imitating the meshing of two gears, of which one is the gear blank and the other the gear shaping cutter.

A gear shaping cutter is basically a gear of a hard material on which the teeth are appropriately relieved at angles α and γ to make flank and rake surface respectively and convert the simple gear into a cutting tool (Figures 6.27 and 6.28). In view of the clearance angle α , the diameter of the cutter varies along its height. The basic design of the cutter is done corresponding to the section II–II in which the basic cutter parameters module m and cutter tooth thickness S_d is taken the same as of the gear to be cut, All other parameters such as number of cutter teeth Z_c , pitch circle diameter of the cutter D_{pc} , etc., are different from that of the gear to be cut.

In order that the involute of the cutter teeth does not get distorted after resharping, it is essential that the involute in any section other than II–II should be generated from the same base circle of diameter $D_b = P_{pc} \cos \theta$ that was used for generating the involute in section II–II; here θ is the pressure angle of the gear and also that of the cutter and D_{pc} is the pitch circle diameter of the cutter.

To comply with this condition, the gear teeth would be thinner in section III–III and thicker in section I–I. Correspondingly, the cutter teeth in section I–I are thinner and those in section III–III are thicker than the cutter teeth in section II–II.

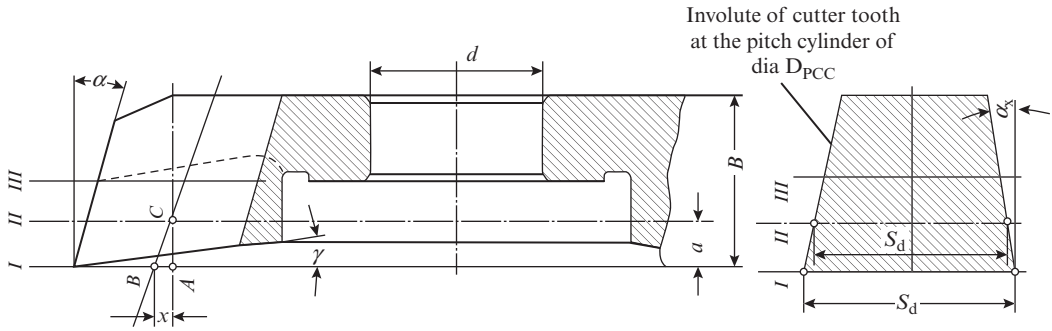


Figure 6.27 Main design parameters of gear shaping cutter

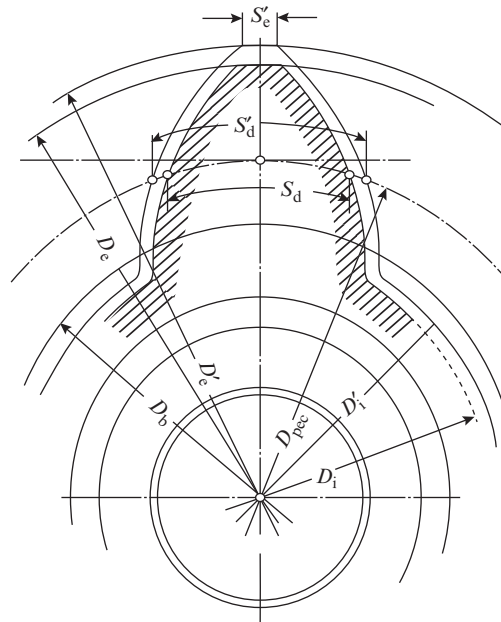


Figure 6.28 Parameter of gear shaping cutter tooth

When using a new cutter, cutting is done by section I–I, which is equivalent to cutting by a basic rack displaced by a distance $+x$. Similarly, after resharpening several times, when cutting is done by section III–III of the cutter, it would be equivalent to cutting by a basic rack displaced by a distance $-x$.

In the section II–II, the thickness of the cutter tooth at the pitch circle diameter is the same as that of the gear to be cut, that is, $S_d = \frac{\pi m n}{2}$ and the gear produced has normal teeth of addendum and dedendum equal to $1.25 m$ each (Figure 6.28). When cutting is done by any other section of

the shaping cutter, the gear is produced with modified teeth and the tooth parameters depend on the magnitude of displacement of the basic rack x .

For section I–I the displacement x (Figure 6.27) is found from the following relation (ignoring γ):

$$a = \frac{x}{\tan \alpha} \quad (6.24)$$

It is customary to represent $x = \xi m$, where ξ is known as extension coefficient.

The thickness of cutter tooth in section I–I at the pitch circle diameter will be

$$S'_d = S_d + 2a \tan \alpha_x \quad (6.25)$$

where α_x is the clearance angle on the side face of the cutter tooth in section I–I which is given by the following relation:

$$\tan \alpha_x = \tan \alpha \tan \theta$$

Hence, on substituting for S'_d , a , and x , we obtain:

$$S'_d = \frac{\pi m}{2} + \frac{2\xi m}{\tan \alpha} \tan \alpha \tan \theta = m \left(\frac{\pi}{2} + 2\xi \tan \theta \right) \quad (6.26)$$

In section I–I the tooth addendum is

$$1.25m + a \tan \alpha = 1.25m + x = 1.25m + \xi m = m(1.25 + \xi)$$

and the dedendum is

$$1.25m - a \tan \alpha = 1.25m - x = 1.25m - \xi m = m(1.25 - \xi)$$

A very important issue in design of gear shaping cutter is to determine the value of parameter a . It should desirably be as large as possible to allow larger number of resharpenings, and hence longer overall life of the cutter. For a given gear of module m and pressure angle θ ,

$$a_{\max} = \frac{\xi_{\max} m}{\tan \alpha} \quad (6.27)$$

The maximum value of ξ_{\max} is limited by the minimum permissible thickness of the cutter tooth at the addendum S'_c in section I–I, because an extremely thin tooth at the addendum will lead to rapid wear of the cutter. The minimum permissible value of S'_c for different values of m are given in Table 6.25.

Table 6.25 Minimum value of cutter tooth thickness at the addendum

| | | | | | |
|-----------------|-------------|-------------|-------------|-------------|-------------|
| $m =$ | 1–1.5 | 1.75–2.75 | 3.0–4.0 | 4.25–6.0 | 6.25–8.0 |
| min S'_c , mm | (0.46–0.41) | (0.40–0.31) | (0.30–0.25) | (0.25–0.20) | (0.20–0.10) |

Thickness of the tooth addendum in Section I–I is given by the expression

$$S'_c = D_c \left(\frac{S_d}{mZ_c} + \frac{2\xi \tan \theta}{Z_c} + \text{inv} \theta - \text{inv} \theta_c \right) \quad (6.28)$$

where

$$D_e = \text{addendum diameter of the cutter in section II-II}$$

$$\theta_e = \text{pressure angle of the involute at the tooth tip} = \cos^{-1} \frac{D_b}{D_e} = \cos^{-1} \frac{D_{\text{pcc}} \cos \theta}{D_e}$$

For determining D_e and Z , we have to first finalize the pitch circle diameter of the cutter D_{pcc} . In principle, D_{pcc} should be taken as small as possible as this will minimize the cutter deformation during operation. The following standard values of D_{pcc} are recommended: 25, 38, 50, 75, 100, 125, 160, and 200 mm. Having selected the value of D_{pcc} and knowing the module m , the number of cutter teeth Z_c can be found from the following expression:

$$Z_c = \frac{D_{\text{pcc}}}{m}$$

After calculating Z_c , it is equated to the nearest whole number and the exact value of D_{pcc} is recalculated. The number of cutter teeth usually lies in the range $Z_c = 15-40$.

For the selected values of D_{pcc} , S_d , and Z_c and known value of m , θ , and θ_e , the extension coefficient is determined from Eqn. (6.28) for the appropriate value of S'_c taken from Table 6.25. Now, on substituting for ξ , m , and α in Eqn. (6.27), the value of parameter a can be found.

For 20° pressure angle, the recommended value of clearance angle α is 6° and that of the rake angle γ is 5° for finish cutters and 10° for rough cutters.

Diameter D_e of the addendum circle and dedendum diameter D_i in section II-II are

$$D_e = D_{\text{pcc}} + 2.5m, \quad D_i = D_{\text{pcc}} - 2.5m \quad (6.29)$$

Diameter D'_e of the addendum circle and D'_i of dedendum circle in section I-I are

$$D'_e = D_e + 2x + 2C, \quad D'_i = D_i + 2x + 2C \quad (6.30)$$

where

C = radial gap between the cutter and gear in the basic section II-II; generally = 0.2 mm

x = displacement of the basic rake that is found for the selected values of a and α from Eqn. (6.24)

Cutter height B is taken from standards and bore diameter d from the machine tool manual.

After designing the gear shaping cutter, it is necessary to check that there is no interference between the cutter and the gear to be cut. Depending on the number of teeth of the gear Z_g , this occurs at different values of ξ . If a gear with small number of teeth Z_g is generated by a cutter with large number of teeth, then there is danger of undercutting of the gear teeth. On the other hand, if a cutter of small number of teeth is used to cut a gear with larger number of teeth, there is a tendency to undercut the teeth of the cutter. This is not possible because the cutter is made of harder material than the gear to be cut. What actually happens is that the tips of the teeth on the gear get beveled by the flanks of the cutter teeth.

The condition to prevent under cutting of the gear teeth is

$$D'_e \leq \sqrt{(A \sin \theta)^2 + D_{\text{bc}}^2} \quad (6.31)$$

where

A = center distance between the meshing cutter and gear

D_{bc} = base circle diameter of the cutter

The condition to prevent beveling of the gear teeth is

$$D_{eg} = \leq \sqrt{(A \sin \theta)^2 + D_{bg}^2} \quad (6.32)$$

where

D_{eg} = addendum circle diameter of the gear to be cut

D_{bg} = base circle diameter of the gear to be cut

If either of the two conditions is violated then the cutter design has to be modified either by changing the number of teeth Z_c or by changing the reference distance a which, in turn means changing displacement of the basic rack. Of the two violations, the first one is serious as it adversely affects the strength of the gear teeth. On the other hand, the second violation is not serious and to some extent even desirable because it provides a natural modification of the gear teeth making them stronger.

The check for undercutting can also be carried out with the help of the nomogram in Figure 6.29. For example if $Z_g = 19$ and $\xi_{max} = 0.158$, then from the relevant curve we find that $Z_c = 65$. If we use a cutter with $Z_c > 65$ than undercutting will take place. In case, we want to use a cutter of greater number of teeth, then ξ_{max} will have to be suitable reduced.

Gear shaping is generally used for making spur gears and is particularly suited for gear blanks in which the limited spacing between the gears puts severe constraint on the size and travel of the cutter and leaves gear shaping as the only viable method. Helical gears can be cut on gear shaping machines using special rotary shaping cutter with helical teeth. The helical motion is imparted to the cutter by means of a helical tracer attachment (Figure 6.30). One-half of the attachment is fixed to the reciprocating spindle of the gear shaping machine and the other half to the quill. As the spindle reciprocates, the cutter is simultaneously revolved thanks to the attachment, thereby imparting a helical motion to the cutter. The helix angle and pitch of the tracer attachment are taken the same as that of the gear to be cut.

Example 6.10

Determine the design parameters of a gear shaping cutter for rough cutting of gears of module $m = 2.5$ mm, pressure angle $\theta = 20^\circ$, and number of teeth $Z_g = 75$.

First of all, we finalize the pitch circle diameter of the cutter D_{pcc} . It is recommended that D_{pcc} should be small to minimize cutter deformation. Hence, from among the standard values, we select $D_{pcc} = 50$ mm.

The number of cutter teeth is found as follows:

$$Z_c = \frac{D_{pcc}}{m} = \frac{50}{2.5} = 20$$

As Z_c is in the recommended range of 15–40, the selected value of $D_{pcc} = 50$ mm is accepted.

As recommended, we select clearance angle $\alpha = 6^\circ$ and rake angle $\gamma = 10^\circ$ (for rough cutter).

For $Z_c = 20$ and $Z_g = 75$, from Figure 6.29, we determine $\xi = 0.158$. Now substituting these values in Eqn. (6.27), we determine the following:

$$a = \frac{\xi m}{\tan \alpha} = \frac{0.158 \times 2.5}{\tan 6^\circ} = \frac{0.158 \times 2.5}{0.105} = 3.76 \text{ mm}$$

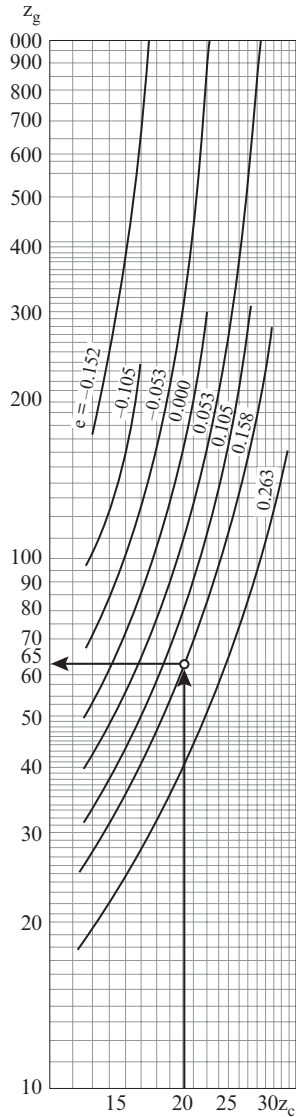


Figure 6.29 Nomogram for determining cutter teeth to make gear without undercutting

Cutter tooth parameters in the design Section (II–II) are as follows:

Addendum height = $1.25\text{ m} = 1.25 \times 2.5 = 3.125\text{ mm}$, dedendum height = $1.25\text{ m} = 1.25 \times 2.5 = 3.125\text{ mm}$, height of tooth = $3.125 + 3.125 = 6.25\text{ mm}$, tooth thickness at pitch circle

$$S_d = \frac{\pi m}{2} = \frac{\pi \times 2.5}{2} = 3.925\text{ mm}$$

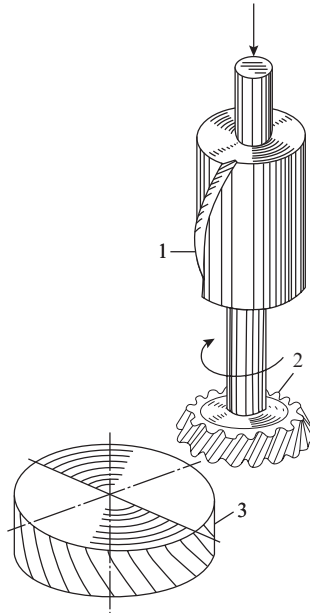


Figure 6.30 Cutting of helical gear with gear shaping cutter

1 - helical tracer attachment, 2 - gear shaping cutter

3 - gear blank

Tooth parameters of the new cutter (in section I-I) are the following:

$$\text{Addendum height} = 1.25 + a \tan \alpha = 1.25 \times 2.5 + 3.76 \times 0.105 = 3.52 \text{ mm}$$

$$\text{Dedendum height} = 1.25 - a \tan \alpha = 1.25 \times 2.5 - 3.76 \times 0.105 = 2.73 \text{ mm}$$

$$\text{Tooth height} = 3.52 + 2.73 = 6.25 \text{ mm}$$

$$\text{Tooth thickness in the pitch circle from Eqn. (6.26)} = m \left[\frac{\pi}{2} + 2\xi \tan \theta \right]$$

$$= 2.5 \left(\frac{3.14}{2} + 2 \times 0.158 \times \tan 20^\circ \right) = 2.5(1.57 + 2 \times 0.158 \times 0.364) = 4.21 \text{ mm}$$

The pitch circle, addendum, and dedendum circle diameters in the design section (II-II) are (see Eqn. 6.29) as follows:

$$D_{\text{pec}} = 50 \text{ mm}$$

$$D_e = D_{\text{pec}} + 2.5m = 50 + 2.5 \times 2.5 = 56.25 \text{ mm}$$

$$D_i = D_{\text{pec}} - 2.5m = 50 - 2.5 \times 2.5 = 43.75 \text{ mm}$$

The pitch circle, addendum, and dedendum circle diameters of the new cutter (in section I-I) are (see Eqn. 6.30):

$$D'_e = D_e + 2\xi m + 2C = 56.25 + 2 \times 0.158 \times 2.5 + 2 \times 0.2 = 57.44 \text{ mm}$$

$$D'_i = D_i + 2\xi m + 2C = 43.75 + 2 \times 0.158 \times 2.5 + 2 \times 0.2 = 44.94 \text{ mm}$$

For cross checking, let us determine S'_c (see Eqn. 6.28); we already know $D_c = 56.25$,

$$S_d = 3.925 \text{ mm}, m = 2.5 \text{ mm}, Z_c = 20, \xi = 0.158, \theta = 20^\circ \text{ inv}20^\circ = \tan 20^\circ - \frac{20 \times \pi}{180} = 0.1494$$

$$\theta_c = \cos^{-1} \frac{D_{pc} \cos \theta}{D_c} = \cos^{-1} \frac{50 \times \cos 20^\circ}{56.25} = \cos^{-1} \frac{50 \times 0.9397}{56.25} = \cos^{-1} 0.8352 = 33^\circ 40'$$

$$\text{inv}33^\circ 40' = \tan 33^\circ 40' - \frac{33^\circ 40' \times \pi}{180} = 0.078483$$

On substituting the above values in Eqn. (6.28), we obtain

$$\begin{aligned} S'_c &= 56.25 \left[\frac{3.925}{2.5 \times 20} + \frac{2 \times 0.158 \times 0.3640}{20} + 0.01494 - 0.078483 \right] \\ &= 56.25(0.0785 + 0.00575 + 0.01494 - 0.078483) \\ &= 56.25 \times 0.02 = 1.125 \text{ mm} \end{aligned}$$

From Table 6.25, the minimum permissible values of S'_c for $m = 2.5l$ lies in the range (0.40–0.31) m , that is, in the given case it should lie between 0.775 mm and 1.0 mm. The calculated value of $S'_c = 1.125$ mm is greater. Hence, the design of the cutter is safe.

The second check against undercutting is carried out according to Eqn. (6.31). We have already determined the following;

$$D'_c = 57.44, D_{bc} = D_{pc} \cos \theta = 50 \times \cos 20^\circ = 50 \times 0.9397 = 46.985 \text{ mm}, \sin \theta = \sin 20^\circ = 0.3420.$$

The distance between the center of the cutter and the gear to be cut is

$$A = \frac{m}{2} (Z_c + Z_g) = \frac{2.5}{2} (20 + 75) = 118.75$$

Hence,

$$\begin{aligned} \sqrt{(A \sin \theta)^2 + (D_{bc})^2} &= \sqrt{(118.75 \times 0.3420)^2 + (46.985)^2} \\ &= \sqrt{(40.6)^2 + (46.985)^2} = \sqrt{1648.36 + 2207.6} = 62.09 \text{ mm} \end{aligned}$$

As D'_c is less than the above value, it can be concluded that the gear produced will be free of undercutting.

6.7.3 Geometry and Design of Hob

As was mentioned in Section 5.7, the hob is a cutting tool that operates on the generation principle for making gears. The hob and the gear to be machined imitate the relative motion of a worm and worm gear, respectively. The hob is obtained by milling flutes on the initial worm and relieving the surfaces behind the cutting edges on the teeth. Hob teeth are form relieved (Figure 5.11).

The main elements of a hob are shown in Figure 6.31, and the profile of hob teeth in a normal section is shown in Figure 6.32. The initial parameters for hob design are module m and pressure angle θ of the gear to be cut. In the normal section (Figure 6.32), the profile of the hob teeth

conforms to that of the normal rack profile at the pitch line, therefore the parameters of hob teeth are obtained as follows:

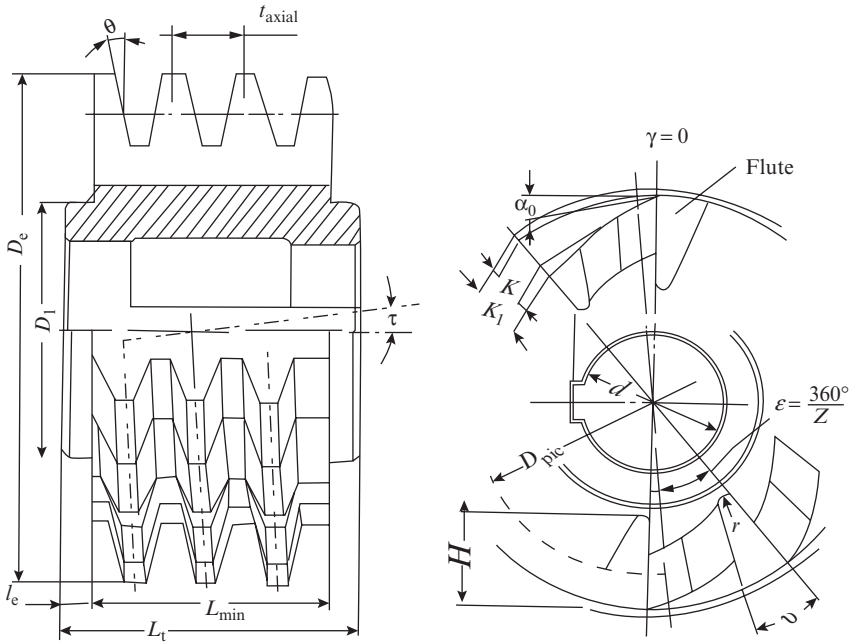


Figure 6.31 Hob and its main parameters

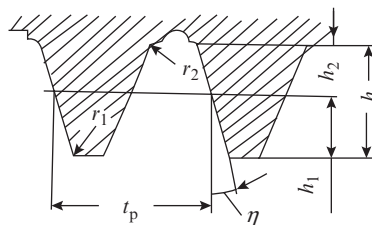


Figure 6.32 Hob tooth profile in normal section

Profile angle η = pressure angle of the gear θ

Addendum $h_1 = 1.25 m$

Dedendum $h_2 = 1.25 m$

Height of tooth $h = h_1 + h_2 = 2.5 m$

Tooth thickness at the pitch circle $S_d = \frac{t_p}{2}$ where t_p is the pitch of the gear to be cut,

$t_p = \pi m = \frac{\pi D_{pcg}}{Z_g}$, where D_{pcg} is pitch circle diameter and Z_g the number of teeth of the gear to be cut;

tooth radius $r_1 = (0.25-0.30) m$ and root fillet $r_2 = (0.20-0.30) m$

The clearance angle at the periphery of hob tooth α_o is related to that on the tooth side surface α_x at diameter D_x by the following relation:

$$\tan \alpha_x = \tan \alpha_o \sin \theta$$

For pressure angle of 20° , the value of α_o should be around $10\text{--}12^\circ$ to ensure that the minimum value of α_x is not less than 4° . Having selected a suitable value of α_o , the magnitude of relief on the peripheral flank of the hob tooth is found from the following relation:

$$K = \frac{\pi D_c}{Z_c} \tan \alpha_o \tag{6.33}$$

where

D_c = hob diameter

Z_c = number of hob teeth.

In ground hobs, a second relieving of the peripheral flank is necessary to provide sufficient space for the grinding wheel. The magnitude of the second relief K_1 is taken as follows:

$$K_1 = (1.2\text{--}1.7) K \tag{6.34}$$

In order to ensure least distortion of the hob tooth profile after resharpener, the rake angle of hobs is taken as $\gamma = 0^\circ$.

(i) *Bore diameter d :*

Like plain milling cutters, hobs are also mounted on an arbor. Therefore, as mentioned in Section 6.4.1, the bore diameter is determined from consideration of strength and stiffness of the arbor under the action of the cutting forces and the nearest higher value from the standard value series is selected.

(ii) *Hob diameter D_c :*

Following the analogy with plain milling cutters, the hob diameter can be found from the following relation, similar to Eqn. (6.16) used for plain milling cutter:

$$D_c = d + 2m + 2H \tag{6.35}$$

where m = thickness of hob body $\geq (0.3\text{--}0.5) d$

H = depth of flute

$$H = h + \frac{K + K_1}{2} + \Delta \tag{6.36}$$

Here, Δ is clearance which is equal to 0.5 mm for normal accuracy hobs and 1–2 mm for precision ground hobs.

Generally, hob diameter $D_c = (2.25\text{--}5.0) d$

(iii) *Number of teeth Z_c :*

As in all multiple tooth cutters, the number of teeth determines the size of teeth and the size of flute between adjacent teeth. The number of teeth can be determined from the following empirical relation:

$$Z_c = \frac{2\pi}{\cos^{-1} \left[1 - \frac{4.4m}{D_c} \right]}$$

Generally, $Z_c = 9-12$ for normal accuracy hobs and $12-16$ for precision ground hobs.

The data for D_e , d , and Z_c given in Table 6.26 can serve as a practical guide and aid in selection of hob parameters.

Table 6.26 Main parameters of hobs

| Module (mm) | Precision hobs | | | Normal accuracy hobs | | |
|----------------|----------------|----------|-----|----------------------|----------|-----|
| | D_e (mm) | d (mm) | Z | D_e (mm) | d (mm) | Z |
| 1.0 | 70 | 32 | 16 | 63 | 27 | 12 |
| 1.5 | 80 | 40 | 16 | 63 | 27 | 12 |
| 2.0 | 90 | 40 | 14 | 70 | 27 | 12 |
| 2.5 | 100 | 40 | 14 | 80 | 32 | 10 |
| 3.0 | 112 | 40 | 14 | 90 | 32 | 10 |
| 4.0 | 125 | 50 | 14 | 100 | 32 | 10 |
| 6.0 | 160 | 60 | 12 | 125 | 40 | 9 |
| 8.0 | 180 | 60 | 12 | 140 | 40 | 9 |
| 10.0 | 225 | 60 | 12 | 160 | 50 | 9 |
| 12.0 | | | | 180 | 50 | 9 |

(iv) Pitch circle diameter D_{pcc} :

Like all cutters with form-relieved teeth, hobs are resharpener by grinding the tooth face, which results in reduction of hob outer diameter D_e and its pitch circle diameter D_{pcc} . For design calculations the following values of D_{pcc} are taken:

$$D_{pcc} = D_e - 2h_1 - 0.5K \text{ for normal accuracy hobs}$$

$$D_{pcc} = D_e - 2h_1 - 0.2K \text{ for precision ground hobs}$$

The above values are based on the assumption that a hob will be resharpener only till its diameter is reduced by one half of the relieved height for normal accuracy hobs and 0.2 of the relieved height for precision ground hobs.

(v) Angle of worm helix τ and flute helix β :

As mentioned earlier in the very beginning a hob cuts gear teeth by imitating as a worm. The angle of worm helix depends on the module of the gear to be cut and the pitch circle diameter of the hob and is given by the following relation:

$$\sin \tau = \frac{t_g}{\pi D_{pcc}} = \frac{\pi m}{\pi D_{pcc}} = \frac{m}{D_{pcc}}$$

where t_g is the pitch of the gear to be cut.

In order to ensure that the rake angle is the same on both side faces of the cutting teeth, the flutes are cut on the hob such that the direction of flute helix is normal to that of the worm helix and the angle of flute helix β is equal to that of the worm helix τ . As can be

seen from Figure 6.33, for the above condition to be satisfied, the pitch of the flute helix t_f should conform to the following relation:

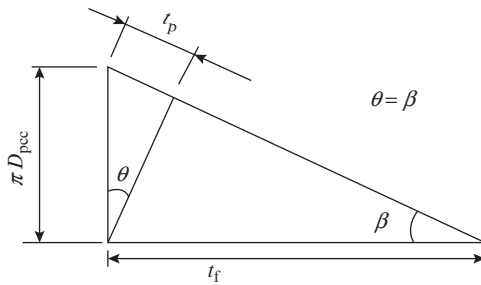


Figure 6.33 Graphic construction for determining flute helix angle

$$t_f = \frac{\pi D_{pcc}}{\tan \beta} = \pi D_{pcc} \cot \beta = \pi D_{pcc} \cot \tau$$

Worm helix angle τ generally lies in the range of 1–5°. However, for gears with very large module it may go up to 10°. For $\tau < 5^\circ$ it is possible to make straight flutes, that is, take $\beta = 0$ without any serious detriment to hob performance, but for higher values of τ , it is necessary to make the flutes with flute helix angle $\beta = \tau$. The axial pitch of the hob teeth which is an important parameter for hob manufacturing is given by the following relation:

$$t_{axial} = \frac{t_g}{\cos \tau}$$

(vi) *Flute parameters:*

The flute shape is determined by the face of one tooth and the back surface of the next tooth (Figure 6.31). As both these surfaces are straight, only three parameters are required to describe the flute, namely flute depth H , flute root radius r and flute angle ν .

Flute depth is found from Eqn. (6.36). The flute root radius can be found from the following empirical relation and the calculated value is rounded off to the following nearest 0.5 mm:

$$r = \frac{\pi(D_e - 2H)}{10Z_c}$$

Flute angle ν is selected depending on the number of teeth Z_c . For $Z_c = 8$, $\nu = 25^\circ$ or 30° , for $Z_c = 10$, $\nu = 22^\circ$, for $Z_c \geq 12$, $\nu = 18^\circ$.

(vii) *Length of hob L*

The minimum length of the cutting portion of the hob should be equal to the length of contact projected on the base line of the rack (Figure 6.34). It may be recalled here that the line of contact of an involute profile is a line making an angle η (equal to pressure angle θ) with the line of centers. From Figure 6.34, it can be noted that length of contact

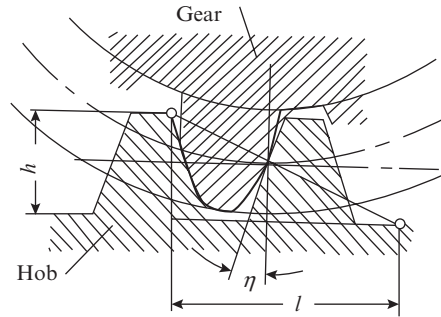


Figure 6.34 Graphic construction to determine the length of cutting portion of hob

$$l = h \cot \eta$$

Considering that one extreme worm of the hob may not participate in the cutting operation after the hob is worn out a little, we find that the minimum length of the hob should be

$$L_{\min} = h \cot \eta + t_g$$

On substituting $\eta = 20^\circ$, that is, $\cot \eta = 2.747$, $t_g = \pi m$ and $h = 2.5 m$ in the above expression, we obtain

$$L_{\min} = 2.5 m \times 2.747 + \pi m \approx 10 m$$

The length of the extensions l_e at the hob end face is taken as $l_e = 4 \text{ mm}$ for $m < 2.75 \text{ mm}$ and $l_e = 5 \text{ mm}$ for $m > 2.75 \text{ mm}$. Thus, the total length of the hob is found as follows:

$$L_t = L_{\min} + 2l_e$$

Generally,

$$L_t = (0.7-0.8) D_e$$

(viii) Diameter of hob face extension D_1 and bore relief d_1 :

The recommendations for determining D_1 and d_1 are as follows:

$$\begin{aligned} D_1 &= D_e - 2H - (1-2) \text{ mm} \\ d_1 &= 1.05d \end{aligned}$$

Hobs can be used for cutting spur as well as helical gears. For cutting spur gear, the hob is set at an angle equal to the worm helix angle τ . When a helical gear of angle ψ is to be cut, then the hob is set at an angle $\psi \pm \tau$; the + sign is used when the hob helix and gear helix are in the same direction and the - sign when they are in opposite directions.

Example 6.11

Determine the design parameters of a precision hob for making gear of module $m = 10 \text{ mm}$ and pressure angle $\theta = 20^\circ$

The parameters of the hob teeth are (see Figure 6.32)

$$\text{Height of addendum } h_1 = 1.25 m = 10 \times 1.25 = 12.50 \text{ mm}$$

$$\text{Height of dedendum } h_2 = 1.25 m = 10 \times 1.25 = 12.50 \text{ mm}$$

Height of the tooth $h = h_1 + h_2 = 12.50 + 12.50 = 25.0$ mm

Tooth thickness at pitch circle diameter $S_d = \frac{\pi m}{2} = \frac{3.14 \times 10}{2} = 15.70$ mm

Tooth radius $r_1 = (0.25-0.30)$ m; we take $r_1 = 0.3$ m = $0.3 \times 10 = 3.0$ mm

Root fillet radius $r_2 = (0.2-0.30)$ m, we take $r_2 = 0.2$ m = $0.2 \times 10 = 2.0$ mm

From Table 6.26, for the given value of $m = 10$, we select the following parameters of precision hob: hob diameter $D_e = 225$ mm, bore diameter $d = 60$ mm, number of hob teeth $Z = 12$.

As per recommendation, for the precision hob we select $\alpha_o = 10^\circ$ and $\gamma = 0^\circ$. Now applying Eqn. (6.33), we obtain relief on the peripheral flank:

$$K = \frac{\pi D_e}{Z_c} \tan \alpha_o = \frac{\pi \times 225}{12} \times \tan 10^\circ \approx 10 \text{ mm}$$

For the second relief K_1 , we refer to Eqn. (6.34) and assuming a value 1.5, we find

$$K_1 = 1.5K = 1.5 \times 10 = 15 \text{ mm}$$

Depth of flute H is found from Eqn. (6.36). Assuming $\Delta = 1.0$ mm, we obtain

$$H = h + \frac{K + K_1}{2} + \Delta = 25.0 + \frac{10 + 15}{2} + 1.0 = 38.5 \text{ mm}$$

On substituting the values of D_e , d , h , and H in Eqn. (6.35), we find

$$m = \frac{D_e - d - 2h}{2} = \frac{225 - 60 - 2 \times 38.5}{2} = 44.0 \text{ mm}$$

As m is greater than the recommended value, the selected values of D_e , d , h , and H are accepted. Pitch circle diameter of precision hob is

$$D_{\text{pec}} = D_e - 2h_1 - 0.2K = 225 + 2 \times 125 - 0.2 \times 10 = 198 \text{ mm}$$

Angle of worm helix is found from the following relation:

$$\tau = \sin^{-1} \left(\frac{m}{D_{\text{pec}}} \right) = \sin^{-1} \left(\frac{10}{198} \right) = \sin^{-1} (0.0505) = 2^\circ 54'$$

Pitch of the flute:

$$t_f = \pi D_{\text{pec}} \cot \tau = 3.14 \times 198 \times \cot 2^\circ 54' = 3.14 \times 198 \times 19.64 = 12210 \text{ mm}$$

Flute depth has already been determined as follows:

$$H = 38.5 \text{ mm}$$

Flute root radius $r = \frac{\pi (D_e - 2H)}{10Z_c} = \frac{\pi (225 - 2 \times 38.5)}{10 \times 12} = 3.9 \text{ mm}$

Flute angle ν is selected as $\nu = 18^\circ$ (as recommended for $Z = 12$).

Hob length $L = 10 \text{ m} + 2l_c$; taking $l_c = 5$ mm, we obtain

$$L = 10 \times 10 + 2 \times 5 = 110 \text{ mm}$$

Diameter of hob face extensions is

$$D_1 = D_w - 2H - (1-2) = 225 - 2 \times 38.5 - 2 = 146 \text{ mm}$$

Review Questions

- 6.1 Design a rectangular bent shank turning tool for the data given as follows: tool overhang = 50 mm, cutting force = 200 kgf, bending strength of tool material = 20 kgf/mm², modulus of elasticity of tool material = 2×10^4 kgf/mm², permissible deflection of tool tip = 0.5 mm
- 6.2 Design a round section boring tool for the data given as follows: tool overhang = 30 mm, cutting force = 150 kgf. The rest of the data is the same as in Q 6.1.
- 6.3 Design a square section boring tool for the data of Q 6.2.
- 6.4 Design a rectangular shank facing tool for the data given in Q 6.1. Ignore the deflection of tool tip as it is not of much relevance in a facing operation.
- 6.5 For the part shown in Example 6.3, design a flat form tool both by graphical construction and analytical method.
- 6.6 For the part shown in Figure 6.12(a), design a flat form tool both by graphical construction and analytical method.
- 6.7 For the part shown in Figure 6.13, design a circular form tool both by graphical construction and analytical method.
- 6.8 Determine the design parameters of drill specified in Review Question 5.3.
- 6.9 Determine the design parameters of drill specified in Review Question 5.4.
- 6.10 Determine the design parameters of a solid HSS plain milling cutter for machining of a medium carbon steel job of width 40 mm with a machining allowance of 6.0 mm.
- 6.11 Determine the design parameters of an assembled plain milling cutter with cemented carbide blades for machining a mild steel job of width 80 mm with a machining allowance of 6.0 mm
- 6.12 Determine the design parameters of a solid HSS face milling cutter for machining a medium carbon steel job of width 40 mm.
- 6.13 Determine the design parameters of an assembled face milling cutter with HSS blades for machining a mild steel job of width 80 mm.
- 6.14 Determine the design parameters of a rising tooth round broach for enlarging a 19 mm diameter drilled hole to 20 mm in a job of length 40 mm made of mild steel (HB220).
- 6.15 For the data given in Q 6.14, determine the design parameters of a progressive cut (group cut) broach.
- 6.16 Determine the design parameters of a spline broach for making a splined hole of external diameter 20 mm, internal diameter 17 mm, width of spline 5 mm and number of splines 6. The hole is pre drilled to a diameter 16.2 mm in a medium steel job of length 50 mm.

- 6.17 Determine the design parameters for a machine tap for making M20 thread in a medium steel part.
- 6.18 Determine the design parameters for a hand tap set for making M20 thread in a mild steel part.
- 6.19 Determine the design parameters for a thread cutting die for making M16 thread in an alloy steel part.
- 6.20 Determine the design parameters of a module cutter for making spur gear of module $m = 8$ mm, number of teeth $Z = 30$ and pressure angle $\theta = 20^\circ$.
- 6.21 Determine the design parameters of a rough hob for making a spur gear of module $m = 10$ mm and pressure angle $\theta = 20^\circ$.
- 6.22 Determine the design parameters of a precision hob for making a spur gear of module $m = 8$ mm and pressure angle $\theta = 20^\circ$.
- 6.23 Determine the design parameter of a gear shaping cutter for making a gear of module $m = 6$ mm and number of teeth $Z = 80$. Select pitch circle diameter of the cutter $D_{\text{pcc}} = 100$ mm

Chapter

7

DESIGN OF JIGS AND FIXTURES

7.1 Introduction

Before carrying out a machining operation, it is first necessary to place, orient, and hold the workpiece properly to establish its correct dimensional and positional relationship with respect to the cutting tool. In job shop and small lot production, the position of the feature to be machined is marked manually using surface gauges by inscribing layout lines on the job surface. Alignment of the job parallel, perpendicular, or at angle to the machine tool table is carried out using tool room straight edges, angle plates, slip gauges, dial indicator, protractor, angle gauges, etc. An example of setting up a job is shown in Figure 7.1 in which the layout lines are shown marked, and the required position of the workpiece is obtained by raising or lowering its sides by means of jacks (or adjustable wedges) on which it rests. This method of setting up the workpiece is cumbersome and is time-consuming. The reliability of setting depends on the operator skill, and the accuracy of the setting is inconsistent.

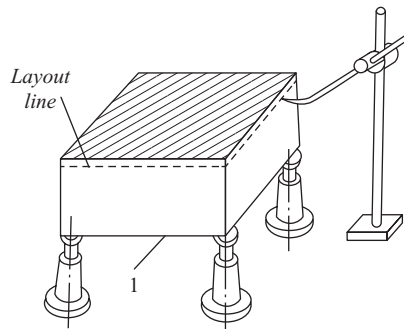


Figure 7.1 Setting up of work piece with the help of layout lines

In batch production and even more so in large lot and mass production, the manual setting up is replaced by a suitably designed workpiece positioning and holding device known as fixture. In machining operations using long cutting tools such as drills, reamers, etc., guiding of the cutting tool also becomes important. The fixtures for such operations carry out tool guiding in addition to the workpiece positioning and holding functions. Such fixtures are known as jigs.

The use of jigs and fixtures eliminates the laborious process of marking and thus eliminates the costly setting up of each workpiece on the machine tool according to the layout lines. It also

increases the machining accuracy and reliability of production by eliminating alignment errors. The other associated advantages arising from the above two key benefits from the use of jigs and fixtures are as follows:

- (i) There is higher productivity due to the reduction of the non-productive time.
- (ii) There is higher productivity due to the possibility of simultaneously machining several components in a single setting.
- (iii) Properly designed fixtures allow rigid clamping of the work piece, which enables machining at higher cutting speed and feed, thereby reducing the machining time and increasing productivity.
- (iv) Freedom from the dependence on the operator's skills allows for consistent setting, which in turn provides better reproducibility of dimensional accuracy.
- (v) Higher uniformity of dimensional tolerances reduces the production cost by simplifying quality control and cutting down assembly time.
- (vi) Simplification of the location and clamping of workpieces allows for the replacement of highly skilled operators by operators of lower skills, thereby reducing production cost.

The design requirements for jigs and fixtures are related to their purpose and must therefore be carefully decided based on economic as well as technical considerations. If the main purpose of a jig or fixture is to expand the process capability of the machine tool, then cost is the predominant criterion. These jigs/fixtures must be reasonably cheap to be economically feasible. If the main purpose is to increase productivity, then factors (i) through (iii) listed above should be considered, and the design that provides the maximum overall economic effect from all the factors should be selected.

If the main purpose of a jig/fixture is to provide higher accuracy, then the design should be based on a comprehensive *error analysis*. Errors can in general be classified as errors of form and size and of relative location of a feature with respect to another. The first type of error is practically independent of the jig/fixture used, but the second type of error strongly depends on the rigor of the error analysis that serves as the platform of the jig/fixture design. The total error consists of a large number of error components as follows:

- (a) Error of machine tool in idle condition.
- (b) Error of locating the jig/fixture on the machine tool.
- (c) Error of the locating surfaces of the jig/fixture with respect to the mounting surfaces.
- (d) Error of locating the component on the fixture.
- (e) Error caused by clamping.
- (f) Error of tool setting and guidance.
- (g) Error caused by deformation due to insufficient rigidity of the machine tool, workpiece, fixture, or cutting tool.
- (h) Error caused by wear of the cutting tool.

Not all the errors listed above occur in every machining operation. In addition, the errors that occur in an operation on one machine (say making of hole on lathe) may significantly differ from the errors in the same operation carried out on another machine (say making a hole on drilling machine) due to the differences in the locating surfaces adopted in the two cases. Analysis of locating errors in various locating schemes used in practice for components of variety of geometrical shape is therefore the corner stone of jig/fixture design.

Aside from the above requirements, it is important that jigs/fixtures should have convenient control elements that are safe to operate and ensure ease of location, clamping, unclamping, removal of component, and access for cleaning and maintenance.

Multiple position jigs/fixtures are equipped with indexing devices to change the position of the workpiece with respect to the cutting tool without altering its position on the fixture.

As regards clamping of the workpiece on small jig/fixtures, the clamping may be achieved by manually applying the required clamping force directly on the clamping element. However, on large jigs/fixtures, it may be necessary to use a suitable mechanism for amplification of the applied manual force to obtain the desired clamping force on the component. For very large clamping force requirements, manual clamping may be dispensed with altogether and replaced by a power device.

Finally, all the elements of jigs/fixtures must be mounted on a body of a suitable shape and size and with mounting features that are commensurate with the machine tool for which the jig/fixture is designed. For example, if the fixture is being made for a milling machine that has T-slots on the table, then the underside of the fixture body should have matching block(s) called tennon strips along its length.

Based on the above discussion, the main elements of fixture may be identified as follows:

1. Locating elements that determine the position of the workpiece with respect to the cutting tool.
2. Clamping elements for securing the workpiece to ensure that the position in which it is located is not disturbed during the cutting operation.
3. Mechanism for mechanical amplification of the clamping force.
4. Power device for application of large clamping force.
5. Indexing device for use in multiple position jigs and fixtures.
6. Body, base, or frame for mounting all the above elements and for mounting the fixture on the machine tool.
7. Jigs consist of all the above-mentioned elements, but they are additionally equipped with tool-guiding elements.

7.2 Location Principles, Methods, and Elements

A body in space has six degrees of freedom, three linear movements in the direction of X, Y, Z coordinate axes, and three rotational movements about each of the above axis. The location of a component implies depriving it of its degrees of freedom in order to fix its position with respect to the cutter. Typical configuration of industrial components consists of a combination of flat, circular, and irregular surfaces. Each of these surfaces may be rough or finished. A finished surface is one that is obtained by machining to specific tolerances, depending on the required accuracy. A rough surface is one that exists on the blank prior to machining. Based on the method employed in the making of the blank, the rough surface will be characterized by the accuracy of the concerned method, for example, casting, forging, rolling, welding, etc.

For the purpose of location, preference is given to flat and circular surfaces, because irregular surfaces, if used for location, add to the complexity of design of the jig/fixture. In addition, machined surfaces are preferred for location, because they provide more accurate, consistent, and reliable location. Among the large number of surfaces of a part, the correct selection of the surfaces to be used for location is crucial to the process of fixture design. An understanding of the role of various surfaces of a part in the accuracy of location, and hence the achievable accuracy of machining, is extremely important and is discussed below.

7.2.1 Concept of Design, Setting, and Measuring Datum Surfaces

A datum is something known as a basis for reference. A design datum is the name given to a line, point, or surface from which the designer specifies a particular dimension. The line, point, or surface may be a physical feature or even a virtual feature such as the axis of a shaft. In order to

produce the desired design dimension, the production engineer makes use of production datum surfaces that are of two types: setting up and measuring datum surfaces. The setting-up datum surface of a part is the surface with which it contacts the locating elements of the fixture to fix the location of the workpiece in the required direction. The measuring datum surface of a part is the surface from which measurements are made on the work piece.

To illustrate the concepts, consider the machining of a step as shown in Figure 7.2. As shown in Figure 7.2(a), surface 1 serves as the design, setting as well as measuring datum for step 2. In Figure 7.2(b), surface 3 is the design as well as measuring datum for step 2, whereas surface 1 is the setting datum. If for some reason, the production engineer introduces a dimension $T = H - h$ (Figure 7.3(c)), then surface 3 will remain the design datum, but surface 1 will become the setting and measuring datum.

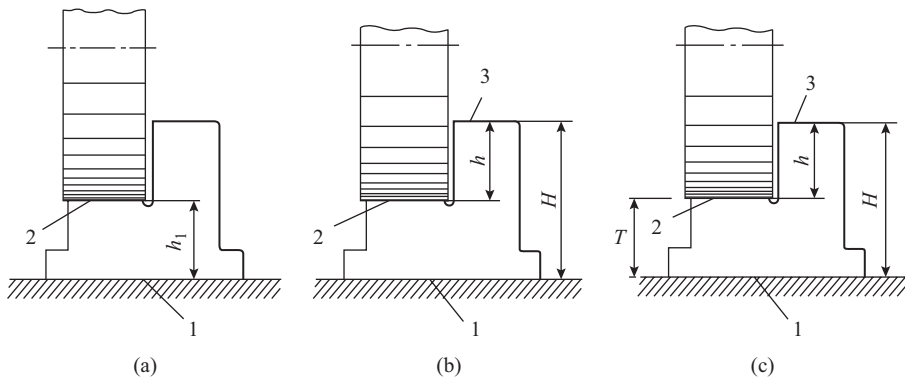


Figure 7.2 Schematic explaining the concept of data: (a) common design, setting, and measuring data, (b) common design and measuring data, and (c) common setting and measuring data

The number of setting surfaces depends on the number of dimensions required to locate the machined surface. For instance, as shown in Figure 7.3(a), for machining the plain surface of height H , only surface 2 is required as the setting datum. However, for machining of the step shown in Figure 7.3(b) two-dimensions, L and H , are required to locate the machined surface, therefore surfaces 1 and 2 are used as setting datum for the respective dimension.

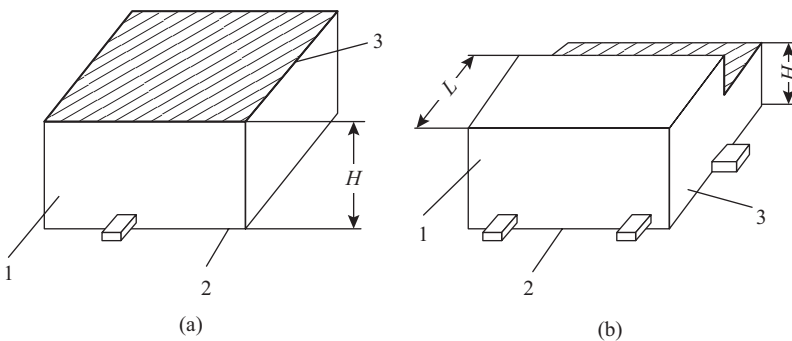


Figure 7.3 Example illustrating location datum surfaces: (a) single-location datum, and (b) two-location datum

The selection of correct setting datum surface is extremely important. Consider the case of machining of step shown in Figure 7.2(a) and suppose that the designer has specified the dimension h_1 with tolerance as 20 ± 0.20 mm. As the design, setting, and measuring datums are represented by surface 1, the tolerance of ± 0.20 mm specified by the designer is available for the machining operation in full.

Now consider the case shown in Figure 7.2(b), where the designer has specified the dimension $h = 30 \pm 0.20$, so that the design tolerance on the step is the same as in the previous case. However, as the design and measuring datum for the step in this case is surface 3, the production engineer will first have to machine surface 3 of nominal height $H = 50$ mm with respect to the setting datum 1. Now if the tolerance on machining of surface 3 is ± 0.10 mm, then the dimension H will be obtained in the range of 50 ± 0.10 mm. Consequently, the machining tolerance available for obtaining the design dimension h will be $(\pm 0.20) - (\pm 0.10) = \pm 0.10$. It can thus be noted that the machining tolerance range actually available for obtaining the step with the same design tolerance has become narrower.

Finally, consider the case shown in Figure 7.2(c). Here, the production engineer has decided to make step 2 by using the setting datum 1 as the measuring datum to achieve the dimension $T = 20$ mm. As the design datum continues to be surface 3, which has a machining tolerance of ± 0.10 , the production engineer will have to machine the dimension T with a machining tolerance of $(\pm 0.20) - (\pm 0.10) = \pm 0.10$ mm in order to obtain the dimension $h = 30 \pm 0.20$ mm.

The foregoing analysis brings us to the important conclusion that wherever the setting datum, measuring datum or both do not coincide with the design datum, then one of them becomes an intermediate datum, and its machining tolerance becomes a sort of locating error that reduces the available tolerance by a corresponding amount. To extend the logic further, consider the case shown in Figure 7.4 in which two steps of design dimensions $h_1 = 15 \pm 0.20$ and $h_2 = 20 \pm 0.35$ have to be machined. Here, the setting datum is surface 1, whereas surfaces 2 and 3 are the design and measuring datums for h_1 and h_2 , respectively. Again if the machining tolerance for dimension $H = 50$ is ± 0.10 mm, then the available tolerance for dimension h_1 will be $(\pm 0.20) - (\pm 0.10) = \pm 0.10$ mm and the available tolerance for dimension h_2 will be $(\pm 0.35) - (\pm 0.10) - (\pm 0.20) = \pm 0.05$ mm. Machining of dimension h_1 involved one intermediate datum 2, whereas the machining of dimension h_2 involved two intermediate datums 2 and 3. We see that the introduction of an extra intermediate datum has drastically reduced the available machining tolerance for dimension h_2 .

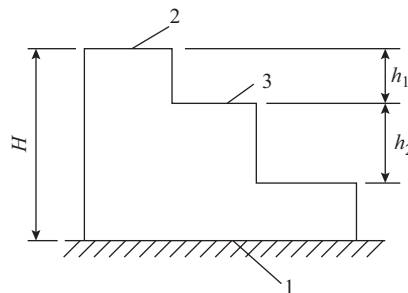


Figure 7.4 Example illustrating the concept of intermediate datum and locating error

The implication of narrow available tolerance on a dimension is that it increases the required precision of machining, thereby increasing the machining cost. With too many intermediate datums, the available tolerance may become extremely small or even zero in which case the machining of

the surface becomes impossible. The available tolerance on the final dimension may be enhanced by reducing the tolerance on the intermediate datum (s). Such a balancing of tolerance may make it possible to machine all the surfaces, but the enhanced machining cost would still have to be borne; only the requirement of higher precision of machining and the burden of additional cost will be transferred from the last dimension to the intermediate datum (s).

Example 7.1

For the part shown in Figure 7.2(c), determine the available tolerance on dimension T for the following values of H and h :

- (a) $H = 15_{-0.070}^{-0.020}$ mm, $h = 3^{+0.12}$ mm
- (b) $H = 15_{-0.12}$ mm, $h = 3^{+0.12}$ mm
- (c) $H = 15_{-0.24}$ mm, $h = 3^{+0.06}$ mm

For case (a):

The tolerance range on dimension $H = 0.050$ mm and that on dimension $h = 0.12$ mm. Therefore, the tolerance range on dimension $T = 0.12 - 0.058 = 0.07$ mm.

For case (b):

The tolerance range on both H and h is 0.12 mm. Therefore, the tolerance range on $T = 0.12 - 0.12 = 0$.

For case (c):

The tolerance range on $H = 0.24$ mm and that on $h = 0.06$ mm. Therefore, the tolerance range on $T = 0.06 - 0.24 = -0.18$ mm.

The conclusion is that for making step 2, it is not possible to introduce the technological dimension T in cases (b) and (c).

Example 7.2

For the part shown in Figure 7.2(c), if the given values are $H = 15_{-0.070}^{-0.020}$ mm and $h = 3^{+0.12}$ mm, determine the dimension T with tolerances.

For the given values of H and h , we find $H_{\max} = 15.0 - 0.02 = 14.98$ mm and $H_{\min} = 15.0 - 0.07 = 14.93$ mm

$$h_{\max} = 3 + 0.12 = 3.12 \text{ mm}, h_{\min} = 3.0 \text{ mm}$$

In addition, it can be found that

$$T_{\min} = H_{\max} - h_{\max} = 14.98 - 3.12 = 11.86 \text{ mm}$$

$$T_{\max} = H_{\min} - h_{\min} = 14.93 - 3.0 = 11.93 \text{ mm}$$

Taking the nominal value of $T = 12.0$ mm, we find the upper deviation = $12.0 - 11.93 = 0.07$ mm and the lower deviation as $12.0 - 11.86 = 0.04$ mm, Hence, the dimension T with tolerance is $12_{-0.14}^{-0.07}$ mm.

When a flat surface of a workpiece is used for location by placing it on a flat base of the fixture, the location will be unstable, unless both the surfaces are ideally flat. Therefore, it becomes necessary to reduce the contact area of the locating surface. Three pin locators of sufficient strength and rigidity can theoretically simulate a flat surface. Therefore, location of flat surface of the

workpiece on three pins substituting for flat base of fixture is adopted in practice as it ensures exact repeatability of location. If four locating pins are used, it will again introduce instability, if the workpiece surface is not perfectly true. This can be easily observed by comparing two tables: one with three legs and the other with four legs. The table with three legs will stand stable on an uneven floor, whereas the table with four legs will wobble on an uneven floor, because one leg will not contact the floor. It may therefore be concluded that it is unwise to use more locating points than the barest minimum that are necessary for location.

The 3-2-1 and six-point principles of location The general principle of location is best illustrated for a prismatic part (Figure 7.5(a)) for which the fixture with the locating elements is shown in Figure 7.5(b). When surface *A* of the part is placed on pins (1), (2), and (3), it deprives the part of three degrees of freedom, namely vertical translatory motion in *Z* direction and rotation about *X*- and *Y*- axes. When surface *B* of the part is placed against pins (4) and (5), it deprives the part of two more degrees of freedom, namely translatory motion in the *X*-direction and rotation about *Z*-axis. Finally, when surface *C* of the part is placed against pin (6), the last remaining degree of freedom, which is translatory motion in the *Y*-direction is also taken away and the part is completely located. This scheme of location is known as the 3-2-1 principle of location for prismatic parts. An equivalent of the 3-2-1 location scheme is shown in Figure 7.5(c), where pins (4) and (5) are replaced by strip (1), pin (6) is retained as such and is labeled 2, and pins 1, 2, and 3 are replaced by two strips 3 and 4. The important general conclusion that emerges from the above discussion is the six-point principle, which states that irrespective of part geometry, six location points are sufficient for its location, depriving it of all the six degrees of freedom.

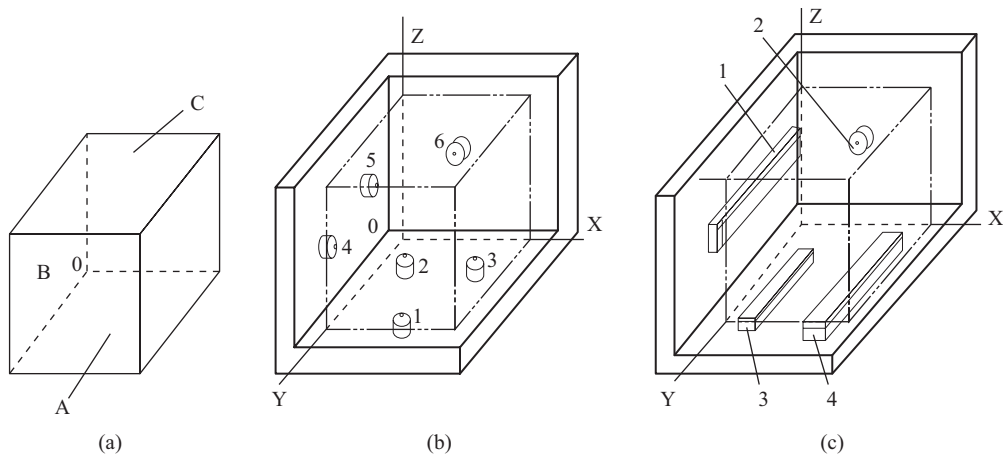


Figure 7.5 Schematic explaining the 3-2-1 principle of location: (a) sample prismatic part, (b) location with the help of rest buttons, and (c) location with the help of rest pads

To illustrate the validity of the six-point principle, consider the machining of a straight step on a prismatic part (Figure 7.6(a)). The fixture shown in Figure 7.5(c) is adopted for location of the part, except that an extra strip is mounted on the vertical wall of the fixture, thereby adding two

extra (redundant) locating points. It is assumed that the base and vertical wall of the fixture are at perfect right angle to each other. If the base and side of the part are also perfectly perpendicular to each other, then on application of the clamping force, the location of the part will not be disturbed and the machined step will be horizontal (Figure 7.6(b)). However, if the base and side of the part are not perpendicular to each other, then depending on whether the angle between the two is $90 + \gamma$ or $90 - \gamma$, the part location will change under the effect of clamping force Q as shown in Figures 7.6(c) and (d), respectively. As a result of this, the step machined on the part will taper in one direction or the other. However, if the fixture with six point location had been used for locating the part with nonperpendicular sides, the location would not have been disturbed by application of the clamping force and the machined step would be straight.

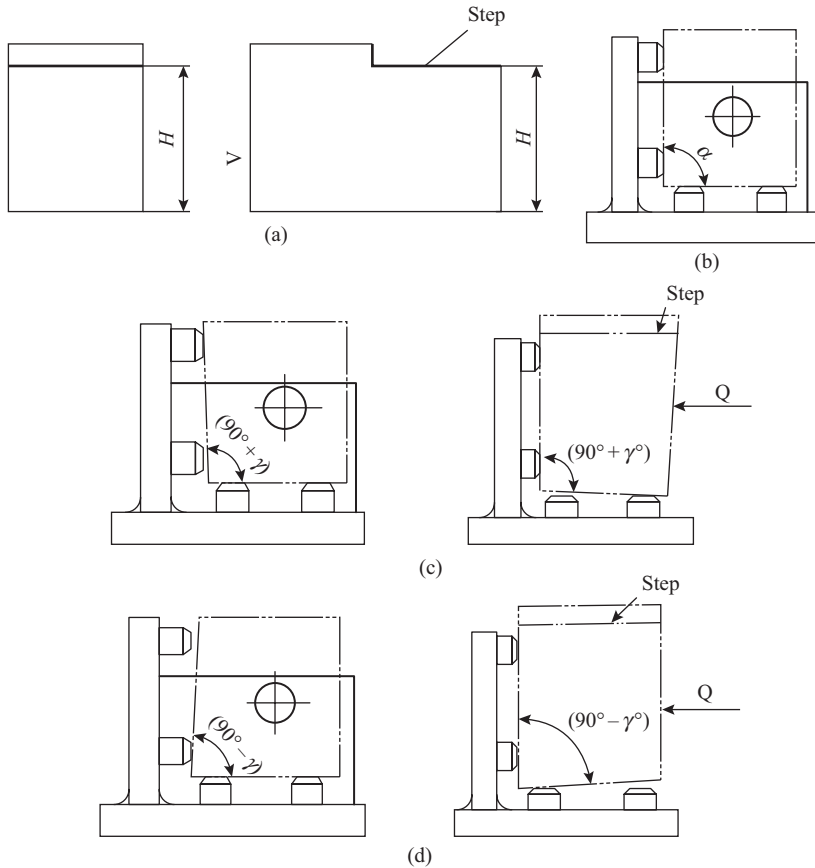
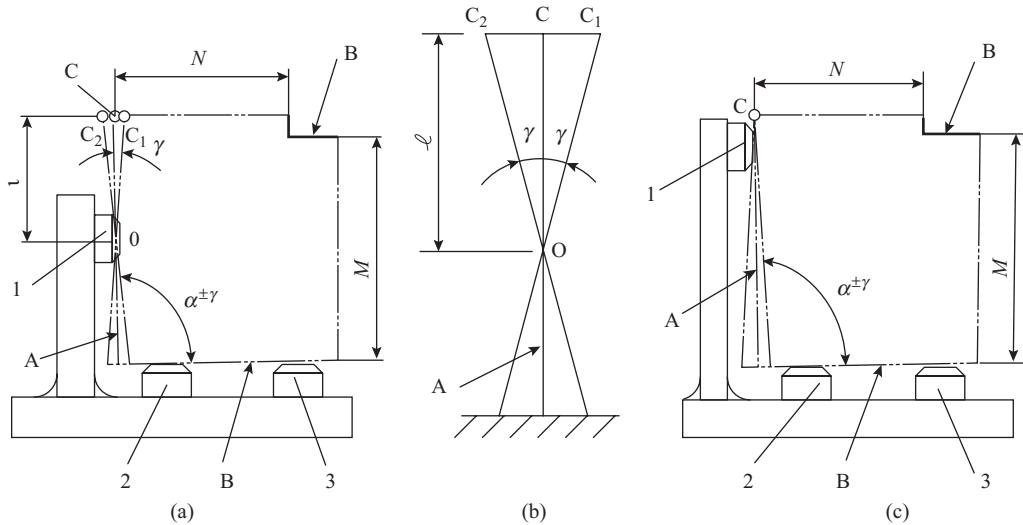


Figure 7.6 Example explaining the deviation from six-point principle of location: (a) sample part, (b) location when sides of work piece are perpendicular, (c) location when angle between sides of work piece is more than 90° , and (d) location when angle between sides of work piece is less than 90°

Example 7.3

For machining of step, the work piece is located in a fixture by the 3-2-1 principle as shown in Figure E7.3a. Determine the locating error on dimensions N and M , if the angle between the sides of the work piece in a lot is in the range $\alpha \pm \gamma$.



The setting datum B for all the work pieces of the lot as regards dimension M is constant and coincides with the plane of rest pads (2) and (3); therefore, there is no locating error on dimension M .

For dimension N , the setting datum A in contact with rest pad 1 may occupy two extreme positions as shown in the geometrical construction as shown in Figure E7.3b, where O represents the centre of rest pad 1 and l represents the distance from O to the top surface of the workpiece.

The maximum deviation of the setting datum A at the top surface on which dimension N is to be made is $C_1C_2 = 2 CC_1 = 2l \tan \gamma$. This represents the locating error. For the given tolerance $\pm \gamma$ on the corner angle, the locating error can be reduced by reducing l , that is, shifting the rest pad towards the point C . In fact, if the centre of the rest pad O is made coincident with C , the locating error will become zero as shown in Figure E15.1(c).

Based on the foregoing discussion, the following points may be made regarding the broad principles of location:

- (i) As far as possible, try to ensure that the design, setting, and measuring datum surfaces are the same.
- (ii) As the location accuracy of part depends on the machining accuracy of the datum surfaces, prefer the surfaces machined with highest accuracy as setting and measuring datums.
- (iii) Prefer the surfaces that provide maximum stability and undergo least deformation on clamping as setting and measuring datums.
- (iv) Try to select a single setting and measuring datum for all machining operations to be carried out on a given component. If this is impossible, then try to keep the number of setting and measurement datum changes to the minimum possible.
- (v) Do not over locate, which means use only the essential minimum number of locating points required for a particular surface and do not duplicate a location.
- (vi) The locating points for a surface should be placed as far as possible from each other to minimize the effect of inaccuracies in the workpiece and the locating elements.

An important factor concerning location is the selection of the first (rough) setting datum, which is used for producing the first machined surface. This surface is then used as the setting datum for subsequent operations. The guidelines for selection of the first rough datum are as follows:

- (a) If all the surfaces of a part are not to be machined, then select one of the rough surfaces that remains unmachined in the final component as the first setting datum for coordination between the rough and machined surfaces. However, among the rough surfaces avoid uneven surfaces such as parting surfaces of forgings, cast surfaces with traces of gating system, etc., for stability of locating and clamping.
- (b) If all the surfaces of a part are machined, then select the surface with the least machining allowance as the first setting datum.

The general requirements to locating elements are as follows:

- (1) The number and arrangement of locating elements should ensure easy location and stability of the workpiece.
- (2) When an irregular or rough surface is used for location, the contact area of the workpiece surface and locating element should be restricted to reduce the effect of roughness and unevenness of the surface.
- (3) Locating elements should be rigid and wear resistant, but they should not damage the location surface of the workpiece, especially if the latter is a finished surface.
- (4) For easy maintenance, the locating elements should be replaceable.
- (5) When an irregular or rough surface is used for location, it is necessary to have flexibility in location (e.g. spring loaded or adjustable locating element) to avoid redundancy.

From the point of view of location, most engineered parts can be placed in one of the following categories:

- Prismatic parts
- Long cylindrical parts
- Short cylindrical parts
- Parts with through hole
- Parts with flat base and two predrilled holes
- Parts with center holes at the end faces

The location scheme, analysis of locating error, and the locating elements used for each of the above category of parts will be discussed in the section that follows.

7.2.2 Locating Scheme, Error Analysis, and Elements for Prismatic Parts

Prismatic parts are located by the 3-2-1 principle described above (see Figure 7.5). Generally, the largest flat surface of the part is selected as the main setting datum for removing three degrees of freedom. The locating error that occurs in prismatic parts has been discussed earlier in Section 7.2.1 and may be summarized as follows:

- (i) There is no locating error when the setting and measuring data coincide with the design datum.
- (ii) If the design or measuring datum does not coincide with the setting datum, then a location error is introduced. The magnitude of this error is equal to the machining tolerance of the design/measuring datum surface.
- (iii) If there are more than one noncoinciding design/measuring datums for obtaining a dimension, then the sum of the machining tolerances of all such datums constitutes the locating error.

The locating elements used for prismatic parts are rest buttons (Figure 7.7) and pads (Figure 7.8). Flat-headed rest buttons (Figure 7.7(a)) are used for locating flat machined surfaces and spherical or knurled head buttons for unmachined surfaces to restrict the area of contact. Rest buttons may be permanent or replaceable. Permanent buttons are press fitted in the fixture body directly, but the replaceable ones are inserted with sliding fit in a bush that is press fitted in the fixture body. Rest pads have two counterbored holes through while they are secured to the fixture body. The pads may be flat (Figure 7.8(a)) or with beveled slots (Figure 7.8(b)). The former are used on vertical wall of the fixture and the latter are used on the horizontal base for the reason that small chips and swarf that accumulate under the screw head in horizontal pads can be easily cleaned when there is a slot around the screw head.

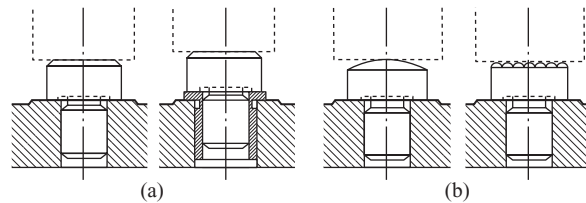


Figure 7.7 Rest buttons: (a) for finish machined surfaces and (b) for rough surfaces

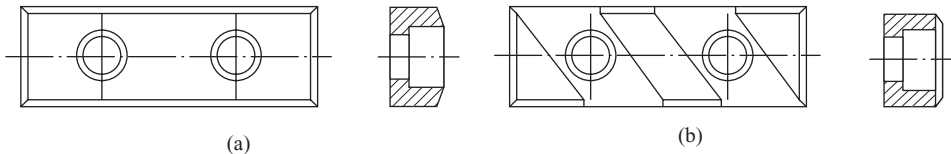


Figure 7.8 Rest pads: (a) flat for vertical surfaces and (b) with beveled slots for horizontal surfaces

Adjustable rest buttons are used for locating rough and irregular surfaces and for accommodating parts of same geometry but with variations in dimensions. Examples of adjustable rest buttons are shown in Figure 7.9. The position of rest button shown in Figure 7.9(a) is varied by a tightening screw (1) and the position is fixed by means of a lock nut (2). In the quick action system shown in Figure 7.9(b), the position of the adjustable button (2) is changed by raising the wedge (1) that is moved by the pushing screw (5). This position is locked by rotating the screw (5) with the help of a knob (6). This forces the ball (4) to move forward and push the woodruff keys (3) outward to jam against the bore and thus lock the position of the rest button. A self-setting type of adjustable rest known as spring jack is shown in Figure 7.9(c). Button 1 is pushed by precompressed spring (4) to contact the locating surface. The size and precompression of the spring is selected in such a way that it does not displace the workpiece. The position of the rest button is locked by tightening the screw (3) with the help of a knob (5). The pin (2) serves to restrict the upward movement of the rest button when the screw is loosened.

7.2.3 Locating Scheme, Error Analysis, and Elements for Long Cylindrical Parts

The basic element used for locating a cylindrical part is a V-block (Figure 7.10). When a cylindrical shaft is placed on the V-block 1, it contacts each face of the block along a line. Each line represents two locating points. Thus, by merely placing a cylindrical shaft on a V-block, four degrees

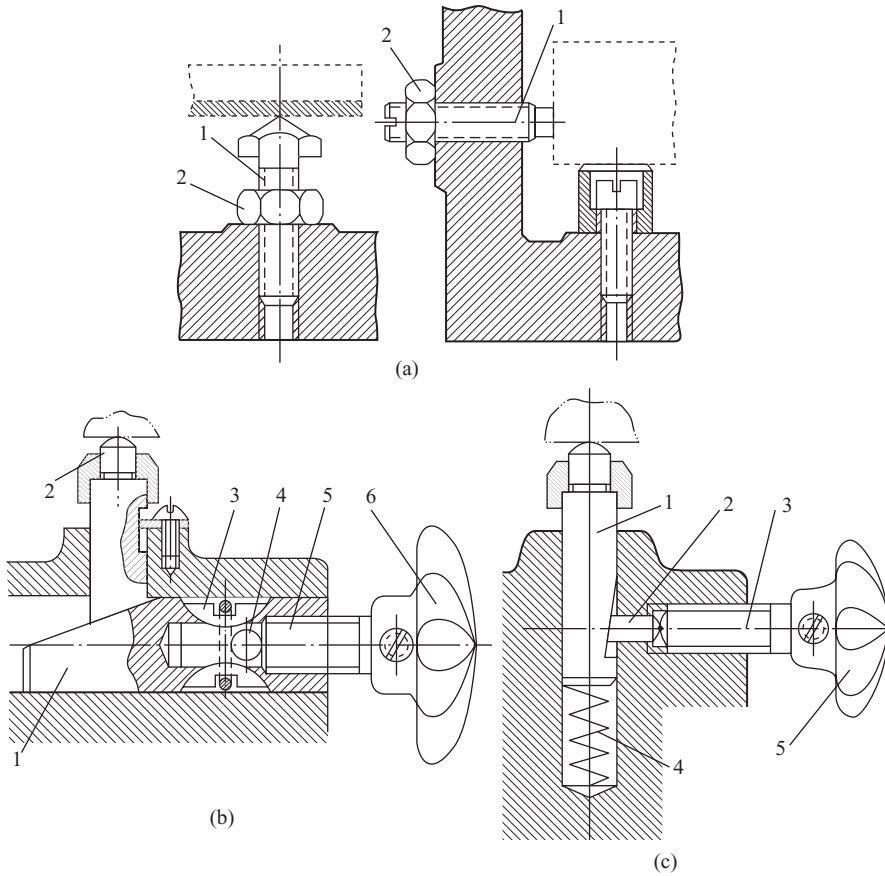


Figure 7.9 Adjustable rest buttons: (a) with screw and lock nut, (b) quick acting with sliding wedge, and (c) spring jack

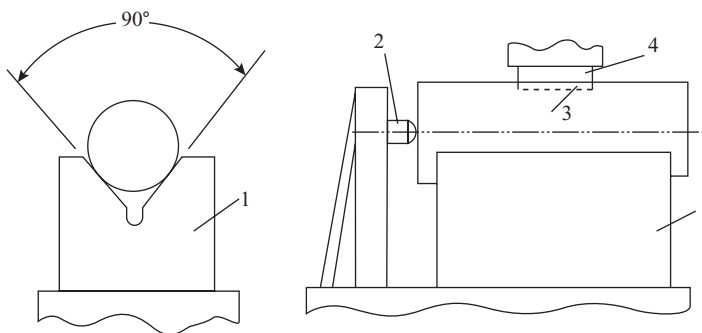


Figure 7.10 Location of long cylindrical work piece in V-block

of freedom are removed. The two degrees that remain are the linear movement along the length of the V-block and rotation of the shaft about its axis. The linear movement is taken away by using a step 2. For restricting the rotation, a feature is required on the cylinder. If such a feature, say a keyway (2) exists, then the rotation can be removed by inserting a key (4) of appropriate size in the keyway. In cylindrical shafts, often removal of four degrees of freedom is sufficient for most operations carried out on lathe. If required, the linear location of the cylindrical shaft is achieved by using a center hole in the shaft face using a center as the locating element. The degree of freedom concerning rotation needs to be removed only when two peripheral features on the cylinder must occupy a specific relative position with respect to each other, say a radial hole has to be machined at a given angle with respect to the keyway.

For analysis of locating error, consider the machining of a flat seat on a shaft located on the V-block. The position of the flat seat can be specified in three ways as shown in Figure 7.11.

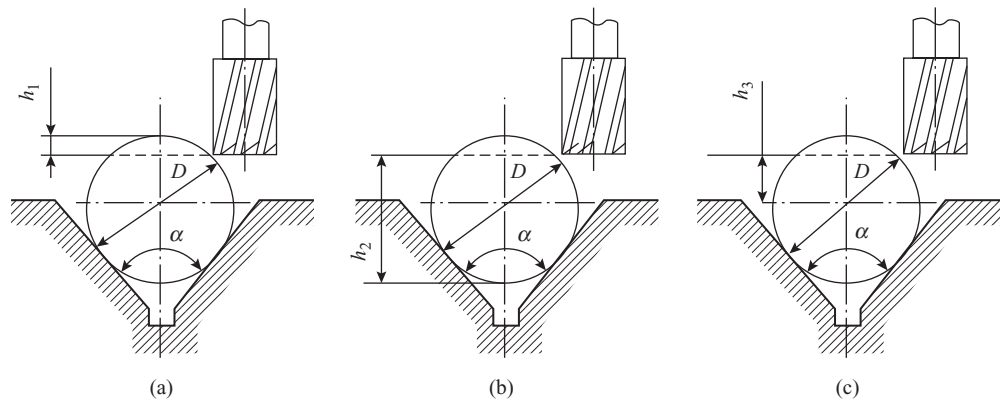


Figure 7.11 Schematic depicting three ways of dimensioning in locating on V-block: (a) from the top of cylindrical work piece, (b) from the bottom of cylindrical work piece, and (c) from the axis of cylindrical work piece

Based on the tolerance δD on the shaft diameter, its size may vary between D_{\min} and D_{\max} as shown in Figure 7.12. Accordingly, the locating error will be Δh_1 , Δh_2 and Δh_3 for the manner of specifying the position of flat seat adopted in Figures 7.11(a) through (c), respectively.

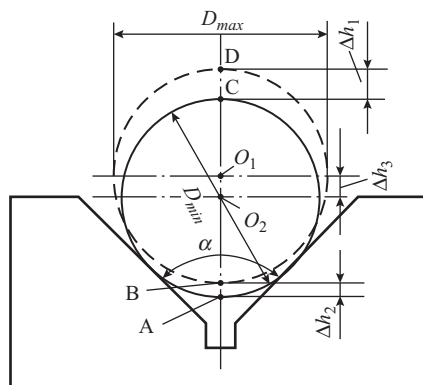


Figure 7.12 Schematic for calculation of locating error in location of cylindrical shaft on a V-block

From Figure 7.12, it can be noted that

$$\begin{aligned}
 \Delta h_1 &= (O_1D + O_1E) - (O_2C + O_2E) \\
 &= \left(\frac{D_{\max}}{2} + \frac{D_{\max}}{2 \sin \frac{\alpha}{2}} \right) - \left(\frac{D_{\min}}{2} + \frac{D_{\min}}{2 \sin \frac{\alpha}{2}} \right) \\
 &= \left(\frac{D_{\max} - D_{\min}}{2} \right) - \frac{1}{\sin \frac{\alpha}{2}} \left(\frac{D_{\min} - D_{\max}}{2} \right) \\
 &= \frac{\delta D}{2} + \frac{\delta D}{2 \sin \frac{\alpha}{2}} \\
 \Delta h_1 &= \frac{\delta D \left(1 + \sin \frac{\alpha}{2} \right)}{2 \sin \frac{\alpha}{2}} \tag{7.1}
 \end{aligned}$$

In a similar manner,

$$\begin{aligned}
 \Delta h_2 &= (O_1E - O_1B) - (O_2E - O_2A) \\
 &= \left(\frac{D_{\max}}{2 \sin \frac{\alpha}{2}} - \frac{D_{\max}}{2} \right) - \left(\frac{D_{\min}}{2 \sin \frac{\alpha}{2}} - \frac{D_{\min}}{2} \right) \\
 &= \left(\frac{D_{\min} - D_{\max}}{2} \right) + \frac{1}{\sin \frac{\alpha}{2}} \left(\frac{D_{\max} - D_{\min}}{2} \right) \\
 &= -\frac{\delta D}{2} + \frac{\delta D}{2 \sin \frac{\alpha}{2}} \\
 \Delta h_2 &= \frac{\delta D \left(1 - \sin \frac{\alpha}{2} \right)}{2 \sin \frac{\alpha}{2}} \tag{7.2}
 \end{aligned}$$

Finally, it can be found that

$$\begin{aligned}
 \Delta h_3 &= O_1E - O_2E \\
 &= \frac{D_{\max}}{2 \sin \frac{\alpha}{2}} - \frac{D_{\min}}{2 \sin \frac{\alpha}{2}}
 \end{aligned}$$

$$= \frac{1}{\sin \frac{\alpha}{2}} \left(\frac{D_{\max} - D_{\min}}{2} \right)$$

$$\Delta h_3 = \frac{\delta D}{2 \sin \frac{\alpha}{2}} \quad (7.3)$$

For different values of angle α , the locating errors are tabulated (see Table 7.1).

Table 7.1 Locating errors for different values of angle α of the V-block

| Locating error | V-block angle α , degrees | | |
|----------------|----------------------------------|-----------------|-----------------|
| | 60 | 90 | 120 |
| Δh_1 | 1.5 δD | 1.21 δD | 1.07 δD |
| Δh_2 | 0.5 δD | 0.21 δD | 0.08 δD |
| Δh_3 | δD | 0.7 δD | 0.58 δD |

Thus, it can be concluded that for the three ways of specifying the position of the flat seat, it is best to use the dimension h_2 as it involves the least location error. A question that arises is, why is the locating error not zero in any of the three cases? The simple answer is that the design and measuring datum was the top point of the shaft for h_1 , bottom print of the shaft for h_2 , and center of the shaft for h_3 , but none of them coincided with the setting datum that are the lines of contact between the shaft and the V-block faces. An important conclusion is that the locating error decreases with the increase of V-angle. Let us now consider the location of cylindrical shaft on a flat surface. The equivalent of the three ways of specifying the position of the flat seat will now be as shown in Figure 7.13. For the purpose of calculation of locating error, location on a flat surface can be locked upon as location in a V-block with included angle $\alpha = 180^\circ$. Therefore, substituting $\alpha = 180^\circ$ in Eqn. (7.1) through Eqn. (7.3), we obtain

$$\Delta h_1 = \delta D, \Delta h_2 = 0, \Delta h_3 = 0.5D$$

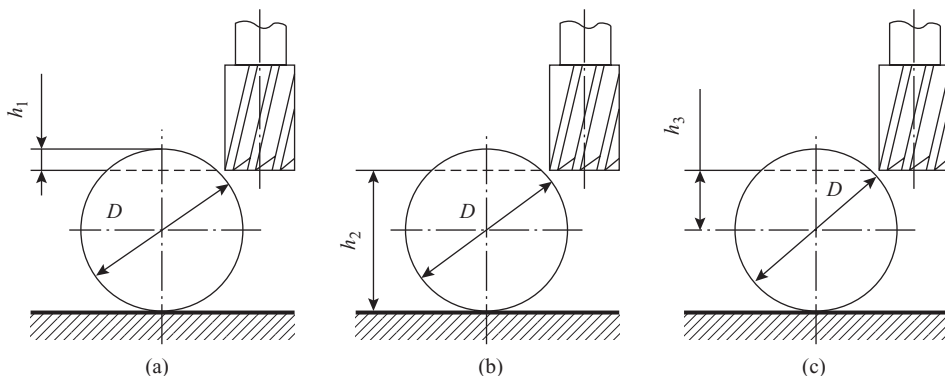
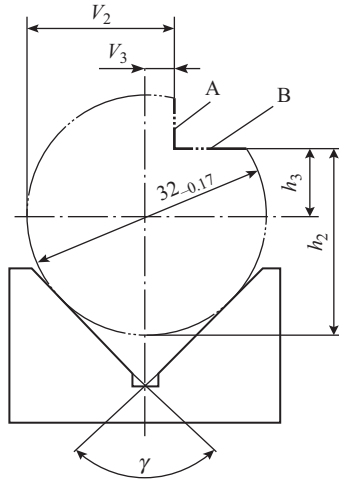


Figure 7.13 Schematic depicting three ways of dimensioning in locating on flat surface: (a) from the top of cylindrical workpiece, (b) from the bottom of cylindrical workpiece, and (c) from the axis of cylindrical workpiece

Example 7.4

For the cylindrical shaft of diameter $32_{-0.17}$ mm located in a V-block of angle 90° , determine the locating error and the available tolerance range for machining of steps *A* and *B* in the following two cases:

- A* and *B* are specified from the axis of the workpiece by dimensions $V_3 = 3 \pm 0.1$ mm, $h_3 = 8 \pm 0.1$ mm.
- A* and *B* are specified from the end points by dimension $V_2 = 19 \pm 0.1$ mm and $h_2 = 24 \pm 0.1$ mm.

**For case (a):**

There is no change in the location of the shaft axis in the vertical direction with variation of the shaft diameter; therefore for step *A*, the location error is zero. Hence, the available tolerance range for machining step *A* = 0.2 mm

For step *B* the locating error is given by Eqn. (7.3). The tolerance on shaft diameter $\delta D = 0.17$ mm. On substituting this value, we obtain the locating error for step *B*:

$$= \frac{\delta D}{2 \sin 45^\circ} = 0.71 \times 0.17 = 0.12 \text{ mm}$$

The tolerance range on h_3 is 0.2 mm. Hence, the available tolerance range for machining step *B* = $0.2 - 0.12 = 0.08$ mm

For case (b):

For step *A*, the locating error is equal to the difference in the maximum and minimum values of the shaft radius. For the given shaft dimension, $D_{\max} = 32.0$ mm and $D_{\min} = 32 - 0.17 = 31.83$ mm. Therefore, locating error is

$$\frac{32.0 - 31.83}{2} = 0.085 \text{ mm}$$

The tolerance range on $V_2 = 0.2$. Hence, the available tolerance range for machining step *A* = $0.2 - 0.085 = 0.115$ mm.

For step *B*, the locating error is given by Eqn. (7.2). On substituting $\delta D = 0.17 \text{ mm}$ and $\alpha = 90^\circ$ in Eqn. (7.2), we obtain the locating error for step *B*:

$$= \frac{0.17(1 - \sin 45^\circ)}{2 \sin 45^\circ} = 0.21 \times 0.17 = 0.036 \text{ mm}$$

Hence, the available tolerance for machining of step *B* = $0.2 - 0.036 = 0.164 \text{ mm}$

Three types of V-blocks used for location of cylindrical shafts are shown in Figure 7.15. Wide V-block shown in Figure 7.15(a) is used for finish machined locating surfaces, whereas the narrow V-block (Figure 7.15(b)) and location on four rest pins (Figure 7.15(c)) are used for the location of rough machined and very rough machined or unmachined shafts, respectively.

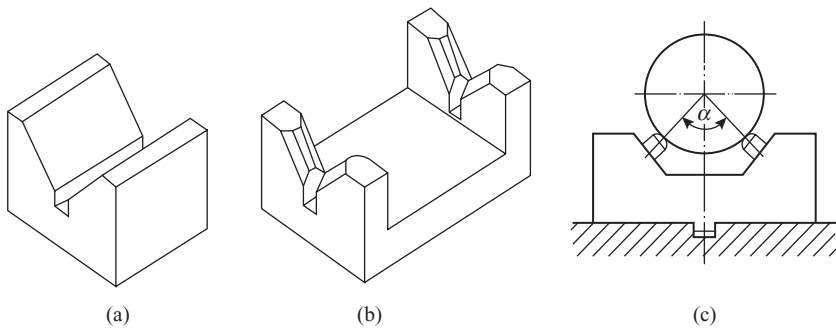


Figure 7.15 V-blocks for location of long cylindrical workpieces: (a) for finish machined shafts, (b) for rough machined shafts, and (c) for very rough machined or unmachined shafts

Self-centering devices are also used for location of cylindrical shafts. Figure 7.16 shows two such devices: one operating with three jaws (Figure 7.16(a)) and the other operating with two V-blocks (Figure 7.16(b)). In these devices, the locating elements (jaws or V-blocks) move simultaneously by equal amount towards the center or away from it. The advantage of these devices is that they combine in themselves both the locating as well as the clamping function. Three-jaw lathe chucks are the most common example of the device operating on the principle illustrated in Figure 7.16(a).

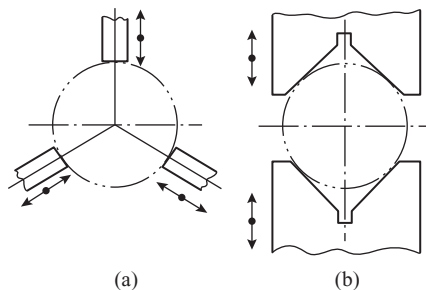


Figure 7.16 Location of cylindrical workpiece in self-centering devices: (a) three-jaw device and (b) device with two V-blocks

When the axis of the workpiece to be located is fixed, then sliding V-locators are employed to accommodate variation in the size of the cylindrical shaft. Two such locators are shown in Figure 7.17.

The locator shown in Figure 7.17(a) is positioned by a hand-operated screw and that shown in Figure 7.17(b) by a hand-operated cam. A spring bearing against a fixed pin ensures firm contact between the sliding block and cam and also brings back the V-block when the cam is released.

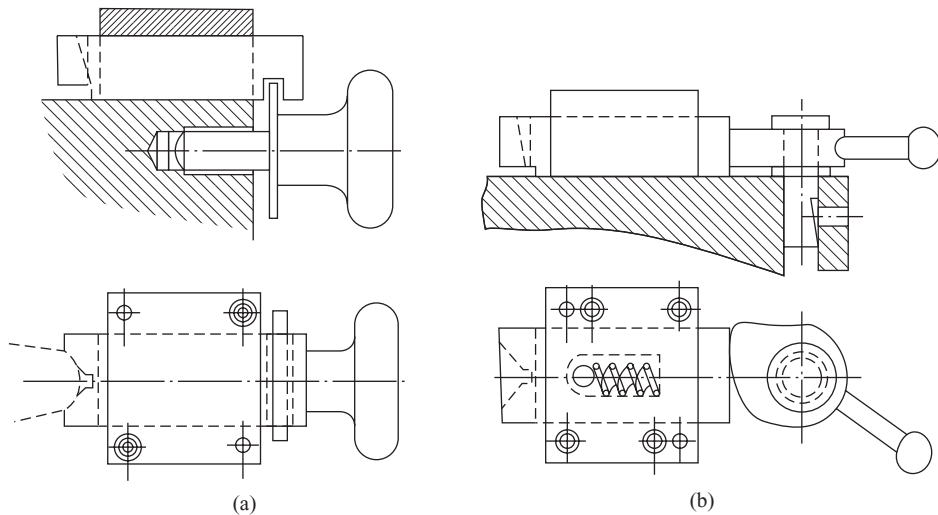


Figure 7.17 Sliding V-locators: (a) with hand-operated screw and (b) with a hand-operated cam

7.2.4 Locating Scheme, Error Analysis, and Elements for Short Cylindrical Parts

In short cylindrical parts such as rings and discs, the axial dimension is much smaller than the radial dimension. Therefore, despite being cylindrical parts, they cannot be located using V-blocks as this does not provide stable location. The face of such parts has the maximum surface area; therefore, it is used as the main setting datum. The basic device used for locating such parts is a self-centering chuck (Figure 7.18). The face of the workpiece rests on the horizontal face of the jaw steps, thereby removing three degrees of freedom. Two more degrees of freedom are removed when the vertical face of the jaw steps is used to locate the cylindrical portion of the workpiece (Figure 7.18(a)). The last remaining degree of freedom, that is, rotation of the workpiece is removed, if needed, by using a feature such as a keyway on the cylindrical portion of the workpiece as discussed for long cylindrical parts. The most common use of self-centering chucks is on lathe machines (Figure 7.18(b)), but they can also be used for quick and efficient location and clamping of stationary parts for drilling (Figure 7.18(a)) and other similar operations.

The locating error of the axial features of short cylindrical parts is governed by the principles discussed for prismatic parts, and that of the radial dimensions by the principles discussed for long cylindrical parts.

7.2.5 Locating Scheme, Error Analysis, and Elements for Parts with Through Hole

Workpieces with through hole are located using a pin or mandrel. Location on pin is used for short workpieces (Figure 7.19(a)) and on mandrel for long workpieces (Figure 7.19(b)). In either case, four degrees of freedom are removed by the pin or the mandrel. The fifth degree of freedom

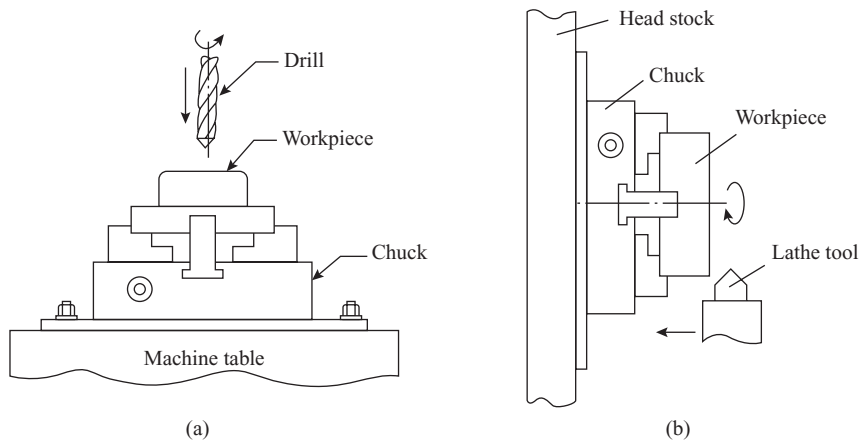


Figure 7.18 Location of short cylindrical workpieces in self-centering chuck: (a) for stationary workpiece and (b) for rotating workpiece

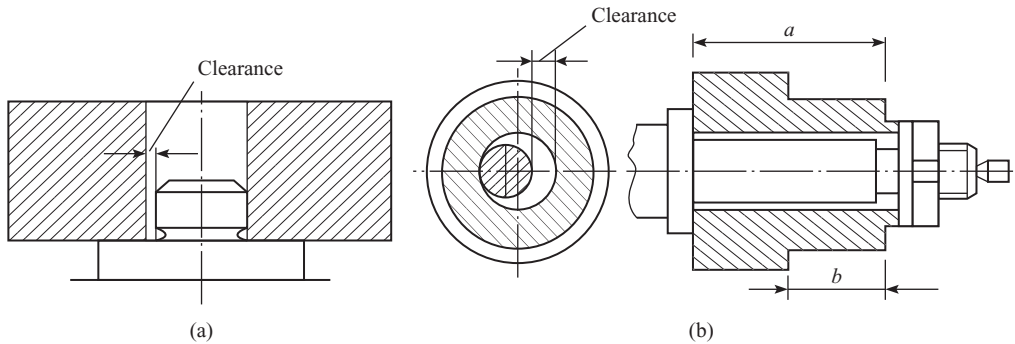


Figure 7.19 Location of workpiece with through hole: (a) on pin for short workpieces and (b) on mandrel for long workpieces

that is axial displacement of workpiece is removed by the shoulder of the pin/mandrel. As in the case of cylindrical parts, the sixth degree of freedom, that is, rotation of the workpiece is removed, if needed by using a feature such as a keyway on the outer surface of the workpiece.

The workpiece is mounted on the pin or mandrel with a clearance. Due to this clearance, the design datum (axis of the hole) is displaced from the setting up datum (axis of the pin or mandrel), resulting in eccentricity equal to half the clearance. The maximum clearance between the hole and the locating element is expressed as follows:

$$S_{\max} = S_{\min} + \delta_h + \delta_l$$

where S_{\min} is the minimum clearance required to mount the workpiece hole on the locating element, δ_h is the tolerance on hole diameter, and δ_l is the tolerance on diameter of the locating element.

The eccentricity between the axis of the workpiece hole and the axis of the locating element comprises $0.5 S_{\max}$ and is reflected as radial run out of the external surface of the workpiece equal

The out-of-perpendicularity of the axis of a hole from its face is expressed as $n:100$ mm. For the adopted location scheme shown in the figure above, the maximum and minimum clearance is found as follows:

Minimum clearance $S_{\min} = D_{\min} - d_{\max} = 30.0 - (30 - 0.025) = 0.025$ mm

Maximum clearance $S_{\max} = D_{\max} - d_{\min} = (30 + 0.05) - (30 - 0.085) = 0.135$ mm

From the geometrical construction shown in the figure above,

$$MN:MP = n:100$$

wherefrom,

$$MP = \frac{MN}{n} \times 100$$

As $MP = l$ represents the length of the pin and MN represents diametric clearance, we may write the above expression as follows:

$$l = \frac{S}{n} \times 100$$

Now substituting $l = 50$ mm, we find

$$n_{\min} = \frac{0.025}{50} \times 100 = 0.05 \text{ mm per } 100 \text{ mm}$$

$$n_{\max} = \frac{0.135}{50} \times 100 = 0.270 \text{ mm per } 100 \text{ mm}$$

The maximum height of pin is governed by the minimum clearance. For the given data of the hole and pin dimensions, the permissible minimum height of the pin is found as follows:

$$l = \frac{S_{\min}}{0.07} \times 100 = \frac{0.025}{0.07} \times 100 = 35.70 \text{ mm}$$

If the pin height is greater than 35.70 mm, then it would not be possible to locate the hole of size D_{\min} .

In short workpieces due to small guiding length, this misalignment can jam the workpiece when it is being lifted (Figure 7.21). To avoid this problem, the height of the pin has to be restricted and may be determined from the following relation:

$$H \leq \frac{l + 0.5D}{D} \sqrt{2DS_{\min}}$$

where D is the hole diameter, l is the distance of the hole axis from the edge of workpiece, and S_{\min} is the minimum clearance between the hole and pin.

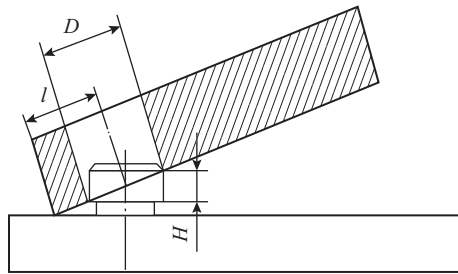


Figure 7.21 Schematic illustrating jamming of workpiece with through hole during removal from fixture

The use of a spherical pin (Figure 7.22) can also help in avoiding the problem of jamming between the hole and pin.

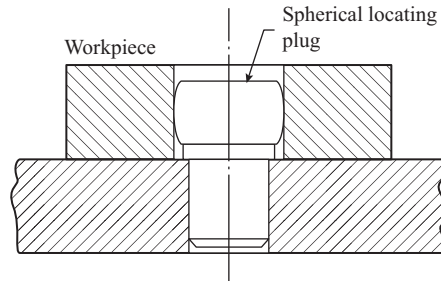


Figure 7.22 Spherical pin for location of workpiece with through hole

In long parts with hole, sometimes the location is carried out on a taper mandrel (Figure 7.23). The taper is very small and lies in the range from 1:1,500 to 1:2,000, which means that the diameter of the mandrel varies from 0.05 to 0.075 mm per 100 mm length of the mandrel. The mandrel is forced into the hole by means of a hand press called mandrel press. The interference between the hole and mandrel prevents the workpiece from slipping during machining. As coaxiality between the hole and mandrel is ensured, the radial locating error is eliminated. However, the disadvantage of taper mandrels is that axial location of the workpiece is not possible.

Pin-type locating elements are shown in Figure 7.24. Permanent pins are press fitted in the fixture body (Figures 7.24(a) and (b)), whereas replaceable pins are mounted with a sliding fit in a

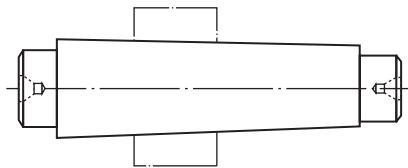


Figure 7.23 Taper mandrel

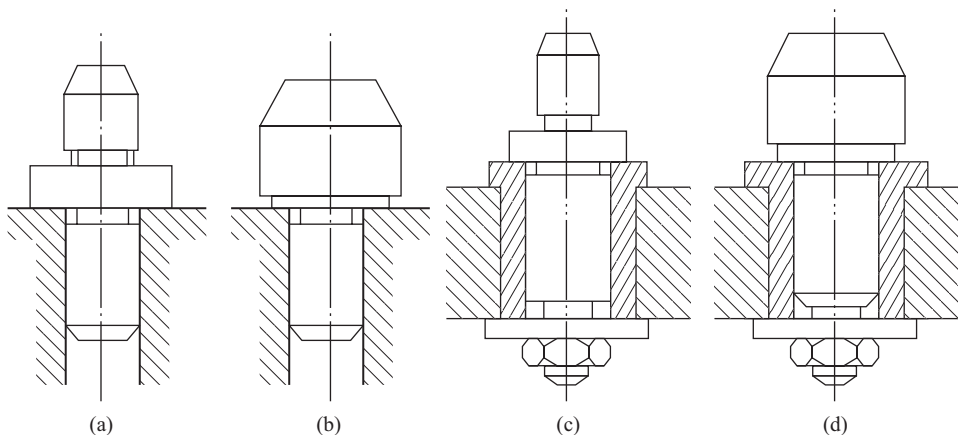


Figure 7.24 Locating pins for location of short workpiece with through hole: (a) permanent with shoulder, (b) permanent plain, (c) replaceable with shoulder, and (d) replaceable plain

bush which is press fitted in the fixture body (Figures 4.24(c) and (d)). Replaceable pins are used in fixtures that are used extensively and are therefore subjected to relatively faster wear and tear. Pins with shoulders (Figures 7.24(a) and (c)) should have a generous chamfer to enable the workpiece to be placed easily on the pin.

Mandrels used for locating of long workpieces are of two types: solid and expanding. Two types of solid mandrels are shown in Figure 7.25. The taper mandrel shown in Figure 7.23 has been described earlier. The cylindrical solid mandrel shown in Figure 7.25(a) forms a heavy interference fit with the workpiece hole. Axial location of the workpiece is possible with the help of spacer rings. The provision of the groove (1) enables both faces of the workpiece to be machined in one setting. Journal (2) has a slightly smaller diameter than that of the hole to facilitate easy insertion of the workpiece and to prevent misalignment when the workpiece is pressed on the locating surface of the mandrel with hand press. In view of the coaxiality of the workpiece hole and mandrel, there is no radial location error in this case. In the mandrel shown in Figure 7.25(b), the workpiece is mounted with a clearance. Axial location of the workpiece is done by the mandrel shoulder (1) and rotation of the workpiece is prevented by the key (2). If the workpiece design does not incorporate a keyway, then its rotation is prevented by tightening the nut (3).

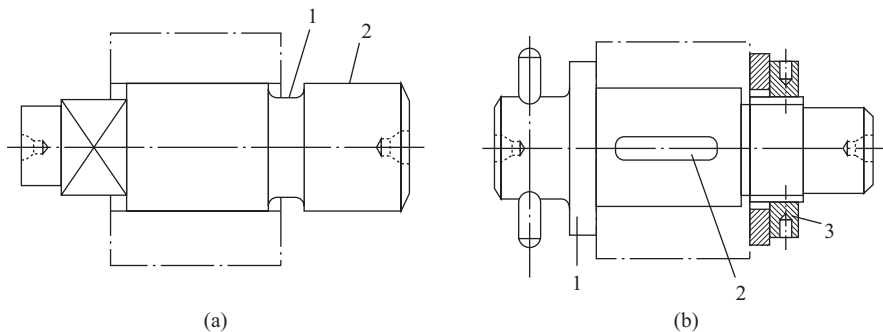


Figure 7.25 Mandrels for location of long workpiece with through hole: (a) cylindrical solid and (b) cylindrical solid with shoulder

Expanding mandrels serve for location and clamping both. Three designs of expanding mandrels are shown in Figure 7.26. The expanding mandrel shown in Figure 7.26(a) is meant for machining of the workpiece between centers. When the nut (5) is advanced, it pushes forward the spring sleeve (3) toward the left, which expands as it moves along the tapered portion (4) of the mandrel. The expanding mandrel grips workpiece (2) from inside thus providing the clamping force. On completion of machining, the nut (1) is rotated, pushing the sleeve (3) toward the right, thereby loosening its grip on the hole and allowing easy removal of the workpiece.

In the expansion mandrel shown in Figure 7.26(b), the spring sleeve (2) is made to expand by rotating the tapered mandrel (1) with a wrench. As the sleeve expands, it grips the hole and clamps the workpiece. In the design shown in Figure 7.26(c), the spring sleeve is replaced by three serrated jaws (1) which expand when the tapered mandrel (2) is moved toward the left, gripping the hole and clamping the workpiece (3). This design is preferred for thick-walled parts. A common feature of all expanding mandrels is that they ensure coaxiality of the hole and mandrel; therefore, the radial locating error in all of them is zero.

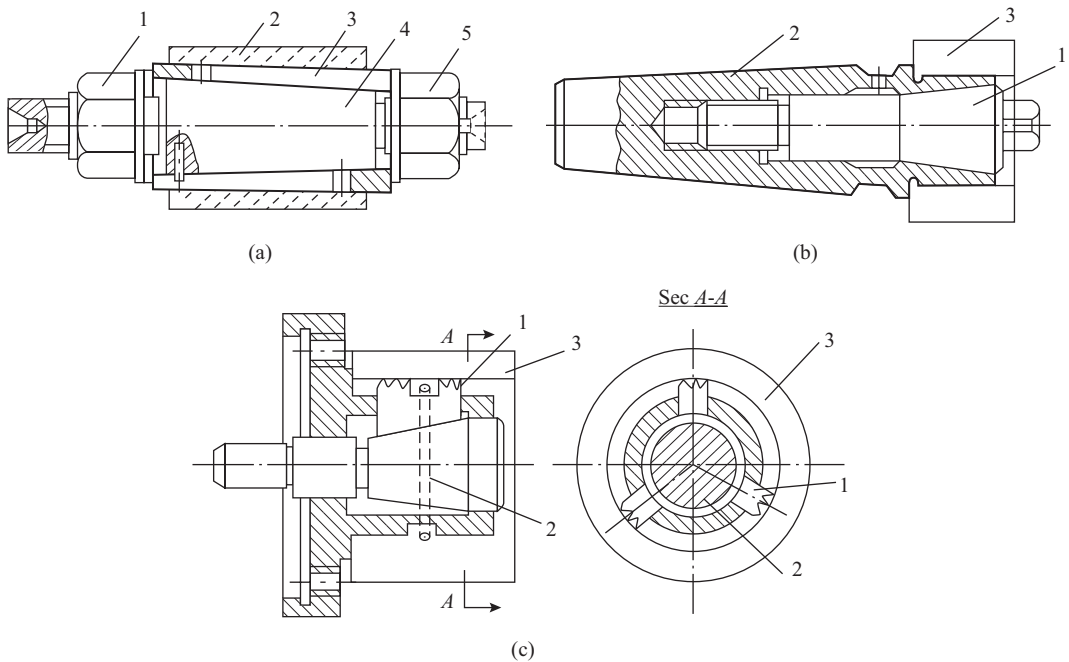


Figure 7.26 Expanding mandrels: (a) for machining of workpiece between centers, (b) for machining of light and thin-walled workpiece, and (c) for machining heavy and thick-walled workpiece

7.2.6 Locating Scheme, Error Analysis, and Elements for Parts with Flat Base and Two Predrilled Holes

For parts such as plates, frames, beds, housings, etc., location from a flat surface and two holes with parallel axes is commonly used (Figure 7.27) using a flat plate and two pins.

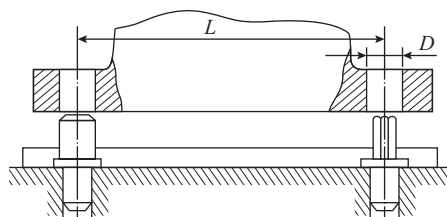


Figure 7.27 Location of workpiece with flat base and two holes

This location scheme eliminates all six degrees of freedom and is conducive to a simple design of the jig or fixture. For the purpose of error analysis, let us assume that the distance between the axes of the two holes of diameter D (radius R) is L and the tolerance on this dimension is $\pm \delta/2$.

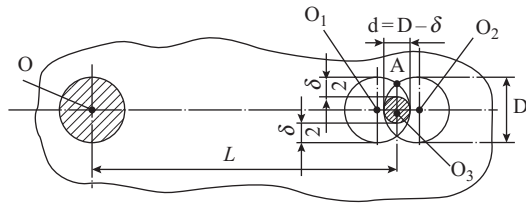


Figure 7.28 Schematic for analysis of locating error in locating the workpiece on flat plate and two cylindrical pins

This means that in the batch of parts to be located, the distance between hole axes may vary from $L - \frac{\delta}{2}$ to $L + \frac{\delta}{2}$. As shown in Figure 7.28, if the hole on the left is located on a pin of the same diameter as that of the hole at O , then the second hole may occupy two extreme positions O_1 and O_2 , respectively, separated by δ . To ensure location of the second hole, the maximum possible radius of the second pin is $r = \frac{D}{2} - \frac{\delta}{2}$ or its diameter $d = D - \delta$ and it should be located at O_3 equal to L from O . Now, if we have a part in the production lot in which the distance between the two holes happens to be exactly equal to L , then it will have a clearance of

$$\pm(R - r) = \pm \left[\frac{D}{2} - \left(\frac{D}{2} - \frac{\Delta}{2} \right) \right] = \pm \frac{\Delta}{2}.$$

If the second pin is made of the shape corresponding to overlap of the two extreme hole positions, then the clearance is reduced to $\pm a$, where

$$a = R - O_3A = R - \sqrt{O_2A^2 - O_2O_3^2}$$

$$a = \frac{D}{2} - \sqrt{\left(\frac{D}{2}\right)^2 - \left(\frac{D}{2} - \frac{\Delta}{2}\right)^2}$$

Obviously, the second shape of the pin should be preferred as it provides less clearance, and hence less locating error. However, fabricating a pin of this shape is difficult; therefore, a diamond pin (Figure 7.29) which is close to the overlap profile is used in actual practice. The dimensions of the diamond pin are found from the following relation:

$$e = \frac{2R\Delta - \Delta^2 - c^2}{2c}$$

where

$$c = \frac{\delta + \delta_1 - 2\Delta_1}{2}$$

2Δ = clearance on the diamond pin

$2\Delta_1$ = clearance on the cylindrical pin

R = radius of the hole

δ = tolerance on dimension L of the workpiece

δ_1 = tolerance on dimension L of the fixture

The condition $\delta_1 + \delta_2 > 2\Delta_1$ is a necessary one; otherwise, it is impossible to use a diamond locating pin.

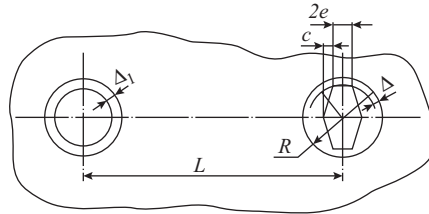


Figure 7.29 Location of workpiece on flat plate: one cylindrical pin and one diamond pin

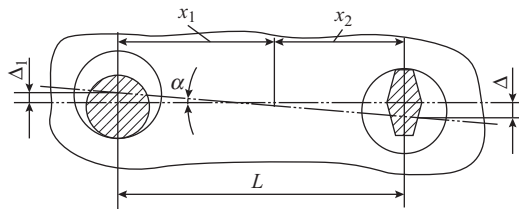


Figure 7.30 Schematic for analysis of misalignment error in locating the workpiece on flat plate and two cylindrical pins

Due to clearance between the workpiece holes and the pins on which they are located, the workpiece suffers misalignment from its center position (Figure 7.30). The maximum misalignment error occurs when the holes are placed with respect to the pins as shown in the figure. If the eccentricity of the round and diamond pin is Δ and Δ_1 , respectively, then

$$x_1 = \Delta_1 \cot \alpha, \quad x_2 = \Delta \cot \alpha$$

$$x_1 + x_2 = L = (\Delta + \Delta_1) \cot \alpha$$

$$\cot \alpha = \frac{L}{\Delta + \Delta_1}$$

Hence,

$$\alpha = \tan^{-1} \left[\frac{\Delta + \Delta_1}{L} \right]$$

As α is small, we may represent

$$\alpha = \frac{\Delta + \Delta_1}{L}$$

It can thus be noted that to minimize the misalignment error, holes that are farthest apart should be used for location.

The problem of jamming when the workpiece is being lifted, which was discussed for single-pin location (Figure 7.21) earlier is present in two-pin location too (Figure 7.31). Assuming that $D = D_1$ and $l = L_1$, the maximum permissible height of the pins that precludes the jamming is found from the following relation:

$$H = \frac{L + l + 0.5D}{L + D} \sqrt{2(L + D)\Delta_{\min}}$$

where Δ_{\min} is the minimum clearance between the hole and pin.

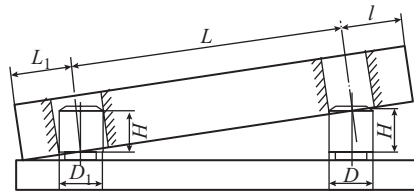


Figure 7.31 Schematic illustrating jamming of workpiece located on flat plate and two pins during removal from fixture

Location of this category of parts is done using cylindrical pins shown in Figure 7.24 and diamond pin shown in Figure 7.32, which like the cylindrical pins may be with or without shoulder as shown in Figures 7.32(a) and (b), respectively. In addition, like cylindrical pins, diamond pins too may be permanent and replaceable.

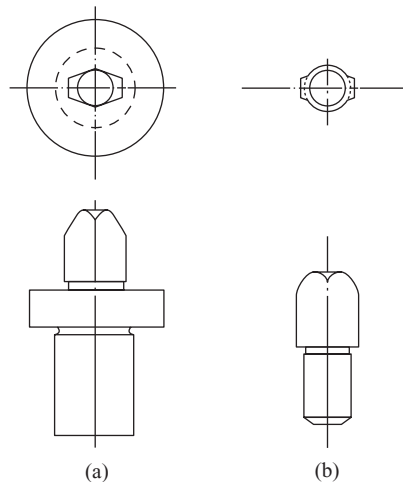


Figure 7.32 Diamond pin: (a) with shoulder and (b) plain

Finally, a few words of description may be in order to facilitate proper use of term for various pin sizes. Very short pins in which the top flat surface of the pin is used for locating flat surface of the

workpiece are known as buttons or rest buttons (Figure 7.7). Pins that are used for location of holes are longer than buttons. With increasing length, they are referred as pin, plug, and mandrel.

7.2.7 Locating Scheme, Error Analysis, and Elements for Parts with Center Holes at End Faces

Workpieces having center holes as setting datums are located between centers. When a workpiece with center holes at both end faces is located between two centers, it is deprived of five degrees of freedom and the only degree of freedom that remains is the possibility of workpiece rotation about its own axis (Figure 7.33(a)). Location between rigid centers produces radial as well as axial locating error. The radial error arises from the absence of coaxiality between the axis of the center hole (design datum) and the axis of the center (setting up datum). This eccentricity is reflected as radial runout of the supported end of the workpiece and represents the locating error. This error is generally expressed by the following empirical relation:

$$\epsilon_r = 0.25 \delta D$$

where δD is the tolerance on the workpiece diameter.

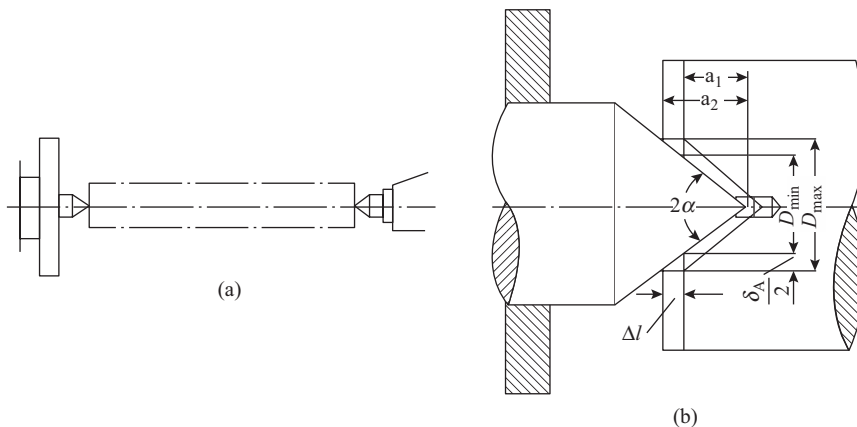


Figure 7.33 Location of workpiece between centers: (a) schematic of location and (b) schematic for analysis of locating error

Axial locating error occurs due to variation in the depth of the center hole (Figure 7.33(b)), which results in the contacting diameter of the counter sunk portion of the center hole to vary between

D_{\min} and D_{\max} . The variation in lengthwise location $\Delta l = a_2 - a_1$ is therefore found as

$$\Delta l = \frac{\frac{\delta A}{2}}{\tan \alpha} = \frac{\delta A}{2 \tan \alpha}$$

where δA is the tolerance on the diameter of the counter sunk portion of the center hole for the lot and α is the half angle of the center.

For common centers of cone angle 60° , the axial locating error varies from 0.1 to 0.25 mm. This error can be eliminated by using a floating center (Figure 7.34). Here, variation of the diameter of center hole does not affect the axial location of the workpiece as its end face is always located by the face of the sleeve of the center.

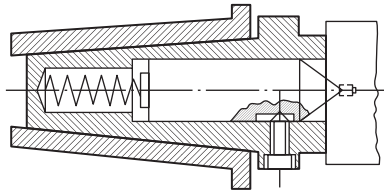


Figure 7.34 Floating center

The different types of centers used for location are shown in Figure 7.35. The solid center shown in Figure 7.35(a) is the most commonly used center. The half center shown in Figure 7.35(b) is used when the workpiece face has to be machined right up to the edge of the center hole. Figure 7.35(c) shows a truncated center that is used for supporting workpieces with large size center hole. The reverse center shown in Figure 7.35(d) is used to support small workpieces in which center holes cannot be made. An external matching tapered extension is made on such workpieces that enters the center hole in the reverse center.

All the centers described till now are known as the so-called *dead centers* as they remain stationary when the workpiece rotates. At high rotational speed of the workpiece, the friction between the rotating workpiece and stationary center can generate intense heat and cause excessive wear of the center and the center hole. In such cases, it is advisable to use a revolving center. Figure 7.35(e) shows a revolving center with roller bearings although revolving centers may also be made with ball bearings.

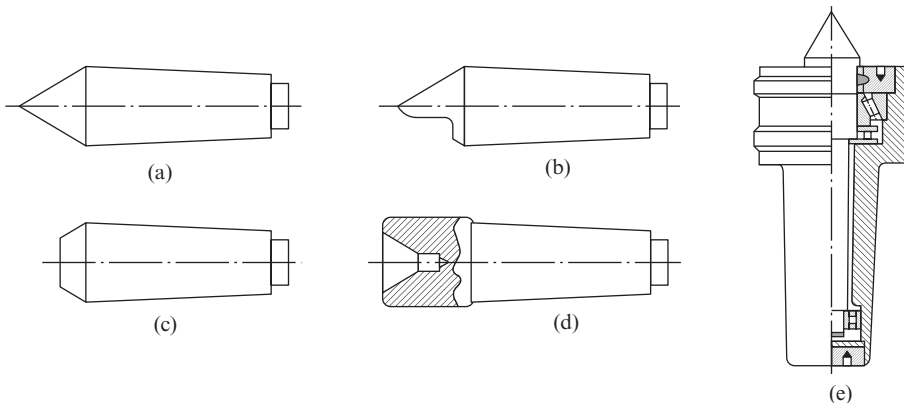


Figure 7.35 Types of centers: (a) solid center, (b) half center, (c) truncated center, (d) reverse center, and (e) revolving center

7.3 Clamping Principles, Methods, and Elements

The main function of clamping is to ensure dependable contact between the workpiece and locating elements and to prevent displacement and vibration of the workpiece during the cutting operation. Displacement of the workpiece may be caused by the cutting forces and its own weight. Clamping devices of jigs and fixtures should therefore satisfy the following requirements:

- (i) They should be simple, robust, reliable, and convenient to maintain.
- (ii) They should ensure that the position of the workpiece after location is not disturbed by clamping.

- (iii) The clamping force should be sufficient to ensure reliable clamping but not excessive to avoid damage to the workpiece surface by denting or deformation.
- (iv) The time of loosening and tightening of the clamp should be as short as possible, and the movement of the lever, screw, cam, etc., of the clamping device should be strictly limited.
- (v) They should be ergonomically designed in terms of operator effort and safety.

No clamping is required for very heavy stable workpieces whose weight is much more than the cutting force produced during the cutting operation and if the direction of the cutting forces is such that it cannot disturb the setting of the workpiece achieved by its location.

7.3.1 Clamping Principles

Many of the requirements to the design of clamping element of jigs and fixtures are intimately linked to the proper selection of the point and direction of application of the clamping force and use of the clamping force of correct magnitude, which ensures reliable clamping without disturbing the workpiece location or damaging it.

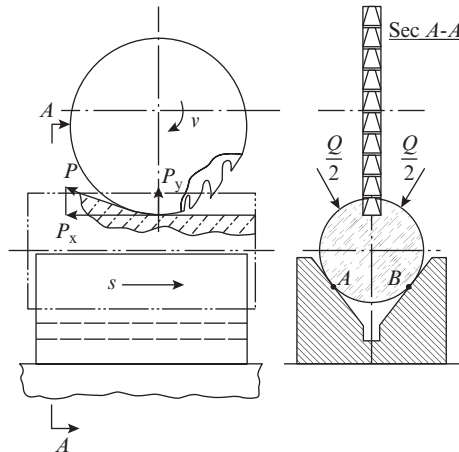


Figure 7.36 Schematic to illustrate the selection of point and direction of application of clamping force in fixture that removes four degrees of freedom

The direction and point of application of the clamping force should be selected based on the location scheme used for a particular workpiece, and it should be directed on to a locating element or near it. Consider the milling of a groove on a cylindrical shaft located in a V-block as shown in Figure 7.36. It is evident that under the effect of force P_x , the workpiece can slide along the length of the V-block. This can be prevented by applying two forces $\frac{Q}{2}$ directed on to the setting datums A and B . Obviously, the magnitude of force $\frac{Q}{2}$ should be such that the frictional forces at the contacting surfaces are sufficient to prevent the workpiece from sliding.

Now consider the case of milling of a groove in the same cylindrical shaft that is located as shown in Figure 7.37. In this case, the possibility of sliding of the workpiece along the length of the V-block has been eliminated by using a stop button. However, the workpiece may be lifted by the moments $P_x a + P_y x$. In this case, the clamping force Q of proper magnitude should be applied as shown in Figure 7.37 to prevent the workpiece from tilting.

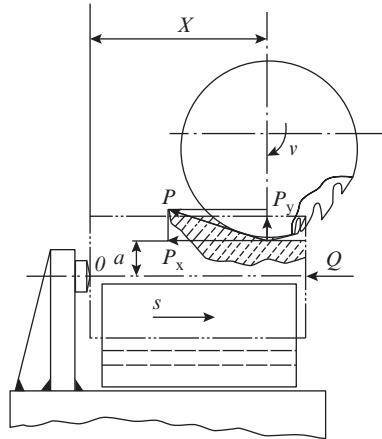


Figure 7.37 Schematic to illustrate the selection of point and direction of application of clamping force in fixture that removes five degrees of freedom

Thus, it can be noted that the location scheme plays an important role in deciding the point and direction of application of the cutting force. Therefore, while choosing the locating scheme, preference should be given to locating surface that allows the clamping force to be directed on to a locating element or near it as in Figure 7.37.

To ensure proper contact between the workpiece and the locating element, the clamping force should be directed perpendicular to the locating element (Figure 7.38(a)). If this is not possible, then the clamping force should be applied on workpiece surface that allows it to be pressed simultaneously against two locating elements (Figure 7.38(b)).

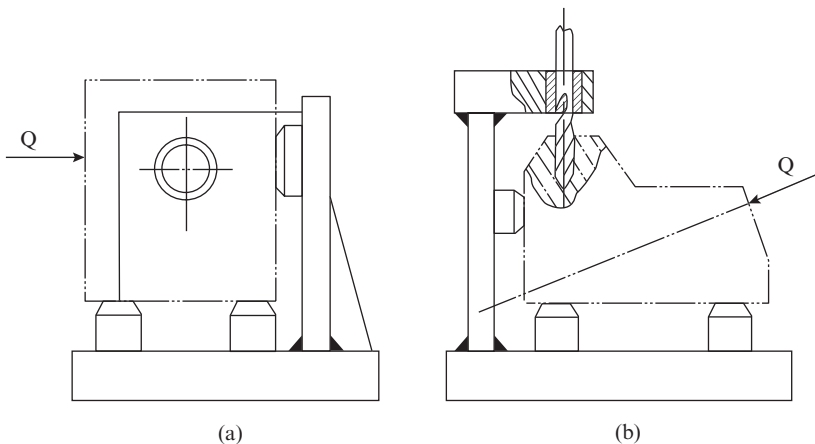


Figure 7.38 Schematic to illustrate correction direction of clamping force: (a) force directed perpendicular to locating element and (b) force directed between two locating elements

To prevent deformation of workpieces with flanges during clamping, the point of application of the clamping force should be directed on to the locating element (Figure 7.39(a)). Deviation from this principle will result in deformation as shown in Figure 7.39(b).

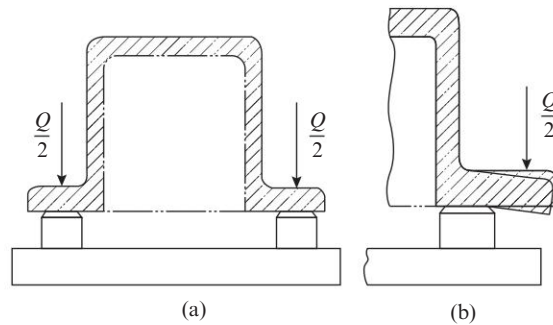


Figure 7.39 Schematic to illustrate application of clamping force on workpiece with flange: (a) correct application and (b) wrong application

While clamping flexible and weak sections, the clamping force should not be applied at a point that may cause the wall to bend or deflect (Figure 7.40(a)). Application of the force at two points near the vertical walls will avoid this problem (Figure 7.40(b)).

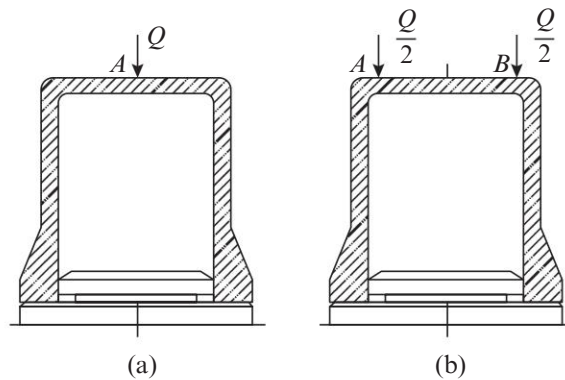


Figure 7.40 Schematic to illustrate application of clamping force on flexible and deformable workpieces: (a) correct application and (b) wrong application

To prevent damage to the workpiece surface during clamping, it is desirable to reduce the pressure at the contact location by distributing the clamping force between several points or a continuous area with the help of pads (1) as shown in Figure 7.41.

For weak and unstable appendages, it may be necessary to use supplementary location and clamping close to the site of the machining operation. For example, the location and clamping of the main body of the workpiece (1) shown in Figure 7.42 is carried out by the 3-2-1 principle and application of two forces Q_1 . However, for straddle milling of the block faces of the appendage, an additional adjustable locating rest button (2) and clamping force Q_2 have been used to ensure stability of the machining operation.

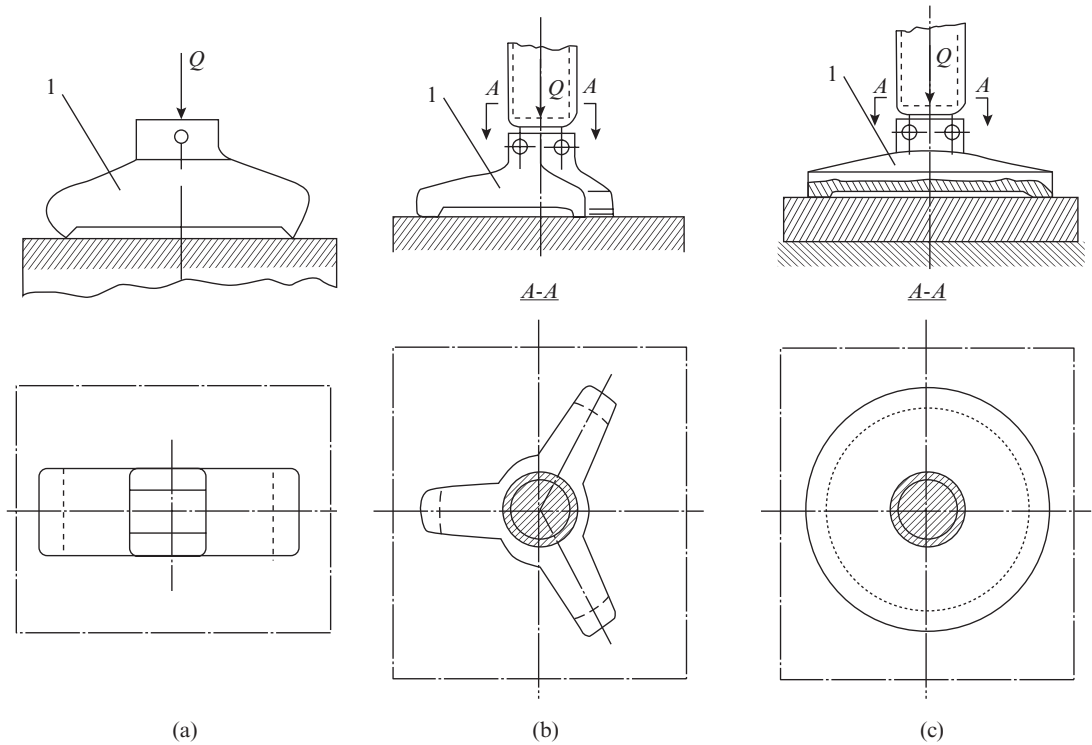


Figure 7.41 Distribution of clamping force by use of pads: (a) on two points, (b) on three points, and (c) on continuous ring-shaped area

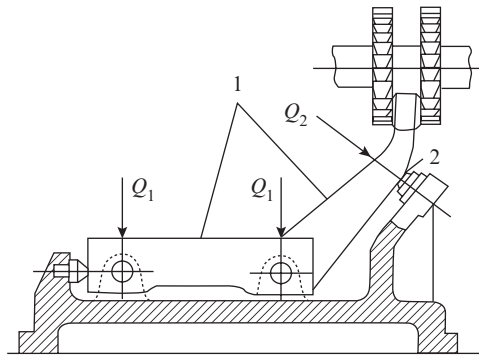


Figure 7.42 Supplementary location for unstable appendage

7.3.2 Clamping Force Calculation

During a machining operation, the workpiece is subjected to cutting forces that tend to push, rotate, and lift it based on the direction and point of application of the forces. This tendency is opposed by the clamping force, reaction of the supports, and frictional forces. The cutting forces and torques are calculated by applying the theoretical and empirical relations given in Chapter 3.

The support reactions and frictional forces depend on the location scheme and the nature of possible displacements of the workpiece during the machining operation, namely sliding, rotation, or lifting. Based on this background, the general procedure for clamping force calculation may be outlined as follows:

- (i) Sketch the force diagram, depicting the cutting, clamping, and reactive forces.
- (ii) Decide the possible displacements of the workpiece during the machining operation, namely sliding, rotation, or tilting.
- (iii) Based on the identified possible displacements, estimate the frictional forces and add them to the force diagram prepared in step (1) above.
- (iv) Take projections of all the forces in the direction of the possible linear displacement, moment of all the forces about the point of possible tilting and moment of all the forces about the axis of possible rotation. Write the equilibrium equations for all possible displacements.
- (v) Calculate the clamping force using the equilibrium equations obtained in step (4) above.
- (vi) Use a factor K to account for increase of cutting force due to tool wear, hard spot, sudden increase of allowance, etc., and to provide a margin of safety. Generally, coefficient K is taken as 1.5 for finishing cuts and 2.5 for rough cuts.

The general procedure of clamping force calculation is now illustrated for a few typical machining operations.

Clamping force calculation in machining of groove with end mill cutter Consider the machining of a groove on the surface of a prismatic part using an end mill cutter (Figure 7.43). For the 3-2 location scheme adopted for the part, the forces are shown on the schematic diagram. As the sixth degree of freedom has not been eliminated, the possible displacement is sliding of the workpiece under the action of cutting force P_y .

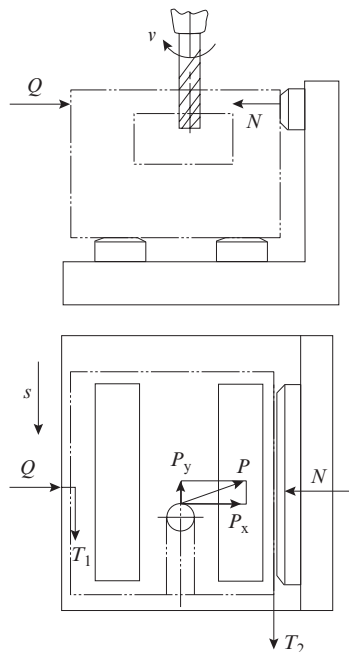


Figure 7.43 Schematic for calculation of clamping force to prevent sliding of workpiece in groove milling operation

Taking projection of all the forces on the X -axis, we find that support reaction:

$$N = Q + P_x$$

where Q is the clamping force.

The frictional force T_1 between the clamping element and workpiece and T_2 between the locating pad and workpiece are $T_1 = f_1 Q$ and $T_2 = f_2 N$, respectively, where f_1 is the coefficient of friction between the clamping element and workpiece and f_2 is the coefficient of friction between the locating pad and the workpiece.

Now taking the projections of all the forces in the Y -direction, which is the direction of possible displacement and using safety factor K , the force equilibrium equation can be written as follows:

$$T_1 + T_2 = KP_y$$

On substituting for T_1 , T_2 , and N , we obtain

$$f_1 Q + f_2 (Q + P_x) = KP_y$$

wherefrom

$$Q = \frac{KP_y - f_2 P_x}{f_1 + f_2}$$

Clamping force calculation in machining of flat surface with plain milling cutter For the location scheme adopted for machining flat surface on a prismatic part with a plain milling cutter, the forces are shown in Figure 7.44. In this case too, the sixth degree of freedom (linear displacement perpendicular to the X - Y plane in Z -direction) has not been eliminated, but this is not necessary as there is no force component in the Z -direction.

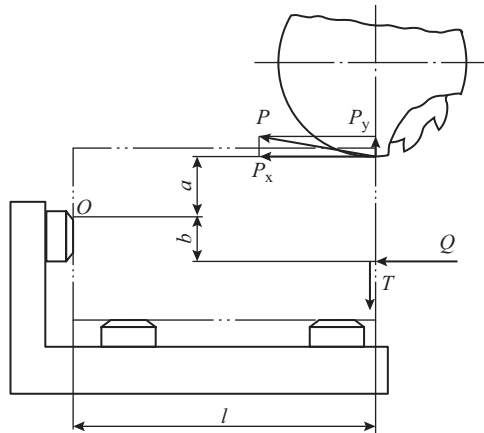


Figure 7.44 Schematic for calculation of clamping force to prevent tilting of workpiece in plain milling operation

In the given case, the possible displacement is tilting of the workpiece about point O due to the moments $P_x a + P_y l$. To counter this tilting, a clamping force Q is applied to produce an opposing balancing moment. Here, it is important to explain the following two factors:

- (1) As the workpiece lifts due to moment $P_x a$, the vertical face of the workpiece slides against the clamping element, thereby giving rise to frictional force $T = fQ$, where f is the coefficient of friction between the clamping element and the workpiece.
- (2) The force component P_y produces a moment $P_y x$ about point O , where x is the distance of the current location of the cutter from point O . The maximum value of this moment $P_y l$ occurs when $x = l$ at the commencement of cut.

Bearing the above factors in mind and taking the moments of all the forces about point O and using safety factor K , the equilibrium equation may be written as follows:

$$Qb + Tl = K(P_x a + P_y l)$$

On substituting $T = fQ$, we obtain

$$Q = \frac{K(P_x a + P_y l)}{b + fl}$$

It is evident from the above relation, that the larger the distance b at which we apply the clamping force from the point of tilting O , the smaller is the magnitude of clamping force Q .

Clamping force calculation in drilling of hole in cylindrical workpiece located in a V-block For the location scheme of the workpiece for drilling a hole shown in Figure 7.45, the forces are shown in Figure 7.45.

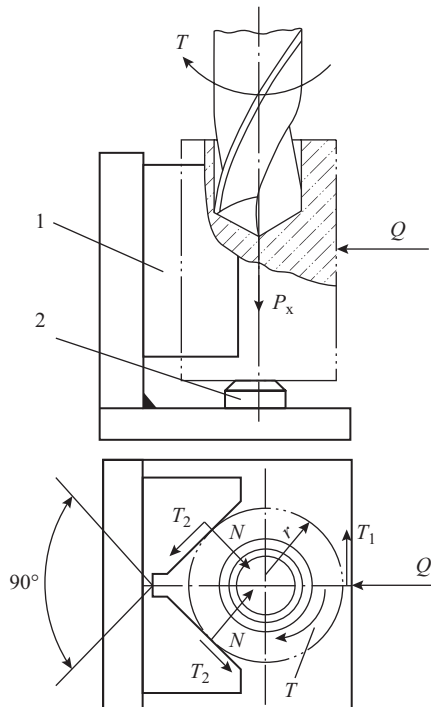


Figure 7.45 Schematic for calculation of clamping force to prevent sliding and rotation of workpiece located in V-block in a drilling operation

The cutting forces produced in drilling operation are torque T and thrust P_x . In this case, the only possible displacement of the workpiece is rotation about its axis due to torque T . The clamping force Q produces a reaction N at each of the contact surface of the V-block. As the workpiece rotates, the reactive force N produces a friction force T_2 on each face of the V-block and a friction force T_1 between the clamping element and the workpiece. Here, $T_1 = f_1 Q$, where f_1 is the coefficient of friction between the workpiece and the clamping element and $T_2 = f_2 N$, where f_2 is the coefficient of friction between the workpiece and the V-block face.

Now taking moment of all the forces about the workpiece axis and using safety factor K , the equilibrium equation may be written as follows:

$$2T_2 r + T_1 r = KT$$

where r is the radius of the workpiece.

Here, it may pertinent to note that the thrust force P_x and the reaction that it produces on the rest button are coincident with the workpiece axis, and therefore do not produce any moment about this axis.

Assuming the included angle of the V-block to be 90° and taking the projection of all the forces in the horizontal direction we find that

$$Q = 2N \sin 45$$

wherefrom

$$N = \frac{Q}{2 \sin 45} = \frac{\sqrt{2}}{2} Q$$

On substituting for T_1 and T_2 in the equilibrium equation, we obtain

$$2f_2 N r + f_1 Q r = KT$$

Now, on substituting for N in the above relation, we obtain

$$2f_2 \frac{\sqrt{2}}{2} Q r + f_1 Q r = KT$$

wherefrom

$$Q = \frac{KT}{(\sqrt{2}f_2 + f_1)r}$$

Clamping force calculation in drilling of hole in cylindrical workpiece clamped in three-jaw chuck on a lathe While drilling a hole in a workpiece clamped in a three-jaw chuck on a lathe (Figure 7.46), the workpiece is subjected to two displacements, sliding along the length of the jaws due to thrust force P_x and rotation about its axis due to torque T . If a clamping force Q is applied on each jaw, then a linear frictional force $T_1 = f_1 Q$ and a rotational frictional force $T_2 = f_2 Q$ will be produced at each jaw. Here, f_1 and f_2 represent the linear and rotational coefficient of friction, respectively, between the workpiece and jaw.

Keeping in mind that the clamping device is a three-jaw chuck, the equilibrium equation for workpiece displacement along the jaws using safety factor K may be written by taking the projection of the forces in the horizontal direction as follows:

$$3T_1 = KP_x$$

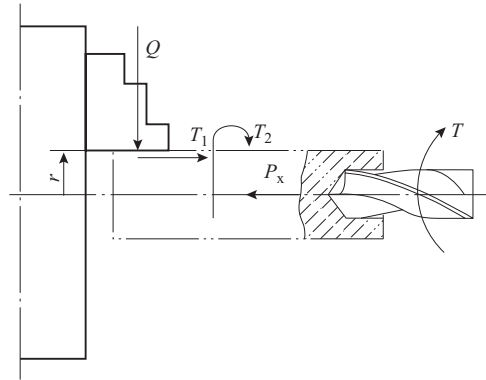


Figure 7.46 Schematic for calculation of clamping force to prevent sliding and rotation of workpiece located in three-jaw chuck in drilling operation

On substituting for T_1 , we obtain

$$3f_1Q = KP_x$$

wherefrom

$$Q = \frac{KP_x}{3f_1}$$

Similarly, the equilibrium equation for workpiece rotation about its axis using safety factor K may be written by taking the moment of all the forces about the axis as follows:

$$3T_2r = KT$$

where r is the radius of the workpiece

On substituting for T_2 , we obtain

$$3f_2Qr = KT$$

wherefrom

$$Q = \frac{KT}{3f_2r}$$

Of the two values obtained, the larger one is used in design calculations. The total clamping force to be applied will obviously be $3Q$.

Clamping force calculation in turning operation on workpiece clamped in a three-jaw chuck on a lathe In a turning operation on a workpiece clamped in a 3-jaw chuck, the workpiece is subjected to three cutting force components P_x , P_y and P_z (Figure 7.47).

As in the case of drilling discussed earlier, the possible workpiece displacements are sliding along the length of the jaws due to force P_x and rotation about the axis due to force P_z . Force component P_y can cause deflection of the workpiece, but not its displacement. Similarly, force component P_x can cause tilting of the workpiece about the clamping point, but this is constrained by the adopted locating scheme and is therefore unable to cause any displacement. As described in the case of drilling, we have linear frictional force $T_1 = f_1 Q$ and rotational frictional force $T_2 = f_2 Q$ acting at each jaw of the three-jaw chuck, where f_1, f_2 , and Q are the same as defined in the previous case.

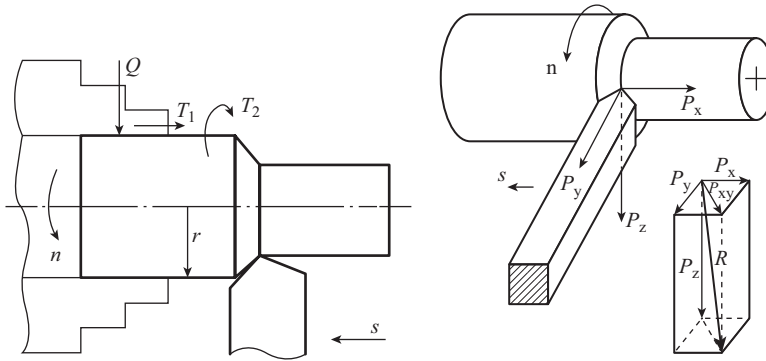


Figure 7.47 Schematic for calculation of clamping force to prevent sliding and rotation of workpiece located in a three-jaw chuck in turning operation

The equilibrium equation for workpiece displacement is obtained by taking the projections of all the forces on the horizontal axis as follows:

$$3T_1 = KP_x$$

On substituting for T_1 , we obtain

$$Q = \frac{KP_x}{3f_1}$$

Similarly, the equilibrium equation for workpiece rotation is obtained by taking the moments of all the forces about the axis as follows:

$$3T_2 r = KP_z r$$

where r is the radius of the workpiece

On substituting for T_2 , we obtain

$$Q = \frac{KP_z}{3f_2}$$

Generally, P_z is (2–4) times greater than P_x , therefore the clamping force obtained from consideration of workpiece rotation is used in design calculations. The total clamping force to be applied will obviously be $3Q$.

In the expressions for clamping force, the coefficients of friction may be taken as follows:

- (i) Contact between machined surface and rest pad $f = 0.10 - 0.15$
- (ii) Contact between machined surface and flat rest button $f = 0.16 - 0.18$
- (iii) Contact between machined surface and rest button with spherical top and contact along a line $f = 0.18 - 0.30$
- (iv) Contact with rest buttons with rough top, jaws, etc., $f = 0.50 - 0.70$

Clamping errors depend on the design of the fixture, size and shape of the workpiece, accuracy of the locating surface and the clamping force. A judicious selection of the point and direction of application of the clamping force is of utmost importance in minimizing the deformation of the workpiece and fixture components and thereby minimize the clamping errors. In this regard, the use of reinforcement ribs and stiffeners aimed at enhancing the overall structural rigidity also plays an important role in reducing the clamping errors. In view of the large number of factors involved and the variability of the clamping force itself, it is extremely difficult to analytically estimate clamping errors. Where these errors become significant, an experimental determination is generally resorted to for deciding the corrective measures

7.3.3 Clamping Mechanisms and Applied Force Calculation

Clamping of workpiece in a jig or fixture is carried out with a clamping device. A clamping device consists of three main components as follows:

- (i) Device for application of force; force application may be manual or powered using pneumatic, hydraulic, hydropneumatic, vacuum, and magnetic devices.
- (ii) Mechanism for conversion of applied force into clamping force.
- (iii) Clamping element for the application of the clamping force on the workpiece at the right point (s) in the right direction.

Clamping mechanisms and their analysis are presented in this section. The next two sections will be devoted to description of the large variety of clamping elements that are used in tooling practice to cater to the workpieces of various geometrical configurations and the description of power drives.

Based on the principle of operation, clamping mechanisms are classified as screw type, eccentric or cam type, wedge type, lever or pivot type, toggle type, and rack and pinion type. Some clamping devices use a combination of mechanisms such as screw-lever type, eccentric-lever type, wedge-lever type, etc. Analysis of the basic clamping mechanisms is discussed below. The analysis of the combination-type clamping mechanisms can be carried out on the basis of the analysis of the simple mechanisms.

The efficiency of clamping mechanisms is defined by a term called *amplification factor*, which represents the ratio of the output force of mechanism to the applied force.

Screw-type clamping mechanism This mechanism is simple in design, reliable in operation, has a large amplification factor and is self-locking. It is used only in manually operated jigs and fixtures. The main element of this mechanism is a screw with metric thread that transmits the clamping force either through the screw (Figures 7.48(a), (b), and (c)) or the nut (Figure 7.48(d)).

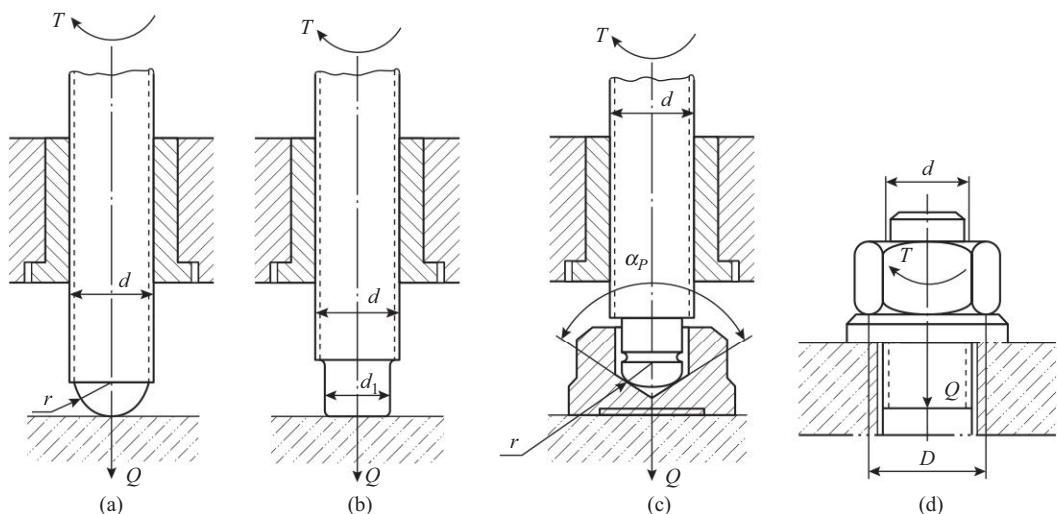


Figure 7.48 Screw-type clamping mechanisms: (a) screw with spherical face, (b) screw with flat face, (c) screw with pad, and (d) tightening force applied through nut

The diameter of the screw is determined from strength consideration and may be found from the expression:

$$d = C \sqrt{\frac{Q}{\sigma_p}}, \text{ mm} \tag{7.4}$$

where

Q is the required clamping force, kilogram

σ_p is the permissible tensile strength of the screw material; it may be taken as 8–10 kgf/mm² for mild steel screws

C is the safety factor; it may be taken as 1.4 for coarse pitch metric thread

In order to obtain the clamping force Q , the torque that needs to be applied on the screw head or the nut is given by the following expression:

$$T = r_m Q \tan(\alpha + \varphi_e) + T_{fr}, \text{ kgf-mm} \tag{7.5}$$

where

r_m is the mean diameter of the thread, millimeter

α is the helix angle of the thread, degrees

φ_e is the effective friction angle, degrees

T_{fr} is the friction torque at the end face of the nut or the screw, kilogram-force millimeter

The coefficient of effective friction f_e is related to the coefficient of sliding friction f by the following relation:

$$f_e = \frac{f}{\cos \alpha / 2}$$

For $\alpha = 60^\circ$, $f_e = 1.15 f$. Hence, at $f = 0.1$, $f_e = 0.115$ and $\varphi_e = \tan^{-1} 0.115 = 6^\circ 40'$ and at $f = 0.15$, $f_e = 0.1725$ and $\varphi_e = \tan^{-1} 0.1725 = 10^\circ 30'$.

The friction torque at the end face of the nut (Figure 7.48(d)) is given by the following expression:

$$T_{fr} = \frac{1}{3} f Q \frac{D_{ex}^3 - D_{in}^3}{D_{ex}^2 - D_{in}^2}, \text{ kgf-mm} \tag{7.6}$$

where D_{ex} and D_{in} represent the external and internal diameter respectively of the nut face.

For coarse-pitch metric thread, at $f = 0.15$, the standard values of the various parameters are as follows: $\alpha = 2^\circ 30'$ (for metric thread M8–M52), $\varphi = 10^\circ 30'$, $r_m = 0.45 d$.

On substituting these values in Eqs (7.5) and (7.6), we obtain

$$T \approx 0.1dQ + 0.05Q \frac{D_{ex}^3 - D_{in}^3}{D_{ex}^2 - D_{in}^2}, \text{ kgf-mm} \tag{7.7}$$

In order to produce torque T , a force P has to be applied on an arm of length l such that $T = Pl$.

On substituting this value in the above expression, we obtain the following expression for calculation of applied force P :

$$P = \frac{Q}{l} \left[0.1d + 0.05 \frac{D_{ex}^3 - D_{in}^3}{D_{ex}^2 - D_{in}^2} \right], \text{ kgf} \tag{7.8}$$

When the force is applied directly by the end face of the screw as in Figures 7.48(a), (b), and (c), then in Eqs (7.4) to (7.8), we put $D_{in} = 0$ and D_{ex} is understood to represent the diameter of the end face of the screw. Accordingly, the modified expression for force applied through the end face of screw is obtained as follows:

$$P = \frac{Q}{l} [0.1d + 0.05d], \text{ kgf} \quad (7.9)$$

Using Eqn. (7.9), simplified expressions for force P applied through the end face of screw can be derived.

Screw with spherical face (Figure 7.48(a))

In this case, due to point contact, the frictional torque component of the end face is absent, hence

$$P \approx \frac{Qd}{10l}, \text{ kg}$$

Screw with flat face (Figure 7.48(b))

$$P \approx (0.1d + 0.5d_1) \frac{Q}{l}, \text{ kg}$$

Screw with pad to avoid damage to surface (Figure 7.48(c))

$$P \approx (0.1d + 0.5r \cot \frac{\alpha_p}{2}) \frac{Q}{l}, \text{ kg}$$

where

r = radius of the spherical end of the screw, in millimeter

α_p = taper angle of the pad hole

Using Eqn. (7.8) and assuming $D_{in} = d$, the simplified expressions for force P applied through the nut face are obtained as follows:

For $D_{ex} = 1.7 d$,

$$P \approx \frac{Qd}{5l} \text{ kg}$$

For $D_{ex} = 2.0 d$,

$$P \approx \frac{Qd}{4.5l} \text{ kg}$$

The applied force must be checked to ensure that the clamping force Q does not exceed the maximum limit Q_{max} , which is found from Eqn. (7.4) as follows:

$$Q_{max} \leq \frac{\sigma_p d^2}{C^2}$$

On substituting $C = 1.4$, the above expression yields the following relation:

$$Q_{max} \leq 0.5d^2 \sigma_p \quad (7.10)$$

Taking the standard length of the tightening wrench which is generally $l = 14d$, the clamping force obtained is approximately 140 P for clamping force transmitted through the end face of the screw and (65–70) P for the clamping force transmitted through the end face of the nut.

Example 7.6

A workpiece is clamped by a screw clamp using M10 screw with a spherical face. If the required clamping force is 500 kg, determine the force to be applied on the screw handle of length 60 mm if the coefficient of friction is 0.15.

For the given M10 screw, $d = 10$ mm, $r_m = 4.5$ mm, $\phi_e = 10'30'$, and $\alpha = 2'30'$.

On substituting the above values in Eqn. (7.5) and taking $T_{fr} = 0$ for screw with spherical face, we find

$$P \times 60 = 4.5 \times 500 \times \tan(2'30' + 10'30')$$

$$P = \frac{4.5 \times 500 \times 0.231}{60} = 8.66 \text{ kg}$$

From the simplified relation, we obtain

$$P \approx \frac{Qd}{10l} = \frac{500 \times 10}{10 \times 60} = 8.33 \text{ kg}$$

The two values are fairly close and confirm the assumptions made in deriving the simplified relations.

Example 7.7

For the data given in Example 7.6, determine the applied force, if the screw has a flat face of diameter 7 mm.

From Eqn. (7.6), substituting $D_{ex} = 0$ and $D_{in} = 7$ mm, we find

$$T_{fr} = \frac{1}{3} \times 0.15Q \times 7 = 0.35Q$$

Now from Eqn. (7.5), we find

$$P \times 60 = 4.5 \times 500 \times 0.231 + 0.35 \times 500 = 11.58 \text{ kg}$$

From the simplified relation, we obtain

$$P = (0.1d + 0.05d_1) \frac{Q}{l} = \frac{500}{60} (0.1 \times 10 + 0.05 \times 7) = 11.25 \text{ kg}$$

Again, we find that the two values are fairly close

Eccentric-type clamping mechanism The main element of eccentric-type clamping mechanism is an eccentric, which may be circular or with a curved profile. Eccentric mechanisms are easy to manufacture and take much less time to apply the clamping force as compared to the screw mechanism. They are therefore also referred to as quick acting clamps. Their amplification factor is less than that of screw clamps; however, the clamping force that eccentric mechanism produces is sufficient for many jobs. Eccentric mechanism is used only in manually operated devices; therefore, it must be designed to ensure self-locking. The analysis is given below for a circular eccentric, but the basic approach of this analysis can also be easily adapted for an eccentric with curved profile.

A circular eccentric consists of a disc with a hole that is located with eccentricity relative to the external cylindrical surface (Figure 7.49(a)). Point A of smallest radius of the eccentric is placed opposite surface B of the workpiece on which the clamping force is to be applied. A gap m is maintained in this position for ease of setting of the workpiece. To clamp the workpiece, eccentric 1 is rotated by means of handle 2, displacing it from the initial position by angle α (Figure 7.49(b)) till the eccentric touches the workpiece surface B. After this, a force applied to the handle serves to press the eccentric against the workpiece surface, thereby clamping the workpiece.

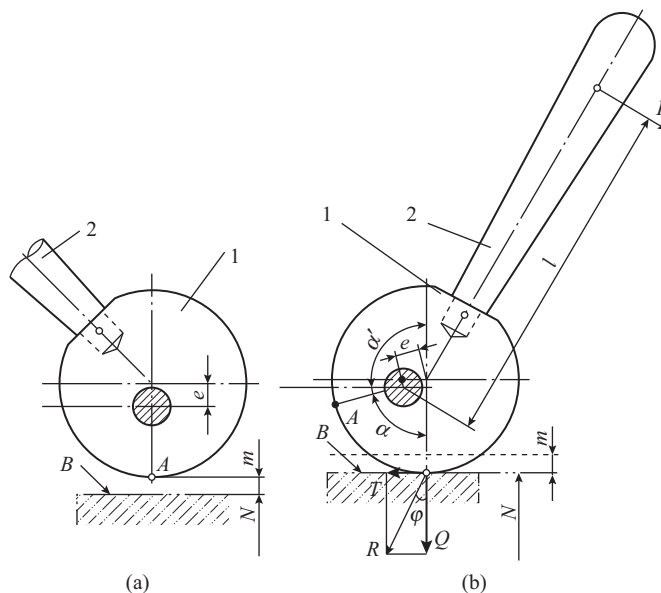


Figure 7.49 Eccentric-type clamping mechanism: (a) in initial position and (b) in clamping position

The angle of rotation of the eccentric α depends on the tolerance on dimension N of the workpiece. Therefore, angle α may vary depending on the actual dimension of a particular workpiece in a lot. Eccentricity e is decided by taking into consideration the desired gap m and the tolerance on dimension N to ensure that the eccentric does not have to be rotated through more than 150° to reach the point at which the clamping action begins. For a mechanism operating in dry condition

(without lubrication), assuming coefficient of friction between the eccentric and workpiece $f = 0.15$, the eccentricity for ensured self-locking is given by the following expression:

$$e \leq 0.05D \quad (7.11)$$

where D is the diameter of the external circular profile of the eccentric.

The applied force P is related to the clamping force Q by the following expression:

$$P \approx \frac{Qe}{l} [1 + \sin(\alpha' + \phi)], \text{ kg} \quad (7.12)$$

where

l = length of handle arm, mm

e = eccentricity, mm

ϕ = friction angle, degrees

$\alpha' = 180 - \alpha$, where α is the angle of rotation of the eccentric from its initial position

From Eqn. (7.12), it can be noted that the most unfavorable condition in which the eccentric produces the minimum clamping force occurs when $\sin(\alpha' + \phi)$ is maximum, that is, $\sin(\alpha' + \phi) = 1$ or $\alpha' + \phi = 90^\circ$. At $f = 0.12 - 0.15$, the friction angle $\phi \approx 8^\circ$, hence maximum $\alpha' = 82^\circ$. This corresponds to angle of rotation $\alpha = 180 - \alpha' \approx 100^\circ$.

It is good practice to use the middle portion of the eccentric that is actually close to $\alpha \approx 100^\circ$. Bearing this in mind, a simplified form of Eqn. (7.12) which is useful for design calculations is obtained by putting $\sin(\alpha' + \phi) = 1$ as follows:

$$P \approx \frac{2Qe}{l} \quad (7.13)$$

Width B of eccentric can be found from the following relation assuming Poisson's ratio $\mu = 0.25$ for both the eccentric and the workpiece materials and also assuming that both have the same modulus of elasticity

$$B = 0.035 \frac{QE}{D\sigma_b^2}, \text{ mm} \quad (7.14)$$

where

σ_b = permissible bearing stress; it may be taken as 1.5–2.0 kgf-mm²

E = modulus of elasticity of the eccentric and workpiece materials, kgf-mm²

Combining Eqs (7.11) and (7.12) and assuming $l = 2D$, which is typical for eccentric mechanisms, we find

$$P = \frac{2Qe}{l} = \frac{2Q \times 0.05D}{2D} = 0.05Q$$

Hence,

$$Q = 20P$$

Thus, we see that typical amplification factor for eccentric mechanism is 20 which is considerably less than that of the screw mechanism.

Example 7.8

A workpiece is clamped by an eccentric clamp of diameter 50 mm and eccentricity 2.5 mm. If the coefficient of friction is 0.15 and the eccentric is rotated through 100° to execute the clamping, determine the force to be applied on the handle of length 100 mm in order to obtain a clamping force of 500 kg.

Referring to Eqn. (7.12), we find

$$e = 2.5 \text{ mm}, l = 100 \text{ mm} \quad \alpha' = 180 - 100 = 80^\circ$$

$$\phi = \tan^{-1} f = \tan^{-1} 0.15 = 8^\circ$$

On substituting these values in Eqn. (7.12), we obtain

$$P = \frac{500 \times 2.5}{100} [1 + \sin(80 + 8)] = 24.99 \text{ kg}$$

From the simplified relation, we obtain

$$P = \frac{2Qe}{l} = \frac{2 \times 500 \times 2.5}{100} = 25.0 \text{ kg}$$

Different types of eccentrics are shown in Figure 7.50. A solid circular eccentric is shown in Figure 7.50(a) and a forked circular eccentric in Figure 7.50(b). The latter has less circular

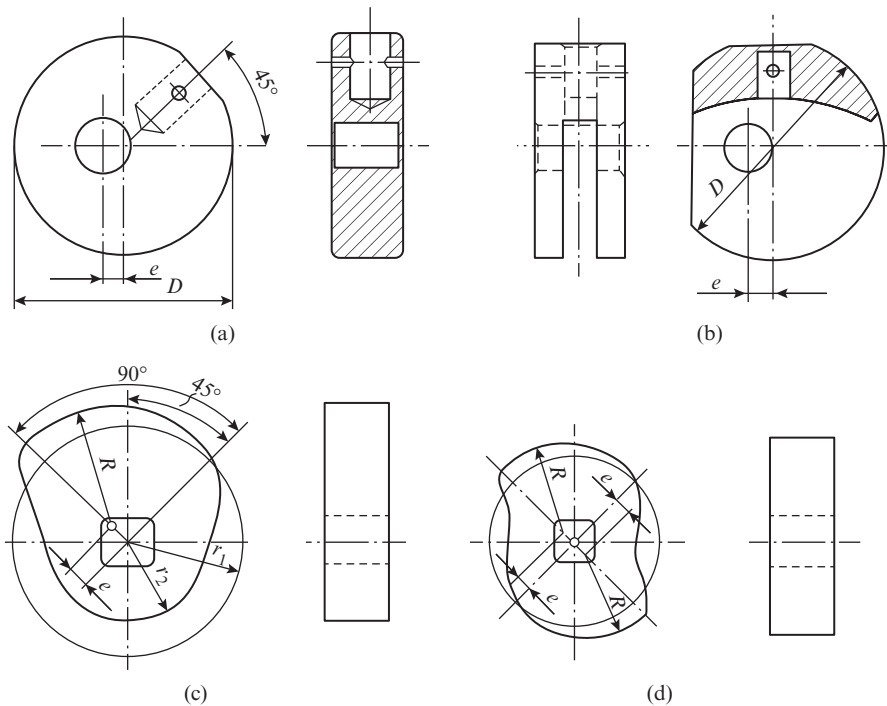


Figure 7.50 Type of eccentrics: (a) solid circular eccentric, (b) forked circular eccentric, (c) single-profile eccentric cam, and (d) double-profile eccentric cam

profile available for clamping as part of the profile is truncated. Two designs of cam-type eccentrics are shown in Figures 7.50(c) and (d). The operating segments of these eccentric are also made as circular arcs with the axis displaced relative to the axis of the cam centre hole. The circular eccentrics and cam-type eccentrics with circular profile are easy to manufacture, but their rotation is limited to 150–160°, which restricts the throw to a maximum of 2 e.

For greater throw, cam-type eccentrics with curved profile are used. The curved profile may be an involute, Archimedean spiral or logarithmic spiral. These eccentrics allow rotation of the order of 300–320°, which explains the greater throw available with these mechanisms. An additional advantage of these eccentrics is that the self-locking ability either increases (for involutes and Archimedean spiral) or remains constant (logarithmic spiral) with the angle of rotation, unlike circular eccentrics which suffer from reduced self-locking ability at large angles of rotation.

Wedge-type clamping mechanism Wedge-type mechanisms are generally used as intermediate element in clamping devices with power drive. They are compact and easy to manufacture and also allow the applied force to be amplified and changed in direction.

A simple wedge mechanism is shown in Figure 7.51. Taking the projections of forces in the horizontal direction, we find

$$F_1 = Q \tan \phi_1, \quad F_2 = Q \tan(\alpha + \phi) \tag{7.15}$$

Hence from the condition of equilibrium of the forces in the horizontal direction, we see that applied force $P = F_1 + F_2$, i.e.

$$P = Q [\tan(\alpha + \phi) + \tan \phi_1] \text{ kg} \tag{7.16}$$

where

Q = clamping force

α = wedge angle

$\phi = \tan^{-1} f$ = friction angle on the inclined surface A of the wedge

$\phi_1 = \tan^{-1} f_1$ = friction angle on the base B of the wedge

f = coefficient of friction between wedge 1 and plunger 2

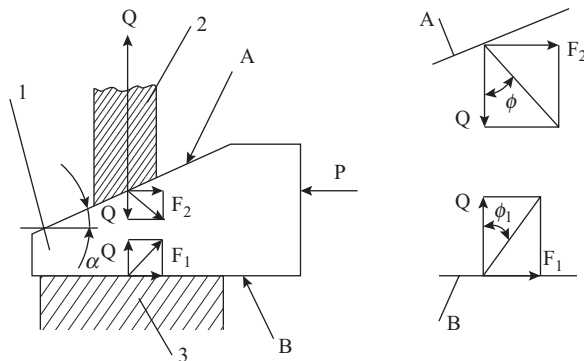


Figure 7.51 Simple wedge-type clamping mechanism

f_1 = coefficient of friction between wedge 1 and fixture body 3

For self-locking of the mechanism, the following condition should be satisfied:

$$\alpha < \varphi + \varphi_1$$

Self-locking wedge-type mechanisms are sometimes made with two inclined surfaces at angle α and β , respectively (Figure 7.52). While sliding over face 1 at angle β plunger 2 quickly approaches the workpiece surface on which the clamping force is to be applied. Now moving along the less steep face 3 of angle α , the clamping is actually executed.

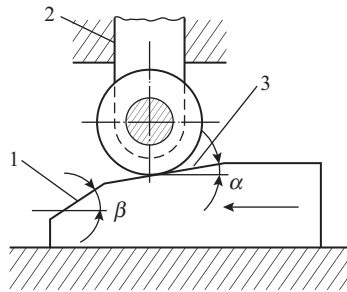


Figure 7.52 Wedge mechanism with two inclined surfaces

The wedge is generally finish machined; therefore, the coefficient of friction f and f_1 lie between 0.1 and 0.15. At $f = f_1 = 0.1$, $\varphi = 5^\circ 43'$ and at $f = 0.15$, $\varphi = 8^\circ 30'$. Therefore, the condition for self-locking for friction only on the inclined surface is $\alpha < 5^\circ 43'$ at $f = 0.1$ and $\alpha < 8^\circ 30'$ at $f = 0.15$. For friction on inclined face and base, the condition for self-locking is $\alpha < 2 \times 5^\circ 43'$, that is, $\alpha < 11^\circ$ at $f = 0.1$ and $\alpha < 2 \times 8^\circ 30'$, $\alpha < 17^\circ$ at $f = 0.15$.

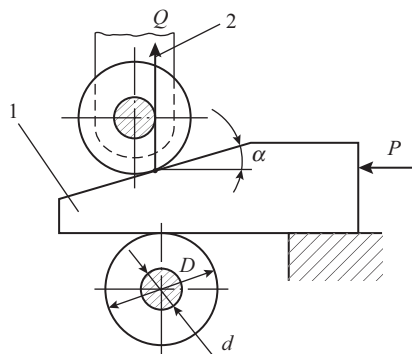


Figure 7.53 Wedge mechanism with roller followers

To reduce friction, wedge mechanisms are often used in combination with roller followers (Figure 7.53), which allows the clamping force Q to be increased by 30–50 percent for the same applied force P . The relation between P and Q is in the case also expressed by Eqn. (7.15) but with modified values of friction angle.

$$P = Q[\tan(\alpha + \phi_{rf}) + \tan \phi_{1rf}] \text{ kg} \tag{7.17}$$

Here ϕ_{rf} and ϕ_{1rf} are the coefficient of rolling friction that are found from the following relations:

$$\tan \phi_{rf} = \frac{d}{D} \tan \phi; \quad \tan \phi_{1rf} = \frac{d}{D} \tan \phi_1$$

where D and d represent the roller diameter and the centre hole diameter of the roller, respectively

Wedge mechanisms with roller followers are mostly power driven; therefore, they are free from the need of self locking. Consequently, the wedge angle α in these mechanisms is usually $\geq 10^\circ$.

In jigs and fixtures, wedge mechanisms are used in various configurations as shown in Figure 7.54, including two wedge-plunger mechanisms without rollers (Figures 7.54(a) and (b)) and two with roller followers (Figures 7.54(c) and (d)). Consider the case depicted in Figure 7.54(a).

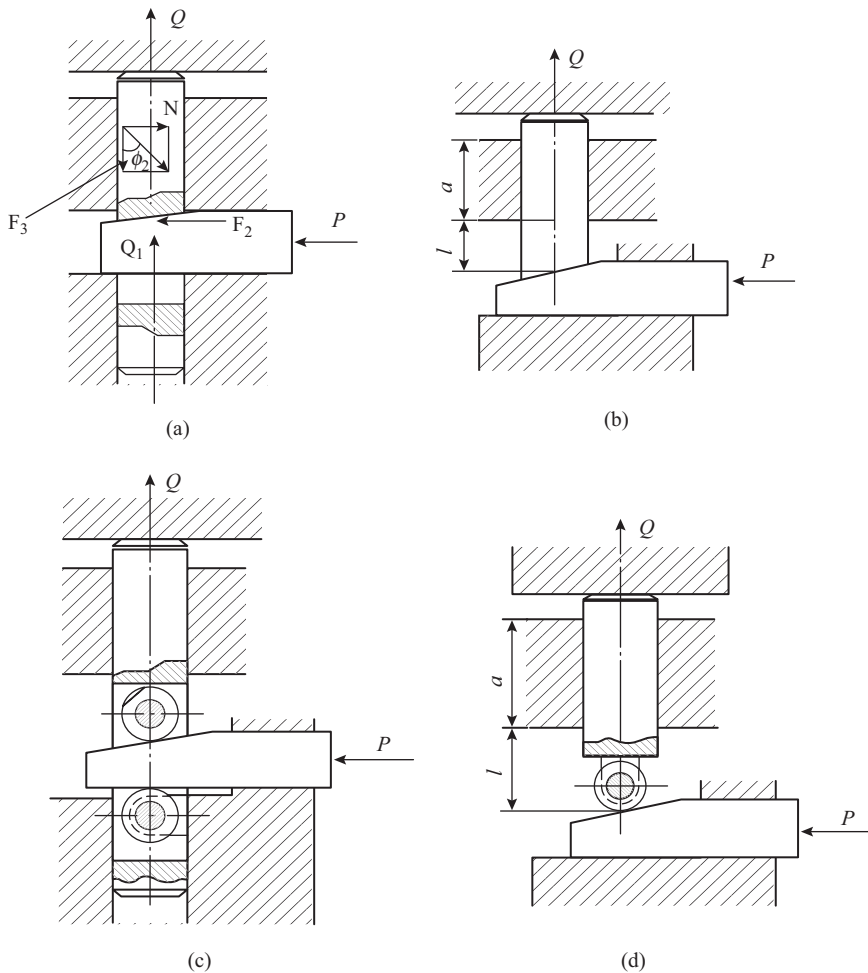


Figure 7.54 Wedge mechanism with plunger followers: (a) with two plungers, (b) with single plunger, (c) with two roller plungers, (d) with single roller plunger

From the conditions of equilibrium, we see that

$$F_2 = N,$$

$$Q = Q_1 - F_3 = Q_1 - N \tan \phi_2 = Q_1 - F_2 \tan \phi_2$$

We know from Eqs (7.15) and (7.16) that

$$Q_1 = \frac{P}{\tan(\alpha + \phi) + \tan \phi_1} \text{ and}$$

$$F_2 = \frac{P \tan(\alpha + \phi)}{\tan(\alpha + \phi) + \tan \phi_1}$$

where P is the applied force and ϕ , ϕ_1 , and ϕ_2 represent the friction angle on the inclined surface of wedge, base of wedge, and the vertical plunger side, respectively.

On substituting for Q_1 and F_2 in the expression of Q above, we obtain

$$Q = \frac{P}{\tan(\alpha + \phi) + \tan \phi_1} - \frac{P \tan(\alpha + \phi)}{\tan(\alpha + \phi) + \tan \phi_1} \tan \phi_2$$

$$Q = \frac{P[1 - \tan(\alpha + \phi)] \tan \phi_2}{\tan(\alpha + \phi) + \tan \phi_1}$$

where from

$$P = Q \frac{\tan(\alpha + \phi) + \tan \phi_1}{1 - \tan(\alpha + \phi) \tan \phi_2} \quad (7.18)$$

Similar relations can be derived for the other mechanisms of Figure 7.54 and the final expressions are given below.

For the wedge-cum-single plunger mechanism shown in Figure 7.54(b),

$$P = Q \frac{\tan(\alpha + \phi) + \tan \phi_1}{1 - \tan(\alpha + \phi) + \tan \phi_{2p}} \quad (7.19)$$

where

$$\tan \phi_{2p} = \frac{3l}{a} \tan \phi_2$$

For the wedge-cum-double plunger with roller followers shown in Figure 7.54(c).

$$P = Q \frac{\tan(\alpha + \phi_{rf}) + \tan \phi_{1rf}}{1 - \tan(\alpha + \phi_{rf}) + \tan \phi_2} \quad (7.20)$$

For the wedge-cum-single plunger with roller follower shown in Figure 7.54(d),

$$P = Q \frac{\tan(\alpha + \phi_{rf}) + \tan \phi_1}{1 - \tan(\alpha + \phi_{rf}) + \tan \phi_{2rf}} \quad (7.21)$$

where

$$\tan \varphi_{2rf} = \frac{3l}{a} \tan \varphi_2$$

Angles φ_{rf} and φ_{1rf} have already been defined with reference to Eqn. (7.17).

For approximate evaluation of the amplification factor of wedge consider Eqn. (7.16). The amplification factor is determined by the term $[\tan(\alpha + \phi) + \tan \phi_2]$. For the condition of friction only on the inclined face, taking $\phi = \phi_1 = 5^\circ 43'$ at $f = 0.1$ and $\alpha = 5^\circ 43'$ to ensure self-locking, we find from Eqn. (7.16) that

$$\begin{aligned} P &= Q[\tan(5^\circ 43' + 5^\circ 43') + \tan 5^\circ 43'] \\ &\approx 0.3 Q \end{aligned}$$

Hence, the amplification is only about 3.33 times. For the plunger with roller, it is of the order of 4.5 times. The small value of amplification factor of wedge-type mechanism as compared to the screw-type and eccentric-type mechanisms explains why the wedge type mechanisms are not suitable for manual operation and are meant mostly to serve as intermediate mechanism between the power drive and the clamping element.

Example 7.9

A workpiece is clamped by a wedge clamp of wedge angle 12° . If the coefficient of friction between the wedge and plunger and the wedge and fixture body is 0.15, determine the pulling force to be applied on the wedge to obtain a clamping force of 500 kg on the plunger. Also check the mechanism for self-locking.

First of all, we check the condition of self-locking, for the given values of $f = f_1 = 0.15$, we find $\varphi = \varphi_1 = \tan^{-1} 0.15 = 8.0^\circ$. As wedge angle $\alpha = 12^\circ$ is less than $\phi + \phi_1$, the condition of self-locking is satisfied.

On substituting the given values in Eqn. (7.16), we obtain

$$P = 500 [\tan(12 + 8) + \tan 8] = 257 \text{ kg}$$

Example 7.10

For the data given in Example 7.9, determine the pulling force, if plungers with roller followers are used. The roller and roller pin diameter is 20 and 5 mm, respectively.

The coefficients of rolling friction are found from the expressions for the already known values of $\varphi = \varphi_1 = 8.0^\circ$

$$\tan \varphi_{rf} = \tan \varphi_{1rf} = \frac{d}{D} \tan 8 = \frac{6}{20} \tan 8^\circ = 0.045,$$

Hence,

$$\varphi_{rf} = \varphi_{1rf} = 2^\circ 30'$$

On substituting these values in Eqn. (7.17), we obtain

$$P = 500 [\tan(12 + 2^\circ 30') + \tan 2^\circ 30'] = 151.8 \text{ kg}$$

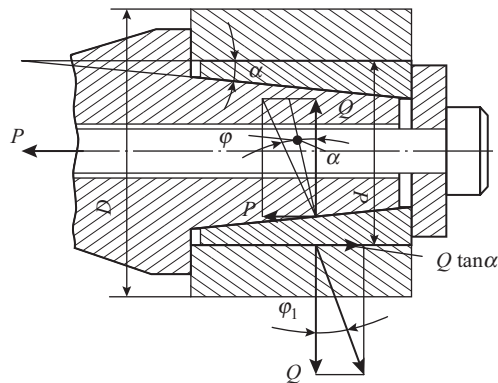


Figure 7.55 Schematic for establishing relation between clamping force and drawing force in expanding mandrel

Expanding mandrels that are used for location and clamping of workpiece with holes also employ a wedge mechanism. In the expanding mandrel shown in Figure 7.55, the relation between the drawing force P and clamping force Q is the same as in a single taper wedge and is given by Eqn. (7.16). The required axial force depends on cutting force P_z and is determined by the condition that the cutting moment should be less than the clamping moment, that is

$$P_z \frac{D}{2} < Q \frac{d}{2}$$

where from

$$Q = \frac{P_z D}{d}$$

Here,

D = diameter of the workpiece

d = diameter of the expanding mandrel

On substituting this value of Q in Eqn. (7.16) and introducing safety factor K for the cutting force, the following relation is obtained for the pulling force in an expanding mandrel:

$$P = \frac{P_z DK}{d} [\tan(\alpha + \phi) + \tan \phi_1]$$

Here, α , ϕ , and ϕ_1 have the same meaning as in Eqn. (7.16).

Spring collet chucks that are used for location and clamping of cylindrical workpieces on the external diameter also use a wedge mechanism (Figure 7.56). The drawing force required to clamp the workpiece in this case is given by an expression similar to Eqn. (7.15) as follows:

$$P = (P_1 + Q) \tan(\alpha + \phi) \quad (7.22)$$

Here,

α = half-included angle of the collet taper

ϕ = friction angle

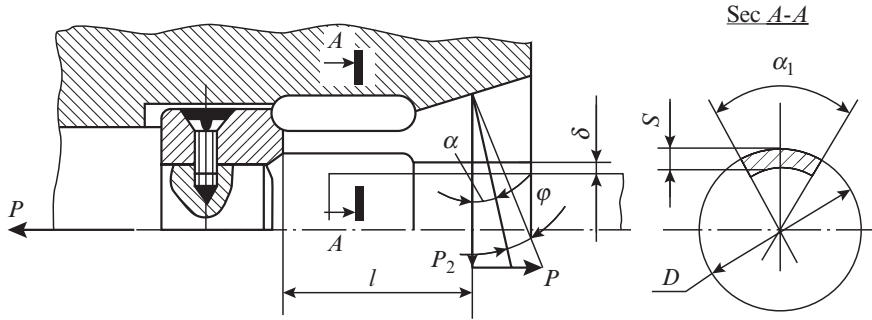


Figure 7.56 Schematic for establishing relation between clamping force and drawing force in spring collet chuck

$P_1 = \frac{3EI\delta z}{l^3}$ represents the force required to close the jaws till they come in contact with the

work surface

Q = clamping force exerted by all the jaws of the collet

E = modulus of elasticity of collet steel = 2.1×10^6 kgf-cm²

l = distance from root of jaw to the middle of taper

δ = deflection of the jaw which is equal to the clearance between the collet and workpiece before clamping

z = number of jaws of the collet

I = moment of inertia of the collet root section

$$I = \frac{D^3 S}{8} \left[\alpha_1 + \sin \alpha_1 \cos \alpha_1 - \frac{2 \sin^2 \alpha_1}{\alpha} \right]$$

where

α_1 = angle through which the jaw extends circumferentially in degrees

D = outside diameter of the jaws

S = thickness of the jaws

Lever-type clamping mechanisms These mechanisms consist of simple or pivoted straps that are pressed against the work surface generally by means of a screw or eccentric mechanism. Some common configurations of lever mechanisms are shown in Figure 7.57.

For the lever mechanisms shown in Figures 7.57(a) through (c), the applied force P and clamping force Q are related by the following expression:

$$Q = \eta \frac{l_1}{l_2} P, \text{ kg} \quad (7.23)$$

In the lever mechanism shown in Figure 7.57(d), P and Q are related by the following expression:

$$Q = \eta \frac{l}{L} P, \text{ kg} \quad (7.24)$$

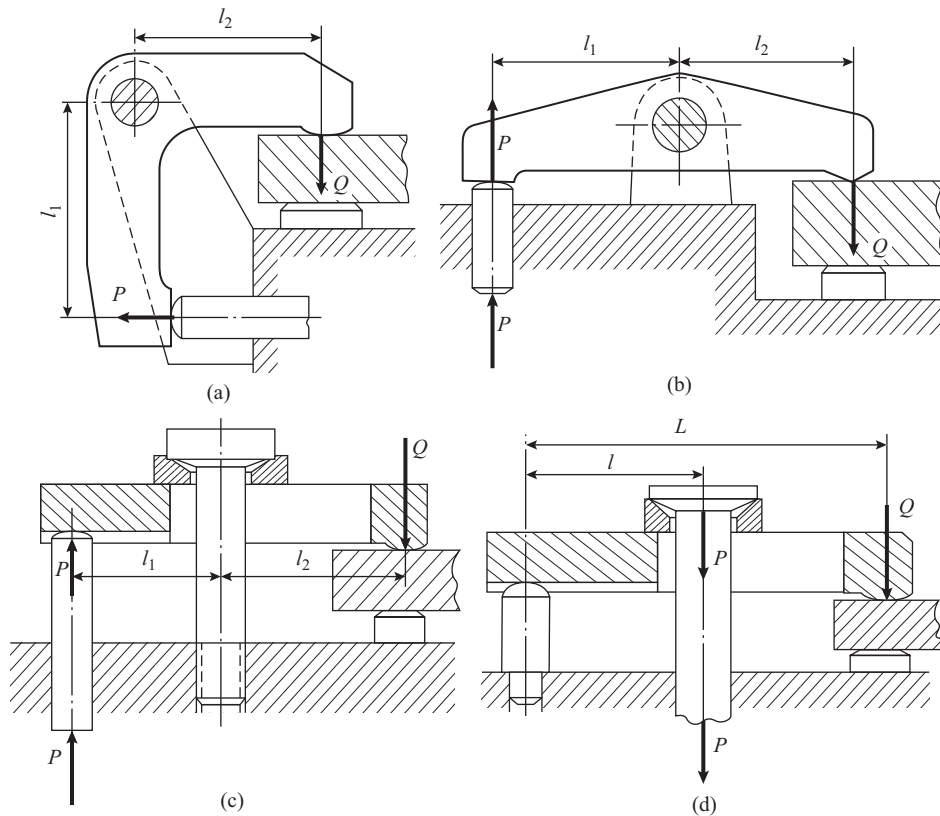


Figure 7.57 Lever-type clamping mechanisms: (a) with double-end bent lever clamp, (b) with double-end straight lever clamp, (c) with clamp supported in the middle, and (d) with clamp supported at one end

In Eqs (7.23) and (7.24), l_1 , l_2 , l , and L represent arms of the lever and η is an efficiency coefficient that accounts for frictional losses in the joints; generally, $\eta \approx 0.95$.

Self-centering three-jaw chuck is one of the most popular fixture used on lathe, turret lathe, and several other machine tools for location and clamping of cylindrical parts. A self-centering three-jaw chuck (Figure 7.58) basically consists of a combination of three clamping mechanisms:

- (i) A lever mechanism involving moments Pl and P_3r_1 about the axis of the small bevel gear
- (ii) A second lever mechanism involving moments P_2r_2 and P_1r_m about the axis of the spiral gears
- (iii) Wedge mechanism with plunger in which the spiral and the rack at the back of the jaw constitutes the wedge, developing force Q_1 and the three jaws themselves act as plungers

The analysis of this mechanism is very complex. However, the end result in terms of relation between the maximum torque on the tightening key and the total clamping force produced by the three jaws is given in Table 7.2.

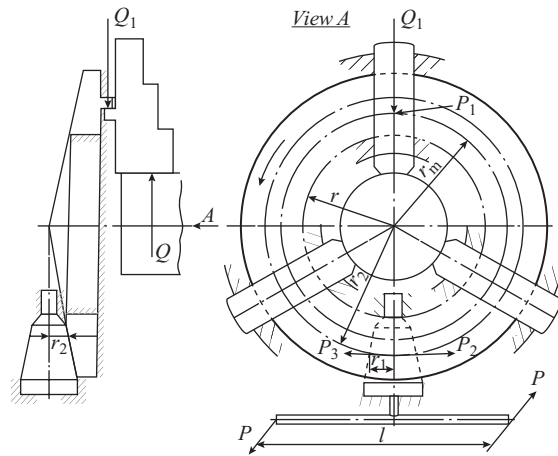


Figure 7.58 Schematic of mechanisms in a self-centering 3-jaw chuck

Table 7.2 Clamping force in a three-jaw chuck

| Diameter of chuck mm | Maximum torque on tightening key (kgf-cm) | Total clamping force in 3-jaws(kgf) |
|-------------------------|--|--|
| 80 | 3.5 | 800 |
| 100 | 5.0 | 900 |
| 125 | 7.5 | 1,700 |
| 160 | 12.5 | 2,500 |
| 200 | 16.0 | 3,000 |
| 250 | 18.0 | 4,500 |
| 320 | 20.0 | 5,500 |
| 400 | 28.0 | 6,500 |
| 500 | 36.0 | 8,500 |
| 630 | 46.0 | 10,500 |

Toggle-type clamping mechanisms These mechanisms use hinged rigid links for movement of the clamping element and exerting the desired clamping force on the workpiece. They are used in manually operated as well as powered clamping devices. Toggle mechanisms come in a very wide range of configurations. Two configurations namely the single-link and double-link toggle mechanisms that are commonly employed in clamping devices are discussed here.

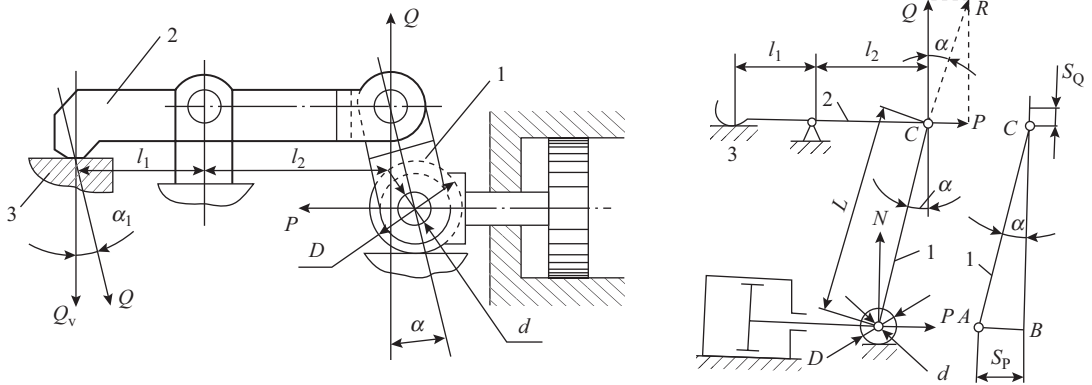


Figure 7.59 Force analysis in a single-link toggle mechanism

The schematic of a single-link toggle mechanism is shown in Figure 7.59. As link 1 rotates, it clamps workpiece 3 by applying pressure through link 2 (strap). The applied force P and reaction N of roller support produce a resultant R directed along link 1. On being resolved at the hinge C , force R yields forces Q and P . For an ideal mechanism (ignoring frictional losses),

$$Q = \frac{P}{\tan \alpha} \quad (7.25)$$

Hence at $\alpha = 0$, an ideal toggle mechanism can theoretically produce vertical force $Q = \infty$. In a real mechanism, the following relation holds good:

$$Q = \frac{P}{\tan(\alpha + \beta) + \tan \phi_{\text{fr}}} \quad (7.26)$$

where β is a supplementary angle that accounts for frictional losses due to sliding friction in the hinged joints and is found from the following expression:

$$\sin \beta = \frac{df}{L} \quad (7.27)$$

where

f = coefficient of sliding friction in the hinged joint and the roller axle

d = diameter of the hinge and the roller axle

L = length of the link

In Eqn. (7.26), ϕ_{fr} is the coefficient of rolling friction that accounts for frictional losses on the roller surface. It is found from the following relation,

$$\tan \phi_{\text{fr}} = \frac{d}{D} \tan \phi_1$$

where

- φ_1 = friction angle at the roller under sliding friction
- d = diameter of roller axle
- D = diameter of the roller

An important characteristic of toggle mechanisms is the available travel margin for clamping. For the position of the link shown in Figure 7.59, the maximum possible displacement of the input link is AB when the link 1 becomes vertical. From ΔABC , we find

$$S_p = AB = L \sin \alpha$$

The corresponding movement of hinge C is

$$S_Q = L - BC = L - L \cos \alpha$$

$$S_Q = L(1 - \cos \alpha) \tag{7.28}$$

The quantity S_Q represents the available travel margin for bringing the strap into contact with the work surface before applying the clamping force. For $L = 100$ mm, the value of S_Q at $\alpha = 10^\circ$ will be 1.5 mm and at $\alpha = 5^\circ$ it will be 0.5 mm. It is generally recommended to have $\alpha = 10^\circ$ to have some margin for accommodating variation in the workpiece dimensions and yet have a margin of 0.5 mm corresponding to $\alpha = 5^\circ$ for tightening. In view of the short travel margin, toggle mechanisms take very little time in clamping and are therefore categorized as quick acting mechanisms.

Some standard configurations of double-link toggle mechanisms are shown in Figure 7.60. The configurations shown in Figures 7.60 (a) and (b) are single action and those shown in Figures 7.60(c) and (d) are double action.

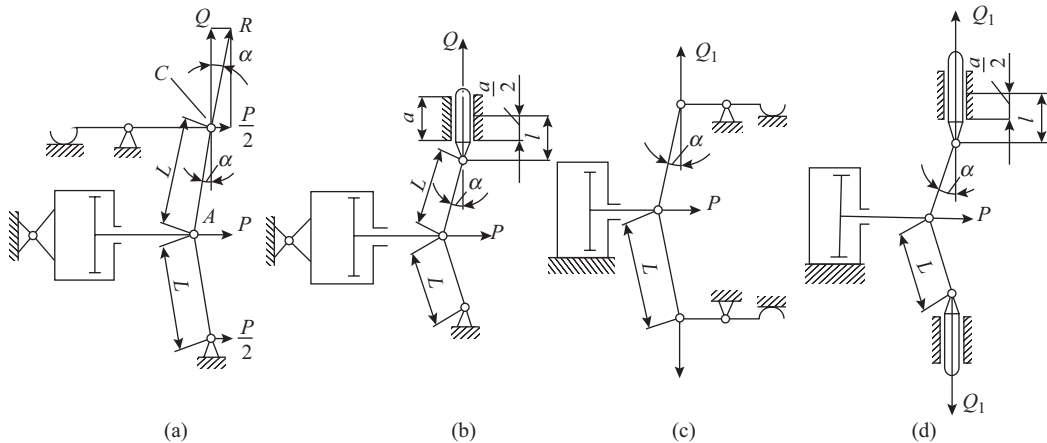


Figure 7.60 Schematic of double-link toggle mechanisms: (a) single-action, (b) single-action with plunger, (c) double-action, and (d) double-action with plungers

For an ideal mechanism (ignoring frictional losses), it can be noted from Figure 7.60(a) that

$$\frac{P/2}{Q} = \tan \alpha$$

Hence,

$$Q = \frac{P}{2 \tan \alpha} \quad (7.29)$$

In a real mechanism, considering friction in the hinged joints, we obtain

$$Q = \frac{P}{2 \tan(\alpha + \beta)} \quad (7.30)$$

Here, β has the same meaning as in the previous case

For the mechanism shown in Figure 7.60(b), the friction in the plunger also has to be taken into consideration. Hence, the relation between P and Q can be obtained as follows:

$$Q = \frac{P}{2} \left[\frac{1}{\tan(\alpha + \beta)} - \tan \phi_{2p} \right] \quad (7.31)$$

where

ϕ_{2p} = friction angle on the plunger side surface

Angle ϕ_{2p} is found from the following relation:

$$\tan \phi_{2p} = \frac{3l}{a} \tan \phi_2$$

where

ϕ_2 = friction angle corresponding to sliding friction condition between the plunger and guideway

a = length of guideway

l = distance from the hinge to the middle of the guideway

For $\frac{l}{a} = 0.7$ and $\tan \phi_2 = 0.1$, $\tan \phi_{2p} = 0.21$

The travel margin of the double-link toggle mechanism is $S_Q = 2L(1 - \cos \alpha)$; that is, it is twice that of the single link mechanism. This happens because of raising of point C due to straightening of the main upper link and also due to raising of point A due to straightening of the lower link.

The double-action toggle mechanisms shown in Figures 7.60(c) and (d) can be looked upon as paired set of the corresponding single-link mechanism. Hence, for the ideal mechanism the total force Q is found as follows:

$$Q_{\text{total}} = 2Q_1 = \frac{P}{\tan \alpha}$$

For a real mechanism without plunger (Figure 7.60(c)), the relation between Q_{total} and P is given by the following expression:

$$Q_{\text{total}} = 2Q_1 = \frac{P}{\tan(\alpha + \beta)} \quad (7.32)$$

For a real mechanism with plunger (Figure 7.60(d)), the relation between Q_{total} and P is given by the expression:

$$Q_{\text{total}} = 2Q_1 = P \left[\frac{1}{\tan(\alpha + \beta)} - \tan \phi_{2p} \right] \quad (7.33)$$

The meaning of the terms β and ϕ_{2p} is the same as explained above for double-link single-action toggle mechanism shown in Figures 7.60(a) and (b).

In all the toggle mechanisms discussed above, the clamping force acting on the workpiece is obtained by multiplying Q with the lever amplification factor (see Eqn. (7.23)).

Rack-and-pinion-type clamping mechanism The schematic of a rack-and-pinion-type clamping mechanism is shown in Figure 7.61. It consists of rack 3 and pinion 5 mounted on shaft 4. When handle 6 is rotated counter clockwise, the rack moves downward to secure the workpiece with strap 2. To retain the clamping force after the operator has removed his hand from the handle, a self-locking device is required as an integral part of the clamping mechanism.

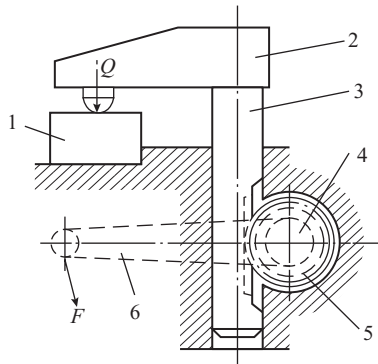


Figure 7.61 Rack-and-pinion-type clamping device

The locking device prevents the pinion from turning in the reverse direction. Locking devices come in various designs. A simple design known as roller lock (Figure 7.62) is described here. It consists of a driving sleeve 3 with a slot for roller 1 which is in contact with a flat on shaft 2 on which the pinion is mounted. Driving sleeve 3 is secured to the handle of the clamping mechanism. When the handle is turned in the direction of arrow, rotation is transmitted to the pinion shaft through roller 1. When the pinion shaft tends to turn in the reverse direction, it jams

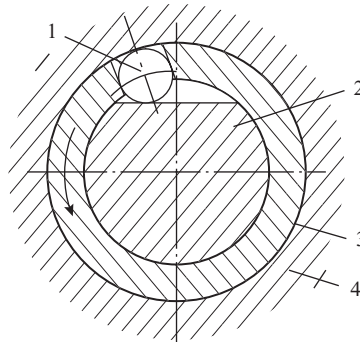


Figure 7.62 Locking device for rack and pinion mechanism

roller 1 between the surface of the bore in body 4 and the flat on shaft 2, thereby locking the system in the clamped position

7.3.4 Clamping Elements and Devices

Clamping devices using screw-type clamping mechanism apply the clamping force on the workpiece either directly as shown in Figures 7.48(a) and (b) or through a pad (Figure 7.48(c)). Generally, a floating pad is preferred as it has the following advantages:

- (i) It reduces the possibility of workpiece displacement during clamping.
- (ii) It compensates for deviation from perpendicularity between the screw toe and workpiece surface.
- (iii) It reduces the possibility of denting of the work surface.
- (iv) It minimizes the possibility of bending of the screw if the surface to be clamped is not perpendicular to the screw axis.

Variations in the design of screw clamps are associated with the manner of retention of the floating pad. A screw clamp with three different designs of floating pad is shown in Figure 7.63.

The simplest and probably the most commonly used clamping element is a strap. All straps operate on the principles of levers. A strap may occupy a fixed position; but in this case, considerable time may be spent in retraction of the strap during loading/unloading of the workpiece. Therefore, to reduce this time, the strap may be provided with a slot and an elongated groove that permits linear withdrawal or with a hole that permits rotational withdrawal by swinging (Figure 7.64). Which of the two is selected depends on the space constraints in each given case.

A strap can be used in combination with all the clamping mechanisms described in Section 7.3.3. Therefore, to distinguish between the large varieties of clamping devices that result from these combinations, often the name of the prominent mechanism is given to the complete device.

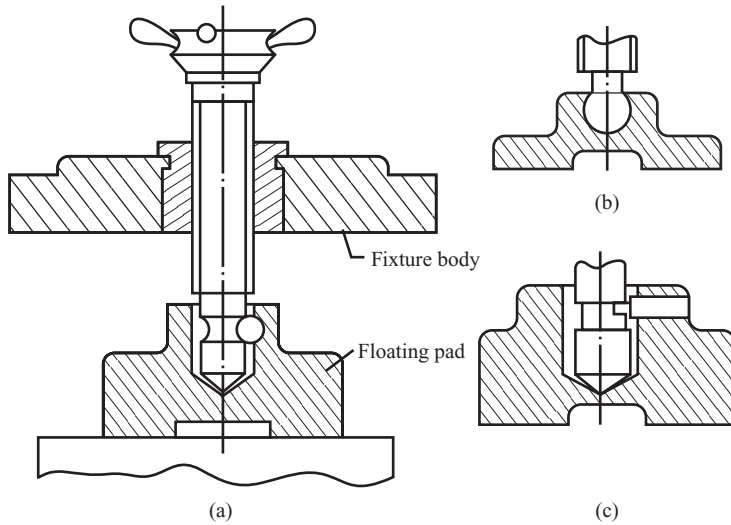


Figure 7.63 Screw clamp with floating pad: (a) with pin for light duty work, (b) with socket joint, and (c) with pin for heavy duty work

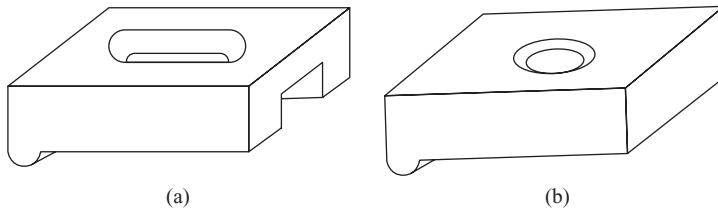


Figure 7.64 Type of straps: (a) slotted strap for liner withdrawal and (b) swinging strap for withdrawal by rotation

Figure 7.65 (a) shows a screw clamp using a slotted strap and Figures 7.65(b) and (c) screw clamps with swinging strap. The heel (fulcrum) may be a pillar pin, fixed extension of the fixture body or an adjustable heel as shown in Figures 7.65(a) (b) and (c), respectively. The design with adjustable heel is the most versatile as it allows setting of the strap height by changing the pin fitted in the fixture body. The screw clamp shown in Figure 7.65(a) is provided with a spherical washer for proper seating of the nut, washer, and strap when the workpiece height varies. The upper part of the spherical washer fits properly under the nut and the lower part fits on the strap even if the stud and strap are not perpendicular to each other. The tightening force in manually operated strap clamps may be applied by hand knobs as shown in Figures 7.65(a) and (b), or by a hexagonal nut as shown in Figure 7.65(c). The different types of handles used in screw and strap clamps are shown in Figure 7.66.

Examples of fixtures in which the strap is used in combination with eccentric, wedge, and toggle mechanism are shown in Figure 7.67. In view of the fact that the clamping time in these designs is much less than in screw clamps, they are also referred to as quick acting clamping devices. The devices in which the strap is provided at the center are also known as pivoted strap clamps.

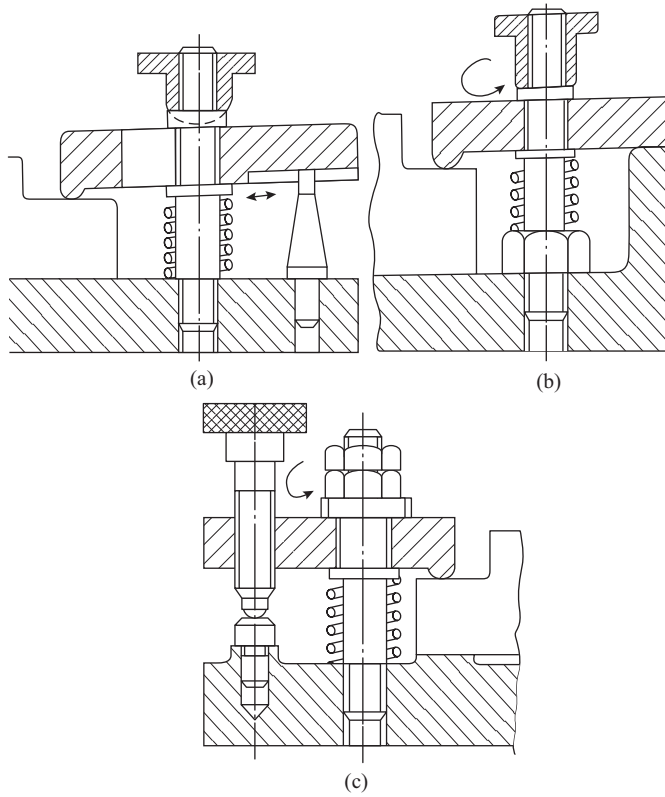


Figure 7.65 Types of screw clamps: (a) with pillar pin and slotted strap, (b) with fixed heel and swinging strap, and (c) with adjustable heel and swinging strap

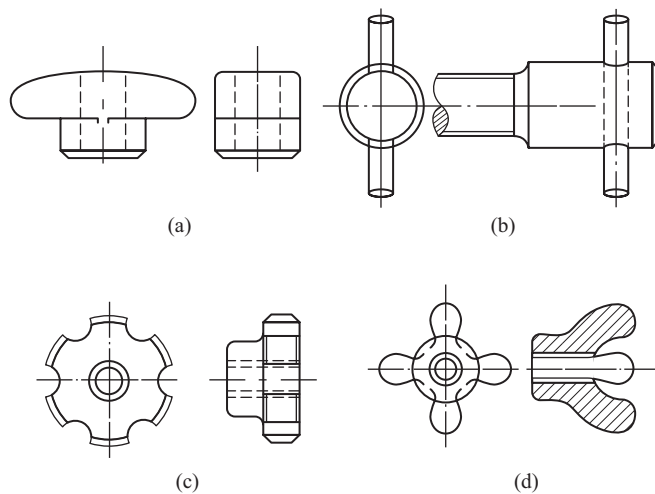


Figure 7.66 Types of handles used in screw clamps: (a) plain flat handle, (b) plain handle with rod, (c) star-shaped handle, and (d) circular fluted handle

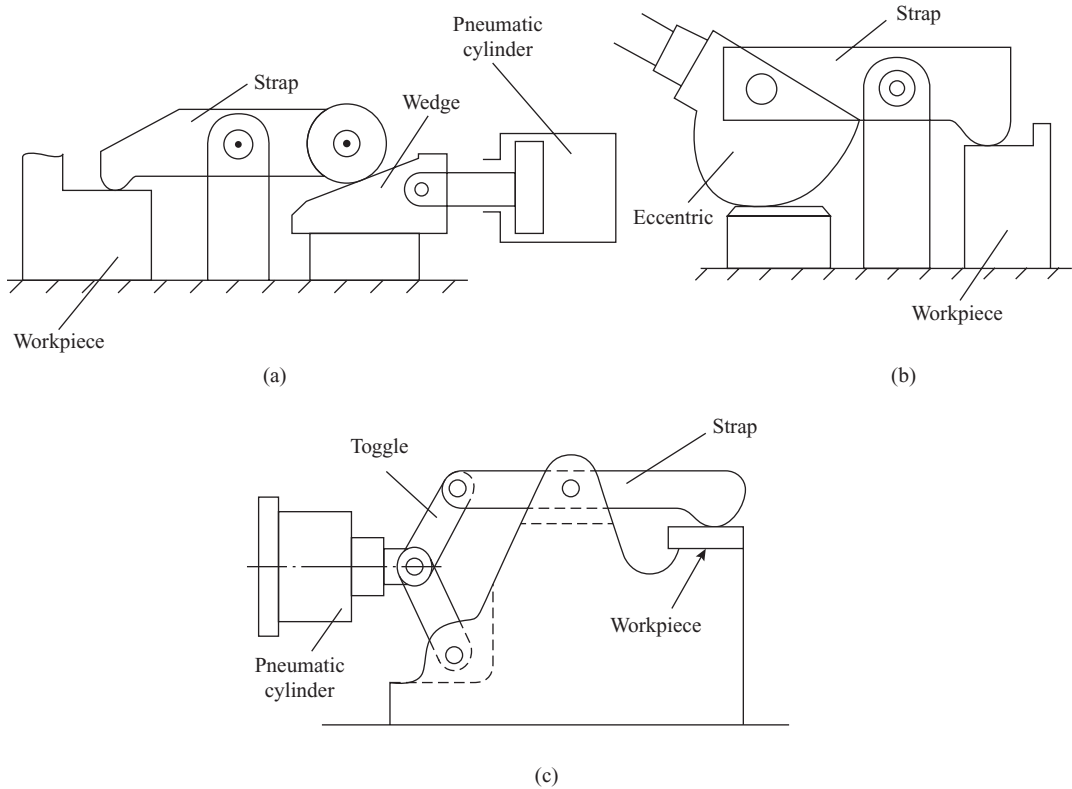


Figure 7.67 Quick acting clamps: (a) air-operated wedge-type pivoted strap clamp, (b) cam-operated pivoted strap clamp, and (c) air-operated toggle strap clamp

To illustrate the manner in which the various features are reflected in naming a particular clamping device, the device shown in Figure 7.67(b) would be called quick acting cam operated pivoted strap clamp and the one shown in Figure 7.67(a) as quick acting pneumatic wedge-type pivoted strap clamp.

In some jigs/fixtures, it is necessary to lift the lid/closing plate of the fixture for loading/unloading of the workpiece. Hinged clamps are found to be useful in this situation. Two designs of hinged clamps are shown in Figure 7.68. In the design shown in Figure 7.68(a), the pillar with the lever nut is swung aside and the hinged lid is lifted for loading/unloading of the workpiece. The floating pad is made integral with the lid, and its shape is decided by the contour of the workpiece to be clamped. In the design shown in Figure 7.68(b), the latch carrying the eye bolt is swung aside for loading/unloading of the workpiece which is located on a cylindrical pin.

One more category of clamps that are useful in the same type of application as hinged clamps and are very simple in design are the so called C-clamps. The simple C-clamp (Figure 7.69(a)) is removed and kept aside to provide access for loading/unloading of the workpiece, whereas the captive C-clamp (Figure 7.69(b)) is swung aside by rotating it about the fixed pin. An added advantage of these clamps is that when the clamp is removed or moved aside, the tightening nut remains in place. Therefore, unloosening the nut by just 1–2 threads is enough for removal of the clamp and a similar small movement of the nut is sufficient for clamping the job. The C-clamps are therefore also referred as quick acting clamps.

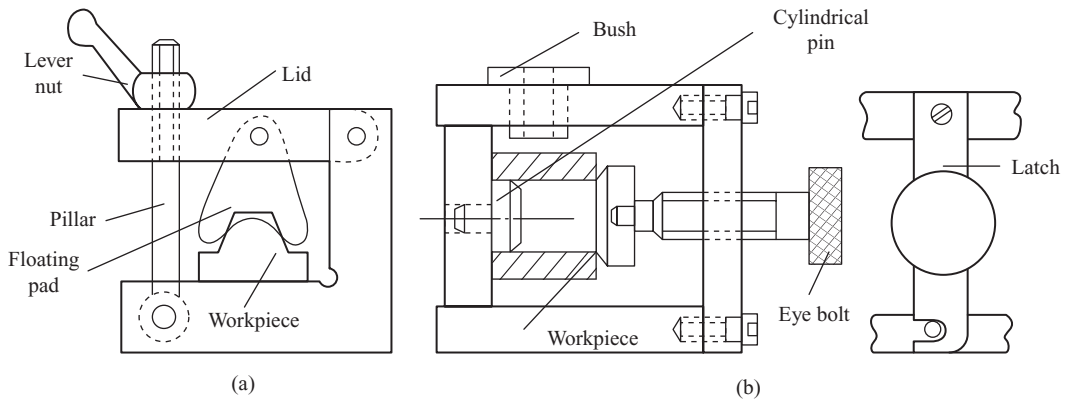


Figure 7.68 Hinged clamps: (a) with pillar and lever nut and (b) with latch and eye bolt

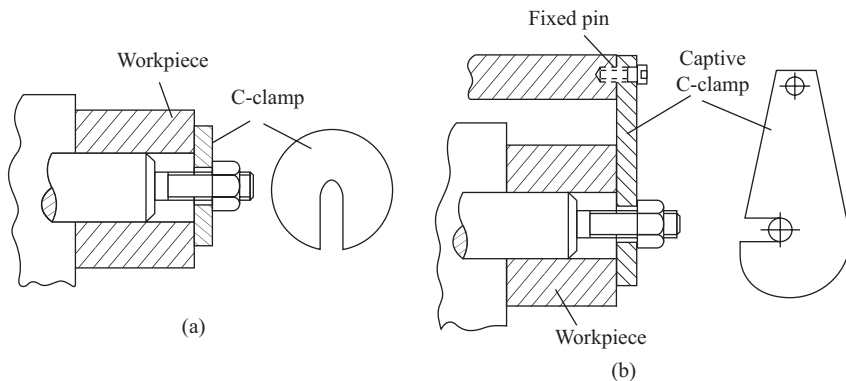


Figure 7.69 Quick acting C-clamps: (a) simple C-clamp and (b) captive C-clamp

Multiple clamping is employed when it is necessary to clamp several workpieces or to apply the clamping force at several points of one job by operating a single screw or handle of the clamping device. The commonly used multiple clamping devices employ pivoted floating pads for equal parallel distribution of the clamping force (Figure 7.70(a)) or parallel distribution with consecutive transmission of the clamping force (Figure 7.70(b)). The ability of the floating pad with well rounded ends to swivel makes it possible to clamp parts with minor difference in height (Figure 7.70(c)).

7.4 Tool Guiding Elements

Cutting tools such as twist drills and reamers have a tendency to deflect during the cutting operation on account of their large length-to-diameter ratio. Guide bushes are used to constrain these tools during operation and eliminate their deflection. Fixtures that use guiding elements are known as jigs. The guide bushes are fitted in a bush plate.

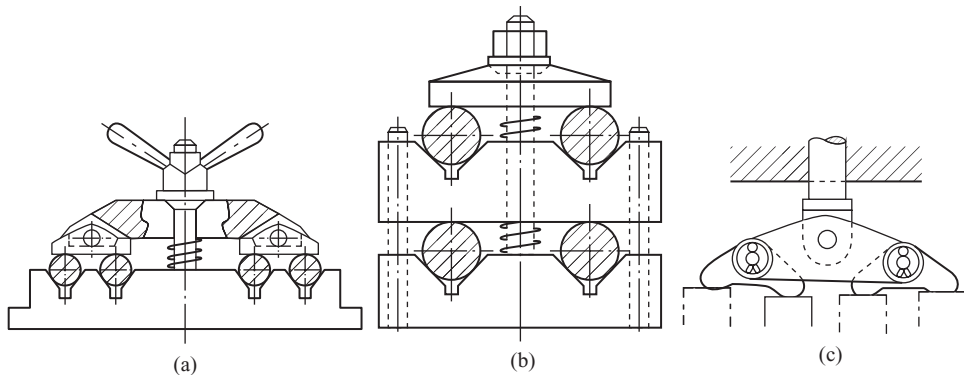


Figure 7.70 Multiple clamping: (a) with parallel distribution of clamping force, (b) with parallel distribution and consecutive transfer of clamping force, and (c) use of swivel pad in multiple clamping

Fixed bushes are used in small lot production. These bushes are press fitted in the bush plate permanently, and therefore cannot be readily removed. If a fixed bush gets worn out, it has to be driven out of the bush plate. This usually damages the bore hole in which the bush is fitted. Therefore the bore hole has to be increased and a new oversized bush is used as replacement for the worn out bush. Fixed bushes may be plain or flanged. A plain bush is shown in Figure 7.71(a). It is simple in design; but despite being press fitted, it suffers from the tendency to gradually push downwards in the bush plate with the passage of time. The flanged bush (Figure 7.71(b)) is free of this shortcoming and also provides more guidance length. The flanged bush is generally preferred, except when two closely spaced holes are to be produced and there is not enough space to accommodate the flanges of two bushes. The height of fixed bush is taken 1.5–2.0 times the diameter of the hole to be machined.

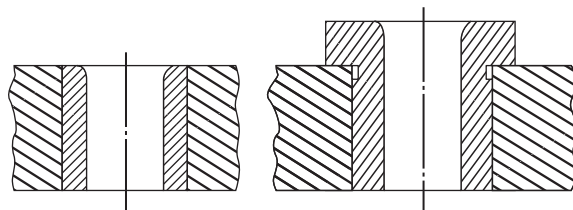


Figure 7.71 Fixed bushes: (a) plain and (b) with flange

When the guide bush is to be used in large lot manufacturing or when tools of different sizes are to be used in machining a single hole, then the wear of the guide bush occurs at a faster rate. The use of fixed bushes becomes uneconomical in such cases, because of the effort, time and cost involved in replacing a worn out bush. Depending on the frequency of changing the bush, renewable or slip bushes are used in these cases. A renewable bush assembly is shown in Figure 7.72. The assembly consists of a liner bush 1 that is press fitted in the bush plate and serves as guide for the renewable bush 2. The latter is assembled with a sliding fit to facilitate easy removal. It is held in place and prevented from rotation by retainer shoulder screw 3. When the renewable bush is worn out, the shoulder screw is removed and the renewable bush is taken out. A new renewable bush is

now placed in the liner bush and secured by means of the shoulder screw 3. Renewable bushes are used in large lot manufacturing where replacement of the bush may become necessary every few hours or days. The height of renewable bush is also taken 1.5–2.0 times the diameter of the hole to be machined.

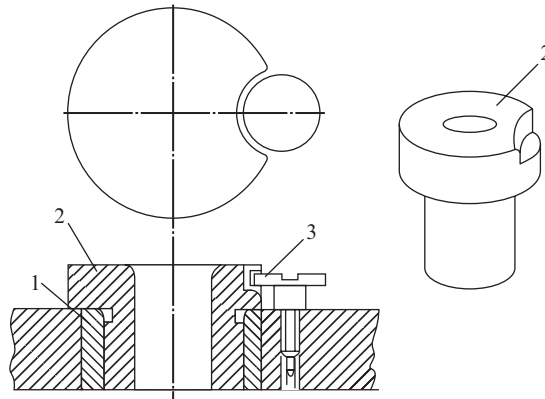


Figure 7.72 Renewable bush

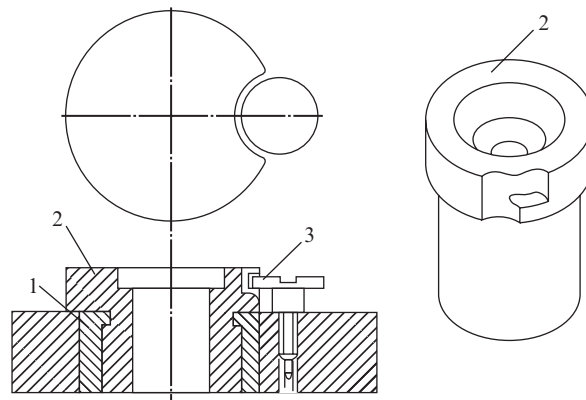


Figure 7.73 Slip bush

When a hole requires operations such as drilling, core drilling, and reaming to be carried out in quick succession, then the guide bushes for these operations should be so designed that they can be replaced very fast, say in a matter of a few seconds. Such a bush known as slip bush is shown in Figure 7.73. The slip bush assembly is basically similar to that of the renewable bush, where the liner bush 1 and shoulder screw 3 serve the same purpose. The difference is in the design of the slip bush 2. The shoulder screw remains in its place during the replacement of the slip bush. For inserting a new bush, it is made to slide past the head of the shoulder screw along the profiled cut in the bush flange and then rotated so that the step comes under the shoulder screw head to prevent the linear displacement or rotation of the bush. For removing a worn-out slip bush, it is

rotated in the opposite direction till the shoulder screw head is aligned with the profiled cut in the bush flange. The latter can now be easily removed by lifting it out of the liner bush. The flange of removable and slip bushes is lightly knurled for ease of handling. The height of the slip bush is taken slightly more than 1.5–2.0 times the diameter of the hole to be machined, but a counter bore at the top restricts the guiding length to 1.5–2.0 times the diameter of the hole as in the fixed and renewable bushes.

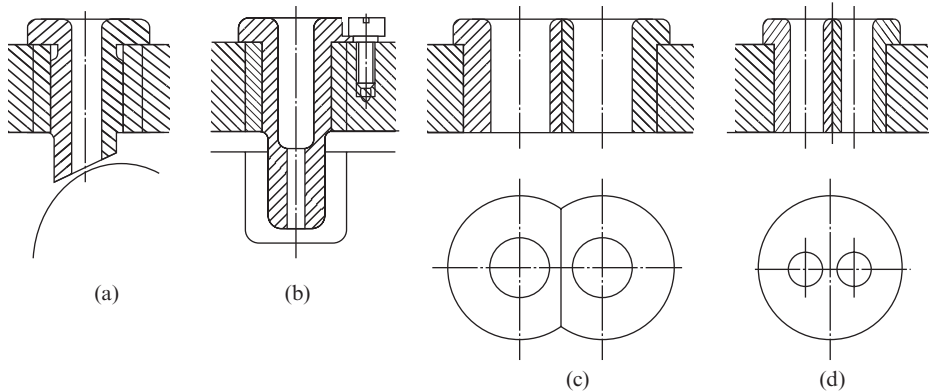


Figure 7.74 Special bushes: (a) for inclined and curved surfaces, (b) for workpiece with deep recess, (c) bushes with truncated heads, and (d) bush with two holes

Special bushes are used for tool guidance in unusual cases. A twist drill tends to slide down when making a hole in an inclined or curved surface due to uneven bending. To avoid this problem, the end face of the bush is modified to match the workpiece surface (Figure 7.74(a)). A long bush is required for drilling a hole in a recess. Therefore in order to reduce friction, it is necessary to restrict the guidance length for which a part of the bore is relieved (Figure 7.74(b)). In addition, when two holes have to be drilled close together, then two bushes with truncated flanges or one bush with two guiding bores may be used (Figures 7.74(c) and (d)).

A few general recommendations that are common for all types of bushes are as follows:

- (i) An adequate chamfer should be provided at the top of the bore hole of bush to facilitate easy enter of the tool.
- (ii) An adequate chamfer should be provided on the external diameter of the bush at the bottom face to facilitate easy assembly of the bush in the liner bush (for renewable and slip bushes) or the bush plate (for fixed bushes).
- (iii) An under cut should be provided at the neck of flanged bushes to ensure that the bush sits flush on the bush plate.
- (iv) In the jig assembly, the distance between the bottom face of bush and the workpiece should be kept at least 0.3 times the diameter of the bore; otherwise, the chip produced in the drilling operation gets trapped in the restricted space, thereby damaging the bush and bush plate and also causing excessive wear of the drill. The maximum value of this distance should not exceed the bore diameter, but should preferably be less than 0.5 times the bore diameter to ensure firm guidance of the tool.

- (i) The nominal size and tolerance on the bore hole of the bush should be selected for a tool of given nominal dimension and tolerance such that the smallest bore hole diameter is greater than the largest tool.
- (ii) Bushes are made of tool steel and are hardened to $HRC = 60 - 65$. Bushes for tools greater than 25 mm diameter are made of low carbon steel and case hardened to $HRC = 60 - 65$. Typically, the wear of the bush per 10m length of machining comprises $4-6 \mu$ for steel workpieces, $3-5 \mu$ for cast iron workpieces and $1-2 \mu$ for aluminum workpieces. Generally, a properly designed bush of appropriate material should need replacement only after machining of 10,000–15,000 workpieces.

7.5 Indexing Devices

Indexing devices are incorporated in multiple station jigs and fixtures to enable multiple operations to be carried out on a workpiece at different positions without disturbing the set-up. In jigs and fixtures, rotary indexing devices are mostly used on account of their greater compactness as compared to linear indexing devices. An indexing device consists of a stationary disc carrying a fixing or locking element such as a ball, peg, or pin and an index plate with as many holes as the number of indexable positions required on the jig or fixture. The stationary disc is attached to the body of the jig/fixture and the index plate to the table on which the workpiece is mounted. To begin the machining of a component the fixing element is inserted in the hole of the index plate corresponding to the position of the first operation on the workpiece. When this operation is completed, the fixing element is withdrawn and the index plate is rotated till the next hole comes in front of the fixing element. The fixing element is now inserted in this hole, thereby positioning the table for the next operation. Each working position is called a station, of which one is generally reserved for loading/unloading of the workpiece and the rest for carrying out the machining operations.

The fixing element may be a cylindrical pin, spherical ball, taper gib, or a tapered peg (Figure 7.75). It is desirable that the operation of the fixing element should be quick; therefore, in most indexing devices, the insertion of the fixing element is executed by spring action. The withdrawal of the fixing element may be manual or mechanized, generally using a rack and pinion mechanism. An indexing device using a spring loaded spherical ball as fixing element is shown in Figure 7.76. Part of the ball is in contact with an indent in the index plate 1 and part of it rests within a hole

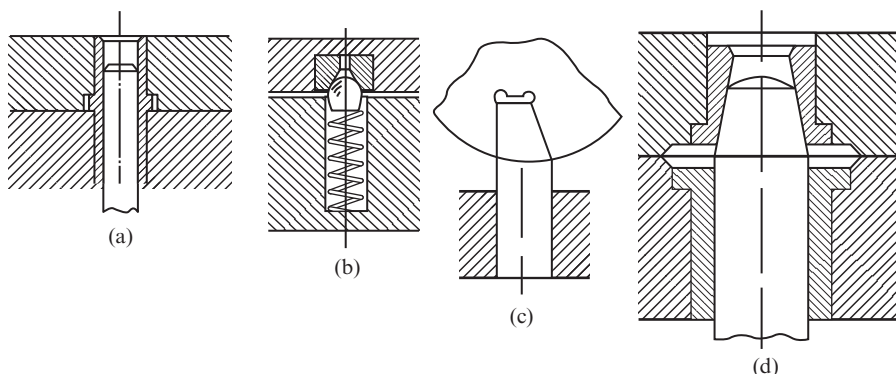


Figure 7.75 Fixing elements in indexing devices: (a) cylindrical pin, (b) spherical ball, (c) taper gib, and (d) tapered peg

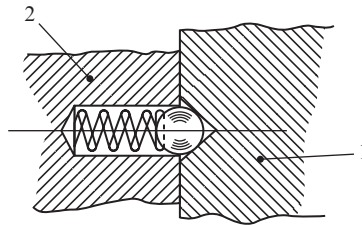


Figure 7.76 Indexing device with spring loaded spherical-ball: 1, index plate and 2, stationary disc

in the stationary disc 2. The rotating member is indexed by hand by applying sufficient torque to push the ball fully into the hole. For carrying out the operation at the next station, the index plate is rotated till the next indent comes in front of the ball. At this moment, the ball is pushed by spring action into the indent, thereby securing the index plate in this position. Though cheap and effective, the spring loaded ball device is not an accurate method of indexing. A major drawback of this device is that it does not provide positive location, therefore involuntary indexing of the index plate may occur if the torque produced during the cutting operation exceeds the indexing torque. An indexing device using cylindrical peg as fixing element is shown in Figure 7.77. The insertion of pin in the hole is under spring action and its withdrawal is manual with the help of a knob. An indexing device using mechanized operation (rack and pinion mechanism) of the fixing element in the form of tapered peg is shown in Figure 7.78. The index plate has tapered holes of matching size and taper angle. Finally, an indexing device using a tapered gib as fixing element is shown in Figure 7.79. Obviously, in this case, the index plate has slots of profile matching the tapered gib instead of holes.

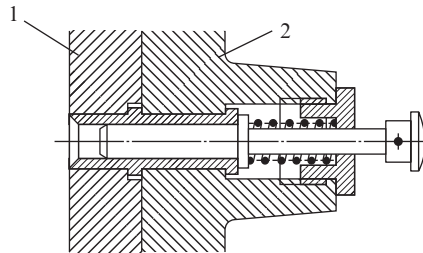


Figure 7.77 Indexing device with spring loaded cylindrical peg: 1, index plate and 2, stationary disc

The devices shown in Figures 7.77 through 7.79 all provide positive location. Of the three type of fixing elements used in positive location indexing devices the cylindrical peg is associated with the maximum positioning error because of the necessity of providing adequate clearance for easy insertion of the peg in the hole. The tapered peg and tapered gib do not need any clearance for insertion and therefore provide more accurate positioning. Between the two, the tapered gib provides more accurate positioning because of less contact surface. However, the indexing device with tapered gib is more costly because precision machining of profiled slots in the index plate requires more skill.

In order to improve the rigidity of the system and reduce vibrations and also to prevent breakage of the fixing element under the effect of cutting force, it is necessary to lock the rotating member

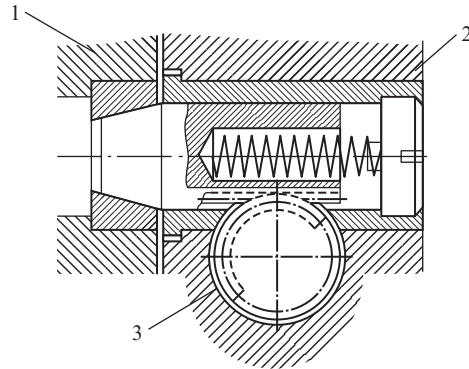


Figure 7.78 Indexing device with tapered peg: 1, index plate; 2, stationary disc; and 3, rack and pinion mechanism

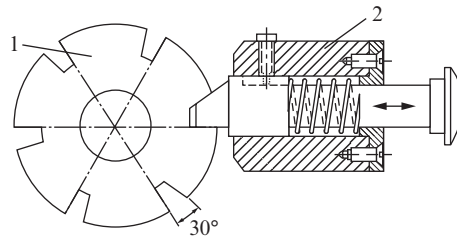


Figure 7.79 Indexing device with taper gib: 1, index plate and 2, stationary block

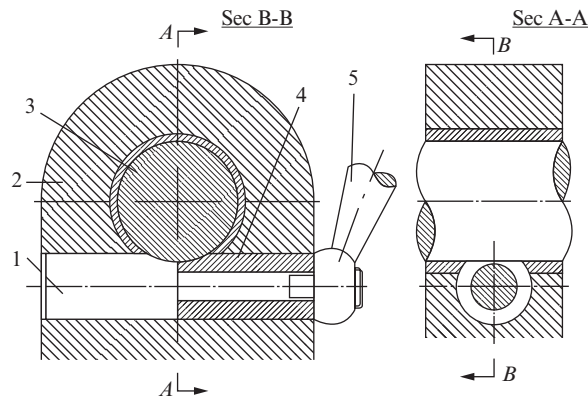


Figure 7.80 Mechanism for locking index plate

with the stationary disc after indexing, independent of and in addition to the locking provided by the fixing element. This is especially important in milling fixtures because of the large cutting forces and impact loading in the milling operation. A variety of designs of locking mechanisms are used in jigs and fixtures. One simple design is shown in Figure 7.80. When handle 5 is rotated,

it pushes sleeve 4 forward. As the gap between screw head 1 and sleeve 4 is reduced, shaft 3 of the rotating member gets locked with the stationary member 2.

7.6 Body of Jigs and Fixtures

The body is the main part of a jig or fixture as it provides the structure on which all the elements (locating, clamping, tool guiding, indexing, and auxiliary elements) are mounted. The shape and dimensions of the body are determined by the selected locating, clamping, and other elements and by the shape, dimensions, and number of workpieces to be machined in one setting.

The body of jig or fixture is required to take up the cutting and clamping forces. It must therefore have sufficient strength, rigidity, and dynamic stability. This should be achieved by proper selection of the body shape and rational use of stiffeners and ribs. Achieving higher strength, rigidity, and dynamic stability by increasing the thickness of the base and walls of the body is not advisable as it increases the weight of the fixture and makes handling difficult, but strategically located apertures and cavities may be provided in the body to reduce its weight without compromising with its strength, rigidity and dynamic stability.

The design of the body should facilitate convenient and rapid loading/unloading of the workpiece and easy disposal of chips and cutting fluid. For this purpose, it is necessary to see that there are no recesses in hard-to-reach places and the chip/cutting fluid disposal surfaces are provided generous inclination angle varying from 30° for machining with flood cooling to 45° for dry machining.

The body should have provision of alignment and clamping on the machine tool with as little loss of time as possible. Lathe fixtures are aligned with the help of tapers and shoulders. In milling fixtures, two short sliding blocks known as tennon strips corresponding to the dimensions of T-slot of milling machine table are provided on the under side of the base of the fixture body for alignment. Slotted lugs in the base are provided for clamping the fixture to the machine table with the help of T-bolts. Alternately, straight flanges at the two ends of the base are provided for clamping with the help of strap clamps. Jigs and fixtures weighing up to 15 kg are handled manually. For heavier jigs and fixtures, provision should be made for eye bolts on the body for ease of lifting with a hoist or crane during installation and removal of the jig/fixture.

The design of jig/fixture body also depends on the material and methods used for its fabrication. Jig and fixture bodies are made by casting, welding, and mechanical assembly of individual components. Cast bodies are made of gray cast iron, welded bodies are fabricated from standard steel sections and components, and assembled bodies are built from individual components and sections with the help of fasteners and adhesives. To illustrate the distinguishing aspects and differences in body design associated with the fabrication, let us consider the example of a jig body. The cast body (Figure 7.81(a)) is made of gray cast iron. The distinguishing feature of this body is provision of bossing at the holes for greater strength. The raised level of the bossings eliminates interference with the adjoining rough surface and makes machining easier. Also stiffeners have been used for enhancing the overall structural rigidity. The welded body (Figure 7.81(b)) is made of steel plates and sections. The bossings and stiffening ribs are also made of steel and welded to the main structure. The assembled body (Figure 7.81(c)) consists of cast T-section comprising the base and column of the fixture and machined plate that is fastened to it by means of screws.

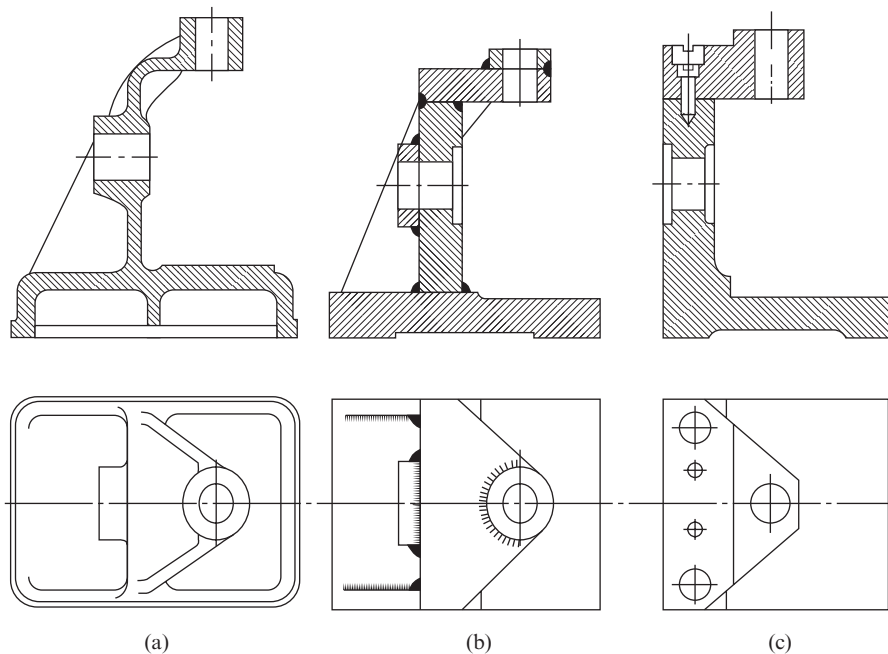


Figure 7.81 Variations in body design based on method of fabrication: (a) cast body, (b) welded body, and (c) assembled body

The bodies of large jigs/fixtures are made from cast iron, especially if they have intricate features. Cast iron is cheap and possesses good strength and rigidity. Cast structures have a tendency to warp with time due to redistribution of internal stresses. Therefore, provision of properly placed stiffeners is important in cast bodies. Welded bodies are generally limited to jigs and fixtures of simple configuration. Welded bodies can be made sufficiently strong and rigid by judicious use of reinforcing ribs, stiffeners, and corner plates. The cost of a welded body can be as much as 50 percent lower than that of a corresponding cast body, and it may also be up to 40 percent lighter in view of the higher strength of steel as compared to cast iron. The main disadvantage of welded bodies is relatively poor accuracy on account of distortion. The assembled bodies are preferred when they can be fabricated from standard blanks and sections, or when some portions of a cast body are difficult to machine on account of poor access. In such cases, machining can be carried out on the concerned component before it is put in the assembled body. All three methods of fabrication are used in manufacturing of jigs and fixtures, and the choice of the method may be determined by the cost effectiveness in each individual case.

To reduce the time spent on design and fabrication of jigs and fixtures, a fair amount of standardization has been achieved for locating, clamping, tool guiding, and indexing elements. However for long, the body which is the main part of a jig/fixture remained a one-off item to be designed and fabricated anew every time. However, attempts have been made at standardization of elements that can be assembled to make a body with minimum or zero machining. A set of 15 such standard elements is shown in Figure 7.82. Each element comes in different standard sizes, thereby allowing a wide range of body configurations to be assembled for drill jigs and milling

fixtures. The plates shown in Figures 7.82(a), through (c) are used as base on which the rest of the elements are mounted. Slotted lugs are provided on the plates shown in Figures 7.82(b) and (c) for clamping on the machine table with the help of T-bolts. The box sections shown in Figures 7.82(d) and (e) can be mounted on the base plate using any of the six sides to suit the given jig or fixture. The channel section shown in Figure 7.82(f) has the same function as the box section. The box and channel sections may be connected to each other or to the plate by means of lug (Figure 7.82(o)). The elements shown in Figures 7.82(f) through (k) are used for creating the necessary features of a given jig or fixture and the elements shown in Figure 7.82 (l) through n are used as reinforcing ribs and stiffeners.

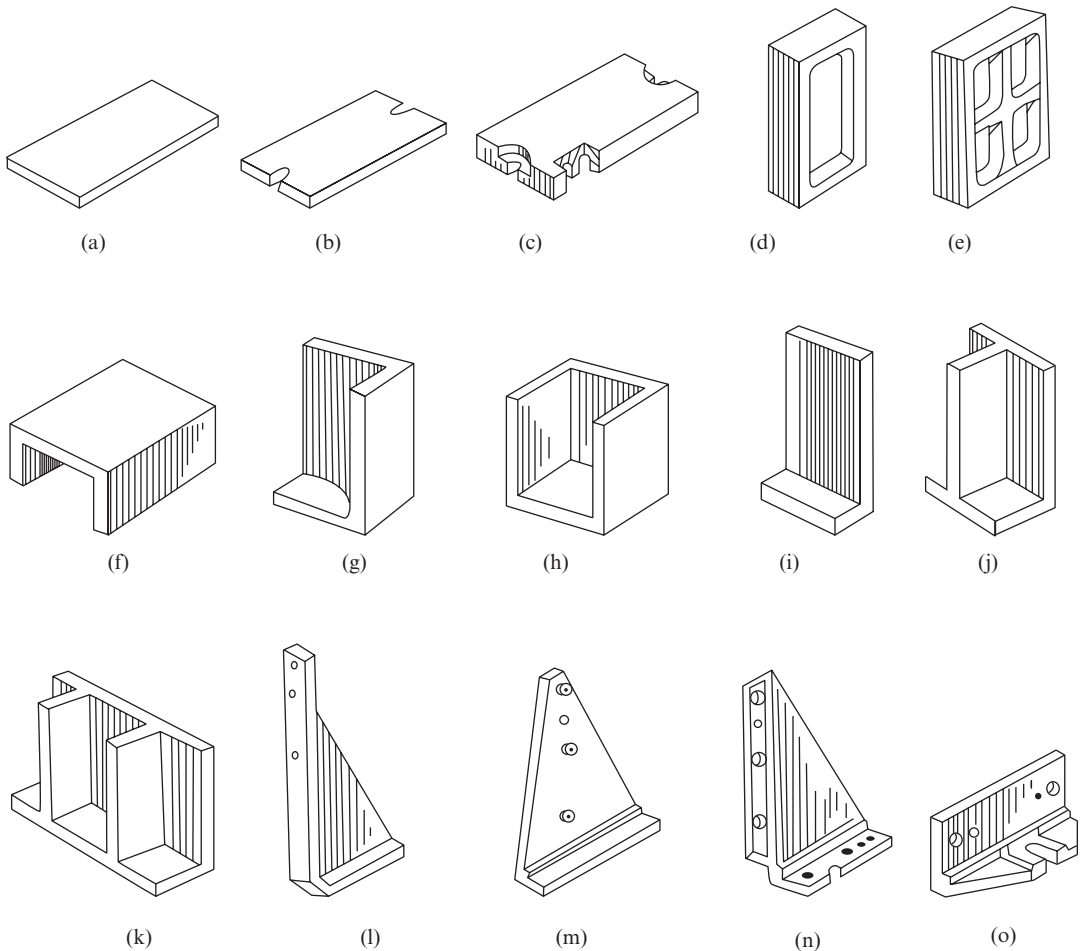


Figure 7.82 Standard elements for jig and fixture body: (a) steel plate; (b) and (c) cast iron plates with slotted lugs; (d) and (e) box sections; (f) channel section; (g) three plate angle piece; (h) open box four plate piece; (i) angle plate; (j) and (k) ribbed angle plates; (l), (m), and (n) reinforcement ribs and stiffeners; and (o) lug

A few examples of built-up bodies from standard elements are shown in Figure 7.83. The body of a milling fixture shown in Figure 7.83(a) consists of plate 1 and box section 2. The body of a drilling jig shown in Figure 7.83(b) consists of base plate 1, channel section 2, and another plate 3. Finally, the body of milling fixture shown in Figure 7.83(c) is assembled from plate 1, angle plate 2, and two reinforcement ribs 3.

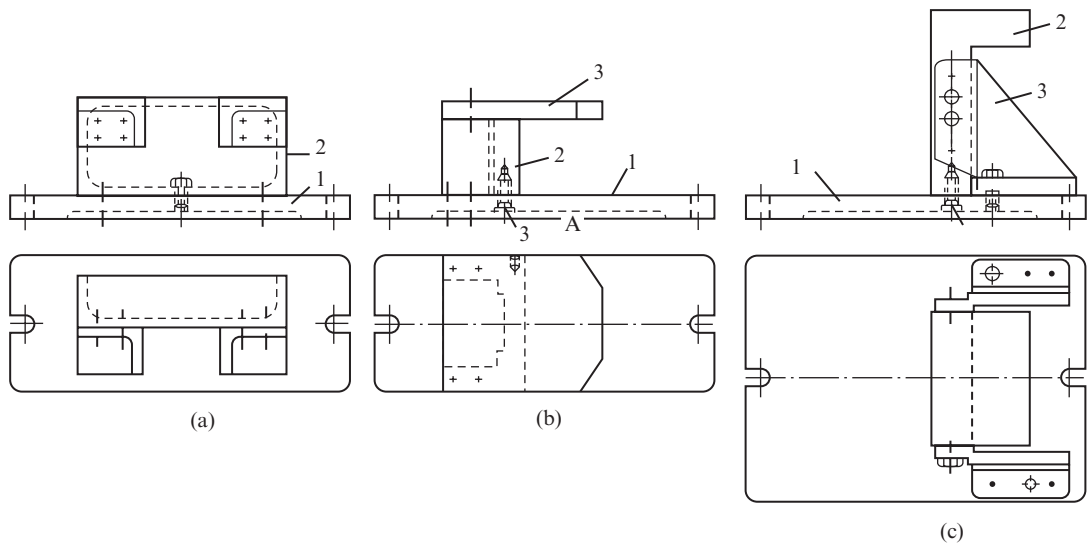


Figure 7.83 Examples of built-up bodies from standard elements: (a) milling fixture assembled using plate and box section, (b) drilling jig assembled using channel section and two plates, and (c) milling fixture assembled using plate, angle plate and two reinforcement ribs

7.7 Power Devices

Power devices are used in jigs and fixtures for clamping of workpieces when the required clamping force is beyond human capability (around 15 kg). They possess several advantages over manual clamping, which justify their wide application in industry; these are as follows:

- (i) reduced handling time
- (ii) uniform clamping force
- (iii) simultaneous clamping of several workpieces in multiple-piece jigs and fixtures; manual clamping in these fixtures leads to unwieldy design and inordinately large clamping time.

Three type of power devices are commonly used in jigs and fixtures – pneumatic, hydraulic, and hydropneumatic. In all these devices, the piston rod is connected to the operating member of the clamping mechanism through which the force has to be applied. The power devices can operate in conjunction with all type of clamping mechanisms, but are easier to incorporate in jigs and fixtures with wedge, lever, and rack-and-pinion-type clamping mechanisms. Direct application of pneumatic or hydraulic pressure for clamping is not advisable because should the air or fluid pressure fall at a critical moment, the clamped workpiece will come loose with all the attendant consequences. On the contrary, when the pressure is applied through a wedge or toggle, the self-locking feature of the mechanism prevents serious accident from happening.

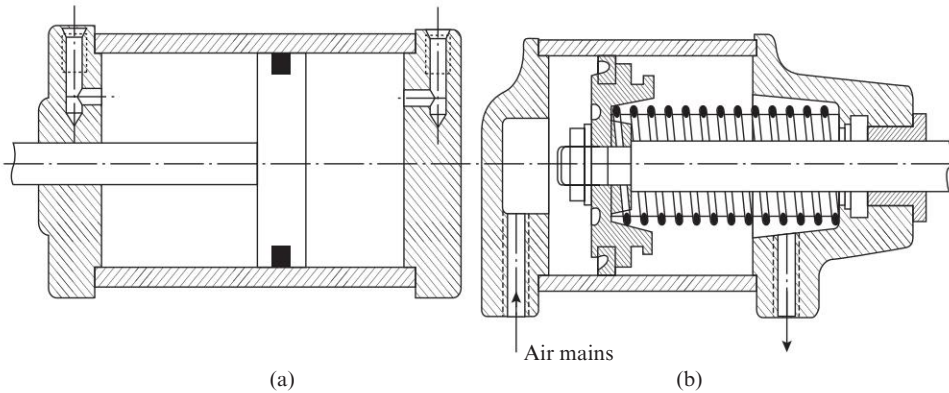


Figure 7.84 Piston-type pneumatic power devices: (a) double action and (b) single action

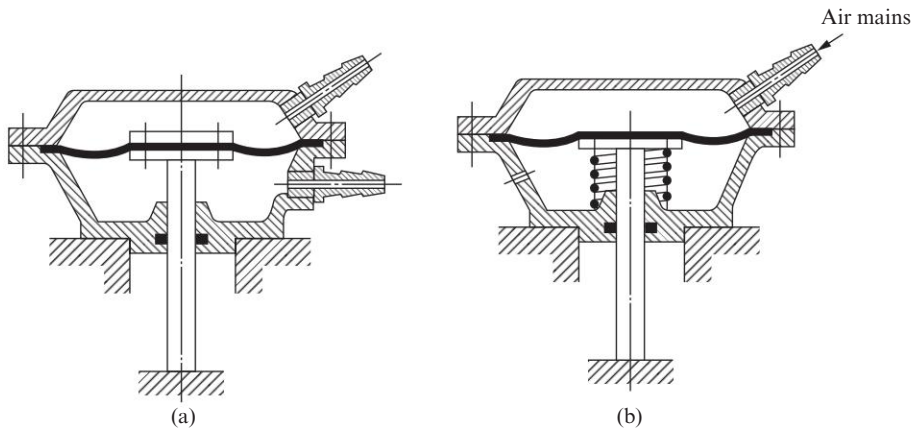


Figure 7.85 Diaphragm-type pneumatic power devices: (a) double action and (b) single action

Pneumatic power devices The pneumatic power devices used in jigs and fixtures are piston type (Figure 7.84) and diaphragm type (Figure 7.85). Both type of devices may be double action (Figures 7.84(a) and 7.85(a)) or single action (Figures 7.84(b) and 7.85(b)). In a double-action device, the rod executes both the clamping and unclamping actions under air pressure. In the single-action devices, the clamping action is executed by movement of the rod under air pressure, but the reverse stroke for unclamping is controlled by spring action. Double-action devices are used in jigs and fixtures with self-locking mechanisms that require larger force for unclamping. In both types of devices, compressed air is supplied at a pressure of 3–6 kgf-cm². Consumption of compressed air is 30–40 percent less in single-action devices, but they develop 5–20 percent less force because part of the energy is used up in overcoming the spring force. Diaphragm devices are simpler, cheaper, and smaller in size as compared with piston devices, but their small effective stroke is a disadvantage.

The size of the pneumatic device depends on the force that needs to be developed. Pneumatic cylinders are used in size range of 50–300 mm bore diameter. Cylinders less than 50 mm are seldom used, and that too only for operating workpiece ejectors in jigs and fixtures. Cylinders over 300 mm diameter are unwieldy, and it becomes expedient to replace the pneumatic device by a hydraulic or hydropneumatic device. Diaphragm devices generally have diaphragms in the range

of 175–225 mm diameter, which allows them to develop force in the range 250–600 kgf and rod stroke in the range 30–35 mm.

Easy availability of compressed air in almost all engineering plants and its relatively low cost and the simplicity of supplying it to machine tools are the reasons for the popularity of pneumatic devices. Other factors responsible for the use of pneumatic device are quick response, simple control, and insensitivity to temperature variations. Compressed air facilitates maintenance and cleaning of jigs and fixtures as swarf is blown away under air pressure. Ordinarily, the standard pressure of compressed air in the shop mains ranges from 5–6 kgf-cm². Therefore, considering pressure losses in the pipelines and the fact that compressed air may be in use simultaneously at a number of stations, it is advisable to assume a pressure of 3–4 kgf-cm² for calculations.

The main drawback of pneumatic devices is their inability to develop operating pressure above 6 kg/cm², which results in large size of these devices. For jigs and fixture where large clamping force is required, the use of pneumatic devices becomes infeasible because of their unwieldy size. In such cases, it is advisable to use hydraulic devices. These devices can develop pressure of up to 100 kgf-cm², which makes them very compact. Generally, hydraulic cylinders of diameter range 20–50 mm are able to generate sufficient force for clamping requirements of most jigs and fixtures. Other features in favor of hydraulic devices are self-lubrication of the cylinder, incompressibility of the working fluid that eliminates jerks and unsteady movement, and absence of water condensation encountered in pneumatic devices. On the flip side, hydraulic devices are more expensive and sensitive to temperature variations as the viscosity of working fluid changes with temperature.

Hydraulic power devices These are piston-type devices and may be single action or double action. The operating principle of hydraulic devices is similar to that of the piston type pneumatic device, except that the operating fluid is oil and not compressed air. Unlike pneumatic devices that get compressed air from main line, hydraulic devices are independent installations that include an electric motor, hydraulic pump, oil tank, direction control valves, pressure valves, etc. (Figure 7.86).

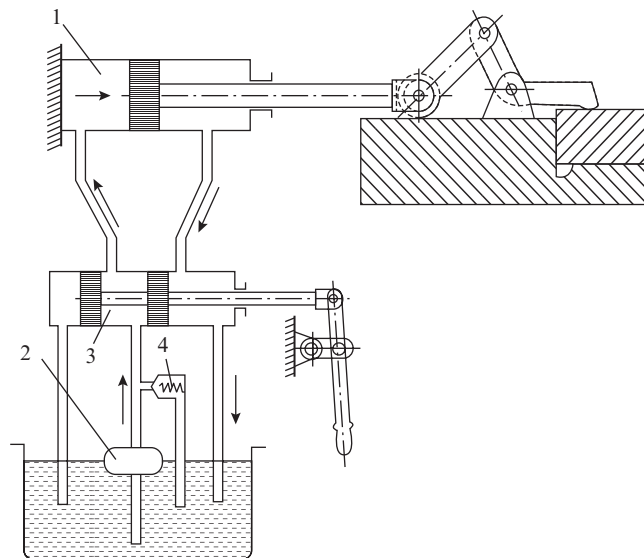


Figure 7.86 Schematic of hydraulic system of power device: (1) hydraulic cylinder, (2) hydraulic pump, (3) direction control valve, and (4) overflow valve

Depending on the available power, one such installation may serve one or more hydraulic cylinders of jigs and fixtures. In machine tools with hydraulic drive, the independent installation may be dispensed with and a branch from the main hydraulic system may be diverted to supply oil to the hydraulic cylinder of the jig or fixture.

It can be noted from the foregoing discussion that if the main hydraulic system of machine tool cannot be utilized for operating a jig or fixture, then the overall cost of an independent hydraulic device becomes prohibitive, unless the oil supply system can serve several jigs and fixtures simultaneously. The cost of hydraulic cylinder is also high because it operates at high pressure, which mandates a more rugged design and high quality sealing to prevent leakage.

Hydro-pneumatic devices These devices use a combination of pneumatic and hydraulic principles in an air-to-oil pressure booster in which low pressure of compressed air mains supplied to a piston-type pneumatic cylinder is boosted to a high pressure of up to 100 kgf/cm² in a hydraulic cylinder. The principle of operation of such a hydro-pneumatic device can be explained with the help of Figure 7.87.

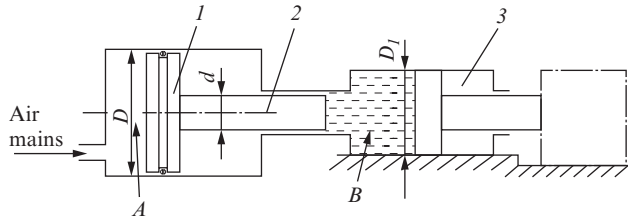


Figure 7.87 Schematic of hydro-pneumatic device: 1, pneumatic cylinder; 2, piston rod; and 3, hydraulic cylinder

When compressed air is supplied to the head end A of the pneumatic cylinder, the following force acts on piston 1.

$$Q_1 = \frac{\pi D^2}{4} p_{ca}, \text{ kg}$$

where

D = diameter of the pneumatic cylinder, centimeter

p_{ca} = pressure of compressed air, kgf/cm²

Piston rod 2 will transmit a force

$$Q_2 = \eta Q_1$$

where η is a coefficient that accounts for frictional losses

In view of the constriction around piston rod 2 the pressure transmitted to chamber B will be

$$p = \frac{Q_2}{\frac{\pi d^2}{4}}$$

where d is the diameter of the piston rod

On substituting for Q_2 in the above expression, we obtain

$$p = \eta \frac{\pi D^2}{4} p_{ca} \frac{4}{\pi d^2}$$

$$p = p_{ca} \eta \left(\frac{D}{d} \right)^2 \text{ kgf/cm}^2 \quad (7.34)$$

It can be noted that the larger the difference between piston diameter D and rod diameter d , the higher is the boost of pressure. As this enhanced pressure acts on the piston of the hydraulic cylinder, it produces a much higher force Q on the piston of the hydraulic cylinder than was available in the rod end of the pneumatic cylinder.

$$Q = p \frac{\pi D_1^2}{4} \eta_d = p_{ca} \eta \eta_d \left(\frac{D}{d} \right)^2 \frac{\pi D_1^2}{4} \quad (7.35)$$

where η_d is the coefficient of efficiency of the device
Denoting the force on the piston of the pneumatic cylinder as

$$Q_1 = p_{ca} \frac{\pi D^2}{4}$$

We may write Eqn. (7.35) as follows:

$$Q = \eta \eta_d Q_1 \left(\frac{D_1}{d} \right)^2 \quad (7.36)$$

The relation between the stroke of pneumatic cylinder L and that of the hydraulic cylinder L_h can be found from the condition of constant volume of the working fluid, that is,

$$\frac{\pi d^2}{4} L = \frac{\pi D_1^2}{4} L_h$$

Considering the volumetric (leakage) losses, the above expression can be written as follows:

$$L = \frac{1}{\eta_v} L_h \left(\frac{D_1}{d} \right)^2 \quad (7.37)$$

where

η_v = coefficient of volumetric losses in the system

If one hydropneumatic booster serves several hydraulic cylinders, then Eqn. (7.37) takes the form

$$L = \frac{1}{\eta_v} L_h \left(\frac{D_1}{d} \right)^2 n \quad (7.38)$$

where n = number of hydraulic cylinders

The consumption of compressed air in one clamping cycle is found from the following expression:

$$V = \frac{\pi}{4} D^2 L \quad (7.39)$$

Example 7.11

The following data are given for a hydropneumatic system: $D = 20$ cm, $d = 4$ cm, $D_1 = 8$ cm, $p_{ca} = 4$ kgf/cm², $\eta_d = 0.8$, $\eta = 0.95$, and $\eta_v = 0.95$. Determine the following:

- (i) Pressure in the hydraulic cylinder
- (ii) Gain in hydraulic force
- (iii) Loss in stroke length of hydraulic cylinder
- (iv) Loss in stroke length if number of hydraulic cylinders is 3
- (v) Consumption of compressed air in one clamping cycle for $L_h = 1$ cm

(i) From Eqn. (7.34), we find

$$p = 4 \times 0.95 \left(\frac{20}{4} \right)^2 = 95 \text{ kgf-cm}^2$$

(ii) From Eqn. (7.36), we find

$$\frac{Q}{Q_1} = 0.95 \times 0.8 \left(\frac{8}{4} \right)^2 = 3.04$$

(iii) From Eqn. (7.37), we find

$$\frac{L}{L_h} = \frac{1}{0.95} \left(\frac{8}{4} \right)^2 = 4.2$$

(iv) From Eqn. (7.38), we find

$$\frac{L}{L_h} = \frac{1}{0.95} \left(\frac{8}{4} \right)^2 \times 3 = 12.6$$

(v) From Eqn. (7.39), we find

$$V = \frac{\pi}{4} \times (20)^2 \times 4.2 = 1318.8 \text{ cm}^3$$

In hydropneumatic devices, the oil used in the hydraulic cylinder is only moving to and fro and not being circulated; therefore, the elaborate system consisting of hydraulic pump, oil tank, valves, etc., is no more required. Further, the application of pressure booster reduces compressed air consumption by up to 90 percent. The main drawback of the hydropneumatic device is the relatively small stroke of the hydraulic piston since the gain of force is due to the loss in travel.

Vacuum-operated power devices These devices are used for holding thin-walled and deformable workpieces of flat or concave shape. The principle of a vacuum-operated device is illustrated in Figure 7.88(a). The workpiece is placed on rubber washer 3 placed in groove 4 in body 1 of the device. Inside the body, there is chamber A that is connected to a vacuum pump. When air is pumped out of this chamber, the workpiece is pulled toward the plate surface and is held by atmospheric pressure (Figure 7.88(b)). The holding force can be found from the following expression:

$$Q = p A K - F$$

A = area of the chamber

K = coefficient of tightness of the vacuum chamber

$p = p_a - p_c$ is the excess pressure, where p_a is the atmospheric pressure and p_c is the pressure in the chamber after creation of vacuum

F = elastic force of the compressed rubber washer

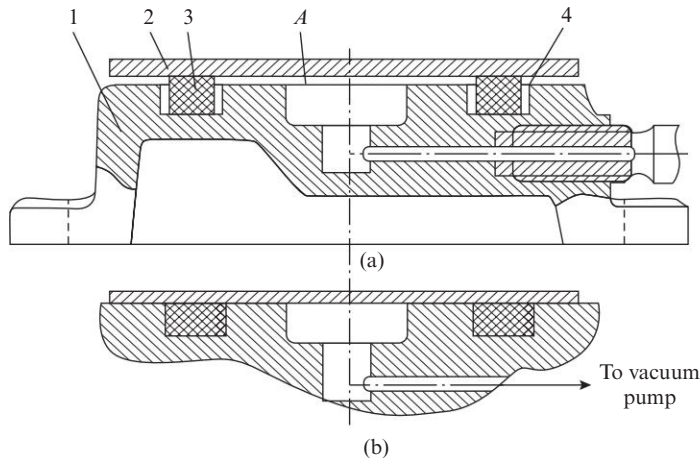


Figure 7.88 Principle of vacuum clamping

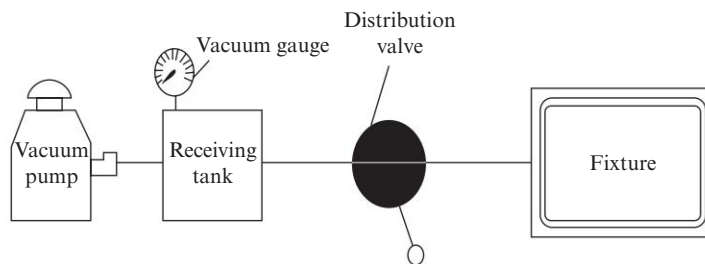


Figure 7.89 Vacuum clamping system

Generally, p_c is kept 0.1–0.15 kgf/cm², because creation of greater vacuum is expensive and associated with technical problems of maintaining the vacuum without any substantial enhancement in the holding force. The degree of tightness depends on the quality of sealing of the vacuum chamber and coefficient K generally varies from 0.8 to 0.85. The overall system of vacuum device is shown in Figure 7.89. Here, it is important to point out that the capacity of the receiver tank should be more than the volume of the vacuum chamber to ensure that development of vacuum is not slowed down. Generally, the holding force produced by vacuum device is sufficient only for finishing operations.

Magnetic devices These devices use the energy of magnetic field to clamp the workpiece. The magnetic flux may be produced by electromagnetic or permanent magnets. In a device with permanent magnets, the elementary magnets are housed in the base of the device and the workpiece is placed on the top plate so that the magnetic flux passes through it and holds the workpiece against the plate by exerting a pulling force (Figure 7.90). An electromagnetic clamping chuck

consists of several elementary electromagnetic circuits that are fed from a DC power source. A commonly used electromagnetic chuck is shown in Figure 7.91. Electromagnetic or magnetic plates and chucks can be used for clamping workpieces made of materials of high magnetic permeability such as steel and cast iron. The magnetic field of these devices affects a large surrounding area and may magnetize the cutting tool and adversely affect its performance. Therefore, magnetic chucks are mostly used in surface grinding machines, because the abrasive tool is not affected by the magnetic field. However, now these chucks are increasingly being used in milling, shaping, and drilling machines too by taking special measures to isolate the cutting tool from the influence of the magnetic field.

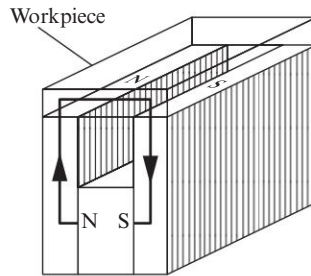


Figure 7.90 Principle of magnetic plate with permanent elementary magnetic system

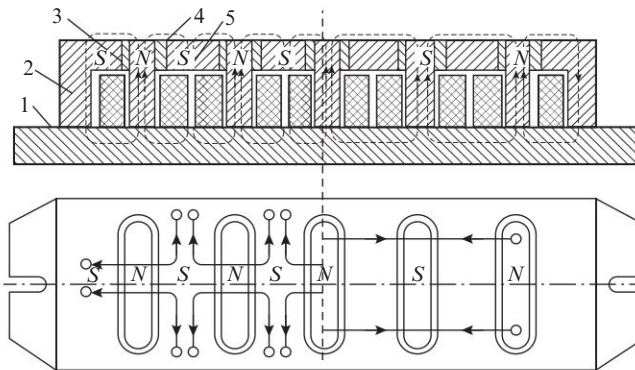


Figure 7.91 Schematic of electromagnetic clutch: 1, base; 2, body; 3, electromagnet cores; 4, nonmagnetic spacers; and 5, electromagnetic coils

The main advantage of magnetic devices is the simplicity of their operation, because it is sufficient to press a switch to activate or deactivate the magnetic field and carry out the clamping or unclamping operation. Magnetic devices can develop attraction force of up to 3 kgf/cm^2 , and magnetic chucks are currently produced with holding plate size up to $100 \times 100 \text{ mm}$. While remaining clamped on the magnetic chuck, the workpiece gets magnetized; therefore after completion of machining, it has to be demagnetized in a special apparatus. Magnetic devices have very high efficiency and can reduce the handling time on clamping and releasing the workpiece by a factor of 5 to 8 compared with machine vices. Generally, magnetic devices with permanent magnets are preferred because they are safer, consume no electrical power, and have long service life of 8–10 yr.

Review Questions

- 7.1 In a fixture using dual-pin location, one of the pins is shaped as a diamond pin because
- it has high wear resistance
 - it is easy to clamp
 - it is easy to restore for reuse after wear
 - it can accommodate variation of the distance between hole axes

- 7.2 Match the components used in jigs and fixtures with their functions

| | Components | Functions |
|----|--------------------|--|
| A. | Spring jack pin | 1. To guide drill during machining |
| B. | V-locator | 2. To provide multiple position machining |
| C. | Fixed bush | 3. To locate cylindrical objects |
| D. | Indexing mechanism | 4. To locate workpiece whose dimension is subject to variation |

- (a) A2B3C4D1 (b) A4B3C1D2
(c) A3B2C1D4 (d) A1B3C4D2

- 7.3 Match the components used in jigs and fixtures with their functions

| | Components | Functions |
|----|------------|---|
| A. | Rest pad | 1. Location of bush |
| B. | Mandrel | 2. Location of external cylindrical profile |
| C. | V-block | 3. Location of shaft with through hole |
| D. | Short pin | 4. Location of flat surface |

- (a) A3 B1 C2 D4 (b) A2B3C4D1
(c) A4B3C2D1 (d) A1B4C2D3

- 7.4 How many degrees of freedom of a workpiece must be eliminated for its complete location in a jig/fixture?
- (a) 6 (b) 5 (c) 4 (d) 3
- 7.5 For locating a cast housing with a flat base and two pre drilled holes, the best combination of locating elements for minimum locating error is
- 1 flat plate, 1 cylindrical pin, 1 small cylindrical pin
 - 1 flat plate, 1 cylindrical pin, 1 diamond pin
 - 1 flat plate, 2 diamond pins
 - 1 flat plate, 2 identical cylindrical pins
- 7.6 The tolerance specified on a feature *A* is ± 0.2 mm. If machining of this feature involves an intermediate datum *B* with machining tolerance of ± 0.1 mm, the available tolerance range for machining of *A* is
- (a) 0.4 mm (b) 0.3 mm (c) 0.2 mm (d) 0.1 mm
- 7.7 For stable location of a flat surface, the number of rest buttons required is
- (a) 3 (b) 4 (c) 5 (d) 2

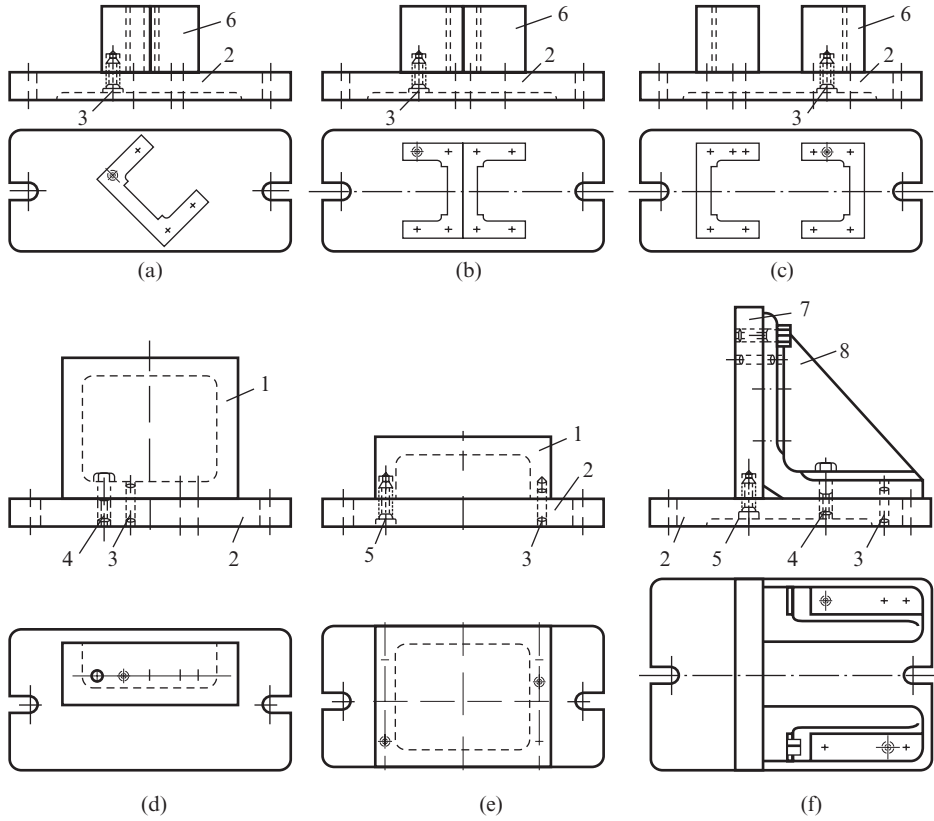
- 7.8 When a flat plate is placed on a plain surface, it is deprived of the following number of degrees of freedom:
 (a) 2 (b) 3 (c) 4 (d) 5
- 7.9 The 3-2-1 scheme of location using rest pads is applicable to the location of
 (a) solid cylindrical parts
 (b) cylindrical parts with through hole
 (c) cylindrical parts with center holes
 (d) prismatic parts
- 7.10 When a cylindrical workpiece is placed on a V-block, it is deprived of the following number of degrees of freedom:
 (a) 2 (b) 3 (c) 4 (d) 5
- 7.11 A shaft of diameter 40 ± 0.1 mm is located in a V-block for machining of a horizontal step 10 ± 0.2 mm measured from the axis of the shaft. If the included angle of the V-block is 90° , the locating error for machining of the step will be
 (a) 0.2 mm (b) 0.4 mm (c) 0.24 mm (d) 0.14 mm
- 7.12 In the above problem, the available tolerance range for machining of the step will be
 (a) 0.26 mm (b) 0.14 mm (c) 0.24 mm (d) 0.4 mm
- 7.13 A V-block with 4 rest pins is used for location of
 (a) short cylindrical parts
 (b) finish machined long cylindrical parts
 (c) unmachined cylindrical parts
 (d) prismatic parts
- 7.14 The locating element suitable for location of short cylindrical parts such as discs is
 (a) flat plate with 2 pins (b) self-centering three-jaw chuck
 (c) V-block (d) flat plate with 2 rest pads
- 7.15 A short workpiece with through hole is located with the help of the following locating element
 (a) V-block (b) flat plate with rest buttons
 (c) flat plate and V-block (d) flat plate with pin
- 7.16 If a cylindrical shaft with a hole of diameter 30 ± 0.05 mm is located using a mandrel of diameter $30_{-0.25}$ mm, the maximum eccentricity of the axis of the workpiece will be
 (a) 0.25 mm (b) 0.2 mm
 (c) 0.15 mm (d) 0.10 mm
- 7.17 Expanding mandrels locate the workpiece from
 (a) inside surface of hole (b) external cylindrical surface
 (c) flat end face of workpiece (d) center hole on end face of workpiece
- 7.18 Location of a workpiece with flat base and two predrilled holes on a plate with two pins deprives it of the following number of degrees of freedom:
 (a) 3 (b) 4 (c) 5 (d) 6
- 7.19 Location of a cylindrical workpiece with center holes between centers deprives it of the following number of degrees of freedom:
 (a) 3 (b) 4 (c) 5 (d) 6

- 7.20** Use of floating pad for clamping in a screw-type device
- (a) reduces location error (b) reduces bending of the screw
(c) reduces clamping force (d) reduces clamping time
- 7.21** Use of a slotted/swinging strap in clamping
- (a) reduces location error (b) reduces workpiece displacement
(c) reduces clamping force (d) reduces clamping time
- 7.22** Among the various clamping mechanisms, the maximum gain of force is achieved in
- (a) lever-type mechanism (b) eccentric mechanism
(c) screw-type mechanism (d) toggle mechanism
- 7.23** Both elements of the pair are quick acting clamps in the following option:
- (a) Screw and wedge (b) eccentric and captive-C
(c) hinged and wedge (d) screw and toggle
- 7.24** In small lot production, the following type of bush is preferred for tool guidance
- (a) fixed flanged bush (b) slip bush
(c) bush with tapered face (d) renewable bush
- 7.25** When several tools are to be guided in quick succession for carrying out different operations at one location, the following guide bush is preferred:
- (a) fixed flanged bush (b) slip bush
(c) bush with tapered face (d) renewable bush
- 7.26** A liner bush is essential in the following pair of bushes:
- (a) fixed plain and slip (b) fixed flanged and renewable
(c) renewable and slip (d) fixed flanged and slip
- 7.27** For positive location in multiple station indexing, the following pair of fixing elements is not suitable:
- (a) cylindrical pin and tapered peg (b) tapered peg and tapered gib
(c) cylindrical pin and tapered gib (d) spherical ball and cylindrical pin
- 7.28** Bodies of large fixtures with intricate details are made by
- (a) adhesive joining (b) mechanical assembly
(c) welding (d) casting
- 7.29** In case of very large clamping force, the following power device is used:
- (a) vacuum (b) pneumatic
(c) hydraulic (d) hydropneumatic
- 7.30** For holding thin-walled and deformable workpieces, the following power device is preferred:
- (a) vacuum (b) pneumatic
(c) hydraulic (d) hydropneumatic
- 7.31** Explain the 3-2-1 principle of location. Distinguish between complete and partial location with simple examples.
- 7.32** What is meant by overlocation? Explain the effect of overlocation on machining accuracy with simple examples
- 7.33** What is the role of jigs and fixtures in a manufacturing process and what are their main advantages?

- 7.34** What are the various objectives for which jigs and fixtures are used in manufacturing? Discuss how these objectives are reflected in the design of jigs and fixtures.
- 7.35** Define and distinguish between design, setting, and measuring datums. Discuss the general principle of selection of setting datum for location of machined surfaces.
- 7.36** Discuss the requirements to locating elements for location of machined and rough surfaces.
- 7.37** Make neat sketches of the locating elements used in location of
- (a) prismatic parts
 - (b) cylindrical parts
 - (c) parts in which holes are used for location
 - (d) parts in which center holes are used for location
- 7.38** What are the main requirements to clamping devices? Discuss the broad principles involved in the design of clamping elements of jigs and fixtures.
- 7.39** Describe the general procedure for clamping force calculation in machining operations.
- 7.40** Name and describe with simple sketches the various clamping mechanisms used in jigs and fixtures.
- 7.41** Make neat sketches of the following clamping devices:
- (a) screw clamp with adjustable pin, slotted strap, and circular fluted handle for tightening
 - (b) screw clamp with pillar pin, swinging strap, and tightening through hexagonal nut
 - (c) double link, single-action toggle with pivoted strap
 - (d) double link, double-action toggle with plungers
 - (e) hydropneumatic, wedge type with roller follower
 - (f) pneumatic, wedge type with pivoted strap
 - (g) eccentric type, with pillar pin and slotted strap; load applied by eccentric in the middle of strap
 - (h) eccentric type with fixed heel and swinging strap; load applied by eccentric on heel
 - (i) two types of hinged clamps
 - (j) two types of C-clamps
- 7.42** Describe with neat sketches the different types of bushes used in jigs and their application.
- 7.43** Describe with neat sketches three types of special bushes used in jigs and their application.
- 7.44** Describe and illustrate with neat sketches the general recommendations for design of bushes used in jigs.
- 7.45** What is the function of indexing devices? Describe with neat sketches the operation of
- (a) rack-and-pinion-operated indexing device with cylindrical pin
 - (b) manually operated indexing device with spherical ball
- 7.46** Discuss the requirements to bodies/frames of jig and fixtures.
- 7.47** Compare the characteristic features of cast, welded and built-up assembled bodies of jigs and fixtures.

7.48 Sketch 3-D views of the jig/fixture bodies shown in the figures below:

- | | | | |
|----------|------------|----------|----------------------|
| 1, box | 2, plate | 3, pin | 4, bolt |
| 5, screw | 6, channel | 7, plate | 8, reinforcement rib |



CLASSIFICATION OF JIGS AND FIXTURES AND THEIR ECONOMIC ANALYSIS

8.1 Classification of Jigs and Fixtures

It was discussed in Section 7.1 that jigs and fixtures eliminate the laborious process of marking in setting up of components for machining. The benefits from use of jigs and fixtures range from improved accuracy and reliability of production to higher productivity, lowering of required operator skills, simpler quality control and shorter assembly time. To realize these benefits across the spectrum of production systems ranging from job shop to large lot and mass production, it is necessary to adopt different strategies to develop a range of jigs and fixtures that are suitable and economically viable for different production systems. For proper appreciation of these strategies and economic analysis of different types of jig and fixtures, it is convenient to classify jigs and fixtures based on their degree of specialization as follows:

- (i) Universal general purpose fixtures (UGPs)
- (ii) Universal adjustable fixtures (UAFs)
- (iii) Special adjustable fixtures (SAFs)
- (iv) Reassemblable fixtures (RAFs)
- (v) Universal built-up fixtures (UBFs)
- (vi) Special fixtures (SPFs)

8.1.1 Universal General-Purpose Fixture(UGP)

Universal general-purpose fixtures (UGPs) are used for locating and clamping a variety of parts of different shapes and sizes. These fixtures are simple in design and do not require any modification or adjustments for accommodating various parts. A UGP typically consists of a body and a clamping device that may be manually operated or powered. UGP fixtures are suitable for job shop and small lot manufacturing in small and medium manufacturing enterprises. Universal three-jaw chucks and indexing heads and vices are typical examples of UGP fixtures.

The schematic of a UGP fixture and some of its applications are illustrated in Figure 8.1. As mentioned earlier, the fixture consists of body 1 and clamping device with drive 2 (Figure 8.1(a)). There are only two locating surfaces A that are common to all applications. The absence of any other locating surface sometimes necessitates prior marking and partial setting up of the part to be machined with the help of layout lines (see Figure 7.1). In view of this, a skilled setter/operator is required on machines tools using UGP fixtures. In addition, with the restrictions on the number of available locating surfaces, it is not possible to machine some parts at all. In others, machining

may be possible but with reduced accuracy. The use of the fixture shown in Figure 8.1(a) in three different applications is illustrated in Figures 8.1(b), (c) and (d).

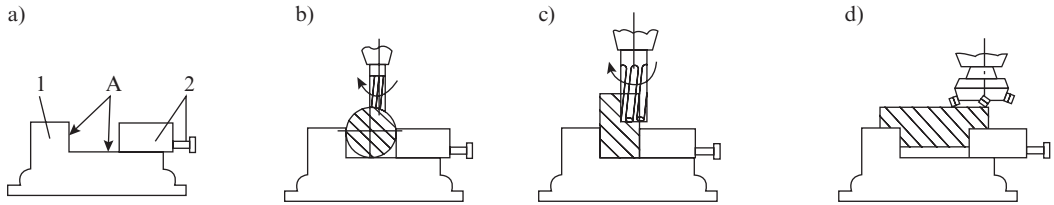


Figure 8.1 Universal general-purpose fixture: (a) schematic of the fixture, (b) milling of flat on a cylindrical shaft, (c) slot milling, and (d) face milling

8.1.2 Universal Adjustable Fixture(UAF)

Universal adjustable fixtures (UAFs) consist of a set of permanent components and replaceable elements for location and tool guiding, etc. Generally, the permanent components are the body and the clamping mechanism. However, some fixtures of this type may also include indexing elements. The replaceable elements used for locating the part and tool guidance are part specific, which allows machining of parts with the same accuracy as in special fixtures (SPFs). In terms of part geometry and size, the range of parts that can be machined using UAF is restricted by geometry and size of the body. In view of the above, UAFs are suitable for part families of similar shape, size and features identified by applying the concepts of group technology. Parts that differ significantly from the families associated with a particular UAF cannot be machined by this UAF. UAFs are suitable for small- and medium-lot batch production in small and medium manufacturing enterprises, especially if the shop layout is organized on group technology principles. Typical examples of UAF are chucks with replaceable jaws, adjustable machine vices, plate jigs, etc.

The schematics of a UAF and some of its applications are illustrated in Figure 8.2. The fixture consists of permanent body 1 and replaceable elements 2 (Figure 8.2(a)). The use of this fixture in three different applications, using a different set of replaceable elements in each case, is illustrated in Figures 8.2(b), (c) and (d).

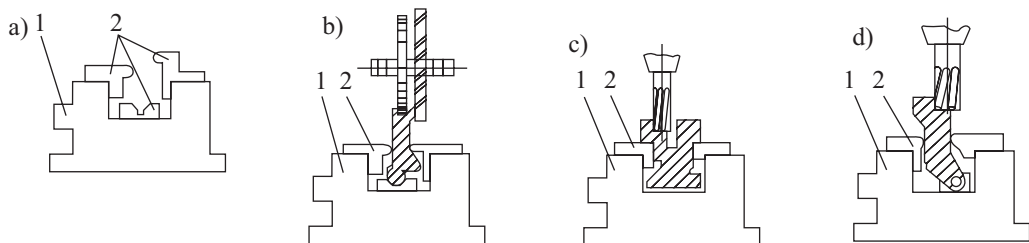


Figure 8.2 Universal adjustable fixture: (a) schematic of the fixture, (b) gang milling of groove and face on lever, (c) slot milling on housing, and (d) slot milling on lever

8.1.3 Special Adjustable Fixture(SAF)

Special adjustable fixtures (SAFs) fixtures are meant for parts that have similar design and production features and use the same set of location surfaces for setting up different parts. They also consist of permanent components (mainly body of the fixture) and sets of replaceable components that are part specific. Thus, in a way they are quite similar to UAF. The main difference between UAF and SAF lies in the following:

- Replaceable elements in SAF are adjustable, which makes it possible to accommodate a larger range of parts of the same type.
- SAF employs a higher degree of mechanization.

Thanks to the above two features, SAF are suitable for medium- and large-lot production. To illustrate the principle of SAF, consider the fixture shown in Figure 8.3. Parts 2 shown in Figures 8.3(a) and (b) belong to one part family. Although similar in design, they have differences in dimensions and geometrical features, namely location of the hole to be drilled and the size of the center hole. The parts are clamped by tightening screw 4. As the screw moves downward, the taper pushes the plunger 5 outward, thereby gripping the center hole and clamping the part. It becomes possible to accommodate these parts on a single fixture by adjusting the position of bush plate 3 and using replaceable plunger 5 of suitable dimensions. SAFs are suitable for medium- and large-lot batch production in medium manufacturing enterprises.

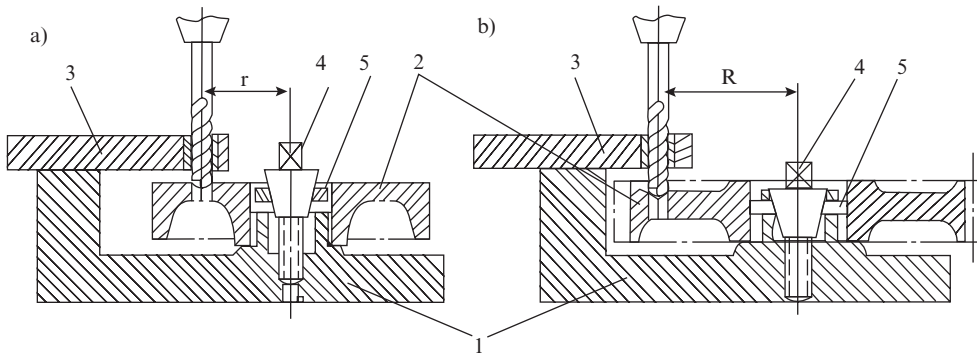


Figure 8.3 Special adjustable fixture: (a) hole drilling in pulley and (b) hole drilling in gear

8.1.4 Reassemblable Fixture(RAF)

Reassemblable fixtures (RAFs) are assembled from standard components and units. Each configuration represents an SPF meant for a particular part. When the fixture is not required, it is disassembled and the components and units can be utilized for assembling a new fixture. The range of fixtures that can be assembled depends on the components and units available in the standard set. If the necessary components and units are available in the set, then a fixture can be assembled in a short time. This significantly reduces the preproduction preparatory time, which is an important factor in the efficiency of modern manufacturing enterprises operating on the principle of multiple product batch production.

The functioning principle of RAF is illustrated in Figure 8.4. The standard set (Figure 8.4(a)) consists of three components 1, 2, 3 and one unit 4, which are used to assemble two fixtures shown in Figures 8.4(b) and (c) for drilling hole in a crank and milling a groove in a housing, respectively.

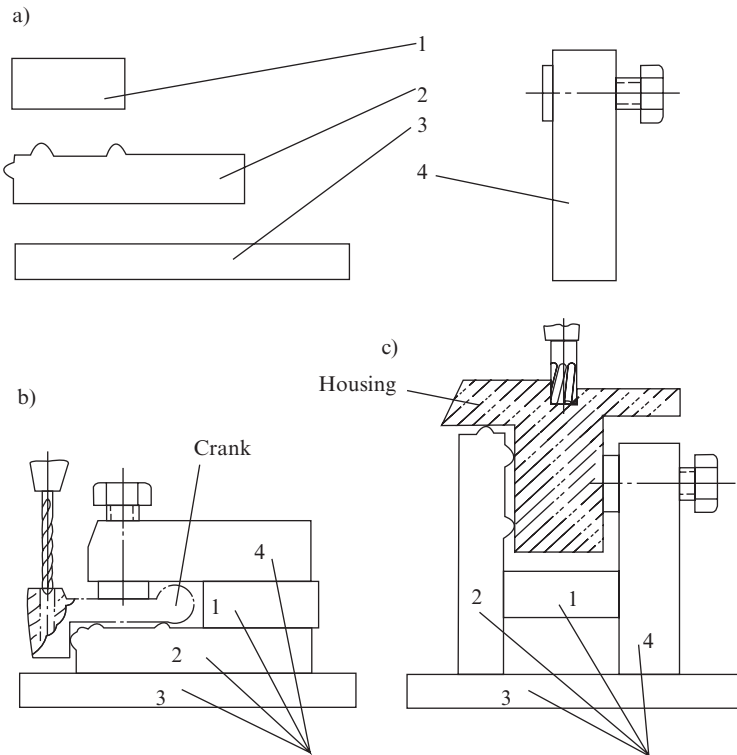


Figure 8.4 Reassemblable fixture: (a) standard set of components, (b) fixture for drilling hole in a crank, and (c) fixture for milling groove in housing

RAFTs consist of 80–90 percent standard parts and the rest that are part specific. In order to be able to assemble a variety of fixtures, the plant must maintain a large inventory of various standard components and units, especially for fixture bodies (see Figure 7.82), drive units, and clamping mechanisms. The cost of such an inventory can be quite high; therefore, RAFTs are generally affordable only for large enterprises involved in multiple product batch manufacturing in medium- to large-lot sizes.

8.1.5 Universal Built-Up Fixture(UBF)

Universal built-up fixtures (UBFs) are an extension of the underlying principles of RAFTs in the sense that they rely on extensive standardization of the components and units of jigs and fixtures and are much bigger in terms of the size of inventory and the variety and range of jigs and fixtures that can be assembled. Diversity of product and specialization creates special requirements within individual firms. It is therefore not surprising that firms prepare their own standards, building their inventory of UBF set gradually over years. For this, a detailed analysis of individual items that recur constantly is made. The range of sizes for each such item is then decided. These items in their identified size range are then included in the set of components suitable for standardization.

A complete UBF set consists of eight groups of standard components and units that cover all the elements of jigs and fixtures. The details of one such typical set are given in Table 8.1.

Table 8.1 *Typical standard components and units in UBF set*

| Group | Components and units | Quantity | | | Percentage by numbers |
|---------------------------|---|----------|-------|-------------------|-----------------------|
| | | Types | Sizes | Approximate total | |
| 1. Base | Square, rectangular and round plates, angle plates, and rings | 11 | 16 | 200 | 1 |
| 2. Body and housing | Square and rectangular pads, V-blocks, angle plates, joining plates, spacers, channels, box sections, etc. | 28 | 96 | 2,000 | 10 |
| 3. Locating elements | Keys, pins, plugs, rest buttons and pads, bushings, fixing pins and dowels, locking devices, etc. | 13 | 168 | 2,800 | 14 |
| 4. Guiding elements | Fixed, replaceable and slip bushes, bush plates, pads, etc. | 5 | 89 | 600 | 3 |
| 5. Clamping elements | Straight, bent and fork straps, contoured clamps, etc. | 14 | 21 | 800 | 4 |
| 6. Fastening elements | Screws, bolts, studs, nuts, washers, etc. | 19 | 85 | 12,000 | 60 |
| 7. Miscellaneous elements | Hinges and swiveling straps, eccentrics, handles, springs, axles, centres, lugs, forks, shaped pins, lock rings, caps, etc. | 24 | 41 | 1,200 | 6 |
| 8. Disassemblable units | Locking devices with index plates, rotary tables, vice-type clamps, swing bolt holders, etc. | 36 | 45 | 400 | 2 |
| Grand total | | 150 | 410 | 20,000 | 100 |

A representative sample of the components of UBF set is shown in Figure 8.5. The base components of Group 1 provide the base on which the whole jig/fixture is assembled. They have rectangular or radial network of T-slots on their working surface to secure other elements of the jig/fixture and suitable holes/lugs for mounting the jig/fixture on the machine tool table. The body- and housing-type parts of Group 2 have the largest variety in terms of types and sizes that are the main factors in the ability of UBF set to be assembled into a wide range of jigs/fixtures of different sizes. The components of this group have keys and tennon strips matching the keyways and T-slots in the base on which they are assembled. A typical set of standard components and sections used in Groups 1 and 2 was shown in Figure 7.82. The purpose, types, and varieties of the components of Group 3 (locating elements), Group 4 (guiding elements), and Group 5 (clamping elements) have been discussed and described in detail in Sections 7.2, 7.4, and 7.3, respectively. The components of Group 7 cover a wide range that are required in one or the other fixture, but in view of their large variety cannot be included in any of the Groups 1–5. The purpose of the components of Group 6 is evident from its name, and these are used for securing the various elements of jigs and fixtures. The components of UBF are interchangeable and are fastened together in the assembly of a particular fixture by means of keys, studs, screw, bolts, and T-bolts.

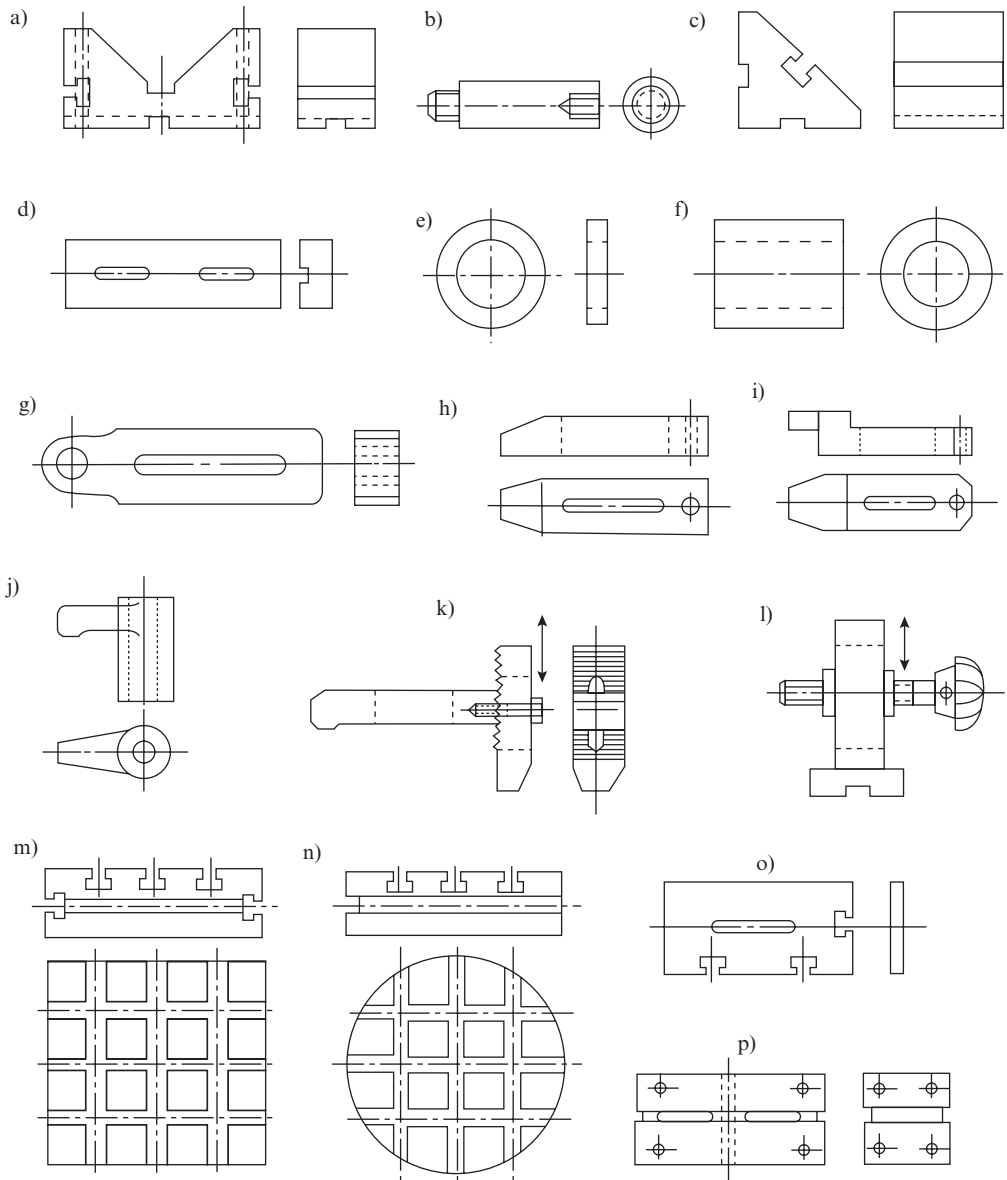


Figure 8.5 Sample components of universal built-up fixture set: (a) V-block, (b) coupler pin, (c) angle plate, (d) rest pad, (e) washer, (f) bush, (g) finger-type clamp, (h) straight clamp, (i) goose neck clamp, (j) swivel clamp, (k) adjustable clamp, (l) adjustable screw clamp, (m) square base, (n) circular base, (o) plate, and (p) adaptor block

The disassemblable units listed in Group 8 of Table 8.1 find wide application in multipurpose jigs and fixtures, speed up their assembly, and contribute to their compact and efficient design and easy maintenance. A representative sample of these units is shown in Figure 8.6. The standard components of UBF set may also be used for assembling adjustable units that can be quickly and easily reset to accommodate different workpieces. This saves precious time, as by readjustment

one is able to avoid assembling of a new fixture, which is naturally a more lengthy process. A few examples of such adjustable units are shown in Figure 8.7.

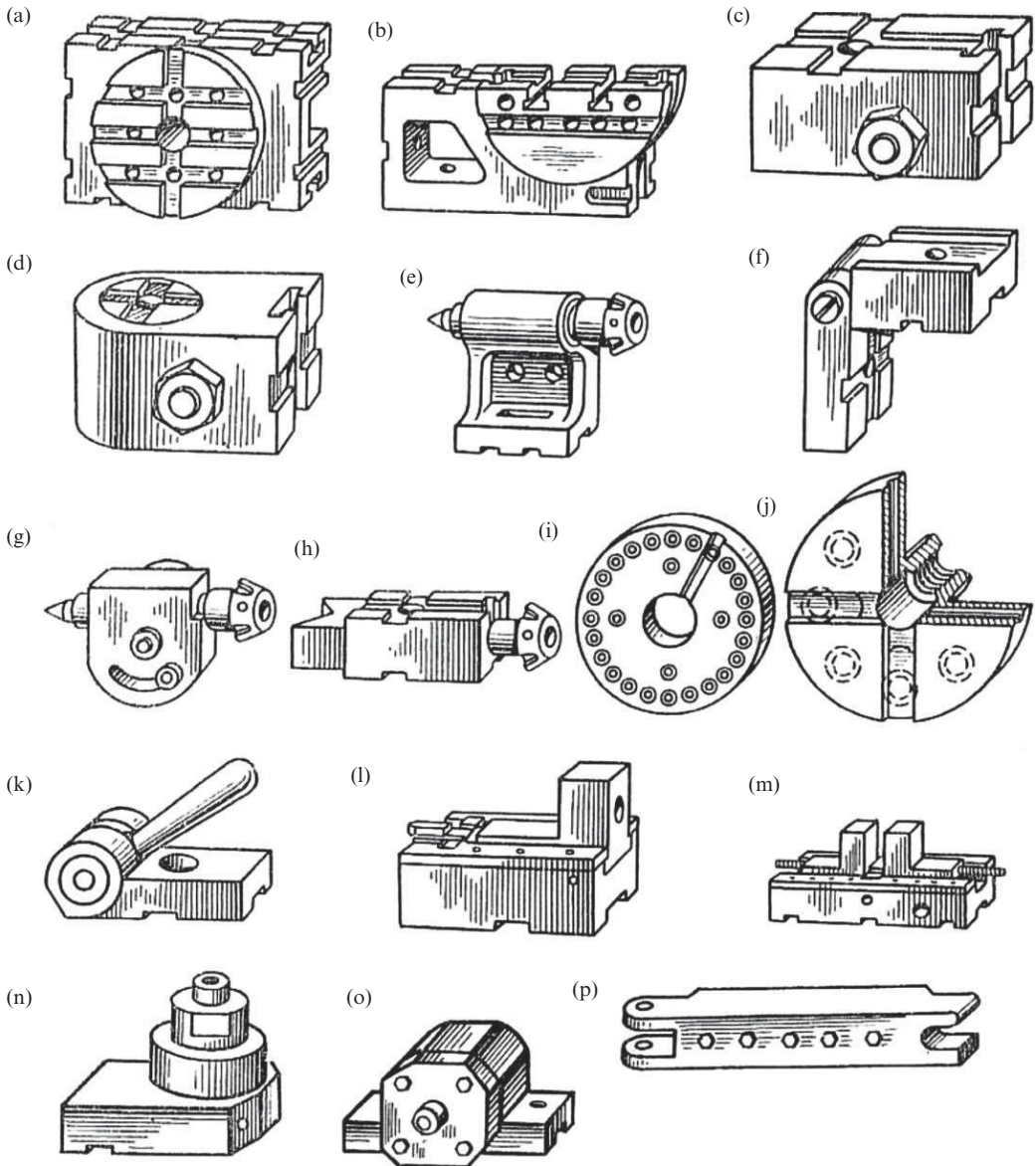


Figure 8.6 Sample disassemblable units built from components of UBF set (a) housing, (b) height element, (c), (d) support blocks, (e) fixed center, (f) angle block, (g) adjustable centre, (h) adjustable V-block, (i) index plate, (j) face plate, (k) cam block, (l), (m) housing, (n) hydraulic power device, (o) pneumatic power device, and (p) latch

A drill jig assembled from standard components of UBF set is shown in Figure 8.8. Main supporting block 2 is mounted on base 1. Guiding supports 3 are mounted on supporting block 2. Adjustable bush plates 4 are guided along the guide way in 3, and their position is secured by means

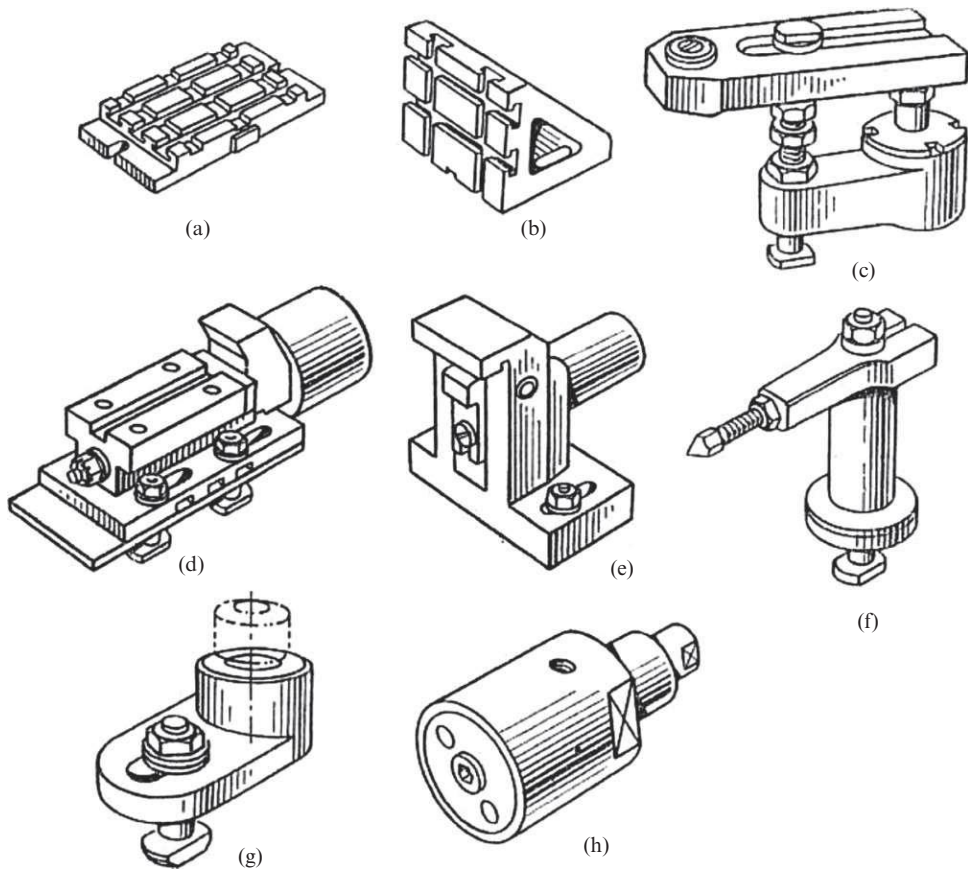


Figure 8.7 Sample adjustable devices built from UBF set: (a) plate, (b) angle plate, (c) adjustable strap, (d) horizontal clamp, (e) vertical clamp, (f) adjustable stop, (g) base lock, and (h) hydraulic cylinder

of nut 8. Pad 6 is used for locating the part and C-clamp 7 for clamping it. The drill is guided by bush 5 that may be a fixed or renewable bush depending on the scale of production (see Section 7.4).

Figure 8.9 shows a milling fixture assembled from standard components of UBF set. Rectangular locating blocks 2 are mounted on base 1 in perpendicular T-slots. The workpiece may be clamped by flat strap clamp 3 or by means of side clamps 4 that are tightened with the help of spherical washer 5 and nut 6. The fixture shown in Figure 8.9 can hold 2 workpieces; but as the design is modular, it can be easily enhanced to accommodate more workpieces.

As is evident from Table 8.1, a full UBF set consists of a total of 20,000 components, which is adequate for simultaneous assembly of 150–200 fixtures. The components of UBF set are made of high-quality alloyed steels and machined to a high degree of precision. Therefore, typical service life of a UBF set may be as high as 15–20 years. From the practice of industrial use of UBF set, it has been observed that about 60 percent of the fixtures assembled from UBF set are for drilling, 37 percent for milling, 7 percent for lathe operations, and the rest for other machine tools.

The main drawback of UBF is its high initial cost. Small and medium enterprises that cannot afford to invest in the full set can start with a limited set of 1,000–2,500 components that would allow them to assemble the most in-demand fixtures to being with. With time, such enterprises can then upgrade the UBF set to full strength.

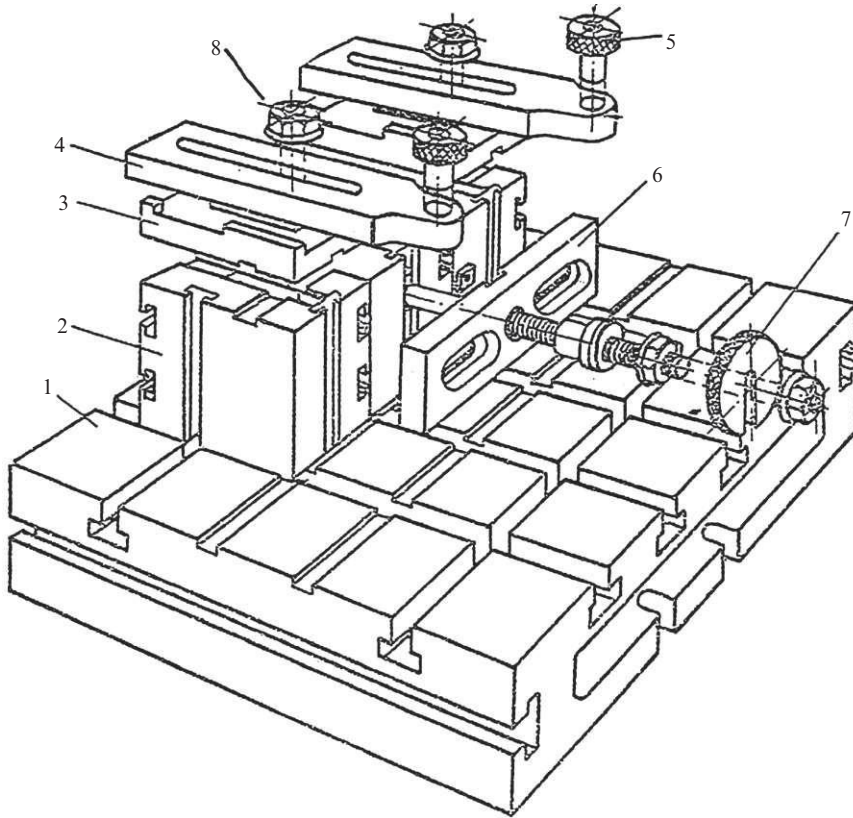


Figure 8.8 Drill jig assembled from components of UBF set

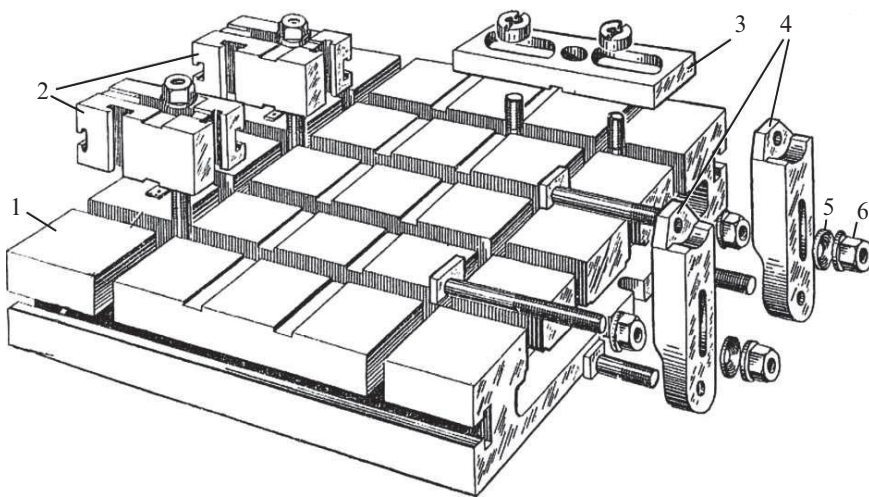


Figure 8.9 Milling fixture assembled from components of UBF set

In view of the immense benefits of UBF, two strategies that make them affordable for small and medium enterprises have been devised. One strategy is to divide the full UBF set into three series based on size as small, medium, and large. The small series is meant mainly for instrumentation making plants, the medium series for general manufacturing plants, and the large series for heavy engineering plants. The throat of the T-slot size and the fastening screw size is also standardized for these three series. T-slot neck of 8 mm and threaded fasteners of size M8 are used for the small series. The corresponding dimensions are 12 mm and M12 for medium series and 16 mm and M16 for the large series. An enterprise can choose to invest only in the series that matches its product profile and thus cut down on the initial investment. The other strategy is for an autonomous organization to centrally maintain a full UBF set and supply assembled fixtures on demand to customer enterprises on rental basis. Experience of industrial use of UBF based on this strategy shows that the average duration of rental of an assembled fixture is about 15 days, including 1 day for assembly, 2 for packing and transportation, and 1 for dismantling. A complete UBF set costs upward of \$1,00,000 with annual maintenance cost of about 3 percent of the initial investment. However, notwithstanding the high initial cost, the break-even period of UBF set is about 3 years, subject to reasonable good utilization.

8.1.6 Special Fixtures(SPF)

An SPF is designed for a particular part for carrying out a specific operation. These fixtures generally involve the complete design and fabrication exercise every time a new fixture is required. Consequently, the time, effort, and cost of making SPFs are very high, and the use of these fixtures is economically feasible only in stable large lot and mass production. These fixtures are assembled by using both standard components and special elements. By increasing the use of standard components and increasing their versatility by making them adjustable, a SPF can be adapted to serve as an SAF and even a UAF.

As mentioned above, the design of SPFs is generally part and operation specific. We also know that various machining operations have an intimate relation with particular machine tools. For example the machine tools of lathe group are primarily used for machining of axi symmetric components, drilling machines for drilling and allied operations, milling machines for machining of plane surfaces and so on. In view of the above, although each SPF is supposed to be unique, a degree of similarity can be discerned in fixtures designed for a particular type of machine tool, say a lathe or milling machine. Similarly, there would be substantial differences between a fixture designed for a lathe and one designed for a milling machine and often, these differences will be similar in nature, irrespective of the variety of individual parts. Keeping the foregoing in mind, it is customary to classify SPFs based on their association with machine tools as lathe fixtures, milling fixtures, drilling fixtures, and so on. Some of these fixtures are described below with the main objective of illustrating how the various aspects of the design of jigs and fixtures discussed in Chapter 7 are applied in actual practice.

Lathe Fixtures The standard fixture for turning and allied operations on lathe is the lathe chuck. Two, three, and four jaw chucks of various sizes are available as standard accessories with lathes. Pneumatic chucks are used for quick clamping of workpieces in medium and large lot batch manufacturing and mass production. Collets are preferred over chucks for holding bar stock. Many varieties and sizes of collets are available for round, square, and hexagonal sections. In case of workpieces with through holes, taper, and solid mandrels are used for location and expanding mandrels for location as well as clamping by gripping of the bore hole. Workpieces with center holes are located between centres and clamped by using face plate and dog carrier. Many of these elements have been described in Sections 7.3, 7.4, 7.5 and 7.7. In any case all these

elements are made by specialist firms and are commercially available in a variety of designs and size. It is therefore not necessary to consider them in detail.

Some parts such as castings and forgings can not be readily mounted by any of the standard methods and a special lathe fixture for work holding may be required. The general principles of locating and clamping discussed in Chapter 7 also apply to the design of lathe fixtures. However, in view of the fact that lathe fixtures rotate during the machining operation, there are additional factors that need to be considered in their design, namely:

- (i) clamps and work holding devices should not be loosened by centrifugal force
- (ii) workpiece should be gripped by the largest diameter
- (iii) fixture should be well balanced; counter weights may be used on irregular shaped parts to avoid vibrations, especially at high speed
- (iv) projections and sharp corners should be avoided as they may not be visible in rotation.

Special lathe fixtures are usually designed by adapting a chuck, face plate and mandrel or a combination of these for the specific part. Axi-symmetric components are held in standard three-jaw self centering chuck. Parts that require eccentric rotation and those with minor deviation from cylindrical shape can be machined in four-jaw chucks in which each jaw moves independently. Difficulty arises in machining of odd shape parts such as castings and forgings.

If such parts are to be machined in a chuck, the jaws of the standard chuck are removed and replaced by special jaws known as top jaws. The top jaws available from the chuck companies in soft state are machined to the desired shape commensurate with part geometry for better grip. These jaws are then hardened or retained in soft state as desired and put back in the chuck. Serrations may be made on the jaw teeth for better grip on rough workpieces. In addition to serrations, the gripping surface of the jaws may be strengthened by insertion of hardened cone point screws and pins. The cone points sink into the workpiece surface ahead of the serrations and provide better grip on difficult to hold surfaces.

One more method of holding irregular shape workpiece in chucks is based on the use of rocking jaws. For instance, on a three jaw chuck two jaws are made solid and the third rocking jaw adjusts itself to the uneven surface. A jaw with a pad provides more gripping area and distributes the clamping pressure more evenly. Such a set of pads provides grip on six equally spaced areas. One such chuck with padded jaws—two solid and one rocking is shown in Figure 8.10(a). When all the jaws of a chuck are made rocking and with pads, they are known as wrap around jaws (Figure 8.10(b)). Such jaws are particularly useful on fragile parts for gentle gripping.

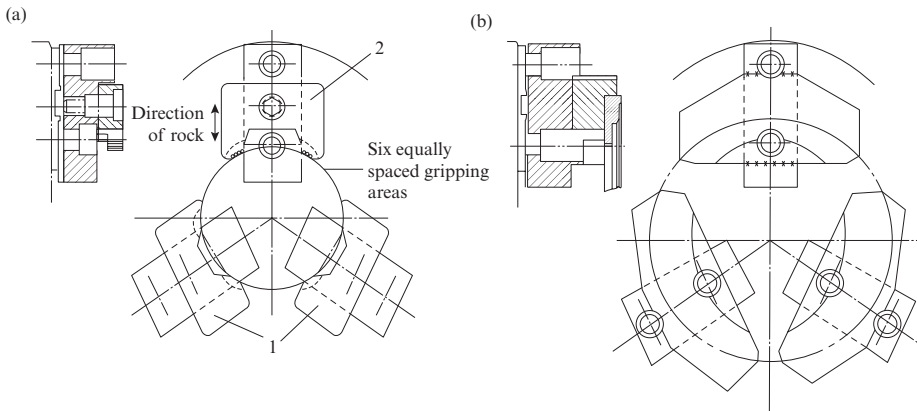


Figure 8.10 Chucks with special jaws (a) chuck with one rocking jaw for holding irregular shape workpiece 1- solid jaws, 2- rocking jaw and (b) chuck with wraparound jaws for holding fragile parts

When an irregular shaped part is to be held on a face plate, the SPF is designed for it applying the general principles and elements of location and clamping discussed in Chapter 7. The base on which this SPF is assembled may be a flat plate or angle plate, which is located on the face plate by means of two dowel pins. It is secured to the face plate either with the help of screws inserted through face plate openings into tapped holes in the base or by means of T-bolts inserted in the T-slots on the face plate.

Grinding fixtures These fixtures are used for work holding on grinding machines. For cylindrical grinding operations, there is large degree of similarity between grinding and lathe fixtures. As in lathes, solid cylindrical workpieces are held in chucks or supported between centers and clamped by means of face plate. Mandrels are used for external cylindrical grinding of workpieces with through hole, whereas chuck is the standard fixture for internal cylindrical grinding. Therefore, the discussion related to lathe fixtures is to a large extent applicable to grinding fixtures too. Surface grinding machines use fixtures that are similar to milling fixtures. Magnetic chucks are also used for directly holding workpieces for all grinding operations, but their use is more common on surface grinding machines. The design of special grinding fixtures for cylindrical grinding operation follows the same procedure as for special lathe fixtures.

Some conditions are unique to grinding process or machine and therefore need to be considered and reflected in the design of grinding fixtures. As grinding is a finishing operation, the allowable limits of locating errors in grinding operations are relatively narrower than in conventional machining operations. Therefore, locating methods must be precise and exacting, and locating elements machined to a high accuracy. Similarly, clamping force should be precise so as to ensure secure clamping without deflecting the workpiece. Grinding is an abrasive cutting operation that is carried out at very high cutting speeds. Abundant coolant supply at the point of wheel-work contact is therefore important to counter the effect of intense localized heating and minimize the resulting workpiece distortion under thermal effect. While designing grinding fixtures, care should be taken to see that it does not obstruct free flow of coolant to the wheel-work contact and free escape of the used coolant and the sludge formed by grinding.

Drill jigs These are devices used for carrying out drilling and allied operations such as core drilling, reaming, tapping, etc. The term *fixture* is used for the devices for other operations such as milling, broaching, shaping, etc. A drill jig for drilling and reaming radial hole in a bush is shown in Figure 8.11. The workpiece 11 is located on locating pin 1 with a flange which removes 5 degrees of freedom. Clamping is done by C-clamp 2 which is tightened by clamping nut 3. Liner bush 4 is permanently fitted in bush plate 9 and accommodates slip bushes 5 and 6 for guiding the drill and reamer, respectively. Retaining screw 7 prevents rotation of the bushes during operation. The jig body 8 is a welded structure strengthened by a stiffening rib 10.

A swinging latch jig for drilling two holes in a solid prismatic part is shown in Figure 8.12. The workpiece 1 is located by the 3–2–1 principle. Hinged pillar 2 with flange nut is used to clamp the latch 3 that carries guide bushes 4 and 5. Clamping force on the workpiece is applied by means of thumb screw 6. Here, it is important to note that the latch must not be directly used for clamping the workpiece, but only as a clamp bar in conjunction with an independent clamping device. Also a proper gap should be provided between the latch and the workpiece. In the absence of this gap, the position of the latch will be affected by deviation from parallelness between the latch and workpiece and will be reflected in a corresponding deviation of the axis of the drilled holes from the vertical.

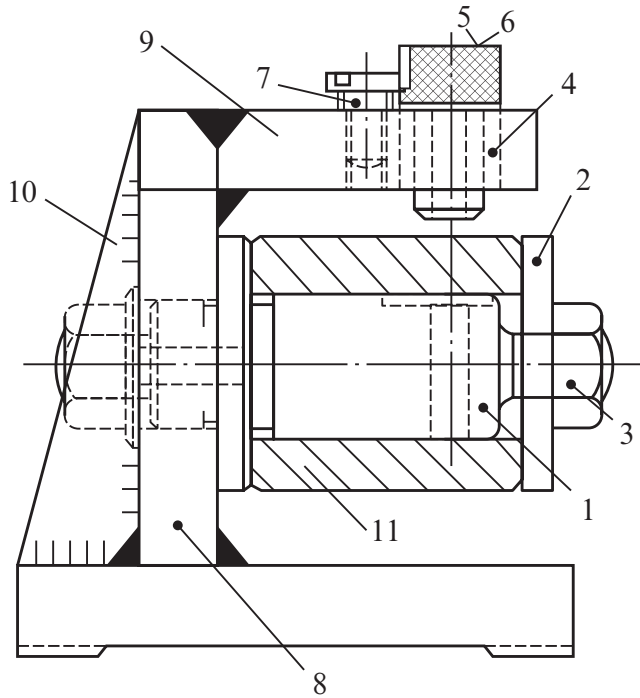


Figure 8.11 Construction details of drill jig

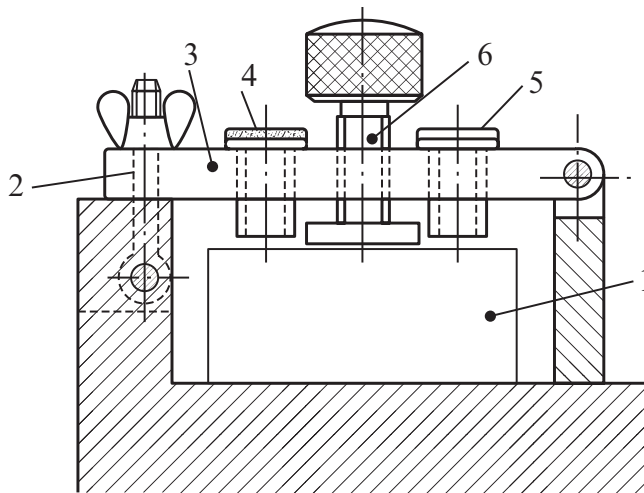


Figure 8.12 Construction details of swinging latch jig

An index jig for making 6 holes of diameter 4 mm in a job (Figure 8.13(a)) is shown in Figure 8.13(b). The workpiece 8 is located on flanged pin 10 and prevented from rotation by key 11. The angle 30° between the hole axis and job face is set by mounting pin 10 at the same angle

with respect to the base of the jig body 5. Clamping is done with the help of C-clamp 12 which is tightened by rotating star wheel 1 that pulls rod 3 forward. The workpiece is removed by rotating the star wheel in the opposite direction, which allows spring 4 to push back the C-clamp and release the workpiece. For drilling of 6 holes, indexing disc 7 is mounted on the locating pin 10. The indexing disc has 6 equal spaced recesses that mate with the fixing element 13 of a pawl and ratchet mechanism. The indexing disc is rotated by means of wheel 2. Bush plate 6 is secured to the top of body 5 and carries bush 9 for guiding the drill.

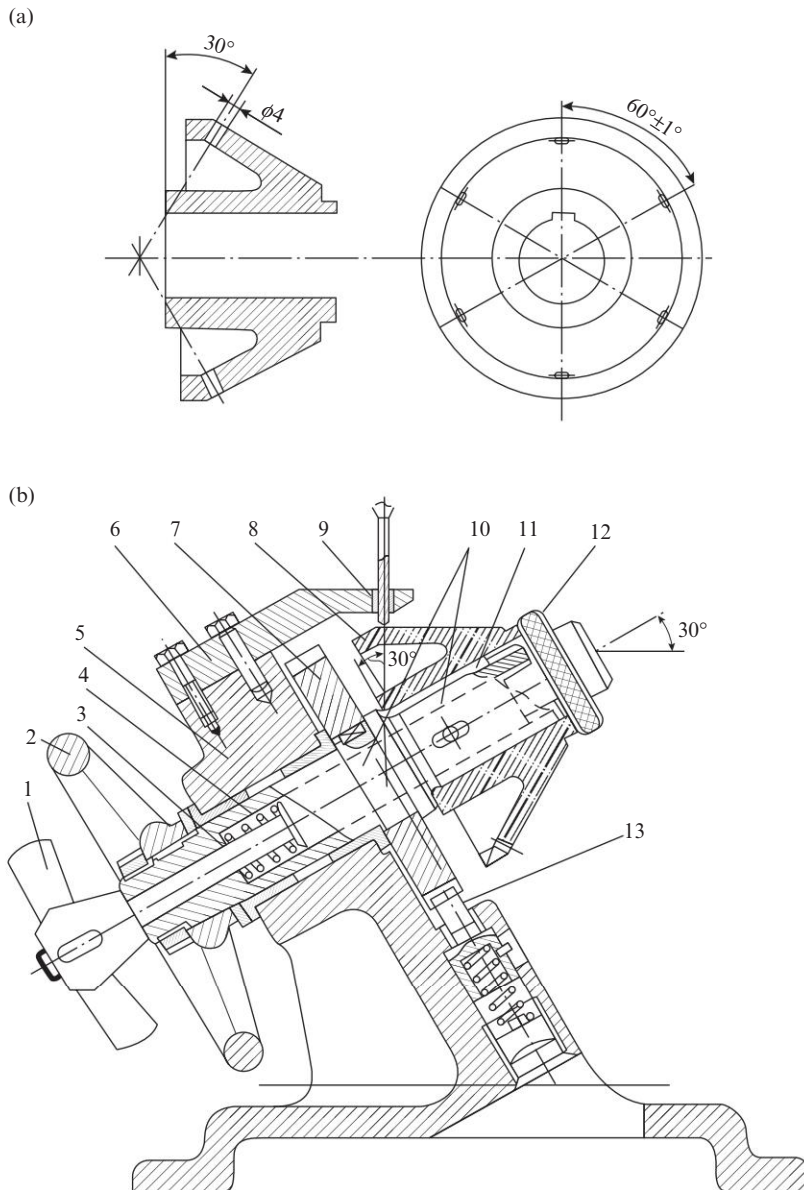


Figure 8.13 Indexing jig: (a) workpiece and (b) construction details of jig

Milling Fixtures These are used for holding prismatic workpiece to carry out various operations on milling machines. The most economical and popular method of holding small components is by using standard vices. It is very easy to clamp workpieces with parallel sides in a vice. However, for other shapes, special jaws may be required. Three such special jaws are shown in Figure 8.14. The special jaw shown in Figure 8.14(a) is suitable for holding cylindrical workpieces. The pair of jaws shown in Figure 8.14(b) is suitable for holding thin sheet. Here, the stop pin prevents bending of the sheet during the clamping action. The extended special jaws shown in Figure 8.14(c) are suitable for holding large workpieces. Here, the guide pin is required for alignment.

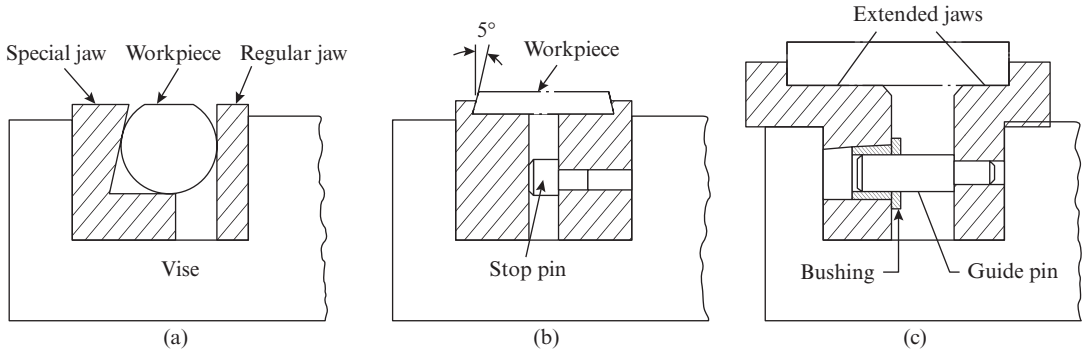


Figure 8.14 Special jaws for milling vices: (a) for holding cylindrical workpiece, (b) for holding thin sheet, and (c) for holding large workpieces

A fixture for end milling a groove in an aluminum die-cast part is shown in Figure 8.15. The part is located with the help of pin 1 and a small diamond pin 3 that is press fitted in the fixture base 2 for which suitable holes are available in the workpiece. Clamp 4 is tightened against the part with the help of cap screw 5. A slot in the top plate 6 of the welded fixture body provides access to the end mill cutter in the work area. As the cutting force is small, it is possible to perform the operation against the clamp, although such an arrangement is generally better avoided. The fixture is located on the machine table with the help of tennon strips 7 and secured with the help of T-bolts for which elongated slots are provided at both ends of the fixture base.

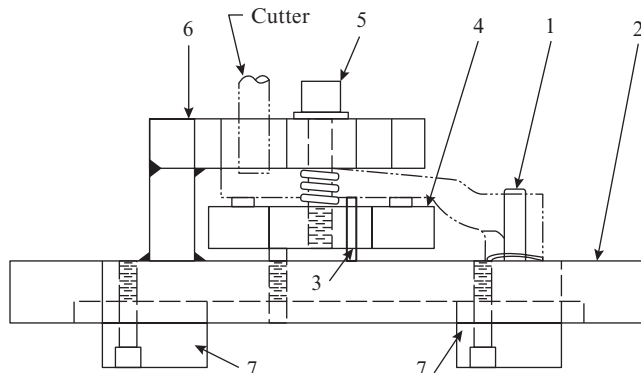


Figure 8.15 Milling fixture for end milling

A fixture for straddle milling a block is shown in Figure 8.16. Two locators 1 of the wedge type ensure sidewise location of the workpiece by approximately centering on the rest surface. In order not to interfere with the cutters that mill the top surface, a bell crank-type clamp 2 is used. Pressure on the clamp is applied by tightening screw 6 that presses on hardened rest button 3 to avoid indentation of the fixture body. As part of setting up operation, the fixture is centralized between the straddle milling cutters. The depth of cutter is set with the help of set block 5 and feeler gauge of appropriate thickness. The fixture is located on the machine table by means of tennon strips 4 and secured to it with the help of T-bolts and straps.

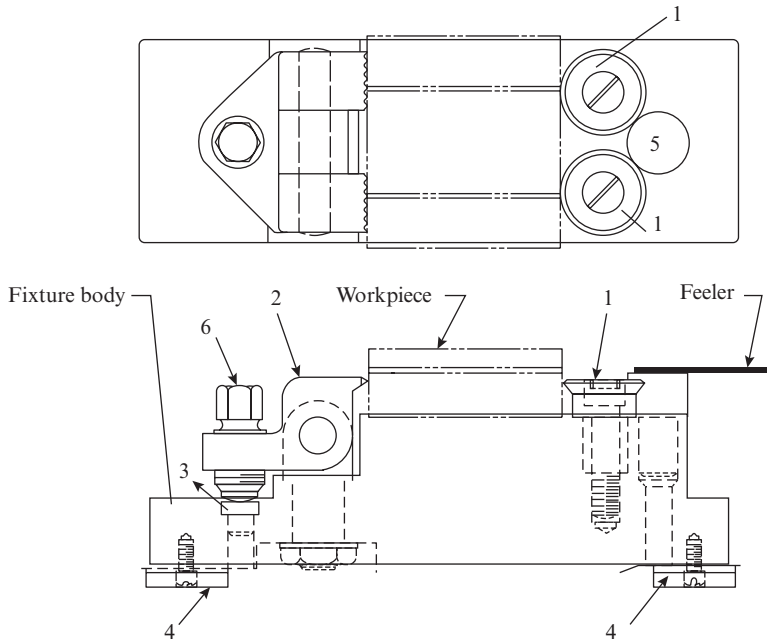


Figure 8.16 Milling fixture for straddle milling

A fixture for straddle milling of the shoulders in a collar (Figure 8.17(a)) is shown in Figure 8.17(b). The bore hole of the workpiece is used for locating it on pin 1 that removes 5 degrees of freedom. Side-wise location with the help of block 2 removes the last remaining degree of freedom. Strap 3, supported on pillar pin 4, is used for clamping. Pad 5 ensures even distribution of the clamping force which is applied through cam type eccentric 6. Fixture body 7 has suitable steps on both sides to accommodate the pair of half side milling cutters 8 used in the straddle milling operation. The fixture is located on the machine table by means of tennon strips 9 and holes in the base are used for securing the fixture to the machine table with the help of T-bolts.

Finally, a simple face-milling fixture is shown in Figure 8.18. Workpiece 1 is located on three adjustable rest buttons 2. Fixed pad 3 serves for side-wise location of the workpiece. When strap 4 is tightened, it pushes the workpiece against the fixed pad 3 and clamps it. Setting pin 5 with feeler gauge serves for setting of face milling cutter to the appropriate depth. The fixture is located on machine table by means of tennon strips 8 and secured to it with the help of 4 T-bolts for which elongated slots 6 are provided in the base of fixture body 7.

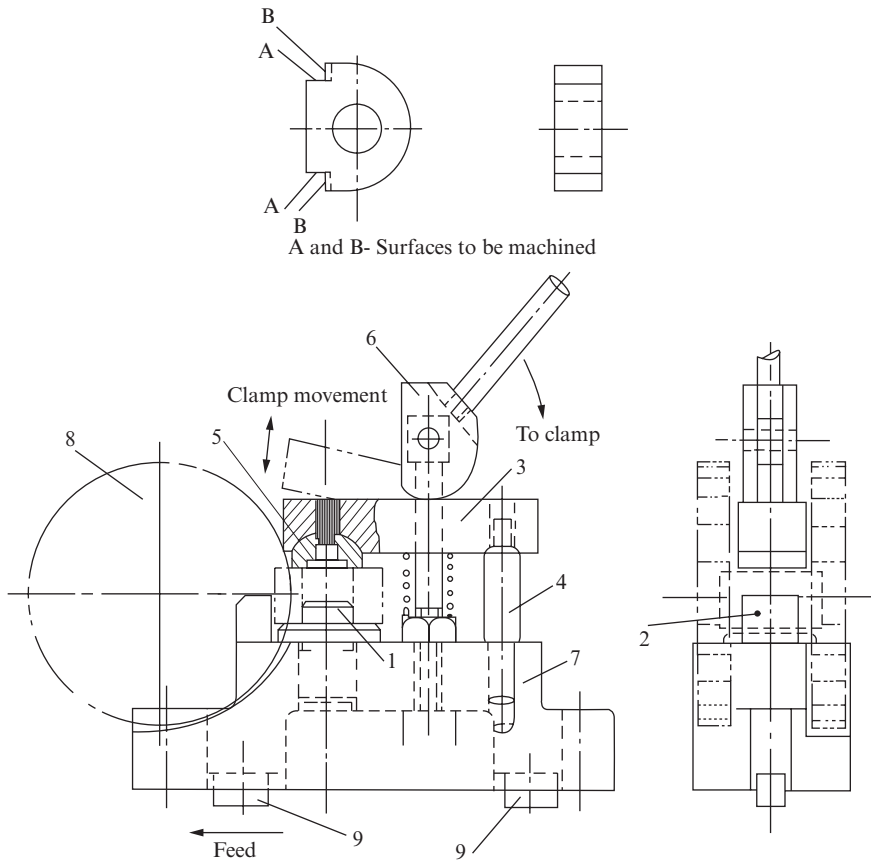


Figure 8.17 Milling fixture with quick acting clamping device

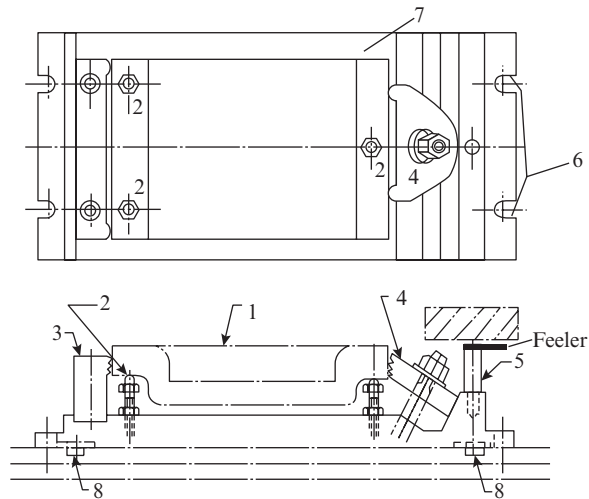


Figure 8.18 Milling fixture for face milling

8.2 Economics of Jigs and Fixtures

The study of the economics of jigs and fixtures has two objectives:

1. Selecting the correct type of fixture from among UGP, UAF, SAF, RAF, UBF, and SPF for a given volume of production and the total period allocated for this purpose.
2. Selecting the most economic design from among the various possible alternatives that are all technically correct.

Here, it is important to remember that fixtures, such as all production equipments have a limited life. Therefore, due consideration must be given to their depreciation. During the life of a jig/fixture, parts may have to be repaired or replaced. This factor should also be considered in the economic analysis. Different fixtures may require change of machine tool and lower or higher operator skills that will be reflected in the operational cost of the fixture. These issues must also be factored in the economic analysis.

The economic effectiveness of the use of a jig or fixture may be expressed by the general condition

$$E \geq P \quad (8.1)$$

where

E = annual savings from the use of jig/fixture

P = annual cost of fixture

The annual economy E may be determined from the following relation:

$$E = (Tc - T_f c_f)Q \quad (8.2)$$

where

T = production time per piece for the given operation without the use of a fixture or with a universal fixture, min

T_f = production time per piece for the given operation using the fixture, min

c = operational cost per minute without use of fixture

c_f = operational cost per minute with fixture

Q = annual production volume of the product

The operational cost consists of the wage rate of the operator with over heads, fixed overheads including cost of machine with accessories per minute (depreciation) and variable overheads arising from running cost such e.g. on coolant, tool usage, etc.

8.2.1 Calculation of Annual Cost of Fixture

The annual cost of an SPF may be expressed by the following general relation

$$P = C \left(i + r + t + \frac{1}{N} \right) + Si \quad (8.3)$$

where

C = cost of fixture

i = annual rate of interest payable on investment, expressed as a decimal

r = yearly percentage of cost for repair, upkeep and maintenance, expressed as a decimal

t = yearly percentage of cost for taxes, insurance, etc., expressed as a decimal

N = years for recovering the cost of fixture out of savings

S = difference between the unamortized and salvage value of old fixture

In industrial practice, the period of amortization of special equipments is generally taken as $N = 2$ years and $r = 0.1$. Representing the contribution of i , t , and S by a common yearly percentage of cost coefficient K , we may write Eqn. (8.3) as follows:

$$P = 0.5C + C(0.1 + K)$$

$$P = (0.6 + K)C \tag{8.4}$$

Example 8.1

A fixture is designed for a part that brings down the time per piece from 26 to 16 min. If the cost of the fixture is ₹ 30,000 = 00 and the operator wage rate is ₹ 36 = 00/hr, determine the annual production volume for break even, given that $N = 2$ years, $i = r = t = 10$ percent, $S = ₹ 2,000 = 00$

Applying Eqn. (8.3), we find the annual cost of the fixture as

$$P = 30,000(0.1 + 0.1 + 0.1 + 0.5) + 2,000 \times 0.1 = ₹ 24,200 = 00$$

Assuming that the same operator wage rate applies for carrying out the operation with or without the fixture, the annual savings from the use of fixture is found from Eqn. (8.2) as follows:

$$E = (26 - 16) \frac{36}{60} Q$$

Applying Eqn. (8.1), the break even is found from the condition

$$(26 - 16) \frac{36}{60} Q \geq 24,200$$

$$6Q \geq 24,200$$

wherefrom

$$6Q \geq 4033$$

For a quick estimation of fixture cost C , it is convenient to classify SPFs into groups based on their degree of complexity that is expressed in terms of the number of components in the fixture. Such a classification is given in Table 8.2. The cost of a fixture of Group 1 is taken as reference value C_1 and the cost of the fixtures of the other groups is found in first approximation by using the values given in Column 4 of the table as multiplication factors.

Table 8.2 Classification of SPFs in groups based on complexity and values of cost multipliers for various groups

| Group | Description of fixture | No of components in fixture | Multiplication factor |
|-------|---|-----------------------------|-----------------------|
| I | Small fixtures with simple body and simple locating and clamping elements, e.g. simple supports, mandrels, replaceable jaws, etc. | ≤ 5 | 1 |

(Continued)

Table 8.2(Continued)

| Group | Description of fixture | No of components in fixture | Multiplication factor |
|---|---|---|------------------------------|
| II | Small fixtures of simple-to-medium complexity in operation with body of medium complexity and simple-to-medium complexity clamping, e.g. chucks, expansion mandrels, etc. | < 5 | 1–2 |
| | | 5–10 | 2–3.5 |
| | | 10–15 | 3.5–5.0 |
| | | | |
| III | 1. Small- and medium-size fixtures with body and clamping elements of medium complexity | 10–15 | 5.0–7.0 |
| | | 15–20 | 7.0–9.0 |
| | | 20–25 | 9.0–11.0 |
| | 2. Small fixtures with complex bodies | | |
| | 3. Medium-size fixtures with simple body | | |
| | IV | 1. Small fixtures with complex bodies and complex clamping elements | 20–25 |
| 25–30 | | | 17.0–20.0 |
| 30–35 | | | 20.0–22.0 |
| 2. Medium-size fixtures with medium complexity body and clamping | | 35–40 | 22.0–25.0 |
| 3. Large fixtures with medium complexity body and simple clamping | | | |
| V | | 1. Medium-size fixtures, complex in operation with complex body and clamping elements | 35–40 |
| | 40–45 | | 39.0–42.0 |
| | 45–50 | | 42.0–46.0 |
| | 2. Large fixtures, simple in operation with complex body and medium complexity clamping | 50–55 | 46.0–49.0 |
| | | | |
| VI | 1. Large-size fixtures complex in operation with multiple wall body and medium-to-complex clamping | 50–55 | 72.0–75.0 |
| | | 55–60 | 75.0–81.0 |
| | | 60–65 | 81.0–86.0 |
| | | 65–70 | 86.0–90.0 |
| | 2. Medium- and large-size fixtures with pneumatic or hydraulic powered clamping | 70–75 | 90.0–95.0 |
| | | 75–80 | 95.0–100.0 |
| | | 80–85 | 100.0–104.0 |
| | | 85–90 | 104.0–109.0 |
| | | 90–95 | 109.0–113.0 |

For a universal general-purpose fixture (UGP), the annual cost is found from the following relation:

$$P_{UGP} = \frac{(0.6 + K)C_{UGP}}{m} \quad (8.5)$$

where

C_{UGP} = cost of general purpose fixture

m = number of times the fixture is used in a year for different operations

Here, it has been assumed that the fixture is amortized in 2 years and rates for i , r , t , and S are applied the same as in Eqn. (8.4).

For UAF and SAFs, the cost consists of the cost of permanent components and the replaceable elements. If it is assumed that the cost of permanent components is fully amortized in 2 years and that of the replaceable components in 1 year and the same rates for i , t , and S are applied as for the SPF, then the expression for annual cost of a UAF/SAF can be written as follows:

$$P_{UAF/SAF} = \frac{(0.6 + K)C_{UAF/SAF}^p}{m} + (1.1 + K)C_{UAF/SAF}^r \quad (8.6)$$

where

$C_{UAF/SAF}^p$ = cost of the set of permanent components

$C_{UAF/SAF}^r$ = cost of replaceable components of the fixture

m = number of times the permanent components are used in various fixtures in a year

The annual cost of an RAF may be determined from the following relation:

$$P_{RAF} = \frac{(0.6 + K)C_{RAF}^p}{m} + (1.1 + K)C_{sc} + C_A n \quad (8.7)$$

where

C_{RAF}^p = cost of the set of permanent components

C_{RAF}^r = cost of replaceable components of the fixture

m = number of fixtures assembled from the permanent set in a year

C_A = cost of assembling the given fixture once

n = number of times the given fixture is assembled in a year

The annual cost of a UBF is determined using a formula similar to that for RAF, except that the number of years for amortization of the UBF set is more. While writing the formula, it is also assumed that notwithstanding the large variety of parts in the UBF set, some special parts are required for the given fixture:

$$P_{UBF} = \frac{\left(\frac{1}{M} + 0.1 + K\right)C_{UBF}}{m} + 1.1C_{sc} + C_A n \quad (8.8)$$

Here,

C_{UBF} = cost of UBF set

M = number of years for amortization of UBF set

The rest of the symbols have the same meaning as in Eqn. (8.6).

It may be noted here that Eqs (8.5) through (8.8) have been derived by assuming 2-year period for amortization of fixture and 10 percent cost of fixture as expenses on its repair and maintenance. For other values, the general expression given by Eqn. (8.3) may be used.

8.2.2 Relative Economic Analysis

The feasibility of different type of fixtures mainly depends on the product life (in months) and the utilization of the fixture that may be expressed by the following relation:

$$K = \frac{T_f n}{A} \tag{8.9}$$

where

T_f = production time per piece for the given operation using a particular fixture

n = number of times the operation is carried out in a given time span (month)

A = availability of fixture in the same time span (month)

Depending on the product life (in months) and the utilization of fixtures, the feasible zones for various types of fixtures have been determined. and the summary of this analysis is given in Figure 8.19.

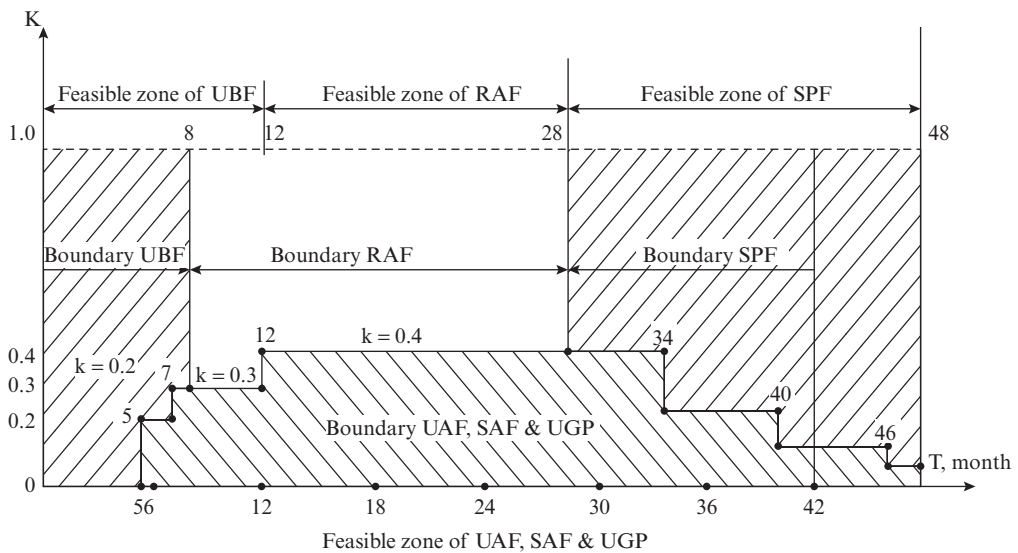


Figure 8.19 Feasible zones of application for various types of fixtures depending on coefficient of utilization K and product life T

Break-even analysis One of the main objectives of relative economic analysis is to determine the break even for a selected fixture. In Eqn. (8.2), representing $s = (TC - T_f C_f)$ as the saving in direct operating cost per piece and using an overhead factor (load factor) L on the labour saved expressed as a decimal, we can write Eqn. (8.1) as follows:

$$Qs(1 + L) \geq P \tag{8.10}$$

By substituting the expression for P from Eqs (8.3)–(8.8), the break even can be determined for a given type of fixture. For instance, if we substitute for P from Eqn. (8.3) in Eqn. (8.10), the break even for special fixture(SPF) is found from the following relation:

$$Qs(1+L) \geq C \left(i+r+t+\frac{1}{n} \right) + Si$$

wherefrom

$$Q \geq \frac{C \left(i+r+t+\frac{1}{n} \right) + Si}{s(1+L)} \quad (8.11)$$

If the simplified relation for P represented by Eqn. (8.4) is substituted in Eqn. (8.10), the break even is obtained for an SPF from the following relation:

$$Q_{\text{SPF}}s(1+L) \geq (0.6+K)C$$

wherefrom

$$Q_{\text{SPF}} \geq \frac{(0.6+K)C}{s(1+L)} \quad (8.12)$$

Example 8.2

A milling fixture costing ₹ 20,000 = 00 is used for producing 5 batches in a year involving a setting up cost of ₹ 500 = 00 each time. Given $N = 2$ years, $i = r = t = 0.1$, $S = 0$, labor saving per part $s = ₹ 5 = 00$ and overhead factor on labour saved $L = 50$ percent. Determine the annual production volume to ensure 15 percent profit on investment.

Referring to Eqn. (8.3), the annual cost of fixture

$$P = 20,000(0.1+0.1+0.1+0.5) = ₹ 16,000 = 00$$

Annual setting up cost = $500 \times 5 = ₹ 2,500 = 00$

Profit on investment = $0.15 \times 20,000 = ₹ 3,000 = 00$

Hence, total annual desired return

$$= 16,000 + 2,500 + 3,000 = ₹ 21,500 = 00$$

The break even is obtained by applying Eqn. (8.10)

$$Q \times 5(1+0.5) \geq 21,500$$

wherefrom

$$Q \geq \frac{21,500}{7.5} = 2867$$

Expression of break even for other types of fixtures can be similarly derived by substituting the appropriate value of P from Eqs (8.5) through (8.8) in Eqn. (8.10).

For a UGP, P is substituted from Eqn. (8.5), and we obtain

$$Q_{\text{UGP}} \geq \frac{(0.6+K)C_{\text{UGP}}}{ms(1+L)} \quad (8.13)$$

For a UAF or SAF, P is substituted from Eqn. (8.6) and we obtain

$$Q_{\text{UAF/SAF}} \geq \frac{1}{s(1+L)} \left[\frac{(0.6+K)C_{\text{UAF/SAF}}^P}{m} + (1.1+K)C_{\text{UAF/SAF}}^T \right] \quad (8.14)$$

For an RAF, P is substituted from Eqn. (8.7) and we obtain

$$Q_{\text{RAF}} \geq \frac{1}{s(1+L)} \left[\frac{(0.6+K)C_{\text{RAF}}^P}{m} + (1.1+K)C_{\text{sc}} + C_A n \right] \quad (8.15)$$

For a UBF, P is substituted from Eqn. (8.8) and we obtain

$$Q_{\text{UBF}} \geq \frac{1}{s(1+L)} \left[\frac{\left(\frac{1}{M} + 0.1 + K \right) C_{\text{UBF}}}{m} + 1.1C_{\text{sc}} + C_A n \right] \quad (8.16)$$

Total cost analysis Having selected the type of fixture based on product life and utilization and validated it by break-even analysis, the next task is to evaluate the various design alternatives from the view point of cost. If the design alternatives use the same machine and cutting tool, then only the cost components related to machining and the fixture are considered in the comparative analysis. The cost of an operation in this case is given by the expression for an SPF as follows:

$$C_0 = T_f c_f (1+L) + \frac{C}{Q} (0.6+K) \quad (8.17)$$

It may be pertinent to note here that the second term in Eqn. (8.17) represents the fixture cost per part for an SPF and is obtained from Eqn. (8.4).

For two competing alternatives 1 and 2 that are both technically correct, the break even can be found by equating the cost values C_{01} and C_{02} , that is,

$$T_{f1} c_{f1} (1+L) + \frac{C_1}{Q} (0.6+K) = T_{f2} c_{f2} (1+L) + \frac{C_2}{Q} (0.6+K)$$

wherefrom

$$(T_{f1} c_{f1} - T_{f2} c_{f2})(1+L) = \frac{1}{Q} (0.6+K)(C_2 - C_1)$$

Hence,

$$Q = \frac{(0.6+K)(C_2 - C_1)}{(1+L)(T_{f1} c_{f1} - T_{f2} c_{f2})} \quad (8.18)$$

By carrying out similar exercise for all the technically correct design alternatives, it is possible to ascertain the feasible annual production volume range for each design alternative and choose the appropriate one for the given production volume.

If the design alternatives involve change to a machine tool of a different type or of the same type but different configuration or accuracy, then the related cost difference must be factored in the calculation of operation cost. The expression for operation cost in this case is

$$C_o = T_f c_f (1+L) + \frac{C}{Q} (0.6+K) + \frac{\left[C_m \left(i+r+t+\frac{1}{N_m} \right) + S_m i \right]}{60H} T_f \quad (8.19)$$

where

C_m = cost of machine tool

H = total running time of machine in a year, in hours

N_m = years allowed for amortization of machine tool

The last term in Eqn. (8.19) represents the product of machine rate with overheads per minute and the production time per piece. Expressions similar to Eqs (8.17) and (8.19) can be derived for other types of fixtures by representing the fixture cost per part with Eqn. (8.5) for UGP, Eqn. (8.6) for UAF/SAF, Eqn. (8.7) for RAF and Eqn. (8.8) for UBF. The comparative analysis among competing alternatives to arrive at the expression of break can be carried out in a manner similar to that adopted for SPF to derive Eqn. (8.18).

Example 8.3

The time per piece on an operation by using a fixture is 20 min. The numerical values of the factors associated with the annual cost of the machine tool and fixture are $C_m = ₹ 3,00,000 = 00$, $N_m = 10$ years, $S_m = 0$, $H = 2,000$ hr, $C = ₹ 20,000 = 00$, $N = 2$ years, $S = 0$. For the machine tool and fixture, all the interest rates i , r , and t expressed as decimal are 0.1. The operator wage rate is ₹ 36 = 00/hr. If the cost of the operation is not to exceed ₹ 40 = 00, determine the annual production value for break even.

Referring to Eqn. (8.19), we find the cost of the operation as (assuming $L = 0$)

$$C_o = \frac{20}{60} \times 36 + \frac{20,000(0.1+0.1+0.1+0.5)}{Q} + \frac{3,00,000(0.1+0.1+0.1+0.1)}{2,000} \times \frac{20}{60}$$

$$C_o = 12 + \frac{16,000}{Q} + 20$$

On equating this to the limiting cost value of ₹ 40 = 00, we obtain

$$12 + \frac{16,000}{Q} + 20 = 40$$

$$\frac{16,000}{Q} = 8$$

wherefrom

$$Q = 2,000$$

Review Questions

- 8.1** The common fixture for holding prismatic parts is
 (a) V-block (b) chuck
 (c) vice (d) mandrel
- 8.2** The common fixture for holding short cylindrical workpieces on the cylindrical surface is
 (a) V-block (b) chuck
 (c) vice (d) collet
- 8.3** The common fixture for holding bar stock is
 (a) V-block (b) mandrel
 (c) vice (d) collet
- 8.4** Chuck with a rocking jaw is used for gripping
 (a) uneven rotational parts (b) finish machined rotational parts
 (c) small-size bar stock (d) prismatic parts
- 8.5** Magnetic plate is used for holding workpiece on
 (a) lathe (b) milling machine
 (c) cylindrical grinding machine (d) surface grinding machine
- 8.6** Lathe chuck is typical example of a
 (a) universal general-purpose fixture (b) universal built-up fixture
 (c) special fixture (d) special adjustable fixture
- 8.7** Among the following, the type of fixture that has maximum versatility is
 (a) special fixture (b) reassemblable fixture
 (c) special adjustable fixture (d) reassemblable adjustable fixture
- 8.8** Tennon strips are mounted to the base of milling fixture for the purpose of
 (a) locating the workpiece (b) clamping the workpiece
 (c) guiding the cutting tool (d) aligning the fixture on machine table
- 8.9** Milling fixture is secured to machine table by means of
 (a) hexagonal bolt (b) stud
 (c) screw (d) T-bolt
- 8.10** Elongated grooves in the base of milling fixture are provided by clamping the fixture to machine table by means of
 (a) flat strap (b) T-bolt
 (c) hexagonal bolt (d) goose neck strap
- 8.11** In solved Example 8.1, determine the annual production volume for break even if the time per piece with fixture is 20 min and the fixture cost is amortized over a period of 3 years.
- 8.12** In solved Example 8.1, if the use of fixture allows hiring of an operator of lower skill level whose wage rate is 25 percent less, how will it affect the annual production volume for break even?
- 8.13** In solved Example 8.3, if the machine running hours in a year is enhanced to 4,000 by operating in two shifts and the number of years for amortization of the machine tool is reduced to 5 years, how will it affect the annual production volume for break even?

- 8.14** In solved Example 8.3, if the annual production volume is to be produced in 5 lots of 400 parts each, determine the cost of operation if the setting up cost for each lot is ₹ 1,000 = 00.
- 8.15** In solved Example 8.2, determine overhead factor on labour saved if the cost of the fixture is ₹ 30,000 = 00 and the annual production volume is 5,000 pieces.
- 8.16** In solved Example 8.2, determine the annual production volume for break even if the production is to be done in 10 batches and the desired profit on investment is 20 percent.

BIBLIOGRAPHY

Acherkan, N.; Metal Cutting Machine Tools. Moscow: State Scientific and Technical Publishing House of Machine Building Literature; **1958** (in Russian).

Acherkan, N.; Metals Handbook. Moscow: Mashinostroenie Publishers; **1966** (in Russian).

Anserov, M. A.; Fixtures for Metal Cutting Machine Tools. Leningrad: Mashinostroenie Publishers; **1975** (in Russian).

Arshinov, V. A and Alekseev, G. A.; Metal Cutting and Cutting Tools. Moscow: Mashinostroenie Publishers; **1964** (in Russian).

Armarego, E. T. A.; and Brown, R. H.; The Machining of Metals. New Jersey: Prentice Hall; **1969**.

Belyaev, N. M.; Strength of Materials. Moscow: Mir Publishers; **1979**.

Bhattacharya, A.; and Ham, I.; Design of Cutting Tools: Use of Metal Cutting Theory. Michigan: ASME; **1969**.

Bhattacharya, A.; and Sen, G. C.; Principles of Machine Tools. Calcutta: New Central Book Agency (P) Ltd.; **1973**.

Bhattacharya, A.; Metal Cutting Theory and Practice. Calcutta: New Central Book Agency (P) Ltd.; **1996**.

Bobrov, V. F.; Fundamentals of the Theory of Metal Cutting. Moscow: Mashinostroenie Publishers; **1964** (in Russian).

Boothroyd, G.; Fundamentals of Metal Machining and Machine Tools. Tokyo: McGraw Hill; **1975**.

Danilevsky, V.; Manufacturing Engineering. Moscow: Mir Publications; **1973**.

DeGarmo, P. E.; Black, J. T.; and Kohser, R. A.; Materials and Processes in Manufacturing. 8th edition, New Delhi: Prentice-Hall of India Pvt. Ltd.; **2001**.

Donaldson, C.; et.al. Tool Design, 3rd edition, New Delhi: Tata McGraw Hill Publishing Co Ltd.; **1992**.

Dubinina, N. P.; et.al. Technology of Metals and Other Engineering Materials. Moscow: Vyshaya Shkola Publishers; **1969** (in Russian).

Grant, H. E.; Jigs and Fixtures: Non Standard Clamping Devices. New Delhi: Tata McGraw Hill Publishing Co Ltd.; **1972**.

Goroshkin, A. K.; Jigs and Fixtures. Moscow: Handbook, Mir Publishers; **1983**.

Groover, M. P.; Fundamentals of Modern Manufacturing : Materials, Processes and Systems. 2nd edition, New York: John Wiley & Sons; **2004**.

Joshi, P. H.; Jigs and Fixtures. New Delhi: Tata McGraw Hill Publishing Co Ltd.; **1998**.

Kalpakjian, S.; and Schmid, S. R.; *Manufacturing Process for Engineering Materials*. 5th edition, Chennai, India: Pearson; **2009**.

Kovan, V.; *Fundamentals of Process Engineering*. Moscow: Foreign Languages Publishing House.
Kuvshinskii, V. V.; *Milling Operation*. Moscow: Mashinostroenie Publishers; **1977** (in Russian).

Lal, G. K.; *Introduction to Machining Science*. New Delhi: New Age International Publishers; **1996**.

Loktev, D. A.; *Metal Cutting Machine Tools*. Moscow: Mashinostroenie Publishers; **1968** (in Russian).

Mehta, N. K.; *Machine Tool Design & Numerical Control*. 3rd edition, New Delhi: McGraw Hill Education (India) Pvt Ltd.; **2012**.

Nefedov, N. A.; and Osipov, K. A.; *Problems and Examples on Metal Cutting and Cutting Tools*. Moscow: Mashinostroenie Publishers; **1976** (in Russian).

Parsons, S. A. J.; *Production Tooling Equipment: The Design of Jigs, Tools and Gauges*. London: Cleave-Hume Press Ltd.; **1954**.

Pandey, P. C.; and Singh, C.K.; *Production Engineering Sciences*. 6th edition, New Delhi: Standard Publications Distributors; **1992**.

Production Technology, Handbook, HMT Bangalore. New Delhi: Tata McGraw Hill Publishing Co Ltd.; **1999**.

Ranganath, B.T.; *Metal Cutting and Tool Design*. 2nd edition. New Delhi: Vikas Publishing House Pvt. Ltd.; **1999**.

Rodin, P.; *Design and Production of Metal Cutting Tools*. Moscow: Mir publishers; **1968**.

Romanov, K. F.; *Cutting Tools, Lecture Notes for UNIDO Course*. Published by People's Friendship University, Moscow: **1975**.

Rowe, G. W.; *An Introduction to the Principles of Metal Working*. London: Edward Arnold Ltd; **1968**.

Shaw, M. C.; *Metal Cutting Principles*. 2nd edition, New York: Oxford University Press; **2005**.

Utkin, N. F.; *Fixtures for Machining Operations*. Leningrad: Lenizdat Publishers; **1969** (in Russian).

Vladimirov, V.; *Dies, Moulds and Jigs*. Moscow: Mir Publishers; **1972**.

Wilson, F. W.; and Holt, J. M.; *Handbook of Fixture Design*. New York: McGraw Hill Book Co Inc.; **1962**.

Zorev, N. N.; *Investigation of Elements of Mechanics of Metal Cutting*. Moscow: Mashgiz; **1952**.

INDEX

3-2-1 Principles of location 321

A

Actual clearance and rake angles 211
Annual cost of fixture 419
Assembled bodies of fixtures 387
Auxiliary motions 3

B

Body of jigs or fixtures 386
Boring operation 9
Braze tools 250
Break-even analysis 423
Built-up bodies 389
Built-up edge 121
Bush plate 379
Bush 380

- Fixed 380
- Flanged 380
- Liner 380
- Plain 380
- Renewable 380
- Slip 381
- Special 382

C

Cast bodies of fixtures 386
Centers 344

- Dead 344
- Half 344
- Reverse 344
- Revolving 344
- Solid 344
- Truncated 344

C-clamps 378

- Captive 378

Chip 81

- Conical 81
- Continuous 77
- Cylindrical 81
- Discontinuous 76

Element 78
Partially continuous 77
Ribbon 81
Snarled 81
Spiral 81
Types of chips 76
Washer type 81
Chip breaking 80
Chip breakers 80

- Attached obstruction type 82, 85
- Groove type 82
- Step obstruction type 82, 83

Chip curling 78
Chip flow control 78
Chip formation 2, 55

- Simplified model 58
- Single-shear plane model 56
- Thick plastic zone model 57

Chip reduction coefficient 71
Chucks 33, 367

- Spring collet 367
- Self-centering 333

Clamping devices 344

- Requirements of 344

Clamping force calculation 348, 349

- General procedure 349
- In drilling of hole 351
- In machining of flat surface with plain milling cutter 350
- In machining of groove with end mill cutter 349
- In turning operation 353

Clamping mechanisms 355

- Eccentric-type 358
- Expanding mandrels 367
- Lever-type 368
- Rack-and-pinion-type 374
- Screw-type 355
- Spring collet chucks 367
- Toggle-type 370
- Wedge-type 362

Clamping principles 344, 345
Classification of jigs and fixtures 402

- Reassemblable fixture 404
- Special adjustable fixture 404

- Universal adjustable fixture 403
- Universal built-up fixture 405
- Universal general-purpose fixture 402
- Core drilling operation 21
- Counterboring operation 22
- Countersinking operation 22
- Crater wear 139
- Cutting 89
 - Oblique 89
 - Orthogonal 90
- Cutting force 124
 - Effect of cutting speed 126
 - Effect of cutting-edge inclination angle 131
 - Effect of feed and depth of cut 126
 - Effect of nose radius 131
 - Effect of primary cutting-edge angle 128
 - Effect of rake angle 128
 - Effect of work material 124
- Cutting speed 4
- Cutting temperature 191

D

- Datum 317
 - Design 317
 - Intermediate 319
 - Measuring 318
 - Setting-up 318
- Design of broach 278
 - Area of space between broach teeth 280
 - Check for strength 284
 - Chip breaking grooves 282
 - Core diameter 288
 - Length of broach 283
 - Number of flutes 288
 - Number of teeth 282
 - Pitch of the cutting teeth 281
 - Progressive cut method 278
 - Rise per tooth 280
 - Rising-tooth method 278
 - Tap length 290
- Design of circular form tool 256
 - By analytical method 258
 - By graphical method 257
 - Determination of profile 258
 - Determination of diameter 256
- Design of drills 266
 - Auxiliary flank height and width 268
 - Core diameter 267
 - Diameter of drill 267
 - Length of drill 268
 - Thickness of cutting blade 267
- Design of face milling cutters 276
 - Cutter diameter 276
 - Cutter length 276
 - Number of teeth 276
- Design of flat form tool 262
 - By analytical method 262
 - By graphical method 262
 - Determination of auxiliary features 262
 - Determination of profile 262
- Design of hob 306
 - Angle of worm helix 309
 - Bore diameter 308
 - Depth of flute 308
 - Flute parameters 310
 - Height of teeth 307
 - Hob diameter 308
 - Length of hob 310
 - Number of teeth 308
 - Pitch circle diameter 309
 - Tooth thickness 307
- Design of module cutter 296
 - Bore diameter 298
 - Cutter diameter 298
 - Geometry of module cutter teeth 297
 - Number of teeth 299
 - Profile of module cutter 296
 - Width of module cutter 299
- Design of gear shaping cutter 299
 - Check for under cutting 303
 - Condition to prevent under beveling 303
 - Condition to prevent under cutting 302
 - Cutter height 302
 - Extension coefficient 301
 - Thickness of cutter tooth 301
 - Thickness of tooth addendum 301
- Design of plain milling cutter 272
 - Bore diameter 273
 - Cutter diameter 273
 - Cutter length 275
 - Number of teeth 274
- Design of single-point tool 246
 - Tool shank based on strength 247
 - Tool shank for stiffness 248
- Design of Taps 287
 - Core diameter 288
 - Design of threaded portion 287
 - Flute profile 289
 - Number of flutes 288
 - Tap length 290

- Design of thread cutting dies 292
 - Bore diameter 298
 - Condition to prevent under cutting 302
 - Cutter diameter 298
 - Cutter height 302
 - Diameter and pitch circle diameter of clearance holes 293
 - Die mounting 294
 - Geometry of module cutter teeth 297
 - Height of die 294
 - Number of clearance holes 292
- Determination of auxiliary features 260
- Disposable insert tools 250
- Down milling 25
- Drill flute 269
- Drill jigs 413
- Drilling operation 19
- Drills with cylindrical shank 268
- Drills with tapered shank 268
- Dynamic shear stress 104
 - Bridgman's relation 104
 - Rosenberg and Eremin's relation 107
 - Zorev's relation 106

E

- Eccentrics 361
 - Types of 361
- Economics of jigs and fixtures 419
- Economics of machining 191
- Effect of feed on rake and clearance angle 211
- Effect of tool setting on rake and clearance angles 210
- Energy relations 96
- Error analysis for long cylindrical parts 325
- Error analysis for parts with center holes 343
- Error analysis for parts with flat base and two predrilled holes 339
- Error analysis for parts with through hole 333
- Error analysis for short cylindrical parts 333
- Expanding mandrels 367
- Exponent of tool life 151

F

- Fabricated bodies 386
- Facing operation 9
- Feasible zones of application of fixtures 423
- Flank wear 138
- Floating pad 375
- Force relations 92

- Forces in drilling 117
 - Thrust 118
 - Torque 117
- Forces in milling 119
- Form tools 214
- Form-relieved cutters 223
 - Circular 214
 - Flat 214

G

- Gear cutting methods 243
 - Gear hobbing 243
 - Gear shaping 243
 - Using a module cutter 244
- Geometry of broach 230, 243
- Geometry of drill 216
 - Actual clearance and rake angles on a drill 219
 - Chisel edge angle 220
 - Helix angle 220
 - Lip angle 217, 220
- Geometry of face milling cutter 227
- Geometry of form tool 214
- Geometry of milling cutters 223
- Geometry of plain milling cutter 225
 - Clearance angle 225
 - Helix angle 226
 - Rake angle 226
- Geometry of single-point thread cutting tool 235
- Geometry of single-point tool 46
 - Machine tool reference system 46
 - Orthogonal system 46
- Geometry of taps 240
- Geometry of thread chasers 237
- Geometry of thread-cutting die 241
- Grinding 41
 - External cylindrical 41
 - Internal cylindrical 43
 - Surface 44
- Grinding fixtures 413
- Guide bushes 379

H

- Handles used in screw clamps 377
- Heat sources in metal cutting 134
 - Flank-machined surface interface 134
 - Primary shear zone 134
 - Tool-chip interface 134

Hinged clamps 378
Hydro-pneumatic devices 392

I

Indexing 31
 Angular 35
 Based on continuous rotation 36
 Differential 33
 Plain 33
Indexing devices 383
Index jig 414

J

Jigs and fixtures 316
 Advantages 316
 Design requirements 316
 Elements of fixtures 317
 Error analysis 316

L

Latch jig 413
Lathe fixtures 411
Locating elements 324
Locating error 319
Locating pins 337
Location principles 317
Locking device 374

M

Machinability 179
Machinability index 183
Machining time 5
Magnetic devices 395
Mandrels 338
 Expanding 338
 Solid 338
 Taper 337
Mechanics of cutting process 88
Merchant's circle 93, 102
Microchipping of cutting edge 137
Milling cutters 24
 Angle cutter 24
 End milling cutter 24
 Face milling cutter 24
 Form cutter 24
 Plain milling cutter 24
 Side milling cutter 24

Milling fixtures 416
Misalignment error 341
Morse taper 269
Multiple clamping 379

O

Optimum tool angles 212
 Auxiliary cutting-edge angle 213
 Clearance angle 212
 Cutting-edge inclination angle 213
 Primary cutting-edge angle 213
 Rake angle 212

P

Pin 340
 Diamond pin 340
Power devices 389
 Hydraulic 391
 Pneumatic 390
 Vacuum-operated 394
Profile sharpened cutters 223

Q

Quick acting cam operated clamping devices 378
Quick acting clamping devices 376
Quick acting pneumatic wedge-type clamping devices 378

R

Reaming 22
Rest buttons 325
Rest pads 325
Restriction effect of auxiliary cutting edge 90
Rough setting datum 323

S

Screw clamp 375
Screw clamp using a slotted strap 376
Screw clamp with floating pad 375, 376
Screw clamps with swinging strap 376
Selection of depth of cut 195
Selection of feed 195
 Constraint on strength of weak element in feed mechanism 196
 Constraint on surface roughness 198
 Constraint on tool deflection 197

- Constraint on workpiece deflection 197
 - Power constraint 195
 - Torque constraint 196
- Seats for bits in brazed single-point tools 250
- Selection of optimum cutting speed 199
 - Maximum production rate criterion 201
 - Maximum profit criterion 203
 - Minimum cost criterion 199
- Shapes of cemented carbide bits 249
- Shapes of disposable inserts 252
- Shaping operations 39
- Shear angle 72
- Shear angle relations 107, 116
 - Ernst and Merchant's 107
 - Kronenberg's 111
 - Lee and Shaffer's 113
 - Merchant's second 109
- Shear plane temperature 188
- Shear strain 73
- Slotting operations 39
- Special jaws for milling vices 416
- Spherical pin 337
- Spherical washer 376
- Spot facing operation 23
- Stagnant zone 122
- Standard components and units of fixtures 406
- Standard elements for jig and fixture body 388
- Strap 375
 - Slotted 376
 - Swinging 376
- Strap clamp 378
- Surface finish 180

T

- Taper turning 11
- Tapping operation 23
- Taylor's constant 151
- Taylor's generalized tool life equation 155
- Taylor's tool life equation 151
- Temperature relations for various heat sources 185
 - Continuous point source 187
 - Moving plane source 187
- Thread chasers 238
 - Block type 238
 - Circular 238
 - Shank type 238
- Thread cutting 14, 234
 - Multiple-point tool (chaser) 234
 - Single-point tool 234
- Tolerance 319
 - Available 319
 - Design 319
- Tool angles in the machine tool reference system 50
- Tool angles in the orthogonal system 48
- Tool failure by plastic deformation 137
- Tool-chip interface temperature 190
- Tool holders 252
 - Bridge-type 252
 - Center-lock-type 253
 - Pin-type 253
- Tool life 149, 163, 175
 - Effect of clearance angle 176
 - Effect of cutting-edge inclination angle 178
 - Effect of intermittent cutting 179
 - Effect of nose radius 179
 - Effect of primary cutting angle 177
 - Effect of rake angle 175
 - Effect of tool material 165
 - Effect of work material 163
- Tool life testing 158
 - Accelerated tool life testing 158
 - Facing test 159
 - Variable speed test 162
- Tool materials 165
 - Alloyed steels 166
 - Cast alloys 168
 - Cemented carbides 169
 - Ceramics 173
 - Coated bits 172
 - Cubic boron nitride 174
 - Diamond 173
 - Double (P-group) carbides 170
 - High carbon steels 166
 - High-speed steels 166
 - Single (K-group) carbides 170
 - Superhard materials 173
 - Triple (M-group) carbides 171
 - Tungsten less cemented carbides 172
- Tools used in lathe operations 7
 - Bent shank facing tool 7
 - Parting and grooving tool 7
 - Round-nose tool 7
 - Straight shank turning tool 7
 - Turning and facing tool 7
- Tool wear criteria 142
- Tool wear mechanisms 146
 - Abrasion wear 147
 - Adhesive wear 147

- Chemical wear 149
- Diffusion wear 148
- Top jaws 412
- Total cost analysis 425
- Turning operation 7

U

- Undeformed chip 58
 - In drilling 59
 - In face milling 64
 - Parameters 58
 - In plain milling 60
 - In turning 59
- Up milling 25

V

- V-block 325, 332
- V-locators 332
 - Sliding 332

- Velocity 95
 - Chip 95
 - Cutting 95
 - Shear 95
- Velocity relations 95

W

- Wear criterion 144
 - Bright band criterion 146
 - for crater wear 144
 - for flank wear 142
 - Force criterion 146
 - Processing criterion 146
- Wear curves 140
- Welded bodies of fixtures 386, 387
- Working motions 2
 - Feed motion 2
 - Primary cutting motion 2
 - Rotary 2
 - Translatory 2